EFFECT OF SOFT STORY ON SEISMIC PERFORMANCE OF REINFORCED CONCRETE BUILDINGS

A THESIS SUBMITTED TO
THE GRADUATE SCHOOL OF NATURAL AND APPLIED SCIENCES
OF
MIDDLE EAST TECHNICAL UNIVERSITY

BY
VESİLE HATUN AKANSEL

IN PARTIAL FULFILLMENT OF THE REQUIREMENTS
FOR
THE DEGREE OF DOCTOR OF PHILOSOPHY
IN
CIVIL ENGINEERING

SEPTEMBER 2017

Approval of the Thesis:

EFFECT OF SOFT STORY ON SEISMIC PERFORMANCE OF REINFORCED CONCRETE BUILDINGS

submitted by **VESİLE HATUN AKANSEL** in partial fulfilment of the requirements for the degree of **Doctor of Philosophy in Civil Engineering Department, Middle East Technical University** by,

Prof. Dr. Gülbin DURAL ÜNVER _____
Dean, Graduate School of **Natural and Applied Sciences**

Prof. Dr. İsmail Özgür YAMAN _____
Head of Department, **Civil Engineering**

Prof. Dr. Ahmet YAKUT _____
Supervisor, **Civil Engineering Department, METU**

Prof. Dr. Polat GÜLKAN _____
Co-advisor, **Civil Engineering Department, NCC, METU**

Examining Committee Members:

Prof. Dr. Murat Altuğ ERBERİK _____
Civil Engineering Department, METU

Prof. Dr. Ahmet YAKUT _____
Civil Engineering Department, METU

Assoc. Prof. Dr. Özgür KURÇ _____
Civil Engineering Department, METU

Assoc. Prof. Dr. İlker KAZAZ _____
Civil Engineering Department, Erzurum Technical University

Assoc. Prof. Dr. Özgür AVŞAR _____
Civil Engineering Department, Anadolu University

Date:
21.09.2017

I hereby declare that all information in this document has been obtained and presented in accordance with academic rules and ethical conduct. I also declare that, as required by these rules and conduct, I have fully cited and referenced all material and results that are not original to this work.

Name, Last Name: Vesile Hatun AKANSEL

Signature:

ABSTRACT

EFFECT OF SOFT STORY ON SEISMIC PERFORMANCE OF REINFORCED CONCRETE BUILDINGS

AKANSEL, Vesile Hatun

Ph.D., Department of Civil Engineering

Supervisor: Prof. Dr. Ahmet Yakut

Co-advisor: Prof. Dr. H. Polat Gülkan

September 2017, 168 pages

Real structures are almost always irregular, as perfect regularity is an idealisation that very rarely occurs. Structural irregularities may vary dramatically in their nature and, in principle, are very difficult to define. In comparison with research efforts dealing with horizontally irregular structures, studies aimed at predicting the behavior of structures with rough layouts in elevation are small in number. Due to drawbacks of irregular structures under seismic excitations, engineers are less confident to design these type of buildings. Vertical irregularities designated in buildings are due to many reasons such as strength, stiffness and mass irregularities and the dynamic behavior of the structures are related with those three parameters. The objective of this study is to carry out a comprehensive research to investigate the effect of vertical irregularities especially soft story on seismic response of structures and to examine efficiency and validity of code specified definitions of vertical irregularities. Typical RC Frames were selected from code designed buildings according to TEC 2007 and irregularities were introduced to reference (base case) frames. Definition of soft story irregularity was investigated.

Keywords: Reinforced concrete buildings, vertical irregularities, soft story, linear and nonlinear procedures, Nonlinear time history analysis.

ÖZ

BETONARME BİNALARDA YUMUŞAK KATIN DEPREM PERFORMANSINA ETKİSİ

AKANSEL, Vesile Hatun
Doktora, İnşaat Mühendisliği Bölümü
Tez Danışmanı: Prof. Dr. Ahmet Yakut
Tez Eş Danışmanı: Prof. Dr. H. Polat Gülkan

Eylül 2017, 168 sayfa

Gerçek yapılarda mükemmel düzenlilik oldukça nadir görülen bir idealleştirmedir ve hemen hemen her zaman düzensizdir. Yapısal düzensizlikler doğası gereği önemli ölçüde değişir ve teorik olarak tanımlamak oldukça zordur. Plan düzensizlikleri için yapılan araştırmalar ile karşılaştırıldığında, düşey düzensizlik bulunan yapıların yapısal davranışını tahmine yönelik yapılan araştırmaların sayısı azdır. Bu tarz yapıların deprem kuvvetleri altındaki davranışlarındaki belirsizliklerden dolayı mühendisler tasarımı güvensiz bulurlar. Binalarda belirlenen düşey düzensizlikler; kütle, dayanıklılık ve dayanım düzensizliklerinden kaynaklanmaktadır ve yapının dinamik davranışı tam olarak bu üç değişkenden etkilenmektedir. Bu çalışmanın amacı; düşey düzensizlik bulunan yapıların, özellikle yumuşak kat için, sismik tepkilerini araştırmak, kod ve yönetmeliklerde tanımlanan yumuşak kat tanımlarının ne kadar etkin ve geçerli olduğunu araştırılmıştır. Tipik betonarme çerçeveler DBYBHY göre tasarlanmış binalardan seçilmiş ve yumuşak kat düzensizliği, referans çerçevelere tanımlanmıştır. Yumuşak kat düzensizlik tanımlamaları araştırılmıştır.

Anahtar Kelimeler: Betonarme binalar, düşey düzensizlikler, yumuşak kat, lineer ve lineer olmayan analizler, Lineer olmayan zaman tanım alanında dinamik analiz.

To my family

ACKNOWLEDGMENTS

Firstly, I would like to express my sincere gratitude to my advisor Prof. Dr. Ahmet Yakut and co-advisor Prof. Dr. H. Polat Gülkan for their continuous support of my Ph.D study and related research, for their patience, motivation and immense knowledge. Their guidance helped me in all the time of research and writing of this thesis.

Besides my advisors, I would like to thank the rest of my thesis committee: Assoc. Prof. Özgür Kurç, Assoc. Prof. İlker Kazaz, for their insightful comments and encouragement, but also for the hard question which incented me to widen my research from various perspectives.

I am thankful to Prof. Dr. M. Altuğ Erberik, Prof. Dr. Ayşegül Askan Gündoğan, and Prof. Dr. Barış Binici for not hesitating to answer my insignificant questions. I am grateful to my co-advisor Prof. Dr. H. Polat Gülkan, Dr. Engin Karaesmen, Dr. Erhan Karaesmen, H. Hüseyin Güler and Prof. Dr. Mehmet Utku not only for their guidance in academia but also for their valuable experiences in life they shared.

I also would like to word my gratitude to Prof. Dr. P. Jack Moehle for his guidance, endless patience, helpful criticisms and encouragement throughout the one year research experience at University of California, Berkeley.

I thank my fellow collegues; Dr. Abdullah Dilsiz, Levent Mazılıgüney, Koray Kadaş, Murat Şahin, Dr. Özkan Kale, İsmail Ozan Demirel, Dr. Alper Aldemir, Hasan Eser, Erhan Budak, Fırat Soner Alıcı, and Kaan Kaatsız for their friendship and stimulating discussions they made for this study. In particular, I am grateful to Dr. Selim Günay, Dr. Pablo Parra and Dr. Carlos Arteta for their friendship, support, encouragement and helpful comments.

My special thanks goes to Başak Varli Bingöl, Murat Bingöl, Fatima Tekin Kahraman, Abdurrahim Kahraman for being more than a friend. I am thankful to Levent Mazılıgüney, Koray Kadaş, Saeideh Nazirzadeh, Shaghayegh Karimzadeh Naghshineh, Murat Şahin, Oruç Altıntaşı, Eren Yağmur for their precious friendship and the valuable times we spent together.

Last but not the least, I would like to thank to my family: my parents, brother and sister and my little niece, for supporting me spritually throughout writing this thesis and my life in general.

TABLE OF CONTENTS

LIST OF TABLES

TABLES

LIST OF FIGURES

FIGURES

LIST OF SYMBOLS

C_1: A coefficient that consider the ratio of length to width of infill wall

d_b: Rebar diameter

E_c= Modulus of elasticity of reinforced concrete

E_{fr} : Expected modulus of elasticity of frame material

E_{in} : Expected modulus of elasticity of infill materials

E_s= Modulus of elasticity of reinforcing steel

f_b: Compressive strength of brick elements

f_c: Compressive strength of reinforced concrete

f_m: Compressive strength of masonry infill wall

F_m: Maximum axial load capacity of equivalent strut

f_{mo}: Compressive strength of mortar

f_p: Compressive strength of plaster

f_{tp}: Cracking strength of the infill, obtained from a diagonal compression test

F_y: Yield force capacity of the equivalent strut

f_y: Yield stress of reinforcing steel

G_{in}: Tangential elastic modulus of masonry infill

H_{col} : Column height between centerlines of beam

H_{in} : Height of infill panel

I_{col} : Moment of inertia of column

K_1: Initial stiffness of the hysteretic material model

K_3: Post stiffness reduction (or post peak stiffness)

K_m: Secant stiffness calculated at maximum axial force capacity of the equivalent strut model

r_{in} : Diagonal length of infill panel

S_m: Displacement at maximum axial force capacity for equivalent strut material model

S_u: Maximum displacement in the hysteretic model

S_y: Yield displacement

t_{in} : t_w: Thickness of infill panel and equivalent strut

t_p: Thickness of the plaster

z: Contact length

α: A parameter used in the local bond-slip relation and can be taken as 0.4 in accordance with CEB-FIP Model Code 90

α: The ratio of story drift ratio to the drift ratio at modal height, which is calculated as 0.7 times of the story height,

α_2: The ratio of the inelastic roof displacement to the elastic roof displacement

α_{irreg}: The ratio of the inelastic roof displacement of irregular cases to inelastic roof displacement of the base case

η_k: Stiffness irregularity parameter (TEC 2007)

θ: Angle whose tangent is the infill height-to-length aspect ratio, in radians.

CHAPTER 1

INTRODUCTION

1.1. Problem Statement

Actual building structures are almost generally irregular, and regularity is an idealization that is rarely occurring. Structural irregularities may vary dramatically in their nature and are very difficult to define, in principle. The shape of the majority of structures is irregular, both in plan and in elevation. Therefore, studies on vertical irregularities are still state-of-art.

Vertical irregularities designated in buildings are due to many reasons such as strength, stiffness and mass irregularities and the dynamic behavior of the structures are related with those three parameters. Previous researchers focused on mostly strength and stiffness properties of the models employed.

In practice, infill walls may become one of the reasons of vertical irregularity resulting in the soft story. Misapplication or architectural aesthetics may lead to unexpected failures at story columns due to soft story effects. On the other hand, recent studies and seismic performance of RC buildings from recent earthquakes showed that infill walls have a significant effect on the strength capacity of the building and should be modeled in analysis and design. To be able to investigate the effect of vertical irregularities due to infill walls, i.e. soft story effect, a reliable infill wall model with accepTable A1ccuracy that simplifies modeling and decreases computational effort is needed. Thus, macro modeling seems useful due to decreasing the calculation effort and is preferred in this thesis for modeling of infill walls.

Due to the influence of infill walls that are considered to change the failure mechanism, their effect on the response of buildings was investigated in this study. The main focus of this study is soft story mechanism at first story and investigation of the relevant IBC and TEC2007 design parameters.

1.2. Literature survey

In comparison with research efforts dealing with horizontally irregular structures, studies aimed at predicting the behavior of structures with rough layouts in elevation are small in number. Nevertheless, in recent years research activity in this field has been growing. The reasons of the vertical irregularities were classified as mass, stiffness and strength discontinuities and their coupling behaviors. Researchers mostly focused on strength and stiffness irregularities. Mass irregularities are less important when it is compared with stiffness and strength irregularities (Al-Ali (1998)). Soft story mechanism is specified as a stiffness irregularity by codes. The literature on the effect of infill walls on soft story mechanism is limited.

In this thesis, the literature review is separated into three part. The first part is related with the effect of infill walls on the vertical irregularity, especially for the soft story. The second part is related with the modeling techniques of infill wall. The third and the last part is related with the experimental studies done on infilled frames.

1.2.1. The Effect of Infill Walls on Soft Story as a Vertical Irregularity

Open first story is a common architectural use in Turkey for shops, galleries and parking lots. The soft story mechanism and localized damages at between few stories was observed during past earthquakes. In Figure 1-1, the collapse of reinforced concrete buildings due to different type of failure mechanisms are given. First story failure mechanisms prone to occur when the first story infill walls do not exist. (Dolsek and Fajfar (2001), Inel and Ozmen (2008), Sezen et. al. (2003), Naeim et. al. (2000)).

Experimental studies showed that the irregular distribution of the infill walls yield large damage in the frames. (Negro and Colombo (1997) and Lu (2012)) Lu (2012) also tested a strength enhanced specimen by a smoothed overstrength profile and prevented the first story soft story failure.

a) b)

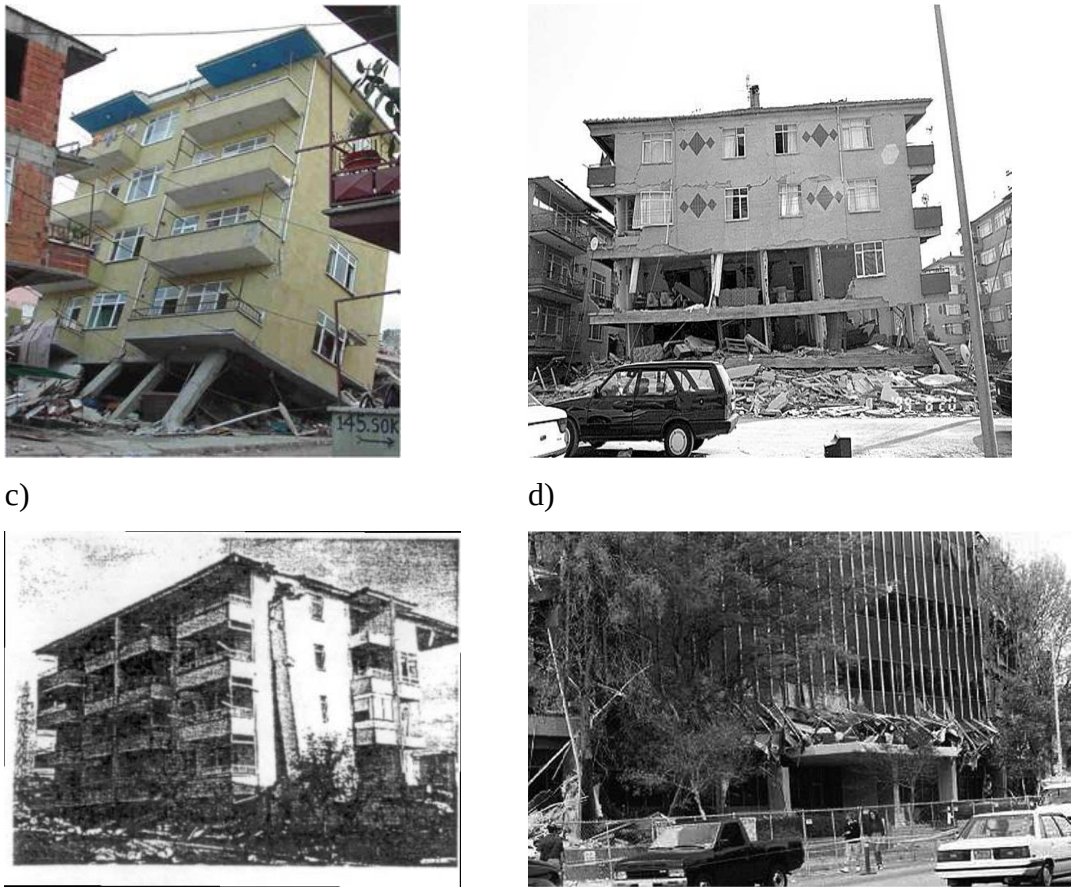

c) d)

Figure 1-1 a) Soft Story Failure (Gölcük, Turkey - 1999), b) Concentration of damage at first two story, 1999 Gölcük, Turkey (Sezen et. al. (2003)), c) Collapse in the bottom two storeys, 1999 Gölcük, Turkey (Dolsek and Fajfar (2001)), d) Collapse of the second floor, 1994 Northridge, USA (Naeim et. al. (2000))

Dolsek and Fajfar (2001), Korkmaz and Ucar (2006), Korkmaz et. al. (2007), Inel and Ozmen (2008), Sattar and Liel (2010), and Aksoy and Özgür (2015) studied reinforced concrete frames with varying infill wall arrangements. The common outcome from these research is that the collapse due to soft story mechanism is the result of the low

global and structural elements' ductility of the bare frames and the infill wall arrangements at the elevation of the building and the story level. Non-existence of the first story infill walls damage the frame almost same as the increased first story height (Inel and Ozmen (2008) and Sattar and Liel (2010)). The presence of infill walls changes the collapse mechanism of the frames. Aksoy and Özgür (2015) also checked the reduction in the shear forces in the columns and checked the values with 0.75 specified value in the RYTEİE 2013 (Principles regarding identification of risky buildings).

Some of the researchers also studied the real structures damaged under the real seismic excitations (Yoshimura (1997) and Verderame et. al. (2010)). Yoshimura (1997) studied a collapsed reinforced concrete building due to soft first story mechanism under the 1995 Hyogoken- Nanbu earthquake. Verderame et. al. (2010) investigated a case study from the 2009 L'Aquila earthquake. Both Yoshimura (1997) and Verderame et. al. (2010) used similar methodologies for the infill walls and included them in the nonlinear models. They obtained the similar damages with the real one and observed the first story failure. Yoshimura (1997) mention that if first story failure mechanism occurs, the collapse may result in with shear strength as low as 60 percent of the total base shear.

As mentioned before, soft story mechanism is a stiffness irregularity, however, the stiffness and strength irregularities may combined in most of the real cases and should be considered together (Sadashiva et. al. (2012)). Due to this relationship, it is needed to review parametric studies done to investigate the effect of vertical irregularities. Some of the studies are given below.

Soni and Mistry (2006) studied on a technical note which is based on the researches done on vertically irregular building frames. They concluded that there is a conflicting conclusion on setback structures, ELF method gives a sufficient results for buildings designed according to the code based limits on drifts. De Stefano and Pintucchi (2008) published a useful review paper related to the irregular building structures not only

regarding vertically but also in the plan. They focused on three area such as plan irregularity, passive control to mitigate the torsional effects and vertical irregularities.

Valmundsson et. al. (1997), Al-Ali and Krawinkler (1998), and Chintanapakdee and Chopra (2004) investigated the effect of stiffness, strength and mass irregularities via a parametric study. They used multistory frames to evaluate the irregularities. Valmundsson et. al. (1997) considered 6 different type of period and Al-Ali and Krawinkler (1998) used 3.0 s first mode period structure and adapted the stiffness and strength at each story by keeping the period as same. Valmundsson et. al. (1997) preferred equivalent lateral load analysis and Al-Ali and Krawinkler (1998), and Chintanapakdee and Chopra (2004) studied additionally nonlinear time history analysis and model pushover analysis. For elastic demand, Al-Ali and Krawinkler (1998) observed that increasing stiffness did not significantly change to the relative contributions of the different modes to elastic story shear and overturning moments as compared with the base case but decreasing the stiffness of one story can alter these contributions. They stated that strength modifications less than 1.2 are sufficient to change the ductility distribution over height from highly nonlinear to a uniform one except the top story. The highest amplification of ductility demands occurs when the weak story is at the mid-height. For the cases with the strong story, the highest amplification of ductility demands occurs at the base. They found that strength reduction factor, 2.0 is sufficient to cause most of the hysteretic energy demands to be dissipated. Their results showed that the cases with combined stiffness and strength irregularities, nonlinear response yields to the strength irregularity cases.

Aghdam and Tariverdilo, (2012) tried to provide straightforward and easy to evaluate numerical criterion to detect vertical stiffness irregularity. They proposed that by taking the ratio of the elastic response (i.e. drift) of the equivalent lateral load analysis result to the time history analysis can be useful to detect the damage localization in height.

Sadashiva et. al. (2012) studied coupled vertical stiffness-strength irregularities of 3, 5, 9, and 15-story steel building frames with a constant mass at each floor level. Structural ductility levels; 1, 2, 3, 4, and 6, and target (design) interstory drift ratios ranging between 0.5 and 3% were used. Inelastic time history analysis was performed to compare the maximum interstory drift ratio demands. They observed and concluded that the ELF method should not be allowed to design the irregular structures because, the codes do not have a systematic quantitative justification for irregularity. They proposed an equation for the stiffness and strength irregularity existence.

Das and Nau (2003) investigated the definition of irregular structures for different vertical irregularities: stiffness, strength, mass, and that due to the presence of nonstructural masonry infill. They observed that the restrictions on the applicability of the equivalent lateral force procedures are unnecessarily conservative for particular types of vertical irregularities considered and these are typically cast-in-place reinforced concrete structures with beams cast monolithically with slabs and supported by columns. They observed and proposed that, if stiffness or strength irregularity exists at the first-story level, a higher overstrength ratio (presently 1.2) can be used for the first story columns. Also, they suggested that design shear should be based on the maximum probable strengths of the captive columns of the buildings with nonstructural infill walls. They observed that ELF (UBC) method has an accepTable A1ccuracy for the design of vertically irregular structures.

1.2.2. Infill Wall Models in Past Studies

The influence of infills within reinforced concrete frame structures is a state-of-art topic for researchers. Infill walls affect the strength, stiffness, ductility with a non-deniable level when the reports of the big earthquakes are investigated. The experimental studies done by many researchers also support the contribution of the infills (Panagiotakos and Fradis (1996), Magenes and Pampanin (2004), Dolsek and Fajfar (2005, 2008), Ercolino et. al. (2012) and Furtado et. al. (2015)). Infill walls may also cause severe damage if the surrounding frame is not well designed for

earthquake forces. Failure mechanisms may change drastically and cause collapse before the real capacity is reached (Ercolino et. al. (2012), Furtado et. al. (2015), and Fiore et. al. (2012a,2012b)).

Material non-linearity is the main factor affecting the nonlinear behavior of the infilled frames. The sources of non-linearity can be grouped for each structural element such as; crushing and cracking of masonry, stiffness and strength degradation for infill panels; cracking of concrete yielding of reinforcement bars and bond slip for surrounding frame; contact length change and degradation of bond-friction mechanisms.

Several models have been developed and used in literature for the design of infill walls such as macro-models and micro models. The developed models can be classified according to their complexity (macro model like equivalent strut model or micro model like finite element models) and the ability to capture the failure mechanisms in the infill walls such as horizontal slip, diagonal cracking or corner crushing.

Tabeshpour et. al. (2012) and Trapani et. al. (2015) studied an extensive literature review which mentions all significant contributions made to infill modeling. Trapani et. al. (2015) observed the most relevant issues for infilled reinforced concrete frames such as;

- Vertical loads transferred to the infills influence both stiffness and strength.
- The strength to assign the equivalent strut depends on shear strength, but different failure mechanisms are also effective.
- Equivalent strut width depends on surrounding frames geometrical and mechanical properties.
- Columns should be checked for shear failure because failure mechanism changes.

In this thesis, macro modeling was preferred for infill wall modeling. Macro models can be investigated through some sub-topics. The first one is the equivalent strut width.

The second important issue is the strength calculation of infill, and the third one is the number of struts in the models.

1.2.2.1. Equivalent Strut width, w

In Table 1-1, proposed w formulas by some researchers are given. Holmes (1981), Paulay and Priestley (1997), and Penelis and Kappos (1992) proposed the equivalent width of the strut as a proportion of the diagonal length of the infill wall. However, b_w, equivalent strut width is not only related with diagonal length but also is related with the frame and infill panel mechanical properties. There are some other aspects to consider in formulating b_w, such as; degradation under cyclic loading, cracking of the panel and adjustment of the parameters during the loading history: high initial stiffness and smaller one at the failure when only the central strip of the panel is working.

Smith and Carter (1970) were among the first authors who studied the concept of the relative stiffness of frame to infill panel. They used some charts to calculate equivalent strut width via contact length definition. In Eq. (1-1), α is the contact length parameter (z) for the surrounding frame, λ is the relative stiffness (Eq (1-2)), and h_{inf} is the height of the infill.

Kadir (1974), Klingner and Bertero (1976), Lliauw and Kwan (1984), Durrani and Luo (1994) , Hendry (1998), Dawe and Seah (1989), and Bertoldi et. al. (1993) , Smith and Carter (1970) and Mainstone (1971) used experimental test results or finite element modeling technics. The proposed equivalent strut width equations in Table 1-1 should be considered with the proposed λ, the relative stiffness parameter. In this way, the results will be consistent with experimental or analytical studies done. Kadir (1974), Hendry (1998) and Dawe and Seah (1989), Saneinejad and Hobbs (1995), and El Dahhakhini et. al. (2003) calculated the λ parameter for columns and beams separately.

Table 1-1 Formulas proposed for equivalent masonry strut's effective width by researchers

Researcher	**w**
Holmes (1981)	$w = 0.33 \cdot d$
Mainstone (1971)	$w = 0.175 \cdot d \cdot (\lambda H_w)^{-0.4}$
Smith and Carter (1970)	From charts via λ *and* α
Liauw and Kwan (1984)	$w = 0.95 \cdot H_w \cdot cos(\theta) \cdot (\lambda H_w)^{-0.5}$
Penelis and Kappos (1992)	$w = 0.25 \cdot d$
Pauley and Priestley (1997)	$w = 0.20 \cdot d$
Durrani and Luo (1994)	$w = 0.32 \cdot d \cdot sin^{1.5}\left(\frac{E_{inf} \cdot t_{inf} \cdot H^4}{m \cdot l \cdot E_c \cdot H}\right)^{-0.1}$ $m = 6 \cdot \left(1 + \frac{6}{\pi} \cdot \tan^{-1}\frac{H \cdot l_t}{L\dot{I}_p}\right)$
Kadir (1974)	$w = \frac{\pi}{2}\left(\frac{1}{4\lambda_p} + \frac{1}{\lambda_T}\right)$
Hendry (1998)	$w = 0.5 \cdot (\alpha_h + \alpha_l)^{0.5}$ $\alpha_h = \frac{\pi}{2}\left(\frac{E_c I_c H}{2E_m t sin(2\theta)}\right)^{1/4}$ $\alpha_l = \pi\left(\frac{E_c I_c l}{2E_m t sin(2\theta)}\right)^{1/4}$
Dawe and Seah (1989)	$w = \frac{2\pi}{3}\left(\frac{\cos\theta}{\lambda_p} + \frac{\sin\theta}{\lambda_T}\right)$
Bertoldi et. al. (1993)	$w = d\left(\frac{K_1}{\lambda H} + K_2\right)$ $\lambda H < 3.14$ | $3.14 < \lambda H < 7.85$ | $\lambda H > 7.85$ K_1: 1.3 | 0707 | 0.47 K_2: −0178 | 0.01 | 0.04

$$\frac{\alpha}{h} = \frac{\pi}{2\lambda h} \tag{1-1}$$

$$\lambda = \left[\frac{E_{inf} \cdot t_{inf} \cdot \sin(2\theta)}{4 \cdot E_{fr} \cdot I_{col} \cdot h_{inf}}\right]^{1/4} \tag{1-2}$$

Papia et.al (2003) and Amato et. al. (2009) proposed a methodology that also considers the vertical load transmission by the frame to infill walls. Amato et.al, (2009),

suggested a simplified tool to take into account the effects of infill walls. They stated that the FEMA approach, proposed by Mainstone (1971), underestimate the stiffening effect of infill wall and lateral strength. Mainstone (1971)'s model does not consider axial stiffness of columns and vertical load occurring after the construction of infills.

1.2.2.2. Strength Calculation and Constitutive Law for the Equivalent Strut

The infill wall modifies the overall strength and stiffness of the system under the seismic excitation. Infilled frames in the non-linear analysis have many uncertainties such as; material characteristic properties and openings that affect the degradation behavior under cyclic loadings.

Uva et. al. (2012) and Trapani et. al. (2015) reviewed the literature for the evaluation of the strength of the equivalent strut. The main inference of the models proposed for the force deformation relationship is the estimation of all possible failure mechanisms, such as; crushing at the center of the panel, crushing of corners, sliding of the bed joints or diagonal tensile failure. Strength capacity can be obtained by calculating all these failure mechanisms. However, stiffness is also as effective as strength in the modeling of the degradation behavior.

As mentioned by Uva et. al. (2012) and Trapani et. al. (2015), the well-known and mostly used force-deformation relationships were proposed by Panagiotakos and Fardis (1996) and Bertoldi et.al (1993). Some simplifications were made for hysteretic model by Dolsek and Fajfar (2005, 2008). The common points of these models are that they are easy to apply for many commercial and open-source software and less computational.

Panagiotakos and Fardis (1996) and Bertoldi et. al. (1993) proposed their constitutive law for the equivalent strut model based on experimental studies. Both methods have a similar point of views to the definition of strength and stiffness. The only difference comes from the effective stiffness definition, K_m. Bertoldi et. al. (1993) arranged force-

deformation relationship around K_m, which is given in Eq.1-10 and Figure 1-3. Panagiotakos and Fardis (1996) assigned and defined stiffness separately in Figure 1-2 by given formulas in Eq.1-3 through 1-7.

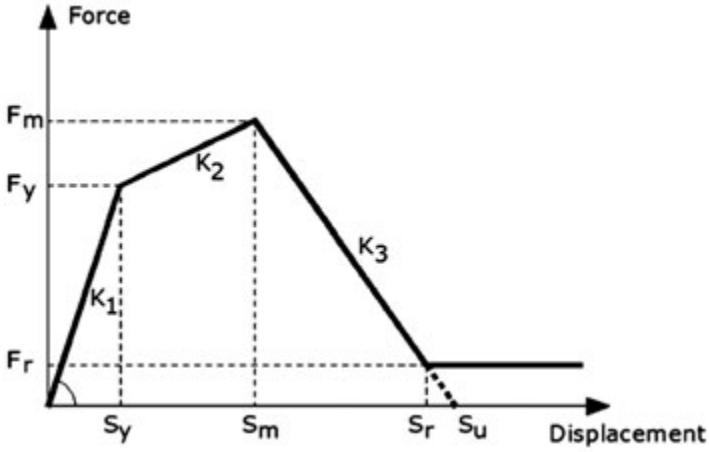

Figure 1-2 Force-Displacement constitutive law proposed in Panagiotakos and Fardis (1996).

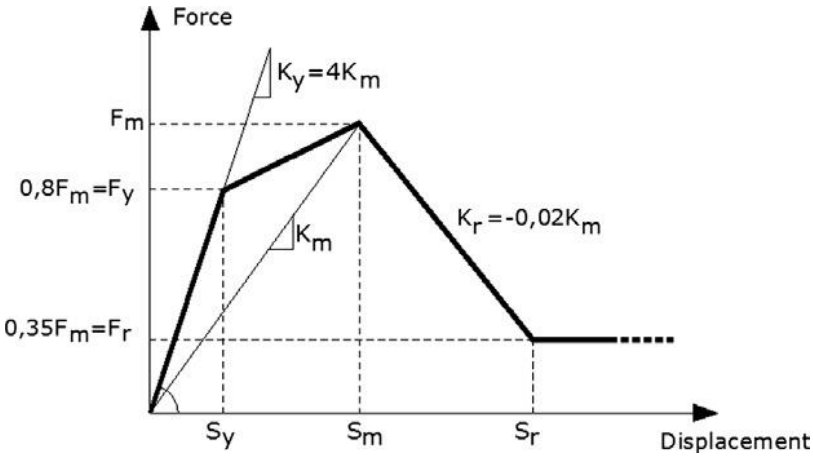

Figure 1-3 Force-Displacement constitutive law proposed in Bertoldi et. al. (1993).

In Eq. 1-3, K_1 is the uncracked stiffness, and F_y is the yielding force at first cracking. f_{tp} is the tensile strength of infill at diagonal compression test. t_w is thickness, L_w and H_w are the length and height of the infill wall, respectively.

$$K_1 = \frac{G_w t_w L_w}{H_w}; \qquad F_y = f_{tp} t_w L_w; \qquad S_y = \frac{F_y}{K_1} \tag{1-3}$$

K_2 is the axial stiffness of the equivalent strut, w, which is calculated from the formula proposed by Klingner and Bertero (1976). Softening stiffness changes in a range as defined in Eq 1-5. In Eq. 1-6, the residual force range is given.

$$K_2 = \frac{E_m w t_w}{d}; \qquad F_m = 1.3F_y; \quad S_m = S_y + \frac{F_m - F_y}{K_2} \tag{1-4}$$

$$0.005K_1 \leq K_3 \leq 0.1K_1 \tag{1-5}$$

$$0 \leq F_r \leq 0.1F_y \tag{1-6}$$

$$S_r \; or \; S_u = S_m + \frac{F_m - F_r}{K_3} \tag{1-7}$$

Dolsek and Fajfar (2005,2008) proposed that F_y=0.6*F_m, Fr=0, and S_m=0.2% in the case of fully infilled and 0.1% for the case of infill with the opening. Residual displacement to displacement at maximum force ratio is proposed as S_r/S_m =5.

Bertoldi et. al. (1993) performed pushover analysis of 10 different frames to modify the infill constitutive law and construct the model by calculating K_m and F_m. Km is given in Eq. (1-8). F_m is calculated by taking into account the minimum of the four possible failure mechanisms of infill walls as given from Eq. 1-9 through Eq. 1-13. These failure mechanisms are crushing at the center of the panel, crushing of the corners, sliding of the bed joints and diagonal tensile failure.

$$K_m = \frac{E_m w t_w}{d} \cos^2 \theta \tag{1-8}$$

$$\sigma_{w1} = \frac{1.16\sigma_{mo} \tan\theta}{K_1 + K_2 \lambda H} \tag{1-9}$$

$$\sigma_{w2} = \frac{1.12\sigma_{mo} \sin\theta \cos\theta}{K_1(\lambda H)^{-0.12} + K_2(\lambda H)^{0.88}} \tag{1-10}$$

$$\sigma_{w3} = \frac{(1.2\sin\theta + 0.45\cos\theta)u + 0.3\sigma_o}{\frac{K_1}{\lambda H} + K_2} \tag{1-11}$$

$$\sigma_{w4} = \frac{0.6\tau_{mo} + 0.3\sigma_o}{\frac{K_1}{\lambda H} + K_2} \tag{1-12}$$

$$F_m = (\sigma_w)_{min} w t_w \cos\theta \tag{1-13}$$

F_m , infill strength capacity, is studied by many researchers in literature, however, in this thesis, the formula proposed by Zarnic and Gostic (1997) was used. They simplified the strength capacity formula by considering a C_1 factor, which considers the wall length to height ratio. This proposed formula includes wall ratio in a way with C_1 factor and calculates max axial load capacity of the strut by considering frame and infill coupling, and the vertical load carried by the infill. The simplified formula is given in Eq 1-14; where f_{tp} is the cracking strength of the infill, obtained from a diagonal compression test, whereas L_{in} and H_{in} are the lengths and the height of the infill.

$$F_m = 0.818\frac{L_{in}t_w f_{tp}}{C_1}\left(1+\sqrt{{C_1}^2+1}\right), \quad C_1 = 1.925\frac{L_{in}}{H_{in}} \tag{1-14}$$

1.2.2.3. Multiple Strut Models

Smith and Carter (1969) proposed a parameter for the interaction of the infill wall and frame as α which is mentioned as z by other researchers for the contact length definition. This parameter helped to construct the multiple strut models. The necessity of contact length z comes from the shear force concentration at the frame member ends due to infill walls. Under seismic excitations, shear forces are lumped in the contact length regions and this behavior increased the shear forces and deformations in the frame members and miscalculation of the bending moments in the frames. In some cases, such as; strong infill with the weak frame, shear failure in surrounding frames may occur. Many researchers (Chrysostomou (1991); Buonopane and Fajfar (1999); El- Dakhakhni (2003, 2004) reported that the shear and bending moment redistribution could not be modeled with single strut model with two loaded corners.

Thiruvengadam, V. (1985) proposed the use of multiple strut models. The model includes moment-resisting frames with vertical and horizontal pin supported strut elements. Shear and axial stiffness of the infill was assigned to the struts.

Chrysostomou (1991) studied a six compression-only strut to model infill walls. Three struts for each direction is defined. The author used contact length as half of the calculated α value according to Eq. 1-1. Crisafulli (1997) used several methods to compare the modeling techniques and multiple strut model proposed by Chysostomou (1991) was one of them. In Figure 1-4, the considered strut models by Crisafulli (1997) are given.

Syrmakezis and Vratsanou (1986) used five parallel struts in each diagonal direction and observed that the different contact length definitions have a significant effect on bending moment distribution on the frame.

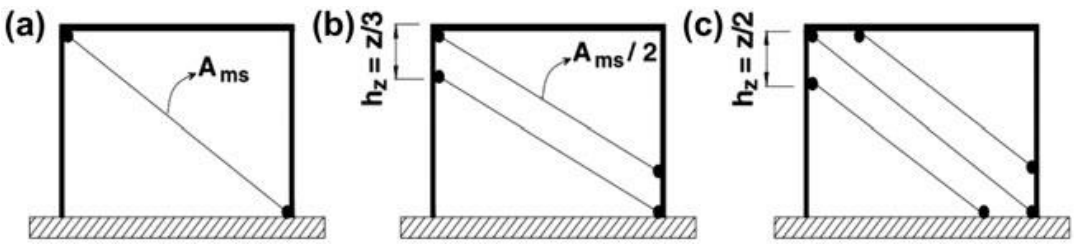

Figure 1-4 Multiple strut configurations from Crisafuli (1997); a) single strut; b) two-strut; c) three-strut model

El-Dakhakhni et. al. (2003, 2004) used the six-strut model by using the different λ and different contact length values for column and beam and compared the monotonic infilled steel frame test results.

Asteris et. al. (2011b) studied a good literature review and case study for macro-modelling of the infilled frames.

1.2.2.4. FEM and Hysteretic models developed for infill walls and case studies

Beyond the single and multiple strut models, there are many other complicated and sophisticated finite element models (FEMs) and hysteretic material models developed for the struts. Micro-modeling techniques are not in the concern of this thesis. Therefore, only a few of them will be mentioned in this part.

Mehrabi et. al. (1997), investigated experimental and analytical studies for infilled reinforced concrete frames with a micro-modeling approach using finite element method. They used smeared crack in their finite element model.

Stavridis and Shing, (2010), used a micro-modelling approach which combines smeared and discrete crack to model infilled reinforced concrete frames. They proposed a systematic approach to calibrate the numerical model. They used experimental studies for validation and gave a sensitivity analysis for modeling parameters. They observed that μ_0, the friction coefficient, value for mortar joint is the most important.

Crisafulli et. al., (2000b), studied and reviewed many macro and micro-modeling approaches in the literature. They mention that the experimental studies for infill and surrounding frames should be investigated in detail to develop more accurate FEM models.

Mohyeddin et. al., (2013), analyzed infilled reinforced concrete frames using finite element modeling with ANSYS. They investigated in-plane and out-of-plane behavior and proposed a simple method to overcome the convergence problem.

Some of the researchers developed a hysteretic model for the simplified macro models. Madan et. al. (1997), Mosallam et. al. (1997) and Crisafulli (1997) are few of these researchers.

Madan et. al. (1997), proposed a hysteretic model for analytical macro model based on equivalent strut approach for representing masonry infill panels in nonlinear analysis of frame structures. They studied many failure modes of the infill panels. Mosalam et. al. (1997), tested gravity-load designed steel frames with various types and configurations of infills and proposed a hysteretic model for infilled frames.

Crisafulli (1997) developed a hysteretic model also for the strut models of infill walls. This hysteretic model is tested for experimental studies, and it is implemented in SeismoStruct software.

Beside all these theoretical studies for modeling the in-plane behavior of infill walls, it is a necessity to mention the case studies performed with these modeling techniques and their observations. Some of these researchers cited in this thesis are Panagiotakos and Fardis (1996), Magenes and Pampanin (2004), Fiore et. al. (2012), Ercolino et.al (2012), and Furtado et. al. (2015).

Panagiotakos and Fardis, (1996), studied a parametric study to understand the nonlinear behavior of infilled frames under seismic excitations. They performed an extensive parametric study which includes SDOF analysis for the elastic period, 4 story building with various infill arrangements to investigate the effect of intensity of ground motions and several reinforced concrete frames with different configurations of infills to understand design under earthquake loadings. They noted that Eurocode 8 is conservative in the design of infilled reinforced concrete buildings for seismic design.

Magenes and Pampanin, (2004), studied existing reinforced concrete structures designed with infill and without infill frames for only under gravity loads. They used the method proposed by Crisafulli (2000) to simulate the axial response of the equivalent struts. They used the pseudo-dynamic response of a four-story building, with infill walls, tested in Italy (Galli (2002)). They gave some performance levels depending on the L/H and strain values.

Oo et. al., (2012), present a simple method derived from the mechanism between infill and reinforced concrete frame. They used two equilibrium, such as static equilibrium of compression balance between the frame-infill interface and lateral displacement compatibility. They found contact length in an iteration and calculated compression strut width regarding contact length. They compared the analytical model with some

experiments. Tests represented the reinforced concrete frames with non-structural infill walls. They obtained good results for strength and stiffness calculation of infill wall.

Fiore et. al. (2012), studied the performance of existing reinforced concrete buildings with infills with low (3-story) and medium (7 stories) height, two cases. They analyzed 3D models, and used equivalent strut model with trilinear hinge model. They also considered the openings in the equivalent strut calculation. The infills used in the models are strong. They used N2 method for the assessment.

Ercolino et. al., (2012), used some dynamic identification data to estimate the mode shapes and frequencies of the infilled RC frames designed according to Eurocode and calibrate the linear structural model of reinforced concrete frame with infill. They only considered the flexural controlled behavior of reinforced concrete frame and didn't observe any significant decrease in displacement capacity for the infilled frames.

Furtado et. al, (2015), proposed a modified equivalent strut model for infill masonry and investigated the seismic response. They studied 3D models and considered only in-plane calibration in their models.

Furtado et. al, (2016), studied in-plane and out-of-plane interaction of masonry infills. They proposed a procedure with element removal option and defined an interaction diagram for masonry infill. They used incremental dynamic analysis to see the seismic response of the proposed procedure and derived the fragility curves.

Decanini et. al., (2004), studied seismic performance of 2-24 storey masonry infilled reinforced concrete frame. They used shear type frames with three types of infill (weak, intermediate and strong) and investigated elastic and inelastic behavior. They observed that for a given type of infill, the strength capacity of the frame increases rather than ductility capacity. For limited ductility levels, they noted that infill might undergo inelastic deformations.

Sanij and Alaghebandian, (2012), compared diagonal strut, three strut and horizontal spring models for infilled reinforced concrete frames. They observed that the horizontal spring model gives less stiff and more ductile behavior.

Su and Shi, (2013), studied displacement-based earthquake loss assessment (DBELA) methodology for reinforced concrete frames with infill masonry panels. They calculated the effective period of the frames based on decided limit states and calculated effective periods. They proposed a simplified equation to find effective period according to ductility level.

1.2.3. Experimental Studies on Infilled Reinforced Concrete Frames

Theoretical applications and developed models have to be verified and validated by experimental studies. In this part, the experimental studies investigated on infilled reinforced concrete or steel frames will be given and discussed.

Flanagan et. al, (1999), performed several bi-directional tests on structural clay tile infilled steel frames to assess in-plane and out-of-plane behavior. They compared the results with few proposed methods in the literature, especially for out-of-plane forces. They observed that only very tall or very thin (h/t) panels might be vulnerable to inertial forces. Interaction of in-plane and out-of-plane forces was not significant at moderate levels of loading. They also observed that after much damage to the infill, there is still a contribution to the lateral strength under combined loading.

Ispir and Ilki, (2013), studied the monotonic and cyclic behavior of unreinforced brick masonry walls. Their studies showed that proportional strain value is between 0.19% - 0.34% and strain value at peak stress is between 0.65% - 0.95%. They have also obtained some relationships for stress strain relationships. Their studies can be an example to strong masonry walls.

Mehrabi et. al., (1996), tested twelve ½ scaled one-bay one-story frame with strong and weak infill walls and frames. They observed a different type of failure mechanisms. First major cracks in weak infilled weak frames occurred at 0.17 story drift and at 0.33 story drift for strong infilled weak frame. Strong frame has first major crack in infill at 0.36 for weak and 0.46 for strong infills.

Huang et. al., (2006), tested six one-bay one-story reinforced concrete frame with half and fully infilled masonry panels. They used CFRP for the columns to strengthen the capacity of the frames.

Mosalam et. al. (1997), tested gravity-load designed steel frames with various types and configurations of infills and proposed a hysteretic model for infilled frames.

Kakaletsis and Karayannis (2008), tested a series of 1/3 scaled one-bay, one-story weak and strong infilled reinforced concrete frames designed according to modern code provisions. They selected infills such that would not cause shear failure in columns and tested bare, fully infilled and infilled with openings frames. They observed that in all tested specimens the first major crack in the infill occurred between 2.54% - 3.87%. The stiffness of the frames for infills with openings 1.57 to 2.5 times of the corresponding bare frame and 2.48 to 2.62 times of bare frame for the case of solid infills. They conclude that the infills, even with openings, improve the strength capacity of the frames.

Asteris et. al. (2011a), tested one-bay, one-story reinforced concrete frames with infill. The experimental specimens are excited to slowly cyclic lateral loads and observed different types of failure modes. They noted that plastic hinge governs the failure mechanism of the frame with infill with window opening at both ends of the columns. The failure mechanism of the frame with door opening has also corner – toe crushing. Both frames have sliding shear mechanisms inside the unreinforced masonry. They observed that first cracking diagonal crack in the infill was observed at a drift of 0.3%

and plastic hinges were developed at the drift of 0.4% at the ends of surrounding columns.

Zovkic et. al., (2012 and 2013), tested ten one-bay, one story infilled reinforced concrete frames and use three types of masonry bricks to represent the soft, medium and strong infilled wall behavior. They observed that in all infilled frames; the first crack occurred around 0.05% story drift and retained their capacity up to 1% story drift.

Markulak et. al. (2013), tested nine one-bay one-story unreinforced masonry infilled steel frame with clay and AAC blocks. They also designed a combined infilled frame from clay and AAC blocks to create a controlled failure mechanism.

Sigmund and Penava, (2013), tested and investigated the influence of the confinement on the infilled frames with an opening on one-bay, one-story 1:2.5 scaled reinforced concrete frames. They used tie columns for openings to preserve the strength, stiffness and ductility. They used analytical methods proposed by other researchers on literature and showed that the calculated drift values are lower; stiffness values are higher and shear capacity of infills are lower than experimental results. They stated that the cracking of infills around 0.05% - 0.1% and suggested as serviceability level or slight damage. They stated the moderate damage level as 0.2-0.3%, 0.5% for heavy damage and 1% for the collapse regarding drift. They also observed that initial stiffness for all experiments is almost 3 times higher than the bare frame.

Sucuoğlu and Siddiqui, (2014), tested an autoclaved aerated concrete (AAC) infilled reinforced concrete frame with PsD testing. They used three level of the earthquake to see the damage levels. They observed infill contribution after 2% interstory drift. They observed a slight shear damage in surrounding columns. They also proposed a simplified method to calculate the infill contribution for design.

1.3. The Objective and Scope

The objective of this study is to investigate the effect of soft story especially due to infill wall arrangements and discontinuities in height for reinforced concrete buildings.

The scope of this thesis is infilled reinforced concrete frames with vertical irregularities and their seismic behavior. The frames are selected from the 3, 5 and 8 story buildings designed according to TEC 2007, TS 500 and TS 498. All frames are designed to prevent the shear failure in columns. In design procedure, infill walls assigned to the system only as mass.

The designed frames are considered as base (reference) frame and the vertical irregularities defined to these frames. These changes are; increased first story height, decreased column dimension at first story columns and increased first story column longitudinal reinforcement area. Code and specification rules for vertical irregularity definitions and parameters are reviewed. The Eurocode 8 takes some precautions for the infilled frames, however, does not use any identifier for vertical irregularities. The FEMA 368-2000, IBC 2012 and the NBC 2005 use the similar definitions for vertical irregularity identification. TEC 2007 uses η_k and η_c parameters for soft and weak story definitions.

In this thesis, the vertical irregularity parameters are investigated through the parameters defined by TEC 2007 and IBC 2012 for soft story and weak story. Some additional parameters for vertical irregularity identification are used such as α: roof drift to drift at effective height, α_2: inelastic displacement to elastic displacement at roof, α_{irreg}: Inelastic roof displacement of the irregular case to the base case. These additional parameters are suggested by Seneviratna and Krawinkler (1997) and Al-Ali and Krawinkler (1998).

The object of this thesis is to investigate the irregularity parameters and to examine their usability for infilled reinforced concrete frames and the limit values.

1.4. Organization of the Dissertation

This thesis includes six chapters. First Chapter is related with the problem statement and the literature studies discussing previous research on relevant topics.

In the second chapter, the vertical irregularities defined in different seismic and design codes are discussed. These codes and specifications are TEC 2007 (Turkish Earthquake Code), Eurocode 8, FEMA 368-2000, IBC 2012 (International Building Code) and NBC 2005 (National Building Code of Canada).

In the third chapter, verification and validation of the modeling of frames were discussed. OpenSees (The Open System for Earthquake Engineering Simulation (McKenna (1997))) software was used for modeling of reinforced concrete frames with infills. Experimental test specimens were studied for comparison of the numerical modeling technique. Infill modelling was discussed and a sensitivity analysis was performed to see the effect of each parameter on the results. As a result of the sensitivity analysis, the modeling parameters and definitions are clarified for the rest of the study.

In the fourth chapter, the building stock in Turkey was discussed, and the representative buildings are introduced. The representative 3, 5, and 8 story buildings were designed according to TEC 2007, TS 500 and TS 498. Then, the representative frames were selected. The vertical irregularities are assigned to these representative frames by considering the strength and stiffness change. The stiffness of the first story is decreased 20 percent to see soft story due to stiffness change. The reinforcement area in the columns is increased 1.5 times to see the strengthening effect.

In the fifth chapter, linear static and nonlinear static analysis were performed. The failure mechanisms of each frame were given regarding immediate occupancy and

collapse presentation limit states. These limit state calculations were discussed. Shear checks of the corresponding frames were considered and done.

In the sixth chapter, the results of the analysis were discussed and some conclusions derived from the study are presented.

CHAPTER 2

VERTICAL IRREGULARITY ON CODES AND SPECIFICATIONS

2.1. Code and Specification Rules for Vertical irregularity

Vertical irregularities are classified into four categories in most of the codes and specifications, and these are named as, soft and weak story irregularities, mass irregularity, and discontinuities at the structural elements in elevation. In this chapter, Turkish Earthquake Code (TEC 2007), Eurocode 8, International Building Code (IBC 2012), FEMA 368, and NBC are briefly described for the vertical irregularity definitions. The focus is on the soft story mechanism.

2.1.1. Turkish Earthquake Code (TEC 2007)

These irregularities are defined in Chapter 2.3 in TEC 2007. Irregularities are divided into two-part: irregularities in plan and vertical irregularities. Vertical irregularities are explained as follows;

<u>B1 – Strength Irregularities between neighbouring stories (Weak Story):</u>

In RC structures, the ratio of the effective shear area of any floor to the one upstairs is called as Strength Irregularity Coefficient, η_{ci}. If this coefficient is smaller than 0.8 as defined in (2-1), it is stated that there exists weak story. The effective shear area at any floor is defined in (2-2).

$$\eta_{ci} = (\sum A_e)_i / (\sum A_e)_{i+1} < 0.8 \qquad (2\text{-}1)$$

$$\sum A_e = \sum A_w + \sum A_g + 0.15 \sum A_k \qquad (2\text{-}2)$$

ΣA_e= Effective shear area at any storey and the earthquake direction under consideration.

ΣA_g= Cross section area of the shear walls parallel to the earthquake direction under consideration at any storey

ΣA_k= Cross section area of the infill walls (except door and windows openings) parallel to the earthquake direction under consideration at any storey

ΣA_w= Effective cross section area of columns (except the overhangs of columns at the perpendicular to the earthquake direction under consideration)

If the total infill wall area of the i'th story is greater than the (i+1)'th story, the infill wall areas are not taken into account when calculating the η_{ci}.

If the η_{ci} is between the range as given in Eq. 2-3, $(\eta_{ci})_{min}$ is multiplied by structural behavior factor of 1.25 and will be applied to the whole building at all earthquake directions. $(\eta_{ci})_{min}$ cannot be smaller than 0.6.

$$0.60 \leq (\eta_{ci})_{min} < 0.80 \qquad (2\text{-}3)$$

<u>B2 – Stiffness Irregularities between neighbouring stories (Soft Story):</u>

The soft story is defined in TEC2007 as; when the ratio of the i'th story average inter story drift ratio to the (i+1) or (i-1)'th story average inter story drift ratio is greater than 2.0 (Eq 2-4). η_{ki} is the stiffness irregularity coefficient. Δ is inter story drift and h is the story height.

$$\eta_{ki} = (\Delta_i / h_i)_{ort} / (\Delta_{i+1} / h_{i+1})_{ort} > 2.0 \text{ or} \qquad (2\text{-}4)$$
$$\eta_{kj} = (\Delta_i / h_i)_{ort} / (\Delta_{i-1} / h_{i-1})_{ort} > 2.0$$

Soft story calculations must be done under the 5% eccentricity consideration.

<u>B3 – Discontinuity of Vertical Structural Elements:</u>

The condition of removing the vertical structural elements (columns, shear walls) of buildings from some of the stories and placing them on the beams or increased column

section edges or placing shear walls onto the columns and beams of the lower story (TEC2007 (Figure 2.4)). These kind of irregularities are out of concern for this study.

2.1.2. Eurocode 8 (EN 1998-1:2004)

In EC8 (EN1998-1:2004), part 4.2.3.3; a building is defined vertically regular, if all columns and shear walls are continuous up to the top of the relevant level if setbacks exist; if the mass of the floor and stiffness of the columns and shear walls do not change significantly in whole height and the ratio of the actual story resistance to the analysis result should not change significantly with the adjacent story. If there exist setbacks in the buildings, some extra precautions should be considered according to part 4.2.3.3 in EC 8. Setbacks are out of concern for this study.

If any of the above is not satisfied, the building will be assumed as non-regular, and the behavior factor q shall be decreased. It should be mentioned that a behavior factor q of up to 1.5 shall be used in deriving the seismic actions, regardless of the structural system and the regularity in elevation.

There is no a specific period calculation equation for irregular structures in Eurocode8, and Equivalent Lateral Force Method (ELF) is not permitted for the design with vertical irregularities.

In EC 8, chapter 5.2.2.2, the behavior factor q, which should be decreased 20% in the case of irregularity in elevation, is discussed. In Eq.2-5, the formula for the calculation of q in the case of vertical irregularity is given.

$$q = q_o \cdot k_w \geq 1.5 \qquad (2\text{-}5)$$

q_o is the basic value of the behavior factor, dependent on the type of the structural system and its regularity in elevation and k_w is the factor reflecting the prevailing failure mode in structural systems with walls (Eq. 2-6). α_o is the prevailing aspect ratio

of the walls of the structural system (Eq 5.3 in EC 8) Basic value of the behavior factor q_0, for systems regular in elevation can be obtained from Table 5.1, EN 1998-1:2004.

$$k_w = \left\{ \begin{array}{c} 1.00, \text{for frame and frame equivalent dual systems} \\ \frac{1+\alpha_o}{3} \leq 1, \text{but not less than 0,5, for wall, wall} - \text{equivalent and torsionally} \\ \text{flexible systems} \end{array} \right\} \quad (2\text{-}6)$$

There are some precautions considered for infill walls existence in EC 8. Infill wall irregularities are mentioned in part 4.3.6.3.2 in EC 8. If there is an infill wall arrangement irregularity at the following two story, seismic action effects are increased by;

$$\eta = (1 + \Delta V_{RW}/\Delta V_{Ed}) \leq q \quad (2\text{-}7)$$

where ΔV_{RW} is the total reduction of the resistance of masonry walls in the storey concerned, compared to the more infilled storey above it; and ΔV_{Ed} is the sum of the seismic shear forces acting on all vertical primary seismic members of the storey concerned. If η is lower than 1.1, magnification of the seismic action can be ignored.

Local effects due to infill walls are covered at part 5.9 in EC 8. The first story is considered as critical and confined, if there exist infill wall and there is no advanced calculation for infill wall in design. If the infill wall height is smaller than surrounding columns, there are two ways to follow for design. The first one is to assume the whole length as a critical region and design confinement according to this. The second way is recalculating the confinement at the clear length of the short column region according to the parts 5.4.2.3 and 5.5.2.2. The moment forces at the end of the short column region are increased 1.1 to 1.3 depending on the ductility level. Confined region for short columns should be extended to l_{cl} (clear length for the column) $+h_c$ (Column dimension, parallel to infill wall). If the infill wall height is less than $1.5h_c$, then the shear force should be resisted by shear reinforcement. If one side of the surrounding columns is in contact with infill wall, these columns whole height are assumed as a critical region. Shear force is considered the minimum of the force

transferred from infill panel and the shear force calculated from increased moments for corresponding ductility class and over-strength factor.

2.1.3. International Building Code (IBC2012)

Different type of irregularities specified in IBC2012 (1705.11) are torsional or extreme torsional irregularity; nonparallel systems irregularity; a stiffness-soft story or stiffness-extreme soft story irregularity; and discontinuity in lateral strength-weak story irregularity. The vertical irregularity conditions are designated according to Table 12.3-2 in ASCE7-10 (Table 2-1).

The soft story is classified into two part as irregular and extreme irregular. If the lateral stiffness is less than 70 percent of the story above or less than 80 percent of the average of the three story above assumed as irregular. It is 1/0.7 =1.43 for the specified value, η_k, for TEC 2007. Extreme irregularity is 1/0.6= 1.67.

The weak story is defined as 20 strength reduction in the story than the above. 35 percent reduction in the strength of the story is assumed as extreme weak story.

There is no a specific period calculation equation for irregular structures in IBC, and Equivalent Lateral Force Method (ELF) is not permitted for the design with vertical irregularities.

Existence of vertical irregularity is direct the designer to change the seismic design category.

Table 2-1 Vertical Structural Irregularities (Table 12.3-2 in ASCE7-10)

Type	Description	Reference Section	Seismic Design Category Application
1a.	**Stiffness-Soft Story Irregularity:** Stiffness-soft story irregularity is defined to exist where there is a story in which the lateral stiffness is less than 70% of that in the story above or less than 80% of the average stiffness of the three stories above.	Table 12.6-1	D, E, and F
1b.	**Stiffness-Extreme Soft Story Irregularity:** Stiffness-extreme soft story irregularity is defined to exist where there is a story in which the lateral stiffness is less than 60% of that in the story above or less than 70% of the average stiffness of the three stories above.	12.3.3.1 Table 12.6-1	E and F D, E, and F
2.	**Weight (Mass) Irregularity:** Weight (mass) irregularity is defined to exist where the effective mass of any story is more than 150% of the effective mass of an adjacent story. A roof that is lighter than the floor below need not be considered.	Table 12.6-1	D, E, and F
3.	**Vertical Geometric Irregularity:** Vertical geometric irregularity is defined to exist where the horizontal dimension of the seismic force-resisting system in any story is more than 130% of that in an adjacent story.	Table 12.6-1	D, E, and F
4.	**In-Plane Discontinuity in Vertical Lateral Force-Resisting Element Irregularity:** In-plane discontinuity in vertical lateral force-resisting elements irregularity is defined to exist where there is an in-plane offset of a vertical seismic force-resisting element resulting in overturning demands on a supporting beam, column, truss, or slab.	12.3.3.3 12.3.3.4 Table 12.6-1	B, C, D, E, and F D, E, and F D, E, and F
5a.	**Discontinuity in Lateral Strength–Weak Story Irregularity:** Discontinuity in lateral strength–weak story irregularity is defined to exist where the story lateral strength is less than 80% of that in the story above. The story lateral strength is the total lateral strength of all seismic-resisting elements sharing the story shear for the direction under consideration.	12.3.3.1 Table 12.6-1	E and F D, E, and F
5b.	**Discontinuity in Lateral Strength–Extreme Weak Story Irregularity:** Discontinuity in lateral strength–extreme weak story irregularity is defined to exist where the story lateral strength is less than 65% of that in the story above. The story strength is the total strength of all seismic-resisting elements sharing the story shear for the direction under consideration.	12.3.3.1 12.3.3.2 Table 12.6-1	D, E, and F B and C D, E, and F

2.1.4. NEHRP Recommended Provisions for Seismic Regulations for Buildings and other Structures (FEMA 368, Edition 2000)

FEMA 368 have similar definitions for vertical irregularities with IBC as given in Table 5.2.3.3 in FEMA 368-2000 and same values are defined for soft, extreme soft and weak stories. The only difference, there is no extreme weak story definition.

FEMA 368-2000 have some restrictions for the analysis of the frames if vertical irregularity exists. The permitted analysis types in (Table 5.2.5.1 FEMA 368) are given for different seismic design categories.

2.1.5. National Building Code of Canada (NBC 2005)

This code has similarities to IBC regarding the definition of the irregularities. Structures having one of the features of Table 4.1.8.6, NBC 2005 are called as irregular. Soft story definitions are same and there are no extreme soft and weak story definitions. In NBC 2005, the reduction in the story strength is not allowed.

Equivalent Lateral Force method can be used only for the irregular buildings when the total height is less than 20 m and the fundamental lateral period is less than 0.5 seconds.

2.2. Discussion of Code and Specification Rules for Vertical irregularity

Code and specification rules for vertical irregularity definitions and parameters are reviewed. The Eurocode 8 takes some precautions for the infilled frames, however, does not use any identifier for vertical irregularities. The FEMA 368-2000, IBC 2012 and the NBC 2005 use the similar definitions for vertical irregularity identification. These three codes and specification define the soft story as the lateral stiffness of the story should not be less than 70% of the adjacent story, and define the weak story as the lateral strength capacity of the floor should not be 80% less than the story above. The extreme weak story irregularity is limited to 65%. TEC 2007 uses η_k and η_c parameters for soft and weak story definitions, respectively. The limit values of 2.0 for soft story and 0.8 and 0.6 for weak story and extreme weak story irregularities are given for η_k and η_c parameters.

In this thesis, the vertical irregularity parameters are investigated through the parameters defined by TEC 2007 and IBC 2012 for soft story and weak story. The corresponding IBC 2012 limit value for η_k is 1/0.7=1.43 and 1/0.6=1.67 for extreme soft story. The limit value for η_c is 0.8 and 0.65 for weak and extreme weak stories.

CHAPTER 3

MODELING AND VERIFICATION

Numerical models must represent the behavior of real-life structures and the physics behind this behavior as much as possible. Modeling technologies are, as important as, experimental studies and it is the cheapest way of research if it is done correctly.

Till to find the best modeling techniques, the experimental studies will be our guide to clarify the numerical models. In this chapter, the numerical modelling approach is described. A sensitivity analysis is performed to see vulnerable parameters in the infill modeling approach. Then experimental studies are used to verify the modeling approach. The calibration of some of the parameters are done via experimental results.

3.1. Modeling of Infilled Reinforced Concrete Frames

Finite element method, which is a numerical technique to find approximate solutions to boundary value problems for partial differential equations was preferred for modeling.

The Open System for Earthquake Engineering Simulation (Opensees, McKenna (1997)), open source software was used for the numerical models. OpenSees has an extensive material, element type and solver database for finite element modeling.

3.1.1. Material Models

Material models used in this thesis are selected from the OPENSEES material database. All the chosen material models are uniaxial and isotropic. In this chapter, general information related to the material models are given.

Concrete 02, Chang& Mander's 1994 concrete material model was preferred. In Figure 3-1, Concrete 02 material model parameters are given. The detailed formulas related to the model can be found on Opensees manual or website (Mazzoni et. al. (2006)). The parameters used in this model are given below.

"uniaxialMaterial Concrete02 $matTag $fpc $epsc0 $fpcu $epsU $lambda $ft $Ets

$matTag	integer tag identifying material
$fpc	concrete compressive strength at 28 days (compression is negative)*
$epsc0	concrete strain at maximum strength*
$fpcu	concrete crushing strength *
$epsU	concrete strain at crushing strength*
$lambda	ratio between unloading slope at $epscu and initial slope
$ft	tensile strength
$Ets	tension softening stiffness (absolute value) (slope of the linear tension softening branch)

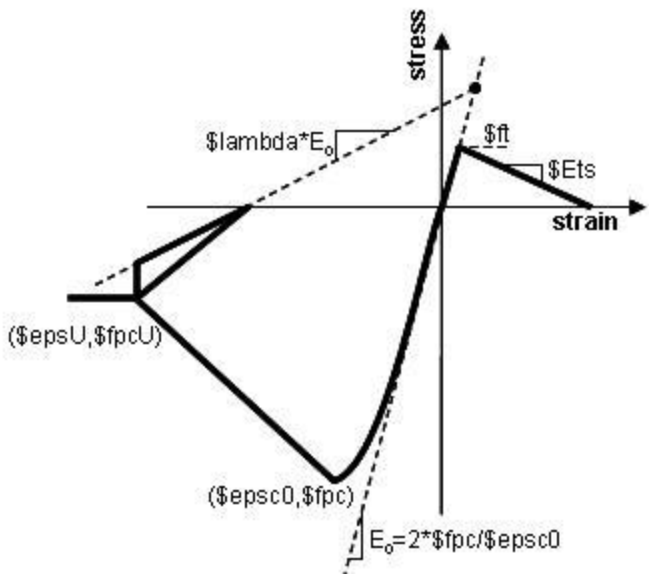

Figure 3-1 Concrete 02 concrete model

The Steel02 material, Giuffré-Menegotto-Pinto model with isotropic strain hardening, was used for rebar material modeling (Figure 3-2). The parameters used in this model are given below.

*"uniaxialMaterial **Steel02** $matTag $Fy $E $b $R0 $cR1 $cR2*

$matTag	integer tag identifying material
$Fy	yield strength
$E0	initial elastic tangent
$b	strain-hardening ratio (ratio between the post-yield tangent and initial elastic tangent)
$R0 $CR1 $CR2	parameters to control the transition from elastic to plastic branches. Recommended values: **$R0**=between 10 and 20, **$cR1**=0.925, **$cR2**=0.15"

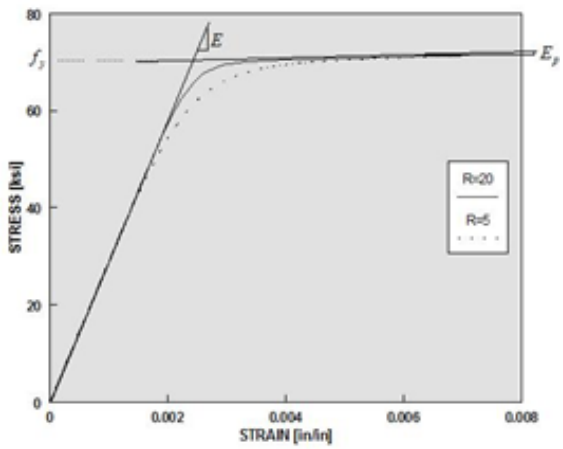

Figure 3-2 Steel02 - Giuffre-Menegotto-Pinto steel material (Mazzoni et. al. (2006))

The uniaxial hysteretic material model was preferred for the infill wall strut model (Figure 3-3). The parameters used in this model are given below. The details of the infill strut model will be provided in the latter parts of this chapter.

*"uniaxialMaterial **Hysteretic** $matTag $s1p $e1p $s2p $e2p <$s3p $e3p> $s1n $e1n $s2n $e2n <$s3n $e3n> $pinchX $pinchY $damage1 $damage2 <$beta>*

$matTag	integer tag identifying material
$s1p $e1p	stress and strain (or force & deformation) at first point of the envelope in the positive direction
$s2p $e2p	stress and strain (or force & deformation) at second point of the envelope in the positive direction
$s3p $e3p	stress and strain (or force & deformation) at third point of the envelope in the positive direction (optional)

$s1n $e1n	stress and strain (or force & deformation) at the first point of the envelope in the negative direction
$s2n $e2n	stress and strain (or force & deformation) at a second point of the envelope in the negative direction
$s3n $e3n	stress and strain (or force & deformation) at the third point of the envelope in the negative direction (optional)
$pinchx	pinching factor for strain (or deformation) during reloading
$pinchy	pinching factor for stress (or force) during reloading
$damage1	damage due to ductility: D1(mu-1)
$damage2	damage due to energy: D2(Eii/Eult)
$beta	power used to determine the degraded unloading stiffness based on ductility, mu-beta (optional, default=0.0)”

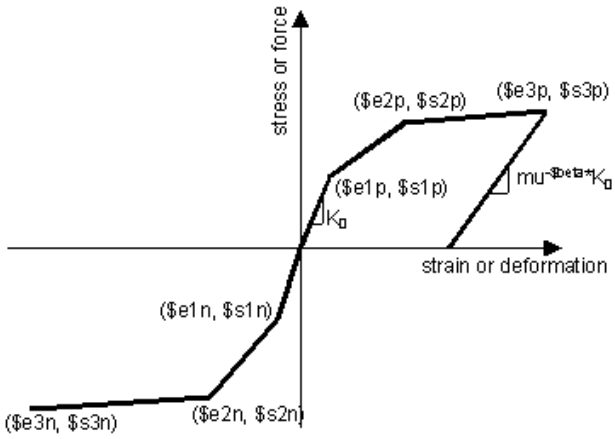

Figure 3-3 Uniaxial hysteretic material model (Mazzoni et. al. (2006))

The method proposed by Zhao and Sritharan (2007) for the BOND SP01 material model was used in models to capture the strain penetration effect at the column end to the footing. Zhao and Sritharan (2007) proposed an equation for the calculation of the yield displacement for the bond slip calculation in Eq.3-1 and Eq. 3-2.

Bond SP01 material model is usable in kips and inches. For SI units it is not applicable. Thus, the bond slip model parameters were calculated for each bar in the section according to given formulas in Eq. 3-1 and Eq. 3-2 and assigned as a new steel material into the model. A new section is defined for the bond slip.

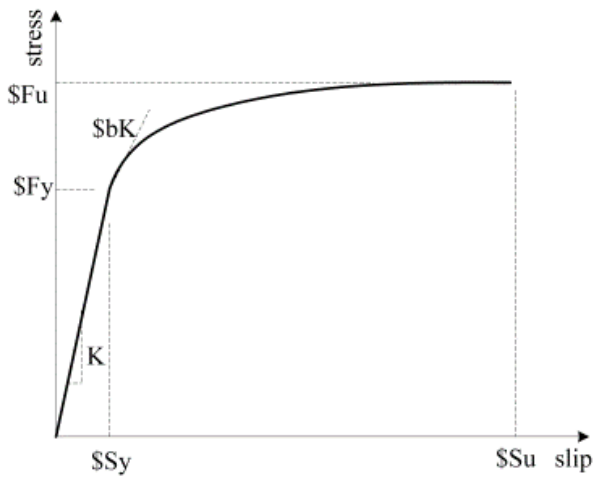

Figure 3-4 a) Bond SP01 uniaxial material model (Mazzoni et. al. (2006))

$$S_y(in) = 0.1\left(\frac{d_b(in)}{4000}\,\frac{f_y(psi)}{\sqrt{f_c'(psi)}}\,(2\cdot\alpha+1)\right)^{1/\alpha} + 0.013\,(in) \tag{3-1}$$

$$S_y(mm) = 2.54\left(\frac{d_b(mm)}{8437}\,\frac{f_y(MPa)}{\sqrt{f_c'(MPa)}}\,(2\cdot\alpha+1)\right)^{1/\alpha} + 0.34\,(mm) \tag{3-2}$$

3.1.2. Modeling of Infill Walls

Fiber sections were defined for each column and beam section. Force-beam-column, force-based, element was chosen due to its high and fast convergence capabilities with less integration point numbers. Force-beam-column element uses Lobatto integration method as default, and there are also options for Legendre, Radau, Newton-Cotes and Trapezoidal methods. In this modeling method, calculations are done at each fiber section with acceptably enough number of defined integration points for each element. A number of integration points were kept small as possible to be able to optimize the solution time with enough accuracy.

ASCE 41 strut model was used to calculate the strut parameters to represent the behavior of infill walled frames (Figure 3-5). Thiruvengadam (1985) proposed the use

of multiple strut models. Chrysostomou (1991) studied a three compression-only strut model for each direction (Figure 3-6). In his study this three strut compression-only strut model was used and a good match with experimental results was observed.

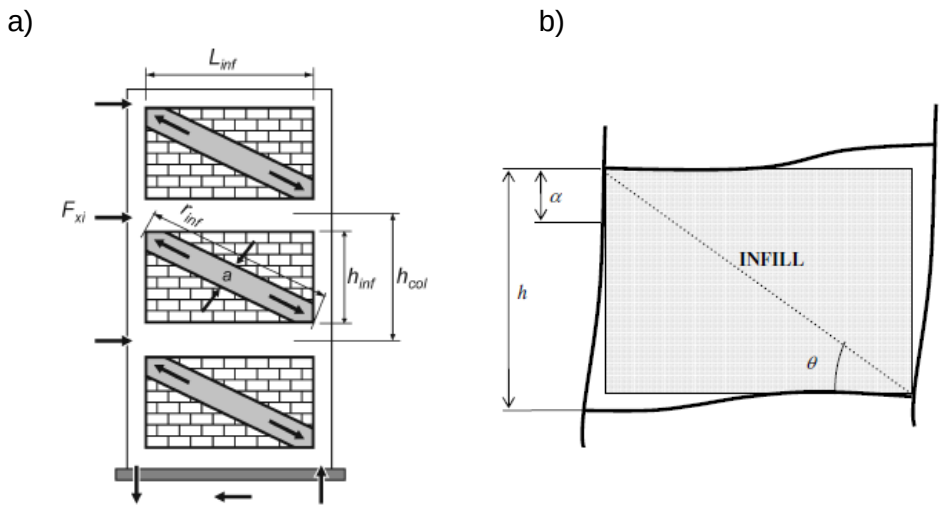

Figure 3-5 a) ASCE41 Concentric compression strut model, b) Smith and Carters' Method (1969) parameters for infill wall

More than one parameter affects the equivalent strut width. The first one is the geometric properties of infill. The panel proportion and panel height are critical parameters. The failure mode changes according to surrounding frame's stiffness. Then, frame and infill properties take an important role on equivalent strut width. ASCE41 equivalent strut model parameters were preferred, and the used formulas are given through Eq.3.3 to Eq.3.5. Mainstone (1971) and Smith and Carter (1969) studies were used for the formulas given in 3-1 to 3-3.

$$w = a = 0.175 \cdot (\lambda_1 \cdot H_{col})^{-0.4} \cdot r_{in} \tag{3-3}$$

$$\lambda_1 = \left[\frac{E_{in} \cdot t_{in} \cdot \sin(2\theta)}{4 \cdot E_{fr} \cdot I_{col} \cdot H_{in}}\right]^{1/4} \tag{3-4}$$

$$z = \frac{\pi}{2 \cdot \lambda_1} \tag{3-5}$$

where;

h_{col} : Column height between centerlines of beam
h_{in} : Height of infill panel
E_{fr} : Expected modulus of elasticity of frame material
E_{in} : Expected modulus of elasticity of infill materials
I_{col} : Moment of inertia of column
r_{in} : Diagonal length of infill panel
t_{in} : Thickness of infill panel and equivalent strut
θ: Angle whose tangent is the infill height-to-length aspect ratio, in radians.
z: Contact length (in calculations half of the calculated values were used.)

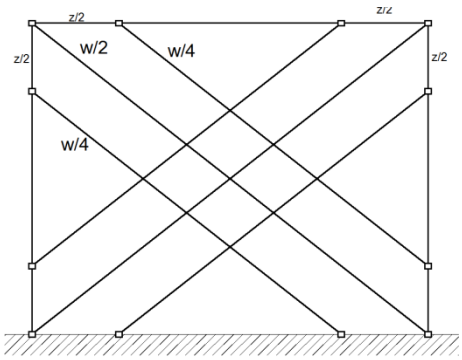

Figure 3-6 Three strut model for each direction proposed by Chrysostomou (1991)

The contact length was used as half of the calculated value given in Eq. 3-3 in numerical models as studied by Chrysostomou (1991) and Crisafulli et. al. (1997 and 2000).

Equivalent strut model is a good approach to estimate the contribution of the infill walls to the frame. However, it is not enough to use it in the nonlinear analysis alone. The strut model needs a material constitutive law for the calculation of the non-linear response. Panagiotakos and Fardis (1996) and Bertoldi et.al (1993) proposed some similar material constitutive relationships for the infill strut model. Details of these two relationships were discussed in Chapter 1.

In this thesis, the material constitutive model from Bertoldi et.al (1993) was modified and studied. In the latter part of this chapter, a sensitivity analysis results will be discussed for the material constitutive law and model parameters. Force deformation relationship used in the modeling given in Figure 3-7. This material constitutive law

was modified with a new formula for F_m, infill strength capacity, by Zarnic and Gostic (1997). This formula includes wall ratio in a way with C_1 factor and gives a good estimate of the maximum axial load capacity of the strut. The formula is given in Eq. 3-6; where f_{tp} is the cracking strength of the infill, obtained from a diagonal compression test, whereas L_{in} and H_{in} are the length and the height of the infill.

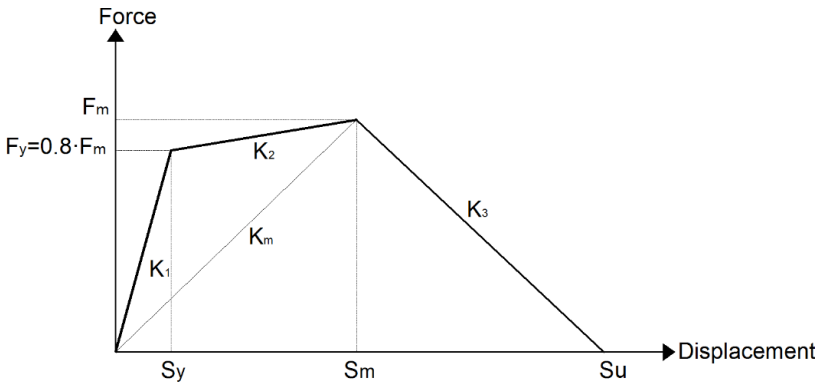

Figure 3-7 Material constitutive law used in this study for equivalent strut model

$$F_m = 0.818\frac{L_{in}t_{in}f_{tp}}{C_1}\left(1+\sqrt{{C_1}^2+1}\right), \quad C_1 = 1.925\frac{L_{in}}{H_{in}} \tag{3-6}$$

Secant stiffness K_m at F_m is calculated from Eq 3-7 which is proposed by Klingner (1976). S_m is calculated as the ratio of the F_m to K_m.

$$K_m = \frac{E_{in}w_{in}t_{in}}{d}\cos^2\theta, \qquad S_m = \frac{F_m}{K_m} \tag{3-7}$$

Yield parameters are calculated according to Eq. 3-8. G_{in} is the tangential elastic modulus of masonry infill.

$$K_y = K_1 = \frac{G_{in}t_{in}L_{in}}{H_{in}}, \qquad F_y = 0.8\cdot F_m = f_{tp}t_{in}L_{in}, \qquad S_y = \frac{F_y}{K_y} \tag{3-8}$$

The ultimate displacement is calculated according to Eq. 3-9. K_3, softening stiffness is in the range of $0.005K1 \leq K_3 \leq 0.1K_1$ according to Uva et. al. (2012), Bertoldi et.al

(1993) and Panagiotakos and Fardis (1996). K_3, post stiffness reduction, is discussed in the latter part of this chapter.

$$S_u = S_m + \frac{F_m}{K_3} \tag{3-9}$$

S_m can be considered as 0.2% in the case of no openings in infill walls and 0.1% for the infill walls with openings (Dolsek and Fajfar (2005, 2008)).

In Figure 3-8, the modeling approach employed in Opeensees is shown. Shear is aggregated into each fiber section with elastic GA rigidity. Shear failure is checked with shear capacity calculated according to TS 500. The material constitutive law, which is obtained using the formulas given by Eq. 3-1 to 3-7, was converted to stress strain relationship to use in the numerical model. Strain compatibility was considered while transforming to stress- strain relationship.

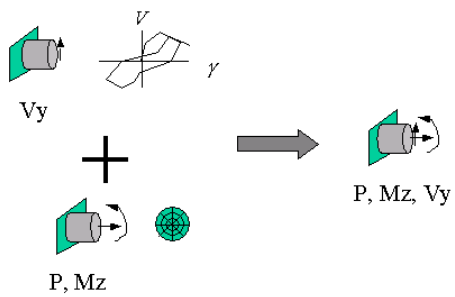

Figure 3-8 Opensees finite element model (Opensees manual)

In linear static and nonlinear static procedures, force-based elements were used. Nonlinear static and time history analysis have many stability and convergence problems. Due to these problems, a convergence algorithm was written which changes and tries different solution algorithms firstly and if does not converge, reduces the tolerance for the iterations. Even if does not converge, elements are changed to displacement beam column elements, and explicit analysis is done by reducing the time increment, d_t. Stability was checked with deformed shape and displacement values after nonlinear analysis, and then the results were used for post-processing.

3.2. Sensitivity Analysis

In this part, the relevant parameters of the infill strut model that affect the total response of the structure will be discussed. The infilled frame model is chosen from the study of Ezzatfar et. al. (2014). The details of the model is given in part 3.1.4.3. These frame is a three story, three bay and mid span is infilled along the height. Sensitivity analysis was considered in two parts. In the first part, as given in Table 3-1, shear strength was kept constant and calculated as a ratio of the compressive strength of the infill wall for each story and E_m, elasticity modulus of infill wall, f_{tp}, shear strength, z, contact length and K_3, post-peak stiffness were selected as sensitivity parameters to study. The shear strength, f_{tp}, was considered to vary in the range of $0.03f_m < f_{tp} < 0.09f_m$. $550f_m$ and $750f_m$ values are chosen for young modulus of the infill walls. These two numbers are mostly used in the literature for the calculation of the young modulus of the masonry infill walls. Contact length was considered as half and the one third of the calculated value according to Eq. 3-5. K_3, post peak stiffness (Figure 3-7), is in the range of $0.005K_1$ and $0.1K_1$.

In Figure 3-9, all part 1 sensitivity analysis results are plotted on the same graph to see the dispersion. It is obvious that there is a huge variance between the results, when we change the values of the parameters for the calculation of equivalent strut model and material constitutive law.

In Table 3-1, in the first 32 cases, the contact length was kept half of the calculated one. In Figure 3-10, these 32 cases were compared in detail. From all graphs given in Figure 3-10, dotted lines represent the cases for $E_m=550*f_m$, and the solid lines represent the cases for $E_m=750*f_m$. It can be observed that the elasticity modulus seems less effective if we are using the same method to calculate equivalent strut width and strength capacity of struts. $E_m=750*f_m$ results in a more brittle behavior when it is compared with $E_m=550*f_m$ results for the degradation part. Higher elasticity modulus decreases the strain capacity of the strut. The shear strength, f_{tp}, was considered to vary in the range of $0.03f_m < f_{tp} < 0.09f_m$. It is clear to say that decrease in the shear

strength resulted in a decrease in the force capacity of the frame. In Figure 3-10, the effect of K_3 stiffness change can be observed. The increase in α, the post peak stiffness multiplier, resulted in a fast decrease in the force capacity as expected.

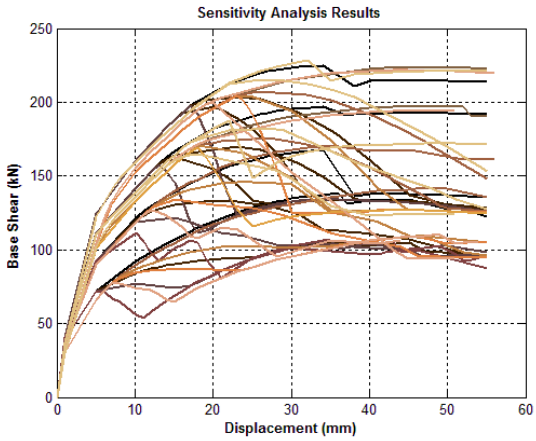

Figure 3-9 Sensitivity analysis Part 1 results with experimental data

The cases for f_{tp}=0.07f_m and f_{tp}=0.09f_m have the best match with different K_3 stiffness values. This discrepancy comes because of the f_{tp} uncertainty. In the last eight cases (Case 33 - Case 40), the results become much stiffer.

The outcomes observed from the first part of the sensitivity analysis are that the f_{tp} and K_3 parameters are sensitive for the material constitutive law and equivalent strut calculation, and young modulus does not change if we use the same material constitutive law and equivalent strut model. It is observed that the decreasing the contact length made the response stiffer, however, we need to fix some parameters to be able to talk the sensitivity of the contact length.

Table 3-1 Sensitivity Analysis Part 1 Cases

CASES	E_{inf} = α *f_m (MPA)	f_{tp}= α *f_m (Mpa)	Contact Length	K_3 = α *K_1
1	750	0.09	z/2	0.005
2	750	0.07	z/2	0.005
3	750	0.05	z/2	0.005

4	750	0.03	z/2	0.005
5	750	0.09	z/2	0.03
6	750	0.07	z/2	0.03
7	750	0.05	z/2	0.03
8	750	0.03	z/2	0.03
9	750	0.09	z/2	0.05
10	750	0.07	z/2	0.05
11	750	0.05	z/2	0.05
12	750	0.03	z/2	0.05
13	750	0.09	z/2	0.1
14	750	0.07	z/2	0.1
15	750	0.05	z/2	0.1
16	750	0.03	z/2	0.1
17	550	0.09	z/2	0.005
18	550	0.07	z/2	0.005
19	550	0.05	z/2	0.005
20	550	0.03	z/2	0.005
21	550	0.09	z/2	0.03
22	550	0.07	z/2	0.03
23	550	0.05	z/2	0.03
24	550	0.03	z/2	0.03
25	550	0.09	z/2	0.05
26	550	0.07	z/2	0.05
27	550	0.05	z/2	0.05
28	550	0.03	z/2	0.05
29	550	0.09	z/2	0.1
30	550	0.07	z/2	0.1
31	550	0.05	z/2	0.1
32	550	0.03	z/2	0.1
33	750	0.09	z/3	0.005
34	750	0.07	z/3	0.005
35	750	0.09	z/3	0.03
36	750	0.07	z/3	0.03
37	550	0.09	z/3	0.005
38	550	0.07	z/3	0.005
39	550	0.09	z/3	0.03
40	550	0.07	z/3	0.03

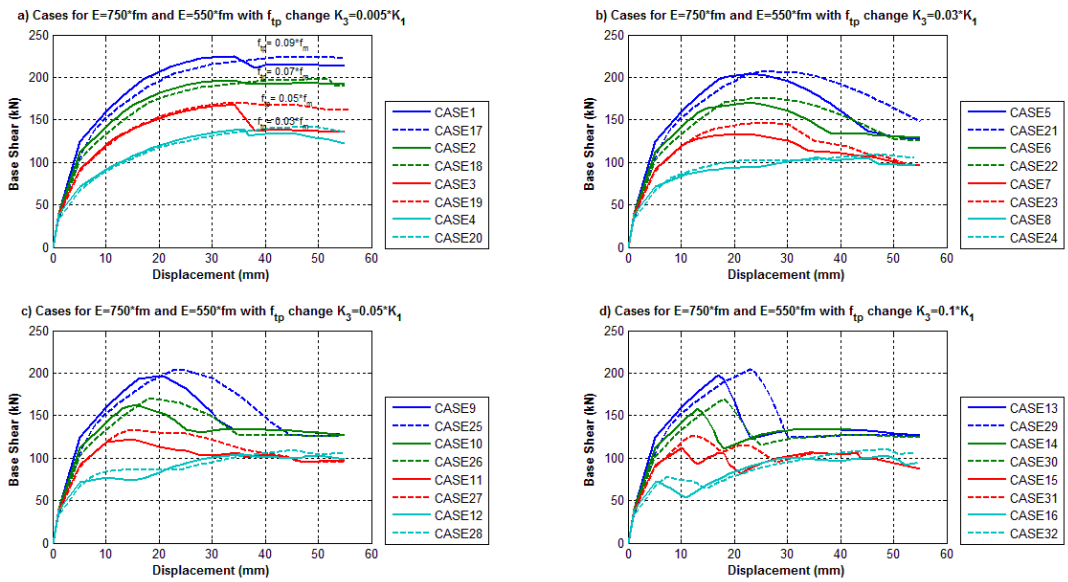

Figure 3-10 Sensitivity analysis Part 1 result comparison.

To decrease the uncertainities comes from the sensitive parameters, we need to fix some of the pre-defined sensitivity variables in part 1 and need to check again for the sensitivity. Therefore, we need to perform another sensitivity analysis that we fixed the young modulus as 550*f_m and f_{tp} calculation with a formulation (Eq. 3-10). In this way, vertical stresses comes from the upper stories will be considered for the f_{tp} calculation.

$$\tau = \tau_o + \mu\sigma \tag{3-10}$$

where τ is the shear stress (f_{tp}), τ_o is the cohesive strength, μ is the friction coefficient an σ is the normal stress under the vertical load. The friction coefficients for weak and strong infills are given as 0.770 and 0.957 by Kakaletsis and Karayannis (2008). τ_o =0.265 MPa was used which is suggested by Begimgil (1991).

In Table 3-2, the studied parameters in part 2 of the sensitivity analysis are given. In this part, f_{tp} was calculated according to Eq. 3-10 for each floor and μ was taken as 0.957. Because, the compressive strength of the infill wall used in the model is

relatively strong (Part 3.1.4.3). In this part, the contact length and K_3, post-peak stiffness were investigated in detail.

In Figure 3-11, sensitivity analysis, part 2 results are plotted. If we calculate the f_{tp} same for each case with Eq. 3-10, the initial stiffness did not show any important difference. However, when the inelastic behavior started after maximum capacity, the results show difference with the change of K_3. It can be seen from Figure 3-11 that the contact length change did not make a huge difference in the force – deformation plot. So, we can say that K_3 is still sensitive to changes and it should be calibrated for the rest of the study. K_3 is also related with the strong and weak infill wall material properties. Therefore, this parameter will be calibrated using the experimental data (Kakaletsis and Karayannis (2008)) for the case study.

Table 3-2 Sensitivity Analysis Part 2 Cases

CASES	**$E_{inf} = \alpha * f_m$ (MPA)**	**Contact Length**	**$K_3 = \alpha * K1$**
1	550	z/2	0.005
2	550	z/2	0.01
3	550	z/2	0.02
4	550	z/2	0.03
5	550	z/2	0.04
6	550	z/2	0.05
7	550	z/2	0.1
8	550	z/3	0.005
9	550	z/3	0.01
10	550	z/3	0.02
11	550	z/3	0.03
12	550	z/3	0.04
13	550	z/3	0.05
14	550	z/3	0.1

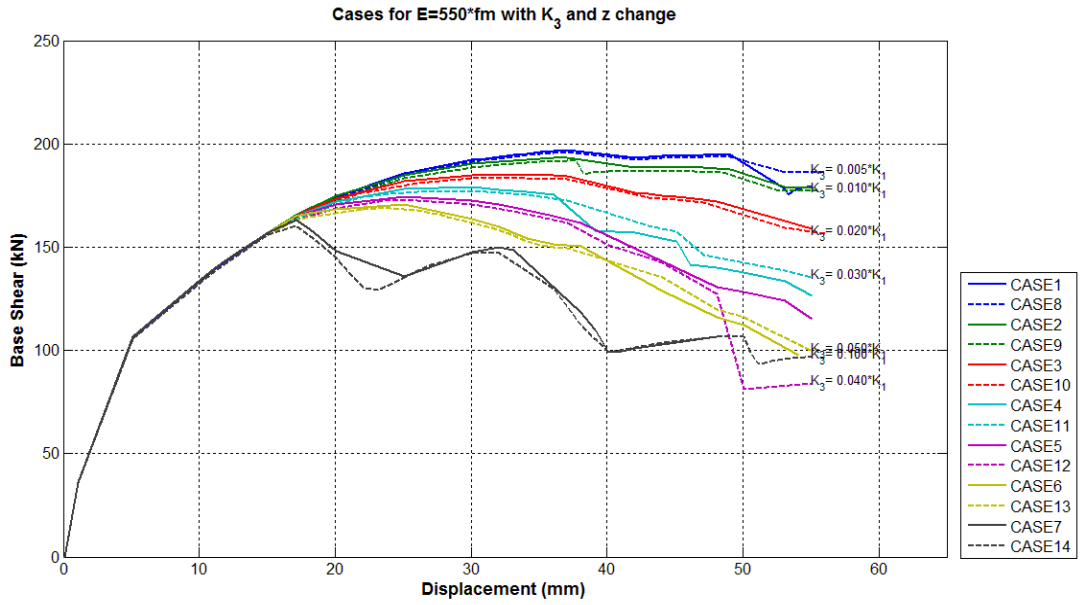

Figure 3-11 Sensitivity analysis Part 2 results compared with PsD test results

Up to this point, step by step the uncertainties in the modeling parameters are tried to be eliminated for the accurate modeling technique. E_m, the elasticity of modulus and z, the contact length parameters, are considered as having less impact. Also, if the infill wall f_{tp} value is calculated according to Eq. 3-10, the results seem much more meaningful.

As mentioned above, the f_{tp}, shear strength under diagonal compression test, has been observed to have an enormous impact on modeling and it seems that it highly depends on the initial shear strength and cohesion under zero vertical loading stress. However, FEMA 273 and ACI 530- 95 only consider the cohesive strength of 0.190 MPa for unreinforced masonry and do not take into account the interaction of infill wall and frame. In TEC (2007) the cohesive strength is 0.12 MPa for typical construction with hollow brick clay. TEC (2007) and ACI530-95 both suggest to take into account the normal stress which comes from the vertical loads. Buonopane and White (1999) observed that the shear strength value is much higher than the suggested values by codes. They observed the average shear strength from the experimental studies as 1.031 MPa. Mehrabi et. al. (1996) also obtained 0.905 MPa average shear strength.

3.3. Verification and Calibration of Numerical Models

Numerical models were verified by using some cyclic, and pseudo-dynamic test results which were studied by Mehrabi et. al. (1996), Kakaletsis and Karayannis (2008) and Ezzatfar et.al (2014) and acceptable results were obtained. Fully infilled frames were considered in verification and validation study. For the material constitutive law, the experimental results were used, if exists and compared with the results for the suggested material constitutive law formulas. Acceptable results obtained for both cases.

3.3.1. Experimental Studies Employed

Mehrabi et. al. (1996) tested 12 one-story-one bay frames with various type of infills. InFigure 3-12, weak and strong frames studied by Mehrabi et. al. (1996) are shown. In this thesis, Specimen 1, Specimen 4 and Specimen 6 were studied. These specimens refer to bare weak frame, weak frame-weak infill and strong frame-weak infill accordingly. In Table 3-3, Table 3-4, and Table 3-5, the material properties and loading details of the experiment setups are given. Details are in Mehrabi et.al (1996). In Figure 3-13, the experimental results are given from the study by Mehrabi (1996).

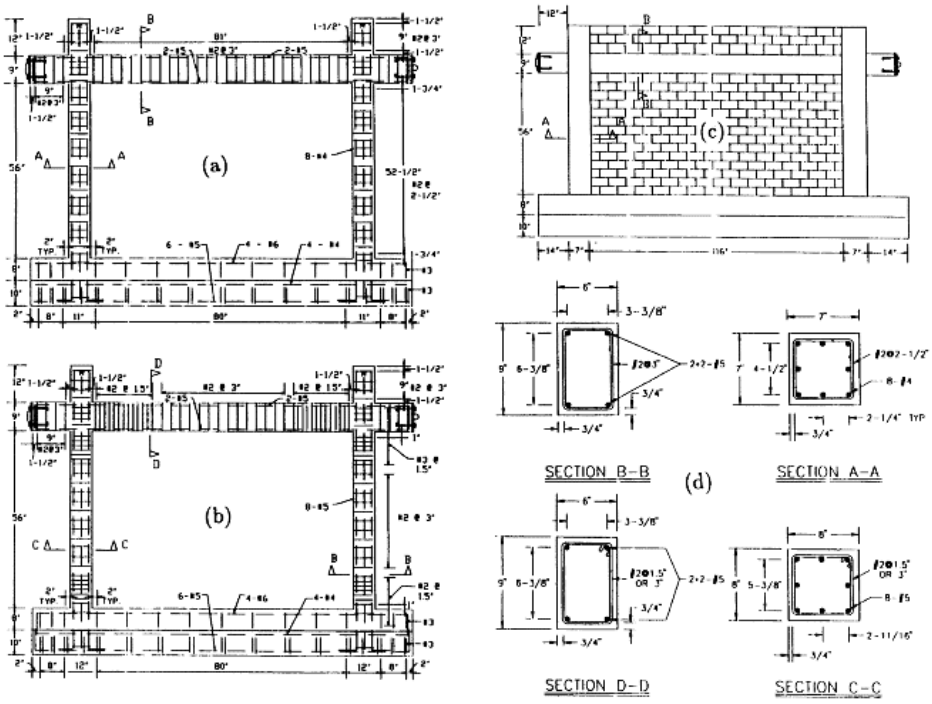

Figure 3-12 Test Specimens (From Mehrabi et.al (1996))

Table 3-3 Average Tensile Strengths of Reinforcing Steel From Mehrabi et. al.(1996)

Bar size (1)	Type of bar (2)	Nominal diameter (in.) (3)	Yield stress (ksi) (4)	Ultimate stress (ksi) (5)
No. 2	Plain	0.25	53.3	65.2
No. 4	Deformed	0.50	61.0	96.0
No. 5	Deformed	0.625	60.0	96.0

Table 3-4 Test Specimens (From Mehrabi et.al (1996))

Specimen number (1)	Type of frame (2)	Type of masonry units (3)	Panel aspect ratio (*h*/*L*) (4)	Lateral load (5)	Vertical Load Distribution (kips)	
					Columns (6)	Beam (7)
1	weak	no infill	0.67	monotonic	66	—
2	weak–repaired (1)*	hollow	0.67	monotonic	66	—
3	weak–repaired (2)*	solid	0.67	monotonic	66	—
4	weak	hollow	0.67	cyclic	44	22
5	weak	solid	0.67	cyclic	44	22
6	strong	hollow	0.67	cyclic	44	22
7	strong	solid	0.67	cyclic	44	22
8	weak–repaired (4)*	hollow	0.67	monotonic	44	22
9	weak–repaired (8)*	solid	0.67	monotonic	44	22
10	weak	hollow	0.48	cyclic	44	22
11	weak	solid	0.48	cyclic	44	22
12	weak–repaired (10)*	solid	0.48	cyclic		33

*Specimen repaired.

Table 3-5 Concrete and Masonry Materials (From Mehrabi et.al (1996))

Specimen number (1)	Frame Concrete: Secant modulus* (ksi) (2)	Frame Concrete: Compressive strength (ksi) (3)	Frame Concrete: Strain at Gpeak stress (4)	Frame Concrete: Modulus of rupture (ksi) (5)	Frame Concrete: Tensile strength (split-cylinder test) (ksi) (6)	Three-Course Masonry Prisms: Secant modulus* (ksi) (7)	Three-Course Masonry Prisms: Compressive strength (ksi) (8)	Three-Course Masonry Prisms: Strain at peak stress (9)	Compressive strength of masonry units (ksi) (10)	Compressive strength of mortar cylinders (ksi) (11)
1	3,180	4.48	0.0018	0.980	0.477	—	—	—	—	—
2	3,180	4.48	0.0018	0.980	0.477	457	1.40	0.0036	2.39	2.30
3	3,180	4.48	0.0018	0.980	0.477	1,381	2.19	0.0029	2.26	2.32
4	2,500	3.89	0.0027	0.705	0.401	667	1.54	0.0030	2.39	2.38
5	2,620	3.03	0.0026	0.635	0.263	1,298	2.01	0.0023	2.26	2.55
6	2,880	3.75	0.0024	0.712	0.455	609	1.47	0.0032	2.39	2.43
7	2,700	4.85	0.0030	0.744	0.328	1,316	1.97	0.0026	2.26	2.25
8	2,500	3.89	0.0027	0.705	0.401	740	1.38	0.0027	2.39	2.25
9	2,500	3.89	0.0027	0.705	0.401	1,195	2.06	0.0026	2.26	1.81
10	2,920	3.90	0.0021	0.689	0.432	572	1.54	0.0036	2.39	1.73
11	2,630	3.73	0.0028	0.617	0.448	1,393	1.66	0.0025	2.26	1.89
12	2,920	3.90	0.0021	0.689	0.432	1,064	1.97	0.0029	2.26	2.59

*At 45% of the compressive strength.

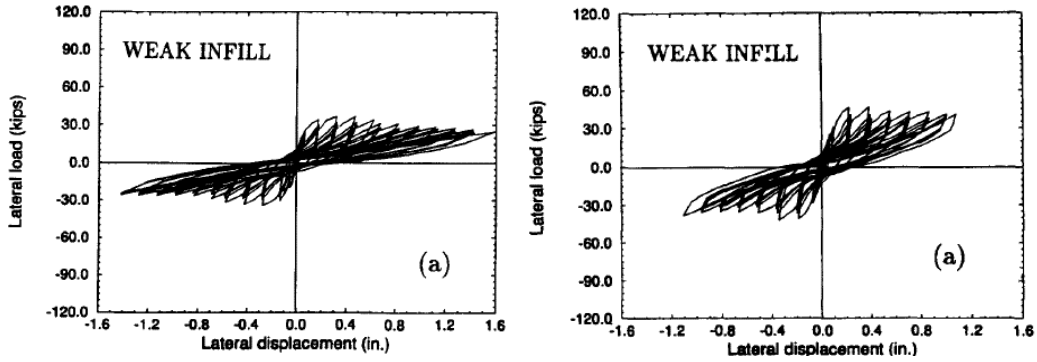

(a) (b)

Figure 3-13 Specimen 4 and Specimen 6 experimental results (From Mehrabi et. al. (1996))

Kakaletsis and Karayannis (2008) tested 1/3 scale one-bay one-story frames that are one bare, two fully infilled and four infilled with openings. They considered two types of infills, regarding strength, such as weak and strong. The authors investigated the effects of openings and compressive strength of masonry.

In Figure 3-14, the details of the test specimen are given from Kakaletsis and Karayannis (2008) study. The compressive strength of the infills is 2.63 MPa for weak infill and 15.8 MPa for strong infill. Elastic modules are 661 MPa and 2837 MPa correspondingly for weak and strong infills. The thickness of the weak infill is 60 mm, and that of strong infill is 52 mm. The compressive stress of concrete was 28.51 MPa,

and the yield stress of the longitudinal and transverse reinforcements were 390.47 MPa and 212.2 MPa, respectively.

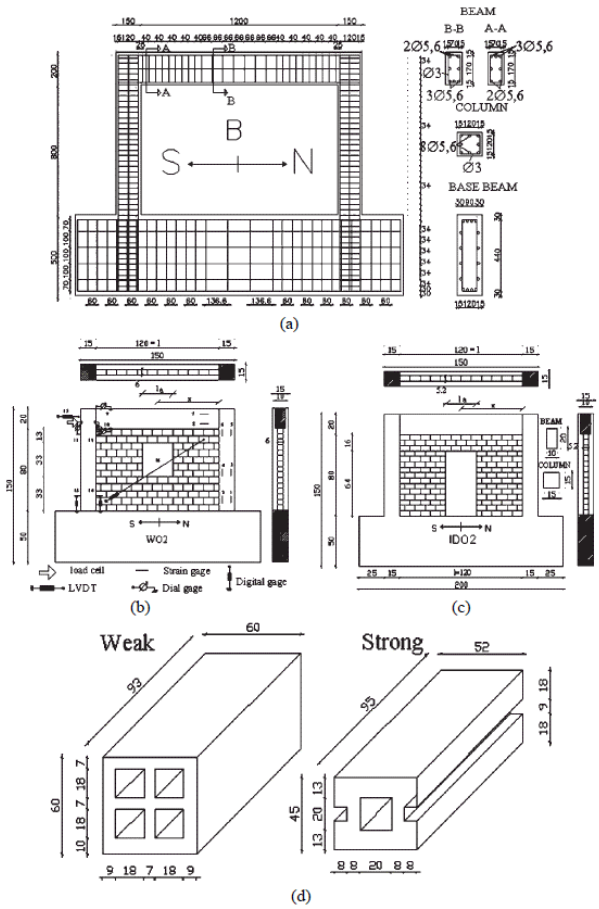

Figure 3-14 Kakaletsis and Karayannis (2008) from Figure 1, details of the test specimen

In Figure 3-15, force displacement hysteresis curves and failure patterns are displayed for specimens S and IS are given for bare, weak infilled and strong infilled frames from the tests of Kakaletsis and Karayannis (2008).

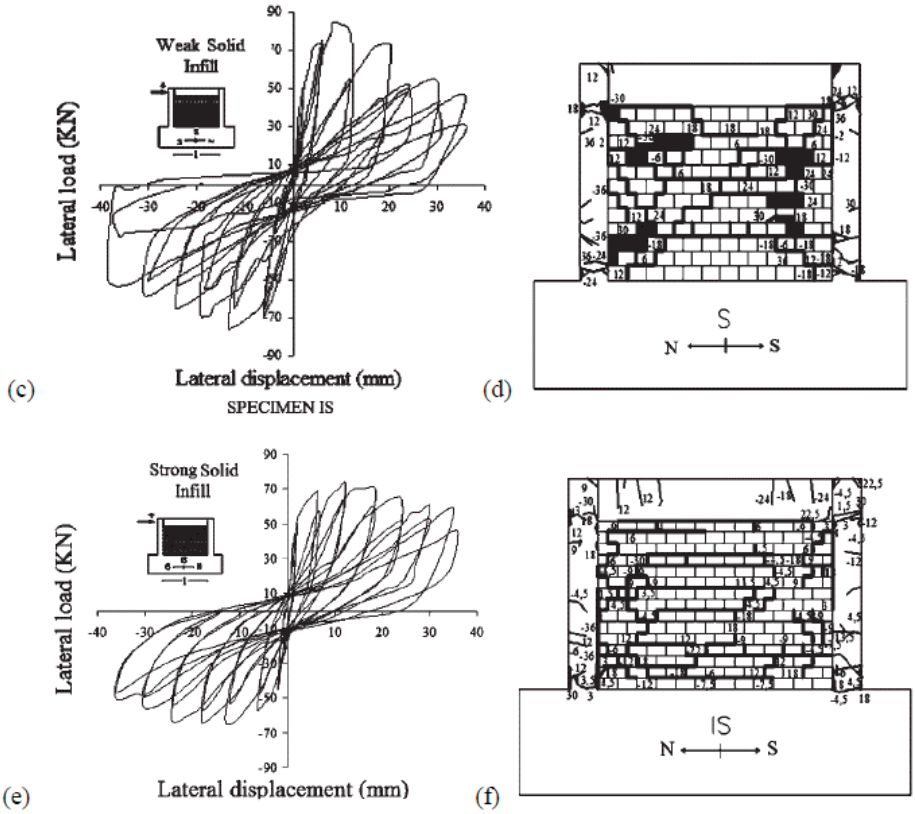

Figure 3-15 Kakaletsis and Karayannis (2008) from Figure 4; hysteresis curves and failure modes.

Kakaletsis and Karayannis (2008) also studied the relationship of the shear strength of the bed joint versus normal stress derived from the cohesion test. In Figure 3-16, this relationship between shear strength at bed joint and normal stress is given for different wall height to length ratio. Using this graph, tensile strength can be calculated and can be compared with the model discussed in part 3.1.2. The friction coefficients for weak and strong infills are determined as 0.770 and 0.957 from , Figure 3-16, respectively. Eq. 3-10 gives the expression for the shear stress. According to Figure 3-16, the cohesive strength is arround 0.267 MPa for weak and 0.17 MPa for strong infills. These cohesive strength numbers are relevant with FEMA-273, "NEHRP recommended provisions", (1997) and ACI 530-95. Infill wall parameters are calculated using Eq. 3-10 and the parameters for the test specimens. The results are given in Figure 3-23 and Figure 3-24 and compared with the experimental hysteresis

backbone envolope curves. It should be considered that the friction coefficient values have a huge variance in test results (Hendry (1998)).

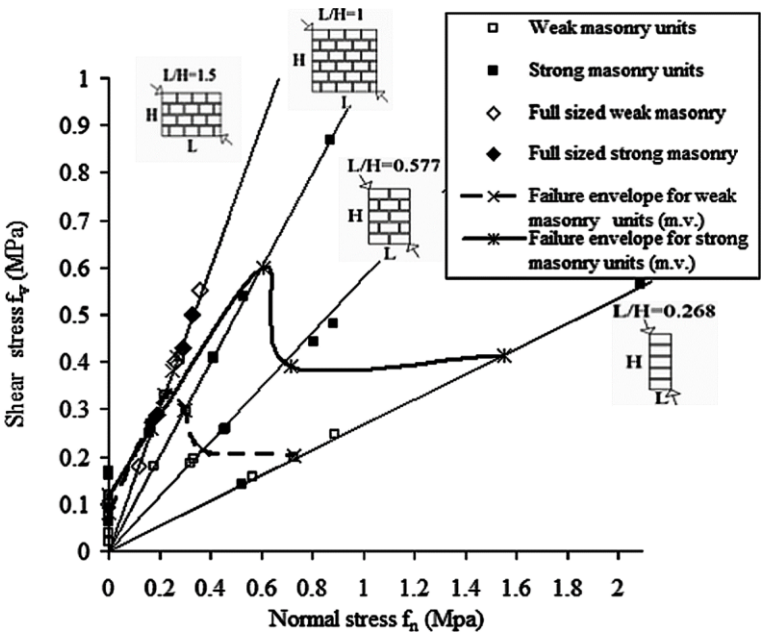

Figure 3-16 Determination of shearing stress for wall cracking. (Kakaletsis and Karayannis (2008))

Ezzatfar et. al. (2014) tested a 3-story, and 3-bay infilled reinforced concrete frame using PsD (Pseudo Dynamic) method. They used a diagonal mass matrix which was consistent with the actual story masses (m1 = 11426 kg, m2 = 11426 kg, m3 = 7925 kg) and defined zero damping to the system. Details of the specimen are given in Figure 3-17. The Specimen 1 at Phase 1 was studied in this thesis. In Phase 1, the specimen was excited under three synthetic ground acceleration records. Fenerci (2013) also investigated the same frame, and some of the figures given below are from his study. Ezzatfar et. al. (2014) used three synthetic ground acceleration records which were generated and scaled to match the site specific spectra of Düzce region. The ground motions used in testing and the corresponding earthquake spectra are shown in Figure 3-18.

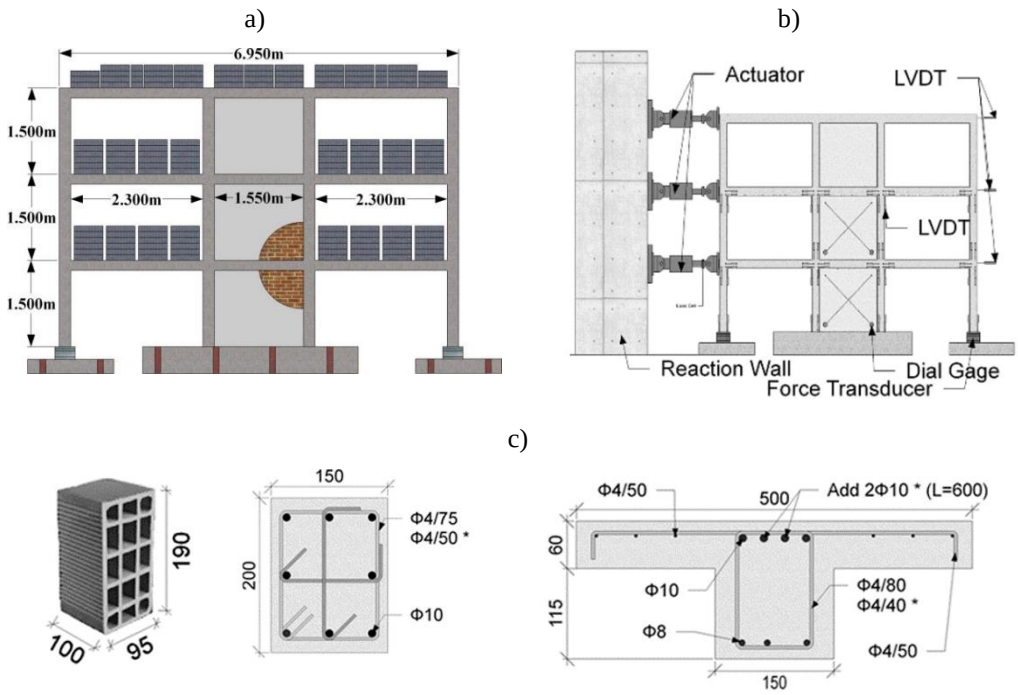

Figure 3-17 Details of Specimen 1 (Ezzatfar et. al. (2014))

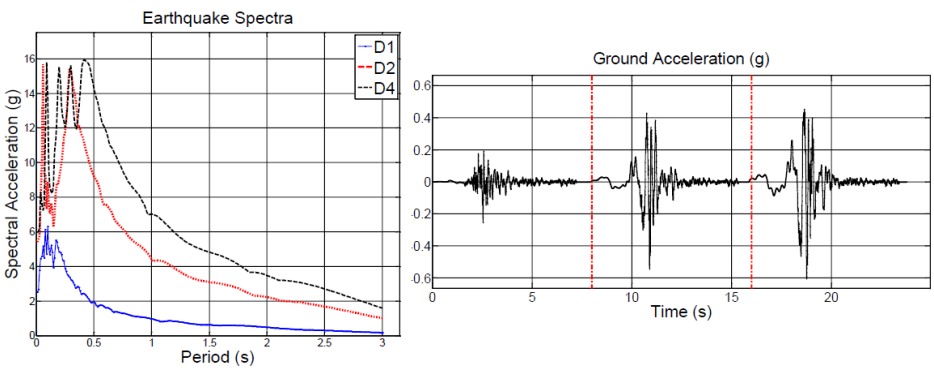

Figure 3-18 Ground Motions Used in Experiments (from Fenerci 2013)

In Figure 3-19, the interstory drift ratios are given by Fenerci (2013). In D1 earthquake, it is reported that the specimen exhibited small displacement values and acted in linear behavior. It was observed that D2 earthquake resulted in interface cracks at the frame-infill wall boundaries and horizontal sliding cracks at the infill and cracks at boundary columns due to frame-infill wall interaction.

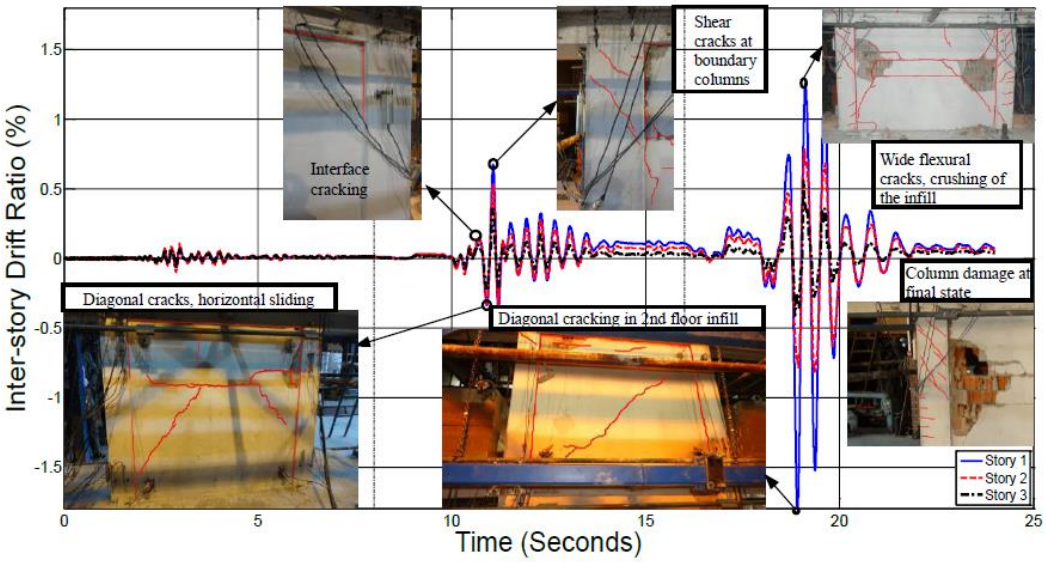

Figure 3-19 Inter-Story Drift Ratio Response along with Damage Patterns for Specimen1 (from Fenerci 2013)

3.3.2. Verification and Calibration of the Model

For verification and calibration, the values of parameters of experiments were compared with the proposed modeling formulas in part 3.1.2.

In Figure 3-20, the monotonic loading experimental result of the bare frame, which is Specimen 1, was compared with the two modeling techniques. In Figure 3-20 a, the bare frame was modelled with forced based elements with fiber sections and Chang and Mander's (1994) material model was used. In Figure 3-20 b, the bond slip is included in the model by using the modified steel material model for the bond slip. It can be observed from Figure 3-20 that bond slip model is necessary for the modeling to be able to capture the initial stiffness. The model worked in infilled frames much better. Mehrabi et. al. (1998) obtained similar results for a bare frame with a different modeling approach.

a) b)

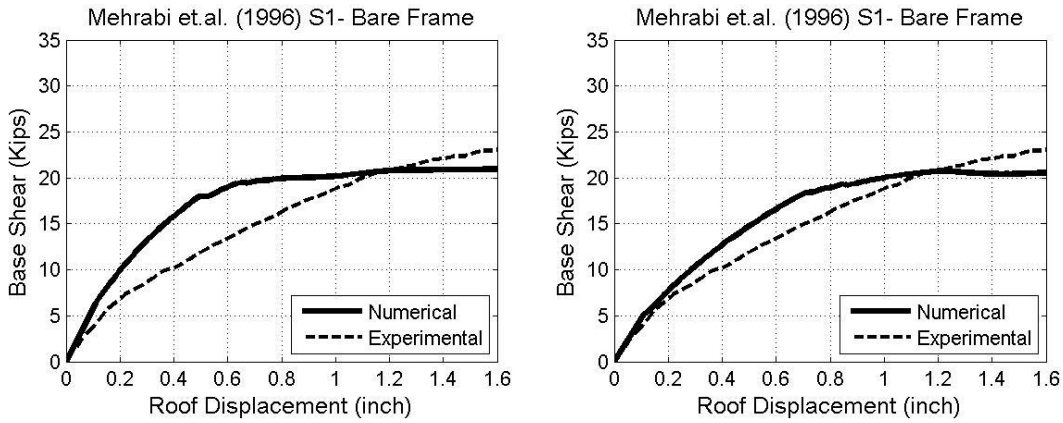

Figure 3-20 Specimen 1 analytical results compared with experimental envelope curves by Mehrabi et. al. (1996) in a) Model without Bond slip effect, b) Model with Bond Slip effect.

In Figure 3-21, the results of the Specimen 4, weak frame-weak infill and Specimen 6, strong frame-weak infill are compared. The bond slip was used in the models. As can be seen, initial stiffness, degradation and strength capacity were captured with an accepTable A1ccuracy. In Figure 3-21, the elasticity modulus is used as given in the experimental study. To verify the modeling technique as given in Part 3.1.2 and disscussed in part 3.2, in Figure 3-22, the modulus of elasticity was calculated with $550f_m$. K_3 was considered as $0.1K_1$ for both In Figure 3-21 and Figure 3-22. The results are similar to each other due to $550f_m$ result in similar values with experimental studies.

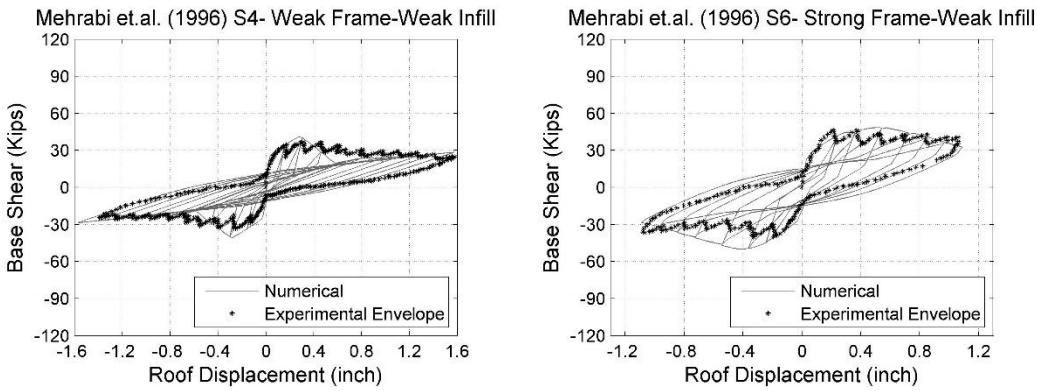

Figure 3-21 Specimen 4 and Specimen 6 Analytical results compared with experimental envelope curve (K_3=0.1K_1.).

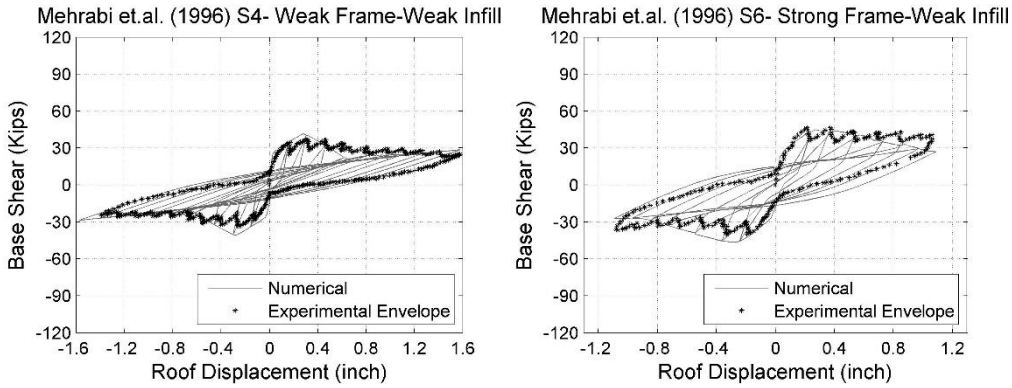

Figure 3-22 Specimen 4 and Specimen 6 Analytical results compared with experimental envelope curve with given material constitutive law (E_m=550f_m and K_3=0.1K_1.).

In Figure 3-23, the analytical results obtained for Specimen S, weak infilled frame, were compared with the experimental ones from Kakaletsis and Karayannis (2008). It has seen that the strength capacity is captured. However, for the weak infill model, (Specimen S), the degradation in the experimental study could not be captured. The weak infill has a low elasticity modulus, and this effect increases the strain values in the material constitutive calculations. Especially the maximum strain and ultimate strain values become larger leading to a stiffer behavior.

In Figure 3-24, the numerical results obtained for the strong infill frame, Specimen IS, were compared with the experimental ones (Kakaletsis and Karayannis (2008)), and a good match was captured. It can be observed that the obtained results for strong infill are much better than that of the weak infill. The post peak stifness is taken as K_3=0.005K_1 for strong infill walls and K_3=0.1K_1 for weak infill walls for the results in Figure 3-23 and Figure 3-24, respectively.

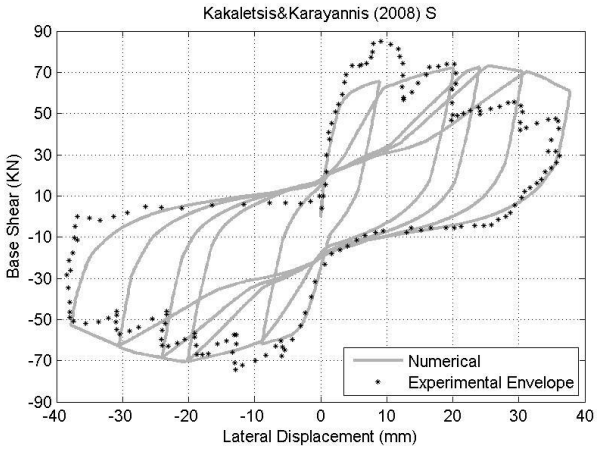

Figure 3-23 Specimen S, weak infill, result comparison with experimental backbone envelope curve

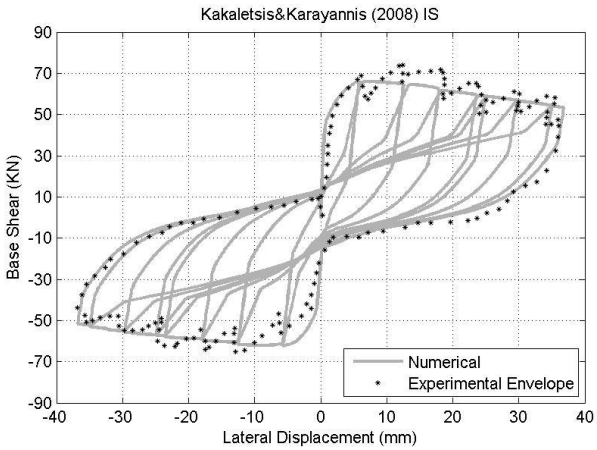

Figure 3-24 Specimen IS, strong infill, result comparison with experimental backbone envelope curve

If we calculate equivalent strut width and strength of the infill with $E_m=550f_m$ and $f_t=(f_t)_{exp}$ according to the part 3.1.2 of this chapter, the results seem to change for the weak infills. It is obvious that the shear strength of the masonry affects the results and the degradation behavior was captured reasonably when $550f_m$ is used for E_m.

In Figure 3-25 and Figure 3-26, the results for weak and strong infill with the parameters calculated from the equations in part 3.2 are shown. The post peak stifness

is calibrated for strong and weak infill walls and K_3=0.005K_1 for strong infill walls and K_3=0.1K_1 for weak infill walls were selected.

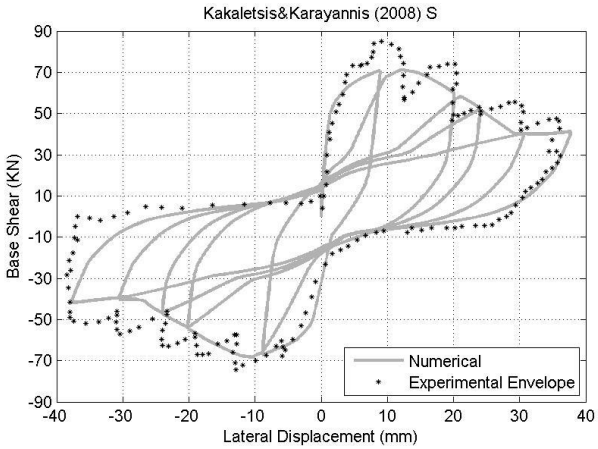

Figure 3-25 Results for Specimen S, weak infill for the method given in part 3.2, E_m=550f_m and f_t=$(f_t)_{exp}$

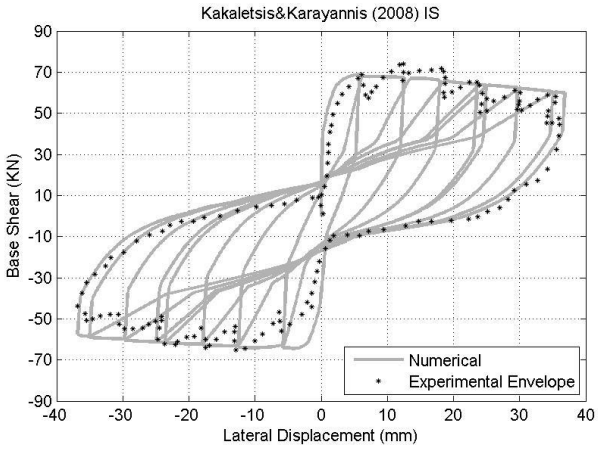

Figure 3-26 Results for Specimen IS, strong infill, a) E=550f_m and f_t=$(f_t)_{exp}$

In the case of Ezzatfar et. al. (2014) study, the shear strength of the infill walls under the diagonal compression test must represent the Turkish construction. Therefore the shear strength was calculated according to Eq. 3-11, which is proposed by Begimgil (1991). The author observed the shear strength for different cracking angles (Figure 3-27) and proposed the formula given in Eq. 3-11, which is relevant to the findings by Yorulmaz (1968) and Sahlin (1971). The increase in the normal stress results in a

change in the shear stress. In Eq. 3-11, 0.265 MPa is used for, τ_o, the cohesive strength and 0.735 is suggested for the μ, friction coefficient. The formula in Eq. 3-11 was derived from the regular mortar type, which is used in Turkish building constructions.

$$\tau = 0.265 + 0.735\sigma \ \ (MPa) \qquad (3\text{-}11)$$

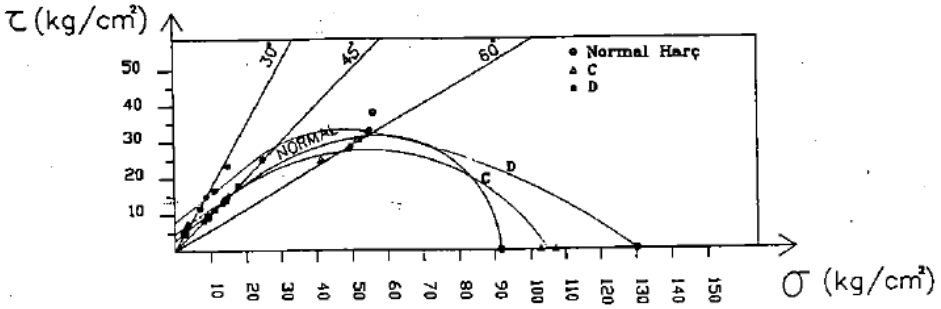

Figure 3-27 Shear Strength vs Normal Stress (Begimgil (1991))

For the modeling of the test specimen of Ezzatfar et. al. (2014), some calculations and assumptions were made. The compressive strength of the infill was calculated from Eq 3-12 which is proposed by Hendry and Malek (1986). The compressive strength of the hollow brick block is f_b=23 MPa, and the compressive strength of the mortar is f_{mo}=4.7 MPa. The calculated masonry compressive strength of the infill is f_m=9.05 MPa. The f_m, compressive strength of the combined infill and plaster was calculated according to Eq. 3-14. The calculated value for combined compressive strength of infill wall is $(f_m)_{infill+plaster}$=8.33 MPa.

$$f_m = 1.242 \cdot {f_b}^{0.531} \cdot {f_{mo}}^{0.208} \qquad \text{(for 102.5 mm thick wall)} \qquad (3\text{-}12)$$

$$f_m = 0.334 \cdot {f_b}^{0.778} \cdot {f_{mo}}^{0.234} \qquad \text{(for 215.0 mm thick wall)} \qquad (3\text{-}13)$$

$$(f_m)_{\text{infill+plaster}} = \frac{(f_m \cdot t_w + f_p \cdot t_p)}{(t_w + t_p)} \ ) \qquad (3\text{-}14)$$

Then f_{tp} values for each floor were calculated with Eq 3-10, and the material constitutive law for infill walls at each floor were obtained. Friction coefficient was taken as 0.957 which is obtained for the strong infills by Kakaletsis and Karayannis

(2008). The reason to use the higher friction coefficient is to have a high compressive strength and having plaster on the infill wall and it is assumed that it increases the friction coefficient. If we considered that the tested shear strength is higher in which is observed by Kakaletsis and Karayannis (2008) and Mehrabi et. al. (1996), this assumption is reasonable.

In Figure 3-28, a numerical model is compared with an experimental pseudo-dynamic test result of the Specimen1 from Ezzatfar et. al. (2014). The base shear was overestimated in one direction. However the interstory drift capacity was captured (Figure 3-29).

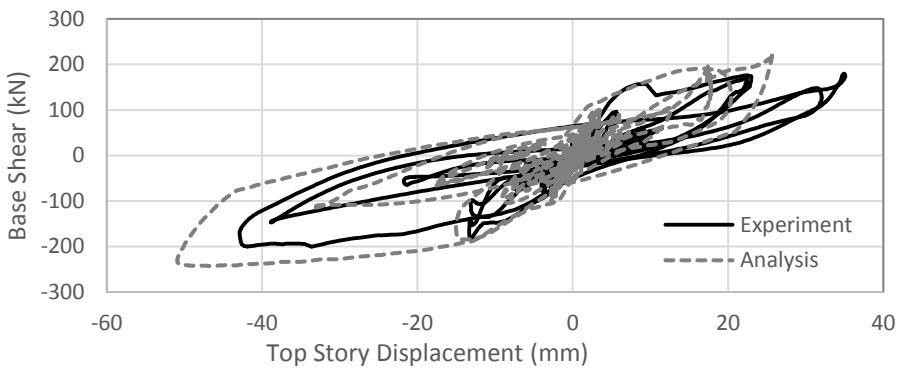

Figure 3-28 Time History Analysis Result Compared with Experimental Pseudo-Dynamic Test Results for All Three Earthquake Motion

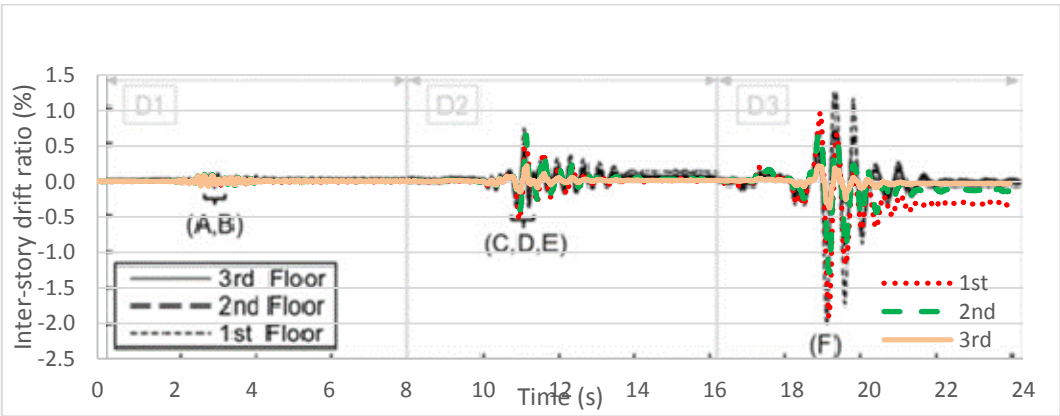

Figure 3-29 Inter story drift ratio values are compared with the test result (Colors for numerical results).

3.4. Discussion of Sensitivity Analysis and Verification and Calibration Results

Throughout the verification and sensitivity analysis, it is observed that calculating the equivalent strut width is not enough for a non-linear analysis and there is a need for a material constitutive law which is suggested by other researchers such as, Panagiotakos and Fardis (1996) and Bertoldi et.al (1993). In this study, the hysteretic model was used and modified with new formulas (Figure 3-7).

ASCE 41 equivalent strut formula (Eq. 3-3) seems to give a good estimate if the material constitutive law is well developed. The contact length definition is a good way to include the effects of the surrounding frame, however, also have some drawbacks. The contact length may change depending on the thickness of the wall and span length and these may result in different contact lengths at each span and will make the modeling complicated. For multistory frames, there is a need for an assumption like using the mean contact length or critical one for each floor or the same span at all floor levels.

Ultimate strain or displacement calculation seems to be effective on degradation depending on the strength type of infill. Therefore, the post peak stiffness, K_3, definition becomes important. For strong infill, $K_3=0.005K_1$ and for the weak infill, $K_3=0.1K_1$ gave a good match with related experimental results.

If it is consistent in calculating the equivalent strut width with the same methodology, E_m seems to be less effective on the results. The contact length change from z/2 to z/3 did not make a huge difference on the results (Figure 3-11).

The f_{tp}, shear strength under diagonal compression test, affect the axial load capacity of the equivalent strut and correspondingly the hysteretic material for degradation behavior. The weak and strong infills have different friction coefficients for different failure angles (Figure 3-27) to calculate f_{tp}.

Most of the infill walls have plaster, and this should be included in the modeling. Eq.3-14 was used to combine the infill and plaster compressive strength and used in the numerical model to compare with experimental results (Ezzatfar et. al. (2014)).

As a result, in the remaining part of this thesis, the following assumptions were made in calculations. The contact length was taken as z/2, where z is calculated according to Eq. 3-5. The friction coefficient was taken as 0.735 and f_{tp} was calculated according to Eq. 3-11, which was proposed by Begimgil (1991). The plaster compressive strength was included into the model through Eq. 3-14. Post peak stiffness was taken as K_3=0.005K_1 and K_3=0.1K_1 for strong and weak infill walls, respectively.

CHAPTER 4

DESCRIPTION OF BUILDINGS SELECTED FROM TURKISH BUILDING STOCK

This chapter presents representative buildings selected from the Turkish building stock, in terms of plans, and their design according to the codes. The selected buildings were designed according to the "Turkish Earthquake Code" (TEC2007) and "Requirements for Design and Construction of Reinforced Concrete Structures" (TS500-2000) and "Design Loads for Buildings" (TS 498). Representative frames from these buildings were selected for the analysis. The vertical irregularities were introduced to these regular frames.

4.1. Literature on Building Stock in Turkey

The buildings were selected according to the statistical parameters which were obtained from the studies of Bal et al. (2007) and Ay (2012). Some of the architectural plans were chosen from the existing buildings but designed according to the codes. First story floor plans were selected and copied to the upper stories to eliminate the irregularities from the layout differences for the design. In reality, however, there are differences at upper stories' layouts including also the distribution and dimensions of non-structural elements. Overhangs at upper stories were not considered for this study.

Ay (2012) reviewed and considered a large database and found some statistical parameters for the building stock in İstanbul. The study differs from the Bal et al. (2008) as this study checks also the number of continuous frames. The number of RC buildings compiled in this statistical study is 33773. The majority of his data is from the Küçükçekmece (29945 buildings), and Zeytinburnu (3034 buildings) building inventories and the most detailed database was from Bakırköy (333) district. All these buildings are reinforced concrete and have the story number varying between 3 and 9 stories. The summary of AY (2012) study is given in Table 4-1 and Table 4-2.

Table 4-1 Statistics for Turkish RC building stock (Ay (2012))

	Mean	Standard Deviation
Ground-story height (m)	3.01	0.39
Upper-story height (m)	2.71	0.20
Ratio of short to long building plan dimension	0.73	0.18
Number of continuous frames along short direction	2.68	1.30
Number of continuous frames along long direction	2.70	1.17
Average span length (if orientation is disregarded) (m)	3.55	0.68

Table 4-2 Statistics for column dimensions (Ay (2012))

Number of Stories	Col. Depth/Col. Width		Ground-story column depth (cm)		Column area decreasing from ground-story to top-story (%)	
	Mean	Std. Dev.	Mean	Std. Dev.	Mean	Std. Dev.
4	1.66	0.35	45.2	8.48	19.0	12.26
5	1.85	0.56	48.4	14.39	24.0	17.85
6	1.86	0.51	49.2	13.42	24.7	18.41
7	2.00	0.64	54.1	16.57	24.4	16.68
8	2.12	0.67	60.3	19.52	30.7	15.15

Bal et. al. (2008 a), studied an extensive database and searched many parameters for the building stock in Marmara Region regarding their statistical characteristics and distributions. Some of the statistical parameters from the Bal et. al. (2008 a) are given in Table 4-3, Table 4-4, and Table 4-5. The column and beam depths and structural wall parameters were statically investigated by Bal et. al. (2008a). Upper and lower boundaries and suggested distribution types were listed as well.

Bal et al. (2008 a) state in their study that the 73.4 percent of the building stock of Marmara Region is RC building with clay or block infill. This number is quite high, and that is another reason why the buildings with infill walls should be investigated in more detail.

Table 4-3 Column depth parameter (Bal et. al. (2008a))

Building type	No. of str.	No. of data	No. of buildings	Mean	COV (%)	A^a	B^a	Suggested distribution	χ^2 test result
Non-compliant									
Dual emergent	⩽3	6	1	0.43	48	0.3	0.8	Normal	10%
	4	12	2	0.47	17	0.3	0.8		
	5	8	1	0.65	8	0.3	0.8		
	6⩾	11	3	0.71	13	0.3	0.8		
Non-compliant									
Dual embedded	⩽3	12	3	0.53	34	0.3	0.9	Normal	10%
	4	19	3	0.58	25	0.3	0.9		
	5	6	1	0.60	26	0.3	0.9		
	6[b]⩾	32	8	0.66	25	0.4	1.0		
Non-compliant									
Frame emergent	⩽3	6	2	0.45	12	0.3	0.6	Log-normal	10%
	4[b]	47	11	0.49	30	0.4	1.0		
	5	35	8	0.65	30	0.4	1.1		
	6⩾	77	16	0.70	29	0.4	1.2		
Non-compliant									
Frame embedded	⩽3	9	1	0.47	19	0.2	0.6	Log-normal	10%
	4[b]	29	6	0.45	43	0.2	1.0		
	5	–	–	–	–	–	–		
	6⩾	7	1	1.00	14	0.6	1.3		
Compliant									
Dual emergent	⩽3	42	10	0.63	23	0.3	1.0	Log-normal	1%
	4	73	16	0.65	32	0.3	1.0		
	5[b]	142	32	0.66	20	0.4	1.0		
	6⩾	52	10	0.72	38	0.4	1.6		
Compliant									
Dual embedded	⩽3	39	10	0.65	31	0.2	1.0	Log-normal	10%
	4	57	10	0.65	25	0.3	1.0		
	5[b]	64	13	0.66	24	0.4	1.0		
	6⩾	45	10	0.78	54	0.4	1.3		
Compliant									
Frame emergent	⩽3	46	12	0.60	36	0.3	1.2	Log-normal	Not sat.[c]
	4[b]	97	17	0.71	28	0.4	1.2		
	5	38	8	0.74	36	0.4	1.4		
	6⩾	24	4	0.85	42	0.4	1.6		
Compliant									
Frame embedded	⩽3	24	6	0.68	45	0.3	1.2	Log-normal	10%
	4	27	7	0.70	35	0.4	1.2		
	5[b]	38	8	0.71	26	0.5	1.2		
	6⩾	10	2	0.83	30	0.5	1.4		

[a] *A* and *B* indicate the lower and the upper bounds of the range in which the suggested distribution could be truncated.
[b] Number of storeys used to define the type of distribution (i.e. log-normal, etc.) and χ^2 test result. In all other cases the type of distribution is found using all of the data for all the numbers of storeys.
[c] The χ^2 test is not satisfied.

Table 4-4 Summary of beam depth (Bal et. al. (2008a))

Building type		No. of data	No. of buildings	Mean	COV (%)	*A*	*B*	Suggested distribution	χ^2 test result
Non-compliant	Dual & Frame emergent	1688	45	0.60	16	0.4	0.8	Log-normal	Not sat.[a]
Non-compliant	Dual & Frame embedded	201	26	0.30	4	0.2	0.3	Exponential (e^{+25x})	10%
Compliant	Dual & Frame emergent	2856	108	0.48	14	0.3	0.6	Normal	Not sat.
Compliant	Dual & Frame embedded	1405	68	0.33	19	0.3	0.6	Exponential (e^{-15x})	Not sat.

[a] The χ^2 test is not satisfied.

Table 4-5 Structural wall (Bal et. al.(2008 a))

Parameter	Building Type			No. of data	No. of buildings	Mean	COV (%)	A[a]	B[a]	Suggested distribution	χ^2 test result
Structural wall thickness (m)	Non-compliant quality			145	37	0.21	13	0.15	0.30	Gama	1%
	Compliant quality			491	109	0.26	10	0.20	0.35	Gama	Not sat.
Structural wall length (m)	Non-compliant	dual	emergent	31	21	2.25	48	1.00	5.50	Log-normal	10%
	Non-compliant	dual	embedded	116	16	1.62	32	1.00	3.50	Exponential ($e^{-0.8x}$)	1%
	Complaint	dual	emergent	275	64	2.43	39	1.75	6.25	Exponential (e^{-x})	Not sat.
	Complaint	dual	embedded	214	45	2.49	40	1.75	6.25	Exponential (e^{-x})	Not sat.

Bal et. al. (2008 a) also listed common deficiencies in the design, based on the poor performance of RC frames during past earthquakes. According to their observations;

- Lack of lateral resistance of the framing system
- Irregularities in strength and stiffness with height
- Irregularities in plan often exist due to constraints on the construction area.
- Poor quality concrete and heavy corrosion at reinforcing bars
- Inadequate reinforcement detailing and confinement of columns and beam-column joints.
- Shallow foundations, footing under individual columns, inadequate tie beams exists in the building stock.

For an accurate estimation of the performance, the infill wall models should also be involved in the numerical models even though there are many uncertainties in their modeling and engineering parameters of material characteristics. The infill material properties were also studied by Bal et. al. (2008a). In Table 4 6, the upper and lower values of the material properties and material constitutive law parameters were given by Bal et. al. (2008a)

Frame types in buildings vary based on their construction or architectural purposes. The density of the infill walls varies from one frame to the other. Due to this reason, different wall distributions also affect the seismic behavior.

Table 4-6 Material properties of Turkish type infill walls (Bal et. al. (2008))

Parameter	Lower bound	Upper bound
Modulus of elasticity, E_m (MPa)	1500	5000
Compressive strentgth, f_m (MPa)	1.9	3.2
Tensile strength[a], f_t (MPa)	1.1	1.3
Strain at max. Stress, ε_m	0.0002	0.0018
Ultimate strain, ε_u	0.0018	0.0040

[a] Tensile strength of the mortar is considered.

4.2. Selected Building Plans and Design According to TEC 2007, TS 498, and TS 500

Building dimensions and plans were selected and modified from the existing structures. The buildings were modified in the perspective of literature review on Turkish building stock to reflect the typical properties. The design was done according to the "Turkish Earthquake Code" (TEC 2007) and "Requirements for Design and Construction of Reinforced Concrete Structures" (TS500 -2000) and "Design Loads for Buildings" (TS 498). The building details, materials and loads used in the design are given in Table 4-7 through Table 4-9.

Table 4-7 Building Details

	Story Height (m)	Total Story Height (m)	Building Area (m^2)	Type
3 Story	3.00	9.00	159.80	Residence
5 Story	3.00	15.00	182.00	Residence
8 Story	3.00	24.00	243.40	Residence

Table 4-8 Material Properties

f_{ck} (MPa)	25
f_{yk} (MPa)	420
E_c (MPa)	30250
E_s (MPa)	200000
Υ_c	1.5
Υ_s	1.15

Table 4-9 Loads used in the design

Concrete density (kN/m^3)	25.0
External wall load -30 cm hollow brick (insulated) (kN/m^2)	4.6
Internal wall load - 20 cm hollow brick (kN/m^2)	3.3
Live load (at rooms) (kN/m^2)	2.0
Live load (at halls and stairs) (kN/m^2)	3.5

Equivalent (Linear) earthquake load analysis was used for the design process. The dimensions are in the range of the statistical studies done by Ay (2012) and Bal et. al. (2008). The soil class was chosen as Z1 (Ta=0.10 s and Tb= 0.30 s) and seismic zone 1 was assumed. PROBINA v.18 (2013) software was used for design. In Figure 4-1, elastic and design spectrums are given. High ductility systems were chosen (R=8) as specified in TEC2007, 2.5.1.6. If the structural system has shear walls, R values are modified by taking into account the base shear contributions to the total system, αs (TEC2007, 2.5.2, 2.5.3, and 2.5.4).

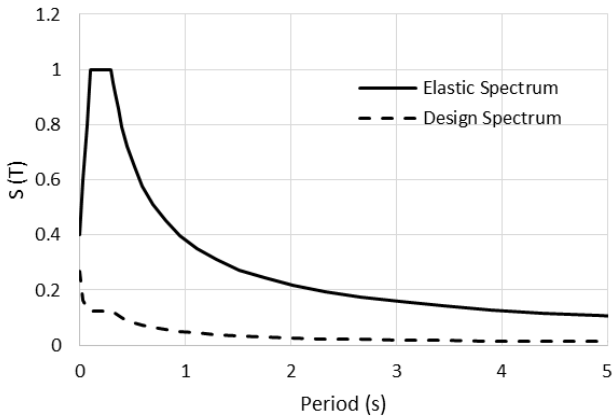

Figure 4-1 Elastic and Design Spectrum

4.2.1. 3-Storey Building and Selected Frame

The first story layout and 3D building model are shown in Figure 4-2, Figure 4-3, and Figure 4-4. The first period of the 3 story building is 0.413 s and the second period is 0.333 s. Story masses for the 1st, 2nd and 3rd floors are 224 tons, 229 tons and 147 tons, correspondingly. Equivalent earthquake loads are applied with 5% eccentricity for the design. In Figure 4-4, the first mode dominant inner frame (F-F axis) was selected for

the analysis. The mass participation ratio is 87% for the chosen direction. The reinforcement details of columns and beams are given in Table A1-1 and Table A1-2 (APPENDIX A).

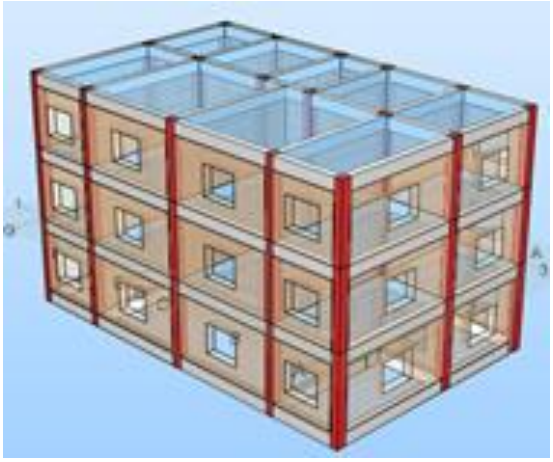

Figure 4-2 Probina model: 3D view of the 3-story building

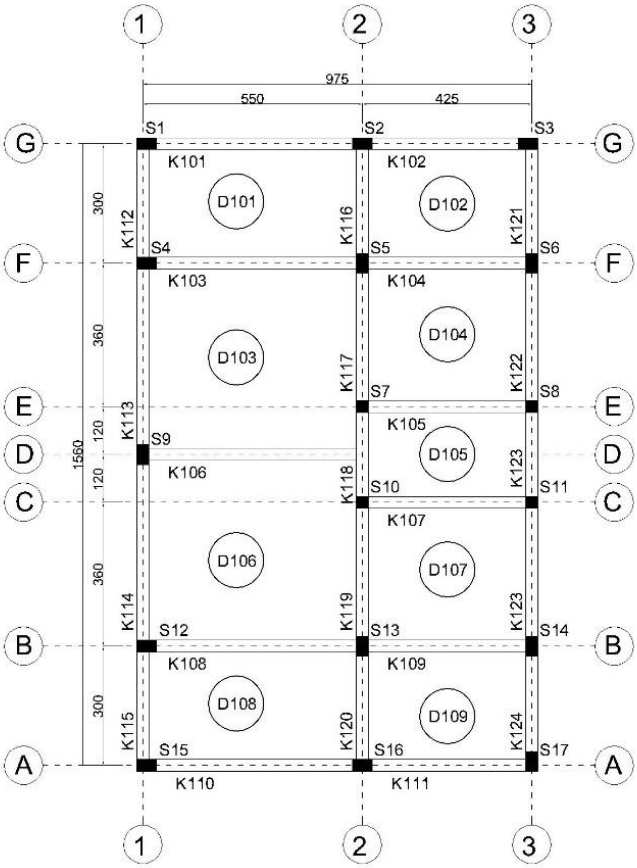

Figure 4-3 Three Storey Building First Story Layout (units are in cm)

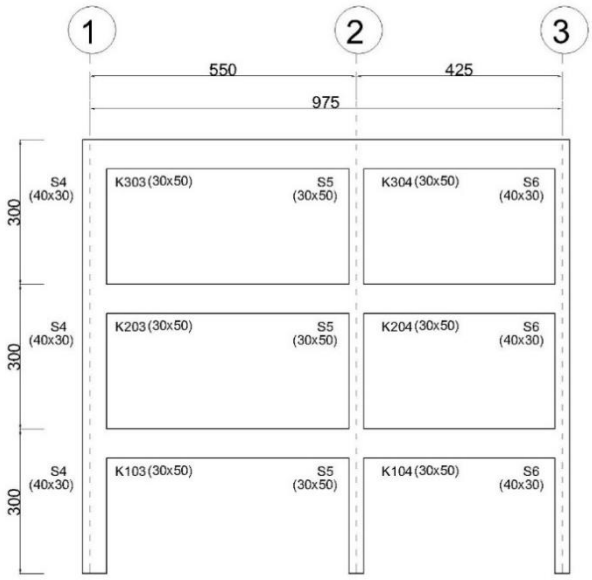

Figure 4-4 3 Storey, F-F axle frame dimensions (units are in cm)

4.2.2. 5-Storey Building and Selected Frame

The first story layout and 3D building model are shown in Figure 4-5 and Figure 4-6. The first period of the 5 story building is 0.461 s and the second period is 0.366 s. Story masses for the floors from first to seventh are 299 tons and for the fifth floor is 200 tons. Equivalent earthquake loads are applied with and 5% eccentricity. In Figure 4-7, the first mod dominant inner frame (F-F axis) was selected. The mass participation ratio is 83.4% for the selected direction. The reinforcement details of columns and beams are given in Table A1-3 and Table A1-4 (APPENDIX A).

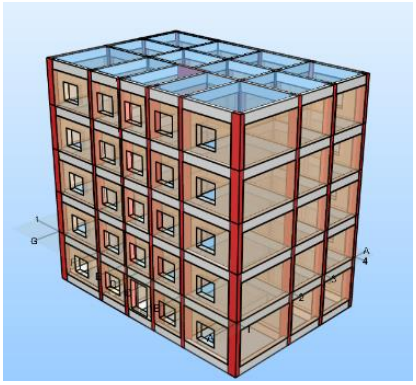

Figure 4-5 Probina model: 3D view of the 5-story building

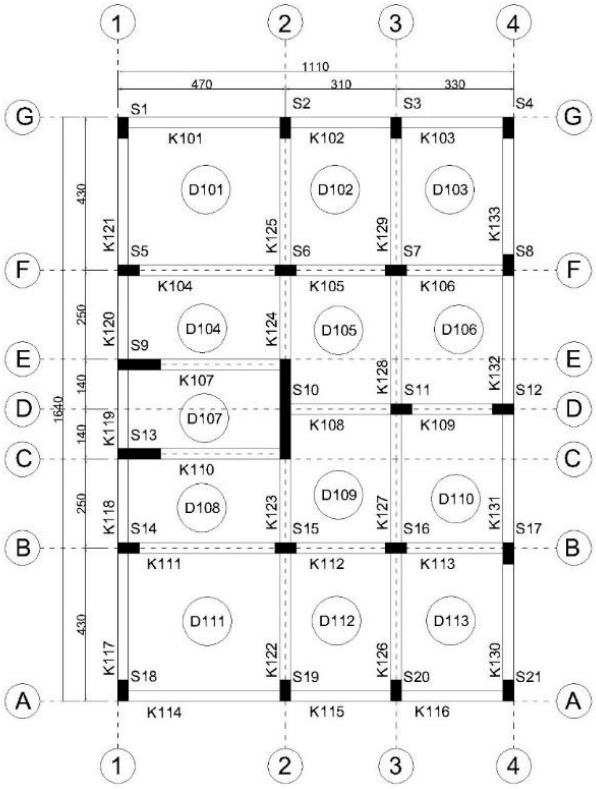

Figure 4-6 5 Story Building First Story Layout (units are in cm)

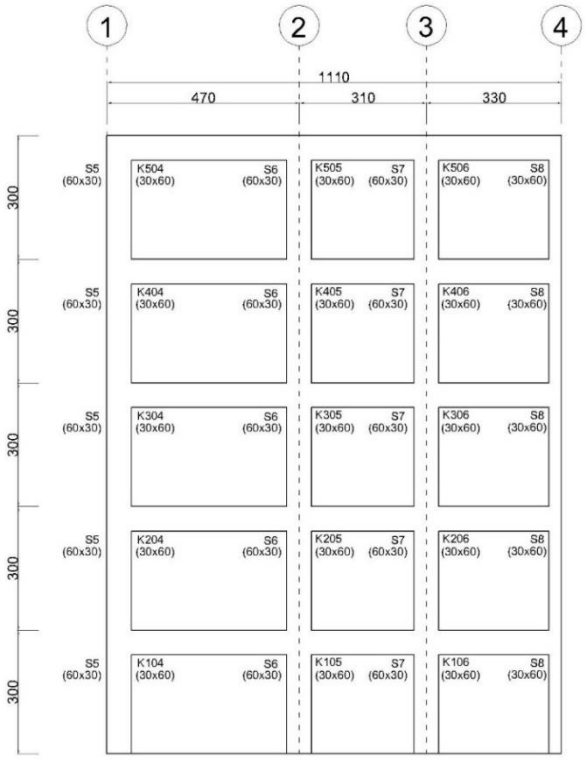

Figure 4-7 5 Storey, F-F axle frame dimensions (units are in cm)

4.2.3. 8-Storey Building and Selected Frame

The first story layout and 3D model of the building are shown in Figure 4-8 and Figure 4-9. The first period of the 8 story building is 0.883 s and the second period is 0.765 s. Story masses for the floors from first to seventh are 341 tons and it is 265 tons for eigth floor. Equivalent earthquake loads are applied with 5% eccentricity. In Figure 4-10, first mode dominant inner frame (F-F axis) was selected. The mass participation ratio is 81.2% for the chosen direction. The reinforcement details of columns and beams are given in Table A1-5 and Table A1-6 (APPENDIX A).

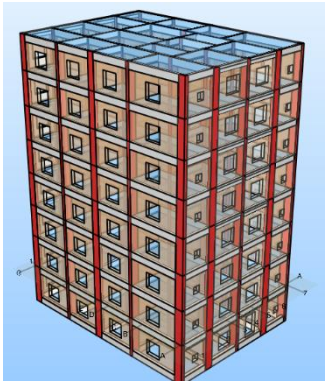

Figure 4-8 Probina model: 3D view of the 8-story building

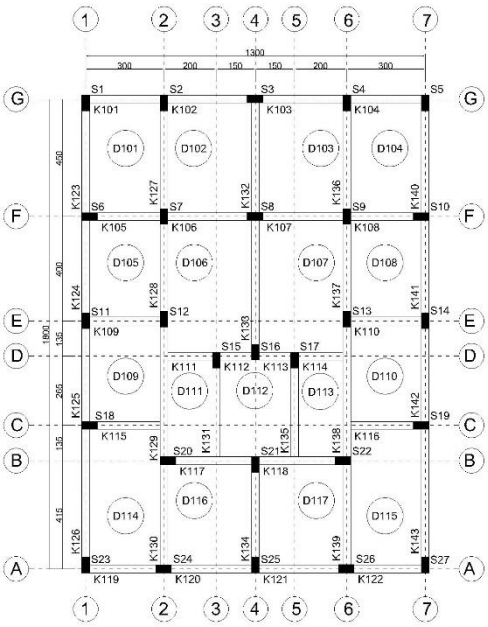

Figure 4-9 8 Story Building First Story Layout (units are in cm)

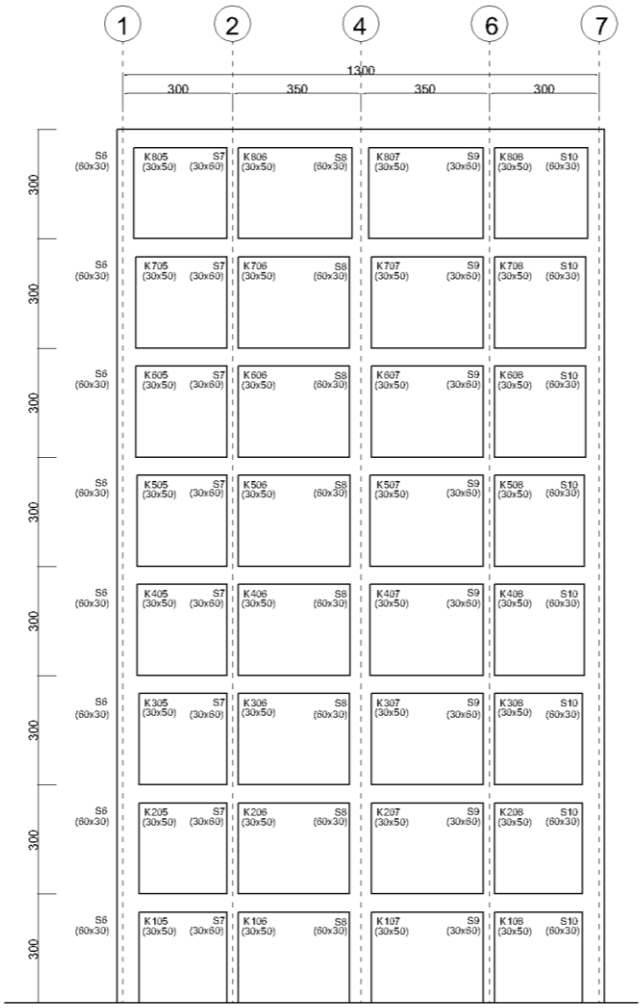

Figure 4-10 8 Story, F-F axle frame dimensions (units are in cm)

4.3. Defining Vertical Irregularities to Regular Frames

TEC and IBC's soft and weak story vertical irregularity parameters (Table 4-10) are calculated for different cases as presented in Table 4-11. The frames are generated from the designed cases. The 3 story, 5 story and 8 story frames are assembled with different infill wall arrangements. The selected frames with different infill wall arrangements are shown in Figure 4-11, Figure 4-12 and Figure 4-13, including also the bare frame. In addition to the cases shown in these figures, these infilled frames were studied without first story infill walls to introduce the soft story effect.

Table 4-10 IBC2012 and TEC2007 Soft and Weak Story Parameters

Parameters	TEC2007		IBC2012	
	irregularity	extreme irregularity	irregularity	extreme irregularity
η_{ki} – Soft Story	2.0	2.0	1/0.7=1.43	1/0.6=1.67
η_{ci} -Weak Story	0.8	0.6	0.8	0.65

Table 4-11 Study Cases for Frames

Varying Parameters	Range
First Story Height (m)	3.0, 4.0, 5.0
Infill wall arrangements	varying in bays
Column dimension multiplier coefficient (CDM)	0.8, 1.0
Column tensile reinforcement multiplier coefficient (RM)	1.0, 1.5

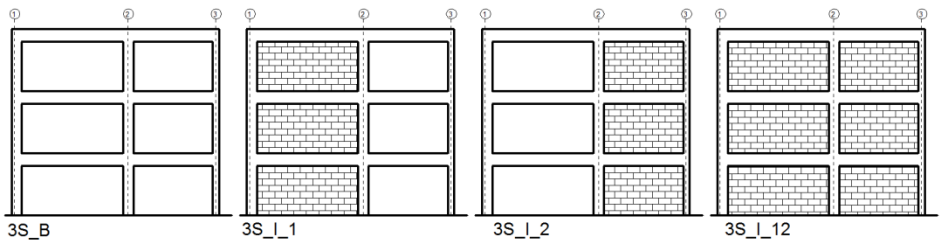

Figure 4-11 3 Story Frames with different infill wall arrangements

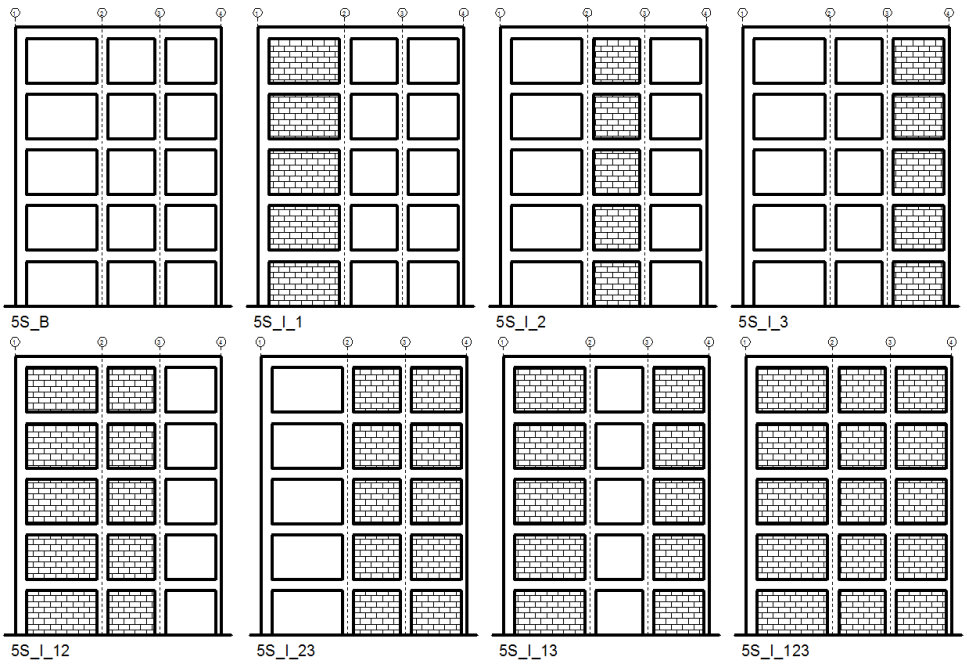

Figure 4-12 5 Story Frames with different infill wall arrangements

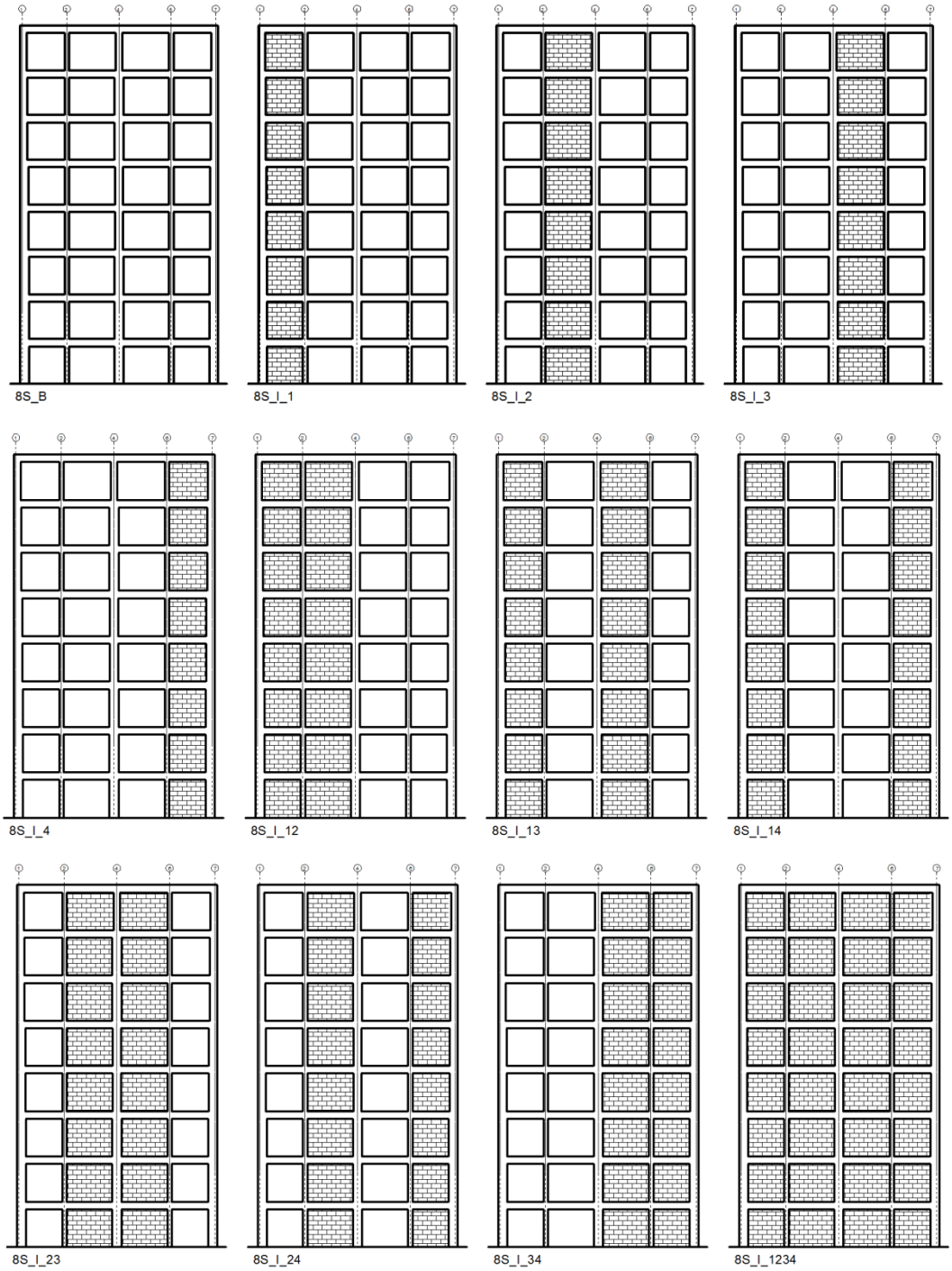

Figure 4-13 8 Story Frames with different infill wall arrangements

Base case terminology is used for the bare frame which has H_1= 3.0 m, CDM=1.0 and RM=1.0 (Table 4-11).

CHAPTER 5

ANALYSIS OF FRAMES AND INTERPRETATIONS OF RESULTS

The selected frames were analyzed using linear and nonlinear analyses procedures to investigate the vertical irregularities, regarding the soft and weak story mechanisms. For linear analysis, equivalent static load and mode superposition (CQC) methods were employed and the pushover analysis and time history analysis were employed for nonlinear analyses. The nonlinear time history analysis was used only for one critical case to check the accuracy of pushover analysis results. The analysis results were evaluated based on the soft story irregularity parameter η_k which is defined in TEC2007. The results were evaluated using some additional parameters that are defined below;

α: the ratio of story drift ratio to the drift ratio at modal height, which is calculated as 0.7 times of the total height,

α_2: the ratio of the inelastic roof displacement to the elastic roof displacement. This parameter is used by Seneviratna and Krawinkler (1997) for regular frames and Al-Ali and Krawinkler (1998) for irregular shear frames.

α_{irreg}: the ratio of the inelastic roof displacement of irregular cases to inelastic roof displacement of the base case (Al-Ali and Krawinkler (1998)).

In Table 4-10, the soft and weak story parameters specified in IBC 2012 and TEC 2007 are given. In this chapter, soft story parameters are discussed and **α, α_2** and **α_{irreg}** parameters are investigated. The soft story irregularity parameter **η_k** and **α** parameter are investigated both in linear and nonlinear analyses. In nonlinear analyses results, **α_2** and **α_{irreg}** parameters are additionally investigated as they were used by other researchers.

The ultimate point was selected based on some assumptions. Global and local failure criterions are defined consistent with other researchers' studies (Zhou et. al. (2014), Priestley et. al. (1996), Kheyroddin and Naderpour (2007), Priestley (2000), Grammatikou et. al. (2016)). The details of the failure criterions are given in part 5.2 in this chapter.

5.1. Linear Procedures

5.1.1. Comparison of Axial Loads on Columns and Struts under Gravity Loads

Including the infill walls load bearing capacity arises the question of how much force will be carried by struts or how the distribution of the forces between the strut and the wall will be. To answer these questions, fully infilled 3, 5 and 8 story frames were selected. The first story height is 3.0 m for all selected frames. The axial forces on the columns were calculated under the gravity loads without infill walls and then compared with the results of the infilled model. The contribution of strut forces were calculated subtracting these two model results. Three strut model changes the distribution of the forces, so, changes the axial forces on the columns. The change is between 0.025 and 0.146 for 3 story frame columns (Table 5-2). The total axial force carried by the struts are between 0.03 and 0.07 times of the axial forces carried by columns (Table 5-3).

Table 5-1 Axial loads on the columns without infill walls in the model for 3 Story frame (Unit: N)

	$F_{Column1}$	$F_{Column2}$	$F_{Column3}$
1st	141084.70	272289.70	131205.00
2nd	83562.98	161657.70	78094.77
3rd	26041.28	51025.85	24984.56

Table 5-2 The ratio of the axial loads comes from the struts to columns for 3 Story frame

	$F_{Strut}/F_{Column1}$	$F_{Strut}/F_{Column2}$	$F_{Strut}/F_{Column3}$
1st	-0.0470	-0.1004	0.0896
2nd	-0.0256	-0.1059	0.1093
3rd	-0.0451	-0.1475	0.0663

Table 5-3 The ratio of the total axial loads comes from the struts to total of columns for 3 Story frame

	$\sum F_{Strut}/\sum F_{Column1}$
1st	0.0408
2nd	0.0332
3rd	0.0690

In Table 5-4, Table 5-5, and Table 5-6, the results are given for 5 story infilled frame. In Table 5-4, the axial loads were calculated without infill walls and in Table 5-5, the ratio of the axial loads coming from the struts to the columns were given. The change is between 0.013 and 0.30.

Table 5-4 Axial loads on the columns without infill walls in the model for 5 Story frame (Unit: N)

	$F_{Column1}$	$F_{Column2}$	$F_{Column3}$	$F_{Column4}$
1st	254930.73	461707.78	416577.65	209800.61
2nd	198131.74	358865.15	323856.47	163123.06
3rd	141332.76	256022.53	231135.29	116445.52
4th	84533.77	153179.90	138414.11	69767.97
5th	27734.78	50337.28	45692.93	23090.43

Table 5-5 The ratio of the axial loads comes from the struts to columns for 5 Story frame

	$F_{Strut}/F_{Column1}$	$F_{Strut}/F_{Column2}$	$F_{Strut}/F_{Column3}$	$F_{Strut}/F_{Column4}$
1st	0.0126	-0.1648	-0.1229	0.2716
2nd	0.0290	-0.1593	-0.1140	0.3030
3rd	0.0400	-0.1672	-0.1261	0.3040
4th	0.0429	-0.1729	-0.1502	0.2866
5th	0.0229	-0.2161	-0.2376	0.2258

In Table 5-6, the ratio of the total axial forces coming from the struts to total axial forces coming from the columns were calculated for each floor and it is in the range of 0.03 to 0.11.

Table 5-6 The ratio of the total axial loads comes from the struts to total of columns for 5 Story frame

	$\sum F_{Strut}/\sum F_{Column1}$
1st	0.0500
2nd	0.0373
3rd	0.0415
4th	0.0531
5th	0.1082

In Table 5-7, Table 5-8, and Table 5-9, the results are given for 8 story infilled frame. In Table 5-7, the axial loads were calculated without infill walls and in Table 5-8, the ratio of the axial loads coming from the struts to the columns were given. The change range is between 0.09 and 0.38. In Table 5-9, the ratio of the total axial forces coming from the struts to total axial forces coming from the columns were calculated for each floor and it is in the range of 0.08 to 0.21.

Table 5-7 Axial loads on the columns without infill walls in the model for 8 Story frame (Unit: N)

	$F_{Column1}$	$F_{Column2}$	$F_{Column3}$	$F_{Column4}$	$F_{Column5}$
1st	295578.40	588567.60	585978.40	588567.60	295578.40
2nd	256001.00	509732.10	507462.20	509732.10	256001.00
3rd	216423.70	430896.60	428945.90	430896.60	216423.70
4th	176846.30	352061.10	350429.70	352061.10	176846.30
5th	137268.90	273225.70	271913.50	273225.70	137268.90
6th	97691.53	194390.20	193397.30	194390.20	97691.53
7th	58114.16	115554.70	114881.10	115554.70	58114.16
8th	18536.78	36719.20	36364.84	36719.20	18536.78

Table 5-8 The ratio of the axial loads comes from the struts to columns for 8 Story frame

	$F_{Strut}/F_{Column1}$	$F_{Strut}/F_{Column2}$	$F_{Strut}/F_{Column3}$	$F_{Strut}/F_{Column4}$	$F_{Strut}/F_{Column5}$
1st	0.1947	-0.2287	-0.1823	-0.2353	0.2796
2nd	0.2340	-0.2223	-0.1671	-0.2206	0.3145
3rd	0.2575	-0.2322	-0.1744	-0.2235	0.3313
4th	0.2669	-0.2368	-0.1785	-0.2249	0.3347
5th	0.2599	-0.2382	-0.1786	-0.2301	0.3243
6th	0.2356	-0.2396	-0.1787	-0.2423	0.3025
7th	0.1886	-0.2446	-0.1831	-0.2657	0.2595
8th	0.0857	-0.3240	-0.2562	-0.3824	0.1594

Table 5-9 The ratio of the total axial loads comes from the struts to total of columns for 8 Story frame

	$\sum F_{Strut}/\sum F_{Column1}$
1st	0.1018
2nd	0.0834
3rd	0.0834
4th	0.0843
5th	0.0881
6th	0.0973
7th	0.1167
8th	0.2091

It is observed that the axial load in outer columns increases and axial forces decreases at the inner columns. The change in the column axial load becomes larger if the number of the story increases. It may go up to 30 percent change. When we look at the total axial forces carried by the infill walls for the floor, the average values are 5 percent, 6 percent and 11 percent for 3, 5 and 8 story infilled frames.

5.1.2. Equivalent Static Load Method (ESL)

Equivalent static load method is a linear analysis procedure where equivalent earthquake loads representing the first mode behavior are determined based on the spectrum. In this thesis, the equivalent static load method is applied according to TEC 2007. The floor weights are calculated with n=0.3 live load reduction factor. Figure

5-1 summarizes the TEC2007 procedure for calculating the lateral forces at floor levels.

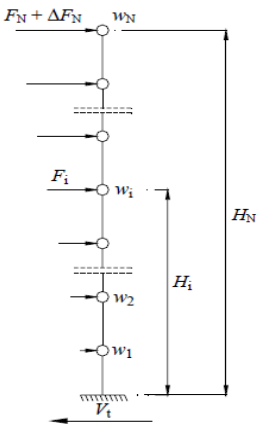

$$V_t = \frac{WA(T_1)}{R_a(T_1)} \geq 0.10\, A_o\, I\, W$$

$$V_t = \Delta F_N + \sum_{i=1}^{N} F_i$$

$$\Delta F_N = 0.0075\, N\, V_t$$

$$F_i = (V_t - \Delta F_N)\, \frac{w_i H_i}{\sum_{j=1}^{N} w_j H_j}$$

Figure 5-1 TEC (2007) Figure 2-6, ESL Method, force distribution

All the selected frames were analyzed using the equivalent static load analysis procedure. The results for one specific case of 3-story frame are shown in Figure 5-2 as an example for the interpretation of the results for α, η_{ki}, and η_{kj}. For this case, it is observed that removal of the first story infill walls increases the soft story parameter, η_k drastically.

In APPENDIX B, the results of α, η_{ki}, and η_{kj} are given for all the cases. All these graphical representations show that the change of the story height is less effective compared to the case of no infill wall at first story. It is worth noting that all designed frame cases, which will be named as *base cases* for the rest of this thesis, satisfy the TEC 2007 code requirements for the soft story irregularity, however, does not satisfy the IBC 2012 requirements.

In Figure 5-3, the first mode periods for the 3 story frames are shown. The x axis represents the frame numbers that are given in APPENDIX A, Table A1-7. For the 3 story base case frame, the first mode period is 0.349 s. The first mode periods of the 5 story and the 8 story frames are given in Figure 5-4 and Figure 5-5, respectively. The first mode periods are 0.386 s and 0.878 s for 5 and 8 story base case frames,

respectively. The x axis labels represent number of corresponding type of frames. For example, 3 story frames has 12 bare frames, 36 infilled frames and 36 infilled frames without first story infill walls.

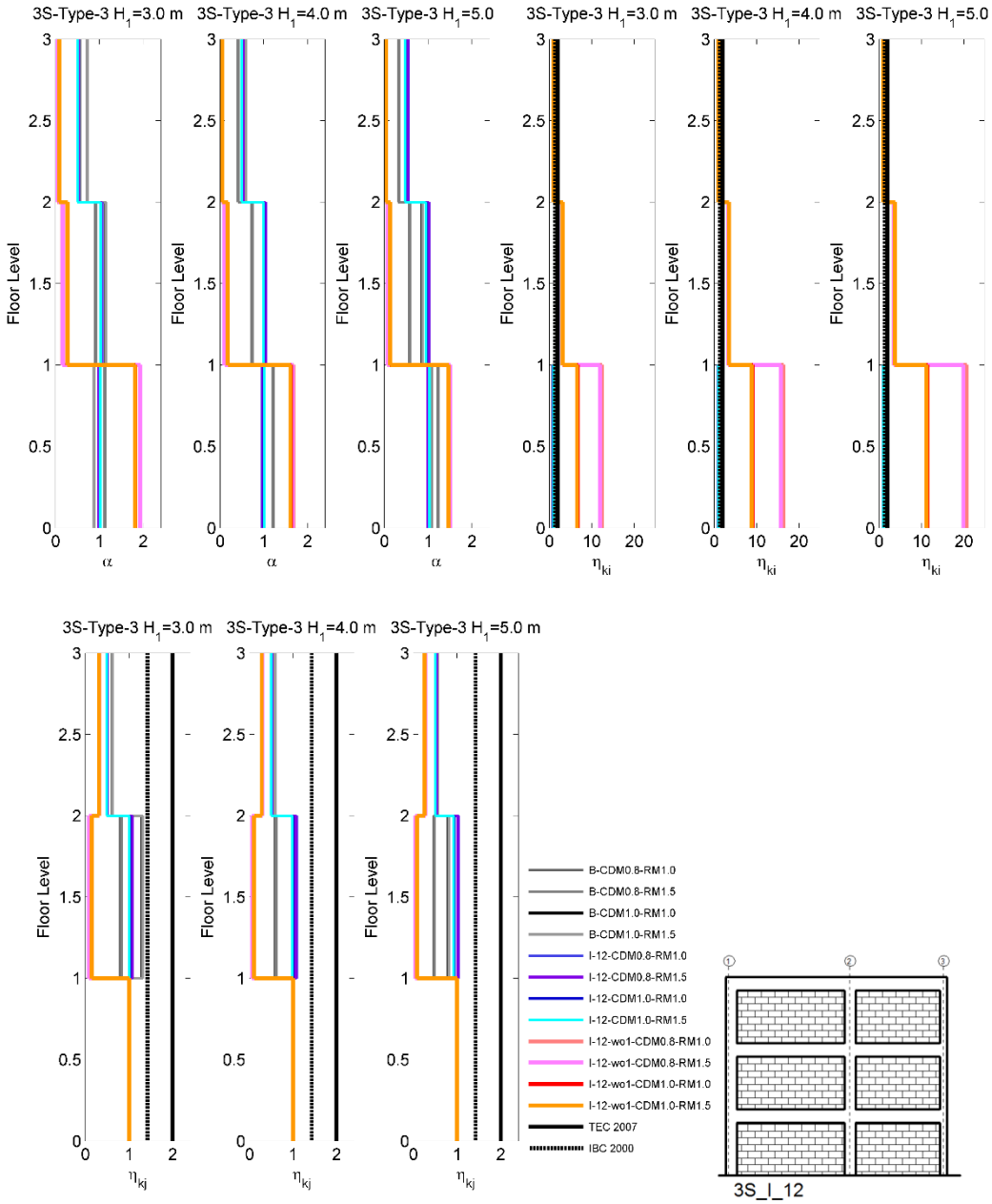

Figure 5-2 3 Story Frame; equivalent static load analysis results for Type 3

In all 3, 5, and 8 story frames, the addition of the infill walls makes them stiffer and removing the first story infill walls makes the frames more flexible. For example,

presence of infill walls reduces the periods approximately to one third of the base case period for 3 story frames, to one half for the 5 and 8 story frames. The infilled frames without first story infill walls become even softer than the base case frames resulting in an increase of the first mode periods of the base case period by a factor of 2 for 3 story frames and 1.5 for 5 story frames. The periods of the base cases and infilled frames without the first story infill walls were almost the same for 8 story frames. The minimum and maximum calculated first periods for each frame type are given in Figure 5-3, Figure 5-4 and Figure 5-5 for 3, 5 and 8 story frames, respectively.

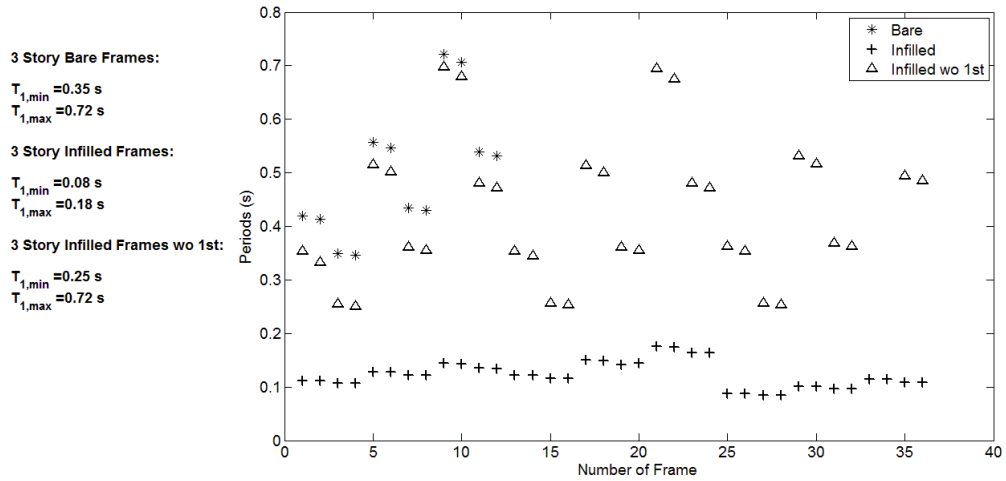

Figure 5-3 3 Story Frames; First mode periods

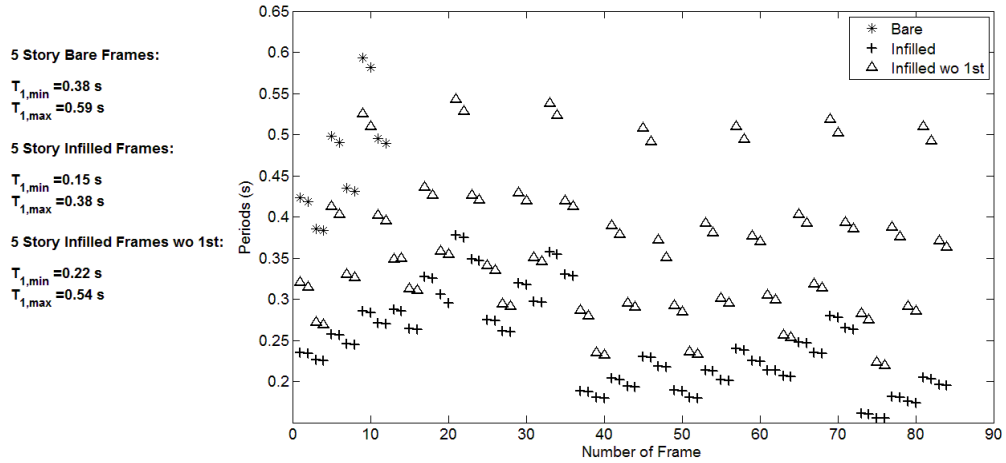

Figure 5-4 5 Story Frames; First mode periods

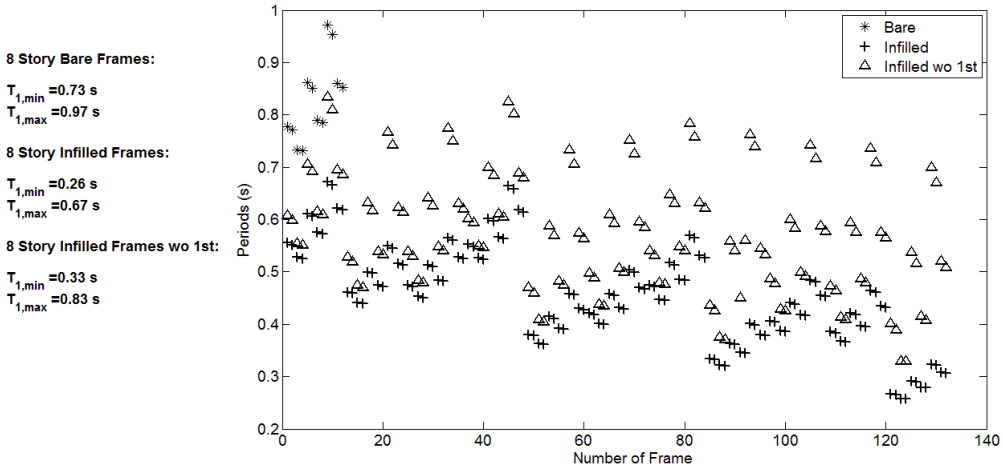

Figure 5-5 8 Story Frames; First mode periods

The results of the equivalent static load analyses, regarding the α, η_{ki}, η_{kj} and η_c parameters are given in APPENDIX B, through Table A2-1 to Table A2-3 for 3, 5, and 8 story frames, respectively.

In Figure 5-6 to Figure 5-8, the α, η_{ki}, and η_{kj} parameters calculated for bare frame cases are presented. For almost all the bare frames, the η_{ki} and η_{kj} parameters are below the limits of 2.0 specified in TEC2007. All the 3 Story bare frames but one satisfy both IBC 2012 and TEC2007 limits. However, 5 and 8 story bare frames with 5.0 m first story height exceed the limit of 1.43 specified in IBC 2012. The mean values of α, η_{ki}, η_{kj}, for all bare frames, are close to 1.0, 1.3 and 1.0, respectively. The maximum values of the α, η_{ki}, and η_{kj}, are given in Table A2-1 to Table A2-3 for the equivalent linear analyses results. All the designed base cases satisfy the code limits. The cases resulting larger values of the α, η_{ki}, and η_{kj} are obtained for the frames where the column dimension multiplier (CDM) is equal to 0.8 and the story height is 5.0 m. The mean values of the frames regarding the α and η_k parameters for the first floor are nearly almost 1.0 for 3 and 5 story frames, and are 0.9 and 0.8 for 8 story frames, respectively.

In Figure 5-9 to Figure 5-11, the α, η_{ki}, η_{kj} parameters computed for the infilled frames are presented. In these cases, the infill walls are continuous along the height of the frames. The maximum value of η_{ki} is approximately 2.0, 1.7 and 1.45 for 3, 5 and 8

story frames, respectively. The average of the α values for the infilled frames are given in Figure 5-9 to Figure 5-11, and these values are close to 1.0. The difference at first story results becomes larger if the number of stories increases. The maximum η_{kj} values are 1.3 for 3 story infilled frames and 1.5 and 1.8 for 5, and 8 story infilled frames, respectively.

In Figure 5-12 to Figure 5-14, the α, η_{ki}, η_{kj} parameters are displayed for the infilled frames without first story infill walls. The maximum α, η_{ki}, η_{kj} parameters are given in Table 5-10, Table 5-11, and Table 5-12. The maximum calculated η_k values exceed the code limit values. The maximum calculated α values vary between 1.1 and 2.9. When the results of the infilled frames without first story infill walls are compared with the infilled frames, α values increase by 1.82, 1.84, and 2.40 times for 3, 5 and 8 story frames, respectively. The η_{ki} values increase by 15.00, 4.60, and 5.00 times, for 3,5 and 8 story frames, respectively. The η_{kj} values reduce by 0.77, 0.73, and 0.78 times for 3, 5 and 8 story frames, respectively for maximum values.

Table 5-10 3 Story frames: Maximum α, η_{ki}, η_{kj} parameters for ESL

3 Story	$\eta_{ki,\,max}$	$\eta_{kj,\,max}$	α_{max}
Bare	2.154	1.315	1.231
Infilled	2.045	1.280	1.145
Infilled wo 1st	20.626	1.000	1.938

Table 5-11 5 Story frames: Maximum α, η_{ki}, η_{kj} parameters for ESL

5 Story	$\eta_{ki,\,max}$	$\eta_{kj,\,max}$	α_{max}
Bare	1.587	1.654	1.321
Infilled	1.603	1.530	1.227
Infilled wo 1st	5.831	1.066	2.191

Table 5-12 8 Story frames: Maximum α, η_{ki}, η_{kj} parameters for ESL

8 Story	$\eta_{ki,\,max}$	$\eta_{kj,\,max}$	α_{max}
Bare	1.443	1.841	1.298
Infilled	1.396	1.778	1.235
Infilled wo 1st	6.303	1.438	2.940

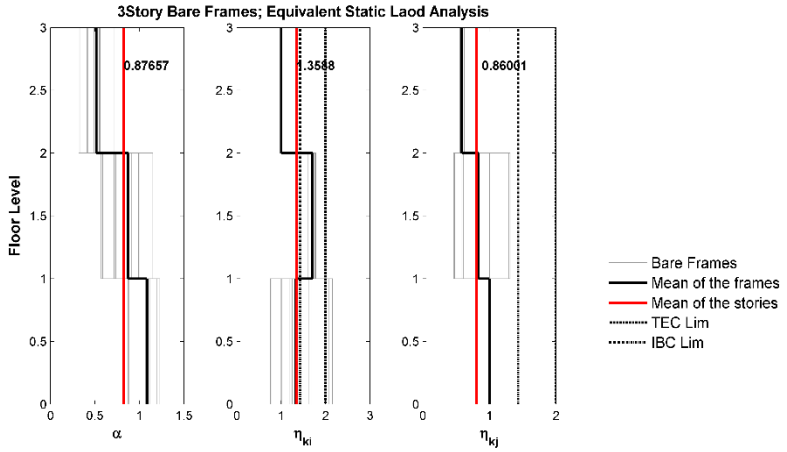

Figure 5-6 3 Story Bare Frames; the α, η_{ki}, η_{kj} results of ESL analysis

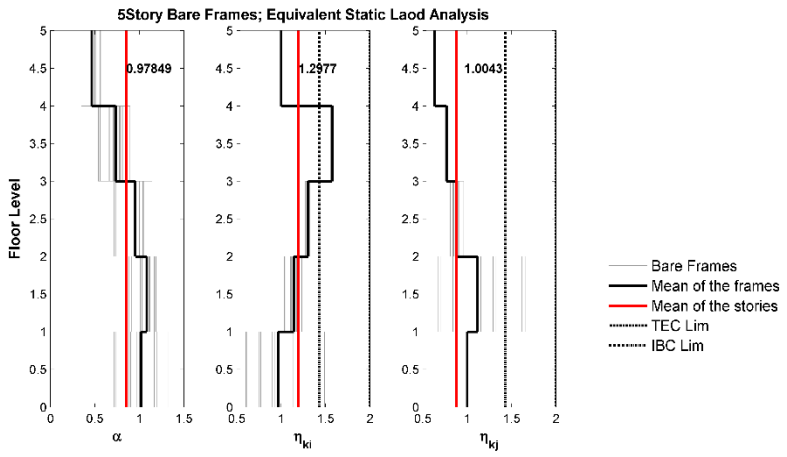

Figure 5-7 5 Story Bare Frames; the α, η_{ki}, η_{kj} results of ESL analysis

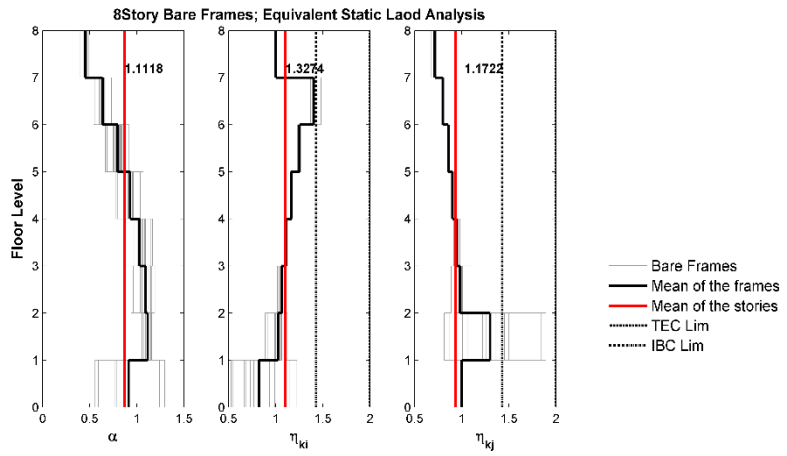

Figure 5-8 8 Story Bare Frames; the α, η_{ki}, η_{kj} results of ESL analysis

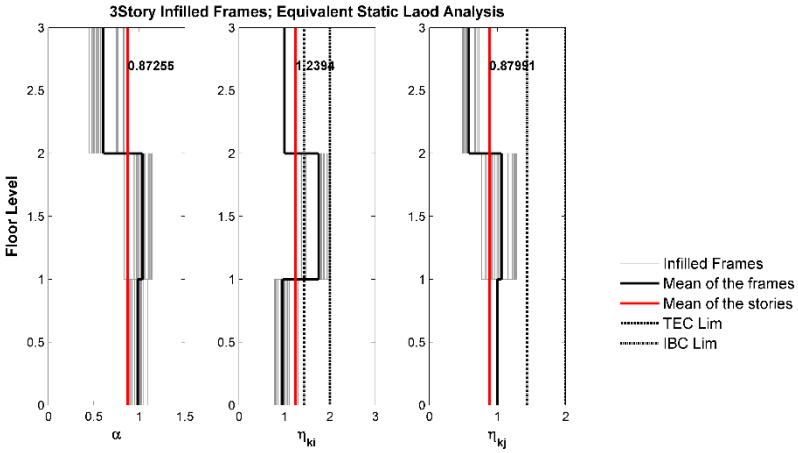

Figure 5-9 3 Story Infilled Frames; the α, η_{ki}, η_{kj} results of ESL analysis

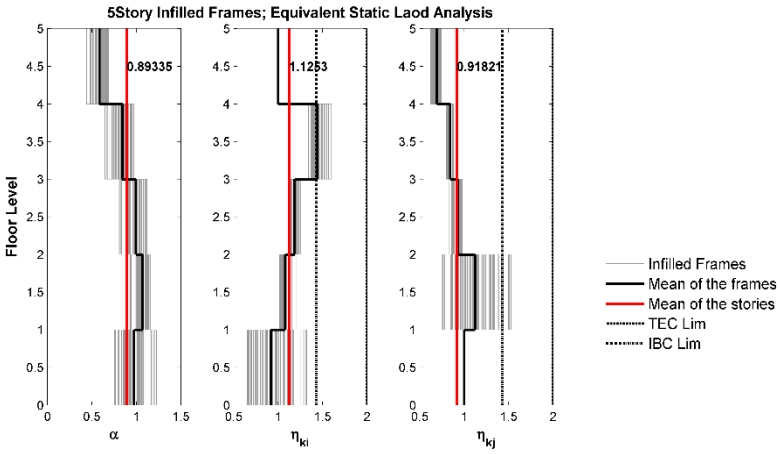

Figure 5-10 5 Story Infilled Frames; the α, η_{ki}, η_{kj} results of ESL analysis

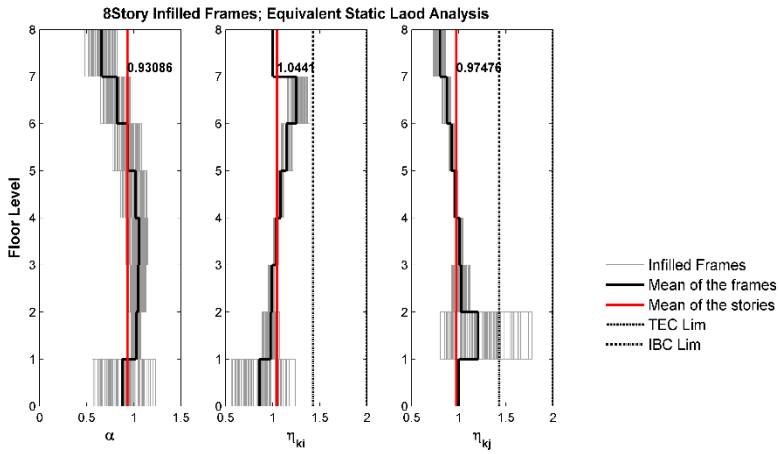

Figure 5-11 8 Story Infilled Frames; the α, η_{ki}, η_{kj} results of ESL analysis

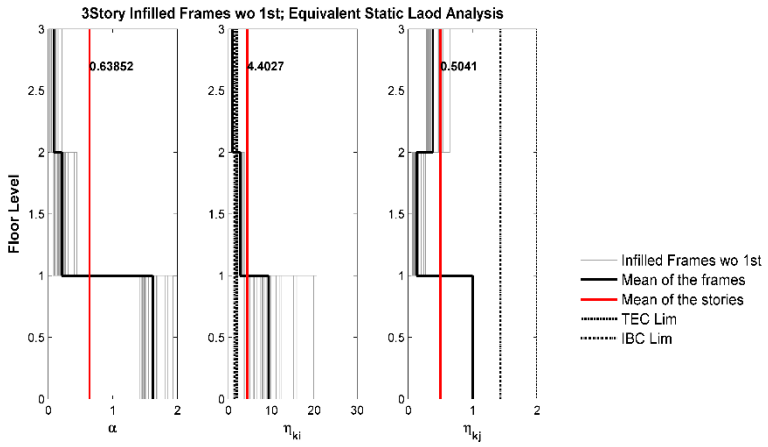

Figure 5-12 3 Story Infilled frames without 1st story infill walls; the α, η_{ki}, η_{kj} results of ESL analysis

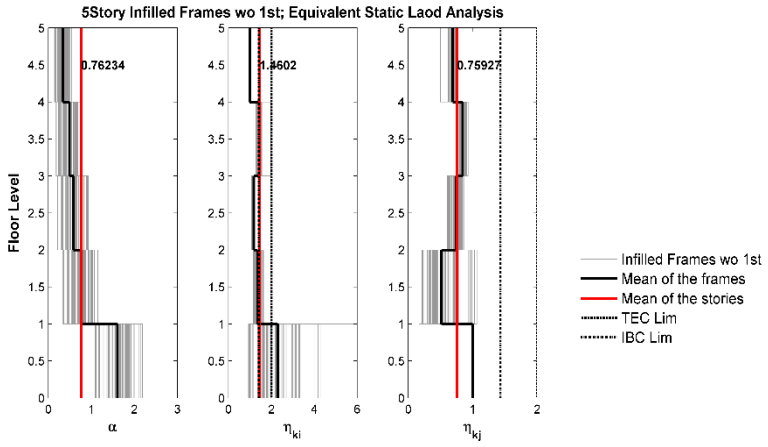

Figure 5-13 5 Story Infilled frames without 1st story infill walls; the α, η_{ki}, η_{kj} results of ESL analysis

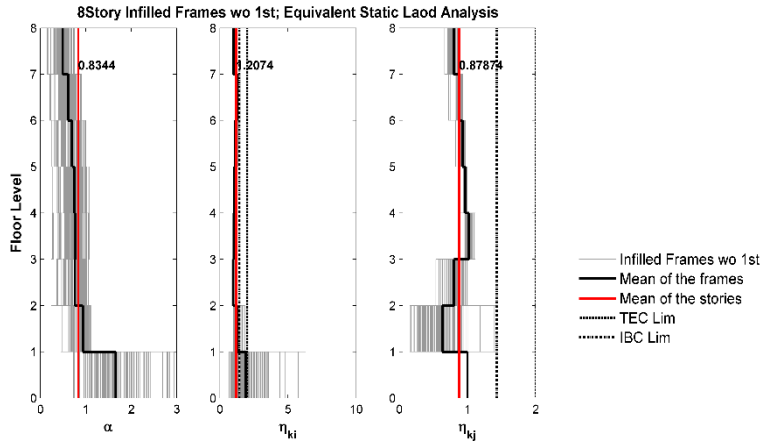

Figure 5-14 8 Story Infilled frames without 1st story infill walls; the α, η_{ki}, η_{kj} results of ESL analysis

In APPENDIX B, each frame type is investigated in detail for all cases. In these detailed figures shown in Figures B-1 to B-21, the equivalent linear analysis results show that for the infilled frame cases, the computed η_{ki} and η_{kj} parameters satisfy the TEC 2007 limits and slightly exceed the IBC 2012 limits in some cases. When the story height is increased, the mean values of α and η_{kj} increase becoming approximately around 1.00. However, evaluation of η_{ki} for 3 Story frames shows that they are much more vulnerable considering the average value exceeding the limits given in TEC2007 and IBC 2012.

Examination of Figures B-1 to B-21 indicate that the cases with a reduction in the first story column dimensions, and the higher first story height than the base case, result in the most critical α, η_{ki}, and η_{kj} values. Despite an increase of 50 percent for the reinforcement areas leading to a decrease in the soft story parameter for these cases, the irregularities are still critical not satisfying the codes in most cases.

ESL analysis results showed that the most critical cases are the ones with infilled frames without first story infill walls where η_{ki} increases drastically.

5.1.3. Mode Superposition Method (MS)

Mode superposition analysis was performed to include higher mode effects in the results of the equivalent static load analysis. The CQC method was preferred to sum up the mode contributions. The number of modes are selected to cover the 90 percent of the first mode mass contribution at the studied direction. TEC 2007 was used for mode superposition analysis and 5 percent damping was assumed for each mode.

In Figure 5-15 to Figure 5-23, the α, η_{ki}, and η_{kj} parameters calculated for 3, 5 and 8 Story frames for mode superposition analysis are presented. The the α, η_{ki}, and η_{kj} parameters of each frame for mode superposition analysis results are given in APPENDIX B, through Figure A2-22 to Figure A2-42. The α, η_{ki}, and η_{kj} values become smaller for the infilled frames. However, the α, η_{ki}, and η_{kj} values for 3 story

frames with full infill walls exceed the TEC 2007 limit, slightly. The most critical cases are the infilled frames without first story infill walls. The α, η_{ki}, and η_{kj} values are higher than the results of the equivalent static analyses ones, slightly (Tables B-4 to B-6).

In Figure 5-15 to Figure 5-17, the α, η_{ki}, and η_{kj} parameters calculated for 3, 5 and 8 story bare frames for mode superposition analysis are presented. All bare cases except two satisfy the η_k limits of 2.00 specified in TEC 2007. 3, 5 and 8 story bare cases with 5.0 m first story height pass the limit of IBC 2012 and TEC 2007. In Figure 5-18 to Figure 5-20, the α, η_{ki}, and η_{kj} results of mode superposition analysis results for infilled frame cases are given for 3, 5 and 8 story frames, respectively. Difference at the first story results becomes larger if the number of stories increases. In Figure 5-21 to Figure 5-23, the α, η_{ki}, and η_{kj} parameters calculated for the 3, 5 and 8 story infilled frames without first story infill walls are presented for mode superposition analysis. The maximum η_k and α values are given in Table 5-13 to Table 5-15.

Table 5-13 3 Story frames: Maximum α, η_{ki}, η_{kj} parameters for MS

3 Story	$\eta_{ki,\,max}$	$\eta_{kj,\,max}$	α_{max}
Bare	2.505	1.828	1.288
Infilled	2.131	1.217	1.131
Infilled wo 1st	26.899	1.000	1.952

Table 5-14 5 Story frames: Maximum α, η_{ki}, η_{kj} parameters for MS

5 Story	$\eta_{ki,\,max}$	$\eta_{kj,\,max}$	α_{max}
Bare	1.535	1.673	1.329
Infilled	1.610	1.600	1.243
Infilled wo 1st	6.042	1.175	2.258

Table 5-15 8 Story frames: Maximum α, η_{ki}, η_{kj} parameters for MS

8 Story	$\eta_{ki,\,max}$	$\eta_{kj,\,max}$	α_{max}
Bare	1.399	1.886	1.296
Infilled	1.542	1.816	1.264
Infilled wo 1st	6.689	1.440	3.091

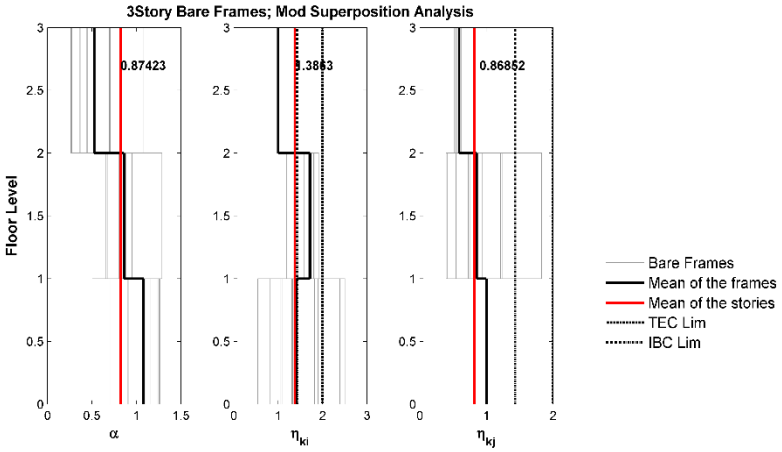

Figure 5-15 3 Story Bare Frames; the α, η_{ki}, η_{kj} results of MS analysis

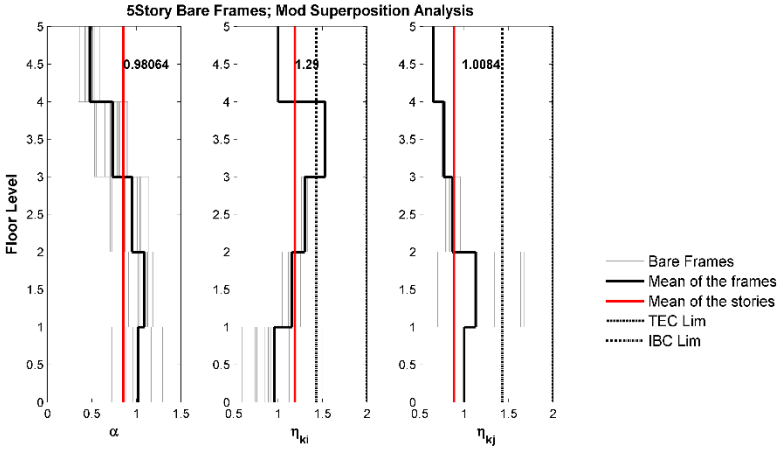

Figure 5-16 5 Story Bare Frames; the α, η_{ki}, η_{kj} results of MS analysis

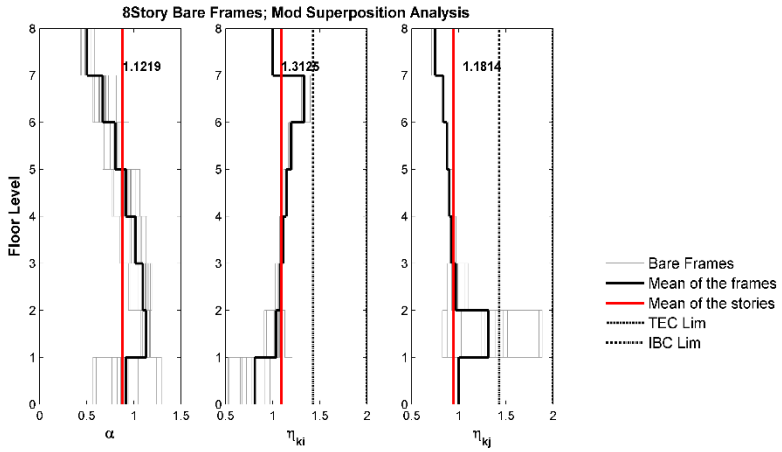

Figure 5-17 8 Story Bare Frames; the α, η_{ki}, η_{kj} results of MS analysis

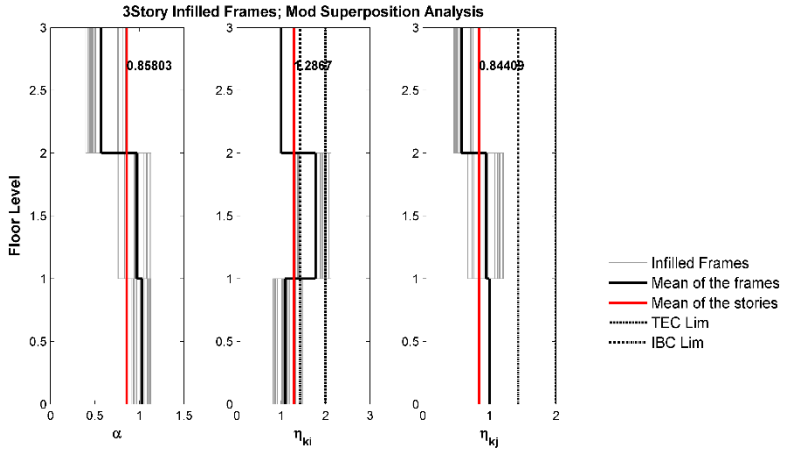

Figure 5-18 3 Story Infilled Frames; the α, η_{ki}, η_{kj} results of MS analysis

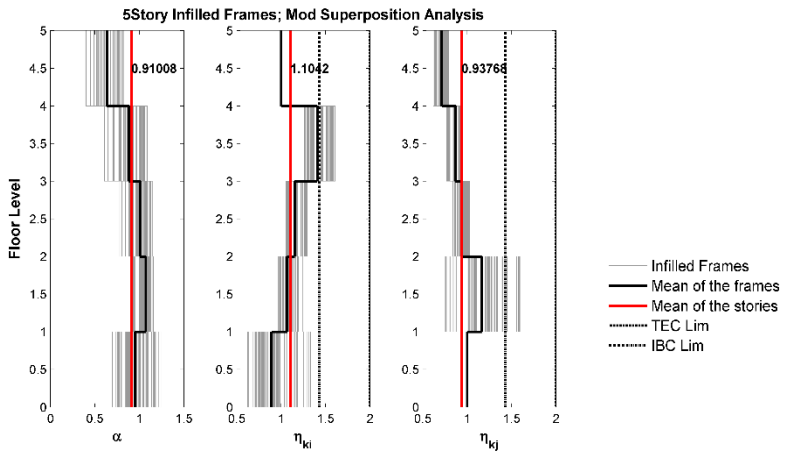

Figure 5-19 5 Story Infilled Frames; the α, η_{ki}, η_{kj} results of MS analysis

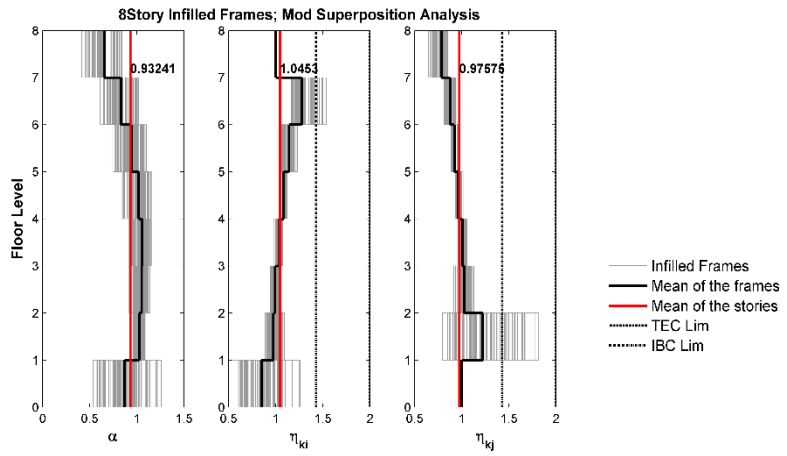

Figure 5-20 8 Story Infilled Frames; the α, η_{ki}, η_{kj} results of MS analysis

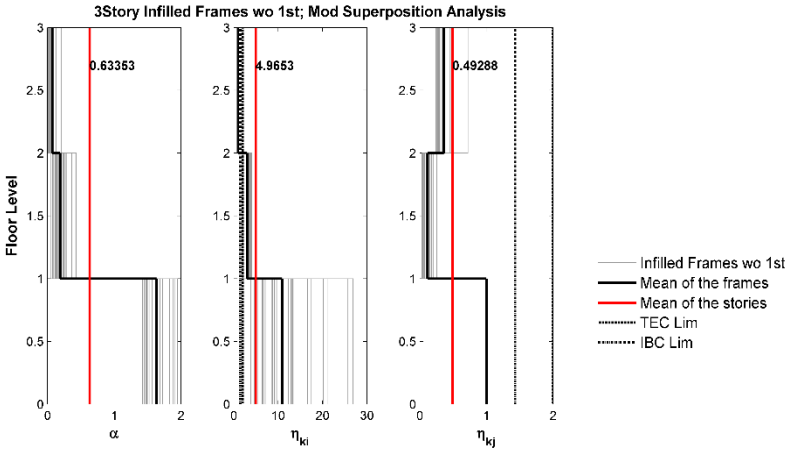

Figure 5-21 3 Story Infilled frames without 1st story infill walls; the α, η_{ki}, η_{kj} results of MS analysis

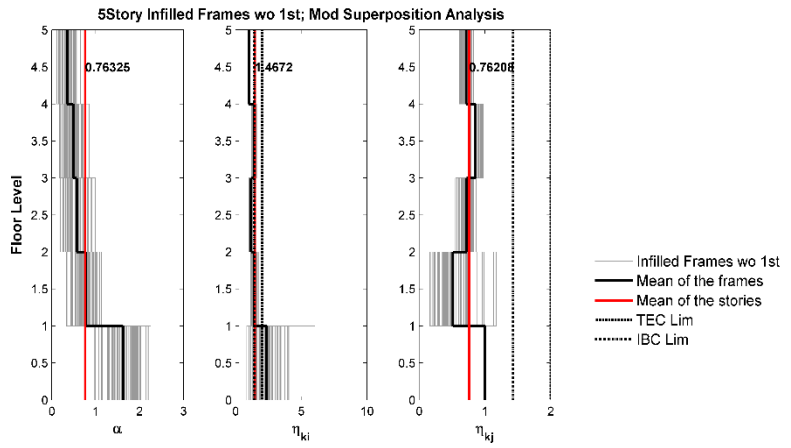

Figure 5-22 5 Story Infilled frames without 1st story infill walls; the α, η_{ki}, η_{kj} results of MS analysis

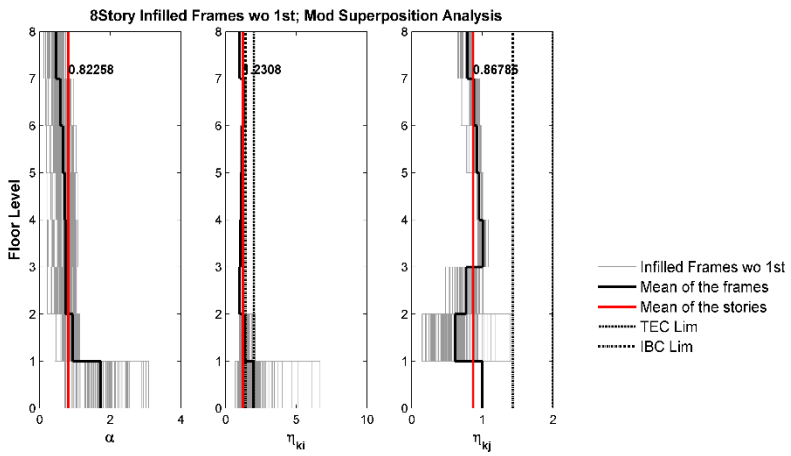

Figure 5-23 8 Story Infilled frames without 1st story infill walls; the α, η_{ki}, η_{kj} results of MS analysis

Examination of Figures B-22 to B-42 indicate that, the cases with a reduction in the first story column dimension, and the higher first story height result in, the most critical α, η_{ki}, and η_{kj} value. Despite an increase of 50 percent for the reinforcement areas leading to a decrease in the soft story parameter for these cases, the irregularities are still critical not satisfying the codes in most.

Mode superposition analysis results showed that the α values and η_{kj} values slightly different than the equivalent static load analysis results and η_{ki}, gives a little bit higher values in mode superposition analysis, especially for 3 story frames for some cases infilled frames without first story infill walls.

5.2. Nonlinear Procedures

Linear analysis results can be used to calculate the α, η_{ki}, and η_{kj} parameters to check the existence of the soft story mechanism according to some specified values in the codes. However, the existence of the soft story mechanisms can only be checked by nonlinear analysis results and hinge mechanisms. Therefore, nonlinear pushover analyses were performed for each frame and soft story mechanism was checked visually to see if the hinges occurred at the bottom and the top side of the columns at ultimate point (Figure 5-24).

The limit values specified in the codes were checked with these visual inspection results. To check the accuracy of the pushover analysis results, nonlinear time history analyses were performed for one critical case.

The visual inspection for soft story mechanism will be discussed in Chapter 6 in detail. In this part, the results of the nonlinear pushover analysis results will be given.

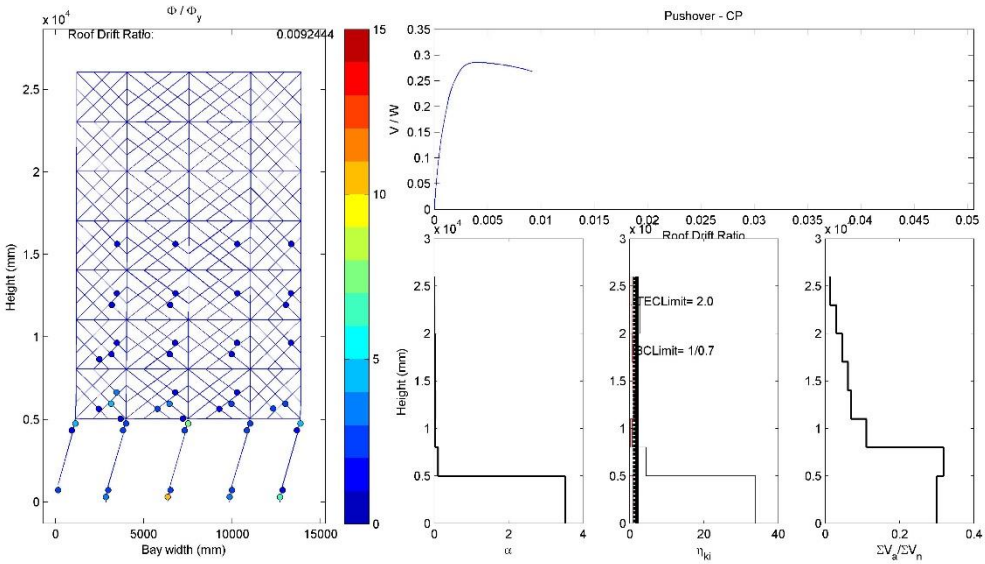

Figure 5-24 Soft story mechanism at ultimate point

5.2.1. Pushover Analyses

Nonlinear pushover analysis was performed to assess the inelastic results for the soft story parameters. The upper triangular, mass normalized, loading pattern was assigned to the nodes at each floor levels. The target displacement for the pushover analysis was calculated according to ASCE 41-13. The ultimate point is calculated based on some assumptions;

- *Global failure criterion:* 20 percent decrease in the base shear capacity is assumed as the ultimate point.
- *Ultimate curvature failure criterion:* The section analysis was performed for each column and beam cross section with corresponding axial loads. The axial loads are calculated from G+nQ, where n, live load multiplier, is 0.3 for residential buildings. The infill loads were also calculated in the relevant frame types. The ultimate curvature was taken as 10 times of the yield curvature which is assumed to correspond to ultimate point (Zhou et. al. (2014), Priestley et. al. (1996), Kheyroddin and Naderpour (2007), Priestley (2000), Grammatikou et. al. (2016)). The moment capacities of the frame

members were calculated using the elastic-perfectly-plastic steel material model.

- *Shear failure criterion:* Shear failure was checked for each frame member. Shear capacity of each frame member was calculated according to TS500. If the shear forces passes the shear capacity, the point is assumed as the ultimate point.

The ultimate point is governed by the first failure of the mentioned failure criterions above. A Matlab script was written for post process to consider the assumptions that were made above (Figure 5-34). The Script reads analysis results and the cross section details for each member ends and run section analysis via OpenSees execuTable A1nd then calculates the yield curvatures, the ultimate curvatures, the moment capacities and the shear capacities to check for the ultimate point. Based on these calculations, the ultimate point was searched in the global and local member responses. The first failure criterion that is reached is assumed as the ultimate point.

The target displacement point in the pushover curve is used to assess the accuracy of the linear analysis methods and the ultimate point is used to observe the occurrence of the soft story mechanism and to assess the performance of the frames regarding the soft story parameters.

5.2.1.1. Pushover analysis results at target displacement (TD)

The pushover analysis results are comparable with the equivalent static load analysis results, if the target displacement is calculated for the same spectrum. Therefore, the target displacement for each frame was calculated by ASCE 41-13 displacement coefficient method.

The details of each frame at the target displacement for the α, η_{ki}, and η_{kj} parameters are given in APPENDIX B, from Figures B-64 to B-84. Examination of Figures B-64 to B-84, indicate that, the most critical α, η_{ki}, and η_{kj} calculations occur at the infilled

frames without first story infill walls. The α, η_{ki}, the η_{kj} values are higher than the results of the equivalent static analysis which are given in Tables B-10 to B-12 of APPENDIX B. These results show that linear analysis procedures are not good at estimating the failure pattern, in other words, underestimate the soft story irregularity.

In Figure 5-25 to Figure 5-27, the α, η_{ki}, and η_{kj} parameters calculated bare frames; in Figure 5-28 to Figure 5-30, these parameters calculated for infilled frames and in Figure 5-31 to Figure 5-33, these parameters calculated for infilled frames without first story infill walls at the target displacement are presented for 3, 5 and 8 story frames. The maximum η_{ki}, η_{kj}, α and additionally α_{irreg} and α_2 values are given in Table 5-16 through Table 5-18 for 3, 5 and 8 story bare frames, respectively. The α_{irreg} parameter is less than one for the infilled frames due to selecting the base case as bare frame and infilled frames without first story infill walls approach to one or more which shows the high irregularity. The maximum η_k results show that even the bare frames exceed the code limits. The α_2 parameter values are almost same for 3 and 5 story relevant frame types at TD.

Table 5-16 3 Story frames: Maximum α, η_{ki}, η_{kj}, α_{irreg}, and α_2 parameters for TD

3 Story	$\eta_{k,\,max,Target}$	$\alpha_{max,Target}$	$\alpha_{irreg,Target}$	$\alpha_{2,Target}$
Bare	3.295	1.317	1.827	1.451
Infilled	5.849	1.479	0.245	1.674
Infilled wo 1st	86.685	2.065	1.597	1.833

Table 5-17 5 Story frames: Maximum α, η_{ki}, η_{kj}, α_{irreg}, and α_2 parameters for TD

5 Story	$\eta_{k,\,max,Target}$	$\alpha_{max,Target}$	$\alpha_{irreg,Target}$	$\alpha_{2,Target}$
Bare	2.007	1.478	1.550	1.666
Infilled	3.530	1.402	0.737	1.529
Infilled wo 1st	25.820	3.158	1.096	1.841

Table 5-18 8 Story frames: Maximum α, η_{ki}, η_{kj}, α_{irreg}, and α_2 parameters for TD

8 Story	$\eta_{k,\,max,Target}$	$\alpha_{max,Target}$	$\alpha_{irreg,Target}$	$\alpha_{2,Target}$
Bare	1.973	1.248	1.210	1.226
Infilled	3.093	1.650	0.510	0.921
Infilled wo 1st	24.020	4.658	0.974	2.140

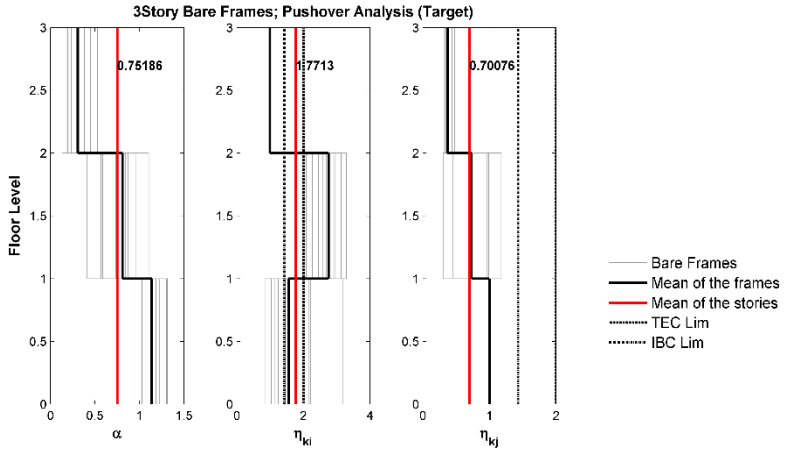

Figure 5-25 3 Story Bare Frames; the α, η_{ki}, η_{kj} results at TD

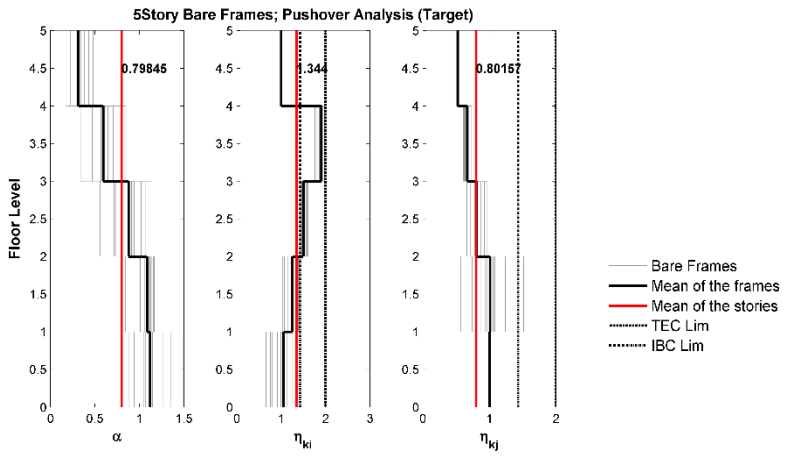

Figure 5-26 5 Story Bare Frames; the α, η_{ki}, η_{kj} results at TD

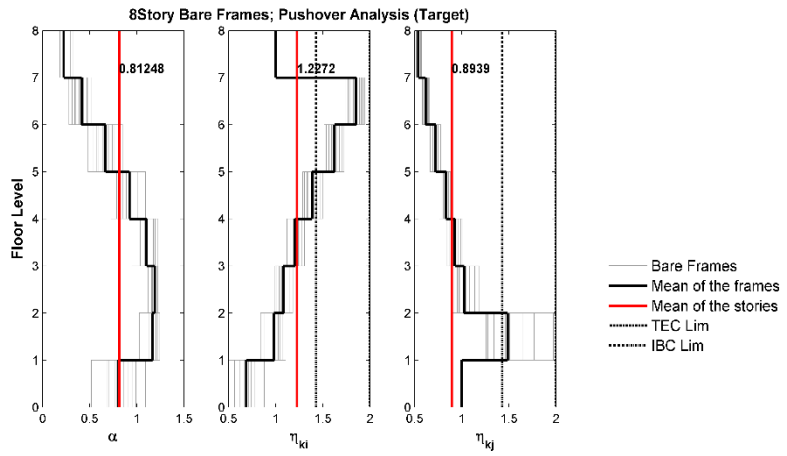

Figure 5-27 8 Story Bare Frames; the α, η_{ki}, η_{kj} results at TD

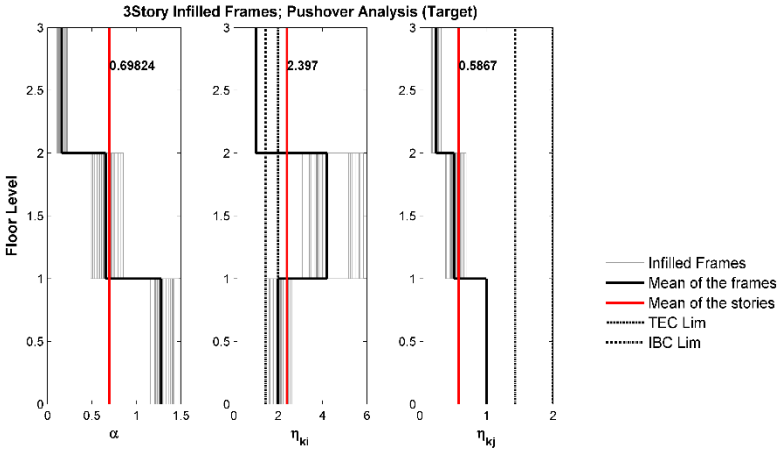

Figure 5-28 3 Story Infilled Frames; the α, η_{ki}, η_{kj} results at TD

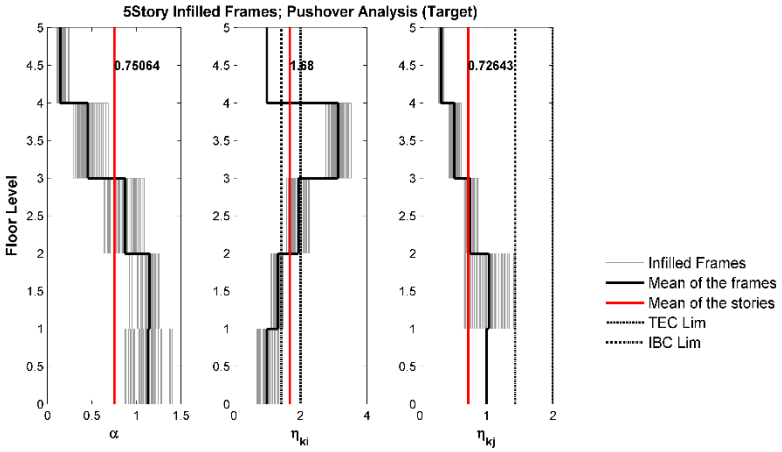

Figure 5-29 5 Story Infilled Frames; the α, η_{ki}, η_{kj} results at TD

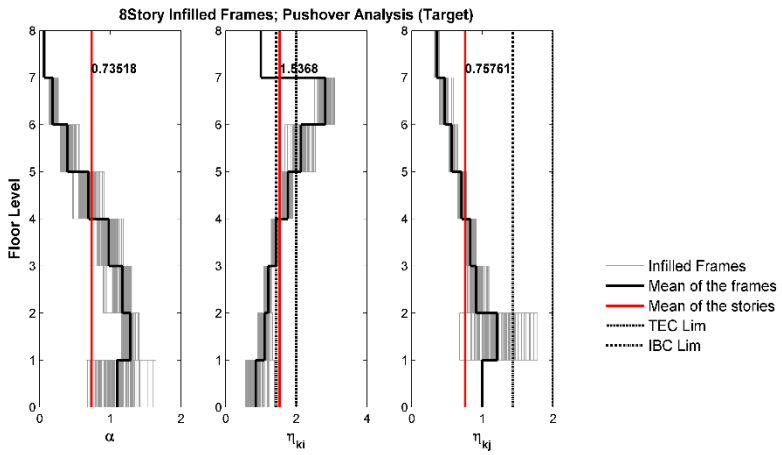

Figure 5-30 8 Story Infilled Frames; the α, η_{ki}, η_{kj} results at TD

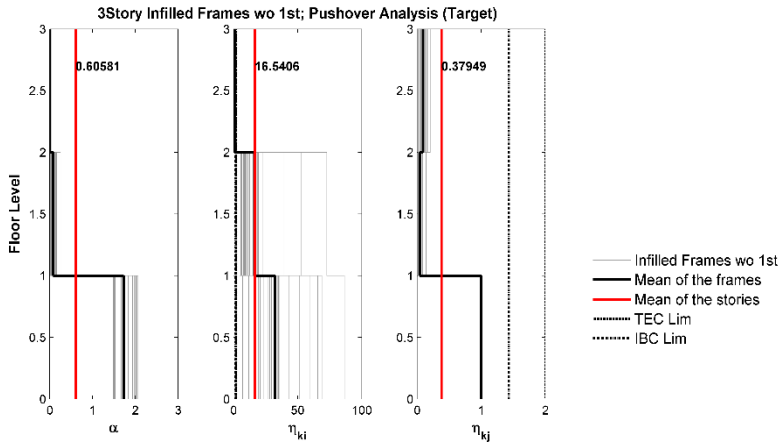

Figure 5-31 3 Story Infilled frames without 1st story infill walls; the α, η_{ki}, η_{kj} results at TD

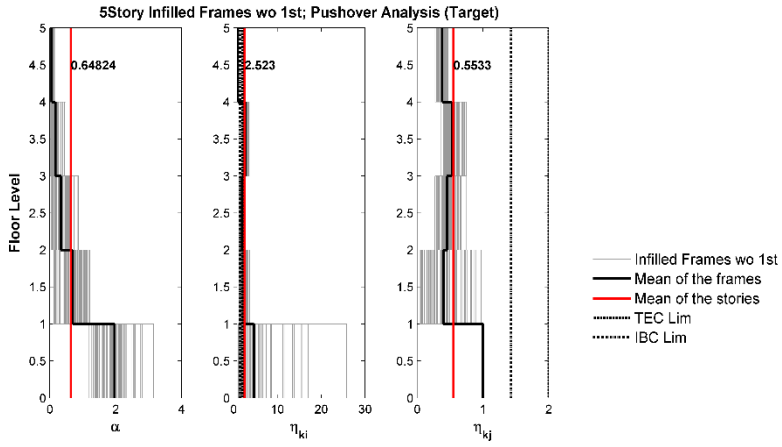

Figure 5-32 5 Story Infilled frames without 1st story infill walls; the α, η_{ki}, η_{kj} results at TD

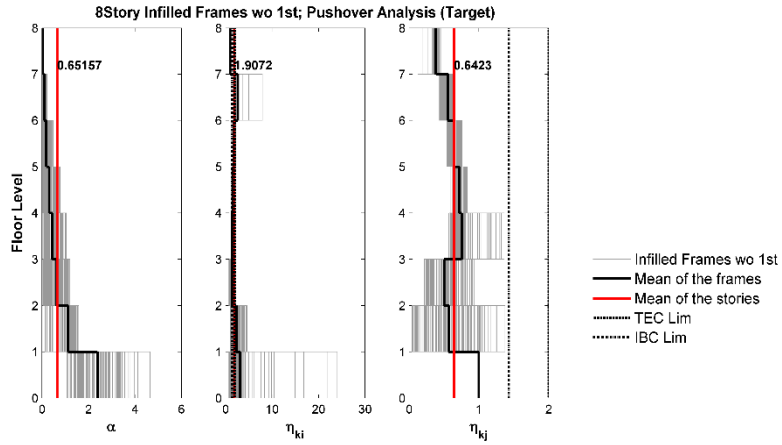

Figure 5-33 8 Story Infilled frames without 1st story infill walls; the α, η_{ki}, η_{kj} results at TD

In Table A2-10 to B-12, the maximum values of α, η_{ki}, η_{kj} parameters at TD are given. The highest α, η_{ki}, η_{kj} parameters occur at the infilled frames without first story infill walls and with the highest first story height. Examination of the results at target displacement shows that the 3 story frames are much more vulnerable than the 5 and 8 story frames. Even the mean of the stories exceed the limit of 2.0, η_k, specified in TEC 2007 for soft story failure. The irregularity values, $\eta_{k,}$ in the frames are extreme if the frames have infills without the first story infill walls. The α parameter seems to change in a narrower range than $\eta_{k.}$

5.2.1.2. Pushover analysis results at ultimate point (UltP)

As mentioned at the beginning of this chapter, the pushover analysis results are evaluated in two parts in this study. The first one is the target displacement values which were calculated according to ASCE 41-13 to compare the linear procedure results and the second one is the ultimate point which is decided based on some assumptions as mentioned before.

In APPENDIX B, the results for the α, η_{ki}, and η_{kj} are given from Figure A2-43 to Figure A2-63 for the pushover analysis results at ultimate point. All these figures show that the most critical cases are the infilled frames without first story infill walls. The α, η_{ki}, and η_{kj} values are higher than the results of the equivalent static analysis (Tables B-7 to B-9 in APPENDIX B) as expected.

In Figure 5-36 to Figure 5-38, the α, η_{ki}, and η_{kj} parameters calculated for bare frames; in Figure 5-39 to Figure 5-41, these parameters calculated for infilled frames and in Figure 5-42 to Figure 5-44, these parameters calculated for infilled frames without first story infill walls for pushover analysis results at the ultimate point are presented for 3, 5 and 8 story, respectively. The maximum η_{ki}, η_{kj}, α and additionally α_{irreg} and α_2 values are given in Table 5-19 through Table 5-21 for 3, 5, and 8 story frames,

respectively. The η_{ki} and η_{kj} calculated at ultimate point for 3 and 5 story bare frames pass the limit of 2.0 specified in TEC2007.

Table 5-19 3 Story frames: Maximum α, η_{ki}, η_{kj}, α_{irreg}, and α_2 parameters for UltP

3 Story	$\eta_{k,\,max,UltP}$	$\alpha_{max,UltP}$	$\alpha_{irregular,UltP}$	$\alpha_{2,UltP}$
Bare	3.886	1.349	1.393	4.985
Infilled	24.168	1.727	0.646	20.684
Infilled wo 1st	136.660	2.080	0.831	5.146

Table 5-20 5 Story frames: Maximum α, η_{ki}, η_{kj}, α_{irreg}, and α_2 parameters for UltP

5 Story	$\eta_{k,\,max,UltP}$	$\alpha_{max,UltP}$	$\alpha_{irregular,UltP}$	$\alpha_{2,UltP}$
Bare	1.989	1.481	1.996	11.551
Infilled	8.318	1.837	1.671	12.132
Infilled wo 1st	47.532	3.307	1.140	10.466

Table 5-21 8 Story frames: Maximum α, η_{ki}, η_{kj}, α_{irreg}, and α_2 parameters for UltP

8 Story	$\eta_{k,\,max,UltP}$	$\alpha_{max,UltP}$	$\alpha_{irregular,UltP}$	$\alpha_{2,UltP}$
Bare	1.696	1.183	1.558	7.387
Infilled	5.822	1.581	0.589	5.328
Infilled wo 1st	52.339	5.125	0.680	8.472

In some cases, η_{ki} values may result in large values due to the soft story failure mechanism and sudden changes in the drift ratios. For example, in Figure 5-34, η_{ki} value pass -1310 (Table A2-7) for the case of 3 story fully infilled frame without first story infill walls with 50 percent increased reinforcement area at first story columns and 5.0 m of first story height. The upper story have a small drift ratio, such as -3e-7, which is actually zero. Thus, η_{ki} becomes larger. If we look at the roof drift ratio at the 2.7 percent, in Figure 5-35, the results are more stable to study the weak and soft story failure mechanism than the ultimate point.

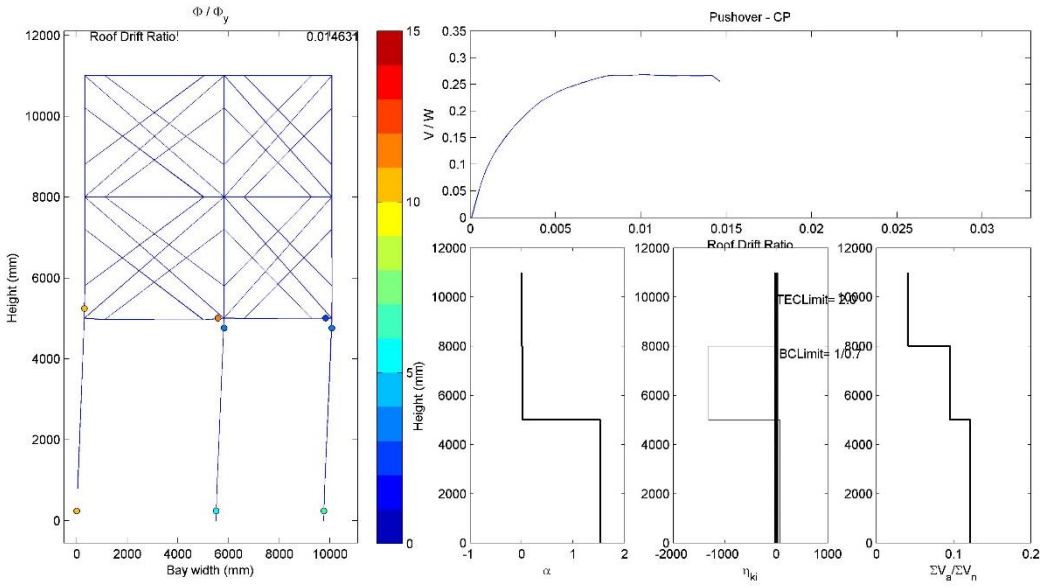

Figure 5-34 Frame: 3_I_12_wo_1_H5.0_CDM1.0_RM1.5, Pushover analysis post processing results at ultimate point

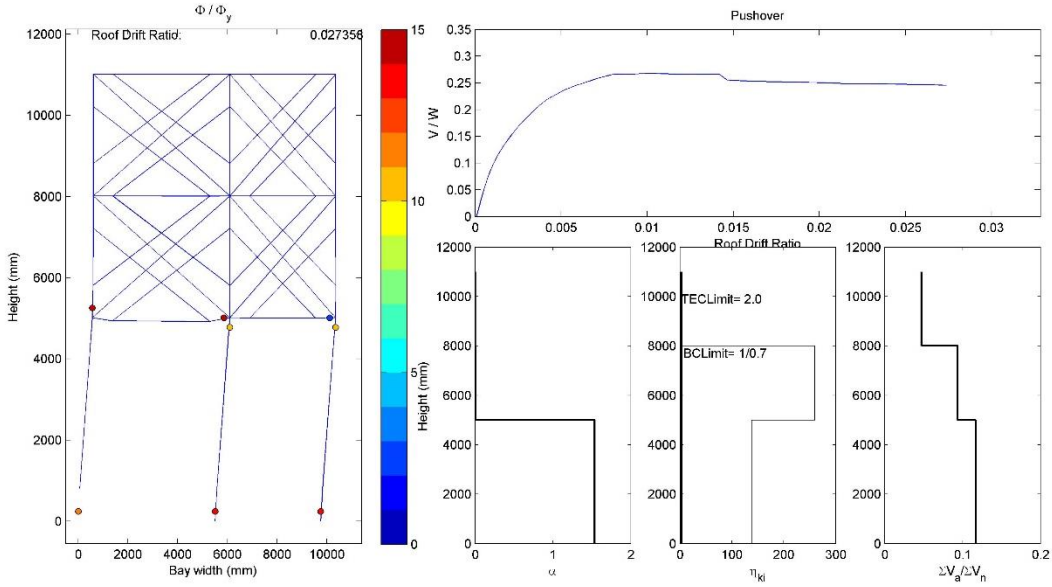

Figure 5-35 Frame: 3_I_12_wo_1_H5.0_CDM1.0_RM1.5, Pushover analysis at 2.7 percent story drift.

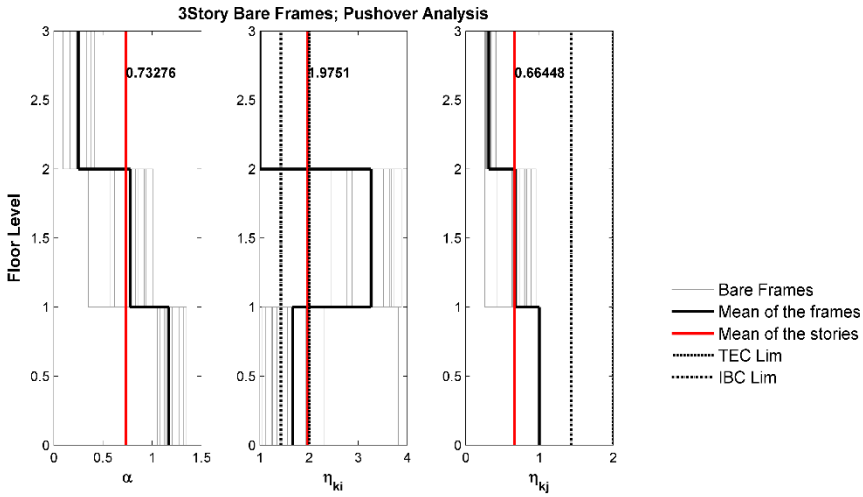

Figure 5-36 3 Story Bare Frames; the α, η_{ki}, η_{kj} results at UltP

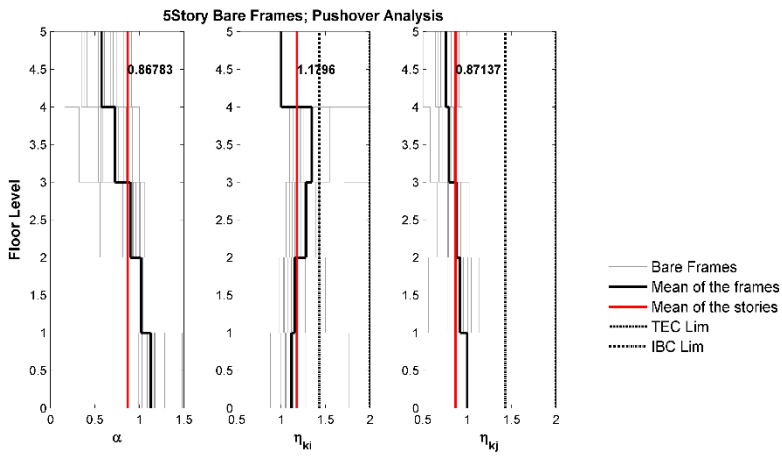

Figure 5-37 5 Story Bare Frames; the α, η_{ki}, η_{kj} results at UltP

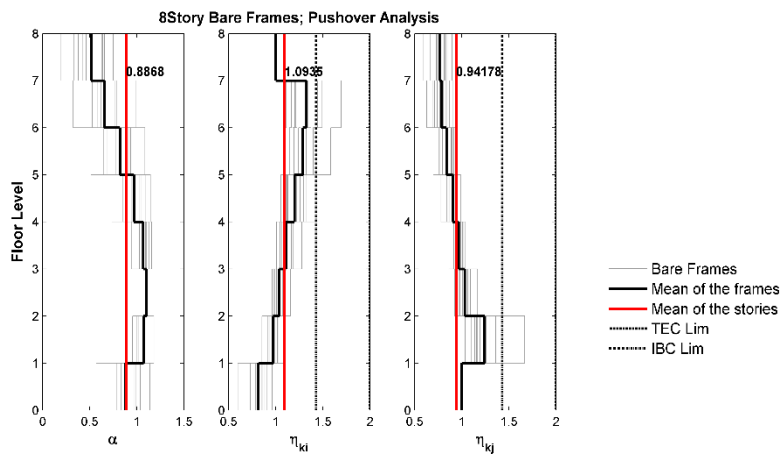

Figure 5-38 8 Story Bare Frames; the α, η_{ki}, η_{kj} results at UltP

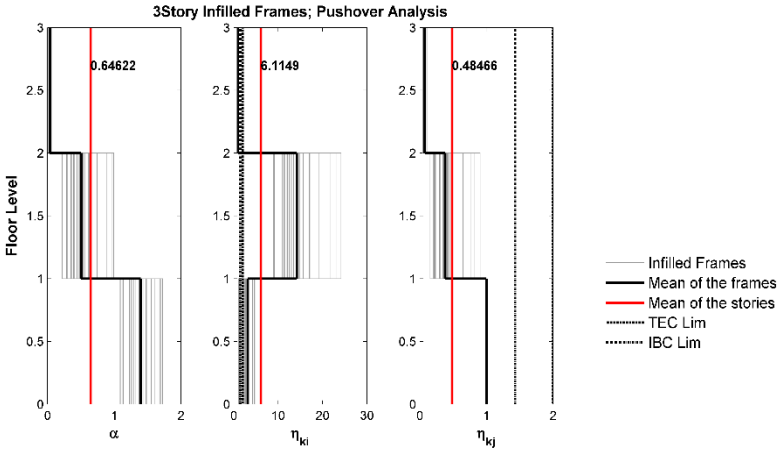

Figure 5-39 3 Story Infilled Frames; the α, η_{ki}, η_{kj} results at UltP

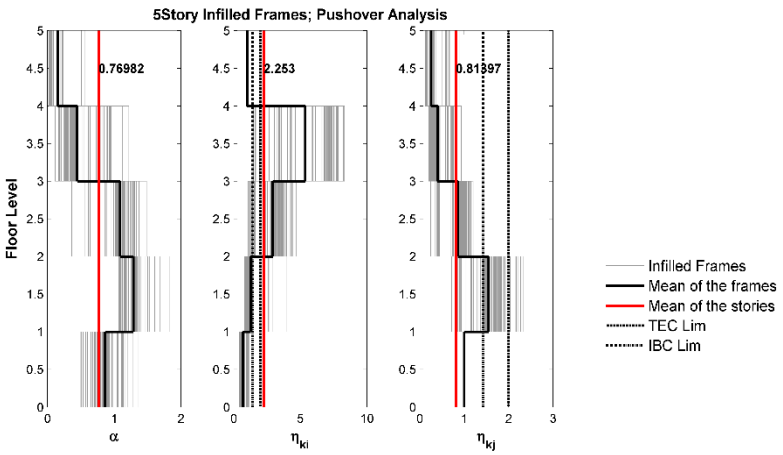

Figure 5-40 5 Story Infilled Frames; the α, η_{ki}, η_{kj} results at UltP

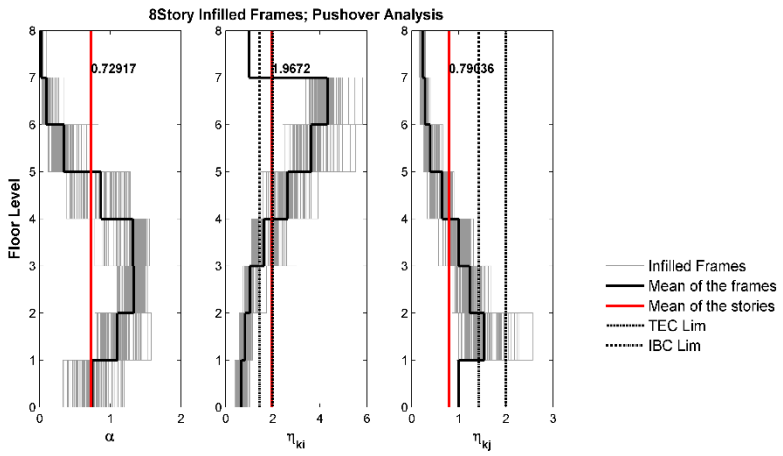

Figure 5-41 8 Story Infilled Frames; the α, η_{ki}, η_{kj} results at UltP

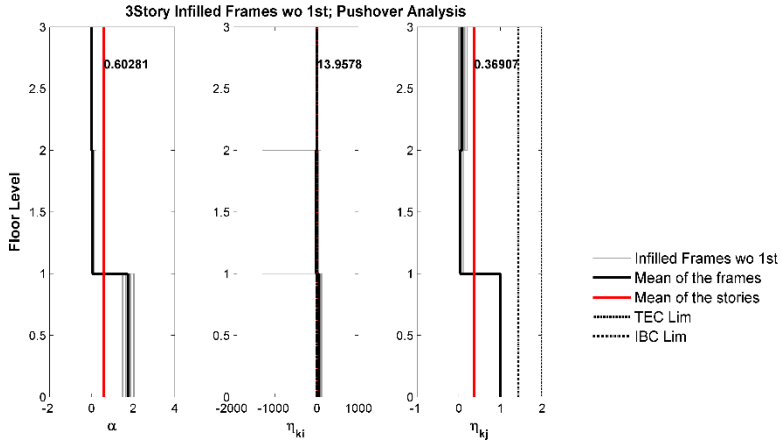

Figure 5-42 3 Story Infilled frames without 1st story infill walls; the α, η_{ki}, η_{kj} results at UltP

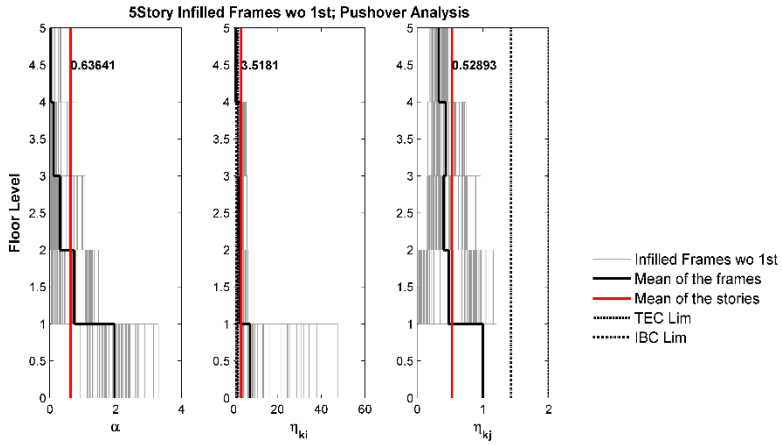

Figure 5-43 5 Story Infilled frames without 1st story infill walls; the α, η_{ki}, η_{kj} results at UltP

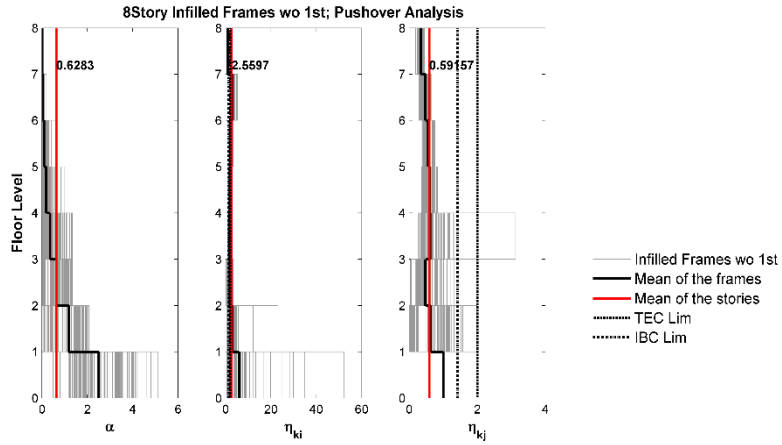

Figure 5-44 8 Story Infilled frames without 1st story infill walls; the α, η_{ki}, η_{kj} results at UltP

5.2.2. Time History Analyses

The dynamic behavior of the frames are tried to be estimated via equivalent static load analysis and pushover analysis. However, the dynamic behavior of the structures under seismic excitations may result in different results. Therefore, time history analyses were performed for one of the critical cases to compare the results of the pushover and equivalent static load analysis results for nonlinear and linear response. This frame is 8 Story fully infilled frame without first story infill walls, with 5.0 m of the first story height. The base case, 8 story bare frame with 3.0 m of the first story height was also analyzed under the linear and nonlinear time history analysis.

The ground motion selection was performed by using the Matlab script provided by Jayaram et. al. (2011). The algorithm generates multiple response spectra from a target distribution then recorded ground motions are selected matching the response spectra with the simulated one. They used a greedy optimization technique to match the target and the sample means and variance.

The spectrum was defined according to TEC2007. The same soil conditions with design case were used to calculate the spectrum. Soil class was chosen as Z1 (Ta=0.10 s and Tb= 0.30 s) and seismic zone 1 was assumed. R was taken as 1.0. Jayaram et. al. (2011) used NGA database for the selection. Selected ground motions are given in Table 5-22. Unscaled ground motions were used. In Table 5-23, the details of the selected ground motions are given. In Figure 5-45a, the spectrum of each ground motion and their median are given and In Figure 5-45b, the mean spectra of the selected ground motions are compared with the TEC 2007 spectrum.

In Figure 5-46, the α, η_{ki}, η_{kj} comparison for linear time history analysis and equivalent static load anlaysis are given. In Figure 5-47, the α, η_{ki}, η_{kj} results are compared for nonlinear time history analysis and pushover analysis . Pushover analysis results were evaluated at TD value which is calculated according to ASCE 41-13. Both linear and nonlinear analysis results are close to time history analysis results. The α

parameter has a good match with time history analysis results. The α_2 parameter,which is inelastic response to elastic response ratio that is suggested by Seneviratna and Krawinkler (1997), has the value of 1.49 for time history analysis result and 1.14 for the pushover analysis results. α_{irreg}, the ratio of the inelastic roof displacement of irregular cases to inelastic roof displacement of the base case that is suggested by Al-Ali and Krawinkler (1998) to determine the irregularity, is much more closer than α_2 parameter to time history analysis results. α_{irreg} parameter is 0.44 for time history analysis results and 0.42 for pushover analysis results.

Table 5-22 Selected ground motions

Record Number	NGA Record Sequence Number	Scale Factor	EQ Name
1	183	1	Imperial Valley
2	184	1	Imperial Valley
3	1511	1	Chi-Chi_ Taiwan
4	169	1	Imperial Valley
5	179	1	Imperial Valley
6	802	1	Loma Prieta
7	292	1	Irpinia_ Italy-01

Table 5-23 Selected ground motions' details

RSN	Magnitude	Mechanism	PGA (g)	Rjb (km)	Rrup (km)	Vs30 (m/sec)
183	6.53	strike slip	0.61	3.86	3.86	206.08
184	6.53	strike slip	0.48	5.09	5.09	202.26
1511	7.62	Reverse Oblique	0.43	2.74	2.74	614.98
169	6.53	strike slip	0.35	22.03	22.03	242.05
179	6.53	strike slip	0.48	4.9	7.05	208.91
802	6.93	Reverse Oblique	0.51	7.58	8.5	380.89
292	6.9	Normal	0.32	6.78	10.84	382

a) b)

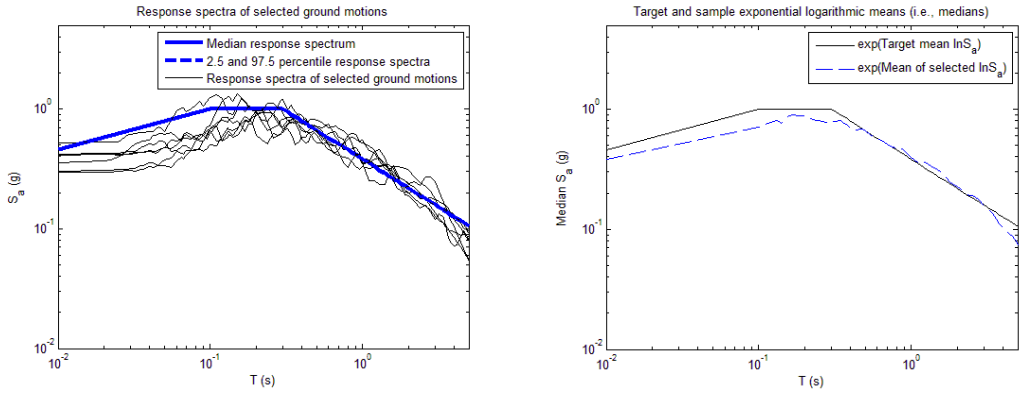

Figure 5-45 Ground Motion Selection

The α parameter is more stable for the comparison of the nonlinear analysis results with the linear analysis results. The increase in α for nonlinear analysis results is arround 20-30 percent . However, the increases in the η_{ki} and η_{kj} are almost 3 times.

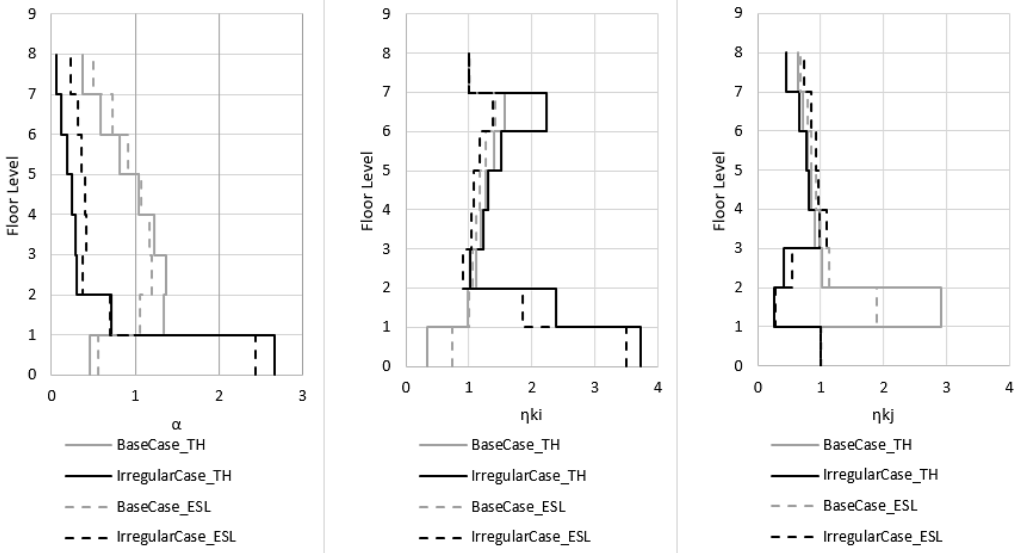

Figure 5-46 Linear TH analysis results

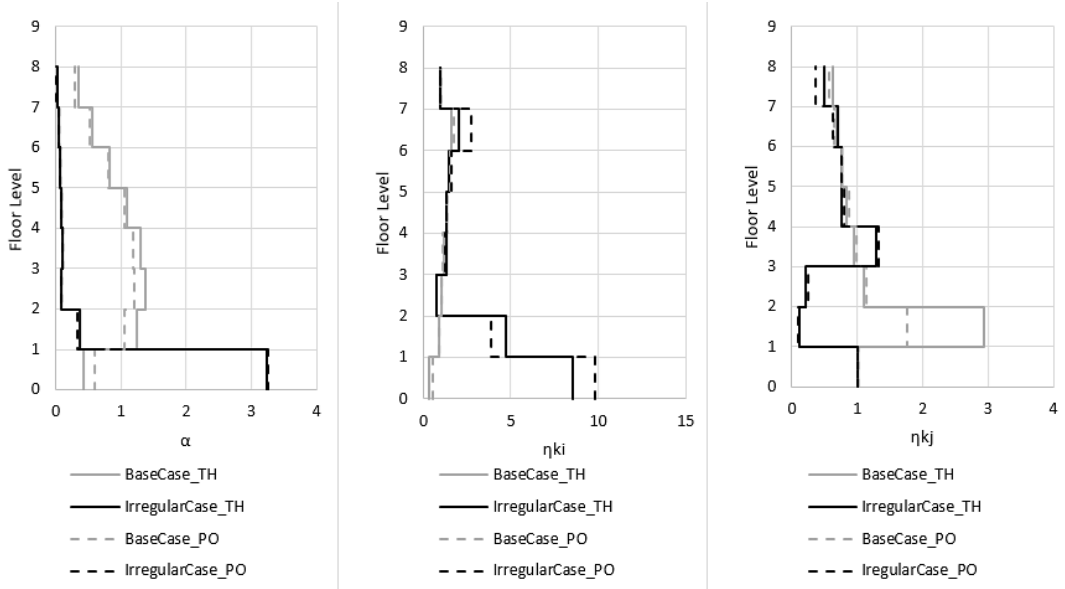

Figure 5-47 Nonlinear TH analysis results

CHAPTER 6

DISCUSSION AND INTERPRETATION OF RESULTS

In this part, the results from the linear and nonlinear analysis are discussed to evaluate the soft story irregularity based on the parameters employed. The, $\boldsymbol{\alpha_2}$ and $\boldsymbol{\alpha_{irreg}}$ parameters were investigated for the vertical irregularity identification and ductility demand under the nonlinear procedures.

6.1. The Linear Analyses Procedure Results

The comparison of the α, η_{ki}, and η_{kj} ratios of mode superposition analysis with equivalent static load analysis results show similar values for all 3, 5 and 8 story frames. 5 Story building results are given as an example. In Figure 6-1 to Figure 6-3, the α, η_{ki}, and η_{kj} parameters calculated for 5 story frames of mode superposition analysis results were compared with equivalent static analysis ones as an example. The mean of the stories of the values of α, η_{ki}, and η_{kj} parameters are almost 1.0 for all the cases.

The 3 story and 8 story frames have similar α, η_{ki}, and η_{kj} ratios. The Infilled frames and infilled frames without first story infill walls have slightly different α, η_{ki}, and η_{kj} ratio values at upper stories. The α parameter only has two large ratio such as, 2.0 and 0.6 for mode superposition analysis to equivalent static load analysis results . The reason for the large values at the upper stories is due to the normalization made at the effective modal height. The difference between all irregularity parameters for infilled frames and infilled frames without first story infill walls (Figure 6-2 and Figure 6-3) are small. The α parameter have higher differences at upper stories than the lower ones due to being normalized with the drift ratio at the effective story height.

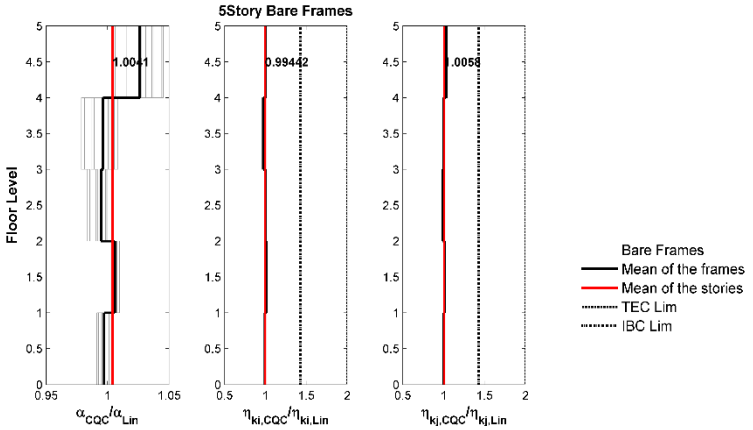

Figure 6-1 5 Story Bare Frames: MS to ESL analysis results for α, η_{ki}, η_{kj}

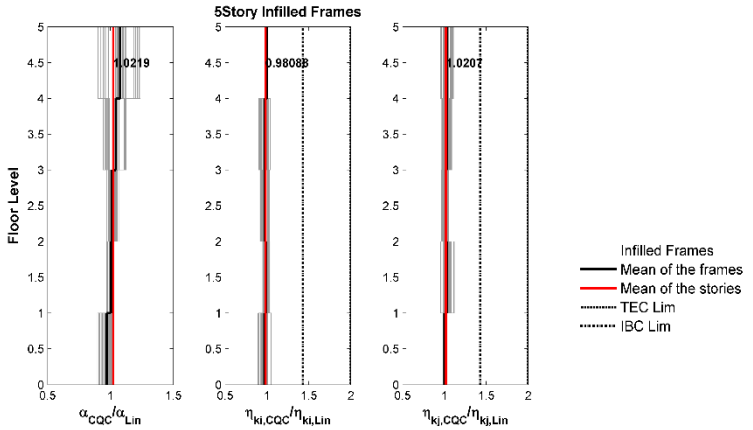

Figure 6-2 5 Story Infilled frames: MS to ESL analysis results for α, η_{ki}, η_{kj}

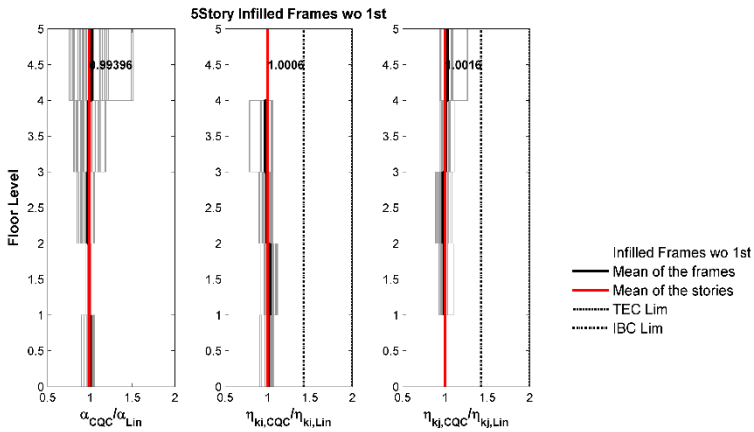

Figure 6-3 5 Story Infilled frames without 1st story infill walls: MS to ESL analysis results for α, η_{ki}, η_{kj}

The comparison of the linear analysis results show that the difference is low and the mean of the stories is close to 1.00 for η_{ki}, parameters. The maximum differences for α parameter occur at the 3 story bare frames of two cases and at the rest, the maximum difference occuring in α parameter is around 20 percent.

6.2. The Nonlinear Procedure Results versus the Linear Procedure Results

In this part, the vertical irregularity parameters are compared at target and ultimate points for the interpretation of soft story parameters. The purpose of these comparisons is that to assess the accuracy of the calculated vertical irregularity parameters for linear procedures and to examine the relationship between the ultimate points and linear procedure results.

6.2.1. The Comparisons at TD with ESL analysis results

The use of ESL method, in other name, equivalent lateral force method is questionable by many researchers, codes and specifications. There are limitations in codes for the use of ESL, however, in most of them another linear procedure, the mode superposition (MS) analysis is suggested. The comparison of the results show that the difference between the MS and the ESL methods is not huge and the values calculated for the soft story irregularity parameters are similar.

In Figure 6-4 to Figure 6-12, the α, η_{ki}, η_{kj} parameters, calculated for 3, 5, and 8 story frames, were compared with pushover analysis results at TD to ESL analysis results for bare frames, infilled frames and infilled frames without the infill walls are given. In Table 6-1, the comparison of the results at TD to ESL analysis results for the maximum calculated α, η_{ki}, η_{kj} parameters are summarized. The maximum ratios occur at the infilled frames without first story infill walls with the highest first story height.

Table 6-1 the summary of maximum α, η_{ki}, η_{kj} ratio values for the pushover analysis results at the target displacement

	Bare		
	3 Story	5 Story	8 Story
$\alpha_{inelas,target}/\alpha_{Lin}$	1.30	1.50	1.80
$\eta_{k,inelas,target}/\eta_{k,Lin}$	1.80	1.30	1.50
	Infilled		
	3 Story	5 Story	8 Story
$\alpha_{inelas,target}/\ \alpha_{Lin}$	1.50	1.45	1.70
$\eta_{k,inelas,target}/\ \eta_{k,Lin}$	3.90	2.50	2.60
	Infilled wo 1st story infill walls		
	3 Story	5 Story	8 Story
$\alpha_{inelas,target}/\ \alpha_{Lin}$	1.20	2.00	1.95
$\eta_{k,inelas,target}/\ \eta_{k,Lin}$	21.0	4.80	7.00

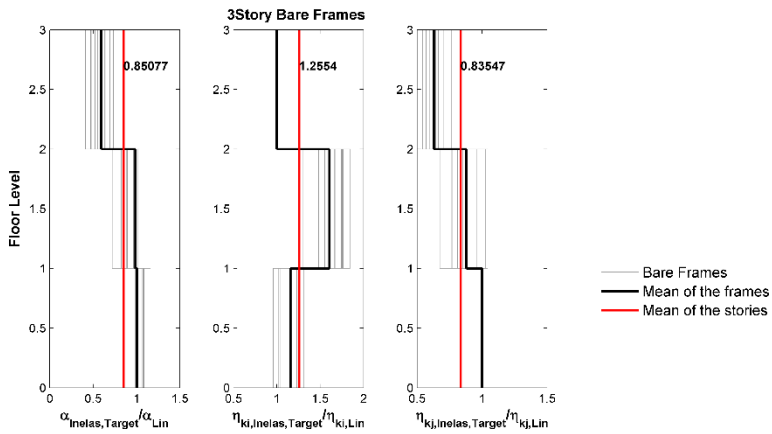

Figure 6-4 3 Story Bare Frames: The results at TD to ESL analysis results for α, η_{ki}, η_{kj}

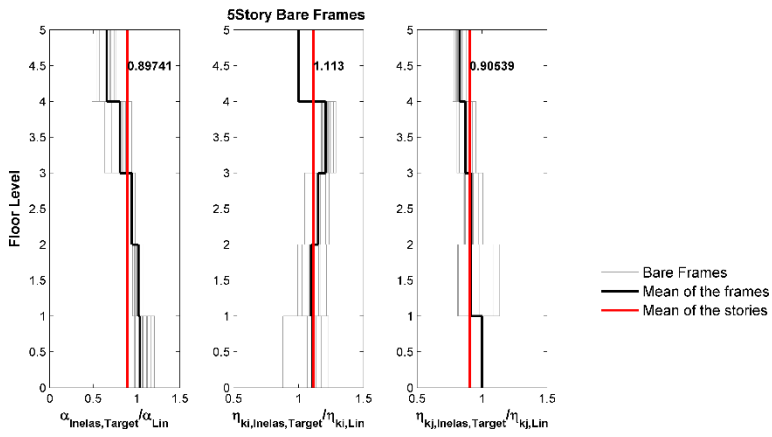

Figure 6-5 5 Story Bare Frames: The results at TD to ESL analysis results for α, η_{ki}, η_{kj}

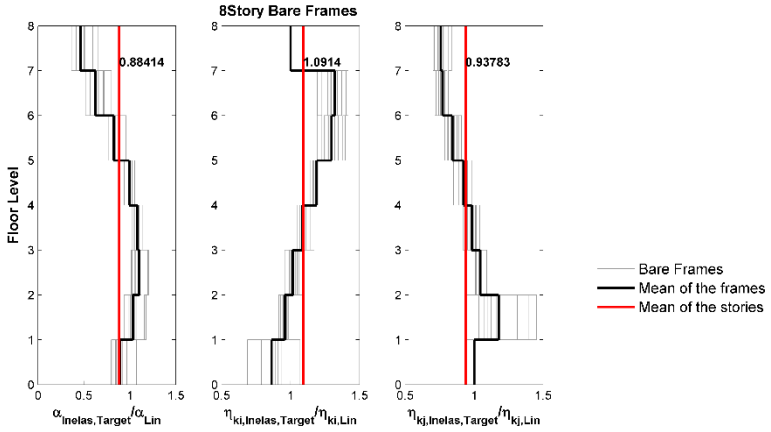

Figure 6-6 8 Story Bare Frames: The results at TD to ESL analysis results for α, η_{ki}, η_{kj}

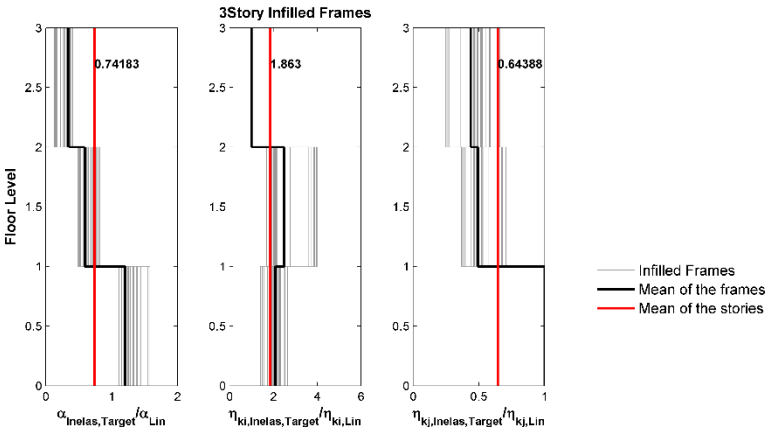

Figure 6-7 3 Story Infilled Frames: The results at TD to ESL analysis results for α, η_{ki}, η_{kj}

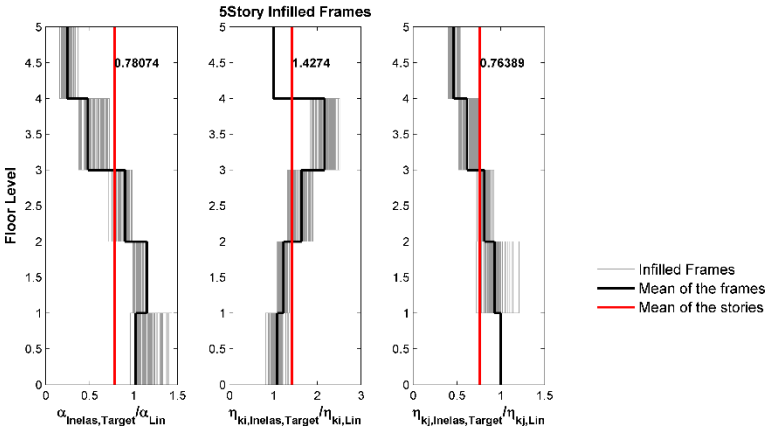

Figure 6-8 5 Story Infilled Frames: The results at TD to ESL analysis results for α, η_{ki}, η_{kj}

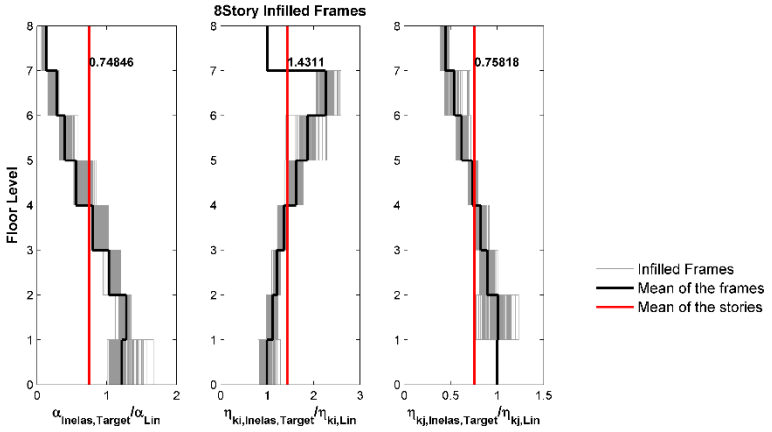

Figure 6-9 8 Story Infilled Frames: The results at TD to ESL analysis results for α, η_{ki}, η_{kj}

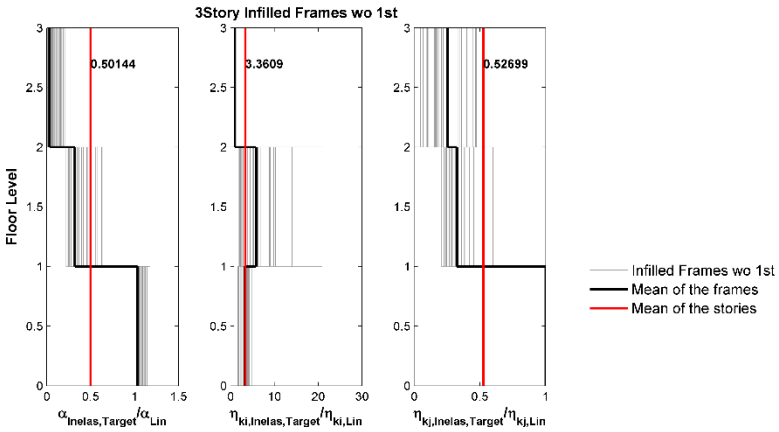

Figure 6-10 3 Story Infilled Frames without 1st story infill walls: The results at TD to ESL analysis results for α, η_{ki}, η_{kj}

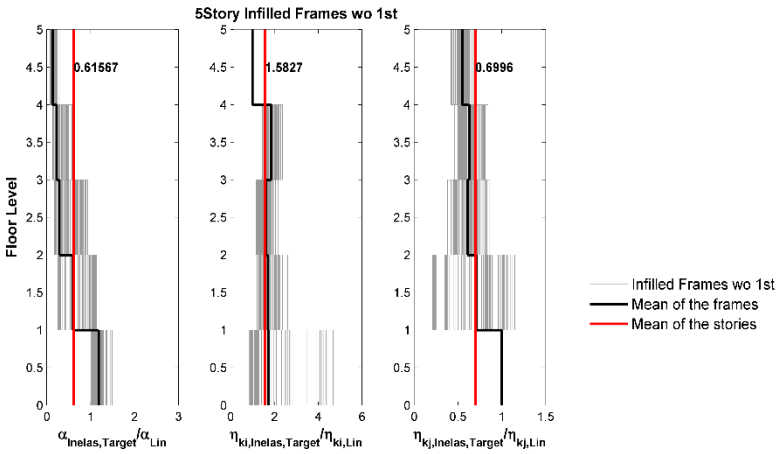

Figure 6-11 5 Story Infilled Frames without 1st story infill walls: The results at TD to ESL analysis results for α, η_{ki}, η_{kj}

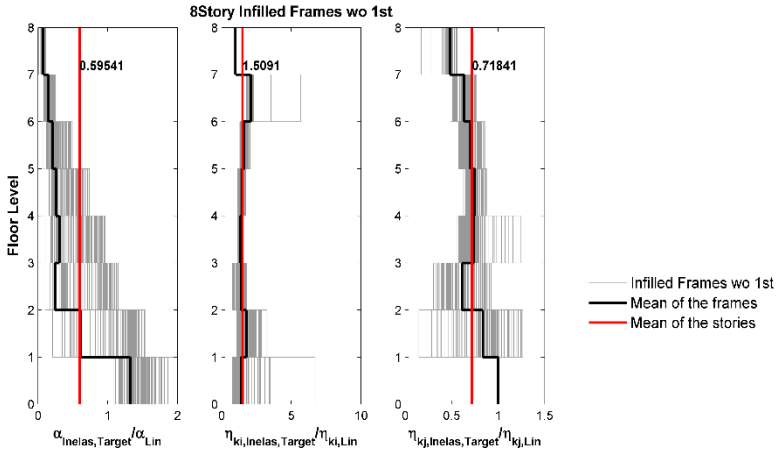

Figure 6-12 8 Story Infilled Frames without 1st story infill walls: The results at TD to ESL analysis results for α, η_{ki}, η_{kj}

6.2.2. The Comparisons at UltP with ESL analysis results

Up to this point, the target displacement point was discussed which is relevant with the linear procedures and design. The performance of the frames can be assessed with ultimate point definition. The ultimate point (UltP) is chosen according to some assumptions as explained at the beginning of this chapter. The infill walls increase the shear forces at the surrounding frames and may change the failure pattern. The failure is expected to propagate faster after the maximum capacity is reached for the infilled frames. Therefore the global failure criterion assumption for 20 percent reduction in base shear capacity was applied.

In APPENDIX C, the pushover curves are given in detail for hinge patterns at ultimate point, target displacement and the pushover curves at the possible last converged step. In the figures of APPENDIX C, the infill cracking strain is given as 0.0002, and the numbers in the legend are multiplied with this. The cracking strain and the ultimate strain changes for each bay of infill walls and that's why the figures for infill failures are representative. However, the cracking strain is around 0.0002 for most of the infill walls and the ultimate strain is approximately vary in the range of 0.002 and 0.0035. Therefore, the infill failures in the figures will give an idea about the condition of the infill walls. The column and the beam hinge patterns represent the situation that exist.

In Figure 6-13 to Figure 6-21, the α, η_{ki}, η_{kj} parameters, calculated for 3, 5, and 8 story frames, were compared with pushover analysis results at TD to ESL analysis results for bare frames, infilled frames and infilled frames without the infill walls are given.

In Table 6-1, the comparison of the results at TD to ESL analysis results for the maximum calculated α, η_{ki}, η_{kj} parameters are summarized. The maximum ratios occur at the infilled frames without first story infill walls with the highest first story height.

Table 6-2 the summary of α, η_{ki}, η_{kj} ratio values for the pushover analysis results at the ultimate point

Bare			
	3 Story	5 Story	8 Story
$\alpha_{inelas,UltP}/\alpha_{Lin}$	1.28	1.30	1.80
$\eta_{k,inelas,\ UltP}/\eta_{k,Lin}$	2.15	1.60	1.50
Infillled			
	3 Story	5 Story	8 Story
$\alpha_{inelas,UltP}/\alpha_{Lin}$	1.76	1.81	1.65
$\eta_{k,inelas,\ UltP}/\eta_{k,Lin}$	15.60	5.60	4.50
Infilled wo 1st story infill walls			
	3 Story	5 Story	8 Story
$\alpha_{inelas,UltP}/\alpha_{Lin}$	1.16	2.05	2.55
$\eta_{k,inelas,\ UltP}/\eta_{k,Lin}$	346.0	8.60	12.00

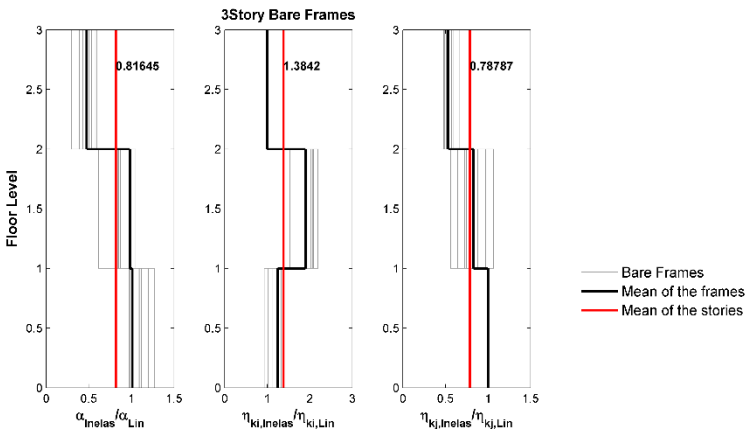

Figure 6-13 3 Story Bare Frames: UltP results to ESL analysis results for the α, η_{ki}, η_{kj} parameters

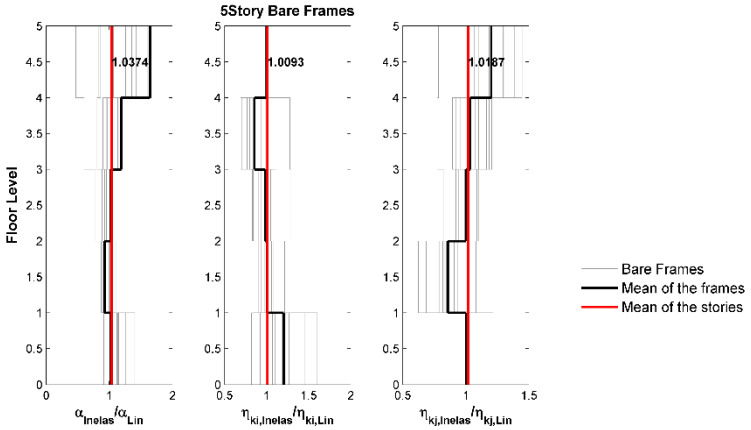

Figure 6-14 5 Story Bare Frames: UltP results to ESL analysis results for the α, η_{ki}, η_{kj} parameters

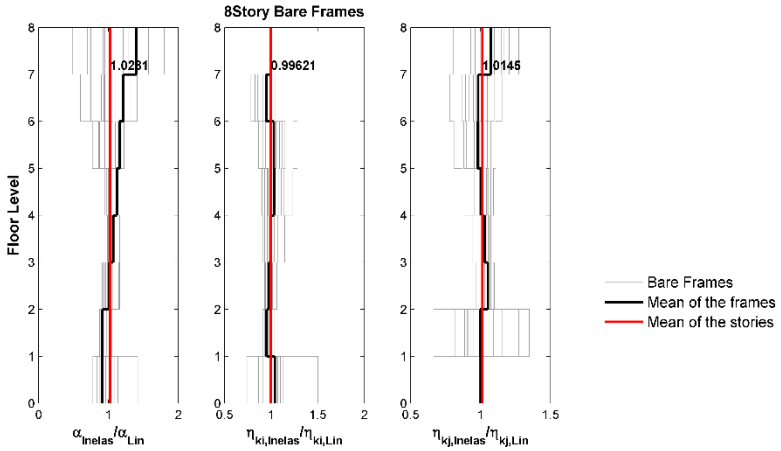

Figure 6-15 8 Story Bare Frames: UltP results to ESL analysis results for the α, η_{ki}, η_{kj} parameters

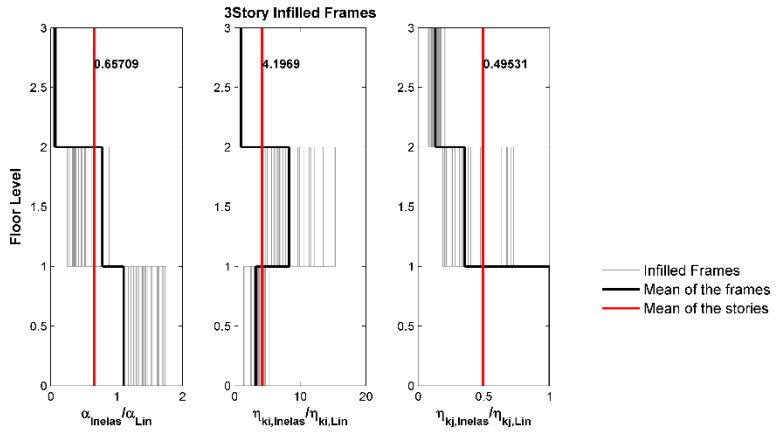

Figure 6-16 3 Story Infilled Frames: UltP results to ESL analysis results for the α, η_{ki}, η_{kj} parameters

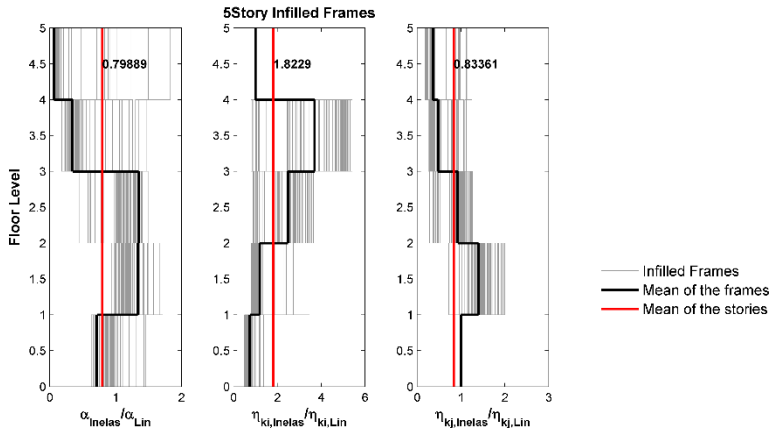

Figure 6-17 5 Story Infilled Frames: UltP results to ESL analysis results for the α, η_{ki}, η_{kj} parameters

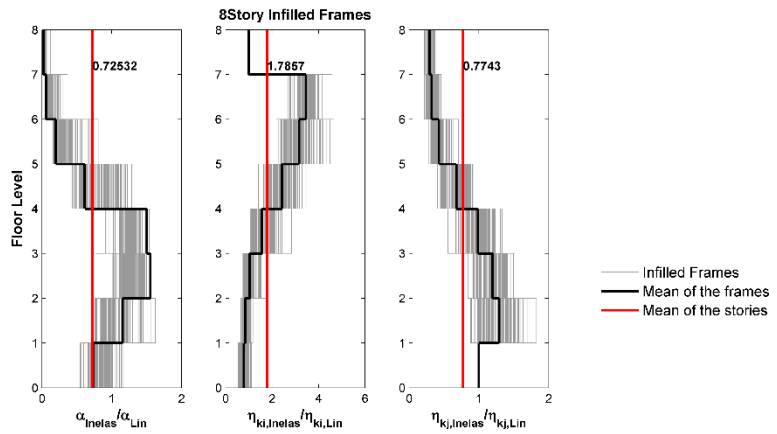

Figure 6-18 8 Story Infilled Frames: UltP results to ESL analysis results for the α, η_{ki}, η_{kj} parameters

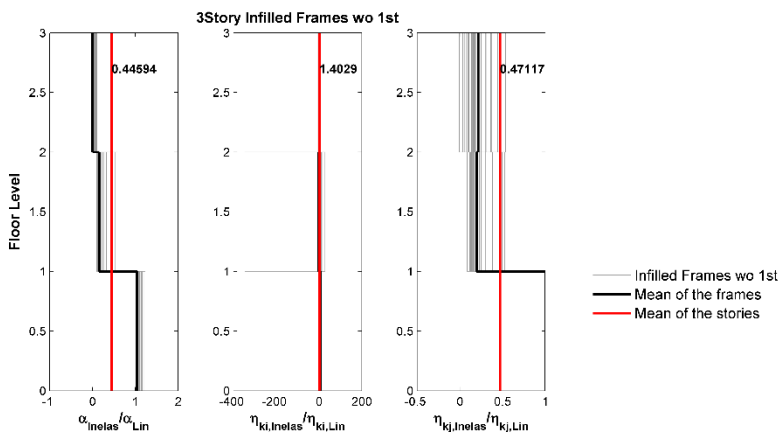

Figure 6-19 3 Story Infilled Frames without 1st story infill walls: UltP results to ESL analysis results for the α, η_{ki}, η_{kj} parameters

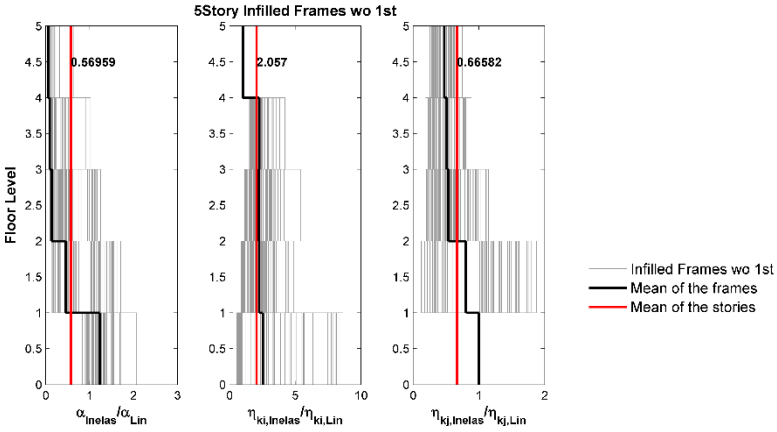

Figure 6-20 5 Story Infilled Frames without 1st story infill walls: UltP results to ESL analysis results for the α, η_{ki}, η_{kj} parameter

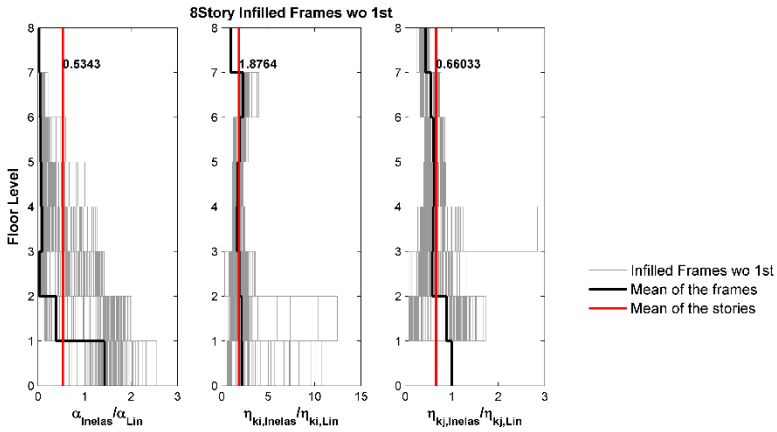

Figure 6-21 8 Story Infilled Frames without 1st story infill walls: UltP results to ESL analysis results for the α, η_{ki}, η_{kj} parameters

6.2.1. The Evaluation of the Parameters with Strength and Stiffness Change

There is a need to evaluate the η_k, α_2 and α_{irreg} parameters to observe the effects of the stiffness and strength changes separately. In Figure 6-22 to Figure 6-25, 5 story frame with 5.0 m of first story height was investigated at UltP for different column dimensions and reinforcement ratios at the first story columns. In Figure 6-22, the hinge pattern is localized between first three stories. The 50 percent increase in the reinforcement ratio for the frame, in Figure 6-23, changes the hinge pattern and first story drift ratio, correspondingly, the η_k and α decrease. In Figure 6-24 and Figure 6-25, the case for the no modification with column dimension was investigated and

the trend is same as in Figure 6-22 and Figure 6-23, the η_k and α decrease in the first story and this is related with the strength change. Thus, it can be noted that the strength change in the floor levels cause the change in the hinge pattern, however the change in the stiffness (the comparison of the Figure 6-22 and 5-77) seems to decrease the η_k and α for UltP, But beyond the UltP, the failure pattern are not same either. Therefore the η_k, α_2 and α_{irreg} parameters are investigated in Figure 6-26 to Figure 6-33 in more detail by separating the changes in column dimension and reinforcement are for bare frame, infilled frame and infilled frame without first story infill walls.

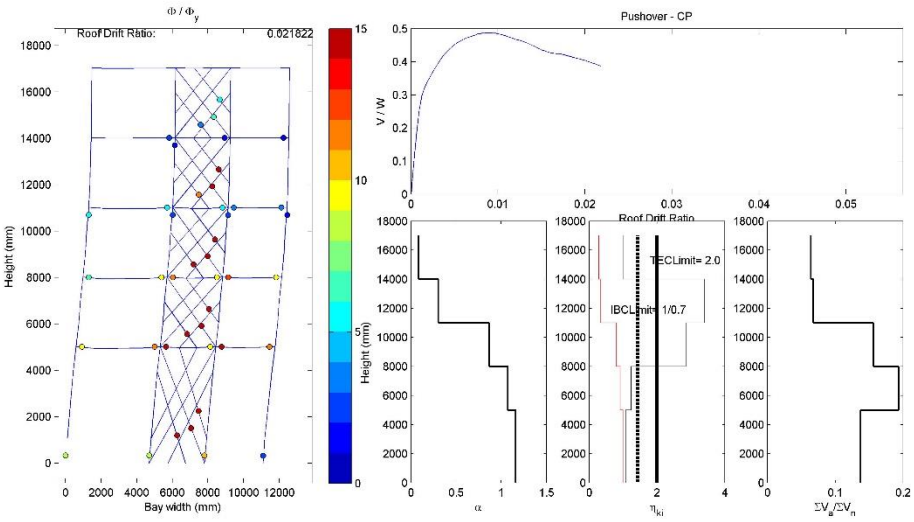

Figure 6-22 The α and η_k results at UltP for 5S_I_2_H5.0_CDM0.8_RM1.0

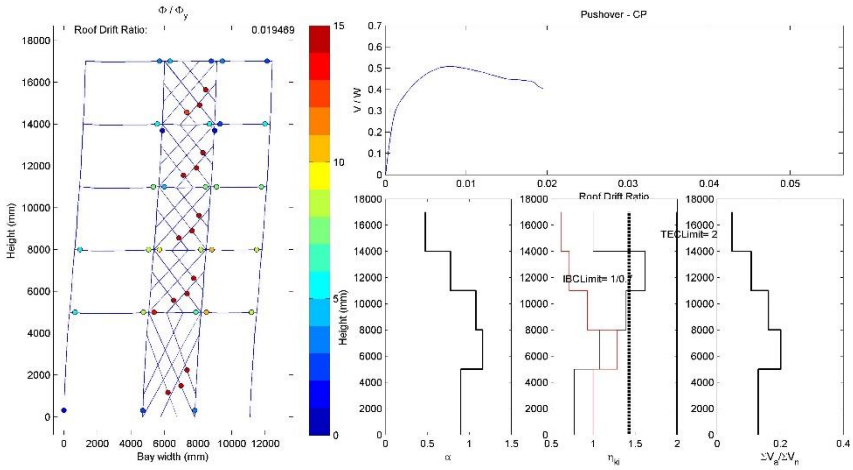

Figure 6-23 The α and η_k results at UltP for 5S_I_2_H5.0_CDM0.8_RM1.5

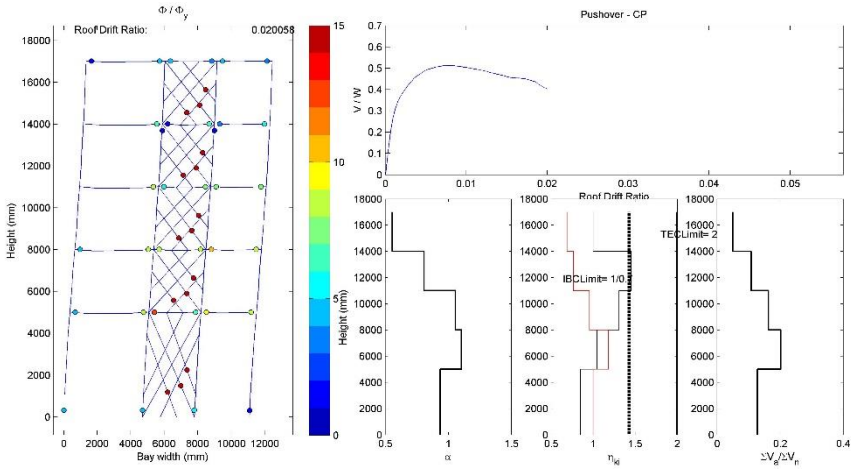

Figure 6-24 The α and η_k results at UltP for 5S_I_2_H5.0_CDM1.0_RM1.0

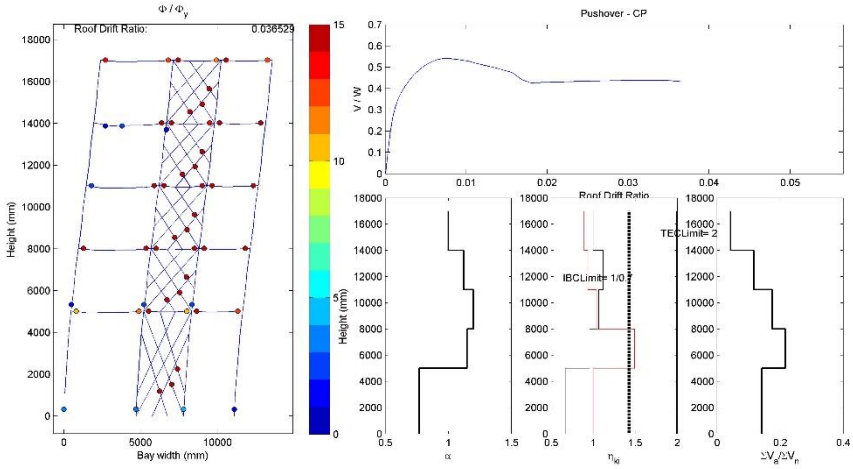

Figure 6-25 The α and η_k results at UltP for 5S_I_2_H5.0_CDM1.0_RM1.5

In Figure 6-26, the α_2 values calculated for 3 Story frames at TD is given. Every following six bar is relevant with the same infill type for 3.0 m, 4.0m and 5.0 m of first story heights for infilled frames and infilled frames without first story infill walls. For example, there is 3 type of infill wall arrangement for 3 story frame and therefore, there are 9 bars in figures for the infilled frames and infilled frames without first story infill walls. The average α_2 values are summarized in Table 6-3. The change of the α_2 values for these two cases of CDM and RM are insignificant for bare frames, slightly decrease for infilled frames and slightly increase for the infilled frames without first story infill walls.

In Figure 6-27, the α_{irreg} values calculated for 3 Story frames at TD is given. Every following three bar is relevant with the same infill type for 3.0 m, 4.0m and 5.0 m of first story heights. The average α_{irreg} values are summarized in Table 6-4. The change of the α_{irreg} values for these two cases of CDM and RM are greater than 1.0 for bare frames and decrease if the stiffness increases. For infilled frames, the α_{irreg} values are smaller than 1 and decrease with stiffness increase. The infilled frames without first story infill walls with decreased stiffness (CDM=0.8), the α_{irreg} values may become greater than 1. The cases with 5.0 m first story height, fully infilled without first story infill walls, these values increase up to 1.5.

Table 6-3 The average α_2 values for 3 story frames regarding the CDM and RM changes at TD

Bare Frames	CDM=0.8	CDM=1.0
RM=1.0	1.35	1.34
RM=1.5	1.34	1.31
Infilled Frames	CDM=0.8	CDM=1.0
RM=1.0	1.37	1.29
RM=1.5	1.33	1.24
Infilled Frames wo 1st	CDM=0.8	CDM=1.0
RM=1.0	1.54	1.62
RM=1.5	1.58	1.62

Table 6-4 The average α_{irreg} values for 3 story frames regarding the CDM and RM changes at TD

Bare Frames	CDM=0.8	CDM=1.0
RM=1.0	1.49	1.24
RM=1.5	1.46	1.20
Infilled Frames	CDM=0.8	CDM=1.0
RM=1.0	0.17	0.15
RM=1.5	0.17	0.14
Infilled Frames wo 1st	CDM=0.8	CDM=1.0
RM=1.0	1.11	0.77
RM=1.5	1.11	0.76

In Figure 6-28, the η_k values calculated for 3 Story frames at TD is given. Every following three bar is relevant with the same infill type for 3.0 m, 4.0m and 5.0 m of first story heights. The average η_k values are summarized in Table 6-5. The change of the η_k values for these two cases of CDM and RM are insignificant for bare frames and infilled frames, and decrease for the infilled frames without first story infill walls if the stiffness and strength increase.

Table 6-5 The average η_k values for 3 story frames regarding the CDM and RM changes at TD

Bare Frames	CDM=0.8	CDM=1.0
RM=1.0	2.93	2.70
RM=1.5	2.88	2.53
Infilled Frames	CDM=0.8	CDM=1.0
RM=1.0	4.21	4.27
RM=1.5	4.26	4.06
Infilled Frames wo 1st	CDM=0.8	CDM=1.0
RM=1.0	50.36	25.27
RM=1.5	37.26	18.95

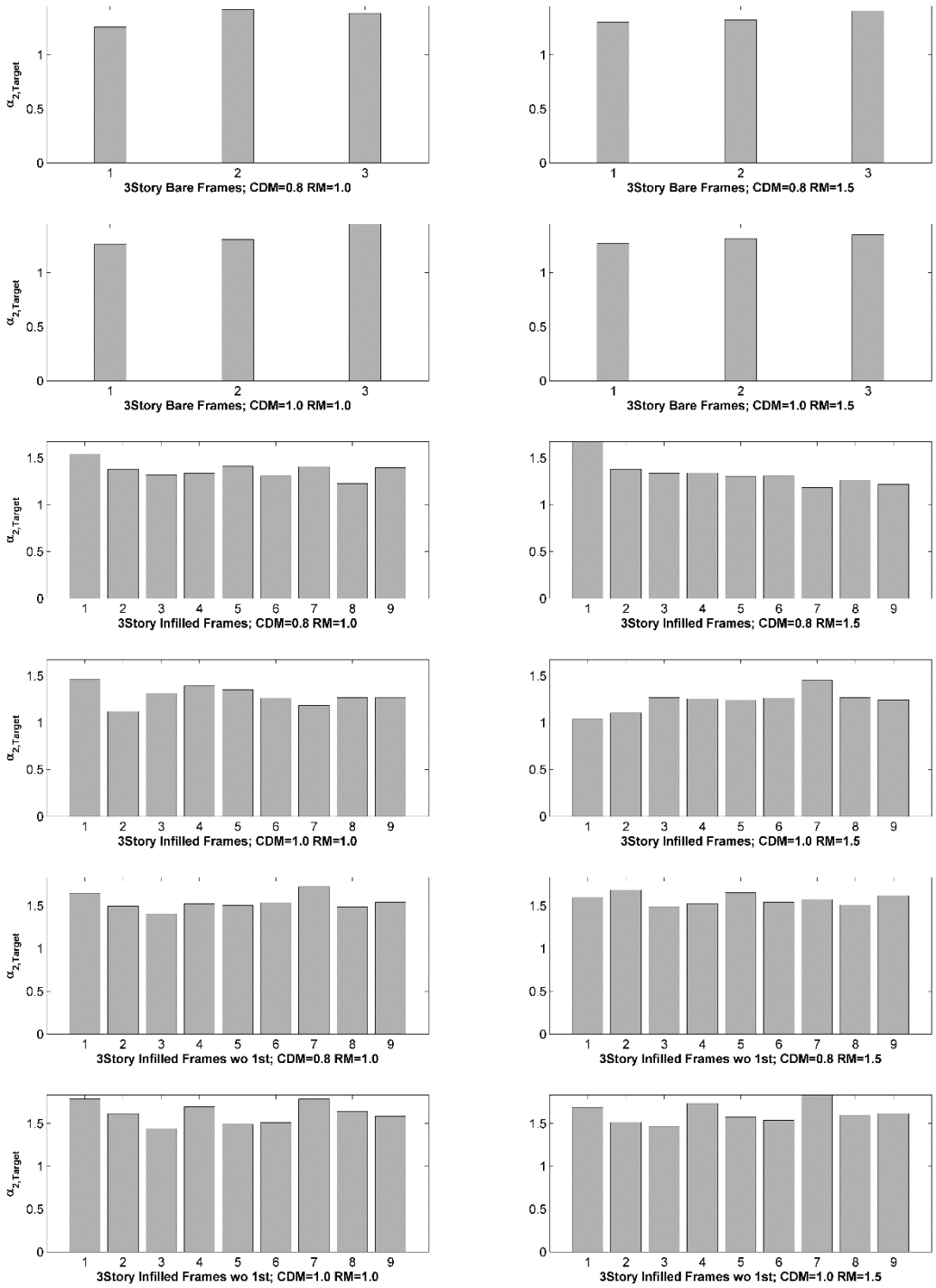

Figure 6-26 The α_2 values calculated for 3 story frames at TD

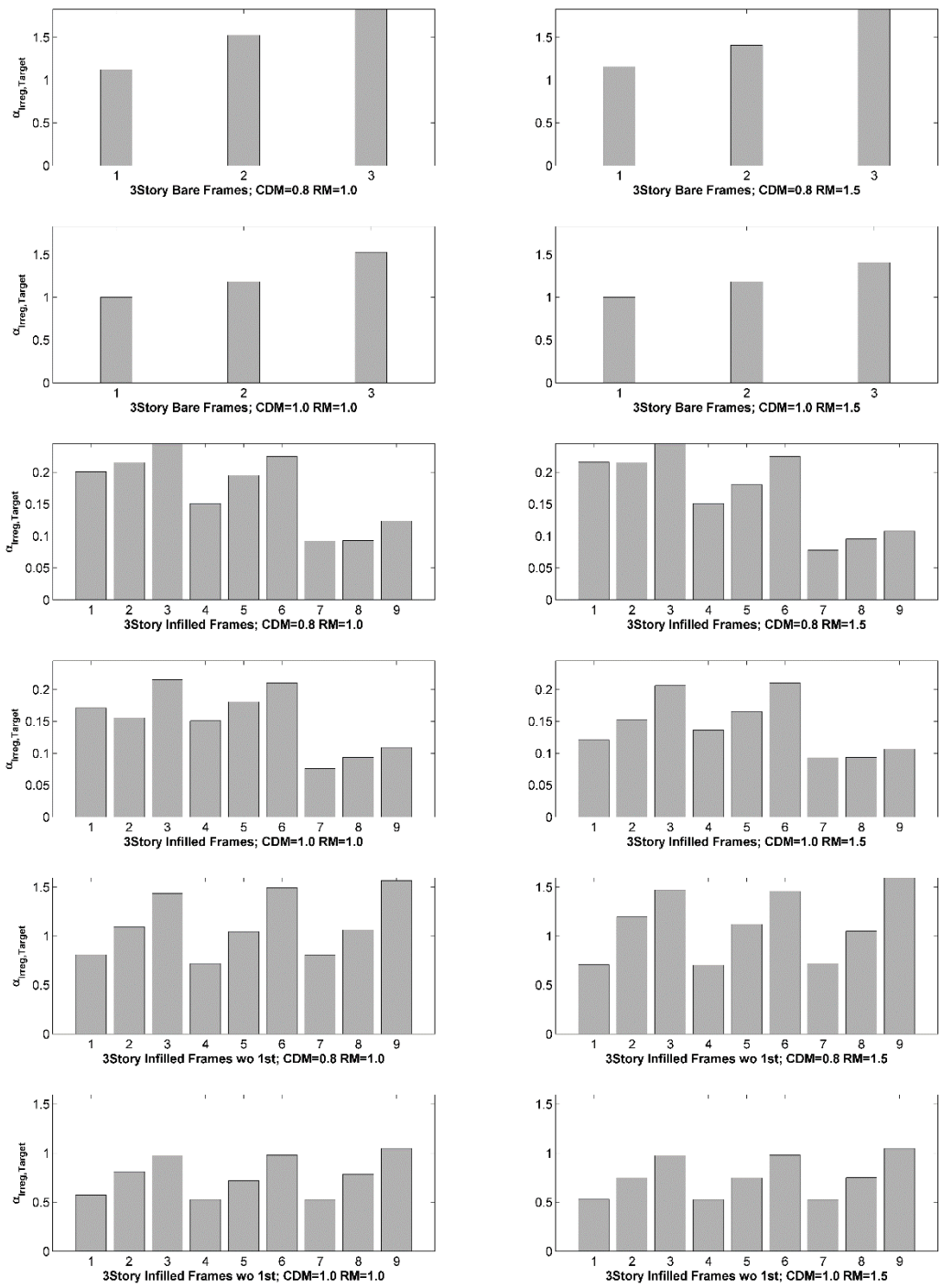

Figure 6-27 The α_{irreg} values calculated for 3 story frames at TD

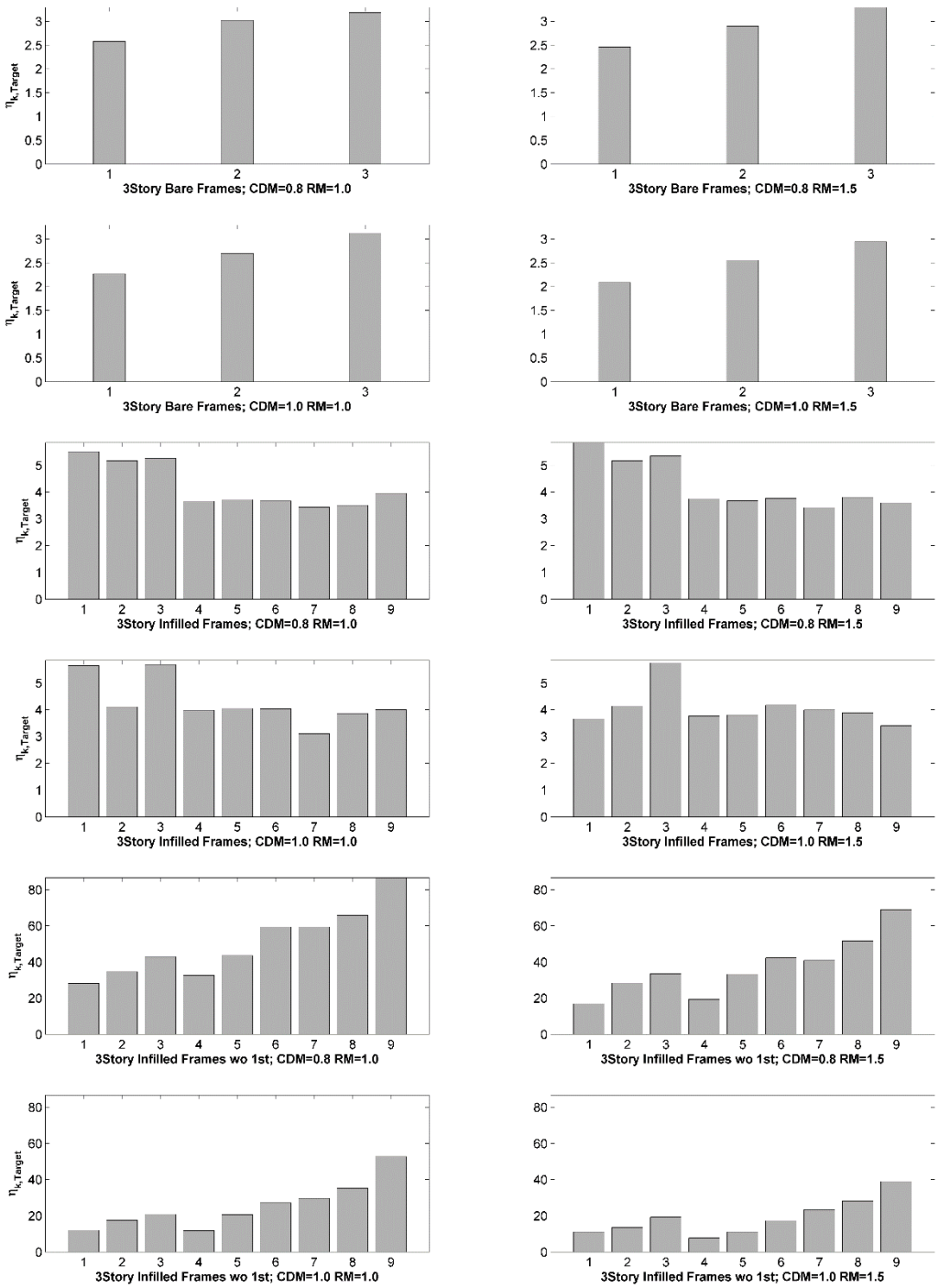

Figure 6-28 The η_k values calculated for 3 story frames at TD

In Figure 6-29, the α_2 values calculated for 5 Story frames at TD is given. Every following six bar is relevant with the same infill type for 3.0 m, 4.0m and 5.0 m of first story heights for infilled frames and infilled frames without first story infill walls. The average α_2 values are summarized in Table 6-6. The change of the α_2 values for these two cases of CDM and RM are insignificant for bare frames, slightly increase for infilled frames and the infilled frames without first story infill walls.

In Figure 6-30, the α_{irreg} values calculated for 5 Story frames at TD is given. Every following three bar is relevant with the same infill type for 3.0 m, 4.0m and 5.0 m of first story heights. The average α_{irreg} values are summarized in Table 6-7. The change of the α_{irreg} values for these two cases of CDM and RM are greater than 1.0 for bare frames and decrease if the stiffness increases. For infilled frames, the α_{irreg} values are less than 1 and almost same as CDM=1.0. The infilled frames without first story infill walls with decreased stiffness (CDM=0.8), the α_{irreg} values are less than 1 and decrease if the stiffness increases. The cases with 5.0 m first story height, fully infilled without first story infill walls, these values increase up to 1.1.

Table 6-6 The average α_2 values for 5 story frames regarding the CDM and RM changes at TD

Bare Frames	CDM=0.8	CDM=1.0
RM=1.0	1.58	1.50
RM=1.5	1.48	1.52
Infilled Frames	CDM=0.8	CDM=1.0
RM=1.0	1.06	1.14
RM=1.5	1.09	1.13
Infilled Frames wo 1st	CDM=0.8	CDM=1.0
RM=1.0	1.30	1.31
RM=1.5	1.26	1.29

Table 6-7 The average α_{irreg} values for 5 story frames regarding the CDM and RM changes at TD

Bare Frames	CDM=0.8	CDM=1.0
RM=1.0	1.34	1.15
RM=1.5	1.24	1.16
Infilled Frames	CDM=0.8	CDM=1.0
RM=1.0	0.44	0.44
RM=1.5	0.45	0.44
Infilled Frames wo 1st	CDM=0.8	CDM=1.0
RM=1.0	0.80	0.64
RM=1.5	0.75	0.62

In Figure 6-31Figure 6-32, the η_k values calculated for 5 Story frames at TD is given. Every following three bar is relevant with the same infill type for 3.0 m, 4.0m and 5.0 m of first story heights. The average η_k values are summarized in Table 6-8. The change of the η_k values for these two cases of CDM and RM are insignificant for bare frames and infilled frames, and decrease for the infilled frames without first story infill walls if the stiffness and strength increase.

Table 6-8 The average η_k values for 5 story frames regarding the CDM and RM changes at TD

Bare Frames	CDM=0.8	CDM=1.0
RM=1.0	1.94	1.89
RM=1.5	1.93	1.85
Infilled Frames	CDM=0.8	CDM=1.0
RM=1.0	3.05	3.18
RM=1.5	3.11	3.18
Infilled Frames wo 1st	CDM=0.8	CDM=1.0
RM=1.0	9.03	3.95
RM=1.5	4.83	3.32

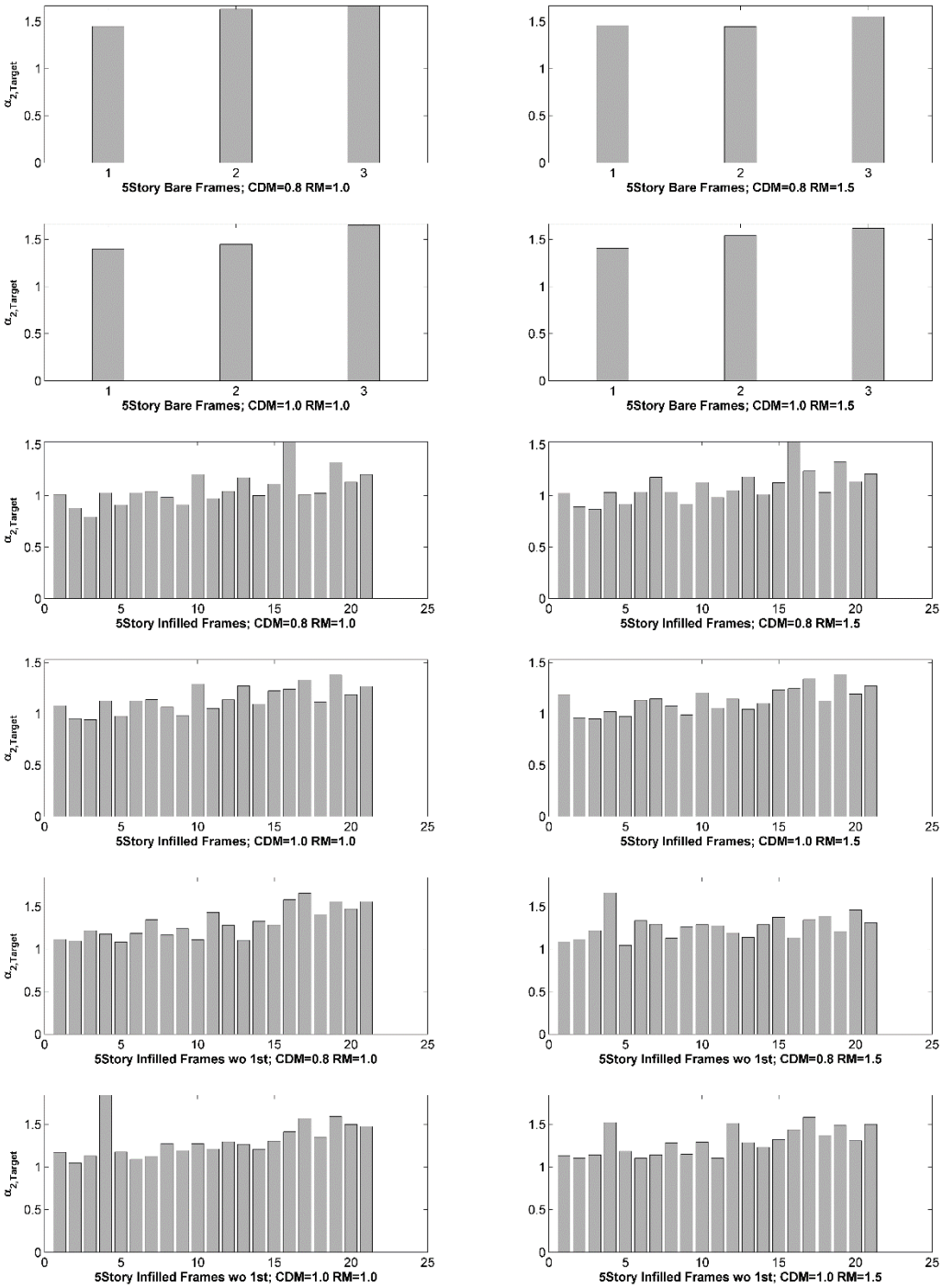

Figure 6-29 The α_2 values calculated for 5 story frames at TD

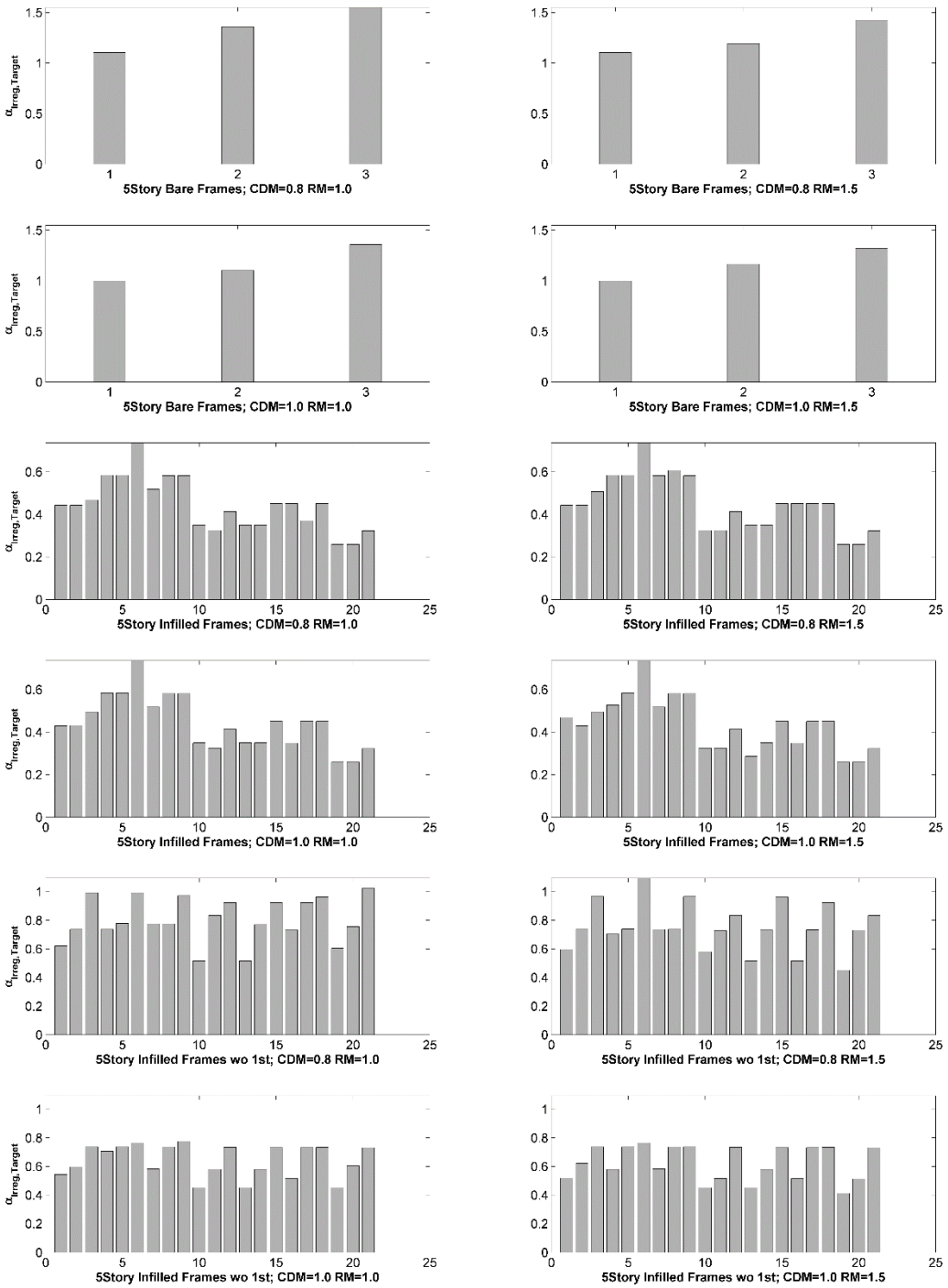

Figure 6-30 The α_{irreg} values calculated for 5 story frames at TD

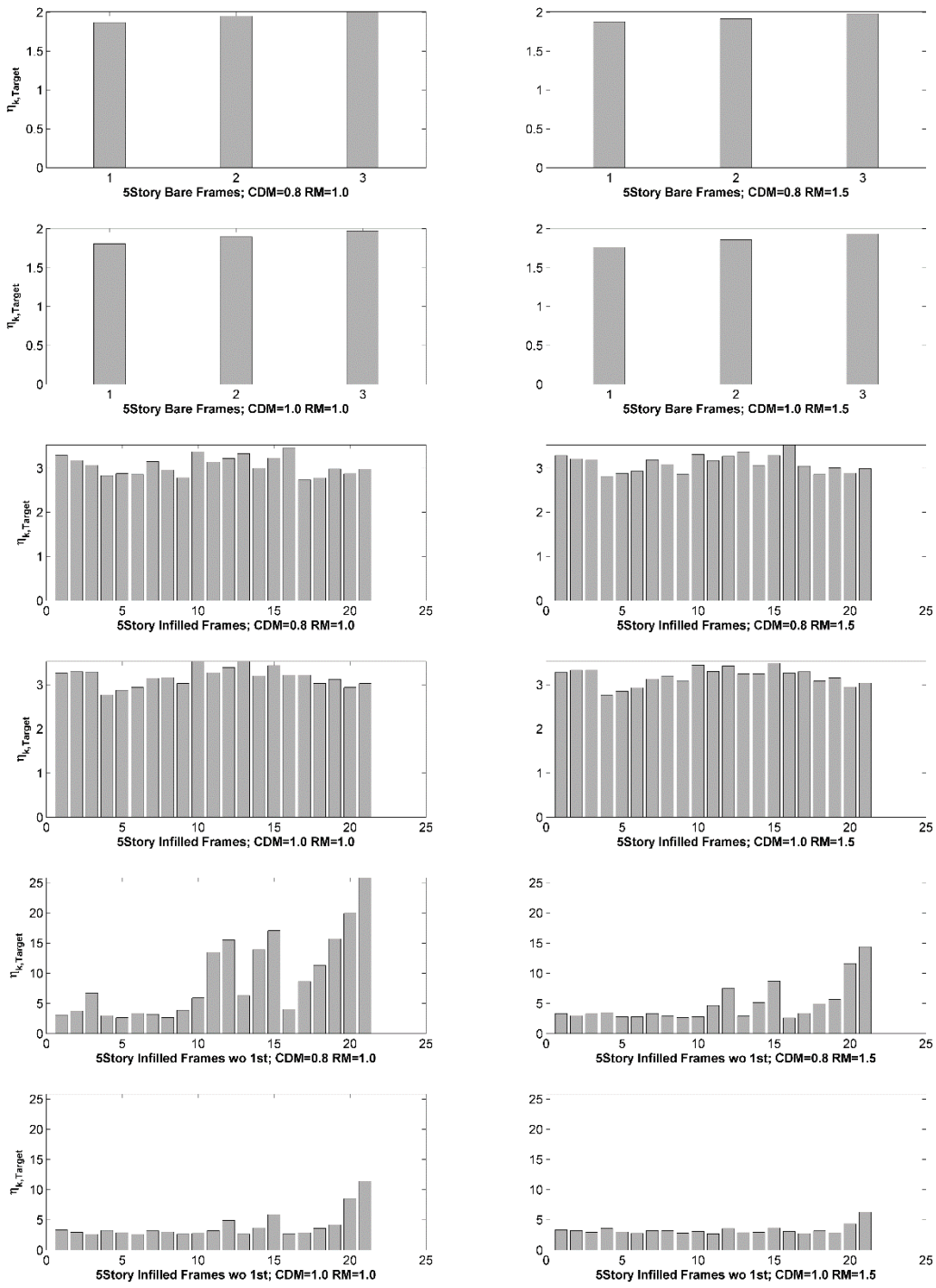

Figure 6-31 The η_k values calculated for 5 story frames at TD

In Figure 6-32, the α_2 values calculated for 8 Story frames at TD is given. Every following six bar is relevant with the same infill type for 3.0 m, 4.0m and 5.0 m of first story heights for infilled frames and infilled frames without first story infill walls. The average α_2 values are summarized in Table 6-9. The change of the α_2 values for these two cases of CDM and RM are insignificant for bare frames, infilled frames and the infilled frames without first story infill walls.

In Figure 6-33, the α_{irreg} values calculated for 8 Story frames at TD is given. Every following three bar is relevant with the same infill type for 3.0 m, 4.0m and 5.0 m of first story heights. The average α_{irreg} values are summarized in Table 6-10 . The change of the α_{irreg} values for these two cases of CDM and RM are greater than 1.0 for bare frames and decrease if the stiffness increases. For infilled frames, the α_{irreg} values are less than 1 and almost same as CDM=1.0. The infilled frames without first story infill walls with decreased stiffness (CDM=0.8), the α_{irreg} values are less than 1 and decrease if the stiffness increases. The cases with 5.0 m first story height, infilled without first story infill walls, these values increase up to 0.7.

Table 6-9 The average α_2 values for 8 story frames regarding the CDM and RM changes at TD

Bare Frames	CDM=0.8	CDM=1.0
RM=1.0	1.21	1.22
RM=1.5	1.22	1.19
Infilled Frames	CDM=0.8	CDM=1.0
RM=1.0	0.74	0.77
RM=1.5	0.74	0.75
Infilled Frames wo 1st	CDM=0.8	CDM=1.0
RM=1.0	1.01	0.91
RM=1.5	0.96	0.92

Table 6-10 The average α_{irreg} values for 8 story frames regarding the CDM and RM changes at TD

Bare Frames	CDM=0.8	CDM=1.0
RM=1.0	1.12	1.04
RM=1.5	1.12	1.03
Infilled Frames	CDM=0.8	CDM=1.0
RM=1.0	0.37	0.37
RM=1.5	0.37	0.36
Infilled Frames wo 1st	CDM=0.8	CDM=1.0
RM=1.0	0.56	0.46
RM=1.5	0.53	0.45

In Figure 6-34Figure 6-32, the η_k values calculated for 8 Story frames at TD is given. Every following three bar is relevant with the same infill type for 3.0 m, 4.0m and 5.0 m of first story heights. The average η_k values are summarized in Table 6-11. The change of the η_k values for these two cases of CDM and RM are insignificant for bare frames and infilled frames, and decrease for the infilled frames without first story infill walls if the stiffness and strength increase.

Table 6-11 The average η_k values for 8 story frames regarding the CDM and RM changes at TD

Bare Frames	CDM=0.8	CDM=1.0
RM=1.0	1.89	1.84
RM=1.5	1.86	1.89
Infilled Frames	CDM=0.8	CDM=1.0
RM=1.0	2.78	2.85
RM=1.5	2.80	2.86
Infilled Frames wo 1st	CDM=0.8	CDM=1.0
RM=1.0	5.84	3.23
RM=1.5	3.72	3.04

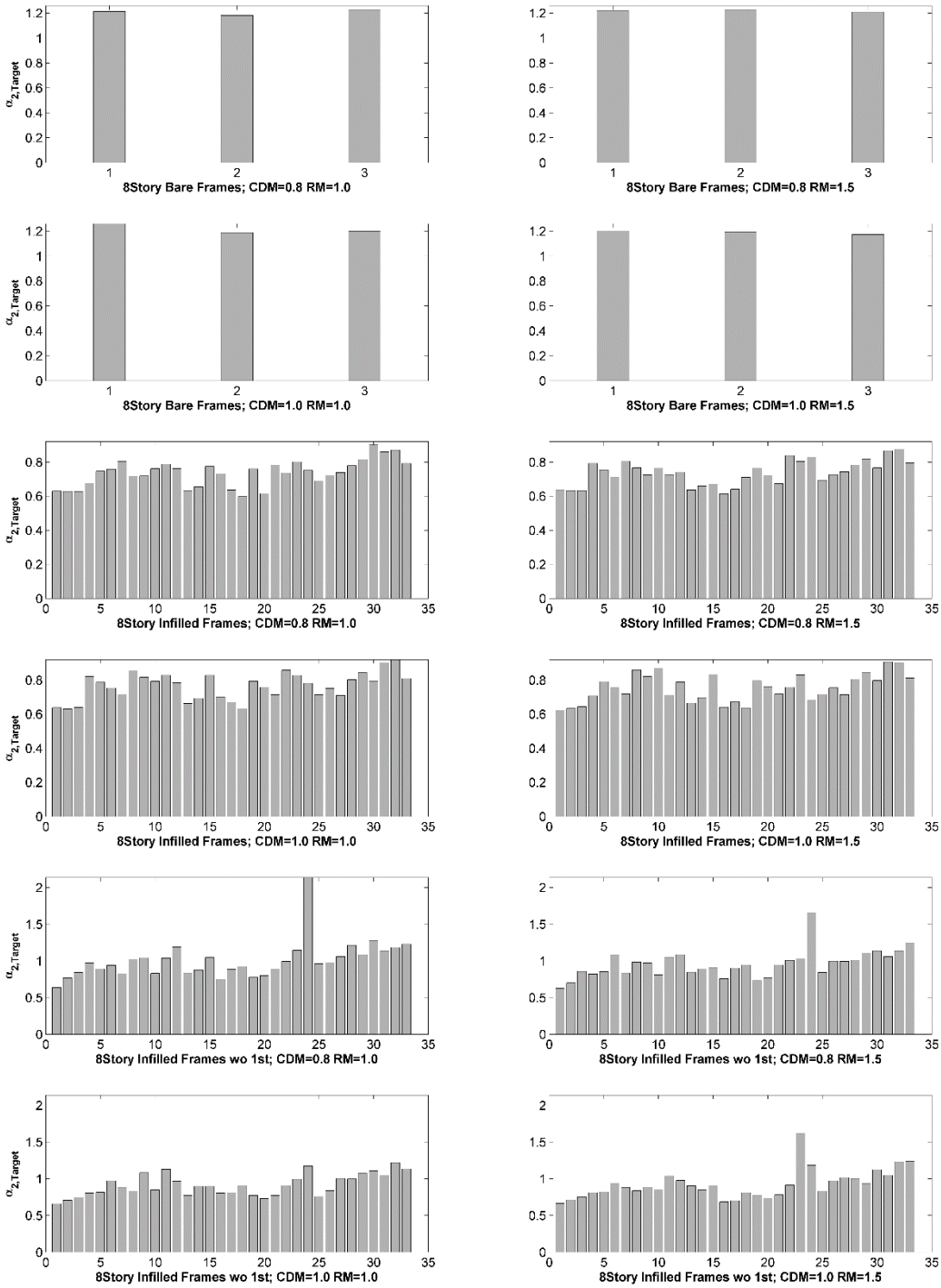

Figure 6-32 The α_2 values calculated for 8 story frames at TD

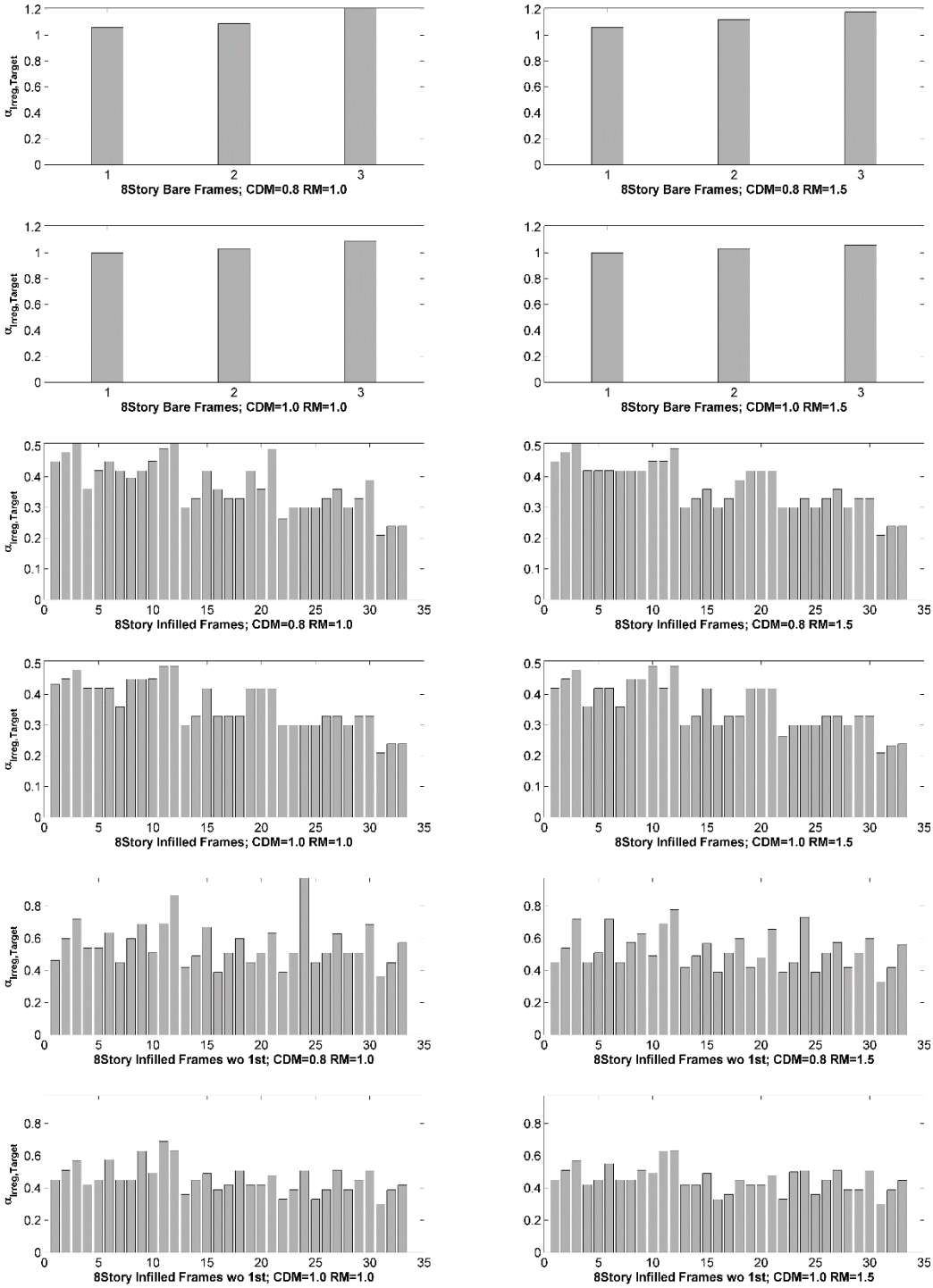

Figure 6-33 The α_{irreg} values calculated for 8 story frames at TD

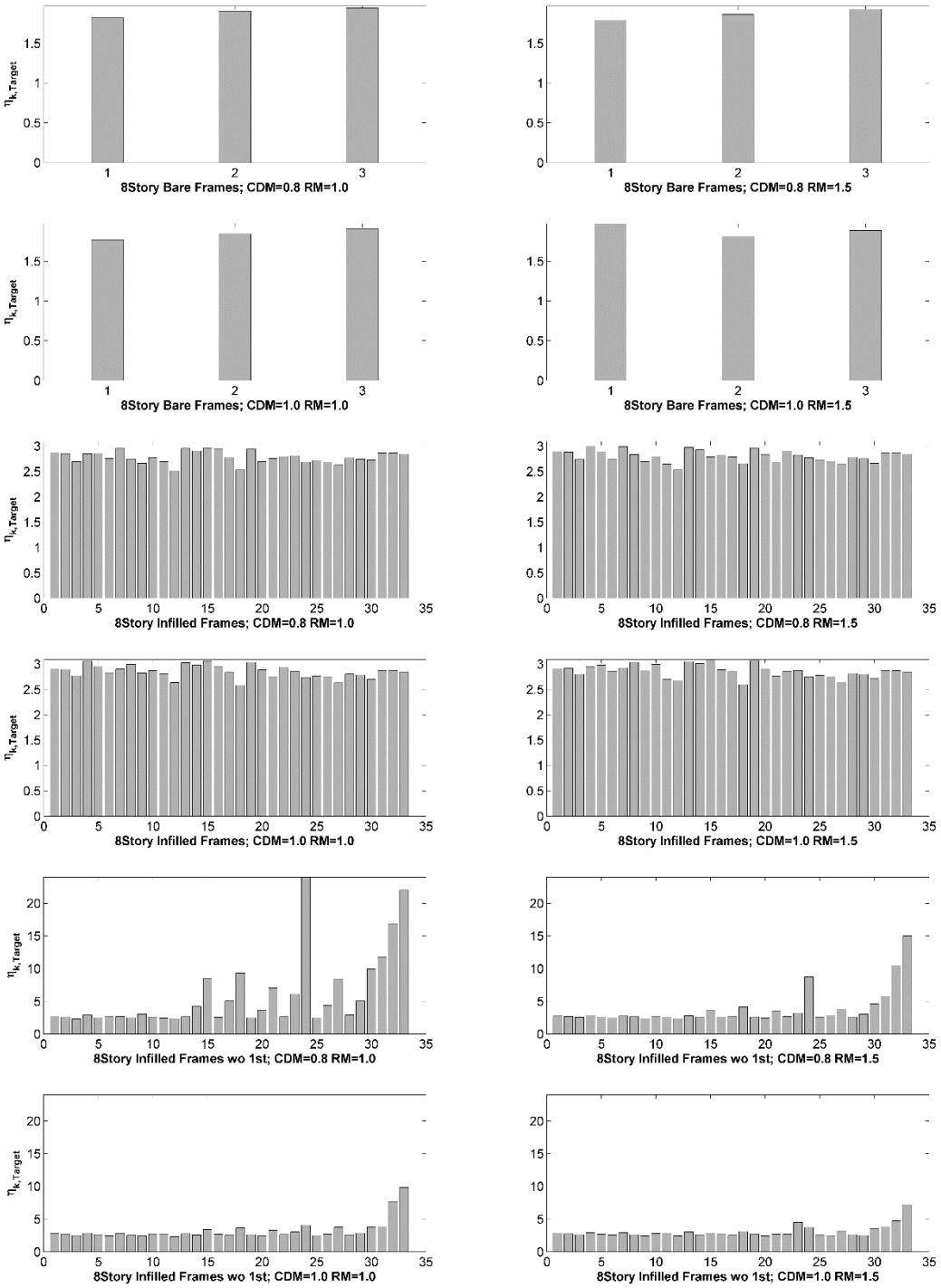

Figure 6-34 The η_k values calculated for 8 story frames at TD

CHAPTER 7

EVALUATION OF THE SOFT STORY MECHANISM

The soft story parameter, η_k, is calculated for all analysis cases and compared with each other. The detailed figures, given in APPENDIX C for the pushover curves for each frame, were evaluated for the soft story mechanism at UltP. A soft story index was created. This evaluation was done with visual inspection and only soft story failure mechanism was investigated. In Figure 7-1, some of the observed failure mechanisms are plotted and the first and the last one are good examples of the soft story mechanisms.

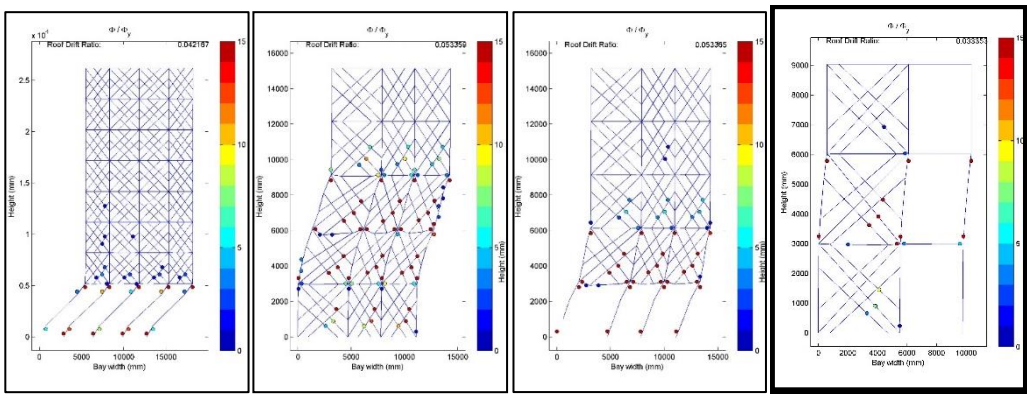

Figure 7-1 Some of the observed failure mechanisms

A Matlab script was written to check the η_k values with the soft story index, to check the compatibility with ESL and MS analysis results. In Table 7-1, the results of this comparison are given. As a reminder, there are 84 3-story, 180 5-story, and 276 8-story frame for each analyses. Thus, the TEC 2007 soft story limit catches approximately 90 percent of the soft story existence for 3, 5 and 8 story frames. The IBC 2012 limit value can catch only 56 percent, 52 percent, and 79 percent of 3, 5, and 8 story frames where soft story exists, respectively.

Table 7-1 The number of frames which satisfy the specified code limit values for the soft story existence, η_k

Number of Stories	ESL		MS (CQC)	
	TEC 2007	IBC 2012	TEC 2007	IBC 2012
3 Story	75	47	72	50
5 Story	161	93	164	99
8 Story	255	217	255	200

If we only look at Table 7-1, it can be said that the TEC 2007 can detect the soft story mechanism with high accuracy, however, when we look at all index for η_k, in one plot for soft story existence, Figure 7-2, the minimum $\boldsymbol{\eta_k}$ value where the soft story exist is **1.42** and is almost same as the IBC 2012 limit value. Thus, we can say that IBC 2012 limit is more conservative than TEC 2012 and it is on the safe side.

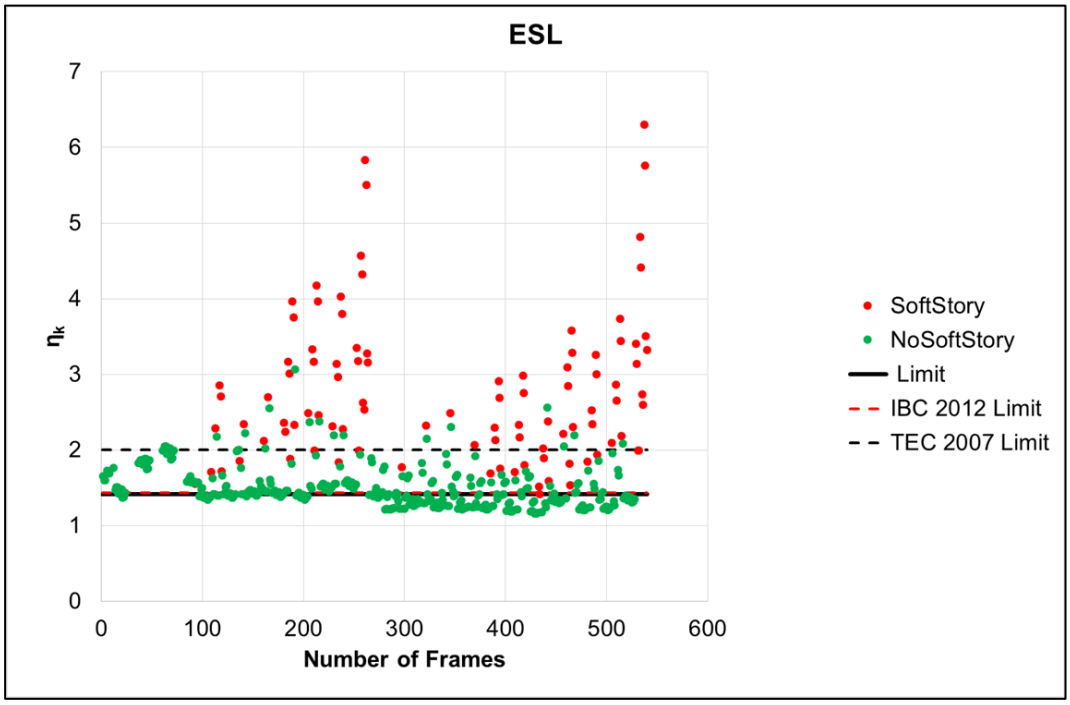

Figure 7-2 The η_k values for all frames under the scope of soft story existence

In Figure 7-3, the α parameter investigated via soft story index to be able to find a relationship between the soft story parameter. It is observed that the minimum **α** value,

where the soft story exists,is **1.08** and for maximum acceptable limit value of α can be selected as **1.3** for the extreme soft story case.

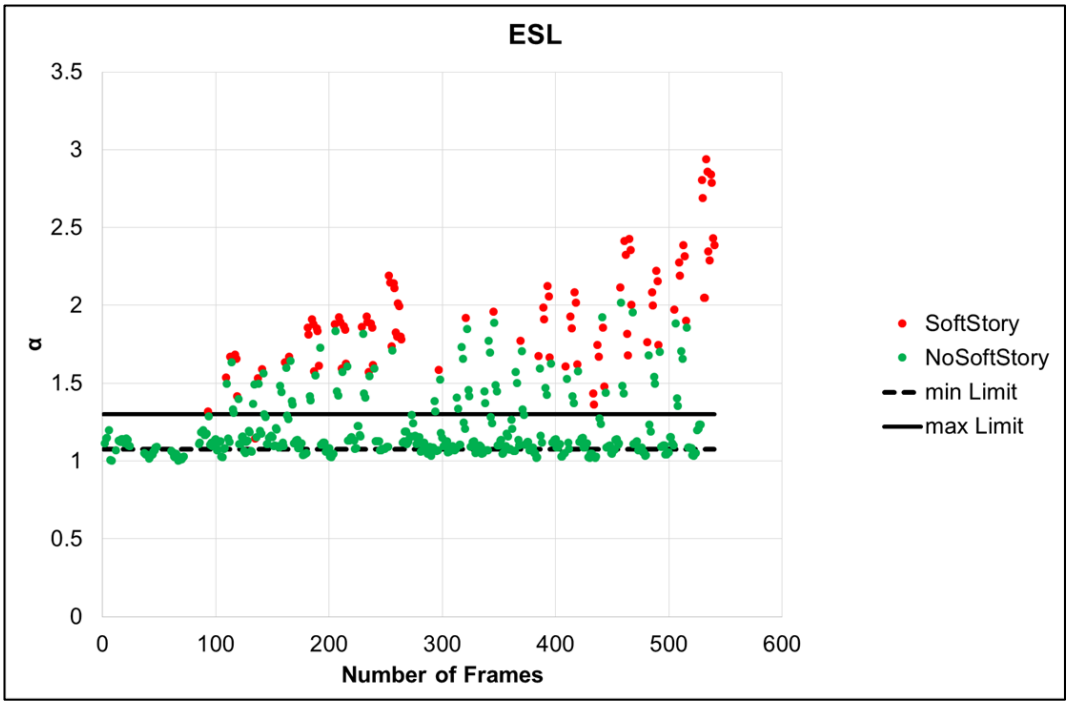

Figure 7-3 The α values for all frames under the scope of soft story existence

In Figure 7-4, the α_2 value is investigated via soft story index to be able to find a relationship with the soft story mechanism. It is hard to say that there is a relationship between the α_2 value and soft story existence.

In Figure 7-5, the α_{irreg} value is investigated via soft story index to be able to find a relationship with the soft story mechanism. It is observed that it is hard to say that there exist a relationship between the α_{irreg} value and soft story mechanism.

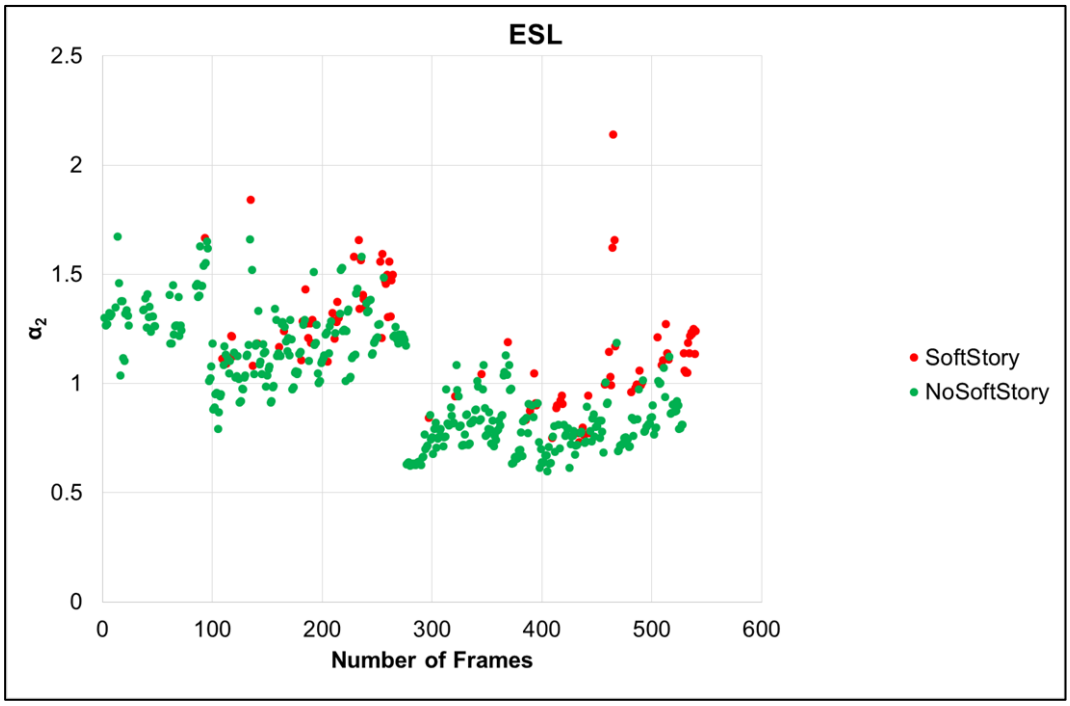

Figure 7-4 The α_2 values for all frames under the scope of soft story existence

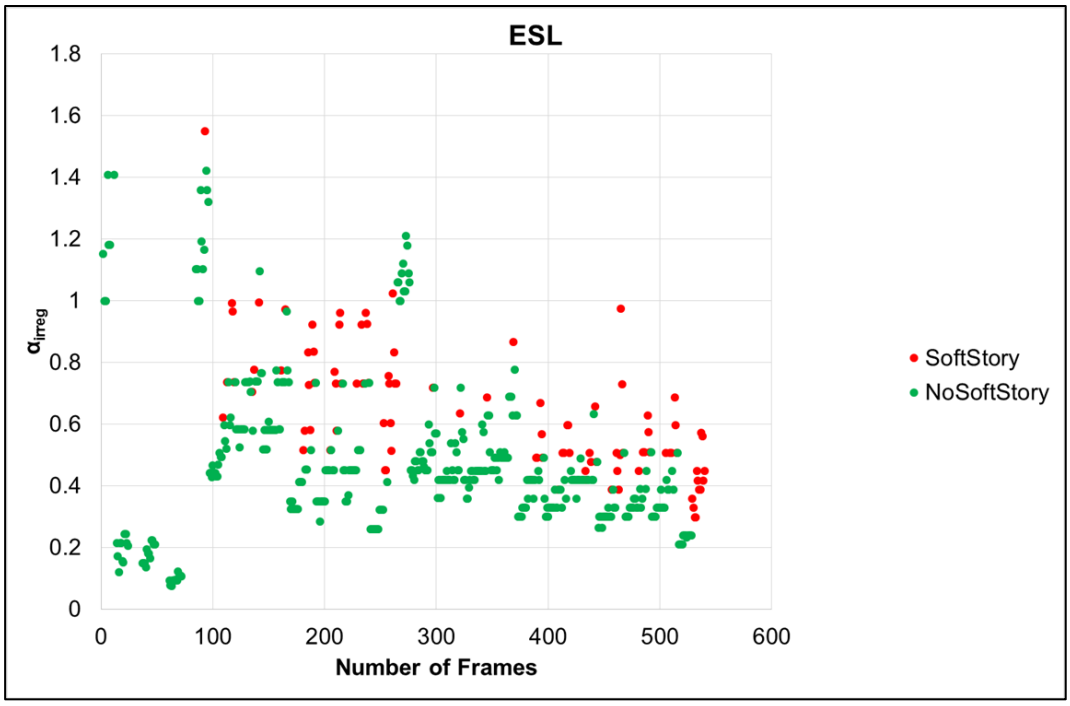

Figure 7-5 The α_{irreg} values for all frames under the scope of soft story existence

CHAPTER 8

CONCLUSIONS AND RECOMMENDATIONS

In this chapter, summary, conclusions, recommendations, and future studies are discussed.

8.1. Summary

In this thesis the effect of the infills of the vertically irregular frames on the structural behavior was studied to investigate the soft story mechanism. First of all, a literature survey was done related with the soft story irregularity for infilled reinforced concrete frames. The vertical irregularity definitions used by codes and the typical mechanical and geometrical characteristics of the building stock of Turkey were investigated. In the review of the codes, irregularity parameters were used mostly to decide the analysis type and to scale the seismic design loads. However, how to determine the vertical irregularity is not clear in most of them. In Eurocode 8, there are some suggestions like scaling the behavior factor and re-arranging the shear reinforcement where the infill walls exist. But, there is not a parameter that defines the soft story irregularity. That is the reason that TEC 2000 and IBC 2012 were used in this thesis to discuss. NBC 2005 and FEMA 368-2000 have similar definitions with IBC 2012 for soft story irregularities.

3, 5 and 8 story buildings were designed according to TEC2007, TS500, TS498 and the characteristic material information was obtained from the literature review for the building stock of Turkey. Probina Orion v.18, (2013) was used for design. Then the frames were selected from these designed buildings. These frames were considered as base cases and vertical irregularities in terms of strength and stiffness were assigned by changing first story column dimensions and reinforcement area and infill wall arrangements in the bays.

In this thesis, only fully infilled bays were studied. Infills with openings are out of concern. In part 4.3, the definition of vertical irregularities and infill wall arrangements are given in detail.

Then, the frames were modelled in OpenSees software. Macro modelling was preferred and ASCE 41, equivalent strut and contact length formulas were used. The calculation of the equivalent strut was not enough to model the nonlinear behavior and the material constitutive law was constructed based on the other researchers' suggestions. In-plane behavior is modelled only. Most of the parameters were clarified based on the literature review, however, there were still uncertainties in the strut material constitutive law, such as shear strength and contact length for the case studies. These uncertainties were tried to be minimized by sensitivity analysis. The infill model and modified material constitutive law seem to give good results with experimental studies.

Selected base cases and created irregular cases were studied under equivalent static load, mode superposition (CQC), nonlinear pushover and time history analysis. The results are discussed in terms of η_{ki}, $\eta_{kj,}$ soft story parameters, and additionally α, α_2 and α_{irreg} parameters which are related to irregularity and ductility. The η_{ki} and $\eta_{kj,}$ parameters are TEC 2007 parameters and they are relevant with IBC 2012 soft story definition. The α, α_2 and α_{irreg} parameters are used and suggested by Seneviratna and Krawinkler (1997) and Al-Ali and Krawinkler (1998).

Linear analysis results were compared to be able to disscuss the useability of the methods. Because, the modern codes uses the vertical irregullarity parameters to decide the analysis method, also. The difference is less between equivalent static load analyses and mode superposition analyses results.

Nonlinear time history analysis was done for one of the critical 8 story frame and the corresponding base case. Results show that the pushover analysis results can be used for the detemination of the soft story irregularities.

Nonlinear analysis results were compared with linear analysis results. Soft story mechanisms for each pushover curve at UltP were visually investigated and a soft story index was created. The η_k and α parameters were evaluated based on this soft story index.

8.2. Conclusions

The main outcomes obtained from the sensitivity analysis and verification studies are given below.

- ASCE 41 equivalent strut formula seems to give a good estimate if the material constitutive law is well developed.
- Three strut macro model seems to give good results with accepTable A1ccuracy for the experimental studies.
- The f_{tp}, shear strength under diagonal compression test, affect the axial load capacity of the equivalent strut width and correspondingly the hysteretic material for degradation behavior. Weak and strong infills have different friction coefficients for different failure angles to calculate the $f_{tp.}$
- Post peak stiffness, K_3, affect the degradation part of the results and should be different for strong and weak infills. In this thesis, K_3=0.005K_1 and K_3=0.1K_1 respectively for strong infill and the weak infill gave a good match with related experimental results.
- If it is consistent in calculating the equivalent strut width with the same methodology, E_m seems to be less effective on the results.

The main conclusions obtained for soft story parameters from the linear and nonlinear analyses results are given as below;

- Linear procedures can predict the soft story failure mechanisms with 90 percent accuracy for ESL with TEC 2007 limit value of 2.0.

- Linear procedures can predict the soft story failure mechanisms with 66 percent accuracy for ESL with IBC 2012 limit value of 1.43.
- The η_k limit specified in TEC 2007 is adequate to detect the soft story. IBC 2012 limit is lower in percentage to detect.
- The η_k limit value of 1.42 that is very close to the value specified in IBC (1.43) is conservative to identify the soft story..
- The α is more stable to see the displaced shape and to get an idea for the location of soft story mechanisms. It is in the range of 1.08 and 3.0. The minimum calculated α value where the soft story exist is 1.08 and can be used as a limit value for soft story detection. α=1.3 can be used for extreme soft story mechanism.
- The infilled frames change the failure pattern and upper stories may fail first.
- The infilled frames without first story infill walls are the most vulnerable to first story failure.
- Almost all of the infilled frames governs the UltP with global failure criterion. Infilled frames without first story infill walls follow the global failure criterion in some cases, but, the ultimate curvature governs the failure in most.
- Pushover analysis results and the soft story indexing according to observations showed that linear analysis procedures can predict the soft story failure, however, the chosen limit value is critical.

8.3. Recommendations for Future Studies

This study governs the in-plane behavior of infilled frames regarding the soft story irregularities. It is obvious that there are many things to do more related with the infilled reinforced concrete building. In this part, recommendations and future study suggestions are given for the investigation of the infill walls on the performance of the reinforced concrete buildings. Some of this suggestions are listed below.

- If the walls have plaster, this should be included in the calculation of the equivalent struts and material constitutive law.

- Using the contact length as half is reasonable.
- Infill walls are considered as full without opening. This effect may be studied. Three strut model give good results, however, should be used with some additional hinges to cover out-of-plane behavior.
- Contact length definition is a good way to include the effects of the surrounding frame, however, also have some drawbacks. The contact length may change depending on the thickness of the wall and span length and these may result in different contact lengths at each span and will make the modeling complicated. For multistory frames, there is a need for an assumption like using the mean contact length or critical one for each floor or same span at all floor levels.
- Out-of-plane behavior was not concerned. Out-of-plane behavior may be concerned with a 3d analysis.

REFERENCES

A. W. Hendry, (1998). “Structural Masonry, 2nd ed.”. Macmillan Press.

Aghdam A. Y. and Tariverdilo S, (2012), “A numerical Criterion to detect Vertical Stiffness Irregularity”, Advances in Structural Engineering, Vol. 15, No. 1

Aksoy, H. B., & Avşar, Ö. (2015), “Considering the Effect of Masonry Infill Walls on the Seismic Behavior of R/C Frames with a Simplified Method”. Pamukkale Üniversitesi Mühendislik Bilimleri Dergisi, 21(3), pp. 115-122.

Al-Ali A. A. K. and Krawinkler H. (1998), “Effects of Vertical Irregularities on Seismic Behavior of Building Structures”, The John A. Blume Earthquake Engineering Center, Stanford University, Report No: 130.

Al-Chaar G., (2002). “Evaluating strength and stiffness of unreinforced masonry infill structures”, US Army Corps of Engineers, Construction engineering research laboratory.

Al-Char K. and Lamb G. E., (2002). “Design of fiber-reinforced polymer materials for seismic rehabilitation of infilled concrete structures”, US Army Corps of Engineers, Construction engineering research laboratory.

Amato G., Cavaleri L., Fossetti M., and Papia M., (2008). “Infilled frames: influence of vertical load on the equivalent diagonal strut model”, Fourteenth World Conference of Earthquake Engineering, 14 WCEE.

Amato G., Fossetti M., Cavaleri L., and Papia M., (2009). “An updated model of equivalent diagonal strut for infill panels”, Fourteenth World Conference of Earthquake Engineering, 14 WCEE.

Asteris P. G., (2003). “Lateral stiffness of brick masonry infilled plane frames”, Journal of Structural Engineering, Vol. 129, No.8, pp. 1071-1079.

Asteris P. G., (2008). “Finite element micro-modeling of infilled frames”, Electronic Journal of Structural Engineering, Vol.8.

Asteris P. G., Kakaletsis S. J., Chrysostomou C. Z., and Smyrou E. E., (2011a). “Failure modes of infilled frames”, Electronic Journal of Structural Engineering, Vol.11, No.1.

Asteris P.G., Antoniou S.T., Sophianopoulos D. S., and Chrysostomou C. Z., (2011b). “Mathematical macromodeling of infilled frames: State of the Art”, Journal of Structural Engineering, Vol. 137, No.12, pp. 1508-1517.

ATC-40 (1996). “Seismic evaluation and retrofit of concrete buildings”, Applied Technology Council, Redwood City, CA.

Ay Bekir Özer, (2012), “A Proposed Ground Motion Selection and Scaling Procedures for Structural Systems”, Middle East Technical University, PhD Thesis, December.

Bal İ. E., Crowley H., and Pinho R., (2008-b), “Displacement-Based Earthquake Loss Assessment for an Earthquake Scenario in Istanbul”, Journal of Earthquake Engineering, 12(S2):12–22.

Bal İ. E., Crowley H., Pinho R., and Gülay F. G., (2008-a), “Detailed Assessment of Structural Characteristics of Turkish RC Building Stock for Loss Assessment Models”, Soil Dynamics and Earthquake Engineering 28, pp. 914–932.

Bal I.E., Crowley H., and Pinho R., (2008). “Displacement-Based Earthquake Loss Assessment for an Earthquake Scenario in Istanbul”, Journal of Earthquake Engineering, 12:S2, 12-22, DOI: 10.1080/13632460802013388.

Beigi, H. A., Sullivan, T. J., Christopoulos, C., & Calvi, G. M. (2015). “Factors influencing the repair costs of soft-story RC frame buildings and implications for their seismic retrofit”. Engineering Structures, 101, 233-245.

Begimgil M., (1991). “Tuğla duvarların kayma dayanımının güçlendirilmesi üzerine deneysel ve analitik bir çalışma”, Türkiye İnşaat Mühendisliği 11. Teknik Kongresi, pp. 167-181.

Benavent-Climent, A., & Mota-Páez, S. (2017). “Earthquake retrofitting of R/C frames with soft first story using hysteretic dampers: Energy-based design method and evaluation”. Engineering Structures, 137, 19-32.

Bertoldi SH, Decanini LD, Gavarini C., (1993). “Telai tamponati soggetti ad azioni sismiche, un modello semplificato: confronto sperimentale e numerico”, Atti del 6 Convegno Nazionale ANIDIS, vol. 2, Perugia, 13–15, [in Italian]. p. 815–24.

Celarec D., Ricci P., and Dolsek M., (2012). “The sensitivity of seismic response parameters to the uncertain modelling variables of masonry-infilled reinforced concrete frames”, Engineering Structures, Vol.35, pp. 165-177.

Chang, G.A., and Mander, J.B., (1994), “Seismic Energy Based Fatigue Damage Ananlysis of Bridge Columns:Part 1 – Evaluation of Seismic Capacity,” NCEER Technical Report No. NCEER-94-0006 State University of New York, Buffalo, N.Y.

Chintanapakdee C. and Chopra A. K. (2004), “Seismic Response of Vertically Irregular Frames: Response History and Modal Pushover Analysis”, Journal of Structural Engineering, Vol. 130, No. 8.

Chrysostomou CZ, (1991), “Effects of degrading infill walls on the nonlinear seismic response of two-dimensional steel frames”, PhD thesis, Cornell University, Ithaca (NY).

Crisafulli F. J., Carr A. J., and Park R., (2000a). “Analytical modelling of infilled frame structures – a general review”, Bulletin of the New Zeland Society for Earthquake Engineering, Vol.33, No.1.

Crisafulli F. J., Carr A. J., and Park R., (2000b). “Capacity design of infilled frame structures”, Twelfth World Conference of Earthquake Engineering, 12 WCEE.

Crisafulli, F.J., (1997). “Seismic behavior of reinforced concrete structures with masonry infills” University of Canterbury, Ph.D. Thesis, Christchurch, New Zealand.

Crisafulli, F.J., Carr, A.J. and Park, R., (2005). “Experimental response of framed masonry structures designed with new reinforcing detail”, Bulletin of the New Zealand Society for Earthquake Engineering, Vol. 38, No. 1, pp 19-32.

Das S. and Nau J. M. (2003), “Seismic Design Aspects of Vertically Irregular Reinforced Concrete Buildings”, Earthquake Spectra, Volume 19, No. 3.

Dawe JL, Seah CK., (1989). “Analysis of concrete masonry infilled steel frames subjected to in-plane loads”. In: Proceeding of the 5th Canadian Masonry Symposium, Vancouver., p. 329–40

De Stefano M. and Pintucchi B. (2008), “A Review of Research on Seismic Behavior of Irregular Building Structures since 2002”, Bulletin of Earthquake Engineering, 6, pp. 285-308.

Decanini L., Mollaioli F., Mura A., and Saragoni R., (2004). “Seismic performance of masonry infilled RC frames”, Thirteenth World Conference of Earthquake Engineering, 13WCEE.

Dolšek, M., & Fajfar, P. (2001). “Soft storey effects in uniformly infilled reinforced concrete frames”. Journal of Earthquake Engineering, 5(1), 1-12.

Dolšek M. and Fajfar P., (2005). “Simplified non-linear seismic analysis of infilled reinforced concrete frames”. Earthquake Eng. Struct. Dynamics, Vol.No:34, pp., 49–66.

Dolsek M., and Fajfar P., (2002). “Mathematical modelling of an infilled RC frame structure based on the results of pseudo-dynamic tests”, Earthquake Engineering and Structural Dynamics, Vol. 31, pp. 1215-1230.

Dolsek M., and Fajfar P., (2008). “The effect of masonry infills on the seismic response of a four-storey reinforced concrete frame – a deterministic assessment”, Engineering Structures, Vol. 30, pp. 1991-2001.

Durrani AJ, Luo YH., (1994). “Seismic retrofit of flat-slab buildings with masonry infills”. In: Proceeding from the NCEER workshop on seismic response of masonry

El Dakhakhni W. W., Egaaly M., and Hamid A., (2003). “Three Strut model for concrete masonry infilled steel frames”, Journal of Structural Engineering, Vol. 129, No. 2.

El-Dakhakhni W.W., Hamid A. A., and Elgaaly M., (2004). “Strength and stiffness prediction of masonry infill panels”, Thirteenth World Conference of Earthquake Engineering, 13WCEE.

Ellul F., and D’Ayala D., (2008). “Push-over nonlinear analysis of infilled frames: realistic FE models of panels and contact”, Fourteenth World Conference of Earthquake Engineering, 14 WCEE.

Elwood, K. J., & Moehle, J. P. (2005). “Axial capacity model for shear-damaged columns”. ACI Structural Journal, 102(4), 578.

Ercolino M., Ricci P., Magliulo G., and Verderame G. M., (2012). “Influence of Infill Panels on the seismic behavior of a RC frame designed according to modern buildings codes”, Fifteenth World Conference of Earthquake Engineering, 15 WCEE.

Erol G., Yuksel E., Saruhan H., Sağbaş G., Tuga P. T., and Karadogan H. F., (2004). “A complementary experimental work on brittle partitioning walls and strengthening by carbon fibers”, Thirteenth World Conference of Earthquake Engineering, 13WCEE.

Ezzatfar, P., Binici, B., Kurc, O., Canbay, E., Sucuoglu, H., and Ozcebe, G., (2014). “Application of mesh reinforced mortar for performance enhancement of hollow clay tile infill walls”, Seismic Evaluation and Rehabilitation of Structures, Vol 26, Springer International Publishing, Switzerland, 171–186.

FEMA-356 (2000). “Prestandard and commentary for seismic rehabilitation of buildings”, FEMA.

FEMA-440 (2005). “Improvement of nonlinear static seismic analysis procedures”, FEMA.

Fenerci A., (2013). “The effect of infill walls on the seismic performance of boundary columns in reinforced concrete frames”, Msc. Thesis, Middle East Technical University, Civil Engineering Department.

Fiore A., Netti A., and Monaco P., (2012a). “The influence of masonry infill on the seismic behaviour of RC frame buildings”, Engineering Structures, Vol.44, pp.133-145.

Fiore A., Porco F., Raffaele D., and Uva G., (2012b). “About the influence of the infill panels over the collapse mechanisms activated under pushover analysis: Two case studies”, Soil Dynamics and Earthquake Engineering, Vol.39, pp. 11-22.

Flanagan R. D., and Bennet R. M., (1999). “Bidirectional behavior of structural clay tile infilled frames”, Journal of Structural Engineering, Vol. 125, No. 3, pp. 236-244.

Flanagan R. D., and Bennet R. M., (2001). “In-plane analysis of masonry infill materials”, Practice Periodical on Structural Design and Construction, Vol. 6, No. 4, pp. 176-182.

Furtado A., Rodrigues H., and Arede A., 2015. “Modelling of masonry infill walls participation in the seismic behaviour of RC buildings using OpenSees”, International Journal of Advanced Structural Engineering, Vol.7, pp. 117-127.

Furtado A., Rodrigues H., Arede A., and Varum H., 2016. “Simplified macro-model for infill masonry walls considering the out-of-plane behaviour”, Earthquake Engineering and Structural Dynamics, Vol.45, pp. 507-524.

Goel R. K., and Chopra A. K., 1997. “Period formulas for moment resisting frame buildings”, Journal of Structural Engineering, Vol. 123, No. 11.

Grammatikou, S., Biskinis, D., & Fardis, M. N., (2016). “Ultimate strain criteria for RC members in monotonic or cyclic flexure”. Journal of Structural Engineering, 142(9), 04016046.

Grimm, C. T., (1988). “Statistical Primer for Brick Masonry”, Masonry: Materials, Design, Construction, and Maintenance, ASTM STP 992, H. A. Harris, Ed., American Society for Testing and Materials, Philadelphia, pp. 169-192.

Hashemi A. and Mosalam K., (2007). “Seismic Evaluation of Reinforced Concrete Buildings Including Effects of Masonry Infill Walls”, Pasific Earthquake Engineering Research Center, UC,Berkeley.

Hendry, A. W., & Malek, M. H., (1986), “Characteristic compressive strength of brickwork walls from collected test results”. MASONRY INT. Masonry Int., (7), 15.

Holmes M. (1981) “Steel frames with brickwork and concrete infilling”. Proc Inst Civil Eng, Part 2, Lond, Vol.19, pp., 473–8.

Huang C. H., Tuan Y. A., and Hsu R. Y., (2006). “Nonlinear pushover analysis of infilled concrete frames”, Earthquake Engineering and Engineering Vibrations, Vol.5, No.2.

Idrizi I.S., Ristic D. N., and Idrizi Z. S., (2012). “Estimation of seismic response improvements on RC buildings with innovative “HD” infil wall panels”, Fifteenth World Conference of Earthquake Engineering, 15 WCEE.

Inel, M., & Ozmen, H. B. (2008). “Effect of infill walls on soft story behavior in mid-rise RC buildings”. In Memorias, Memorias, 14th World Conference on Earthquake Engineering, Beijing, China, Artículo (No. 05-01, p. 0279).

Jayaram, N., Lin, T., & Baker, J. W., (2011). “A computationally efficient ground-motion selection algorithm for matching a target response spectrum mean and variance”. Earthquake Spectra, 27(3), 797-815.

Kakaletsis D. J., and Karayannis C. G., (2008). “Influence of masonry strength and openings on infilled R/C frames under cycling loading”, Journal of Earthquake Engineering, 12:197-221.

Kaushik H. B., Rai D. C., and Jain S. K., (2008). “A rational approach to analytical modeling of masonry infills in reinforced concrete frame buildings”, Fourteenth World Conference of Earthquake Engineering, 14 WCEE.

Kaushik H. B., Rai D. C., and Jain S. K., (2009). “Effectiveness of some strengthening options for masonry-infilled RC frames with open first story”, Journal of Structural Engineering, Vol. 135, No. 8, pp. 925-937.

Kheyroddin A., and Naderpour H., (2007). “Plastic hinge rotation capacity of reinforced concrete beams”, IJCE, Vol.5 No.1.

Kheyroddin, A., & Naderpour, H. (2007). “Plastic hinge rotation capacity of reinforced concrete beams”. International Journal of Civil Engineering, 5(1), 30-47.

Klingner RE, Bertero VV., (1976). “Infilled frames in earthquake-resistant construction”. Report EERC 76-32. Earthquake Engineering Research Center.

Korkmaz A. K., Demir F. and Sivri M., (2007). “Earthquake assessment of RC structures with masonry infill walls”, International Journal of Science and Technology, Vol.2, No.2, pp. 155-164.

Korkmaz, A., & Taner, U. Ç. A. R. (2006). “Effects of Soft Story Irregularıty to Earthquake Behavior of R/C Structures”. Uludağ University Journal of the Faculty of Engineering, 11(2).

Li S., Liu S., Zhai C., and Xie L., (2012). “Unified analysis on progressive and seismic collapse of RC frame structure: the effect of masonry-infilled walls”, Fifteenth World Conference of Earthquake Engineering, 15 WCEE.

Lu, Y. (2002). “Comparative study of seismic behavior of multistory reinforced concrete framed structures”. Journal of structural engineering, 128(2), 169-178.

Lunn D. S., (2013). “Behavior and modeling of infill masonry walls strengthened with FRP using various end anchorages”, Ph.D. Thesis, North Carolina, Raleigh.

Madan A., Reinhorn A. M., and Mander J. B., (1997). “Modeling of masonry infill panels for structural analysis”, Journal of Structural Engineering, Vol.123, No. 10, pp.1295-1302.

Magenes G., and Pampanin S., (2004). “Seismic response of gravity-load design frames with masonry infills”, Thirteenth World Conference of Earthquake Engineering, 13WCEE.

Mainstone RJ., (1971). “On the stiffness and strength of infilled frames”. Proceeding of Institution of Civil Engineers (ICE), Supplement (IV), Paper No. 7360; 57–90.

Markulak D., Radic I., and Sigmund V., (2013). “Cyclic testing of single bay steel frames with various types of masonry infill”, Engineering Structures, Vol. 51, pp. 267-277.

Mazzoni, S., McKenna, F., Scott, M. H., & Fenves, G. L. (2006). “OpenSees command language manual”. Pacific Earthquake Engineering Research (PEER) Center.

McKenna FT, (1997). “Object-oriented finite element programming: frameworks for analysis, algorithms and parallel computing”. PhD thesis, University of California, Berkeley.

McKenna, F. (2011). “OpenSees: a framework for earthquake engineering simulation”. Computing in Science & Engineering, 13(4), 58-66.

Mehrabi A. B., and Shing P. B., (1996). “Finite element modeling of masonry –infilled RC frames”, Journal of Structural Engineering, Vol. 123, No.5, pp. 604-613.

Mehrabi A. B., Shing P. B., Schuller M. P., and Noland J. L., (1996). “Experimental evaluation of masonry –infilled RC frames”, Journal of Structural Engineering, Vol. 122, No.3, pp. 228-237.

Mohyeddin A. Goldsworthy H. M., and Gad E. F., (2013). “FE modeling of RC frames with masonry infill panels under in-plane and out of plane loading”, Engineering Structures, Vol. 51, pp. 73-87.

Morandi, P. Hak, S. Magenes, G. (2013). “Simplified out-of-plane resistance verification for slender clay masonry infills in RC frames”, 15th ANIDIS Convention of Seismic Engineering in Italy, Padova, 30 June – 04 July.

Mosalam K. M., White R. N., and Gergely P., (1997). “Static response of infilled frames using quasi-static experimentation”, Journal of Structural Engineering, Vol. 123, No.11, pp. 1462-1469.

Moyeddin A. Goldsworthy H. M.., and Gad E. F., (2013). “FE modelling of RC frames with masonry infill panels under in-plane and out-of-plane loading”, Engineering Structures, Vol. 51, pp. 73-87.

Negro, P., & Colombo, A. (1997). “Irregularities induced by nonstructural masonry panels in framed buildings”. Engineering Structures, 19(7), 576-585.

Oo M., Oo T., and Sanada Y., (2012). “A simple approach for determining contact length between frame and infill of brick masonry infilled RC frames”, Fifteenth World Conference of Earthquake Engineering, 15 WCEE.

Öztürk M. S., (2005). “Effects of masonry infill walls on the seismic performance of buildings”, Msc. Thesis, Middle East Technical University, Civil Engineering Department.

P. Fajfar and P. Gaspersic (1996), “The N2 method for the seismic damage analysis for RC buildings”, Earthquake Engineering and Structural Dynamics 25, 23}67.

Pampanin S., (2006). “Controversial aspects in seismic assessment and retrofit of structures in modern times: understanding and implementing lessons learned from ancient heritage”, Bulletin of the New Zeland Society for Earthquake Engineering, Vol.39, No.2.

Panagiotakos T. B., and Fradis M. N., (1996). “Eleventh World Conference on Earthquake Engineering”, 11WCEE, Paper No: 25.

Papia, M., Cavaleri, L., & Fossetti, M. (2003). “Infilled frames: Developments in the evaluation of the stiffening effect of infills”. Structural Engineering and Mechanics, Vol.16, pp. 675–693.

PEER (2009), “Strong Ground Motion Database”, Available from: http://peer.berkeley.edu/nga/. 2009.

Penelis GG, Kappos AJ., (1997). “Earthquake-resistant concrete structures”. London: E &FN Spon.

Plumier, A., Doneux, C., Stoychev, L., & Demarcot, T. (2005). “Mitigation of soft storey failures of RC structures under earthquake by encased steel profiles”. In Fourth International Conference on Advances in Steel Structures (Vol. 2, pp. 1193-1198).

Pradhan P. M., (2012). “Equivalent strut width for infilled frames”, Journal of Civil Engineering Research, Vol.2, No. 5, pp. 42-48.

Priestley, M. J. N. (2000). “Performance based seismic design”. Bulletin of the New Zealand society for earthquake engineering, 33(3), 325-346.

Priestley, M. J. N., Seible, F., and Calvi, G. M. S. (1996). “Seismic design and retrofit of bridges”, John Wiley & Sons, New York.

Probina Orion v.18, (2013), Prota Software Company, 06550, Çankaya, Ankara, Turkey

Redmond L., Ezzatfar P., DesRoches R., Stavridis A, Özcebe G. and Kurç Ö., (2015). “Finite Element Modeling of a Reinforced Concrete Frame with Masonry Infill and Mesh Reinforced Mortar Subjected to Earthquake Loading”, Earthquake Spectra, Vol. 32, No. 1, pp. 393–414.

Sadashiva V. K., MacRae G. A., and Deam B. L. (2012), “Seismic Response of Structures with Coupled Vertical Stiffness-Strength Irregularities”, Earthquake Engineering and Structural Dynamics, 41, pp. 119-138.

Sahlin, S., (1971). “Structural Masonry”, Prentice-Hall, Inc., Englewood Cliffs, New Jersey. 290 pp.

Sahoo, D. R., & Rai, D. C. (2013). “Design and evaluation of seismic strengthening techniques for reinforced concrete frames with soft ground story”. Engineering Structures, 56, 1933-1944.

Saneinejad A., and Hobbs B., (1995). “Inelastic design of infilled frames”, Journal of Structural Engineering, Vol. 1121, No.4, pp. 634-650.

Sanij E. D., and Alaghebandian R.,(2012). “Nonlinear earthquake response analysis of RC frames with masonry infills”, Fifteenth World Conference of Earthquake Engineering, 15 WCEE.

Sattar, S., & Liel, A. B. (2010). “Seismic performance of reinforced concrete frame structures with and without masonry infill walls”. In 9th US National and 10th Canadian conference on earthquake engineering.

Seneviratna G.D.P.K. and Krawinkler H. (1997), “Evaluation of Inelastic MDOF Effects for Seismic Design”, The John A. Blume Earthquake Engineering Center, Stanford University, Report No: 120.

Sezen, H., Whittaker, A. S., Elwood, K. J., & Mosalam, K. M. (2003). “Performance of reinforced concrete buildings during the August 17, 1999 Kocaeli, Turkey earthquake, and seismic design and construction practise in Turkey”. Engineering Structures, 25(1), 103-114.

Shing P. B., Stravridis A., Koutromanos I., Willam K., Blackard B., Kyriakides M. A. Billington S.L. , and Arnold S., (2009). “Seismic performance of non-ductile RC frames with brick infill”, ATC& SEI Conference on Improving the Seismic Performance of Existing Buildings and Other Structures.

Sigmund V., and Penava D., (2014). “Influence of openings, with and without confinement, on cyclic response of infilled RC frames - An experimental study”, Journal of Earthquake Engineering, 18:113–146.

Sipos T. K., Sigmund V., and Nyarko M. H., (2013). “Earthquake performance of infilled frames using neural networks and experimental database”, Engineering Structures, Vol. 51, pp. 113-127.

Smith, B.S. and Carter, C. (1969). “A Method of Analysis for Infilled frames”, Proc. ICE, Vol. 44, pp.31-48.

Soni D. P. and Mistry B. B. (2006), “Qualitative Review of seismic Response of Vertically Irregular Building Frames”, ISET Journal of Earthquake Technology, Technical Note, Vol. 43, No. 4.

Stavridis A., and Shing P. B., (2010). “Finite-Element modeling of nonlinear behavior of masonry-infilled RC Frames”, Journal of Structural Engineering, Vol. 136, No.3, pp. 285-296.

Stavridis A., Koutromanos I., and Shing P. B., (2012). “Shake-table test of a three-story reinforced concrete frame with masonry infill walls”, Earthquake Engineering and Structural Dynamics, Vol. 41. Pp. 1089-1108.

Su L., and Shi J., (2013). “Displacement-based earthquake loss assessment methodology for RC frames infilled with masonry panels”, Engineering Structures, Vol. 48, pp. 430-441.

Sucuoğlu H. and Siddiqui U. A., (2014). “Pseudo-dynamic testing and analytical modeling of AAC infilled RC frames”, Journal of Earthquake Engineering, 18:1281–1301.

Sucuoğlu H., (2013). “Implications of masonry infill and partition damage in performance perception in residential buildings after a moderate earthquake”, Earthquake Spectra, Vol.29, No. 2, pp. 661-667.

Sucuoğlu H., and Erberik M. A., (1997). “Performance evaluation of a three-storey unreinforced masonry building during the 1992 Erzincan earthquake”, Vol.26, pp.319-336.

Sucuoğlu H., and McNiven H. D., (1991). “Seismic Shear Capacity of Reinforced Masonry Piers”, Journal of Structural Engineering, Vol.177, No. 7.

Syrmakezis C. A., and Asteris P. G., (2001). “Masonry failure criterion under biaxial stress state”, Journal of Materials in Civil Engineering, Vol.13, No.1, pp.58-64.

Syrmakezis, C. A., and Vratsanou, V. Y. (1986). “Influence of infill walls to RC frames Response.” Proc., 8th European Conf. on Earthquake Engineering, European Association for Earthquake Engineering (EAEE), Istanbul, Turkey, 47–53.

Tabeshpour M. R., Azad A., and Golafshani A. A., (2012). “Seismic behavior and retrofit of infilled frames”, Intech open access publisher.

Taşkın B., and Hasgür Z., (2008). “Investigation of infill wall effect for the seismic performance of a moderately damaged RC building”, Eurocode 8 Perspectives from the Italian Standpoint Workshop, 119-128.

Thiruvengadam, V. (1985). “On the natural frequencies of infilled frames.” Earthquake Eng. Struct. Dyn., 13(3), 401–419.

Trapani F.D., Macaluso G., Cavaleri L., and Maurizio P., (2015). “Masonry infills and RC frames interaction: literature overview and state of the art of macro-modeling approach”, EJECE, Vol.19, No.9, pp. 1059-1095.

Uva G., Raffaele F., Porco F., and Fiore A., (2012). “On the role of equivalent strut models in the seismic assessment of infilled RC buildings”, Engineering Structures, Vol. 42, pp. 83-94.

Valmundsson E. V. and Nau J. M. (1997), “Seismic response of Building Frames with Vertical Structural Irregularities”, Journal of Structural Engineering, Vol. 123, No. 1.

Varadharajan S., Sehgal V. K., and Saini B. (2012), “Seismic Response of Multistory Reinforced Concrete frame with Vertical Mass and Stiffness Irregularities”, The Structural Design of Tall and Special Buildings, DOI: 10.1002/tal.1045.

Verderame, G. M., De Luca, F., Ricci, P., & Manfredi, G. (2011). Preliminary analysis of a soft-storey mechanism after the 2009 L'Aquila earthquake. Earthquake engineering & structural dynamics, 40(8), 925-944.

Yoshimura, M. (1997). Nonlinear analysis of a reinforced concrete building with a soft first story collapsed by the 1995 Hyogoken-Nanbu Earthquake. Cement and Concrete Composites, 19(3), 213-221.

Yorulmaz M and Sözen M. A., (1968). “Behavior of Single-Story Reinforced Concrete Frames with Filler Walls”, SRS 337, University of Illinois, Urbana.

Yuen Y. P., and Kuang J. S., (2012). “Nonlinear response and failure mechanism of infilled RC frame structures under biaxial seismic excitation”, Fifteenth World Conference of Earthquake Engineering, 15 WCEE.

Zarnic R, Gostic S., (1997). “Masonry infilled frames as an effective structural sub-assemblage”. Seismic Design Methodologies for the Next Generation of Codes, Fajfar P, Krawinkler H (eds). Balkema: Rotterdam, pp.335–346.

Zhao, J., and S. Sritharan. (2007), “Modeling of strain penetration effects in fiber-based analysis of reinforced concrete structures”. ACI Structural Journal, 104(2), pp. 133-141.

Zhao, J., and S. Sritharan. (2007). “Modeling of strain penetration effects in fiber-based analysis of reinforced concrete structures”. ACI Structural Journal, 104(2), pp. 133-141.

Zhou, J., He, F., & Liu, T. (2014). “Curvature ductility of columns and structural displacement ductility in RC frame structures subjected to ground motions”. Soil Dynamics and Earthquake Engineering, 63, 174-183.

Zovkic J., Sigmund V., and Guljas I., (2012). “Testing of RC frames with masonry infill of various strength”, Fifteenth World Conference of Earthquake Engineering, 15 WCEE.

Zovkic J., Sigmund V., and Guljas I., (2013). “Cyclic testing of a single bay reinforced concrete frames with various types of masonry infill”, Eathquake Engineering and Structural Dynamics, Vol. 42, pp. 1131-1149.

APPENDICES

A1. BUILDING DETAILS

Table A1-1 Story building F-F axle column reinforcement details

Column	Story	b1	b2	Longitudinal Reinf.	Transverse Reinf.
S4	1	40	30	4x1ø16 + 2x1ø16	ø8/15-10
S4	2	40	30	4x1ø16 + 2x1ø16	ø8/15-10
S4	3	40	30	4x1ø16 + 2x1ø16	ø8/15-10
S5	1	30	50	4x1ø18 + 2x1ø18	ø8/15-10
S5	2	30	50	4x1ø18 + 2x1ø18	ø8/15-10
S5	3	30	50	4x1ø18 + 2x1ø18	ø8/15-10
S6	1	30	40	4x1ø16 + 2x1ø16	ø8/15-10
S6	2	30	40	4x1ø16 + 2x1ø16	ø8/15-10
S6	3	30	40	4x1ø16 + 2x1ø16	ø8/15-10

Table A1-2 Story building F-F axle beam reinforcement details

Beam	bxh	Montage	Top / Left	Top / Right	Bend-up	Bottom	Bottom /Left	Bottom /Right	Left Trans.	Mid. Trans.	Right Trans.
K103	30/50	2ø14	3ø12	3ø12	1ø14	2ø14	1ø12	1ø12	1ø8/10	1ø8/20	1ø8/10
K104	30/50	2ø14	3ø12	3ø12	1ø14	2ø14	1ø12	1ø12	1ø8/10	1ø8/20	1ø8/10
K203	30/50	2ø12	3ø12	3ø12	1ø14	2ø14	1ø12	1ø12	1ø8/10	1ø8/20	1ø8/10
K204	30/50	2ø12	3ø12	3ø12	1ø14	2ø14	1ø12	1ø12	1ø8/10	1ø8/20	1ø8/10
K303	30/50	2ø12	1ø12	1ø12	1ø14	2ø14	1ø12	1ø12	1ø8/10	1ø8/20	1ø8/10
K304	30/50	2ø12	1ø12	1ø12	1ø14	2ø14	1ø12	1ø12	1ø8/10	1ø8/20	1ø8/10

Table A1-3 5Story building F-F axle column reinforcement details

Column	Story	b1	b2	Longitudinal Reinf.			Transverse Reinf.
S5	1	60	30	4x1ø18	+	2x2ø18	ø8/15-8
S5	2	60	30	4x1ø18	+	2x2ø18	ø8/13-10
S5	3	60	30	4x1ø18	+	2x2ø18	ø8/15-10
S5	4	60	30	4x1ø18	+	2x2ø18	ø8/15-10
S5	5	60	30	4x1ø18	+	2x2ø18	ø8/15-10
S6	1	60	30	4x1ø18	+	2x2ø18	ø8/15-8
S6	2	60	30	4x1ø18	+	2x2ø18	ø8/10
S6	3	60	30	4x1ø18	+	2x2ø18	ø8/11-10
S6	4	60	30	4x1ø18	+	2x2ø18	ø8/13-10
S6	5	60	30	4x1ø18	+	2x2ø18	ø8/15-9
S7	1	60	30	4x1ø18	+	2x2ø18	ø8/15-8
S7	2	60	30	4x1ø18	+	2x2ø18	ø8/10
S7	3	60	30	4x1ø18	+	2x2ø18	ø8/11-10
S7	4	60	30	4x1ø18	+	2x2ø18	ø8/13-10
S7	5	60	30	4x1ø18	+	2x2ø18	ø8/15-10
S8	1	30	60	4x1ø18	+	2x2ø18	ø8/15-8
S8	2	30	60	4x1ø18	+	2x2ø18	ø8/10
S8	3	30	60	4x1ø18	+	2x2ø18	ø8/11-10
S8	4	30	60	4x1ø18	+	2x2ø18	ø8/14-10
S8	5	30	60	4x1ø18	+	2x2ø18	ø8/15-10

Table A1-4 5 Story building F-F axle beam reinforcement details

Beam	Story	Dimension	Montage	Top / Left	Top / Right	Bend-up	Bottom	Bottom /Left	Bottom /Right	Left Transverse	Mid Span. Transverse	Right Transverse
K104	1	30/60	2ø16	2ø20	2ø20	1ø18	2ø18	4ø14	4ø14	1ø8/10	1ø8/20	1ø8/10
K105	1	30/60	2ø16	2ø20	2ø20	1ø18	2ø18	4ø14	4ø14	1ø8/7	1ø8/12	1ø8/7
K106	1	30/60	2ø16	2ø20	2ø20	1ø18	2ø18	4ø14	4ø14	1ø8/9	1ø8/20	1ø8/9
K204	2	30/60	2ø16	2ø20	2ø20	1ø18	2ø18	4ø14	4ø14	1ø8/10	1ø8/20	1ø8/10
K205	2	30/60	2ø16	2ø20	2ø20	1ø18	2ø18	4ø14	4ø14	1ø8/7	1ø8/12	1ø8/7
K206	2	30/60	2ø16	2ø20	2ø20	1ø18	2ø18	4ø14	4ø14	1ø8/9	1ø8/20	1ø8/9
K304	3	30/60	2ø16	2ø16	2ø16	1ø14	2ø14	4ø14	4ø14	1ø8/10	1ø8/20	1ø8/10
K305	3	30/60	2ø16	2ø16	2ø16	1ø14	2ø14	4ø14	4ø14	1ø8/8	1ø8/15	1ø8/8
K306	3	30/60	2ø16	2ø16	2ø16	1ø14	2ø14	4ø14	4ø14	1ø8/10	1ø8/20	1ø8/10
K404	4	30/60	2ø14	2ø12	2ø12	1ø14	2ø14	2ø14	2ø14	1ø8/10	1ø8/20	1ø8/10
K405	4	30/60	2ø14	2ø12	2ø12	1ø14	2ø14	2ø14	2ø14	1ø8/10	1ø8/20	1ø8/10
K406	4	30/60	2ø14	1ø12	2ø12	1ø14	2ø14	2ø14	2ø14	1ø8/10	1ø8/20	1ø8/10
K504	5	30/60	2ø12	1ø12	1ø12	1ø14	2ø14	1ø14	1ø14	1ø8/10	1ø8/20	1ø8/10
K505	5	30/60	2ø12	1ø12	1ø12	1ø14	2ø14	1ø14	1ø14	1ø8/10	1ø8/20	1ø8/10
K506	5	30/60	2ø12	1ø12	1ø12	1ø14	2ø14	1ø14	1ø14	1ø8/10	1ø8/20	1ø8/10

Table A1-5 8 Story building F-F axle column reinforcement details

Column	Story	b1	b2	Longitudinal Reinf.			Transverse Reinf.
S6	1	60	30	4x1ø18	+	2x2ø18	ø8/15-8
S6	2	60	30	4x1ø18	+	2x2ø18	ø8/15-8
S6	3	60	30	4x1ø18	+	2x2ø18	ø8/15-10
S6	4	60	30	4x1ø18	+	2x2ø18	ø8/15-10
S6	5	60	30	4x1ø18	+	2x2ø18	ø8/15-10
S6	6	60	30	4x1ø18	+	2x2ø18	ø8/15-10
S6	7	60	30	4x1ø18	+	2x2ø18	ø8/15-10
S6	8	60	30	4x1ø18	+	2x2ø18	ø8/15-10
S7	1	30	60	4x1ø18	+	2x2ø18	ø8/15-8
S7	2	30	60	4x1ø18	+	2x2ø18	ø8/15-8
S7	3	30	60	4x1ø18	+	2x2ø18	ø8/15-8
S7	4	30	60	4x1ø18	+	2x2ø18	ø8/10
S7	5	30	60	4x1ø18	+	2x2ø18	ø8/11-10
S7	6	30	60	4x1ø18	+	2x2ø18	ø8/15-10
S7	7	30	60	4x1ø18	+	2x2ø18	ø8/15-10
S7	8	30	60	4x1ø18	+	2x2ø18	ø8/15-10
S8	1	60	30	4x1ø18	+	2x2ø18	ø8/15-8
S8	2	60	30	4x1ø18	+	2x2ø18	ø8/15-8
S8	3	60	30	4x1ø18	+	2x2ø18	ø8/15-8
S8	4	60	30	4x1ø18	+	2x2ø18	ø8/15-8
S8	5	60	30	4x1ø18	+	2x2ø18	ø8/14-10
S8	6	60	30	4x1ø18	+	2x2ø18	ø8/15-10
S8	7	60	30	4x1ø18	+	2x2ø18	ø8/15-10

Table A1-5 cont.) 8 Story building F-F axle column reinforcement details

Column	Story	b1	b2	Longitudinal Reinf.			Transverse Reinf.
S8	8	60	30	4x1ø18	+	2x2ø18	ø8/15-10
S9	1	30	60	4x1ø18	+	2x2ø18	ø8/15-8
S9	2	30	60	4x1ø18	+	2x2ø18	ø8/15-8
S9	3	30	60	4x1ø18	+	2x2ø18	ø8/15-8
S9	4	30	60	4x1ø18	+	2x2ø18	ø8/10
S9	5	30	60	4x1ø18	+	2x2ø18	ø8/11-10
S9	6	30	60	4x1ø18	+	2x2ø18	ø8/15-10
S9	7	30	60	4x1ø18	+	2x2ø18	ø8/15-10
S9	8	30	60	4x1ø18	+	2x2ø18	ø8/15-10
S10	1	60	30	4x1ø18	+	2x2ø18	ø8/15-8
S10	2	60	30	4x1ø18	+	2x2ø18	ø8/15-8
S10	3	60	30	4x1ø18	+	2x2ø18	ø8/15-8
S10	4	60	30	4x1ø18	+	2x2ø18	ø8/15-10
S10	5	60	30	4x1ø18	+	2x2ø18	ø8/15-10
S10	6	60	30	4x1ø18	+	2x2ø18	ø8/15-10
S10	7	60	30	4x1ø18	+	2x2ø18	ø8/15-10
S10	8	60	30	4x1ø18	+	2x2ø18	ø8/15-10

Table A1-6 8 Story building F-F axle beam reinforcement details

Beam	Story	Dimension	Montage	Top / Left	Top / Right	Bend-up	Bottom	Bottom /Left	Bottom /Right	Left Transverse	Mid Span. Transverse	Right Transverse
K105	1	30/50	2ø12	4ø12	2ø12	1ø14	2ø14	2ø12	2ø12	1ø8/10	1ø8/20	1ø8/10
K106	1	30/50	2ø12	2ø12	2ø12	1ø14	2ø14	2ø12	2ø12	1ø8/10	1ø8/20	1ø8/10
K107	1	30/50	2ø12	2ø12	2ø12	1ø14	2ø14	2ø12	2ø12	1ø8/10	1ø8/20	1ø8/10
K108	1	30/50	2ø12	2ø12	4ø12	1ø14	2ø14	2ø12	3ø12	1ø8/10	1ø8/20	1ø8/10
K205	2	30/50	2ø12	4ø14	2ø12	1ø14	2ø14	3ø12	2ø12	1ø8/10	1ø8/20	1ø8/10
K206	2	30/50	2ø12	2ø12	2ø12	1ø14	2ø14	2ø12	3ø12	1ø8/10	1ø8/20	1ø8/10
K207	2	30/50	2ø12	2ø12	2ø12	1ø14	2ø14	3ø12	2ø12	1ø8/10	1ø8/20	1ø8/10
K208	2	30/50	2ø12	2ø12	4ø14	1ø14	2ø14	2ø12	3ø12	1ø8/10	1ø8/20	1ø8/10
K305	3	30/50	2ø12	3ø14	2ø12	1ø14	2ø14	1ø12	1ø12	1ø8/10	1ø8/20	1ø8/10
K306	3	30/50	2ø12	2ø12	2ø12	1ø14	2ø14	1ø12	3ø12	1ø8/10	1ø8/20	1ø8/10
K307	3	30/50	2ø12	2ø12	2ø12	1ø14	2ø14	3ø12	1ø12	1ø8/10	1ø8/20	1ø8/10
K308	3	30/50	2ø12	2ø12	3ø14	1ø14	2ø14	1ø12	2ø12	1ø8/10	1ø8/20	1ø8/10
K405	4	30/50	2ø12	4ø12	2ø12	1ø14	2ø14	1ø12	1ø12	1ø8/10	1ø8/20	1ø8/10
K406	4	30/50	2ø12	2ø12	2ø12	1ø14	2ø14	1ø12	3ø12	1ø8/10	1ø8/20	1ø8/10
K407	4	30/50	2ø12	2ø12	2ø12	1ø14	2ø14	3ø12	1ø12	1ø8/10	1ø8/20	1ø8/10
K408	4	30/50	2ø12	2ø12	4ø12	1ø14	2ø14	1ø12	1ø12	1ø8/10	1ø8/20	1ø8/10
K505	5	30/50	2ø12	3ø12	1ø12	1ø14	2ø14	1ø12	1ø12	1ø8/10	1ø8/20	1ø8/10
K506	5	30/50	2ø12	1ø12	1ø12	1ø14	2ø14	1ø12	2ø12	1ø8/10	1ø8/20	1ø8/10
K507	5	30/50	2ø12	1ø12	1ø12	1ø14	2ø14	2ø12	1ø12	1ø8/10	1ø8/20	1ø8/10
K508	5	30/50	2ø12	1ø12	3ø12	1ø14	2ø14	1ø12	1ø12	1ø8/10	1ø8/20	1ø8/10

Table A1-6 (cont.) 8 Story building F-F axle beam reinforcement details

Beam	Story	Dimension	Montage	Top / Left	Top / Right	Bend-up	Bottom	Bottom /Left	Bottom /Right	Left Transverse	Mid Span. Transverse	Right Transverse
K605	6	30/50	2ø12	2ø12		1ø14	2ø14	1ø12	1ø12	1ø8/10	1ø8/20	1ø8/10
K606	6	30/50	2ø12			1ø14	2ø14	1ø12	1ø12	1ø8/10	1ø8/20	1ø8/10
K607	6	30/50	2ø12			1ø14	2ø14	1ø12	1ø12	1ø8/10	1ø8/20	1ø8/10
K608	6	30/50	2ø12		2ø12	1ø14	2ø14	1ø12	1ø12	1ø8/10	1ø8/20	1ø8/10
K705	7	30/50	2ø12	1ø12		1ø14	2ø14	1ø12	1ø12	1ø8/10	1ø8/20	1ø8/10
K706	7	30/50	2ø12			1ø14	2ø14	1ø12	1ø12	1ø8/10	1ø8/20	1ø8/10
K707	7	30/50	2ø12			1ø14	2ø14	1ø12	1ø12	1ø8/10	1ø8/20	1ø8/10
K708	7	30/50	2ø12		1ø12	1ø14	2ø14	1ø12	1ø12	1ø8/10	1ø8/20	1ø8/10
K805	8	30/50	2ø12			1ø14	2ø14	1ø12	1ø12	1ø8/10	1ø8/20	1ø8/10
K806	8	30/50	2ø12			1ø14	2ø14	1ø12	1ø12	1ø8/10	1ø8/20	1ø8/10
K807	8	30/50	2ø12			1ø14	2ø14	1ø12	1ø12	1ø8/10	1ø8/20	1ø8/10
K808	8	30/50	2ø12			1ø14	2ø14	1ø12	1ø12	1ø8/10	1ø8/20	1ø8/10

Table A1-7 3 Story Frames

Number	Name of the Frame
1	3S_B_H3.0_CDM0.8_RM1.0
2	3S_B_H3.0_CDM0.8_RM1.5
3	3S_B_H3.0_CDM1.0_RM1.0 (Base Case)
4	3S_B_H3.0_CDM1.0_RM1.5
5	3S_B_H4.0_CDM0.8_RM1.0
6	3S_B_H4.0_CDM0.8_RM1.5
7	3S_B_H4.0_CDM1.0_RM1.0
8	3S_B_H4.0_CDM1.0_RM1.5
9	3S_B_H5.0_CDM0.8_RM1.0
10	3S_B_H5.0_CDM0.8_RM1.5
11	3S_B_H5.0_CDM1.0_RM1.0
12	3S_B_H5.0_CDM1.0_RM1.5
13	3S_I_1_H3.0_CDM0.8_RM1.0
14	3S_I_1_H3.0_CDM0.8_RM1.5
15	3S_I_1_H3.0_CDM1.0_RM1.0
16	3S_I_1_H3.0_CDM1.0_RM1.5
17	3S_I_1_H4.0_CDM0.8_RM1.0
18	3S_I_1_H4.0_CDM0.8_RM1.5
19	3S_I_1_H4.0_CDM1.0_RM1.0
20	3S_I_1_H4.0_CDM1.0_RM1.5
21	3S_I_1_H5.0_CDM0.8_RM1.0
22	3S_I_1_H5.0_CDM0.8_RM1.5
23	3S_I_1_H5.0_CDM1.0_RM1.0
24	3S_I_1_H5.0_CDM1.0_RM1.5
25	3S_I_1_wo_1_H3.0_CDM0.8_RM1.0
26	3S_I_1_wo_1_H3.0_CDM0.8_RM1.5
27	3S_I_1_wo_1_H3.0_CDM1.0_RM1.0
28	3S_I_1_wo_1_H3.0_CDM1.0_RM1.5
29	3S_I_1_wo_1_H4.0_CDM0.8_RM1.0
30	3S_I_1_wo_1_H4.0_CDM0.8_RM1.5
31	3S_I_1_wo_1_H4.0_CDM1.0_RM1.0
32	3S_I_1_wo_1_H4.0_CDM1.0_RM1.5
33	3S_I_1_wo_1_H5.0_CDM0.8_RM1.0
34	3S_I_1_wo_1_H5.0_CDM0.8_RM1.5
35	3S_I_1_wo_1_H5.0_CDM1.0_RM1.0
36	3S_I_1_wo_1_H5.0_CDM1.0_RM1.5
37	3S_I_2_H3.0_CDM0.8_RM1.0
38	3S_I_2_H3.0_CDM0.8_RM1.5
39	3S_I_2_H3.0_CDM1.0_RM1.0

40	3S_I_2_H3.0_CDM1.0_RM1.5
41	3S_I_2_H4.0_CDM0.8_RM1.0
42	3S_I_2_H4.0_CDM0.8_RM1.5
43	3S_I_2_H4.0_CDM1.0_RM1.0
44	3S_I_2_H4.0_CDM1.0_RM1.5
45	3S_I_2_H5.0_CDM0.8_RM1.0
46	3S_I_2_H5.0_CDM0.8_RM1.5
47	3S_I_2_H5.0_CDM1.0_RM1.0
48	3S_I_2_H5.0_CDM1.0_RM1.5
49	3S_I_2_wo_1_H3.0_CDM0.8_RM1.0
50	3S_I_2_wo_1_H3.0_CDM0.8_RM1.5
51	3S_I_2_wo_1_H3.0_CDM1.0_RM1.0
52	3S_I_2_wo_1_H3.0_CDM1.0_RM1.5
53	3S_I_2_wo_1_H4.0_CDM0.8_RM1.0
54	3S_I_2_wo_1_H4.0_CDM0.8_RM1.5
55	3S_I_2_wo_1_H4.0_CDM1.0_RM1.0
56	3S_I_2_wo_1_H4.0_CDM1.0_RM1.5
57	3S_I_2_wo_1_H5.0_CDM0.8_RM1.0
58	3S_I_2_wo_1_H5.0_CDM0.8_RM1.5
59	3S_I_2_wo_1_H5.0_CDM1.0_RM1.0
60	3S_I_2_wo_1_H5.0_CDM1.0_RM1.5
61	3S_I_12_H3.0_CDM0.8_RM1.0
62	3S_I_12_H3.0_CDM0.8_RM1.5
63	3S_I_12_H3.0_CDM1.0_RM1.0
64	3S_I_12_H3.0_CDM1.0_RM1.5
65	3S_I_12_H4.0_CDM0.8_RM1.0
66	3S_I_12_H4.0_CDM0.8_RM1.5
67	3S_I_12_H4.0_CDM1.0_RM1.0
68	3S_I_12_H4.0_CDM1.0_RM1.5
69	3S_I_12_H5.0_CDM0.8_RM1.0
70	3S_I_12_H5.0_CDM0.8_RM1.5
71	3S_I_12_H5.0_CDM1.0_RM1.0
72	3S_I_12_H5.0_CDM1.0_RM1.5
73	3S_I_12_wo_1_H3.0_CDM0.8_RM1.0
74	3S_I_12_wo_1_H3.0_CDM0.8_RM1.5
75	3S_I_12_wo_1_H3.0_CDM1.0_RM1.0
76	3S_I_12_wo_1_H3.0_CDM1.0_RM1.5
77	3S_I_12_wo_1_H4.0_CDM0.8_RM1.0
78	3S_I_12_wo_1_H4.0_CDM0.8_RM1.5
79	3S_I_12_wo_1_H4.0_CDM1.0_RM1.0
80	3S_I_12_wo_1_H4.0_CDM1.0_RM1.5
81	3S_I_12_wo_1_H5.0_CDM0.8_RM1.0
82	3S_I_12_wo_1_H5.0_CDM0.8_RM1.5

83	3S_I_12_wo_1_H5.0_CDM1.0_RM1.0
84	3S_I_12_wo_1_H5.0_CDM1.0_RM1.5

Table A1-8 5 Story Frames

Number	Name of the Frame
1	5S_B_H3.0_CDM0.8_RM1.0
2	5S_B_H3.0_CDM0.8_RM1.5
3	5S_B_H3.0_CDM1.0_RM1.0 (Base Case)
4	5S_B_H3.0_CDM1.0_RM1.5
5	5S_B_H4.0_CDM0.8_RM1.0
6	5S_B_H4.0_CDM0.8_RM1.5
7	5S_B_H4.0_CDM1.0_RM1.0
8	5S_B_H4.0_CDM1.0_RM1.5
9	5S_B_H5.0_CDM0.8_RM1.0
10	5S_B_H5.0_CDM0.8_RM1.5
11	5S_B_H5.0_CDM1.0_RM1.0
12	5S_B_H5.0_CDM1.0_RM1.5
13	5S_I_1_H3.0_CDM0.8_RM1.0
14	5S_I_1_H3.0_CDM0.8_RM1.5
15	5S_I_1_H3.0_CDM1.0_RM1.0
16	5S_I_1_H3.0_CDM1.0_RM1.5
17	5S_I_1_H4.0_CDM0.8_RM1.0
18	5S_I_1_H4.0_CDM0.8_RM1.5
19	5S_I_1_H4.0_CDM1.0_RM1.0
20	5S_I_1_H4.0_CDM1.0_RM1.5
21	5S_I_1_H5.0_CDM0.8_RM1.0
22	5S_I_1_H5.0_CDM0.8_RM1.5
23	5S_I_1_H5.0_CDM1.0_RM1.0
24	5S_I_1_H5.0_CDM1.0_RM1.5
25	5S_I_1_wo_1_H3.0_CDM0.8_RM1.0
26	5S_I_1_wo_1_H3.0_CDM0.8_RM1.5
27	5S_I_1_wo_1_H3.0_CDM1.0_RM1.0
28	5S_I_1_wo_1_H3.0_CDM1.0_RM1.5
29	5S_I_1_wo_1_H4.0_CDM0.8_RM1.0
30	5S_I_1_wo_1_H4.0_CDM0.8_RM1.5
31	5S_I_1_wo_1_H4.0_CDM1.0_RM1.0
32	5S_I_1_wo_1_H4.0_CDM1.0_RM1.5
33	5S_I_1_wo_1_H5.0_CDM0.8_RM1.0

34	5S_I_1_wo_1_H5.0_CDM0.8_RM1.5
35	5S_I_1_wo_1_H5.0_CDM1.0_RM1.0
36	5S_I_1_wo_1_H5.0_CDM1.0_RM1.5
37	5S_I_2_H3.0_CDM0.8_RM1.0
38	5S_I_2_H3.0_CDM0.8_RM1.5
39	5S_I_2_H3.0_CDM1.0_RM1.0
40	5S_I_2_H3.0_CDM1.0_RM1.5
41	5S_I_2_H4.0_CDM0.8_RM1.0
42	5S_I_2_H4.0_CDM0.8_RM1.5
43	5S_I_2_H4.0_CDM1.0_RM1.0
44	5S_I_2_H4.0_CDM1.0_RM1.5
45	5S_I_2_H5.0_CDM0.8_RM1.0
46	5S_I_2_H5.0_CDM0.8_RM1.5
47	5S_I_2_H5.0_CDM1.0_RM1.0
48	5S_I_2_H5.0_CDM1.0_RM1.5
49	5S_I_2_wo_1_H3.0_CDM0.8_RM1.0
50	5S_I_2_wo_1_H3.0_CDM0.8_RM1.5
51	5S_I_2_wo_1_H3.0_CDM1.0_RM1.0
52	5S_I_2_wo_1_H3.0_CDM1.0_RM1.5
53	5S_I_2_wo_1_H4.0_CDM0.8_RM1.0
54	5S_I_2_wo_1_H4.0_CDM0.8_RM1.5
55	5S_I_2_wo_1_H4.0_CDM1.0_RM1.0
56	5S_I_2_wo_1_H4.0_CDM1.0_RM1.5
57	5S_I_2_wo_1_H5.0_CDM0.8_RM1.0
58	5S_I_2_wo_1_H5.0_CDM0.8_RM1.5
59	5S_I_2_wo_1_H5.0_CDM1.0_RM1.0
60	5S_I_2_wo_1_H5.0_CDM1.0_RM1.5
61	5S_I_3_H3.0_CDM0.8_RM1.0
62	5S_I_3_H3.0_CDM0.8_RM1.5
63	5S_I_3_H3.0_CDM1.0_RM1.0
64	5S_I_3_H3.0_CDM1.0_RM1.5
65	5S_I_3_H4.0_CDM0.8_RM1.0
66	5S_I_3_H4.0_CDM0.8_RM1.5
67	5S_I_3_H4.0_CDM1.0_RM1.0
68	5S_I_3_H4.0_CDM1.0_RM1.5
69	5S_I_3_H5.0_CDM0.8_RM1.0
70	5S_I_3_H5.0_CDM0.8_RM1.5
71	5S_I_3_H5.0_CDM1.0_RM1.0
72	5S_I_3_H5.0_CDM1.0_RM1.5
73	5S_I_3_wo_1_H3.0_CDM0.8_RM1.0
74	5S_I_3_wo_1_H3.0_CDM0.8_RM1.5
75	5S_I_3_wo_1_H3.0_CDM1.0_RM1.0
76	5S_I_3_wo_1_H3.0_CDM1.0_RM1.5

77	5S_I_3_wo_1_H4.0_CDM0.8_RM1.0
78	5S_I_3_wo_1_H4.0_CDM0.8_RM1.5
79	5S_I_3_wo_1_H4.0_CDM1.0_RM1.0
80	5S_I_3_wo_1_H4.0_CDM1.0_RM1.5
81	5S_I_3_wo_1_H5.0_CDM0.8_RM1.0
82	5S_I_3_wo_1_H5.0_CDM0.8_RM1.5
83	5S_I_3_wo_1_H5.0_CDM1.0_RM1.0
84	5S_I_3_wo_1_H5.0_CDM1.0_RM1.5
85	5S_I_12_H3.0_CDM0.8_RM1.0
86	5S_I_12_H3.0_CDM0.8_RM1.5
87	5S_I_12_H3.0_CDM1.0_RM1.0
88	5S_I_12_H3.0_CDM1.0_RM1.5
89	5S_I_12_H4.0_CDM0.8_RM1.0
90	5S_I_12_H4.0_CDM0.8_RM1.5
91	5S_I_12_H4.0_CDM1.0_RM1.0
92	5S_I_12_H4.0_CDM1.0_RM1.5
93	5S_I_12_H5.0_CDM0.8_RM1.0
94	5S_I_12_H5.0_CDM0.8_RM1.5
95	5S_I_12_H5.0_CDM1.0_RM1.0
96	5S_I_12_H5.0_CDM1.0_RM1.5
97	5S_I_12_wo_1_H3.0_CDM0.8_RM1.0
98	5S_I_12_wo_1_H3.0_CDM0.8_RM1.5
99	5S_I_12_wo_1_H3.0_CDM1.0_RM1.0
100	5S_I_12_wo_1_H3.0_CDM1.0_RM1.5
101	5S_I_12_wo_1_H4.0_CDM0.8_RM1.0
102	5S_I_12_wo_1_H4.0_CDM0.8_RM1.5
103	5S_I_12_wo_1_H4.0_CDM1.0_RM1.0
104	5S_I_12_wo_1_H4.0_CDM1.0_RM1.5
105	5S_I_12_wo_1_H5.0_CDM0.8_RM1.0
106	5S_I_12_wo_1_H5.0_CDM0.8_RM1.5
107	5S_I_12_wo_1_H5.0_CDM1.0_RM1.0
108	5S_I_12_wo_1_H5.0_CDM1.0_RM1.5
109	5S_I_13_H3.0_CDM0.8_RM1.0
110	5S_I_13_H3.0_CDM0.8_RM1.5
111	5S_I_13_H3.0_CDM1.0_RM1.0
112	5S_I_13_H3.0_CDM1.0_RM1.5
113	5S_I_13_H4.0_CDM0.8_RM1.0
114	5S_I_13_H4.0_CDM0.8_RM1.5
115	5S_I_13_H4.0_CDM1.0_RM1.0
116	5S_I_13_H4.0_CDM1.0_RM1.5
117	5S_I_13_H5.0_CDM0.8_RM1.0
118	5S_I_13_H5.0_CDM0.8_RM1.5
119	5S_I_13_H5.0_CDM1.0_RM1.0

120	5S_I_13_H5.0_CDM1.0_RM1.5
121	5S_I_13_wo_1_H3.0_CDM0.8_RM1.0
122	5S_I_13_wo_1_H3.0_CDM0.8_RM1.5
123	5S_I_13_wo_1_H3.0_CDM1.0_RM1.0
124	5S_I_13_wo_1_H3.0_CDM1.0_RM1.5
125	5S_I_13_wo_1_H4.0_CDM0.8_RM1.0
126	5S_I_13_wo_1_H4.0_CDM0.8_RM1.5
127	5S_I_13_wo_1_H4.0_CDM1.0_RM1.0
128	5S_I_13_wo_1_H4.0_CDM1.0_RM1.5
129	5S_I_13_wo_1_H5.0_CDM0.8_RM1.0
130	5S_I_13_wo_1_H5.0_CDM0.8_RM1.5
131	5S_I_13_wo_1_H5.0_CDM1.0_RM1.0
132	5S_I_13_wo_1_H5.0_CDM1.0_RM1.5
133	5S_I_23_H3.0_CDM0.8_RM1.0
134	5S_I_23_H3.0_CDM0.8_RM1.5
135	5S_I_23_H3.0_CDM1.0_RM1.0
136	5S_I_23_H3.0_CDM1.0_RM1.5
137	5S_I_23_H4.0_CDM0.8_RM1.0
138	5S_I_23_H4.0_CDM0.8_RM1.5
139	5S_I_23_H4.0_CDM1.0_RM1.0
140	5S_I_23_H4.0_CDM1.0_RM1.5
141	5S_I_23_H5.0_CDM0.8_RM1.0
142	5S_I_23_H5.0_CDM0.8_RM1.5
143	5S_I_23_H5.0_CDM1.0_RM1.0
144	5S_I_23_H5.0_CDM1.0_RM1.5
145	5S_I_23_wo_1_H3.0_CDM0.8_RM1.0
146	5S_I_23_wo_1_H3.0_CDM0.8_RM1.5
147	5S_I_23_wo_1_H3.0_CDM1.0_RM1.0
148	5S_I_23_wo_1_H3.0_CDM1.0_RM1.5
149	5S_I_23_wo_1_H4.0_CDM0.8_RM1.0
150	5S_I_23_wo_1_H4.0_CDM0.8_RM1.5
151	5S_I_23_wo_1_H4.0_CDM1.0_RM1.0
152	5S_I_23_wo_1_H4.0_CDM1.0_RM1.5
153	5S_I_23_wo_1_H5.0_CDM0.8_RM1.0
154	5S_I_23_wo_1_H5.0_CDM0.8_RM1.5
155	5S_I_23_wo_1_H5.0_CDM1.0_RM1.0
156	5S_I_23_wo_1_H5.0_CDM1.0_RM1.5
157	5S_I_123_H3.0_CDM0.8_RM1.0
158	5S_I_123_H3.0_CDM0.8_RM1.5
159	5S_I_123_H3.0_CDM1.0_RM1.0
160	5S_I_123_H3.0_CDM1.0_RM1.5
161	5S_I_123_H4.0_CDM0.8_RM1.0
162	5S_I_123_H4.0_CDM0.8_RM1.5

163	5S_I_123_H4.0_CDM1.0_RM1.0
164	5S_I_123_H4.0_CDM1.0_RM1.5
165	5S_I_123_H5.0_CDM0.8_RM1.0
166	5S_I_123_H5.0_CDM0.8_RM1.5
167	5S_I_123_H5.0_CDM1.0_RM1.0
168	5S_I_123_H5.0_CDM1.0_RM1.5
169	5S_I_123_wo_1_H3.0_CDM0.8_RM1.0
170	5S_I_123_wo_1_H3.0_CDM0.8_RM1.5
171	5S_I_123_wo_1_H3.0_CDM1.0_RM1.0
172	5S_I_123_wo_1_H3.0_CDM1.0_RM1.5
173	5S_I_123_wo_1_H4.0_CDM0.8_RM1.0
174	5S_I_123_wo_1_H4.0_CDM0.8_RM1.5
175	5S_I_123_wo_1_H4.0_CDM1.0_RM1.0
176	5S_I_123_wo_1_H4.0_CDM1.0_RM1.5
177	5S_I_123_wo_1_H5.0_CDM0.8_RM1.0
178	5S_I_123_wo_1_H5.0_CDM0.8_RM1.5
179	5S_I_123_wo_1_H5.0_CDM1.0_RM1.0
180	5S_I_123_wo_1_H5.0_CDM1.0_RM1.5

Table A1-9 8 Story Frames

Number	**Name of the Frame**
1	8S_B_H3.0_CDM0.8_RM1.0
2	8S_B_H3.0_CDM0.8_RM1.5
3	8S_B_H3.0_CDM1.0_RM1.0 (Base Case)
4	8S_B_H3.0_CDM1.0_RM1.5
5	8S_B_H4.0_CDM0.8_RM1.0
6	8S_B_H4.0_CDM0.8_RM1.5
7	8S_B_H4.0_CDM1.0_RM1.0
8	8S_B_H4.0_CDM1.0_RM1.5
9	8S_B_H5.0_CDM0.8_RM1.0
10	8S_B_H5.0_CDM0.8_RM1.5
11	8S_B_H5.0_CDM1.0_RM1.0
12	8S_B_H5.0_CDM1.0_RM1.5
13	8S_I_1_H3.0_CDM0.8_RM1.0
14	8S_I_1_H3.0_CDM0.8_RM1.5
15	8S_I_1_H3.0_CDM1.0_RM1.0
16	8S_I_1_H3.0_CDM1.0_RM1.5
17	8S_I_1_H4.0_CDM0.8_RM1.0
18	8S_I_1_H4.0_CDM0.8_RM1.5
19	8S_I_1_H4.0_CDM1.0_RM1.0

20	8S_I_1_H4.0_CDM1.0_RM1.5
21	8S_I_1_H5.0_CDM0.8_RM1.0
22	8S_I_1_H5.0_CDM0.8_RM1.5
23	8S_I_1_H5.0_CDM1.0_RM1.0
24	8S_I_1_H5.0_CDM1.0_RM1.5
25	8S_I_1_wo_1_H3.0_CDM0.8_RM1.0
26	8S_I_1_wo_1_H3.0_CDM0.8_RM1.5
27	8S_I_1_wo_1_H3.0_CDM1.0_RM1.0
28	8S_I_1_wo_1_H3.0_CDM1.0_RM1.5
29	8S_I_1_wo_1_H4.0_CDM0.8_RM1.0
30	8S_I_1_wo_1_H4.0_CDM0.8_RM1.5
31	8S_I_1_wo_1_H4.0_CDM1.0_RM1.0
32	8S_I_1_wo_1_H4.0_CDM1.0_RM1.5
33	8S_I_1_wo_1_H5.0_CDM0.8_RM1.0
34	8S_I_1_wo_1_H5.0_CDM0.8_RM1.5
35	8S_I_1_wo_1_H5.0_CDM1.0_RM1.0
36	8S_I_1_wo_1_H5.0_CDM1.0_RM1.5
37	8S_I_2_H3.0_CDM0.8_RM1.0
38	8S_I_2_H3.0_CDM0.8_RM1.5
39	8S_I_2_H3.0_CDM1.0_RM1.0
40	8S_I_2_H3.0_CDM1.0_RM1.5
41	8S_I_2_H4.0_CDM0.8_RM1.0
42	8S_I_2_H4.0_CDM0.8_RM1.5
43	8S_I_2_H4.0_CDM1.0_RM1.0
44	8S_I_2_H4.0_CDM1.0_RM1.5
45	8S_I_2_H5.0_CDM0.8_RM1.0
46	8S_I_2_H5.0_CDM0.8_RM1.5
47	8S_I_2_H5.0_CDM1.0_RM1.0
48	8S_I_2_H5.0_CDM1.0_RM1.5
49	8S_I_2_wo_1_H3.0_CDM0.8_RM1.0
50	8S_I_2_wo_1_H3.0_CDM0.8_RM1.5
51	8S_I_2_wo_1_H3.0_CDM1.0_RM1.0
52	8S_I_2_wo_1_H3.0_CDM1.0_RM1.5
53	8S_I_2_wo_1_H4.0_CDM0.8_RM1.0
54	8S_I_2_wo_1_H4.0_CDM0.8_RM1.5
55	8S_I_2_wo_1_H4.0_CDM1.0_RM1.0
56	8S_I_2_wo_1_H4.0_CDM1.0_RM1.5
57	8S_I_2_wo_1_H5.0_CDM0.8_RM1.0
58	8S_I_2_wo_1_H5.0_CDM0.8_RM1.5
59	8S_I_2_wo_1_H5.0_CDM1.0_RM1.0
60	8S_I_2_wo_1_H5.0_CDM1.0_RM1.5
61	8S_I_3_H3.0_CDM0.8_RM1.0
62	8S_I_3_H3.0_CDM0.8_RM1.5

63	8S_I_3_H3.0_CDM1.0_RM1.0
64	8S_I_3_H3.0_CDM1.0_RM1.5
65	8S_I_3_H4.0_CDM0.8_RM1.0
66	8S_I_3_H4.0_CDM0.8_RM1.5
67	8S_I_3_H4.0_CDM1.0_RM1.0
68	8S_I_3_H4.0_CDM1.0_RM1.5
69	8S_I_3_H5.0_CDM0.8_RM1.0
70	8S_I_3_H5.0_CDM0.8_RM1.5
71	8S_I_3_H5.0_CDM1.0_RM1.0
72	8S_I_3_H5.0_CDM1.0_RM1.5
73	8S_I_3_wo_1_H3.0_CDM0.8_RM1.0
74	8S_I_3_wo_1_H3.0_CDM0.8_RM1.5
75	8S_I_3_wo_1_H3.0_CDM1.0_RM1.0
76	8S_I_3_wo_1_H3.0_CDM1.0_RM1.5
77	8S_I_3_wo_1_H4.0_CDM0.8_RM1.0
78	8S_I_3_wo_1_H4.0_CDM0.8_RM1.5
79	8S_I_3_wo_1_H4.0_CDM1.0_RM1.0
80	8S_I_3_wo_1_H4.0_CDM1.0_RM1.5
81	8S_I_3_wo_1_H5.0_CDM0.8_RM1.0
82	8S_I_3_wo_1_H5.0_CDM0.8_RM1.5
83	8S_I_3_wo_1_H5.0_CDM1.0_RM1.0
84	8S_I_3_wo_1_H5.0_CDM1.0_RM1.5
85	8S_I_4_H3.0_CDM0.8_RM1.0
86	8S_I_4_H3.0_CDM0.8_RM1.5
87	8S_I_4_H3.0_CDM1.0_RM1.0
88	8S_I_4_H3.0_CDM1.0_RM1.5
89	8S_I_4_H4.0_CDM0.8_RM1.0
90	8S_I_4_H4.0_CDM0.8_RM1.5
91	8S_I_4_H4.0_CDM1.0_RM1.0
92	8S_I_4_H4.0_CDM1.0_RM1.5
93	8S_I_4_H5.0_CDM0.8_RM1.0
94	8S_I_4_H5.0_CDM0.8_RM1.5
95	8S_I_4_H5.0_CDM1.0_RM1.0
96	8S_I_4_H5.0_CDM1.0_RM1.5
97	8S_I_4_wo_1_H3.0_CDM0.8_RM1.0
98	8S_I_4_wo_1_H3.0_CDM0.8_RM1.5
99	8S_I_4_wo_1_H3.0_CDM1.0_RM1.0
100	8S_I_4_wo_1_H3.0_CDM1.0_RM1.5
101	8S_I_4_wo_1_H4.0_CDM0.8_RM1.0
102	8S_I_4_wo_1_H4.0_CDM0.8_RM1.5
103	8S_I_4_wo_1_H4.0_CDM1.0_RM1.0
104	8S_I_4_wo_1_H4.0_CDM1.0_RM1.5
105	8S_I_4_wo_1_H5.0_CDM0.8_RM1.0

106	8S_I_4_wo_1_H5.0_CDM0.8_RM1.5
107	8S_I_4_wo_1_H5.0_CDM1.0_RM1.0
108	8S_I_4_wo_1_H5.0_CDM1.0_RM1.5
109	8S_I_12_H3.0_CDM0.8_RM1.0
110	8S_I_12_H3.0_CDM0.8_RM1.5
111	8S_I_12_H3.0_CDM1.0_RM1.0
112	8S_I_12_H3.0_CDM1.0_RM1.5
113	8S_I_12_H4.0_CDM0.8_RM1.0
114	8S_I_12_H4.0_CDM0.8_RM1.5
115	8S_I_12_H4.0_CDM1.0_RM1.0
116	8S_I_12_H4.0_CDM1.0_RM1.5
117	8S_I_12_H5.0_CDM0.8_RM1.0
118	8S_I_12_H5.0_CDM0.8_RM1.5
119	8S_I_12_H5.0_CDM1.0_RM1.0
120	8S_I_12_H5.0_CDM1.0_RM1.5
121	8S_I_12_wo_1_H3.0_CDM0.8_RM1.0
122	8S_I_12_wo_1_H3.0_CDM0.8_RM1.5
123	8S_I_12_wo_1_H3.0_CDM1.0_RM1.0
124	8S_I_12_wo_1_H3.0_CDM1.0_RM1.5
125	8S_I_12_wo_1_H4.0_CDM0.8_RM1.0
126	8S_I_12_wo_1_H4.0_CDM0.8_RM1.5
127	8S_I_12_wo_1_H4.0_CDM1.0_RM1.0
128	8S_I_12_wo_1_H4.0_CDM1.0_RM1.5
129	8S_I_12_wo_1_H5.0_CDM0.8_RM1.0
130	8S_I_12_wo_1_H5.0_CDM0.8_RM1.5
131	8S_I_12_wo_1_H5.0_CDM1.0_RM1.0
132	8S_I_12_wo_1_H5.0_CDM1.0_RM1.5
133	8S_I_13_H3.0_CDM0.8_RM1.0
134	8S_I_13_H3.0_CDM0.8_RM1.5
135	8S_I_13_H3.0_CDM1.0_RM1.0
136	8S_I_13_H3.0_CDM1.0_RM1.5
137	8S_I_13_H4.0_CDM0.8_RM1.0
138	8S_I_13_H4.0_CDM0.8_RM1.5
139	8S_I_13_H4.0_CDM1.0_RM1.0
140	8S_I_13_H4.0_CDM1.0_RM1.5
141	8S_I_13_H5.0_CDM0.8_RM1.0
142	8S_I_13_H5.0_CDM0.8_RM1.5
143	8S_I_13_H5.0_CDM1.0_RM1.0
144	8S_I_13_H5.0_CDM1.0_RM1.5
145	8S_I_13_wo_1_H3.0_CDM0.8_RM1.0
146	8S_I_13_wo_1_H3.0_CDM0.8_RM1.5
147	8S_I_13_wo_1_H3.0_CDM1.0_RM1.0
148	8S_I_13_wo_1_H3.0_CDM1.0_RM1.5

149	8S_I_13_wo_1_H4.0_CDM0.8_RM1.0
150	8S_I_13_wo_1_H4.0_CDM0.8_RM1.5
151	8S_I_13_wo_1_H4.0_CDM1.0_RM1.0
152	8S_I_13_wo_1_H4.0_CDM1.0_RM1.5
153	8S_I_13_wo_1_H5.0_CDM0.8_RM1.0
154	8S_I_13_wo_1_H5.0_CDM0.8_RM1.5
155	8S_I_13_wo_1_H5.0_CDM1.0_RM1.0
156	8S_I_13_wo_1_H5.0_CDM1.0_RM1.5
157	8S_I_14_H3.0_CDM0.8_RM1.0
158	8S_I_14_H3.0_CDM0.8_RM1.5
159	8S_I_14_H3.0_CDM1.0_RM1.0
160	8S_I_14_H3.0_CDM1.0_RM1.5
161	8S_I_14_H4.0_CDM0.8_RM1.0
162	8S_I_14_H4.0_CDM0.8_RM1.5
163	8S_I_14_H4.0_CDM1.0_RM1.0
164	8S_I_14_H4.0_CDM1.0_RM1.5
165	8S_I_14_H5.0_CDM0.8_RM1.0
166	8S_I_14_H5.0_CDM0.8_RM1.5
167	8S_I_14_H5.0_CDM1.0_RM1.0
168	8S_I_14_H5.0_CDM1.0_RM1.5
169	8S_I_14_wo_1_H3.0_CDM0.8_RM1.0
170	8S_I_14_wo_1_H3.0_CDM0.8_RM1.5
171	8S_I_14_wo_1_H3.0_CDM1.0_RM1.0
172	8S_I_14_wo_1_H3.0_CDM1.0_RM1.5
173	8S_I_14_wo_1_H4.0_CDM0.8_RM1.0
174	8S_I_14_wo_1_H4.0_CDM0.8_RM1.5
175	8S_I_14_wo_1_H4.0_CDM1.0_RM1.0
176	8S_I_14_wo_1_H4.0_CDM1.0_RM1.5
177	8S_I_14_wo_1_H5.0_CDM0.8_RM1.0
178	8S_I_14_wo_1_H5.0_CDM0.8_RM1.5
179	8S_I_14_wo_1_H5.0_CDM1.0_RM1.0
180	8S_I_14_wo_1_H5.0_CDM1.0_RM1.5
181	8S_I_23_H3.0_CDM0.8_RM1.0
182	8S_I_23_H3.0_CDM0.8_RM1.5
183	8S_I_23_H3.0_CDM1.0_RM1.0
184	8S_I_23_H3.0_CDM1.0_RM1.5
185	8S_I_23_H4.0_CDM0.8_RM1.0
186	8S_I_23_H4.0_CDM0.8_RM1.5
187	8S_I_23_H4.0_CDM1.0_RM1.0
188	8S_I_23_H4.0_CDM1.0_RM1.5
189	8S_I_23_H5.0_CDM0.8_RM1.0
190	8S_I_23_H5.0_CDM0.8_RM1.5
191	8S_I_23_H5.0_CDM1.0_RM1.0

192	8S_I_23_H5.0_CDM1.0_RM1.5
193	8S_I_23_wo_1_H3.0_CDM0.8_RM1.0
194	8S_I_23_wo_1_H3.0_CDM0.8_RM1.5
195	8S_I_23_wo_1_H3.0_CDM1.0_RM1.0
196	8S_I_23_wo_1_H3.0_CDM1.0_RM1.5
197	8S_I_23_wo_1_H4.0_CDM0.8_RM1.0
198	8S_I_23_wo_1_H4.0_CDM0.8_RM1.5
199	8S_I_23_wo_1_H4.0_CDM1.0_RM1.0
200	8S_I_23_wo_1_H4.0_CDM1.0_RM1.5
201	8S_I_23_wo_1_H5.0_CDM0.8_RM1.0
202	8S_I_23_wo_1_H5.0_CDM0.8_RM1.5
203	8S_I_23_wo_1_H5.0_CDM1.0_RM1.0
204	8S_I_23_wo_1_H5.0_CDM1.0_RM1.5
205	8S_I_24_H3.0_CDM0.8_RM1.0
206	8S_I_24_H3.0_CDM0.8_RM1.5
207	8S_I_24_H3.0_CDM1.0_RM1.0
208	8S_I_24_H3.0_CDM1.0_RM1.5
209	8S_I_24_H4.0_CDM0.8_RM1.0
210	8S_I_24_H4.0_CDM0.8_RM1.5
211	8S_I_24_H4.0_CDM1.0_RM1.0
212	8S_I_24_H4.0_CDM1.0_RM1.5
213	8S_I_24_H5.0_CDM0.8_RM1.0
214	8S_I_24_H5.0_CDM0.8_RM1.5
215	8S_I_24_H5.0_CDM1.0_RM1.0
216	8S_I_24_H5.0_CDM1.0_RM1.5
217	8S_I_24_wo_1_H3.0_CDM0.8_RM1.0
218	8S_I_24_wo_1_H3.0_CDM0.8_RM1.5
219	8S_I_24_wo_1_H3.0_CDM1.0_RM1.0
220	8S_I_24_wo_1_H3.0_CDM1.0_RM1.5
221	8S_I_24_wo_1_H4.0_CDM0.8_RM1.0
222	8S_I_24_wo_1_H4.0_CDM0.8_RM1.5
223	8S_I_24_wo_1_H4.0_CDM1.0_RM1.0
224	8S_I_24_wo_1_H4.0_CDM1.0_RM1.5
225	8S_I_24_wo_1_H5.0_CDM0.8_RM1.0
226	8S_I_24_wo_1_H5.0_CDM0.8_RM1.5
227	8S_I_24_wo_1_H5.0_CDM1.0_RM1.0
228	8S_I_24_wo_1_H5.0_CDM1.0_RM1.5
229	8S_I_34_H3.0_CDM0.8_RM1.0
230	8S_I_34_H3.0_CDM0.8_RM1.5
231	8S_I_34_H3.0_CDM1.0_RM1.0
232	8S_I_34_H3.0_CDM1.0_RM1.5
233	8S_I_34_H4.0_CDM0.8_RM1.0
234	8S_I_34_H4.0_CDM0.8_RM1.5

235	8S_I_34_H4.0_CDM1.0_RM1.0
236	8S_I_34_H4.0_CDM1.0_RM1.5
237	8S_I_34_H5.0_CDM0.8_RM1.0
238	8S_I_34_H5.0_CDM0.8_RM1.5
239	8S_I_34_H5.0_CDM1.0_RM1.0
240	8S_I_34_H5.0_CDM1.0_RM1.5
241	8S_I_34_wo_1_H3.0_CDM0.8_RM1.0
242	8S_I_34_wo_1_H3.0_CDM0.8_RM1.5
243	8S_I_34_wo_1_H3.0_CDM1.0_RM1.0
244	8S_I_34_wo_1_H3.0_CDM1.0_RM1.5
245	8S_I_34_wo_1_H4.0_CDM0.8_RM1.0
246	8S_I_34_wo_1_H4.0_CDM0.8_RM1.5
247	8S_I_34_wo_1_H4.0_CDM1.0_RM1.0
248	8S_I_34_wo_1_H4.0_CDM1.0_RM1.5
249	8S_I_34_wo_1_H5.0_CDM0.8_RM1.0
250	8S_I_34_wo_1_H5.0_CDM0.8_RM1.5
251	8S_I_34_wo_1_H5.0_CDM1.0_RM1.0
252	8S_I_34_wo_1_H5.0_CDM1.0_RM1.5
253	8S_I_1234_H3.0_CDM0.8_RM1.0
254	8S_I_1234_H3.0_CDM0.8_RM1.5
255	8S_I_1234_H3.0_CDM1.0_RM1.0
256	8S_I_1234_H3.0_CDM1.0_RM1.5
257	8S_I_1234_H4.0_CDM0.8_RM1.0
258	8S_I_1234_H4.0_CDM0.8_RM1.5
259	8S_I_1234_H4.0_CDM1.0_RM1.0
260	8S_I_1234_H4.0_CDM1.0_RM1.5
261	8S_I_1234_H5.0_CDM0.8_RM1.0
262	8S_I_1234_H5.0_CDM0.8_RM1.5
263	8S_I_1234_H5.0_CDM1.0_RM1.0
264	8S_I_1234_H5.0_CDM1.0_RM1.5
265	8S_I_1234_wo_1_H3.0_CDM0.8_RM1.0
266	8S_I_1234_wo_1_H3.0_CDM0.8_RM1.5
267	8S_I_1234_wo_1_H3.0_CDM1.0_RM1.0
268	8S_I_1234_wo_1_H3.0_CDM1.0_RM1.5
269	8S_I_1234_wo_1_H4.0_CDM0.8_RM1.0
270	8S_I_1234_wo_1_H4.0_CDM0.8_RM1.5
271	8S_I_1234_wo_1_H4.0_CDM1.0_RM1.0
272	8S_I_1234_wo_1_H4.0_CDM1.0_RM1.5
273	8S_I_1234_wo_1_H5.0_CDM0.8_RM1.0
274	8S_I_1234_wo_1_H5.0_CDM0.8_RM1.5
275	8S_I_1234_wo_1_H5.0_CDM1.0_RM1.0
276	8S_I_1234_wo_1_H5.0_CDM1.0_RM1.5

A2. THE VERTICAL IRREGULARITY PARAMETERS FOR ANALYSIS RESULTS

The results of the analysis were given in this appendix and the summary of analysis results for each frame was given in Chapter 5 of this thesis. Each analysis part was given separately and in detail for each frame to observe the effect of infill walls on the seismic behavior.

A2.1 Equivalent Static Load Analysis Results

Table A2-1 Soft story, weak story and max alpha values for 3 Story frame for linear analysis results

Frame Type/ Story Level	$\eta_{ki,\,max}$	$\eta_{kj,\,max}$	α_{max}
3S_B_H3.0_CDM0.8_RM1.0	1.659	1.000	**1.133**
3S_B_H3.0_CDM0.8_RM1.5	1.657	1.000	1.116
3S_B_H3.0_CDM1.0_RM1.0	1.602	1.291	1.143
3S_B_H3.0_CDM1.0_RM1.5	1.597	1.315	1.152
3S_B_H4.0_CDM0.8_RM1.0	1.732	1.000	1.212
3S_B_H4.0_CDM0.8_RM1.5	1.732	1.000	1.199
3S_B_H4.0_CDM1.0_RM1.0	1.695	1.000	1.006
3S_B_H4.0_CDM1.0_RM1.5	1.692	1.007	1.004
3S_B_H5.0_CDM0.8_RM1.0	2.154	1.000	1.231
3S_B_H5.0_CDM0.8_RM1.5	2.071	1.000	1.222
3S_B_H5.0_CDM1.0_RM1.0	1.768	1.000	1.077
3S_B_H5.0_CDM1.0_RM1.5	1.766	1.000	1.070
3S_I_1_H3.0_CDM0.8_RM1.0	1.471	1.280	1.135
3S_I_1_H3.0_CDM0.8_RM1.5	1.475	1.267	1.131
3S_I_1_H3.0_CDM1.0_RM1.0	1.504	1.258	1.128
3S_I_1_H3.0_CDM1.0_RM1.5	1.504	1.250	1.125
3S_I_1_H4.0_CDM0.8_RM1.0	1.427	1.279	1.143
3S_I_1_H4.0_CDM0.8_RM1.5	1.427	1.279	1.143
3S_I_1_H4.0_CDM1.0_RM1.0	1.475	1.224	1.117
3S_I_1_H4.0_CDM1.0_RM1.5	1.476	1.216	1.113
3S_I_1_H5.0_CDM0.8_RM1.0	1.370	1.242	1.145
3S_I_1_H5.0_CDM0.8_RM1.5	1.377	1.227	1.136
3S_I_1_H5.0_CDM1.0_RM1.0	1.429	1.164	1.101
3S_I_1_H5.0_CDM1.0_RM1.5	1.432	1.155	1.095
3S_I_1_wo_1_H3.0_CDM0.8_RM1.0	6.561	1.000	1.810
3S_I_1_wo_1_H3.0_CDM0.8_RM1.5	10.208	1.000	1.902

3S_I_1_wo_1_H3.0_CDM1.0_RM1.0	3.764	1.000	1.643
3S_I_1_wo_1_H3.0_CDM1.0_RM1.5	3.675	1.000	1.634
3S_I_1_wo_1_H4.0_CDM0.8_RM1.0	8.438	1.000	1.607
3S_I_1_wo_1_H4.0_CDM0.8_RM1.5	8.183	1.000	1.603
3S_I_1_wo_1_H4.0_CDM1.0_RM1.0	5.037	1.000	1.523
3S_I_1_wo_1_H4.0_CDM1.0_RM1.5	4.928	1.000	1.519
3S_I_1_wo_1_H5.0_CDM0.8_RM1.0	10.248	1.000	1.463
3S_I_1_wo_1_H5.0_CDM0.8_RM1.5	9.950	1.000	1.461
3S_I_1_wo_1_H5.0_CDM1.0_RM1.0	6.188	1.000	1.416
3S_I_1_wo_1_H5.0_CDM1.0_RM1.5	6.054	1.000	1.414
3S_I_2_H3.0_CDM0.8_RM1.0	1.825	1.064	1.053
3S_I_2_H3.0_CDM0.8_RM1.5	1.829	1.047	1.045
3S_I_2_H3.0_CDM1.0_RM1.0	1.867	1.038	1.041
3S_I_2_H3.0_CDM1.0_RM1.5	1.868	1.031	1.038
3S_I_2_H4.0_CDM0.8_RM1.0	1.806	1.000	1.017
3S_I_2_H4.0_CDM0.8_RM1.5	1.814	1.000	1.025
3S_I_2_H4.0_CDM1.0_RM1.0	1.884	1.000	1.041
3S_I_2_H4.0_CDM1.0_RM1.5	1.888	1.000	1.044
3S_I_2_H5.0_CDM0.8_RM1.0	1.746	1.000	1.062
3S_I_2_H5.0_CDM0.8_RM1.5	1.757	1.000	1.068
3S_I_2_H5.0_CDM1.0_RM1.0	1.856	1.000	1.088
3S_I_2_H5.0_CDM1.0_RM1.5	1.862	1.000	1.091
3S_I_2_wo_1_H3.0_CDM0.8_RM1.0	7.893	1.000	1.856
3S_I_2_wo_1_H3.0_CDM0.8_RM1.5	7.562	1.000	1.846
3S_I_2_wo_1_H3.0_CDM1.0_RM1.0	4.254	1.000	1.688
3S_I_2_wo_1_H3.0_CDM1.0_RM1.5	4.149	1.000	1.679
3S_I_2_wo_1_H4.0_CDM0.8_RM1.0	11.634	1.000	1.644
3S_I_2_wo_1_H4.0_CDM0.8_RM1.5	11.110	1.000	1.639
3S_I_2_wo_1_H4.0_CDM1.0_RM1.0	5.980	1.000	1.555
3S_I_2_wo_1_H4.0_CDM1.0_RM1.5	5.811	1.000	1.550
3S_I_2_wo_1_H5.0_CDM0.8_RM1.0	15.963	1.000	1.490
3S_I_2_wo_1_H5.0_CDM0.8_RM1.5	15.230	1.000	1.487
3S_I_2_wo_1_H5.0_CDM1.0_RM1.0	8.095	1.000	1.444
3S_I_2_wo_1_H5.0_CDM1.0_RM1.5	7.865	1.000	1.441
3S_I_12_H3.0_CDM0.8_RM1.0	1.997	1.083	1.064
3S_I_12_H3.0_CDM0.8_RM1.5	2.005	1.068	1.057
3S_I_12_H3.0_CDM1.0_RM1.0	2.044	1.012	1.031
3S_I_12_H3.0_CDM1.0_RM1.5	2.045	1.005	1.027
3S_I_12_H4.0_CDM0.8_RM1.0	1.944	1.082	1.045
3S_I_12_H4.0_CDM0.8_RM1.5	1.953	1.065	1.036
3S_I_12_H4.0_CDM1.0_RM1.0	2.017	1.000	1.003
3S_I_12_H4.0_CDM1.0_RM1.5	2.020	1.000	1.007
3S_I_12_H5.0_CDM0.8_RM1.0	1.879	1.033	1.021

3S_I_12_H5.0_CDM0.8_RM1.5	1.893	1.022	1.014
3S_I_12_H5.0_CDM1.0_RM1.0	1.984	1.000	1.025
3S_I_12_H5.0_CDM1.0_RM1.5	1.990	1.000	1.028
3S_I_12_wo_1_H3.0_CDM0.8_RM1.0	12.316	1.000	1.938
3S_I_12_wo_1_H3.0_CDM0.8_RM1.5	11.879	1.000	1.932
3S_I_12_wo_1_H3.0_CDM1.0_RM1.0	6.730	1.000	1.821
3S_I_12_wo_1_H3.0_CDM1.0_RM1.5	6.556	1.000	1.815
3S_I_12_wo_1_H4.0_CDM0.8_RM1.0	16.328	1.000	1.673
3S_I_12_wo_1_H4.0_CDM0.8_RM1.5	15.740	1.000	1.670
3S_I_12_wo_1_H4.0_CDM1.0_RM1.0	9.096	1.000	1.617
3S_I_12_wo_1_H4.0_CDM1.0_RM1.5	8.871	1.000	1.614
3S_I_12_wo_1_H5.0_CDM0.8_RM1.0	20.626	1.000	1.501
3S_I_12_wo_1_H5.0_CDM0.8_RM1.5	19.883	1.000	1.499
3S_I_12_wo_1_H5.0_CDM1.0_RM1.0	11.462	1.000	1.471
3S_I_12_wo_1_H5.0_CDM1.0_RM1.5	11.173	1.000	1.469

Table A2-2 Soft story, weak story and max alpha values for 5 Story frame for linear analysis results

Frame Type/ Story Level	$\eta_{ki,\,max}$	$\eta_{kj,\,max}$	α_{max}
5S_B_H3.0_CDM0.8_RM1.0	1.581	1.109	1.110
5S_B_H3.0_CDM0.8_RM1.5	1.582	1.155	1.121
5S_B_H3.0_CDM1.0_RM1.0	1.587	1.616	1.186
5S_B_H3.0_CDM1.0_RM1.5	1.587	1.654	1.189
5S_B_H4.0_CDM0.8_RM1.0	1.570	1.000	1.200
5S_B_H4.0_CDM0.8_RM1.5	1.572	1.000	1.167
5S_B_H4.0_CDM1.0_RM1.0	1.582	1.292	1.168
5S_B_H4.0_CDM1.0_RM1.5	1.582	1.326	1.175
5S_B_H5.0_CDM0.8_RM1.0	1.557	1.000	1.321
5S_B_H5.0_CDM0.8_RM1.5	1.559	1.000	1.290
5S_B_H5.0_CDM1.0_RM1.0	1.574	1.072	1.106
5S_B_H5.0_CDM1.0_RM1.5	1.575	1.104	1.119
5S_I_1_H3.0_CDM0.8_RM1.0	1.389	1.273	1.095
5S_I_1_H3.0_CDM0.8_RM1.5	1.392	1.286	1.098
5S_I_1_H3.0_CDM1.0_RM1.0	1.412	1.482	1.137
5S_I_1_H3.0_CDM1.0_RM1.5	1.414	1.499	1.139
5S_I_1_H4.0_CDM0.8_RM1.0	1.367	1.134	1.069
5S_I_1_H4.0_CDM0.8_RM1.5	1.371	1.144	1.072
5S_I_1_H4.0_CDM1.0_RM1.0	1.395	1.293	1.123
5S_I_1_H4.0_CDM1.0_RM1.5	1.397	1.306	1.127
5S_I_1_H5.0_CDM0.8_RM1.0	1.345	1.000	1.029
5S_I_1_H5.0_CDM0.8_RM1.5	1.349	1.000	1.026
5S_I_1_H5.0_CDM1.0_RM1.0	1.377	1.116	1.080
5S_I_1_H5.0_CDM1.0_RM1.5	1.380	1.128	1.085

5S_I_1_wo_1_H3.0_CDM0.8_RM1.0	1.708	1.000	1.538
5S_I_1_wo_1_H3.0_CDM0.8_RM1.5	1.629	1.000	1.497
5S_I_1_wo_1_H3.0_CDM1.0_RM1.0	1.414	1.000	1.146
5S_I_1_wo_1_H3.0_CDM1.0_RM1.5	1.415	1.000	1.123
5S_I_1_wo_1_H4.0_CDM0.8_RM1.0	2.285	1.000	1.670
5S_I_1_wo_1_H4.0_CDM0.8_RM1.5	2.173	1.000	1.637
5S_I_1_wo_1_H4.0_CDM1.0_RM1.0	1.398	1.000	1.332
5S_I_1_wo_1_H4.0_CDM1.0_RM1.5	1.394	1.000	1.310
5S_I_1_wo_1_H5.0_CDM0.8_RM1.0	2.854	1.000	1.683
5S_I_1_wo_1_H5.0_CDM0.8_RM1.5	2.710	1.000	1.659
5S_I_1_wo_1_H5.0_CDM1.0_RM1.0	1.715	1.000	1.417
5S_I_1_wo_1_H5.0_CDM1.0_RM1.5	1.659	1.000	1.398
5S_I_2_H3.0_CDM0.8_RM1.0	1.419	1.240	1.108
5S_I_2_H3.0_CDM0.8_RM1.5	1.421	1.246	1.110
5S_I_2_H3.0_CDM1.0_RM1.0	1.439	1.509	1.155
5S_I_2_H3.0_CDM1.0_RM1.5	1.440	1.530	1.157
5S_I_2_H4.0_CDM0.8_RM1.0	1.395	1.000	1.064
5S_I_2_H4.0_CDM0.8_RM1.5	1.399	1.000	1.054
5S_I_2_H4.0_CDM1.0_RM1.0	1.424	1.208	1.125
5S_I_2_H4.0_CDM1.0_RM1.5	1.427	1.225	1.130
5S_I_2_H5.0_CDM0.8_RM1.0	1.369	1.000	1.195
5S_I_2_H5.0_CDM0.8_RM1.5	1.373	1.000	1.185
5S_I_2_H5.0_CDM1.0_RM1.0	1.400	1.000	1.064
5S_I_2_H5.0_CDM1.0_RM1.5	1.402	1.007	1.061
5S_I_2_wo_1_H3.0_CDM0.8_RM1.0	1.413	1.000	1.366
5S_I_2_wo_1_H3.0_CDM0.8_RM1.5	1.987	1.000	1.494
5S_I_2_wo_1_H3.0_CDM1.0_RM1.0	1.997	1.032	1.146
5S_I_2_wo_1_H3.0_CDM1.0_RM1.5	2.001	1.066	1.156
5S_I_2_wo_1_H4.0_CDM0.8_RM1.0	1.857	1.000	1.533
5S_I_2_wo_1_H4.0_CDM0.8_RM1.5	1.766	1.000	1.498
5S_I_2_wo_1_H4.0_CDM1.0_RM1.0	1.414	1.000	1.196
5S_I_2_wo_1_H4.0_CDM1.0_RM1.5	1.416	1.000	1.175
5S_I_2_wo_1_H5.0_CDM0.8_RM1.0	2.341	1.000	1.591
5S_I_2_wo_1_H5.0_CDM0.8_RM1.5	2.220	1.000	1.563
5S_I_2_wo_1_H5.0_CDM1.0_RM1.0	1.414	1.000	1.303
5S_I_2_wo_1_H5.0_CDM1.0_RM1.5	1.388	1.000	1.284
5S_I_3_H3.0_CDM0.8_RM1.0	1.446	1.192	1.108
5S_I_3_H3.0_CDM0.8_RM1.5	1.449	1.208	1.112
5S_I_3_H3.0_CDM1.0_RM1.0	1.472	1.423	1.151
5S_I_3_H3.0_CDM1.0_RM1.5	1.474	1.441	1.154
5S_I_3_H4.0_CDM0.8_RM1.0	1.422	1.000	1.165
5S_I_3_H4.0_CDM0.8_RM1.5	1.426	1.000	1.153
5S_I_3_H4.0_CDM1.0_RM1.0	1.455	1.077	1.094

5S_I_3_H4.0_CDM1.0_RM1.5	1.457	1.095	1.100
5S_I_3_H5.0_CDM0.8_RM1.0	1.396	1.000	1.213
5S_I_3_H5.0_CDM0.8_RM1.5	1.400	1.000	1.205
5S_I_3_H5.0_CDM1.0_RM1.0	1.431	1.000	1.096
5S_I_3_H5.0_CDM1.0_RM1.5	1.434	1.000	1.086
5S_I_3_wo_1_H3.0_CDM0.8_RM1.0	1.593	1.000	1.485
5S_I_3_wo_1_H3.0_CDM0.8_RM1.5	1.521	1.000	1.445
5S_I_3_wo_1_H3.0_CDM1.0_RM1.0	1.475	1.000	1.118
5S_I_3_wo_1_H3.0_CDM1.0_RM1.5	1.477	1.000	1.096
5S_I_3_wo_1_H4.0_CDM0.8_RM1.0	2.126	1.000	1.634
5S_I_3_wo_1_H4.0_CDM0.8_RM1.5	2.021	1.000	1.599
5S_I_3_wo_1_H4.0_CDM1.0_RM1.0	1.449	1.000	1.290
5S_I_3_wo_1_H4.0_CDM1.0_RM1.5	1.452	1.000	1.268
5S_I_3_wo_1_H5.0_CDM0.8_RM1.0	2.700	1.000	1.672
5S_I_3_wo_1_H5.0_CDM0.8_RM1.5	2.556	1.000	1.644
5S_I_3_wo_1_H5.0_CDM1.0_RM1.0	1.607	1.000	1.385
5S_I_3_wo_1_H5.0_CDM1.0_RM1.5	1.555	1.000	1.365
5S_I_12_H3.0_CDM0.8_RM1.0	1.433	1.338	1.112
5S_I_12_H3.0_CDM0.8_RM1.5	1.436	1.336	1.113
5S_I_12_H3.0_CDM1.0_RM1.0	1.459	1.416	1.133
5S_I_12_H3.0_CDM1.0_RM1.5	1.461	1.423	1.135
5S_I_12_H4.0_CDM0.8_RM1.0	1.405	1.163	1.082
5S_I_12_H4.0_CDM0.8_RM1.5	1.410	1.160	1.083
5S_I_12_H4.0_CDM1.0_RM1.0	1.437	1.218	1.110
5S_I_12_H4.0_CDM1.0_RM1.5	1.439	1.224	1.112
5S_I_12_H5.0_CDM0.8_RM1.0	1.380	1.000	1.041
5S_I_12_H5.0_CDM0.8_RM1.5	1.385	1.000	1.043
5S_I_12_H5.0_CDM1.0_RM1.0	1.416	1.025	1.049
5S_I_12_H5.0_CDM1.0_RM1.5	1.418	1.031	1.052
5S_I_12_wo_1_H3.0_CDM0.8_RM1.0	2.357	1.000	1.859
5S_I_12_wo_1_H3.0_CDM0.8_RM1.5	2.238	1.000	1.814
5S_I_12_wo_1_H3.0_CDM1.0_RM1.0	1.459	1.000	1.418
5S_I_12_wo_1_H3.0_CDM1.0_RM1.5	1.461	1.000	1.391
5S_I_12_wo_1_H4.0_CDM0.8_RM1.0	3.169	1.000	1.911
5S_I_12_wo_1_H4.0_CDM0.8_RM1.5	3.008	1.000	1.880
5S_I_12_wo_1_H4.0_CDM1.0_RM1.0	1.885	1.000	1.576
5S_I_12_wo_1_H4.0_CDM1.0_RM1.5	1.822	1.000	1.552
5S_I_12_wo_1_H5.0_CDM0.8_RM1.0	3.961	1.000	1.855
5S_I_12_wo_1_H5.0_CDM0.8_RM1.5	3.755	1.000	1.834
5S_I_12_wo_1_H5.0_CDM1.0_RM1.0	2.332	1.000	1.614
5S_I_12_wo_1_H5.0_CDM1.0_RM1.5	3.069	1.000	1.728
5S_I_13_H3.0_CDM0.8_RM1.0	1.399	1.325	1.105
5S_I_13_H3.0_CDM0.8_RM1.5	1.403	1.321	1.104

5S_I_13_H3.0_CDM1.0_RM1.0	1.430	1.384	1.118
5S_I_13_H3.0_CDM1.0_RM1.5	1.432	1.389	1.119
5S_I_13_H4.0_CDM0.8_RM1.0	1.370	1.106	1.062
5S_I_13_H4.0_CDM0.8_RM1.5	1.375	1.101	1.061
5S_I_13_H4.0_CDM1.0_RM1.0	1.406	1.151	1.083
5S_I_13_H4.0_CDM1.0_RM1.5	1.409	1.156	1.085
5S_I_13_H5.0_CDM0.8_RM1.0	1.345	1.015	1.029
5S_I_13_H5.0_CDM0.8_RM1.5	1.350	1.008	1.027
5S_I_13_H5.0_CDM1.0_RM1.0	1.384	1.033	1.045
5S_I_13_H5.0_CDM1.0_RM1.5	1.387	1.037	1.047
5S_I_13_wo_1_H3.0_CDM0.8_RM1.0	2.490	1.000	1.880
5S_I_13_wo_1_H3.0_CDM0.8_RM1.5	2.367	1.000	1.836
5S_I_13_wo_1_H3.0_CDM1.0_RM1.0	1.530	1.000	1.449
5S_I_13_wo_1_H3.0_CDM1.0_RM1.5	1.485	1.000	1.422
5S_I_13_wo_1_H4.0_CDM0.8_RM1.0	3.335	1.000	1.925
5S_I_13_wo_1_H4.0_CDM0.8_RM1.5	3.168	1.000	1.894
5S_I_13_wo_1_H4.0_CDM1.0_RM1.0	1.998	1.000	1.595
5S_I_13_wo_1_H4.0_CDM1.0_RM1.5	1.932	1.000	1.571
5S_I_13_wo_1_H5.0_CDM0.8_RM1.0	4.177	1.000	1.866
5S_I_13_wo_1_H5.0_CDM0.8_RM1.5	3.962	1.000	1.845
5S_I_13_wo_1_H5.0_CDM1.0_RM1.0	2.462	1.000	1.627
5S_I_13_wo_1_H5.0_CDM1.0_RM1.5	2.379	1.000	1.609
5S_I_23_H3.0_CDM0.8_RM1.0	1.518	1.250	1.132
5S_I_23_H3.0_CDM0.8_RM1.5	1.522	1.248	1.132
5S_I_23_H3.0_CDM1.0_RM1.0	1.551	1.335	1.152
5S_I_23_H3.0_CDM1.0_RM1.5	1.553	1.343	1.153
5S_I_23_H4.0_CDM0.8_RM1.0	1.484	1.000	1.135
5S_I_23_H4.0_CDM0.8_RM1.5	1.489	1.000	1.134
5S_I_23_H4.0_CDM1.0_RM1.0	1.525	1.010	1.078
5S_I_23_H4.0_CDM1.0_RM1.5	1.528	1.020	1.082
5S_I_23_H5.0_CDM0.8_RM1.0	1.454	1.000	1.227
5S_I_23_H5.0_CDM0.8_RM1.5	1.460	1.000	1.226
5S_I_23_H5.0_CDM1.0_RM1.0	1.501	1.000	1.167
5S_I_23_H5.0_CDM1.0_RM1.5	1.504	1.000	1.161
5S_I_23_wo_1_H3.0_CDM0.8_RM1.0	2.313	1.000	1.862
5S_I_23_wo_1_H3.0_CDM0.8_RM1.5	2.198	1.000	1.817
5S_I_23_wo_1_H3.0_CDM1.0_RM1.0	1.553	1.000	1.433
5S_I_23_wo_1_H3.0_CDM1.0_RM1.5	1.555	1.000	1.406
5S_I_23_wo_1_H4.0_CDM0.8_RM1.0	3.137	1.000	1.928
5S_I_23_wo_1_H4.0_CDM0.8_RM1.5	2.965	1.000	1.894
5S_I_23_wo_1_H4.0_CDM1.0_RM1.0	1.840	1.000	1.572
5S_I_23_wo_1_H4.0_CDM1.0_RM1.5	1.779	1.000	1.548
5S_I_23_wo_1_H5.0_CDM0.8_RM1.0	4.032	1.000	1.883

5S_I_23_wo_1_H5.0_CDM0.8_RM1.5	3.796	1.000	1.859
5S_I_23_wo_1_H5.0_CDM1.0_RM1.0	2.275	1.000	1.616
5S_I_23_wo_1_H5.0_CDM1.0_RM1.5	2.194	1.000	1.597
5S_I_123_H3.0_CDM0.8_RM1.0	1.566	1.301	1.128
5S_I_123_H3.0_CDM0.8_RM1.5	1.571	1.290	1.126
5S_I_123_H3.0_CDM1.0_RM1.0	1.601	1.289	1.129
5S_I_123_H3.0_CDM1.0_RM1.5	1.603	1.289	1.128
5S_I_123_H4.0_CDM0.8_RM1.0	1.528	1.066	1.071
5S_I_123_H4.0_CDM0.8_RM1.5	1.534	1.059	1.069
5S_I_123_H4.0_CDM1.0_RM1.0	1.571	1.064	1.078
5S_I_123_H4.0_CDM1.0_RM1.5	1.574	1.065	1.079
5S_I_123_H5.0_CDM0.8_RM1.0	1.494	1.000	1.079
5S_I_123_H5.0_CDM0.8_RM1.5	1.500	1.000	1.085
5S_I_123_H5.0_CDM1.0_RM1.0	1.544	1.000	1.093
5S_I_123_H5.0_CDM1.0_RM1.5	1.547	1.000	1.093
5S_I_123_wo_1_H3.0_CDM0.8_RM1.0	3.351	1.000	2.191
5S_I_123_wo_1_H3.0_CDM0.8_RM1.5	3.175	1.000	2.146
5S_I_123_wo_1_H3.0_CDM1.0_RM1.0	1.997	1.000	1.739
5S_I_123_wo_1_H3.0_CDM1.0_RM1.5	1.934	1.000	1.709
5S_I_123_wo_1_H4.0_CDM0.8_RM1.0	4.574	1.000	2.142
5S_I_123_wo_1_H4.0_CDM0.8_RM1.5	4.323	1.000	2.113
5S_I_123_wo_1_H4.0_CDM1.0_RM1.0	2.629	1.000	1.824
5S_I_123_wo_1_H4.0_CDM1.0_RM1.5	2.537	1.000	1.801
5S_I_123_wo_1_H5.0_CDM0.8_RM1.0	5.831	1.000	2.012
5S_I_123_wo_1_H5.0_CDM0.8_RM1.5	5.504	1.000	1.995
5S_I_123_wo_1_H5.0_CDM1.0_RM1.0	3.280	1.000	1.800
5S_I_123_wo_1_H5.0_CDM1.0_RM1.5	3.160	1.000	1.783

Table A2-3 Soft story, weak story and max alpha values for 8 Story frame for linear analysis results

Frame Type/ Story Level	$\eta_{ki,\ max}$	$\eta_{kj,\ max}$	α_{max}
8S_B_H3.0_CDM0.8_RM1.0	1.406	1.301	1.120
8S_B_H3.0_CDM0.8_RM1.5	1.408	1.364	1.127
8S_B_H3.0_CDM1.0_RM1.0	1.483	1.893	1.192
8S_B_H3.0_CDM1.0_RM1.5	1.421	1.841	1.191
8S_B_H4.0_CDM0.8_RM1.0	1.388	1.010	1.111
8S_B_H4.0_CDM0.8_RM1.5	1.391	1.067	1.122
8S_B_H4.0_CDM1.0_RM1.0	1.406	1.455	1.150
8S_B_H4.0_CDM1.0_RM1.5	1.408	1.498	1.158
8S_B_H5.0_CDM0.8_RM1.0	1.370	1.000	1.298
8S_B_H5.0_CDM0.8_RM1.5	1.373	1.000	1.243
8S_B_H5.0_CDM1.0_RM1.0	1.391	1.221	1.160
8S_B_H5.0_CDM1.0_RM1.5	1.393	1.261	1.164

8S_I_1_H3.0_CDM0.8_RM1.0	1.230	1.406	1.110
8S_I_1_H3.0_CDM0.8_RM1.5	1.231	1.444	1.114
8S_I_1_H3.0_CDM1.0_RM1.0	1.236	1.741	1.149
8S_I_1_H3.0_CDM1.0_RM1.5	1.236	1.778	1.154
8S_I_1_H4.0_CDM0.8_RM1.0	1.218	1.119	1.062
8S_I_1_H4.0_CDM0.8_RM1.5	1.220	1.149	1.068
8S_I_1_H4.0_CDM1.0_RM1.0	1.226	1.382	1.112
8S_I_1_H4.0_CDM1.0_RM1.5	1.227	1.412	1.117
8S_I_1_H5.0_CDM0.8_RM1.0	1.214	1.009	1.090
8S_I_1_H5.0_CDM0.8_RM1.5	1.215	1.010	1.067
8S_I_1_H5.0_CDM1.0_RM1.0	1.223	1.141	1.049
8S_I_1_H5.0_CDM1.0_RM1.5	1.224	1.170	1.056
8S_I_1_wo_1_H3.0_CDM0.8_RM1.0	1.228	1.019	1.090
8S_I_1_wo_1_H3.0_CDM0.8_RM1.5	1.229	1.020	1.036
8S_I_1_wo_1_H3.0_CDM1.0_RM1.0	1.235	1.390	1.080
8S_I_1_wo_1_H3.0_CDM1.0_RM1.5	1.235	1.438	1.088
8S_I_1_wo_1_H4.0_CDM0.8_RM1.0	1.413	1.011	1.384
8S_I_1_wo_1_H4.0_CDM0.8_RM1.5	1.324	1.012	1.321
8S_I_1_wo_1_H4.0_CDM1.0_RM1.0	1.227	1.079	1.067
8S_I_1_wo_1_H4.0_CDM1.0_RM1.5	1.228	1.119	1.072
8S_I_1_wo_1_H5.0_CDM0.8_RM1.0	1.775	1.005	1.588
8S_I_1_wo_1_H5.0_CDM0.8_RM1.5	1.656	1.006	1.525
8S_I_1_wo_1_H5.0_CDM1.0_RM1.0	1.219	1.011	1.182
8S_I_1_wo_1_H5.0_CDM1.0_RM1.5	1.220	1.012	1.148
8S_I_2_H3.0_CDM0.8_RM1.0	1.296	1.373	1.094
8S_I_2_H3.0_CDM0.8_RM1.5	1.298	1.400	1.097
8S_I_2_H3.0_CDM1.0_RM1.0	1.312	1.630	1.124
8S_I_2_H3.0_CDM1.0_RM1.5	1.313	1.660	1.127
8S_I_2_H4.0_CDM0.8_RM1.0	1.279	1.123	1.056
8S_I_2_H4.0_CDM0.8_RM1.5	1.282	1.144	1.059
8S_I_2_H4.0_CDM1.0_RM1.0	1.298	1.327	1.088
8S_I_2_H4.0_CDM1.0_RM1.5	1.299	1.352	1.092
8S_I_2_H5.0_CDM0.8_RM1.0	1.265	1.000	1.094
8S_I_2_H5.0_CDM0.8_RM1.5	1.268	1.000	1.082
8S_I_2_H5.0_CDM1.0_RM1.0	1.284	1.095	1.071
8S_I_2_H5.0_CDM1.0_RM1.5	1.286	1.116	1.077
8S_I_2_wo_1_H3.0_CDM0.8_RM1.0	1.348	1.000	1.407
8S_I_2_wo_1_H3.0_CDM0.8_RM1.5	1.294	1.000	1.336
8S_I_2_wo_1_H3.0_CDM1.0_RM1.0	1.310	1.142	1.105
8S_I_2_wo_1_H3.0_CDM1.0_RM1.5	1.311	1.186	1.107
8S_I_2_wo_1_H4.0_CDM0.8_RM1.0	1.830	1.000	1.735
8S_I_2_wo_1_H4.0_CDM0.8_RM1.5	1.704	1.000	1.659
8S_I_2_wo_1_H4.0_CDM1.0_RM1.0	1.292	1.000	1.250

8S_I_2_wo_1_H4.0_CDM1.0_RM1.5	1.294	1.000	1.210
8S_I_2_wo_1_H5.0_CDM0.8_RM1.0	2.319	1.000	1.918
8S_I_2_wo_1_H5.0_CDM0.8_RM1.5	2.149	1.000	1.849
8S_I_2_wo_1_H5.0_CDM1.0_RM1.0	1.417	1.000	1.456
8S_I_2_wo_1_H5.0_CDM1.0_RM1.5	1.356	1.000	1.416
8S_I_3_H3.0_CDM0.8_RM1.0	1.254	1.325	1.092
8S_I_3_H3.0_CDM0.8_RM1.5	1.256	1.350	1.095
8S_I_3_H3.0_CDM1.0_RM1.0	1.268	1.563	1.123
8S_I_3_H3.0_CDM1.0_RM1.5	1.269	1.591	1.127
8S_I_3_H4.0_CDM0.8_RM1.0	1.241	1.094	1.053
8S_I_3_H4.0_CDM0.8_RM1.5	1.243	1.114	1.055
8S_I_3_H4.0_CDM1.0_RM1.0	1.257	1.284	1.085
8S_I_3_H4.0_CDM1.0_RM1.5	1.258	1.308	1.090
8S_I_3_H5.0_CDM0.8_RM1.0	1.228	1.000	1.102
8S_I_3_H5.0_CDM0.8_RM1.5	1.231	1.000	1.090
8S_I_3_H5.0_CDM1.0_RM1.0	1.245	1.059	1.047
8S_I_3_H5.0_CDM1.0_RM1.5	1.246	1.080	1.053
8S_I_3_wo_1_H3.0_CDM0.8_RM1.0	1.437	1.006	1.447
8S_I_3_wo_1_H3.0_CDM0.8_RM1.5	1.346	1.007	1.374
8S_I_3_wo_1_H3.0_CDM1.0_RM1.0	1.268	1.065	1.070
8S_I_3_wo_1_H3.0_CDM1.0_RM1.5	1.269	1.105	1.072
8S_I_3_wo_1_H4.0_CDM0.8_RM1.0	1.945	1.001	1.772
8S_I_3_wo_1_H4.0_CDM0.8_RM1.5	1.811	1.002	1.695
8S_I_3_wo_1_H4.0_CDM1.0_RM1.0	1.256	1.005	1.282
8S_I_3_wo_1_H4.0_CDM1.0_RM1.5	1.257	1.005	1.242
8S_I_3_wo_1_H5.0_CDM0.8_RM1.0	2.488	1.000	1.959
8S_I_3_wo_1_H5.0_CDM0.8_RM1.5	2.304	1.000	1.889
8S_I_3_wo_1_H5.0_CDM1.0_RM1.0	1.514	1.000	1.490
8S_I_3_wo_1_H5.0_CDM1.0_RM1.5	1.449	1.001	1.449
8S_I_4_H3.0_CDM0.8_RM1.0	1.241	1.387	1.099
8S_I_4_H3.0_CDM0.8_RM1.5	1.242	1.415	1.103
8S_I_4_H3.0_CDM1.0_RM1.0	1.255	1.643	1.132
8S_I_4_H3.0_CDM1.0_RM1.5	1.256	1.672	1.136
8S_I_4_H4.0_CDM0.8_RM1.0	1.228	1.079	1.048
8S_I_4_H4.0_CDM0.8_RM1.5	1.230	1.105	1.054
8S_I_4_H4.0_CDM1.0_RM1.0	1.244	1.308	1.092
8S_I_4_H4.0_CDM1.0_RM1.5	1.246	1.334	1.097
8S_I_4_H5.0_CDM0.8_RM1.0	1.217	1.000	1.178
8S_I_4_H5.0_CDM0.8_RM1.5	1.219	1.000	1.157
8S_I_4_H5.0_CDM1.0_RM1.0	1.234	1.064	1.073
8S_I_4_H5.0_CDM1.0_RM1.5	1.236	1.088	1.079
8S_I_4_wo_1_H3.0_CDM0.8_RM1.0	1.239	1.000	1.268
8S_I_4_wo_1_H3.0_CDM0.8_RM1.5	1.241	1.000	1.207

8S_I_4_wo_1_H3.0_CDM1.0_RM1.0	1.254	1.192	1.063
8S_I_4_wo_1_H3.0_CDM1.0_RM1.5	1.256	1.232	1.063
8S_I_4_wo_1_H4.0_CDM0.8_RM1.0	1.633	1.000	1.571
8S_I_4_wo_1_H4.0_CDM0.8_RM1.5	1.528	1.000	1.502
8S_I_4_wo_1_H4.0_CDM1.0_RM1.0	1.241	1.000	1.136
8S_I_4_wo_1_H4.0_CDM1.0_RM1.5	1.243	1.000	1.102
8S_I_4_wo_1_H5.0_CDM0.8_RM1.0	2.064	1.000	1.772
8S_I_4_wo_1_H5.0_CDM0.8_RM1.5	1.920	1.000	1.705
8S_I_4_wo_1_H5.0_CDM1.0_RM1.0	1.299	1.000	1.333
8S_I_4_wo_1_H5.0_CDM1.0_RM1.5	1.247	1.000	1.296
8S_I_12_H3.0_CDM0.8_RM1.0	1.247	1.398	1.107
8S_I_12_H3.0_CDM0.8_RM1.5	1.249	1.413	1.108
8S_I_12_H3.0_CDM1.0_RM1.0	1.263	1.566	1.121
8S_I_12_H3.0_CDM1.0_RM1.5	1.264	1.589	1.123
8S_I_12_H4.0_CDM0.8_RM1.0	1.229	1.138	1.071
8S_I_12_H4.0_CDM0.8_RM1.5	1.232	1.148	1.072
8S_I_12_H4.0_CDM1.0_RM1.0	1.249	1.263	1.084
8S_I_12_H4.0_CDM1.0_RM1.5	1.250	1.281	1.087
8S_I_12_H5.0_CDM0.8_RM1.0	1.216	1.022	1.050
8S_I_12_H5.0_CDM0.8_RM1.5	1.216	1.019	1.054
8S_I_12_H5.0_CDM1.0_RM1.0	1.234	1.026	1.021
8S_I_12_H5.0_CDM1.0_RM1.5	1.236	1.042	1.027
8S_I_12_wo_1_H3.0_CDM0.8_RM1.0	1.687	1.037	1.676
8S_I_12_wo_1_H3.0_CDM0.8_RM1.5	1.573	1.037	1.594
8S_I_12_wo_1_H3.0_CDM1.0_RM1.0	1.260	1.031	1.162
8S_I_12_wo_1_H3.0_CDM1.0_RM1.5	1.261	1.031	1.121
8S_I_12_wo_1_H4.0_CDM0.8_RM1.0	2.293	1.044	1.989
8S_I_12_wo_1_H4.0_CDM0.8_RM1.5	2.129	1.044	1.910
8S_I_12_wo_1_H4.0_CDM1.0_RM1.0	1.412	1.038	1.469
8S_I_12_wo_1_H4.0_CDM1.0_RM1.5	1.352	1.038	1.424
8S_I_12_wo_1_H5.0_CDM0.8_RM1.0	2.908	1.053	2.125
8S_I_12_wo_1_H5.0_CDM0.8_RM1.5	2.691	1.052	2.059
8S_I_12_wo_1_H5.0_CDM1.0_RM1.0	1.756	1.046	1.668
8S_I_12_wo_1_H5.0_CDM1.0_RM1.5	1.677	1.045	1.626
8S_I_13_H3.0_CDM0.8_RM1.0	1.207	1.407	1.117
8S_I_13_H3.0_CDM0.8_RM1.5	1.209	1.420	1.119
8S_I_13_H3.0_CDM1.0_RM1.0	1.218	1.561	1.137
8S_I_13_H3.0_CDM1.0_RM1.5	1.219	1.583	1.139
8S_I_13_H4.0_CDM0.8_RM1.0	1.196	1.178	1.088
8S_I_13_H4.0_CDM0.8_RM1.5	1.198	1.187	1.090
8S_I_13_H4.0_CDM1.0_RM1.0	1.209	1.285	1.107
8S_I_13_H4.0_CDM1.0_RM1.5	1.210	1.302	1.110
8S_I_13_H5.0_CDM0.8_RM1.0	1.189	1.044	1.031

8S_I_13_H5.0_CDM0.8_RM1.5	1.190	1.039	1.032
8S_I_13_H5.0_CDM1.0_RM1.0	1.200	1.056	1.049
8S_I_13_H5.0_CDM1.0_RM1.5	1.201	1.071	1.052
8S_I_13_wo_1_H3.0_CDM0.8_RM1.0	1.712	1.054	1.610
8S_I_13_wo_1_H3.0_CDM0.8_RM1.5	1.600	1.055	1.530
8S_I_13_wo_1_H3.0_CDM1.0_RM1.0	1.217	1.057	1.118
8S_I_13_wo_1_H3.0_CDM1.0_RM1.5	1.218	1.057	1.079
8S_I_13_wo_1_H4.0_CDM0.8_RM1.0	2.331	1.056	1.931
8S_I_13_wo_1_H4.0_CDM0.8_RM1.5	2.166	1.057	1.852
8S_I_13_wo_1_H4.0_CDM1.0_RM1.0	1.445	1.058	1.417
8S_I_13_wo_1_H4.0_CDM1.0_RM1.5	1.384	1.058	1.373
8S_I_13_wo_1_H5.0_CDM0.8_RM1.0	2.979	1.059	2.087
8S_I_13_wo_1_H5.0_CDM0.8_RM1.5	2.757	1.060	2.018
8S_I_13_wo_1_H5.0_CDM1.0_RM1.0	1.802	1.061	1.622
8S_I_13_wo_1_H5.0_CDM1.0_RM1.5	1.721	1.062	1.579
8S_I_14_H3.0_CDM0.8_RM1.0	1.171	1.485	1.125
8S_I_14_H3.0_CDM0.8_RM1.5	1.172	1.497	1.127
8S_I_14_H3.0_CDM1.0_RM1.0	1.181	1.635	1.147
8S_I_14_H3.0_CDM1.0_RM1.5	1.182	1.656	1.149
8S_I_14_H4.0_CDM0.8_RM1.0	1.163	1.186	1.086
8S_I_14_H4.0_CDM0.8_RM1.5	1.164	1.196	1.088
8S_I_14_H4.0_CDM1.0_RM1.0	1.173	1.307	1.111
8S_I_14_H4.0_CDM1.0_RM1.5	1.174	1.325	1.114
8S_I_14_H5.0_CDM0.8_RM1.0	1.156	1.024	1.023
8S_I_14_H5.0_CDM0.8_RM1.5	1.157	1.025	1.019
8S_I_14_H5.0_CDM1.0_RM1.0	1.167	1.060	1.045
8S_I_14_H5.0_CDM1.0_RM1.5	1.167	1.077	1.050
8S_I_14_wo_1_H3.0_CDM0.8_RM1.0	1.512	1.046	1.434
8S_I_14_wo_1_H3.0_CDM0.8_RM1.5	1.420	1.047	1.364
8S_I_14_wo_1_H3.0_CDM1.0_RM1.0	1.180	1.051	1.022
8S_I_14_wo_1_H3.0_CDM1.0_RM1.5	1.181	1.052	1.031
8S_I_14_wo_1_H4.0_CDM0.8_RM1.0	2.024	1.041	1.746
8S_I_14_wo_1_H4.0_CDM0.8_RM1.5	1.889	1.042	1.672
8S_I_14_wo_1_H4.0_CDM1.0_RM1.0	1.293	1.046	1.276
8S_I_14_wo_1_H4.0_CDM1.0_RM1.5	1.243	1.047	1.237
8S_I_14_wo_1_H5.0_CDM0.8_RM1.0	2.563	1.040	1.923
8S_I_14_wo_1_H5.0_CDM0.8_RM1.5	2.381	1.041	1.856
8S_I_14_wo_1_H5.0_CDM1.0_RM1.0	1.594	1.043	1.478
8S_I_14_wo_1_H5.0_CDM1.0_RM1.5	1.527	1.044	1.438
8S_I_23_H3.0_CDM0.8_RM1.0	1.337	1.285	1.087
8S_I_23_H3.0_CDM0.8_RM1.5	1.340	1.292	1.087
8S_I_23_H3.0_CDM1.0_RM1.0	1.357	1.405	1.097
8S_I_23_H3.0_CDM1.0_RM1.5	1.359	1.423	1.099

8S_I_23_H4.0_CDM0.8_RM1.0	1.316	1.073	1.050
8S_I_23_H4.0_CDM0.8_RM1.5	1.320	1.077	1.049
8S_I_23_H4.0_CDM1.0_RM1.0	1.340	1.153	1.068
8S_I_23_H4.0_CDM1.0_RM1.5	1.342	1.167	1.072
8S_I_23_H5.0_CDM0.8_RM1.0	1.300	1.000	1.138
8S_I_23_H5.0_CDM0.8_RM1.5	1.304	1.000	1.139
8S_I_23_H5.0_CDM1.0_RM1.0	1.328	1.000	1.106
8S_I_23_H5.0_CDM1.0_RM1.5	1.301	1.000	1.069
8S_I_23_wo_1_H3.0_CDM0.8_RM1.0	2.213	1.018	2.118
8S_I_23_wo_1_H3.0_CDM0.8_RM1.5	2.052	1.018	2.018
8S_I_23_wo_1_H3.0_CDM1.0_RM1.0	1.360	1.009	1.485
8S_I_23_wo_1_H3.0_CDM1.0_RM1.5	1.361	1.009	1.434
8S_I_23_wo_1_H4.0_CDM0.8_RM1.0	3.090	1.032	2.413
8S_I_23_wo_1_H4.0_CDM0.8_RM1.5	2.848	1.032	2.325
8S_I_23_wo_1_H4.0_CDM1.0_RM1.0	1.818	1.022	1.818
8S_I_23_wo_1_H4.0_CDM1.0_RM1.5	1.536	1.000	1.678
8S_I_23_wo_1_H5.0_CDM0.8_RM1.0	3.575	1.000	2.427
8S_I_23_wo_1_H5.0_CDM0.8_RM1.5	3.288	1.000	2.358
8S_I_23_wo_1_H5.0_CDM1.0_RM1.0	2.308	1.036	2.002
8S_I_23_wo_1_H5.0_CDM1.0_RM1.5	2.194	1.035	1.955
8S_I_24_H3.0_CDM0.8_RM1.0	1.227	1.438	1.108
8S_I_24_H3.0_CDM0.8_RM1.5	1.229	1.443	1.109
8S_I_24_H3.0_CDM1.0_RM1.0	1.244	1.545	1.124
8S_I_24_H3.0_CDM1.0_RM1.5	1.245	1.561	1.126
8S_I_24_H4.0_CDM0.8_RM1.0	1.214	1.174	1.069
8S_I_24_H4.0_CDM0.8_RM1.5	1.216	1.177	1.069
8S_I_24_H4.0_CDM1.0_RM1.0	1.231	1.253	1.083
8S_I_24_H4.0_CDM1.0_RM1.5	1.232	1.266	1.086
8S_I_24_H5.0_CDM0.8_RM1.0	1.202	1.000	1.058
8S_I_24_H5.0_CDM0.8_RM1.5	1.204	1.000	1.057
8S_I_24_H5.0_CDM1.0_RM1.0	1.221	1.017	1.033
8S_I_24_H5.0_CDM1.0_RM1.5	1.223	1.030	1.037
8S_I_24_wo_1_H3.0_CDM0.8_RM1.0	1.849	1.023	1.764
8S_I_24_wo_1_H3.0_CDM0.8_RM1.5	1.726	1.023	1.679
8S_I_24_wo_1_H3.0_CDM1.0_RM1.0	1.242	1.023	1.233
8S_I_24_wo_1_H3.0_CDM1.0_RM1.5	1.243	1.023	1.191
8S_I_24_wo_1_H4.0_CDM0.8_RM1.0	2.529	1.023	2.085
8S_I_24_wo_1_H4.0_CDM0.8_RM1.5	2.346	1.023	2.002
8S_I_24_wo_1_H4.0_CDM1.0_RM1.0	1.553	1.023	1.542
8S_I_24_wo_1_H4.0_CDM1.0_RM1.5	1.487	1.023	1.495
8S_I_24_wo_1_H5.0_CDM0.8_RM1.0	3.255	1.025	2.223
8S_I_24_wo_1_H5.0_CDM0.8_RM1.5	3.004	1.025	2.154
8S_I_24_wo_1_H5.0_CDM1.0_RM1.0	1.941	1.024	1.744

8S_I_24_wo_1_H5.0_CDM1.0_RM1.5	1.853	1.024	1.700
8S_I_34_H3.0_CDM0.8_RM1.0	1.245	1.345	1.090
8S_I_34_H3.0_CDM0.8_RM1.5	1.248	1.349	1.090
8S_I_34_H3.0_CDM1.0_RM1.0	1.267	1.429	1.101
8S_I_34_H3.0_CDM1.0_RM1.5	1.269	1.445	1.103
8S_I_34_H4.0_CDM0.8_RM1.0	1.225	1.074	1.044
8S_I_34_H4.0_CDM0.8_RM1.5	1.229	1.078	1.044
8S_I_34_H4.0_CDM1.0_RM1.0	1.251	1.148	1.055
8S_I_34_H4.0_CDM1.0_RM1.5	1.253	1.162	1.058
8S_I_34_H5.0_CDM0.8_RM1.0	1.208	1.000	1.156
8S_I_34_H5.0_CDM0.8_RM1.5	1.212	1.000	1.154
8S_I_34_H5.0_CDM1.0_RM1.0	1.236	1.000	1.112
8S_I_34_H5.0_CDM1.0_RM1.5	1.238	1.000	1.103
8S_I_34_wo_1_H3.0_CDM0.8_RM1.0	2.095	1.009	1.975
8S_I_34_wo_1_H3.0_CDM0.8_RM1.5	1.952	1.009	1.883
8S_I_34_wo_1_H3.0_CDM1.0_RM1.0	1.325	1.007	1.402
8S_I_34_wo_1_H3.0_CDM1.0_RM1.5	1.273	1.007	1.355
8S_I_34_wo_1_H4.0_CDM0.8_RM1.0	2.863	1.009	2.275
8S_I_34_wo_1_H4.0_CDM0.8_RM1.5	2.650	1.009	2.189
8S_I_34_wo_1_H4.0_CDM1.0_RM1.0	1.734	1.006	1.708
8S_I_34_wo_1_H4.0_CDM1.0_RM1.5	1.659	1.006	1.659
8S_I_34_wo_1_H5.0_CDM0.8_RM1.0	3.737	1.013	2.387
8S_I_34_wo_1_H5.0_CDM0.8_RM1.5	3.439	1.013	2.317
8S_I_34_wo_1_H5.0_CDM1.0_RM1.0	2.187	1.009	1.901
8S_I_34_wo_1_H5.0_CDM1.0_RM1.5	2.085	1.009	1.856
8S_I_1234_H3.0_CDM0.8_RM1.0	1.362	1.298	1.088
8S_I_1234_H3.0_CDM0.8_RM1.5	1.367	1.291	1.086
8S_I_1234_H3.0_CDM1.0_RM1.0	1.394	1.277	1.081
8S_I_1234_H3.0_CDM1.0_RM1.5	1.396	1.282	1.081
8S_I_1234_H4.0_CDM0.8_RM1.0	1.333	1.037	1.038
8S_I_1234_H4.0_CDM0.8_RM1.5	1.337	1.031	1.035
8S_I_1234_H4.0_CDM1.0_RM1.0	1.369	1.026	1.050
8S_I_1234_H4.0_CDM1.0_RM1.5	1.372	1.030	1.053
8S_I_1234_H5.0_CDM0.8_RM1.0	1.308	1.000	1.200
8S_I_1234_H5.0_CDM0.8_RM1.5	1.313	1.000	1.208
8S_I_1234_H5.0_CDM1.0_RM1.0	1.346	1.000	1.235
8S_I_1234_H5.0_CDM1.0_RM1.5	1.349	1.000	1.233
8S_I_1234_wo_1_H3.0_CDM0.8_RM1.0	3.403	1.055	2.804
8S_I_1234_wo_1_H3.0_CDM0.8_RM1.5	3.136	1.054	2.690
8S_I_1234_wo_1_H3.0_CDM1.0_RM1.0	1.996	1.035	2.051
8S_I_1234_wo_1_H3.0_CDM1.0_RM1.5	1.996	1.035	2.051
8S_I_1234_wo_1_H4.0_CDM0.8_RM1.0	4.814	1.088	2.940
8S_I_1234_wo_1_H4.0_CDM0.8_RM1.5	4.415	1.088	2.859

8S_I_1234_wo_1_H4.0_CDM1.0_RM1.0	2.734	1.069	2.349
8S_I_1234_wo_1_H4.0_CDM1.0_RM1.5	2.597	1.067	2.291
8S_I_1234_wo_1_H5.0_CDM0.8_RM1.0	6.303	1.115	2.843
8S_I_1234_wo_1_H5.0_CDM0.8_RM1.5	5.761	1.115	2.789
8S_I_1234_wo_1_H5.0_CDM1.0_RM1.0	3.506	1.101	2.431
8S_I_1234_wo_1_H5.0_CDM1.0_RM1.5	3.320	1.100	2.387

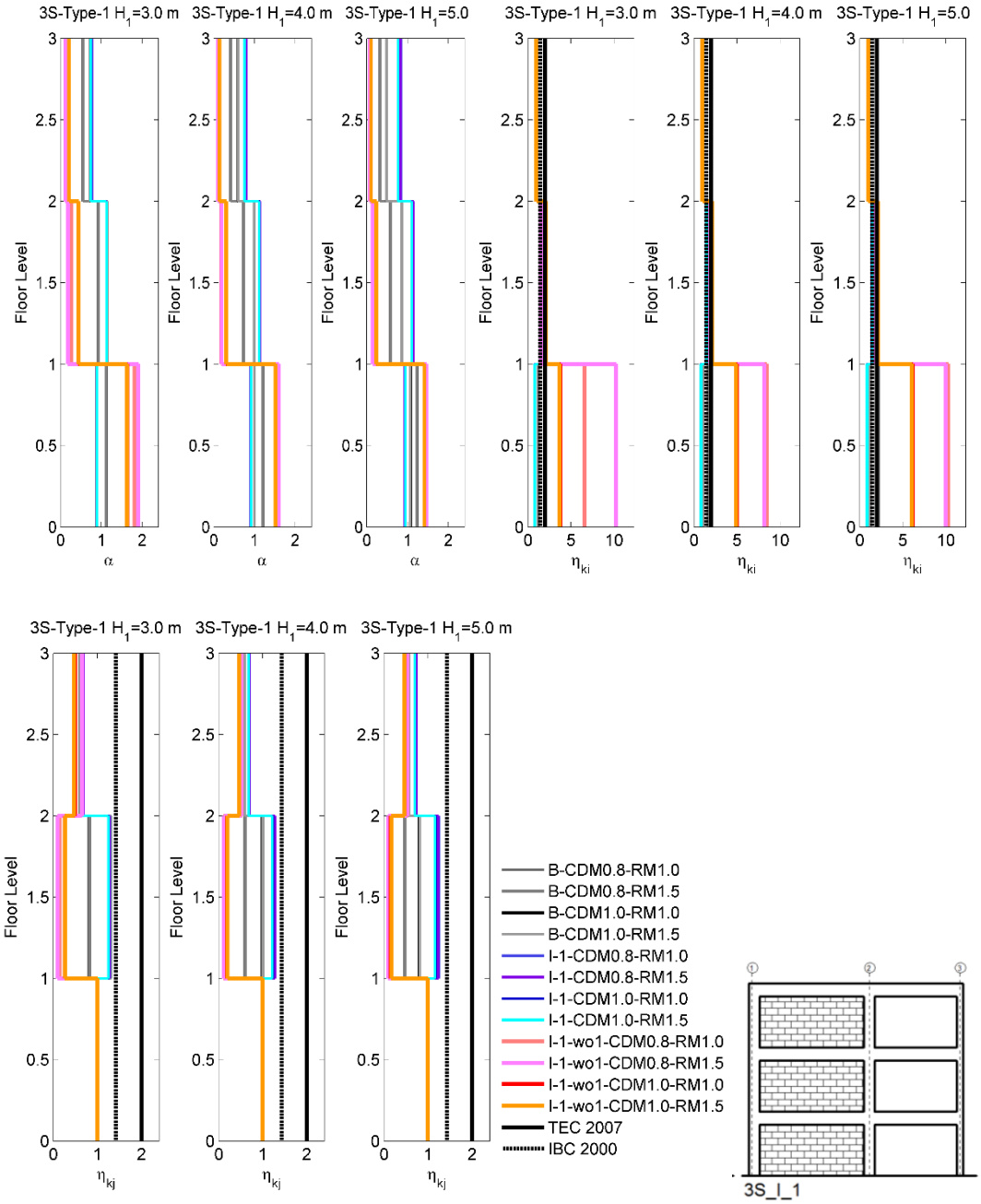

Figure A2-1 3 Story Frame; equivalent static load analysis results for Type 1

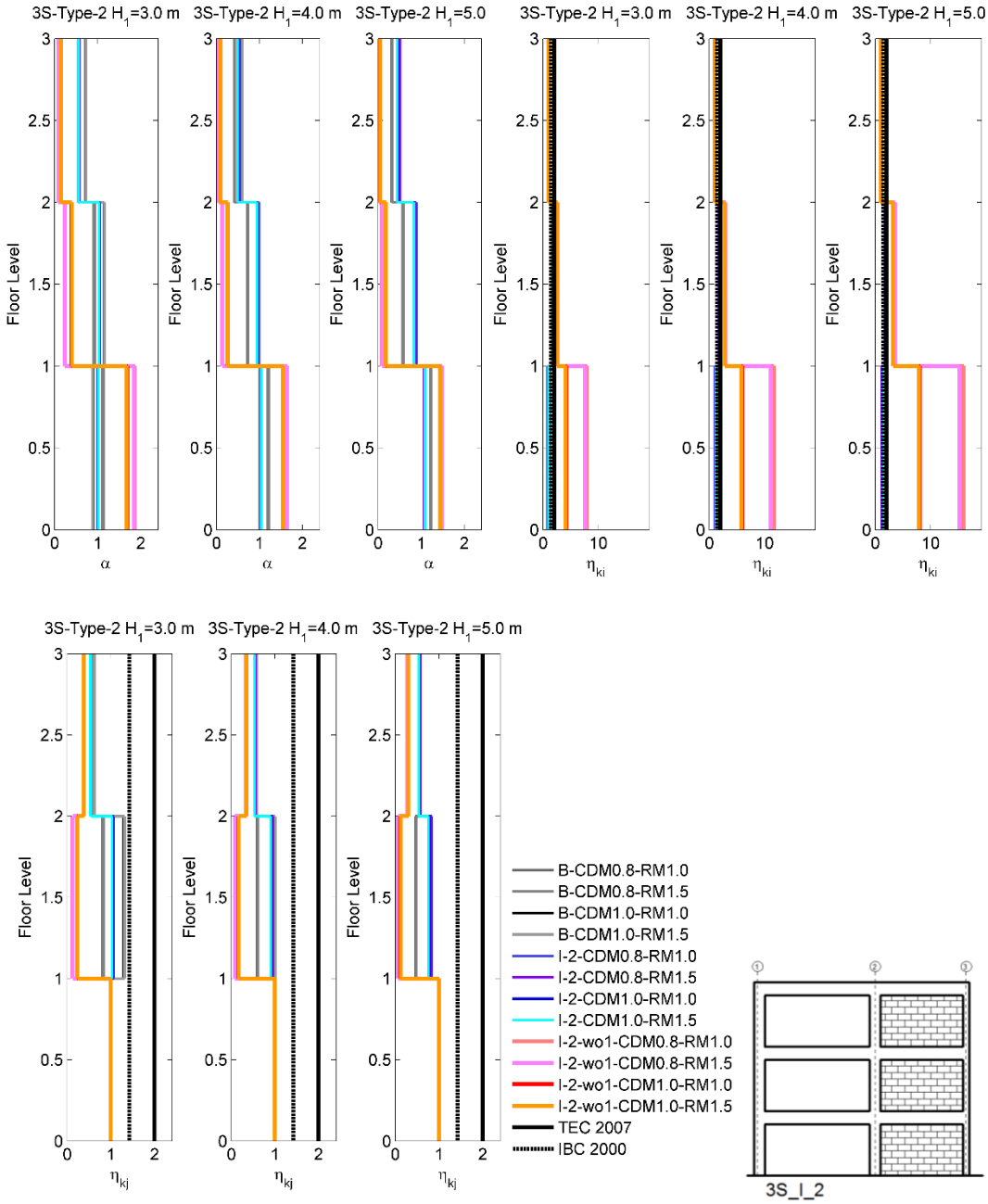

Figure A2-2 3 Story Frame; equivalent static load analysis results for Type 2

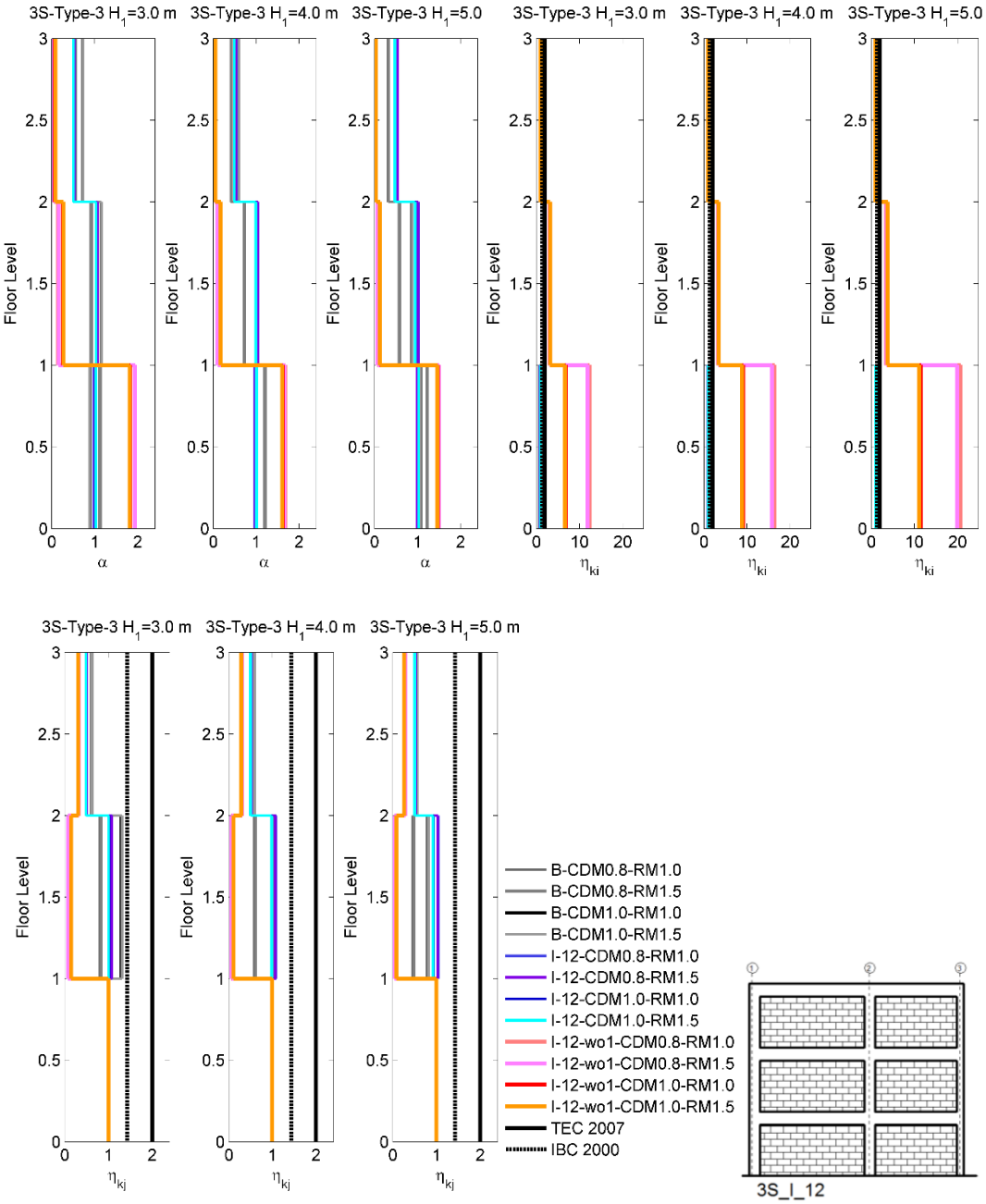

Figure A2-3 3 Story Frame; equivalent static load analysis results for Type 3

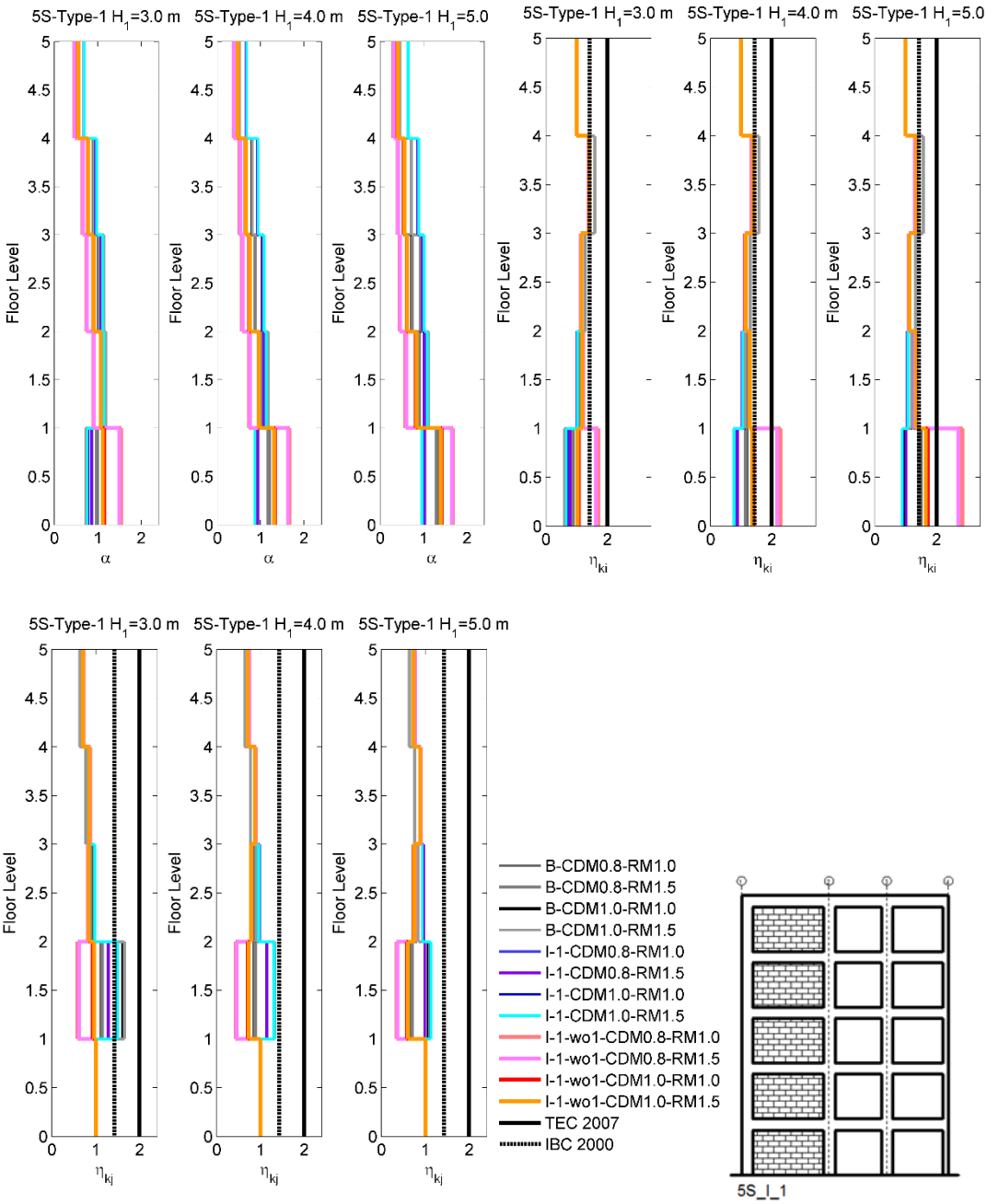

Figure A2-4 5 Story Frame; equivalent static load analysis results for Type 1

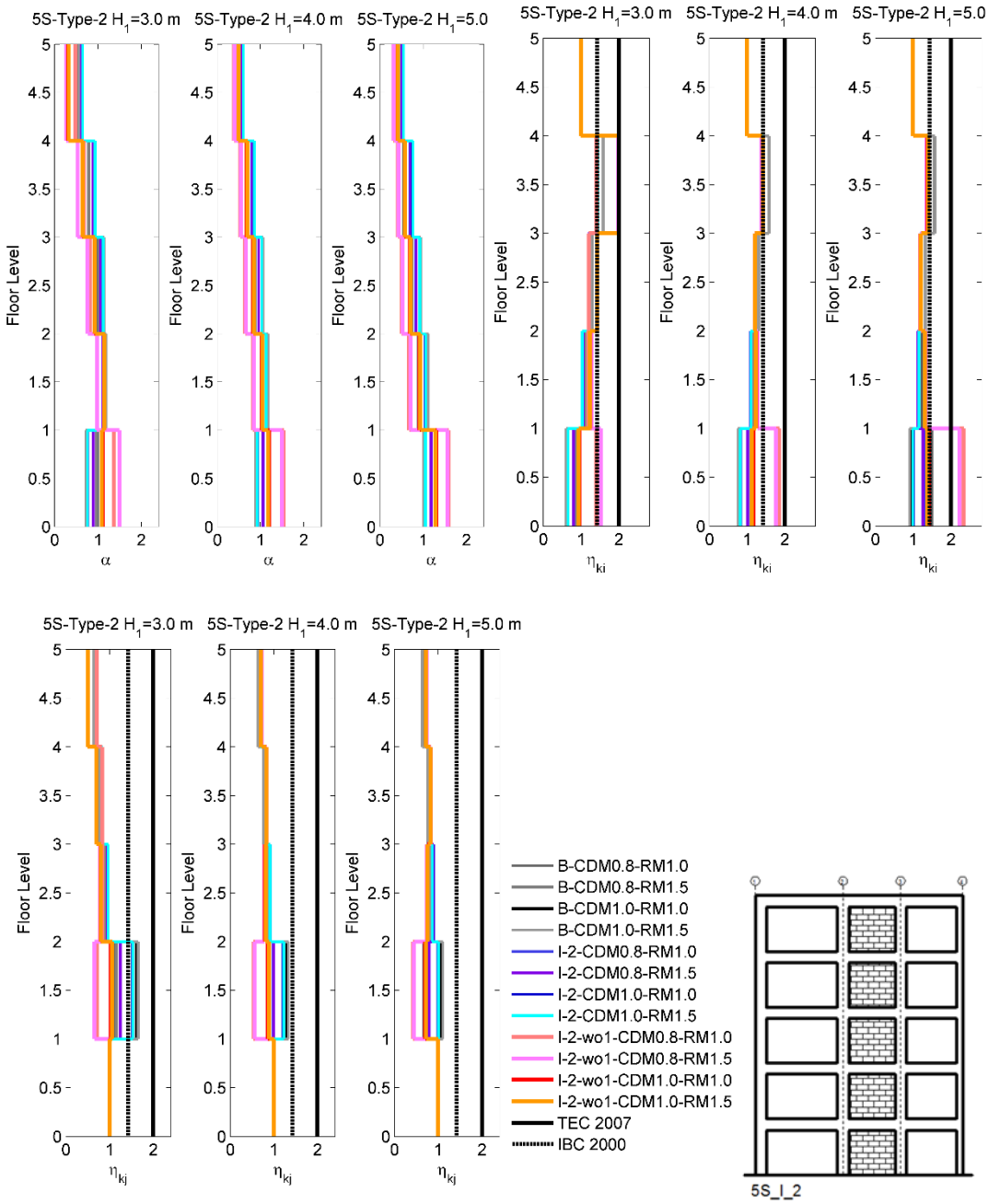

Figure A2-5 5 Story Frame; equivalent static load analysis results for Type 2

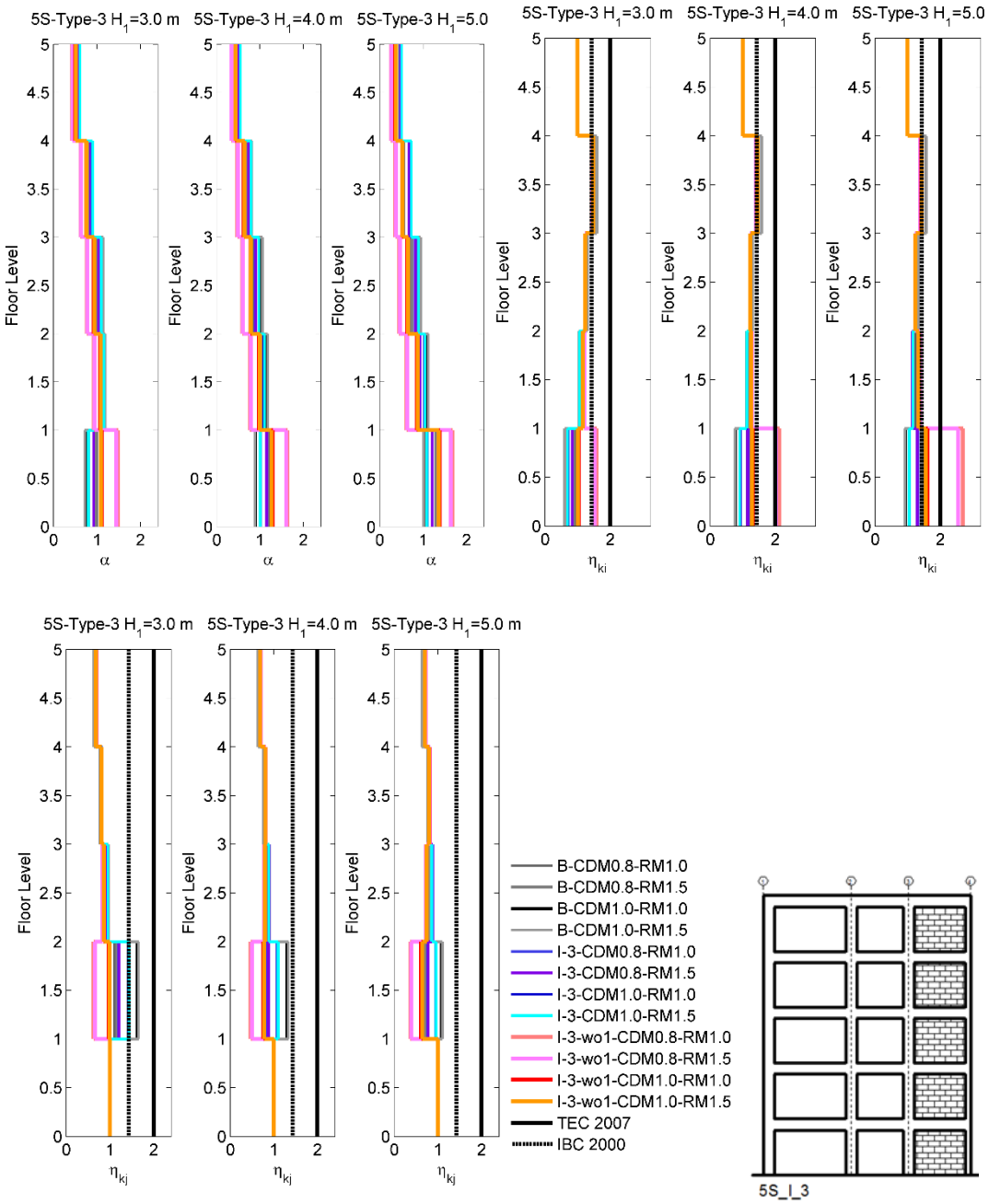

Figure A2-6 5 Story Frame; equivalent static load analysis results for Type 3

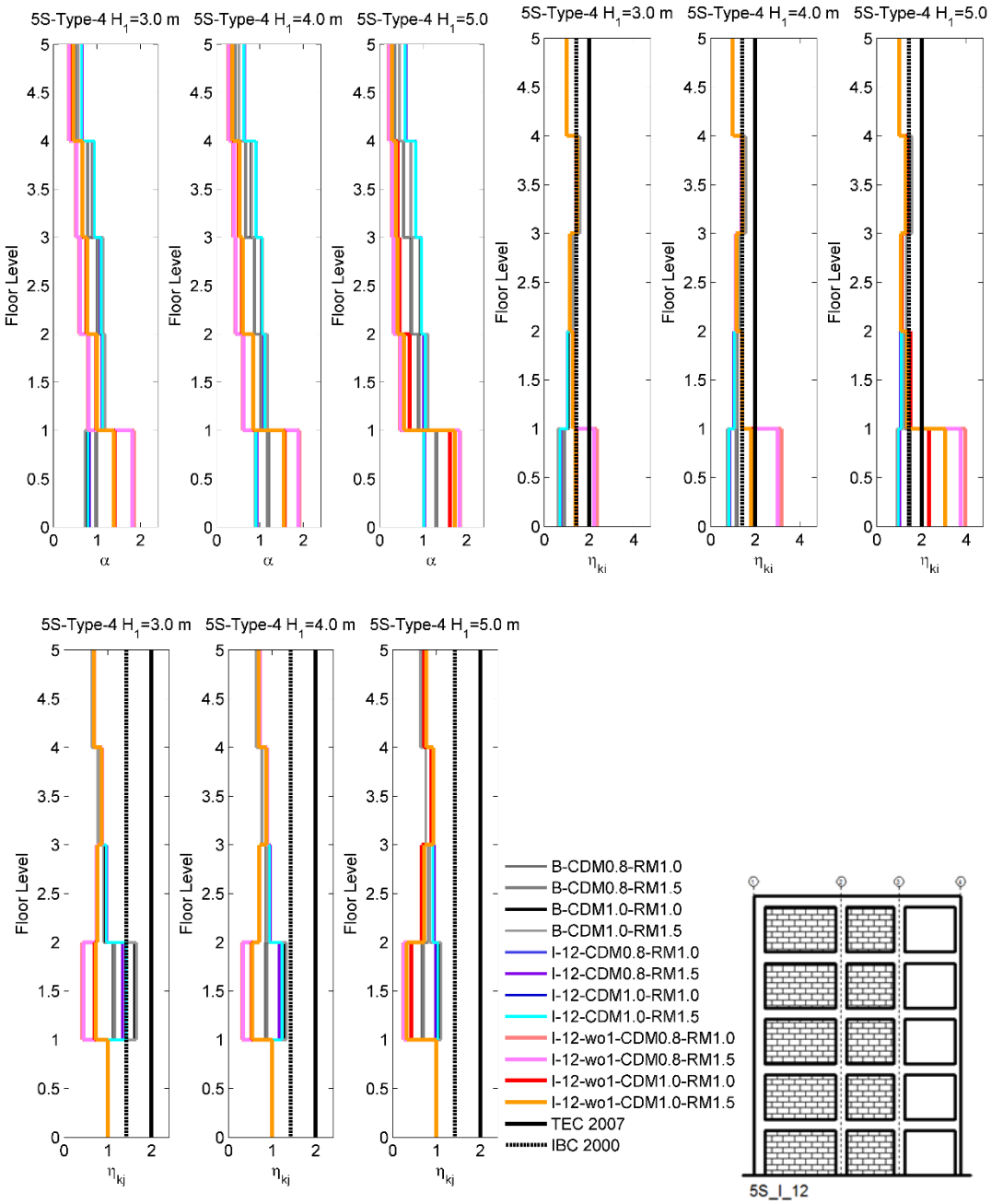

Figure A2-7 5 Story Frame; equivalent static load analysis results for Type 4

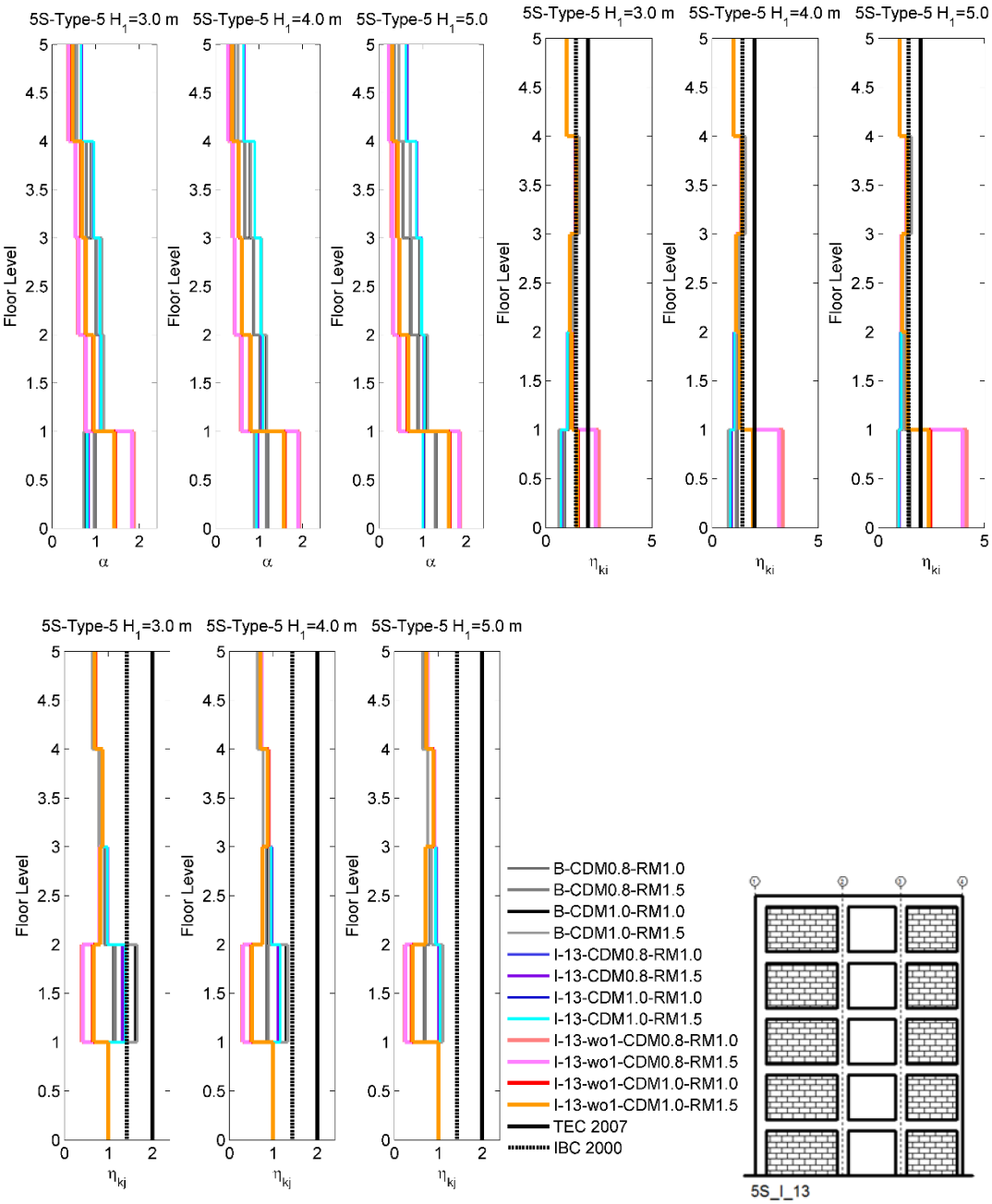

Figure A2-8 5 Story Frame; equivalent static load analysis results for Type 5

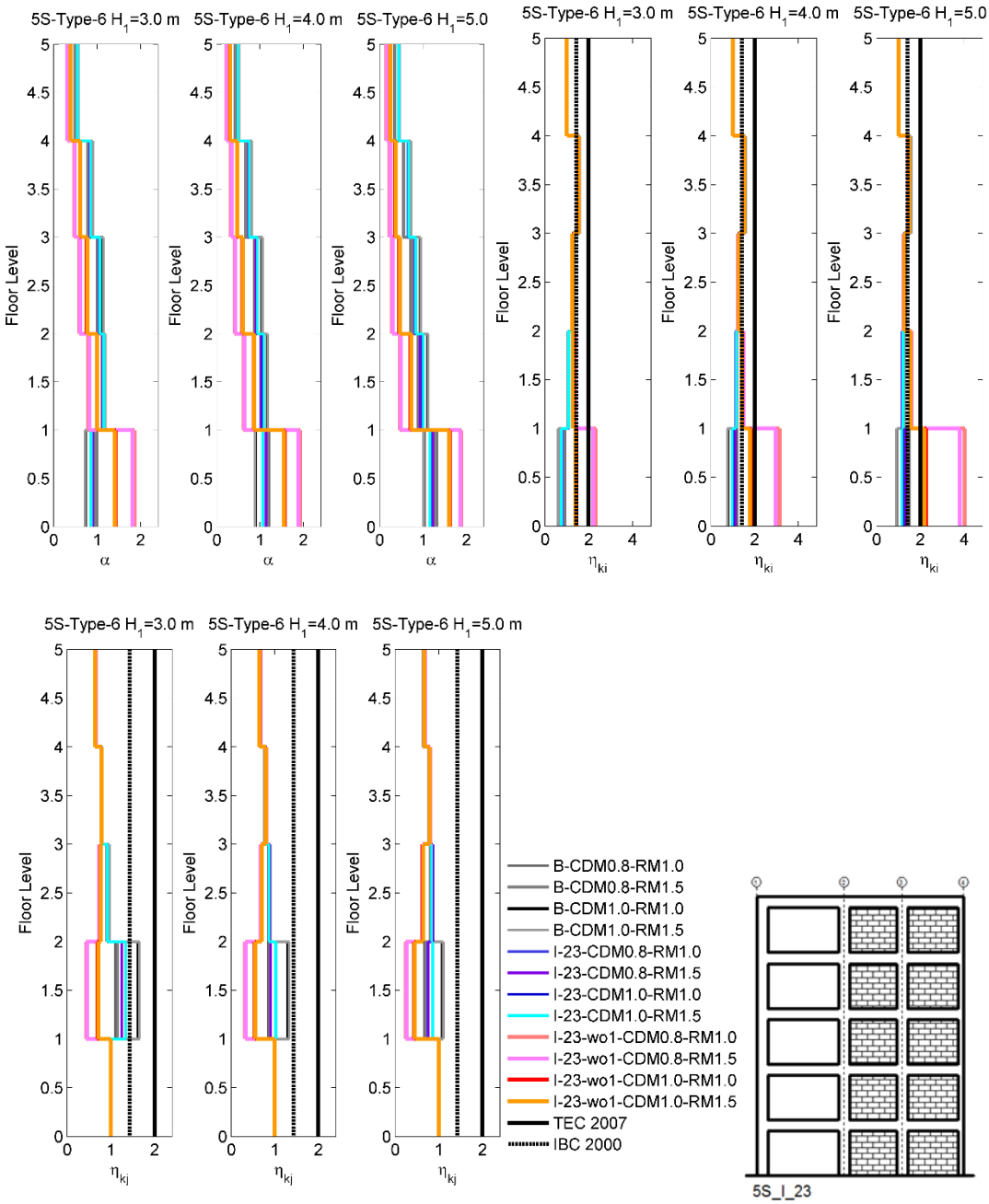

Figure A2-9 5 Story Frame; equivalent static load analysis results for Type 6

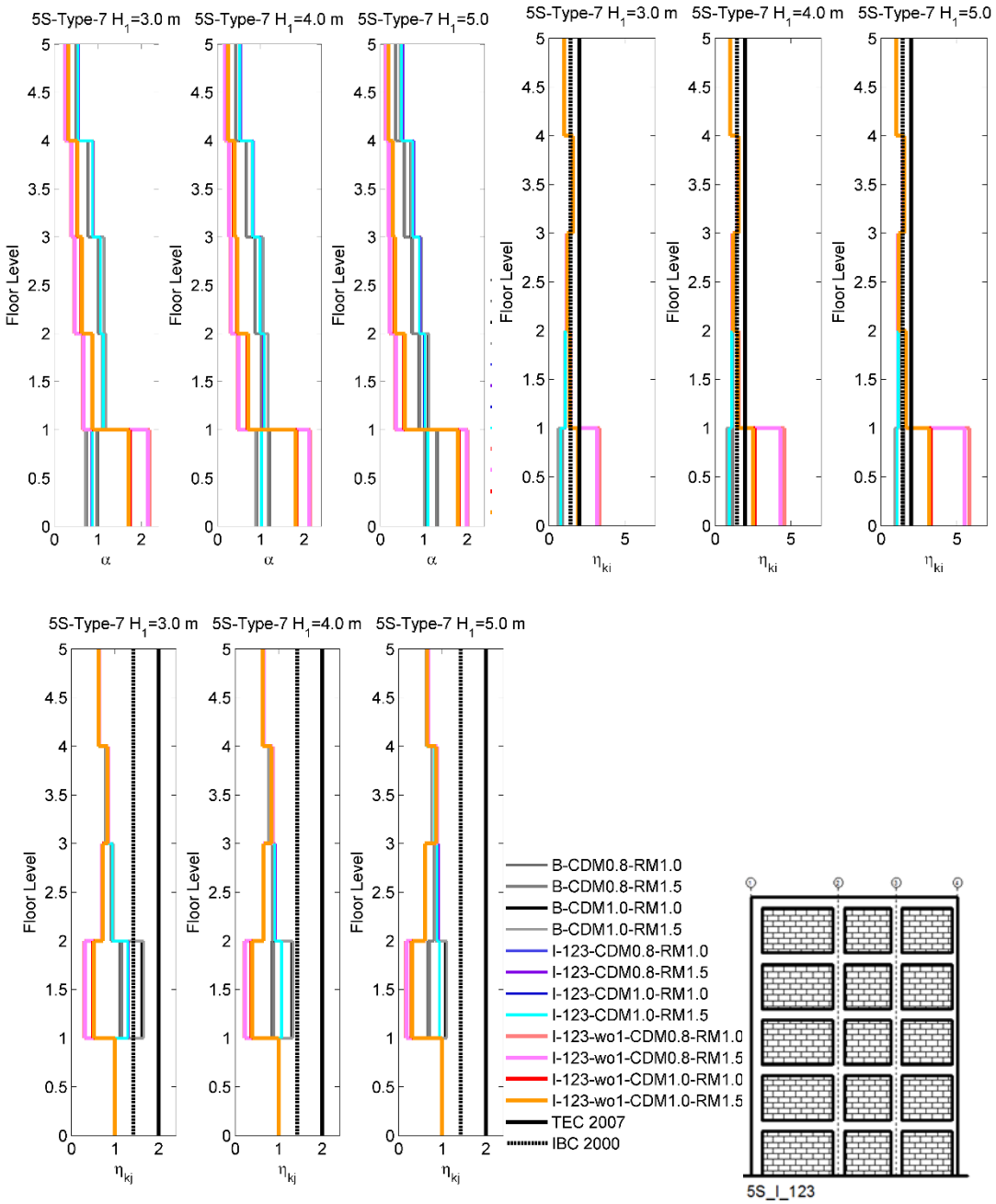

Figure A2-10 5 Story Frame; equivalent static load analysis results for Type 7

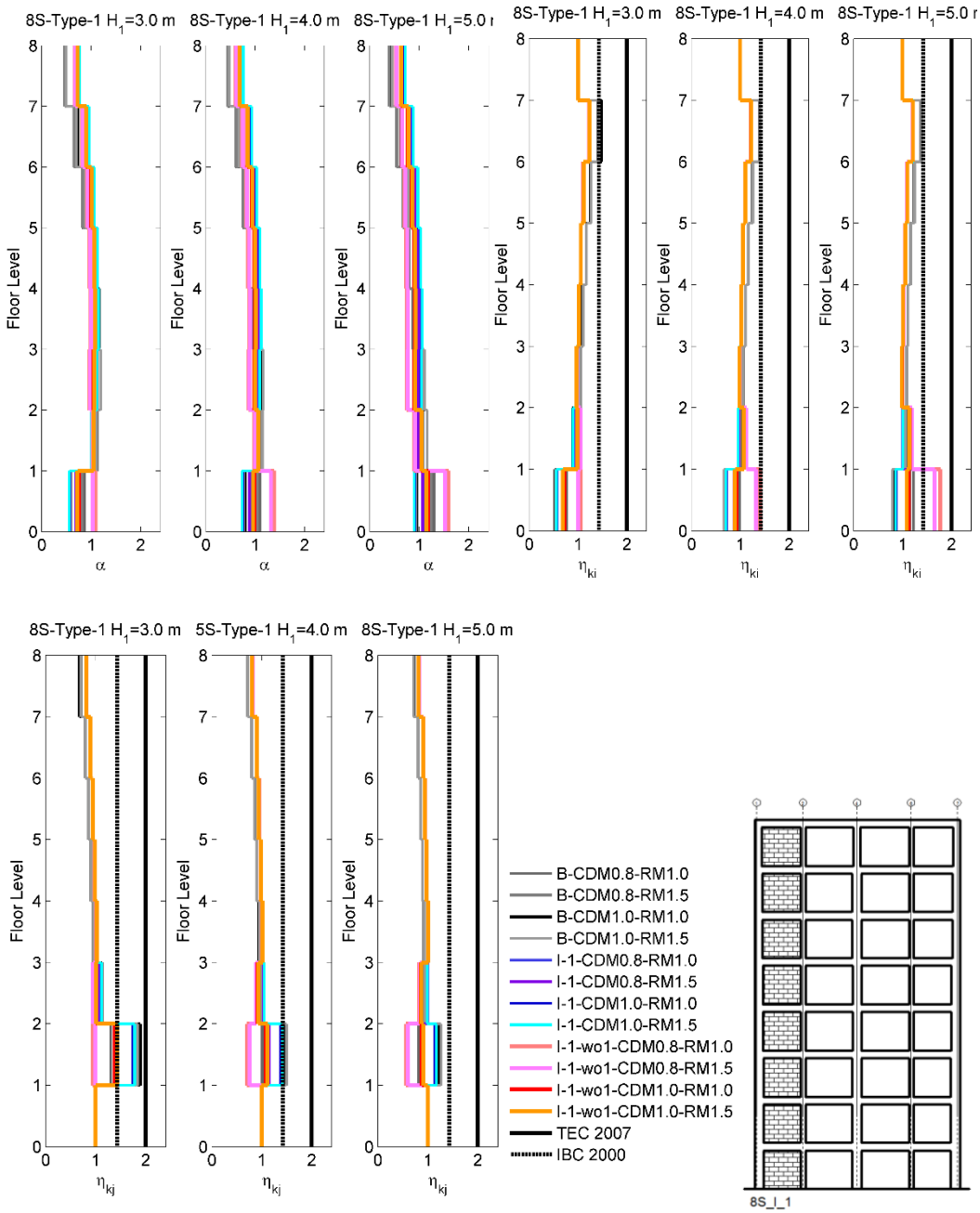

Figure A2-11 8 Story Frame; equivalent static load analysis results for Type 1

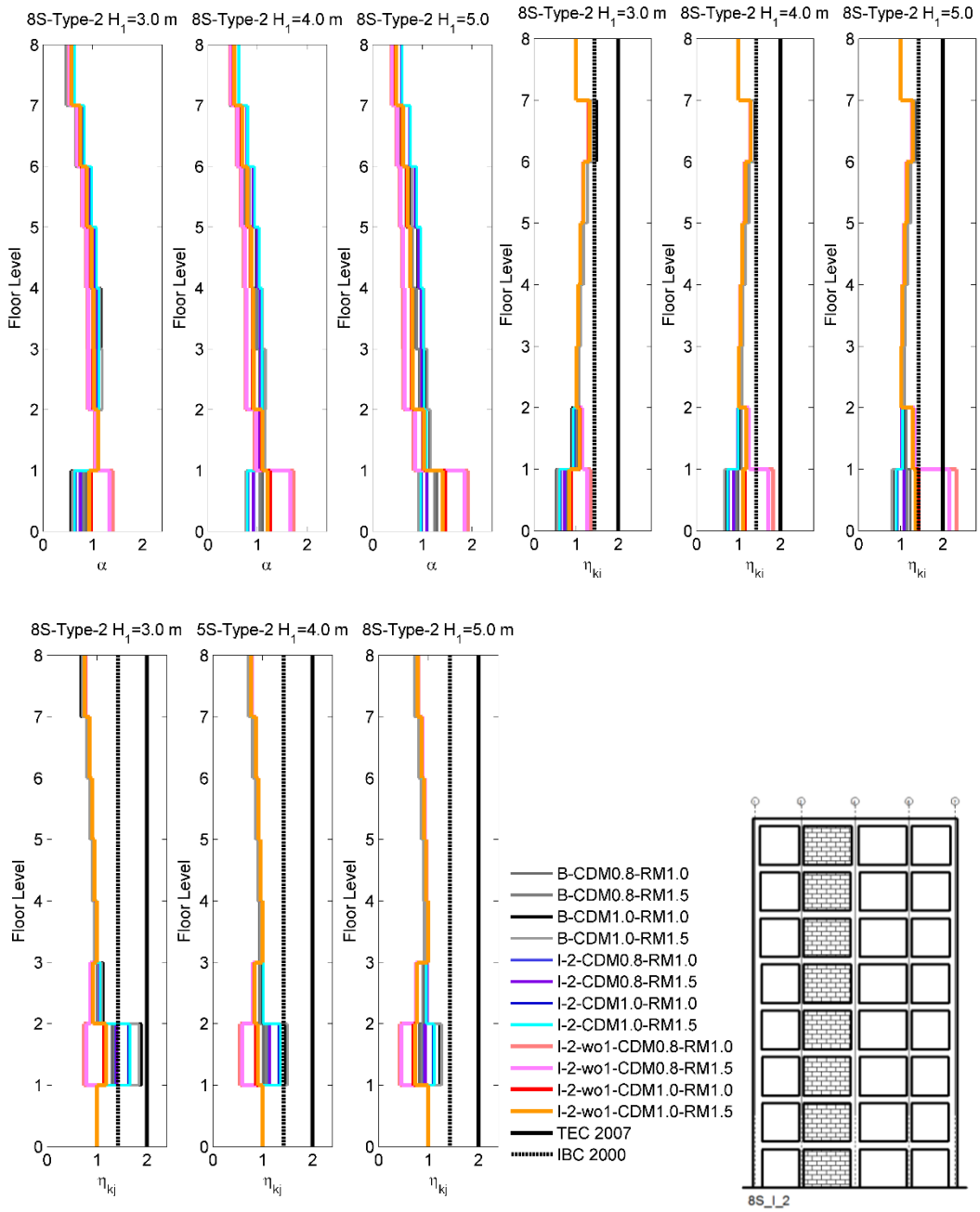

Figure A2-12 8 Story Frame; equivalent static load analysis results for Type 2

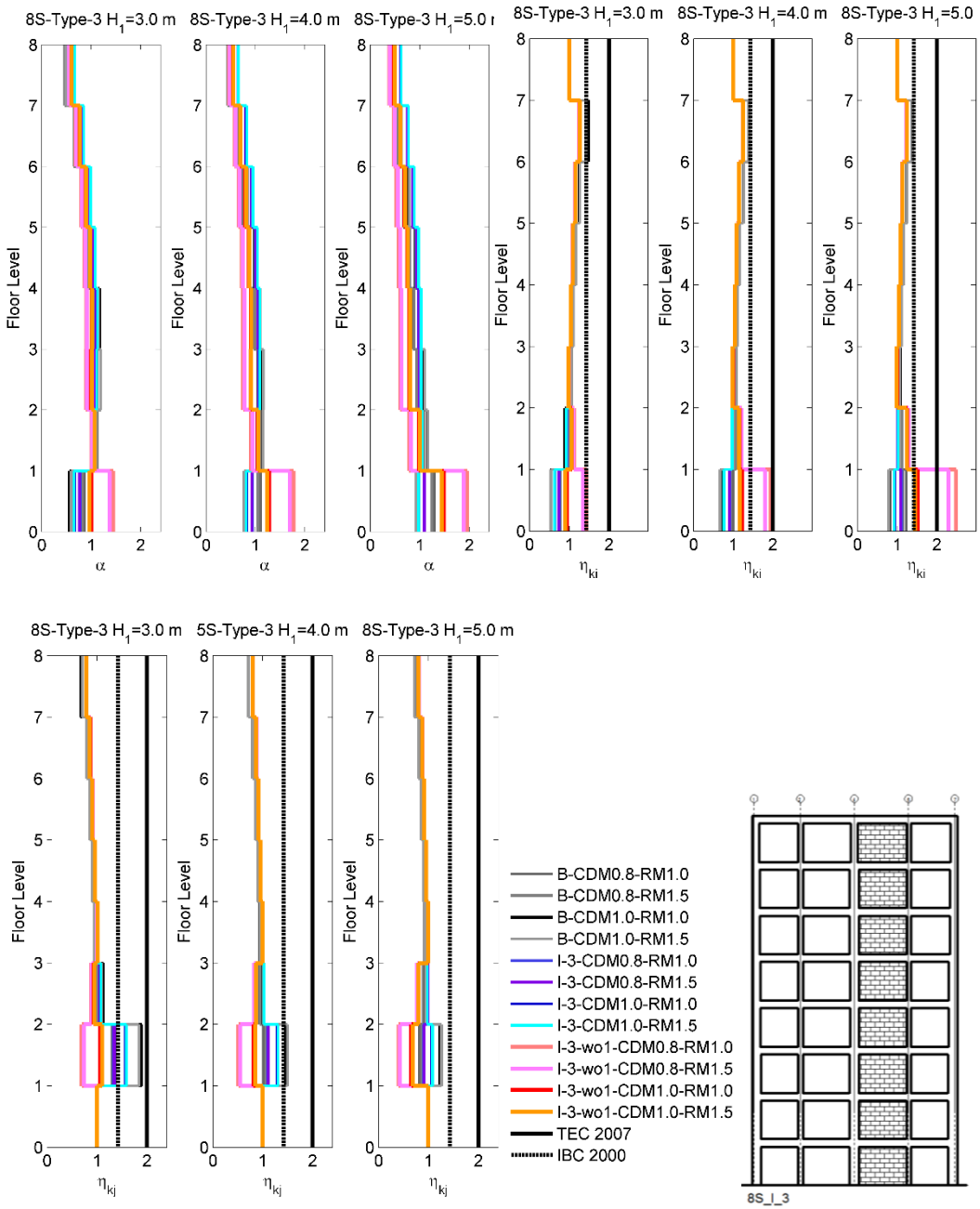

Figure A2-13 8 Story Frame; equivalent static load analysis results for Type 3

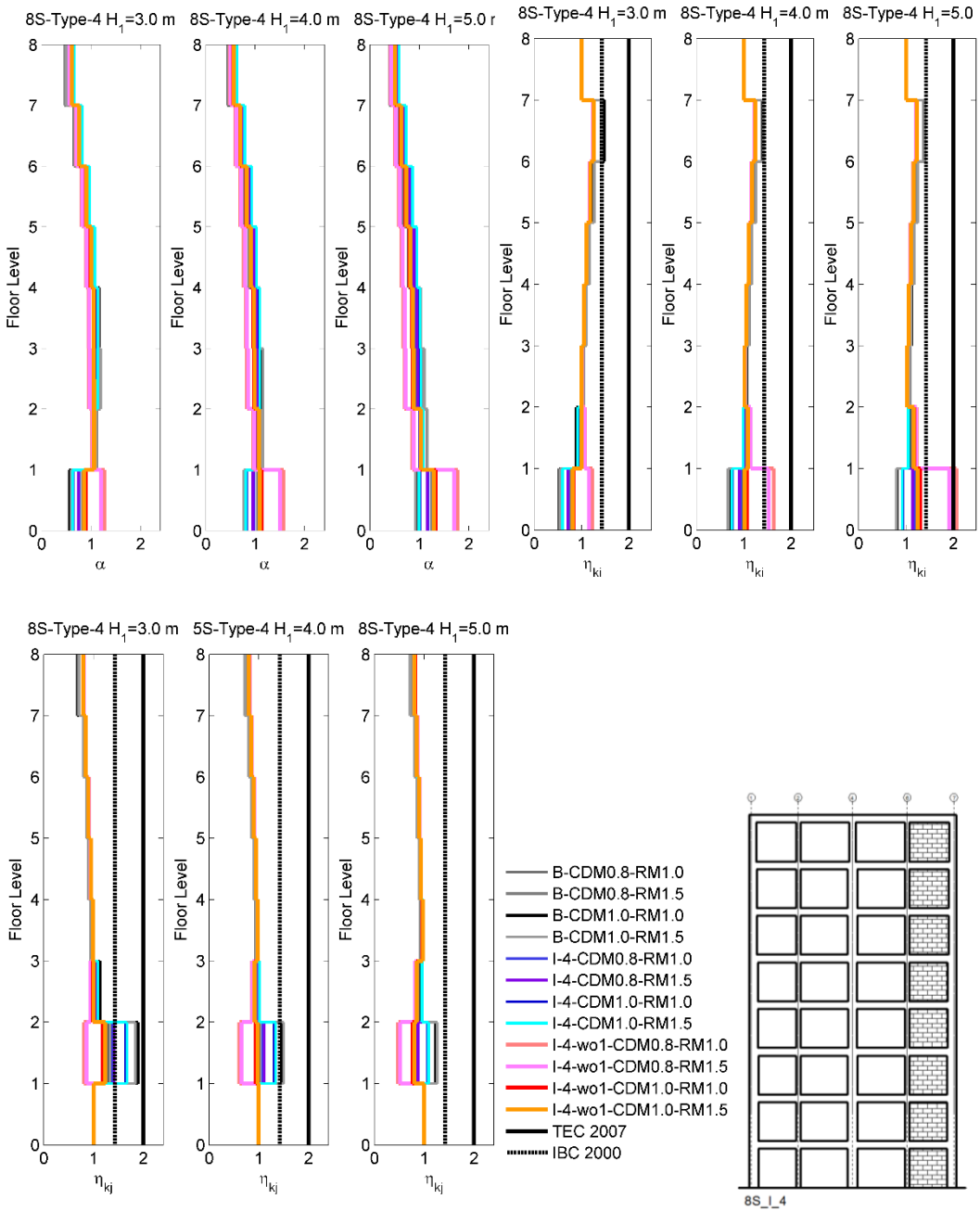

Figure A2-14 8 Story Frame; equivalent static load analysis results for Type 4

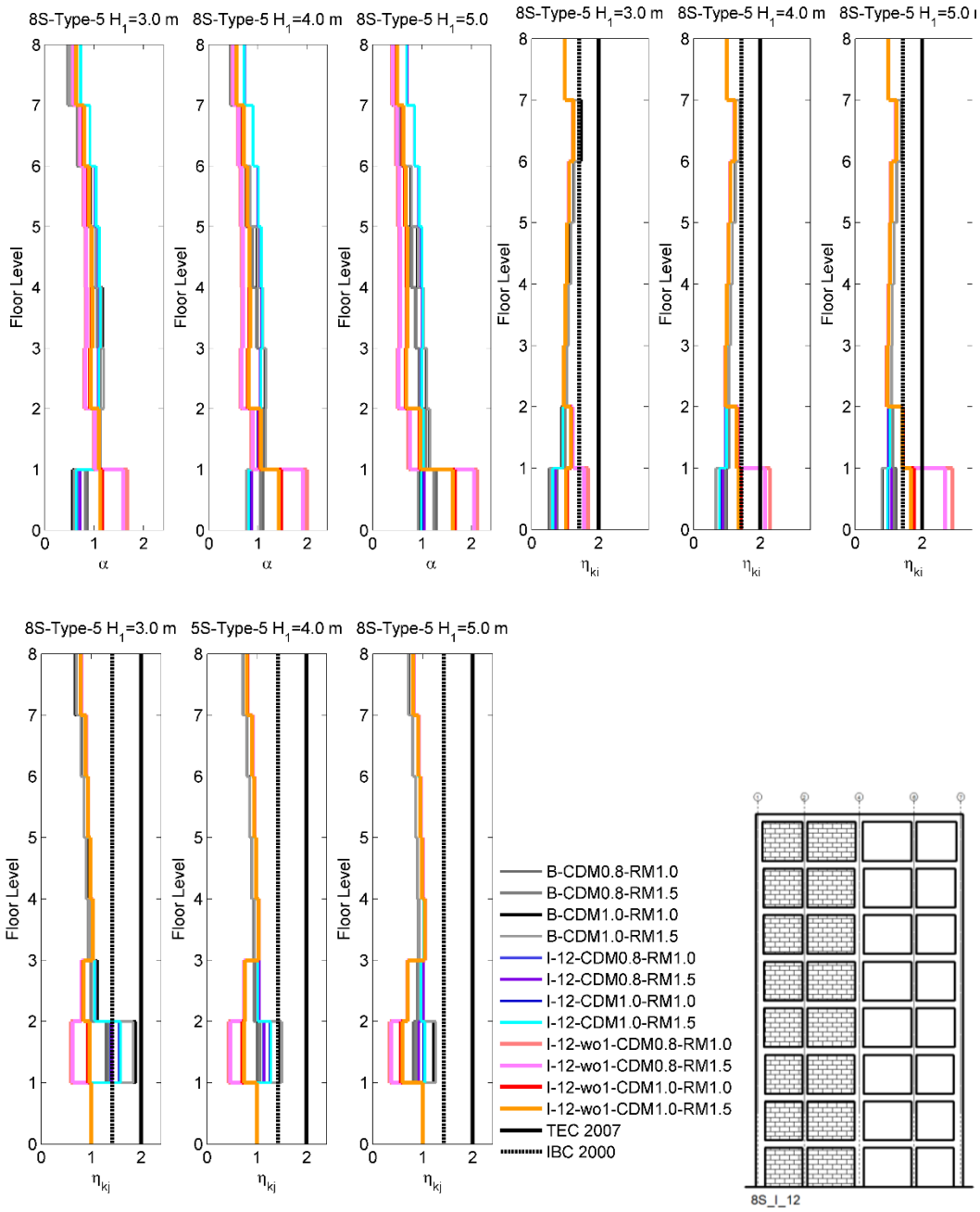

Figure A2-15 8 Story Frame; equivalent static load analysis results for Type 5

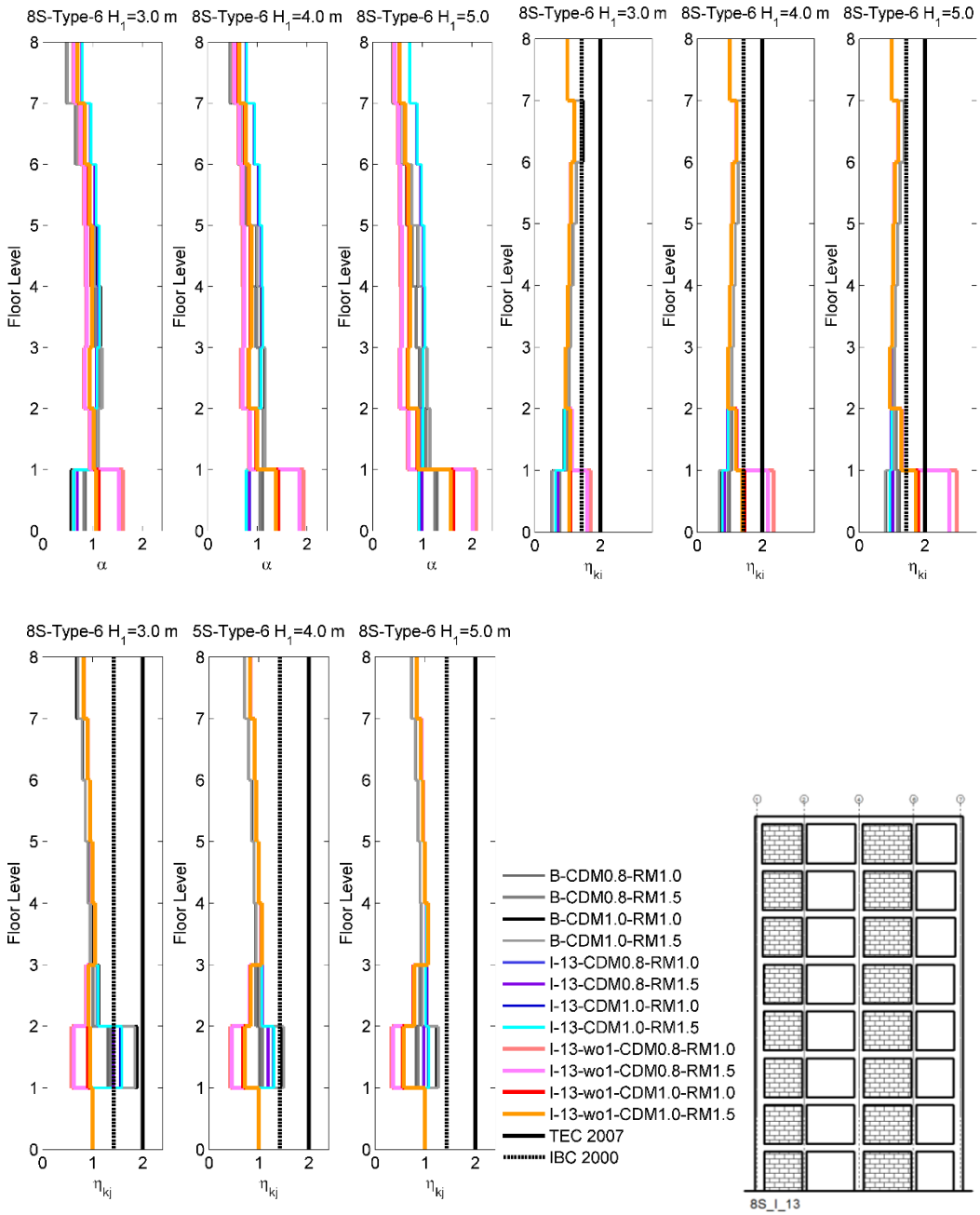

Figure A2-16 8 Story Frame; equivalent static load analysis results for Type 6

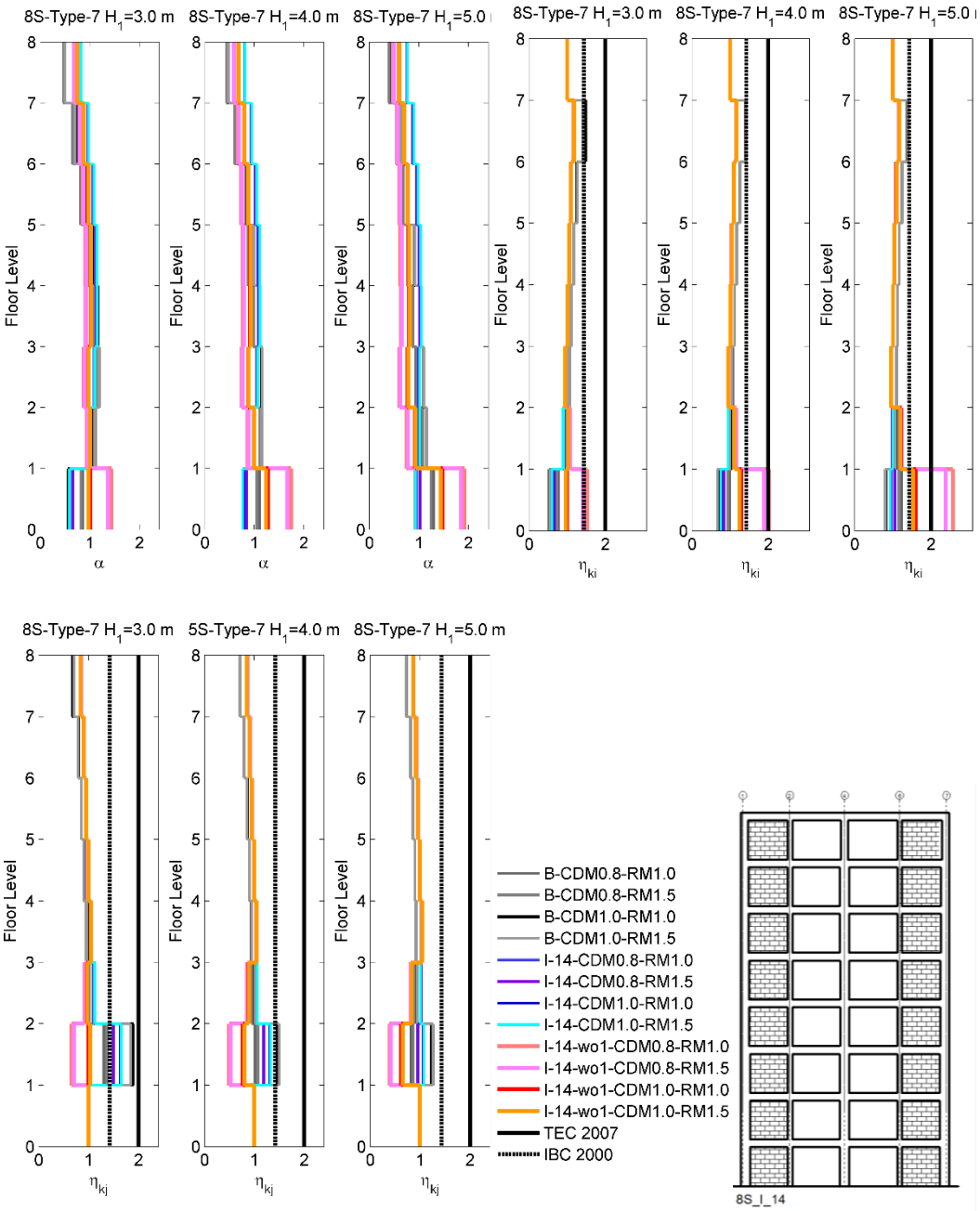

Figure A2-17 8 Story Frame; equivalent static load analysis results for Type 7

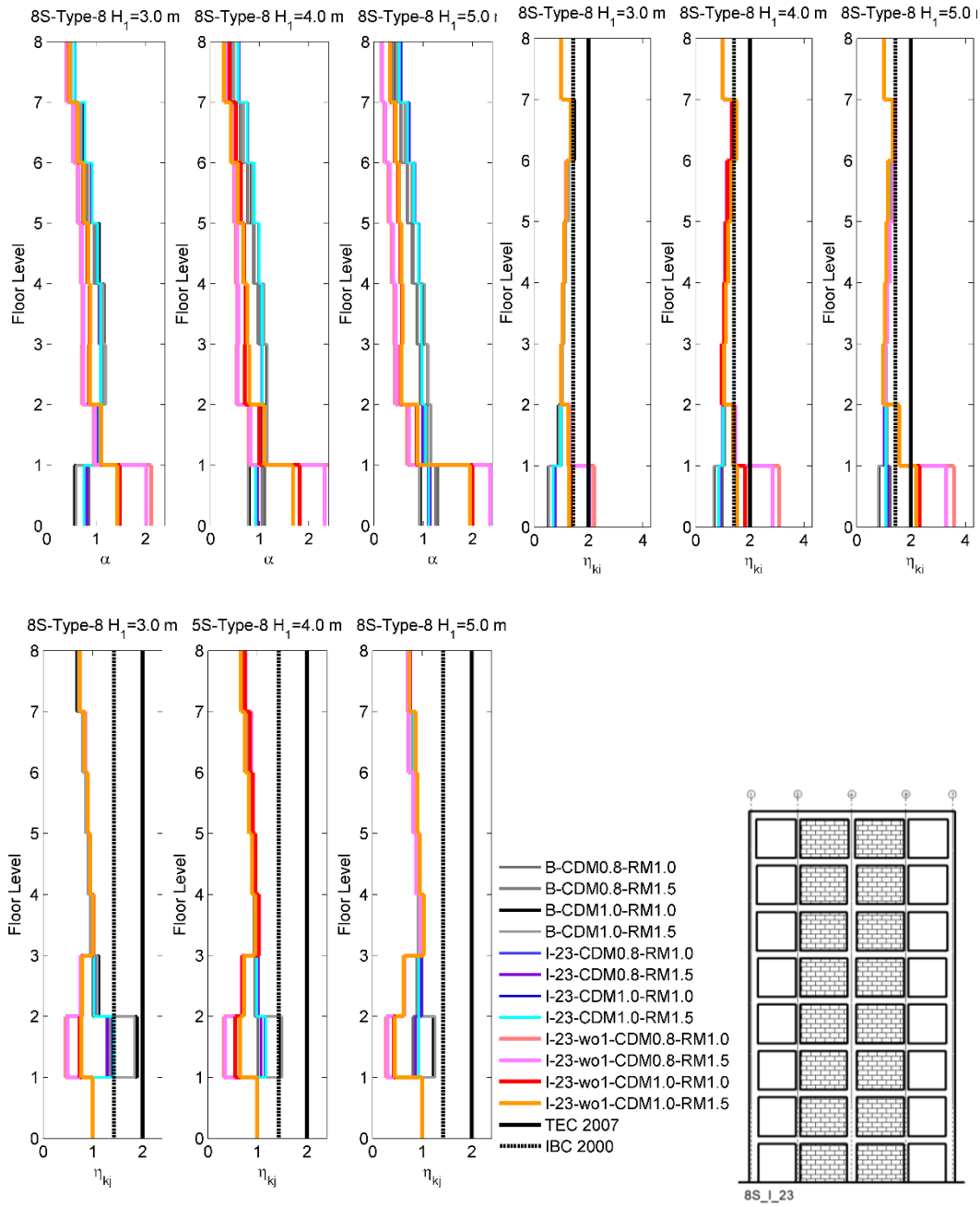

Figure A2-18 8 Story Frame; equivalent static load analysis results for Type 8

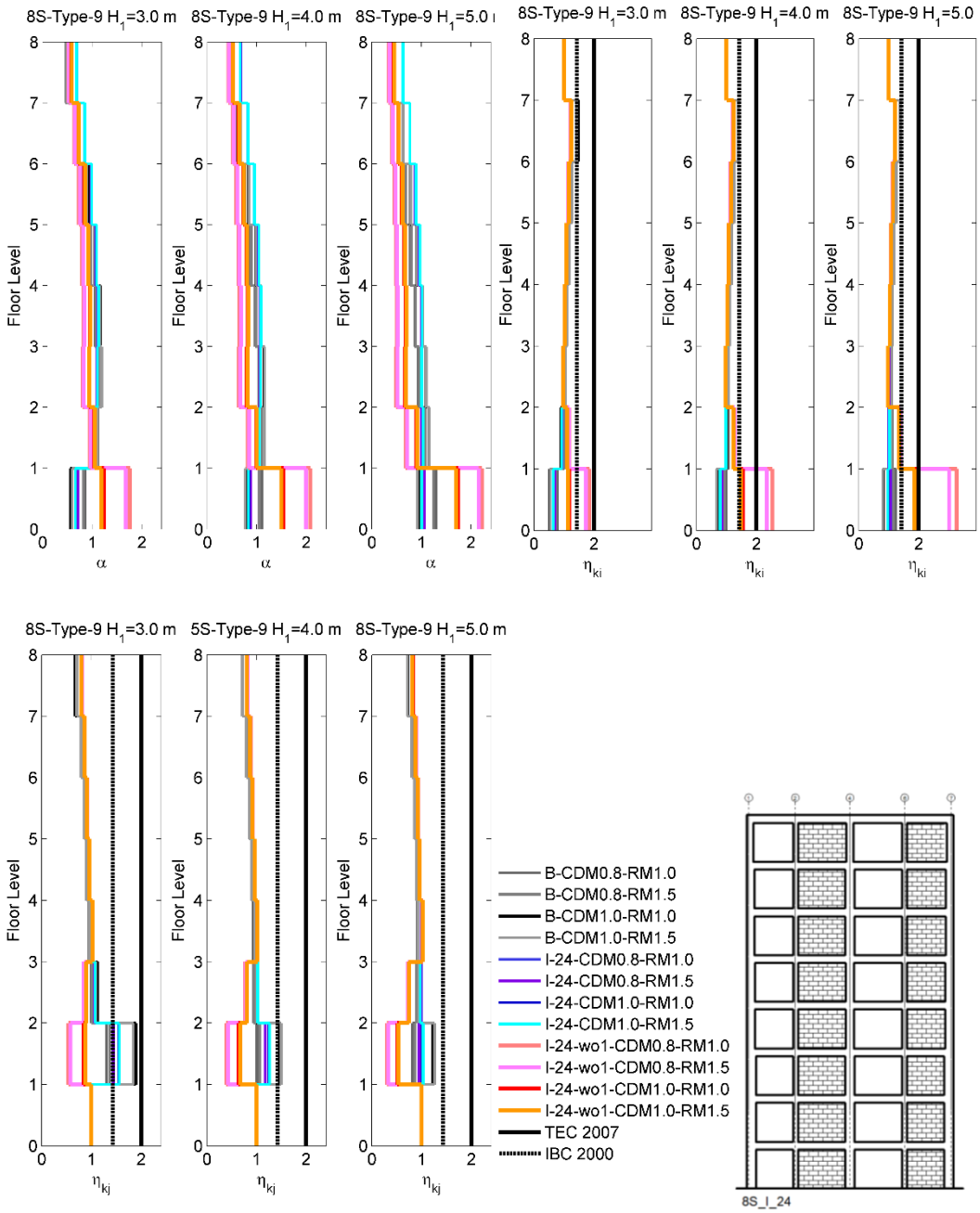

Figure A2-19 8 Story Frame; equivalent static load analysis results for Type 9

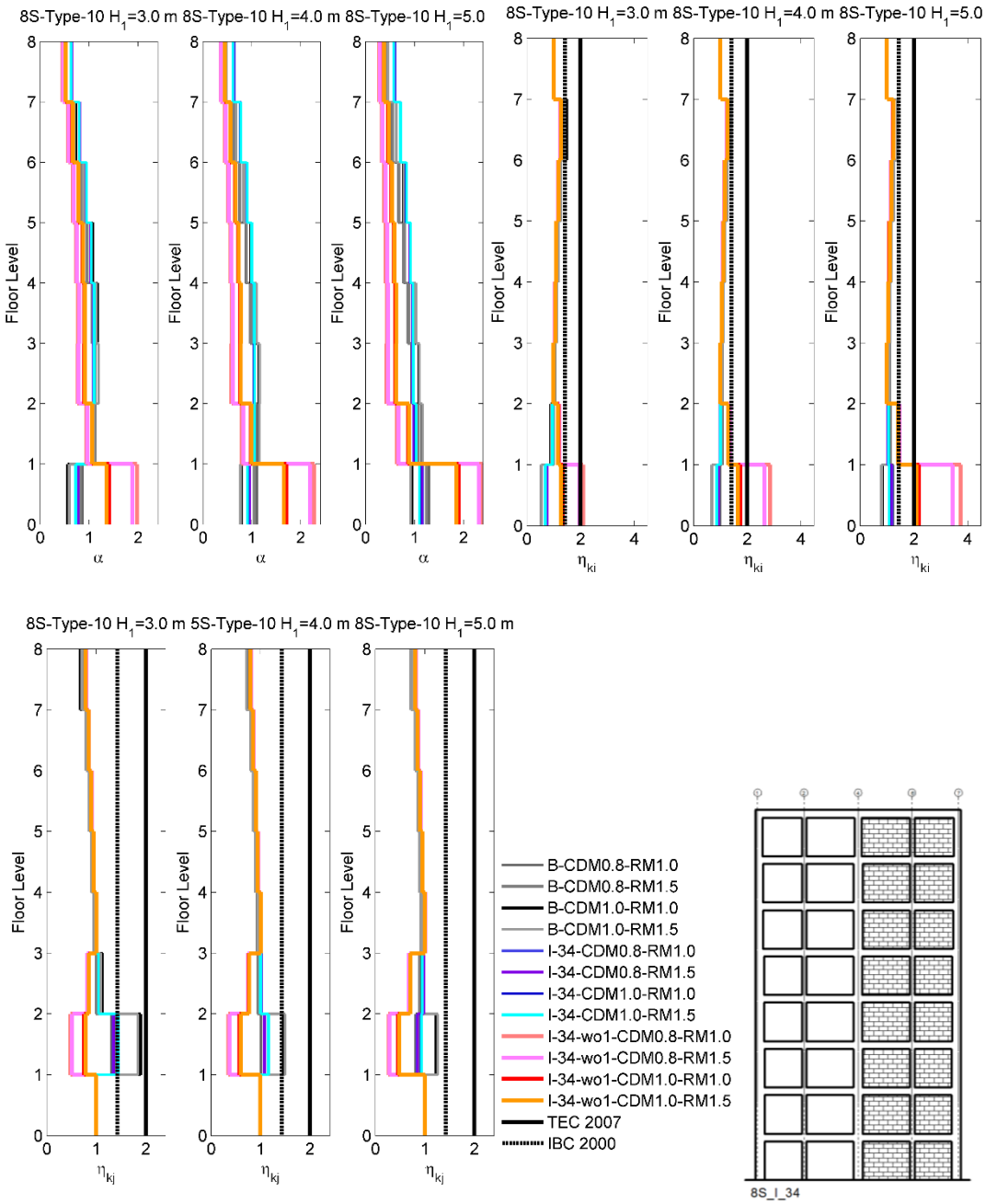

Figure A2-20 8 Story Frame; equivalent static load analysis results for Type 10

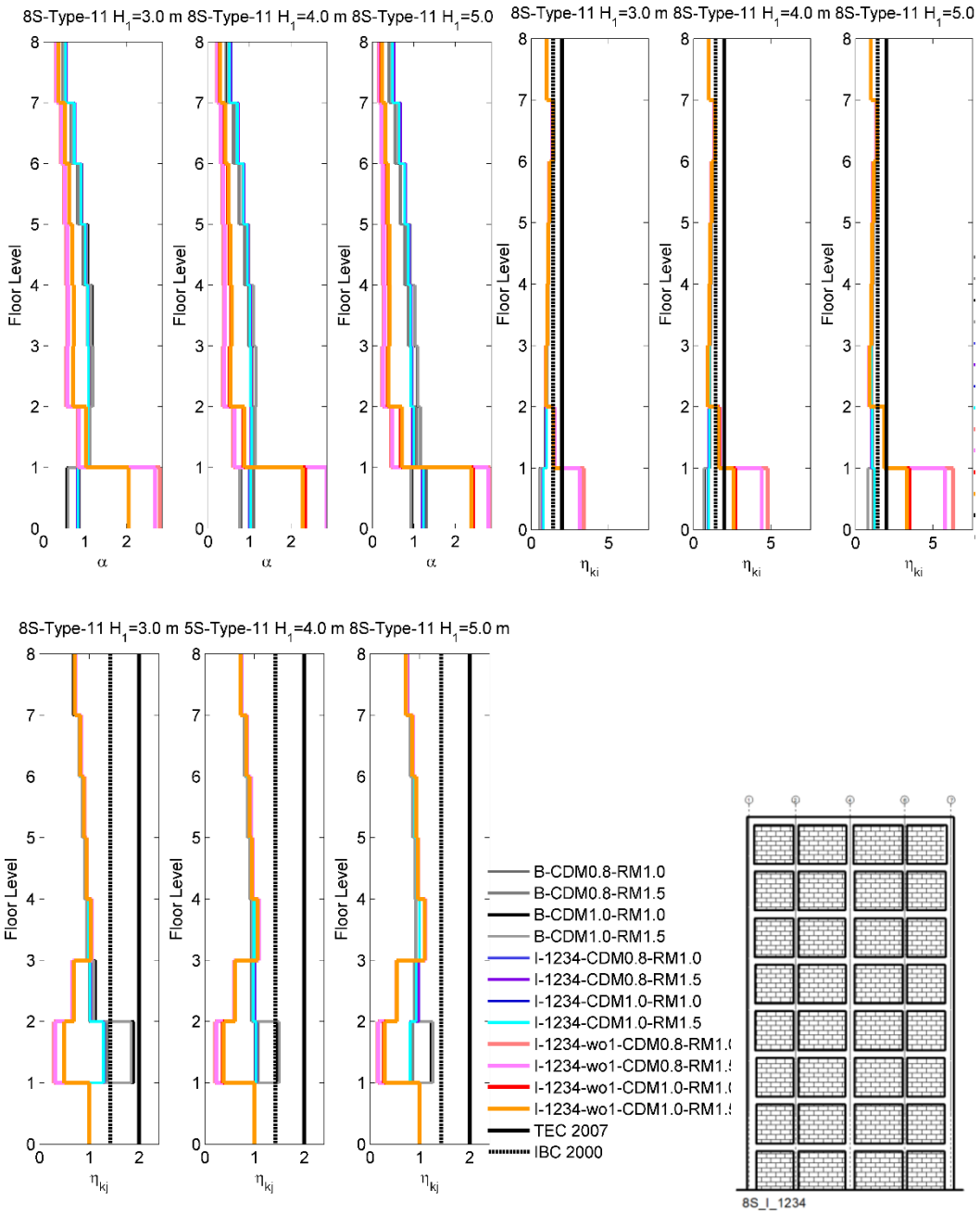

Figure A2-21 8 Story Frame; equivalent static load analysis results for Type 11

A2.2 Mod Superposition Analysis Result

Table A2-4 Soft story, weak story and max alpha values for 3 Story frame for mod superposition analysis results

Frame Type/ Story Level	$\eta_{ki,\ max}$	$\eta_{kj,\ max}$	α_{max}
3S_B_H3.0_CDM0.8_RM1.0	1.190	1.828	1.288
3S_B_H3.0_CDM0.8_RM1.5	1.682	1.000	1.163
3S_B_H3.0_CDM1.0_RM1.0	1.596	1.214	1.113
3S_B_H3.0_CDM1.0_RM1.5	1.589	1.238	1.123
3S_B_H4.0_CDM0.8_RM1.0	1.904	1.000	1.255
3S_B_H4.0_CDM0.8_RM1.5	1.826	1.000	1.240
3S_B_H4.0_CDM1.0_RM1.0	1.721	1.000	1.036
3S_B_H4.0_CDM1.0_RM1.5	1.715	1.000	1.026
3S_B_H5.0_CDM0.8_RM1.0	2.505	1.000	1.267
3S_B_H5.0_CDM0.8_RM1.5	2.392	1.000	1.256
3S_B_H5.0_CDM1.0_RM1.0	1.835	1.000	1.104
3S_B_H5.0_CDM1.0_RM1.5	1.830	1.000	1.096
3S_I_1_H3.0_CDM0.8_RM1.0	1.387	1.090	1.056
3S_I_1_H3.0_CDM0.8_RM1.5	1.393	1.084	1.053
3S_I_1_H3.0_CDM1.0_RM1.0	1.438	1.169	1.091
3S_I_1_H3.0_CDM1.0_RM1.5	1.439	1.164	1.089
3S_I_1_H4.0_CDM0.8_RM1.0	1.363	1.216	1.113
3S_I_1_H4.0_CDM0.8_RM1.5	1.363	1.216	1.113
3S_I_1_H4.0_CDM1.0_RM1.0	1.407	1.150	1.080
3S_I_1_H4.0_CDM1.0_RM1.5	1.409	1.141	1.076
3S_I_1_H5.0_CDM0.8_RM1.0	1.319	1.217	1.131
3S_I_1_H5.0_CDM0.8_RM1.5	1.325	1.200	1.122
3S_I_1_H5.0_CDM1.0_RM1.0	1.372	1.133	1.082
3S_I_1_H5.0_CDM1.0_RM1.5	1.375	1.123	1.076
3S_I_1_wo_1_H3.0_CDM0.8_RM1.0	6.004	1.000	1.785
3S_I_1_wo_1_H3.0_CDM0.8_RM1.5	10.620	1.000	1.907
3S_I_1_wo_1_H3.0_CDM1.0_RM1.0	3.921	1.000	1.657
3S_I_1_wo_1_H3.0_CDM1.0_RM1.5	3.832	1.000	1.649
3S_I_1_wo_1_H4.0_CDM0.8_RM1.0	10.098	1.000	1.629
3S_I_1_wo_1_H4.0_CDM0.8_RM1.5	9.702	1.000	1.624
3S_I_1_wo_1_H4.0_CDM1.0_RM1.0	5.493	1.000	1.540
3S_I_1_wo_1_H4.0_CDM1.0_RM1.5	5.354	1.000	1.535
3S_I_1_wo_1_H5.0_CDM0.8_RM1.0	13.376	1.000	1.480
3S_I_1_wo_1_H5.0_CDM0.8_RM1.5	12.824	1.000	1.478
3S_I_1_wo_1_H5.0_CDM1.0_RM1.0	7.109	1.000	1.431
3S_I_1_wo_1_H5.0_CDM1.0_RM1.5	6.918	1.000	1.429
3S_I_2_H3.0_CDM0.8_RM1.0	1.936	1.000	1.110

3S_I_2_H3.0_CDM0.8_RM1.5	1.938	1.000	1.114
3S_I_2_H3.0_CDM1.0_RM1.0	1.972	1.000	1.101
3S_I_2_H3.0_CDM1.0_RM1.5	1.971	1.000	1.104
3S_I_2_H4.0_CDM0.8_RM1.0	1.882	1.000	1.120
3S_I_2_H4.0_CDM0.8_RM1.5	1.888	1.000	1.123
3S_I_2_H4.0_CDM1.0_RM1.0	1.944	1.000	1.114
3S_I_2_H4.0_CDM1.0_RM1.5	1.939	1.000	1.111
3S_I_2_H5.0_CDM0.8_RM1.0	1.796	1.000	1.124
3S_I_2_H5.0_CDM0.8_RM1.5	1.808	1.000	1.127
3S_I_2_H5.0_CDM1.0_RM1.0	1.911	1.000	1.129
3S_I_2_H5.0_CDM1.0_RM1.5	1.916	1.000	1.130
3S_I_2_wo_1_H3.0_CDM0.8_RM1.0	9.129	1.000	1.886
3S_I_2_wo_1_H3.0_CDM0.8_RM1.5	8.733	1.000	1.878
3S_I_2_wo_1_H3.0_CDM1.0_RM1.0	4.823	1.000	1.729
3S_I_2_wo_1_H3.0_CDM1.0_RM1.5	4.699	1.000	1.721
3S_I_2_wo_1_H4.0_CDM0.8_RM1.0	12.975	1.000	1.654
3S_I_2_wo_1_H4.0_CDM0.8_RM1.5	12.376	1.000	1.650
3S_I_2_wo_1_H4.0_CDM1.0_RM1.0	6.626	1.000	1.572
3S_I_2_wo_1_H4.0_CDM1.0_RM1.5	6.436	1.000	1.567
3S_I_2_wo_1_H5.0_CDM0.8_RM1.0	17.495	1.000	1.494
3S_I_2_wo_1_H5.0_CDM0.8_RM1.5	16.669	1.000	1.492
3S_I_2_wo_1_H5.0_CDM1.0_RM1.0	8.795	1.000	1.451
3S_I_2_wo_1_H5.0_CDM1.0_RM1.5	8.531	1.000	1.448
3S_I_12_H3.0_CDM0.8_RM1.0	2.074	1.000	1.055
3S_I_12_H3.0_CDM0.8_RM1.5	2.083	1.000	1.062
3S_I_12_H3.0_CDM1.0_RM1.0	2.131	1.000	1.086
3S_I_12_H3.0_CDM1.0_RM1.5	2.131	1.000	1.091
3S_I_12_H4.0_CDM0.8_RM1.0	1.984	1.000	1.006
3S_I_12_H4.0_CDM0.8_RM1.5	1.997	1.000	1.009
3S_I_12_H4.0_CDM1.0_RM1.0	2.066	1.000	1.030
3S_I_12_H4.0_CDM1.0_RM1.5	2.068	1.000	1.035
3S_I_12_H5.0_CDM0.8_RM1.0	1.890	1.000	1.013
3S_I_12_H5.0_CDM0.8_RM1.5	1.907	1.000	1.015
3S_I_12_H5.0_CDM1.0_RM1.0	2.014	1.000	1.030
3S_I_12_H5.0_CDM1.0_RM1.5	2.019	1.000	1.033
3S_I_12_wo_1_H3.0_CDM0.8_RM1.0	13.597	1.000	1.952
3S_I_12_wo_1_H3.0_CDM0.8_RM1.5	13.084	1.000	1.947
3S_I_12_wo_1_H3.0_CDM1.0_RM1.0	7.275	1.000	1.840
3S_I_12_wo_1_H3.0_CDM1.0_RM1.5	7.093	1.000	1.834
3S_I_12_wo_1_H4.0_CDM0.8_RM1.0	21.257	1.000	1.690
3S_I_12_wo_1_H4.0_CDM0.8_RM1.5	20.195	1.000	1.687
3S_I_12_wo_1_H4.0_CDM1.0_RM1.0	9.497	1.000	1.622
3S_I_12_wo_1_H4.0_CDM1.0_RM1.5	9.200	1.000	1.618

3S_I_12_wo_1_H5.0_CDM0.8_RM1.0	26.899	1.000	1.510
3S_I_12_wo_1_H5.0_CDM0.8_RM1.5	25.649	1.000	1.508
3S_I_12_wo_1_H5.0_CDM1.0_RM1.0	13.255	1.000	1.480
3S_I_12_wo_1_H5.0_CDM1.0_RM1.5	12.866	1.000	1.478

Table A2-5 Soft story, weak story and max alpha values for 5 Story frame for mod superposition analysis results

Frame Type/ Story Level	$\eta_{ki,\ max}$	$\eta_{kj,\ max}$	α_{max}
5S_B_H3.0_CDM0.8_RM1.0	1.535	1.124	1.121
5S_B_H3.0_CDM0.8_RM1.5	1.535	1.172	1.131
5S_B_H3.0_CDM1.0_RM1.0	1.531	1.636	1.191
5S_B_H3.0_CDM1.0_RM1.5	1.531	1.673	1.192
5S_B_H4.0_CDM0.8_RM1.0	1.531	1.000	1.203
5S_B_H4.0_CDM0.8_RM1.5	1.531	1.000	1.168
5S_B_H4.0_CDM1.0_RM1.0	1.533	1.309	1.175
5S_B_H4.0_CDM1.0_RM1.5	1.533	1.344	1.182
5S_B_H5.0_CDM0.8_RM1.0	1.519	1.000	1.329
5S_B_H5.0_CDM0.8_RM1.5	1.521	1.000	1.296
5S_B_H5.0_CDM1.0_RM1.0	1.530	1.083	1.114
5S_B_H5.0_CDM1.0_RM1.5	1.530	1.115	1.126
5S_I_1_H3.0_CDM0.8_RM1.0	1.267	1.418	1.111
5S_I_1_H3.0_CDM0.8_RM1.5	1.269	1.428	1.113
5S_I_1_H3.0_CDM1.0_RM1.0	1.277	1.588	1.144
5S_I_1_H3.0_CDM1.0_RM1.5	1.278	1.600	1.147
5S_I_1_H4.0_CDM0.8_RM1.0	1.264	1.270	1.096
5S_I_1_H4.0_CDM0.8_RM1.5	1.266	1.277	1.097
5S_I_1_H4.0_CDM1.0_RM1.0	1.277	1.406	1.125
5S_I_1_H4.0_CDM1.0_RM1.5	1.278	1.416	1.128
5S_I_1_H5.0_CDM0.8_RM1.0	1.260	1.094	1.043
5S_I_1_H5.0_CDM0.8_RM1.5	1.262	1.098	1.046
5S_I_1_H5.0_CDM1.0_RM1.0	1.275	1.211	1.094
5S_I_1_H5.0_CDM1.0_RM1.5	1.276	1.221	1.098
5S_I_1_wo_1_H3.0_CDM0.8_RM1.0	1.664	1.000	1.498
5S_I_1_wo_1_H3.0_CDM0.8_RM1.5	1.586	1.000	1.458
5S_I_1_wo_1_H3.0_CDM1.0_RM1.0	1.290	1.000	1.101
5S_I_1_wo_1_H3.0_CDM1.0_RM1.5	1.290	1.000	1.077
5S_I_1_wo_1_H4.0_CDM0.8_RM1.0	2.225	1.000	1.634
5S_I_1_wo_1_H4.0_CDM0.8_RM1.5	2.115	1.000	1.601
5S_I_1_wo_1_H4.0_CDM1.0_RM1.0	1.360	1.000	1.297
5S_I_1_wo_1_H4.0_CDM1.0_RM1.5	1.319	1.000	1.275
5S_I_1_wo_1_H5.0_CDM0.8_RM1.0	2.766	1.000	1.655
5S_I_1_wo_1_H5.0_CDM0.8_RM1.5	2.630	1.000	1.630
5S_I_1_wo_1_H5.0_CDM1.0_RM1.0	1.664	1.000	1.385

5S_I_1_wo_1_H5.0_CDM1.0_RM1.5	1.611	1.000	1.366
5S_I_2_H3.0_CDM0.8_RM1.0	1.362	1.314	1.120
5S_I_2_H3.0_CDM0.8_RM1.5	1.362	1.331	1.123
5S_I_2_H3.0_CDM1.0_RM1.0	1.366	1.559	1.151
5S_I_2_H3.0_CDM1.0_RM1.5	1.367	1.576	1.152
5S_I_2_H4.0_CDM0.8_RM1.0	1.352	1.019	1.054
5S_I_2_H4.0_CDM0.8_RM1.5	1.355	1.035	1.060
5S_I_2_H4.0_CDM1.0_RM1.0	1.372	1.246	1.132
5S_I_2_H4.0_CDM1.0_RM1.5	1.375	1.261	1.135
5S_I_2_H5.0_CDM0.8_RM1.0	1.334	1.000	1.182
5S_I_2_H5.0_CDM0.8_RM1.5	1.336	1.000	1.172
5S_I_2_H5.0_CDM1.0_RM1.0	1.354	1.012	1.062
5S_I_2_H5.0_CDM1.0_RM1.5	1.356	1.029	1.070
5S_I_2_wo_1_H3.0_CDM0.8_RM1.0	1.402	1.000	1.380
5S_I_2_wo_1_H3.0_CDM0.8_RM1.5	1.573	1.000	1.388
5S_I_2_wo_1_H3.0_CDM1.0_RM1.0	1.572	1.137	1.134
5S_I_2_wo_1_H3.0_CDM1.0_RM1.5	1.572	1.175	1.142
5S_I_2_wo_1_H4.0_CDM0.8_RM1.0	1.880	1.000	1.551
5S_I_2_wo_1_H4.0_CDM0.8_RM1.5	1.786	1.000	1.515
5S_I_2_wo_1_H4.0_CDM1.0_RM1.0	1.356	1.000	1.203
5S_I_2_wo_1_H4.0_CDM1.0_RM1.5	1.358	1.000	1.181
5S_I_2_wo_1_H5.0_CDM0.8_RM1.0	2.380	1.000	1.607
5S_I_2_wo_1_H5.0_CDM0.8_RM1.5	2.253	1.000	1.578
5S_I_2_wo_1_H5.0_CDM1.0_RM1.0	1.421	1.000	1.311
5S_I_2_wo_1_H5.0_CDM1.0_RM1.5	1.376	1.000	1.291
5S_I_3_H3.0_CDM0.8_RM1.0	1.459	1.241	1.128
5S_I_3_H3.0_CDM0.8_RM1.5	1.461	1.255	1.132
5S_I_3_H3.0_CDM1.0_RM1.0	1.474	1.451	1.162
5S_I_3_H3.0_CDM1.0_RM1.5	1.475	1.465	1.163
5S_I_3_H4.0_CDM0.8_RM1.0	1.445	1.000	1.168
5S_I_3_H4.0_CDM0.8_RM1.5	1.448	1.000	1.156
5S_I_3_H4.0_CDM1.0_RM1.0	1.472	1.087	1.106
5S_I_3_H4.0_CDM1.0_RM1.5	1.474	1.105	1.112
5S_I_3_H5.0_CDM0.8_RM1.0	1.421	1.000	1.222
5S_I_3_H5.0_CDM0.8_RM1.5	1.425	1.000	1.214
5S_I_3_H5.0_CDM1.0_RM1.0	1.452	1.000	1.100
5S_I_3_H5.0_CDM1.0_RM1.5	1.455	1.000	1.091
5S_I_3_wo_1_H3.0_CDM0.8_RM1.0	1.645	1.000	1.540
5S_I_3_wo_1_H3.0_CDM0.8_RM1.5	1.569	1.000	1.498
5S_I_3_wo_1_H3.0_CDM1.0_RM1.0	1.485	1.000	1.154
5S_I_3_wo_1_H3.0_CDM1.0_RM1.5	1.486	1.000	1.131
5S_I_3_wo_1_H4.0_CDM0.8_RM1.0	2.216	1.000	1.686
5S_I_3_wo_1_H4.0_CDM0.8_RM1.5	2.101	1.000	1.649

5S_I_3_wo_1_H4.0_CDM1.0_RM1.0	1.463	1.000	1.326
5S_I_3_wo_1_H4.0_CDM1.0_RM1.5	1.465	1.000	1.303
5S_I_3_wo_1_H5.0_CDM0.8_RM1.0	2.826	1.000	1.711
5S_I_3_wo_1_H5.0_CDM0.8_RM1.5	2.670	1.000	1.683
5S_I_3_wo_1_H5.0_CDM1.0_RM1.0	1.653	1.000	1.417
5S_I_3_wo_1_H5.0_CDM1.0_RM1.5	1.599	1.000	1.397
5S_I_12_H3.0_CDM0.8_RM1.0	1.302	1.399	1.107
5S_I_12_H3.0_CDM0.8_RM1.5	1.304	1.394	1.106
5S_I_12_H3.0_CDM1.0_RM1.0	1.316	1.449	1.118
5S_I_12_H3.0_CDM1.0_RM1.5	1.317	1.452	1.119
5S_I_12_H4.0_CDM0.8_RM1.0	1.298	1.240	1.085
5S_I_12_H4.0_CDM0.8_RM1.5	1.301	1.236	1.082
5S_I_12_H4.0_CDM1.0_RM1.0	1.316	1.277	1.100
5S_I_12_H4.0_CDM1.0_RM1.5	1.317	1.280	1.101
5S_I_12_H5.0_CDM0.8_RM1.0	1.291	1.045	1.030
5S_I_12_H5.0_CDM0.8_RM1.5	1.294	1.041	1.030
5S_I_12_H5.0_CDM1.0_RM1.0	1.313	1.081	1.057
5S_I_12_H5.0_CDM1.0_RM1.5	1.315	1.085	1.059
5S_I_12_wo_1_H3.0_CDM0.8_RM1.0	2.392	1.000	1.872
5S_I_12_wo_1_H3.0_CDM0.8_RM1.5	2.267	1.000	1.824
5S_I_12_wo_1_H3.0_CDM1.0_RM1.0	1.425	1.000	1.401
5S_I_12_wo_1_H3.0_CDM1.0_RM1.5	1.383	1.000	1.373
5S_I_12_wo_1_H4.0_CDM0.8_RM1.0	3.202	1.000	1.917
5S_I_12_wo_1_H4.0_CDM0.8_RM1.5	3.039	1.000	1.886
5S_I_12_wo_1_H4.0_CDM1.0_RM1.0	1.907	1.000	1.583
5S_I_12_wo_1_H4.0_CDM1.0_RM1.5	1.841	1.000	1.558
5S_I_12_wo_1_H5.0_CDM0.8_RM1.0	3.974	1.000	1.853
5S_I_12_wo_1_H5.0_CDM0.8_RM1.5	3.768	1.000	1.832
5S_I_12_wo_1_H5.0_CDM1.0_RM1.0	2.342	1.000	1.615
5S_I_12_wo_1_H5.0_CDM1.0_RM1.5	3.033	1.000	1.716
5S_I_13_H3.0_CDM0.8_RM1.0	1.339	1.395	1.105
5S_I_13_H3.0_CDM0.8_RM1.5	1.342	1.387	1.104
5S_I_13_H3.0_CDM1.0_RM1.0	1.360	1.414	1.113
5S_I_13_H3.0_CDM1.0_RM1.5	1.362	1.416	1.114
5S_I_13_H4.0_CDM0.8_RM1.0	1.327	1.178	1.073
5S_I_13_H4.0_CDM0.8_RM1.5	1.331	1.173	1.072
5S_I_13_H4.0_CDM1.0_RM1.0	1.352	1.202	1.084
5S_I_13_H4.0_CDM1.0_RM1.5	1.355	1.205	1.085
5S_I_13_H5.0_CDM0.8_RM1.0	1.313	1.083	1.049
5S_I_13_H5.0_CDM0.8_RM1.5	1.317	1.075	1.047
5S_I_13_H5.0_CDM1.0_RM1.0	1.341	1.086	1.058
5S_I_13_H5.0_CDM1.0_RM1.5	1.344	1.088	1.059
5S_I_13_wo_1_H3.0_CDM0.8_RM1.0	2.556	1.000	1.913

5S_I_13_wo_1_H3.0_CDM0.8_RM1.5	2.425	1.000	1.866
5S_I_13_wo_1_H3.0_CDM1.0_RM1.0	1.549	1.000	1.459
5S_I_13_wo_1_H3.0_CDM1.0_RM1.5	1.503	1.000	1.431
5S_I_13_wo_1_H4.0_CDM0.8_RM1.0	3.420	1.000	1.946
5S_I_13_wo_1_H4.0_CDM0.8_RM1.5	3.247	1.000	1.916
5S_I_13_wo_1_H4.0_CDM1.0_RM1.0	2.041	1.000	1.615
5S_I_13_wo_1_H4.0_CDM1.0_RM1.5	1.972	1.000	1.590
5S_I_13_wo_1_H5.0_CDM0.8_RM1.0	4.259	1.000	1.876
5S_I_13_wo_1_H5.0_CDM0.8_RM1.5	4.038	1.000	1.855
5S_I_13_wo_1_H5.0_CDM1.0_RM1.0	2.499	1.000	1.638
5S_I_13_wo_1_H5.0_CDM1.0_RM1.5	2.414	1.000	1.620
5S_I_23_H3.0_CDM0.8_RM1.0	1.581	1.307	1.157
5S_I_23_H3.0_CDM0.8_RM1.5	1.585	1.299	1.156
5S_I_23_H3.0_CDM1.0_RM1.0	1.608	1.340	1.162
5S_I_23_H3.0_CDM1.0_RM1.5	1.610	1.343	1.162
5S_I_23_H4.0_CDM0.8_RM1.0	1.548	1.000	1.138
5S_I_23_H4.0_CDM0.8_RM1.5	1.554	1.000	1.138
5S_I_23_H4.0_CDM1.0_RM1.0	1.590	1.010	1.090
5S_I_23_H4.0_CDM1.0_RM1.5	1.593	1.019	1.093
5S_I_23_H5.0_CDM0.8_RM1.0	1.513	1.000	1.243
5S_I_23_H5.0_CDM0.8_RM1.5	1.521	1.000	1.243
5S_I_23_H5.0_CDM1.0_RM1.0	1.568	1.000	1.184
5S_I_23_H5.0_CDM1.0_RM1.5	1.572	1.000	1.179
5S_I_23_wo_1_H3.0_CDM0.8_RM1.0	2.468	1.000	1.967
5S_I_23_wo_1_H3.0_CDM0.8_RM1.5	2.340	1.000	1.918
5S_I_23_wo_1_H3.0_CDM1.0_RM1.0	1.622	1.000	1.513
5S_I_23_wo_1_H3.0_CDM1.0_RM1.5	1.624	1.000	1.485
5S_I_23_wo_1_H4.0_CDM0.8_RM1.0	3.367	1.000	2.004
5S_I_23_wo_1_H4.0_CDM0.8_RM1.5	3.175	1.000	1.969
5S_I_23_wo_1_H4.0_CDM1.0_RM1.0	1.936	1.000	1.639
5S_I_23_wo_1_H4.0_CDM1.0_RM1.5	1.871	1.000	1.614
5S_I_23_wo_1_H5.0_CDM0.8_RM1.0	4.328	1.000	1.931
5S_I_23_wo_1_H5.0_CDM0.8_RM1.5	4.067	1.000	1.907
5S_I_23_wo_1_H5.0_CDM1.0_RM1.0	2.398	1.000	1.667
5S_I_23_wo_1_H5.0_CDM1.0_RM1.5	2.310	1.000	1.647
5S_I_123_H3.0_CDM0.8_RM1.0	1.556	1.240	1.094
5S_I_123_H3.0_CDM0.8_RM1.5	1.559	1.235	1.094
5S_I_123_H3.0_CDM1.0_RM1.0	1.578	1.230	1.098
5S_I_123_H3.0_CDM1.0_RM1.5	1.579	1.229	1.098
5S_I_123_H4.0_CDM0.8_RM1.0	1.532	1.060	1.059
5S_I_123_H4.0_CDM0.8_RM1.5	1.537	1.053	1.058
5S_I_123_H4.0_CDM1.0_RM1.0	1.567	1.054	1.066
5S_I_123_H4.0_CDM1.0_RM1.5	1.570	1.053	1.067

5S_I_123_H5.0_CDM0.8_RM1.0	1.510	1.000	1.072
5S_I_123_H5.0_CDM0.8_RM1.5	1.516	1.000	1.078
5S_I_123_H5.0_CDM1.0_RM1.0	1.554	1.000	1.089
5S_I_123_H5.0_CDM1.0_RM1.5	1.557	1.000	1.089
5S_I_123_wo_1_H3.0_CDM0.8_RM1.0	3.512	1.000	2.258
5S_I_123_wo_1_H3.0_CDM0.8_RM1.5	3.320	1.000	2.212
5S_I_123_wo_1_H3.0_CDM1.0_RM1.0	2.060	1.000	1.787
5S_I_123_wo_1_H3.0_CDM1.0_RM1.5	1.995	1.000	1.757
5S_I_123_wo_1_H4.0_CDM0.8_RM1.0	4.785	1.000	2.179
5S_I_123_wo_1_H4.0_CDM0.8_RM1.5	4.519	1.000	2.152
5S_I_123_wo_1_H4.0_CDM1.0_RM1.0	2.725	1.000	1.866
5S_I_123_wo_1_H4.0_CDM1.0_RM1.5	2.627	1.000	1.841
5S_I_123_wo_1_H5.0_CDM0.8_RM1.0	6.042	1.000	2.031
5S_I_123_wo_1_H5.0_CDM0.8_RM1.5	5.703	1.000	2.014
5S_I_123_wo_1_H5.0_CDM1.0_RM1.0	3.388	1.000	1.825
5S_I_123_wo_1_H5.0_CDM1.0_RM1.5	3.262	1.000	1.809

Table A2-6 Soft story, weak story and max alpha values for 8 Story frame for mod superposition analysis results

Frame Type/ Story Level	$\eta_{ki,\,max}$	$\eta_{kj,\,max}$	α_{max}
8S_B_H3.0_CDM0.8_RM1.0	1.335	1.325	1.144
8S_B_H3.0_CDM0.8_RM1.5	1.336	1.387	1.145
8S_B_H3.0_CDM1.0_RM1.0	1.399	1.886	1.179
8S_B_H3.0_CDM1.0_RM1.5	1.347	1.854	1.193
8S_B_H4.0_CDM0.8_RM1.0	1.323	1.028	1.130
8S_B_H4.0_CDM0.8_RM1.5	1.325	1.087	1.141
8S_B_H4.0_CDM1.0_RM1.0	1.338	1.474	1.168
8S_B_H4.0_CDM1.0_RM1.5	1.339	1.517	1.166
8S_B_H5.0_CDM0.8_RM1.0	1.308	1.000	1.296
8S_B_H5.0_CDM0.8_RM1.5	1.311	1.000	1.241
8S_B_H5.0_CDM1.0_RM1.0	1.328	1.239	1.175
8S_B_H5.0_CDM1.0_RM1.5	1.329	1.280	1.179
8S_I_1_H3.0_CDM0.8_RM1.0	1.211	1.466	1.116
8S_I_1_H3.0_CDM0.8_RM1.5	1.212	1.501	1.120
8S_I_1_H3.0_CDM1.0_RM1.0	1.216	1.780	1.152
8S_I_1_H3.0_CDM1.0_RM1.5	1.216	1.816	1.156
8S_I_1_H4.0_CDM0.8_RM1.0	1.204	1.170	1.075
8S_I_1_H4.0_CDM0.8_RM1.5	1.205	1.199	1.080
8S_I_1_H4.0_CDM1.0_RM1.0	1.209	1.422	1.121
8S_I_1_H4.0_CDM1.0_RM1.5	1.210	1.451	1.126
8S_I_1_H5.0_CDM0.8_RM1.0	1.206	1.013	1.049

8S_I_1_H5.0_CDM0.8_RM1.5	1.206	1.014	1.029
8S_I_1_H5.0_CDM1.0_RM1.0	1.209	1.171	1.061
8S_I_1_H5.0_CDM1.0_RM1.5	1.210	1.199	1.068
8S_I_1_wo_1_H3.0_CDM0.8_RM1.0	1.210	1.022	1.083
8S_I_1_wo_1_H3.0_CDM0.8_RM1.5	1.211	1.023	1.030
8S_I_1_wo_1_H3.0_CDM1.0_RM1.0	1.215	1.392	1.077
8S_I_1_wo_1_H3.0_CDM1.0_RM1.5	1.216	1.440	1.085
8S_I_1_wo_1_H4.0_CDM0.8_RM1.0	1.416	1.012	1.383
8S_I_1_wo_1_H4.0_CDM0.8_RM1.5	1.326	1.013	1.319
8S_I_1_wo_1_H4.0_CDM1.0_RM1.0	1.210	1.081	1.061
8S_I_1_wo_1_H4.0_CDM1.0_RM1.5	1.211	1.121	1.065
8S_I_1_wo_1_H5.0_CDM0.8_RM1.0	1.789	1.006	1.594
8S_I_1_wo_1_H5.0_CDM0.8_RM1.5	1.667	1.007	1.530
8S_I_1_wo_1_H5.0_CDM1.0_RM1.0	1.204	1.013	1.178
8S_I_1_wo_1_H5.0_CDM1.0_RM1.5	1.205	1.015	1.143
8S_I_2_H3.0_CDM0.8_RM1.0	1.286	1.416	1.099
8S_I_2_H3.0_CDM0.8_RM1.5	1.288	1.439	1.101
8S_I_2_H3.0_CDM1.0_RM1.0	1.304	1.647	1.124
8S_I_2_H3.0_CDM1.0_RM1.5	1.305	1.674	1.127
8S_I_2_H4.0_CDM0.8_RM1.0	1.270	1.161	1.066
8S_I_2_H4.0_CDM0.8_RM1.5	1.272	1.180	1.068
8S_I_2_H4.0_CDM1.0_RM1.0	1.292	1.349	1.092
8S_I_2_H4.0_CDM1.0_RM1.5	1.294	1.372	1.096
8S_I_2_H5.0_CDM0.8_RM1.0	1.256	1.000	1.080
8S_I_2_H5.0_CDM0.8_RM1.5	1.259	1.000	1.070
8S_I_2_H5.0_CDM1.0_RM1.0	1.277	1.107	1.078
8S_I_2_H5.0_CDM1.0_RM1.5	1.279	1.128	1.084
8S_I_2_wo_1_H3.0_CDM0.8_RM1.0	1.376	1.000	1.460
8S_I_2_wo_1_H3.0_CDM0.8_RM1.5	1.287	1.000	1.385
8S_I_2_wo_1_H3.0_CDM1.0_RM1.0	1.303	1.122	1.121
8S_I_2_wo_1_H3.0_CDM1.0_RM1.5	1.304	1.165	1.122
8S_I_2_wo_1_H4.0_CDM0.8_RM1.0	1.878	1.000	1.802
8S_I_2_wo_1_H4.0_CDM0.8_RM1.5	1.746	1.000	1.722
8S_I_2_wo_1_H4.0_CDM1.0_RM1.0	1.284	1.000	1.291
8S_I_2_wo_1_H4.0_CDM1.0_RM1.5	1.286	1.000	1.249
8S_I_2_wo_1_H5.0_CDM0.8_RM1.0	2.392	1.000	1.983
8S_I_2_wo_1_H5.0_CDM0.8_RM1.5	2.212	1.000	1.912
8S_I_2_wo_1_H5.0_CDM1.0_RM1.0	1.445	1.000	1.504
8S_I_2_wo_1_H5.0_CDM1.0_RM1.5	1.382	1.000	1.462
8S_I_3_H3.0_CDM0.8_RM1.0	1.274	1.356	1.095
8S_I_3_H3.0_CDM0.8_RM1.5	1.276	1.378	1.097
8S_I_3_H3.0_CDM1.0_RM1.0	1.287	1.567	1.122
8S_I_3_H3.0_CDM1.0_RM1.5	1.288	1.592	1.125

8S_I_3_H4.0_CDM0.8_RM1.0	1.263	1.120	1.063
8S_I_3_H4.0_CDM0.8_RM1.5	1.265	1.138	1.065
8S_I_3_H4.0_CDM1.0_RM1.0	1.278	1.294	1.088
8S_I_3_H4.0_CDM1.0_RM1.5	1.280	1.316	1.092
8S_I_3_H5.0_CDM0.8_RM1.0	1.250	1.000	1.104
8S_I_3_H5.0_CDM0.8_RM1.5	1.252	1.000	1.093
8S_I_3_H5.0_CDM1.0_RM1.0	1.268	1.061	1.058
8S_I_3_H5.0_CDM1.0_RM1.5	1.269	1.082	1.064
8S_I_3_wo_1_H3.0_CDM0.8_RM1.0	1.494	1.000	1.536
8S_I_3_wo_1_H3.0_CDM0.8_RM1.5	1.398	1.000	1.458
8S_I_3_wo_1_H3.0_CDM1.0_RM1.0	1.287	1.029	1.091
8S_I_3_wo_1_H3.0_CDM1.0_RM1.5	1.288	1.069	1.093
8S_I_3_wo_1_H4.0_CDM0.8_RM1.0	2.033	1.000	1.876
8S_I_3_wo_1_H4.0_CDM0.8_RM1.5	1.888	1.000	1.794
8S_I_3_wo_1_H4.0_CDM1.0_RM1.0	1.275	1.000	1.350
8S_I_3_wo_1_H4.0_CDM1.0_RM1.5	1.277	1.000	1.307
8S_I_3_wo_1_H5.0_CDM0.8_RM1.0	2.612	1.000	2.059
8S_I_3_wo_1_H5.0_CDM0.8_RM1.5	2.413	1.000	1.985
8S_I_3_wo_1_H5.0_CDM1.0_RM1.0	1.567	1.000	1.564
8S_I_3_wo_1_H5.0_CDM1.0_RM1.5	1.498	1.000	1.521
8S_I_4_H3.0_CDM0.8_RM1.0	1.259	1.412	1.108
8S_I_4_H3.0_CDM0.8_RM1.5	1.261	1.436	1.111
8S_I_4_H3.0_CDM1.0_RM1.0	1.275	1.640	1.136
8S_I_4_H3.0_CDM1.0_RM1.5	1.276	1.666	1.139
8S_I_4_H4.0_CDM0.8_RM1.0	1.247	1.089	1.069
8S_I_4_H4.0_CDM0.8_RM1.5	1.249	1.113	1.074
8S_I_4_H4.0_CDM1.0_RM1.0	1.265	1.305	1.097
8S_I_4_H4.0_CDM1.0_RM1.5	1.266	1.330	1.100
8S_I_4_H5.0_CDM0.8_RM1.0	1.236	1.000	1.204
8S_I_4_H5.0_CDM0.8_RM1.5	1.238	1.000	1.183
8S_I_4_H5.0_CDM1.0_RM1.0	1.255	1.054	1.091
8S_I_4_H5.0_CDM1.0_RM1.5	1.257	1.078	1.096
8S_I_4_wo_1_H3.0_CDM0.8_RM1.0	1.288	1.000	1.358
8S_I_4_wo_1_H3.0_CDM0.8_RM1.5	1.257	1.000	1.292
8S_I_4_wo_1_H3.0_CDM1.0_RM1.0	1.273	1.144	1.091
8S_I_4_wo_1_H3.0_CDM1.0_RM1.5	1.274	1.182	1.090
8S_I_4_wo_1_H4.0_CDM0.8_RM1.0	1.709	1.000	1.671
8S_I_4_wo_1_H4.0_CDM0.8_RM1.5	1.597	1.000	1.597
8S_I_4_wo_1_H4.0_CDM1.0_RM1.0	1.259	1.000	1.205
8S_I_4_wo_1_H4.0_CDM1.0_RM1.5	1.260	1.000	1.168
8S_I_4_wo_1_H5.0_CDM0.8_RM1.0	2.164	1.000	1.869
8S_I_4_wo_1_H5.0_CDM0.8_RM1.5	2.010	1.000	1.798
8S_I_4_wo_1_H5.0_CDM1.0_RM1.0	1.347	1.000	1.406

8S_I_4_wo_1_H5.0_CDM1.0_RM1.5	1.293	1.000	1.366
8S_I_12_H3.0_CDM0.8_RM1.0	1.233	1.456	1.119
8S_I_12_H3.0_CDM0.8_RM1.5	1.235	1.467	1.119
8S_I_12_H3.0_CDM1.0_RM1.0	1.246	1.596	1.131
8S_I_12_H3.0_CDM1.0_RM1.5	1.247	1.616	1.133
8S_I_12_H4.0_CDM0.8_RM1.0	1.224	1.204	1.091
8S_I_12_H4.0_CDM0.8_RM1.5	1.225	1.210	1.091
8S_I_12_H4.0_CDM1.0_RM1.0	1.237	1.302	1.099
8S_I_12_H4.0_CDM1.0_RM1.5	1.239	1.319	1.101
8S_I_12_H5.0_CDM0.8_RM1.0	1.213	1.036	1.029
8S_I_12_H5.0_CDM0.8_RM1.5	1.213	1.033	1.026
8S_I_12_H5.0_CDM1.0_RM1.0	1.228	1.056	1.034
8S_I_12_H5.0_CDM1.0_RM1.5	1.229	1.071	1.037
8S_I_12_wo_1_H3.0_CDM0.8_RM1.0	1.711	1.034	1.704
8S_I_12_wo_1_H3.0_CDM0.8_RM1.5	1.594	1.035	1.618
8S_I_12_wo_1_H3.0_CDM1.0_RM1.0	1.243	1.034	1.171
8S_I_12_wo_1_H3.0_CDM1.0_RM1.5	1.244	1.034	1.128
8S_I_12_wo_1_H4.0_CDM0.8_RM1.0	2.346	1.041	2.029
8S_I_12_wo_1_H4.0_CDM0.8_RM1.5	2.174	1.041	1.948
8S_I_12_wo_1_H4.0_CDM1.0_RM1.0	1.430	1.035	1.492
8S_I_12_wo_1_H4.0_CDM1.0_RM1.5	1.368	1.035	1.446
8S_I_12_wo_1_H5.0_CDM0.8_RM1.0	2.987	1.055	2.158
8S_I_12_wo_1_H5.0_CDM0.8_RM1.5	2.760	1.054	2.092
8S_I_12_wo_1_H5.0_CDM1.0_RM1.0	1.785	1.042	1.697
8S_I_12_wo_1_H5.0_CDM1.0_RM1.5	1.704	1.042	1.653
8S_I_13_H3.0_CDM0.8_RM1.0	1.223	1.456	1.125
8S_I_13_H3.0_CDM0.8_RM1.5	1.224	1.464	1.126
8S_I_13_H3.0_CDM1.0_RM1.0	1.231	1.578	1.146
8S_I_13_H3.0_CDM1.0_RM1.5	1.232	1.597	1.149
8S_I_13_H4.0_CDM0.8_RM1.0	1.215	1.233	1.103
8S_I_13_H4.0_CDM0.8_RM1.5	1.216	1.238	1.103
8S_I_13_H4.0_CDM1.0_RM1.0	1.226	1.314	1.116
8S_I_13_H4.0_CDM1.0_RM1.5	1.227	1.330	1.119
8S_I_13_H5.0_CDM0.8_RM1.0	1.207	1.057	1.047
8S_I_13_H5.0_CDM0.8_RM1.5	1.208	1.052	1.047
8S_I_13_H5.0_CDM1.0_RM1.0	1.219	1.077	1.059
8S_I_13_H5.0_CDM1.0_RM1.5	1.220	1.092	1.061
8S_I_13_wo_1_H3.0_CDM0.8_RM1.0	1.767	1.047	1.671
8S_I_13_wo_1_H3.0_CDM0.8_RM1.5	1.648	1.049	1.585
8S_I_13_wo_1_H3.0_CDM1.0_RM1.0	1.232	1.057	1.149
8S_I_13_wo_1_H3.0_CDM1.0_RM1.5	1.233	1.058	1.108
8S_I_13_wo_1_H4.0_CDM0.8_RM1.0	2.422	1.044	2.007
8S_I_13_wo_1_H4.0_CDM0.8_RM1.5	2.246	1.046	1.923

8S_I_13_wo_1_H4.0_CDM1.0_RM1.0	1.483	1.052	1.462
8S_I_13_wo_1_H4.0_CDM1.0_RM1.5	1.419	1.053	1.416
8S_I_13_wo_1_H5.0_CDM0.8_RM1.0	3.114	1.047	2.158
8S_I_13_wo_1_H5.0_CDM0.8_RM1.5	2.875	1.048	2.088
8S_I_13_wo_1_H5.0_CDM1.0_RM1.0	1.855	1.052	1.675
8S_I_13_wo_1_H5.0_CDM1.0_RM1.5	1.770	1.053	1.630
8S_I_14_H3.0_CDM0.8_RM1.0	1.181	1.538	1.131
8S_I_14_H3.0_CDM0.8_RM1.5	1.208	1.485	1.135
8S_I_14_H3.0_CDM1.0_RM1.0	1.191	1.650	1.151
8S_I_14_H3.0_CDM1.0_RM1.5	1.192	1.668	1.154
8S_I_14_H4.0_CDM0.8_RM1.0	1.174	1.231	1.095
8S_I_14_H4.0_CDM0.8_RM1.5	1.176	1.238	1.096
8S_I_14_H4.0_CDM1.0_RM1.0	1.185	1.328	1.115
8S_I_14_H4.0_CDM1.0_RM1.5	1.186	1.344	1.118
8S_I_14_H5.0_CDM0.8_RM1.0	1.167	1.026	1.025
8S_I_14_H5.0_CDM0.8_RM1.5	1.169	1.025	1.026
8S_I_14_H5.0_CDM1.0_RM1.0	1.179	1.072	1.048
8S_I_14_H5.0_CDM1.0_RM1.5	1.180	1.087	1.052
8S_I_14_wo_1_H3.0_CDM0.8_RM1.0	1.567	1.039	1.495
8S_I_14_wo_1_H3.0_CDM0.8_RM1.5	1.469	1.041	1.420
8S_I_14_wo_1_H3.0_CDM1.0_RM1.0	1.190	1.051	1.041
8S_I_14_wo_1_H3.0_CDM1.0_RM1.5	1.191	1.052	1.018
8S_I_14_wo_1_H4.0_CDM0.8_RM1.0	2.104	1.031	1.818
8S_I_14_wo_1_H4.0_CDM0.8_RM1.5	1.960	1.032	1.740
8S_I_14_wo_1_H4.0_CDM1.0_RM1.0	1.322	1.045	1.303
8S_I_14_wo_1_H4.0_CDM1.0_RM1.5	1.279	1.041	1.280
8S_I_14_wo_1_H5.0_CDM0.8_RM1.0	2.676	1.027	1.994
8S_I_14_wo_1_H5.0_CDM0.8_RM1.5	2.481	1.028	1.924
8S_I_14_wo_1_H5.0_CDM1.0_RM1.0	1.643	1.034	1.529
8S_I_14_wo_1_H5.0_CDM1.0_RM1.5	1.573	1.035	1.487
8S_I_23_H3.0_CDM0.8_RM1.0	1.391	1.306	1.097
8S_I_23_H3.0_CDM0.8_RM1.5	1.394	1.310	1.096
8S_I_23_H3.0_CDM1.0_RM1.0	1.416	1.397	1.100
8S_I_23_H3.0_CDM1.0_RM1.5	1.418	1.413	1.102
8S_I_23_H4.0_CDM0.8_RM1.0	1.367	1.099	1.064
8S_I_23_H4.0_CDM0.8_RM1.5	1.371	1.103	1.062
8S_I_23_H4.0_CDM1.0_RM1.0	1.397	1.159	1.075
8S_I_23_H4.0_CDM1.0_RM1.5	1.399	1.171	1.079
8S_I_23_H5.0_CDM0.8_RM1.0	1.347	1.000	1.135
8S_I_23_H5.0_CDM0.8_RM1.5	1.352	1.000	1.139
8S_I_23_H5.0_CDM1.0_RM1.0	1.381	1.000	1.119
8S_I_23_H5.0_CDM1.0_RM1.5	1.384	1.000	1.112
8S_I_23_wo_1_H3.0_CDM0.8_RM1.0	2.307	1.000	2.270

8S_I_23_wo_1_H3.0_CDM0.8_RM1.5	2.136	1.000	2.163
8S_I_23_wo_1_H3.0_CDM1.0_RM1.0	1.416	1.000	1.592
8S_I_23_wo_1_H3.0_CDM1.0_RM1.5	1.419	1.000	1.536
8S_I_23_wo_1_H4.0_CDM0.8_RM1.0	3.263	1.000	2.562
8S_I_23_wo_1_H4.0_CDM0.8_RM1.5	3.000	1.000	2.472
8S_I_23_wo_1_H4.0_CDM1.0_RM1.0	1.893	1.000	1.939
8S_I_23_wo_1_H4.0_CDM1.0_RM1.5	1.523	1.000	1.682
8S_I_23_wo_1_H5.0_CDM0.8_RM1.0	3.679	1.000	2.486
8S_I_23_wo_1_H5.0_CDM0.8_RM1.5	3.373	1.000	2.413
8S_I_23_wo_1_H5.0_CDM1.0_RM1.0	2.410	1.002	2.112
8S_I_23_wo_1_H5.0_CDM1.0_RM1.5	2.288	1.001	2.064
8S_I_24_H3.0_CDM0.8_RM1.0	1.250	1.476	1.113
8S_I_24_H3.0_CDM0.8_RM1.5	1.253	1.475	1.114
8S_I_24_H3.0_CDM1.0_RM1.0	1.270	1.541	1.125
8S_I_24_H3.0_CDM1.0_RM1.5	1.272	1.554	1.127
8S_I_24_H4.0_CDM0.8_RM1.0	1.234	1.209	1.075
8S_I_24_H4.0_CDM0.8_RM1.5	1.237	1.207	1.074
8S_I_24_H4.0_CDM1.0_RM1.0	1.256	1.259	1.083
8S_I_24_H4.0_CDM1.0_RM1.5	1.258	1.270	1.085
8S_I_24_H5.0_CDM0.8_RM1.0	1.218	1.000	1.053
8S_I_24_H5.0_CDM0.8_RM1.5	1.221	1.000	1.054
8S_I_24_H5.0_CDM1.0_RM1.0	1.243	1.018	1.043
8S_I_24_H5.0_CDM1.0_RM1.5	1.245	1.029	1.047
8S_I_24_wo_1_H3.0_CDM0.8_RM1.0	1.944	1.001	1.891
8S_I_24_wo_1_H3.0_CDM0.8_RM1.5	1.812	1.002	1.799
8S_I_24_wo_1_H3.0_CDM1.0_RM1.0	1.266	1.009	1.317
8S_I_24_wo_1_H3.0_CDM1.0_RM1.5	1.268	1.010	1.271
8S_I_24_wo_1_H4.0_CDM0.8_RM1.0	2.670	1.000	2.217
8S_I_24_wo_1_H4.0_CDM0.8_RM1.5	2.471	1.000	2.129
8S_I_24_wo_1_H4.0_CDM1.0_RM1.0	1.620	1.000	1.638
8S_I_24_wo_1_H4.0_CDM1.0_RM1.5	1.550	1.001	1.588
8S_I_24_wo_1_H5.0_CDM0.8_RM1.0	3.449	1.000	2.332
8S_I_24_wo_1_H5.0_CDM0.8_RM1.5	3.176	1.000	2.262
8S_I_24_wo_1_H5.0_CDM1.0_RM1.0	2.028	1.000	1.841
8S_I_24_wo_1_H5.0_CDM1.0_RM1.5	1.933	1.000	1.794
8S_I_34_H3.0_CDM0.8_RM1.0	1.284	1.356	1.097
8S_I_34_H3.0_CDM0.8_RM1.5	1.288	1.356	1.096
8S_I_34_H3.0_CDM1.0_RM1.0	1.314	1.412	1.102
8S_I_34_H3.0_CDM1.0_RM1.5	1.317	1.425	1.103
8S_I_34_H4.0_CDM0.8_RM1.0	1.258	1.085	1.051
8S_I_34_H4.0_CDM0.8_RM1.5	1.263	1.088	1.051
8S_I_34_H4.0_CDM1.0_RM1.0	1.293	1.142	1.062
8S_I_34_H4.0_CDM1.0_RM1.5	1.296	1.153	1.065

8S_I_34_H5.0_CDM0.8_RM1.0	1.235	1.000	1.165
8S_I_34_H5.0_CDM0.8_RM1.5	1.239	1.000	1.165
8S_I_34_H5.0_CDM1.0_RM1.0	1.272	1.000	1.137
8S_I_34_H5.0_CDM1.0_RM1.5	1.275	1.000	1.128
8S_I_34_wo_1_H3.0_CDM0.8_RM1.0	2.241	1.000	2.155
8S_I_34_wo_1_H3.0_CDM0.8_RM1.5	2.084	1.000	2.054
8S_I_34_wo_1_H3.0_CDM1.0_RM1.0	1.404	1.000	1.523
8S_I_34_wo_1_H3.0_CDM1.0_RM1.5	1.348	1.000	1.473
8S_I_34_wo_1_H4.0_CDM0.8_RM1.0	3.075	1.000	2.451
8S_I_34_wo_1_H4.0_CDM0.8_RM1.5	2.838	1.000	2.360
8S_I_34_wo_1_H4.0_CDM1.0_RM1.0	1.834	1.000	1.844
8S_I_34_wo_1_H4.0_CDM1.0_RM1.5	1.752	1.000	1.790
8S_I_34_wo_1_H5.0_CDM0.8_RM1.0	4.032	1.000	2.527
8S_I_34_wo_1_H5.0_CDM0.8_RM1.5	3.700	1.000	2.458
8S_I_34_wo_1_H5.0_CDM1.0_RM1.0	2.317	1.000	2.031
8S_I_34_wo_1_H5.0_CDM1.0_RM1.5	2.205	1.000	1.983
8S_I_1234_H3.0_CDM0.8_RM1.0	1.491	1.146	1.074
8S_I_1234_H3.0_CDM0.8_RM1.5	1.497	1.154	1.073
8S_I_1234_H3.0_CDM1.0_RM1.0	1.538	1.190	1.068
8S_I_1234_H3.0_CDM1.0_RM1.5	1.542	1.196	1.068
8S_I_1234_H4.0_CDM0.8_RM1.0	1.443	1.020	1.037
8S_I_1234_H4.0_CDM0.8_RM1.5	1.450	1.014	1.035
8S_I_1234_H4.0_CDM1.0_RM1.0	1.498	1.006	1.047
8S_I_1234_H4.0_CDM1.0_RM1.5	1.502	1.009	1.050
8S_I_1234_H5.0_CDM0.8_RM1.0	1.403	1.000	1.215
8S_I_1234_H5.0_CDM0.8_RM1.5	1.410	1.000	1.226
8S_I_1234_H5.0_CDM1.0_RM1.0	1.459	1.000	1.264
8S_I_1234_H5.0_CDM1.0_RM1.5	1.464	1.000	1.263
8S_I_1234_wo_1_H3.0_CDM0.8_RM1.0	3.616	1.020	3.024
8S_I_1234_wo_1_H3.0_CDM0.8_RM1.5	3.326	1.019	2.905
8S_I_1234_wo_1_H3.0_CDM1.0_RM1.0	2.096	1.007	2.222
8S_I_1234_wo_1_H3.0_CDM1.0_RM1.5	2.096	1.007	2.222
8S_I_1234_wo_1_H4.0_CDM0.8_RM1.0	5.119	1.052	3.091
8S_I_1234_wo_1_H4.0_CDM0.8_RM1.5	4.686	1.052	3.011
8S_I_1234_wo_1_H4.0_CDM1.0_RM1.0	2.875	1.036	2.504
8S_I_1234_wo_1_H4.0_CDM1.0_RM1.5	2.728	1.035	2.444
8S_I_1234_wo_1_H5.0_CDM0.8_RM1.0	6.689	1.087	2.936
8S_I_1234_wo_1_H5.0_CDM0.8_RM1.5	6.105	1.087	2.886
8S_I_1234_wo_1_H5.0_CDM1.0_RM1.0	3.681	1.068	2.543
8S_I_1234_wo_1_H5.0_CDM1.0_RM1.5	3.483	1.068	2.499

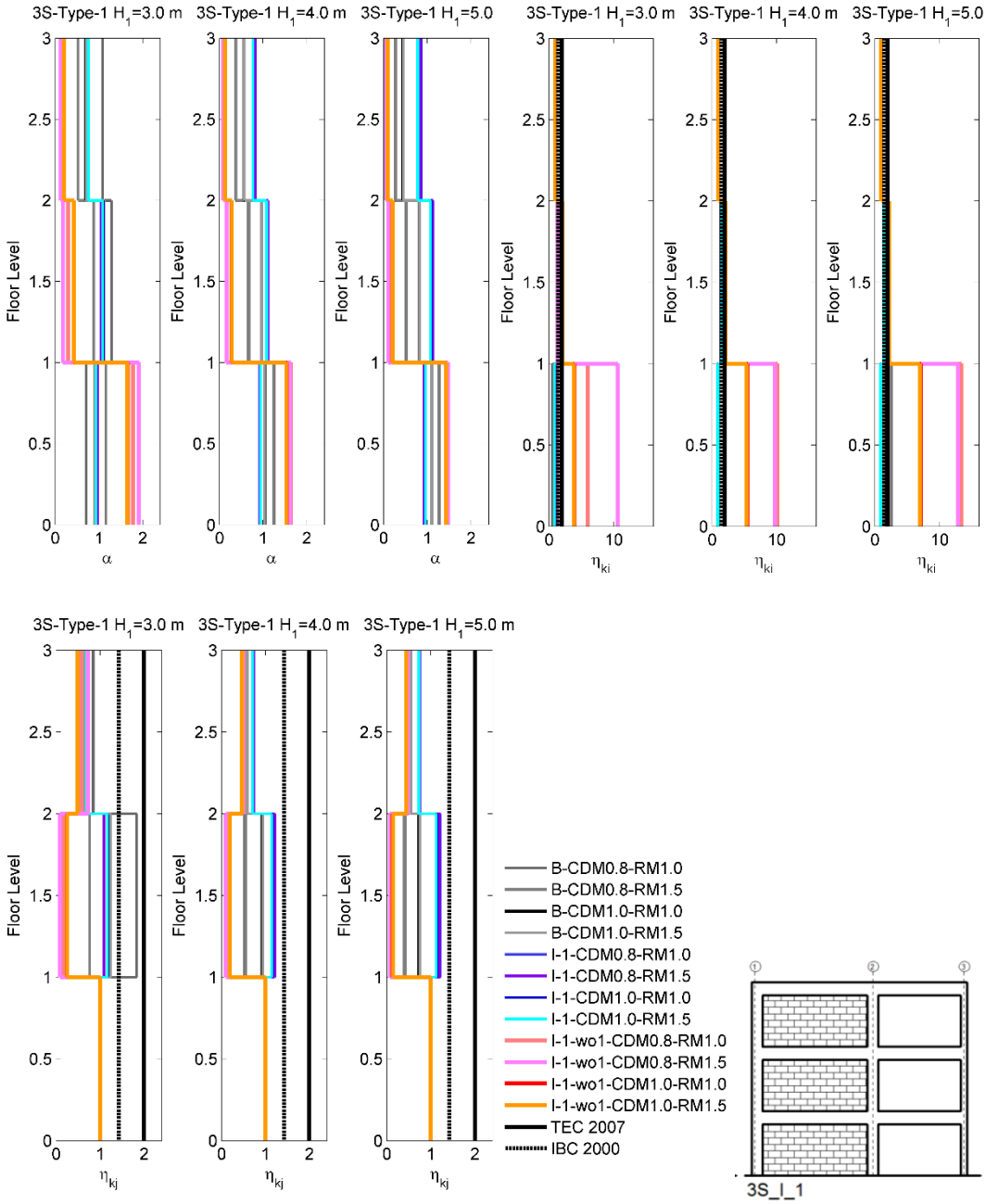

Figure A2-22 3 Story Frame; mod superposition analysis results for Type 1

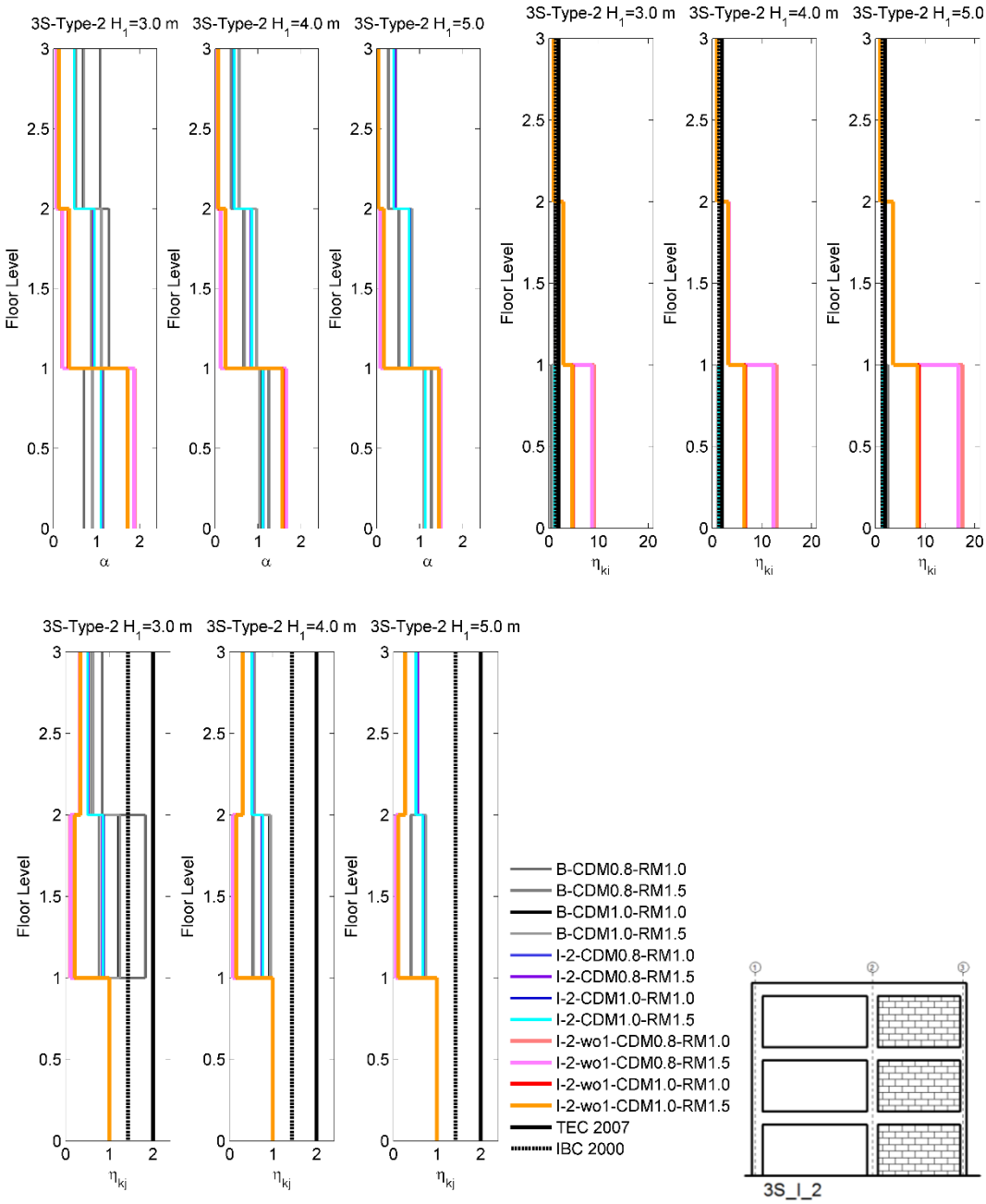

Figure A2-23 3 Story Frame; mod superposition analysis results for Type 2

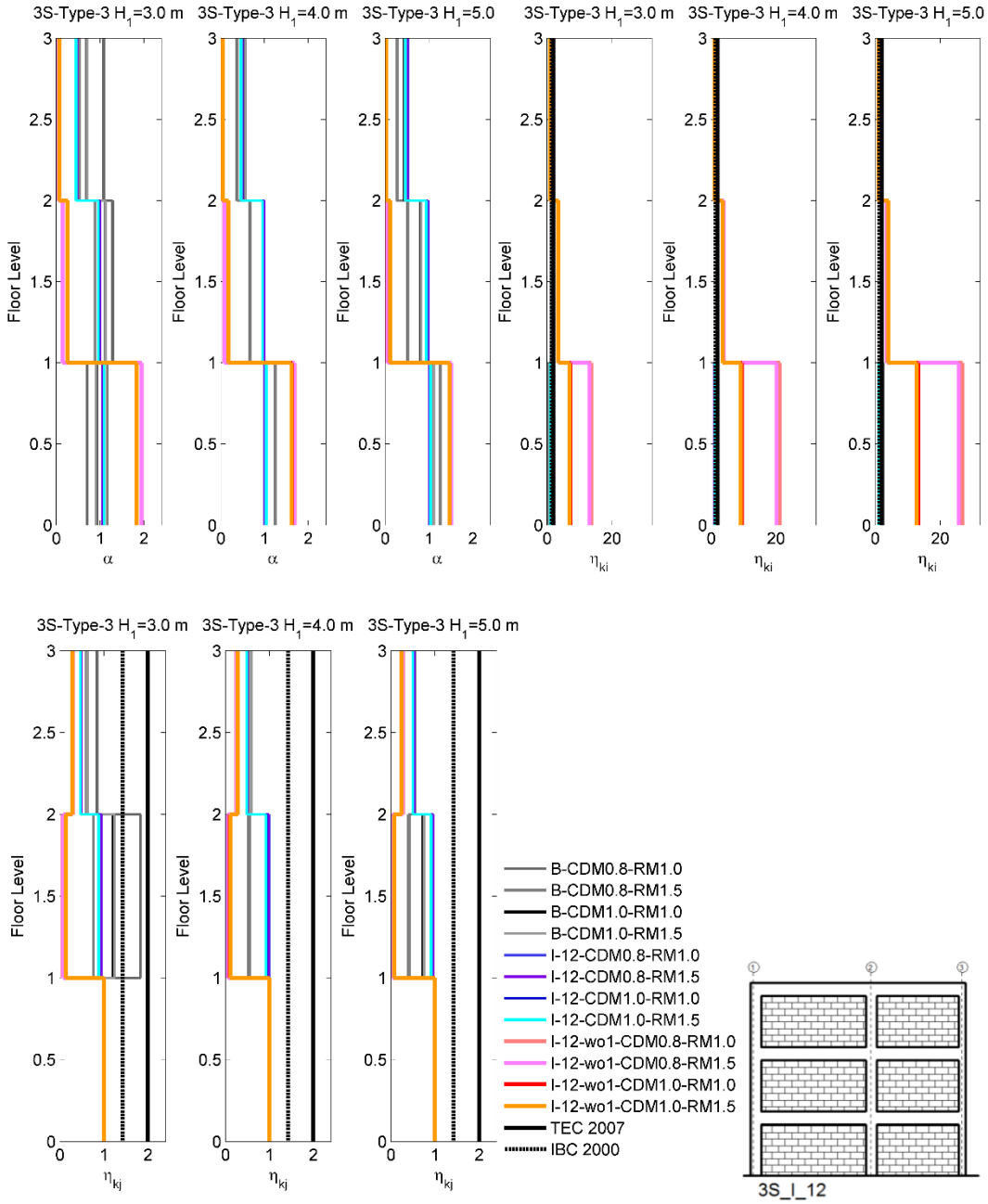

Figure A2-24 3 Story Frame; mod superposition analysis results for Type 3

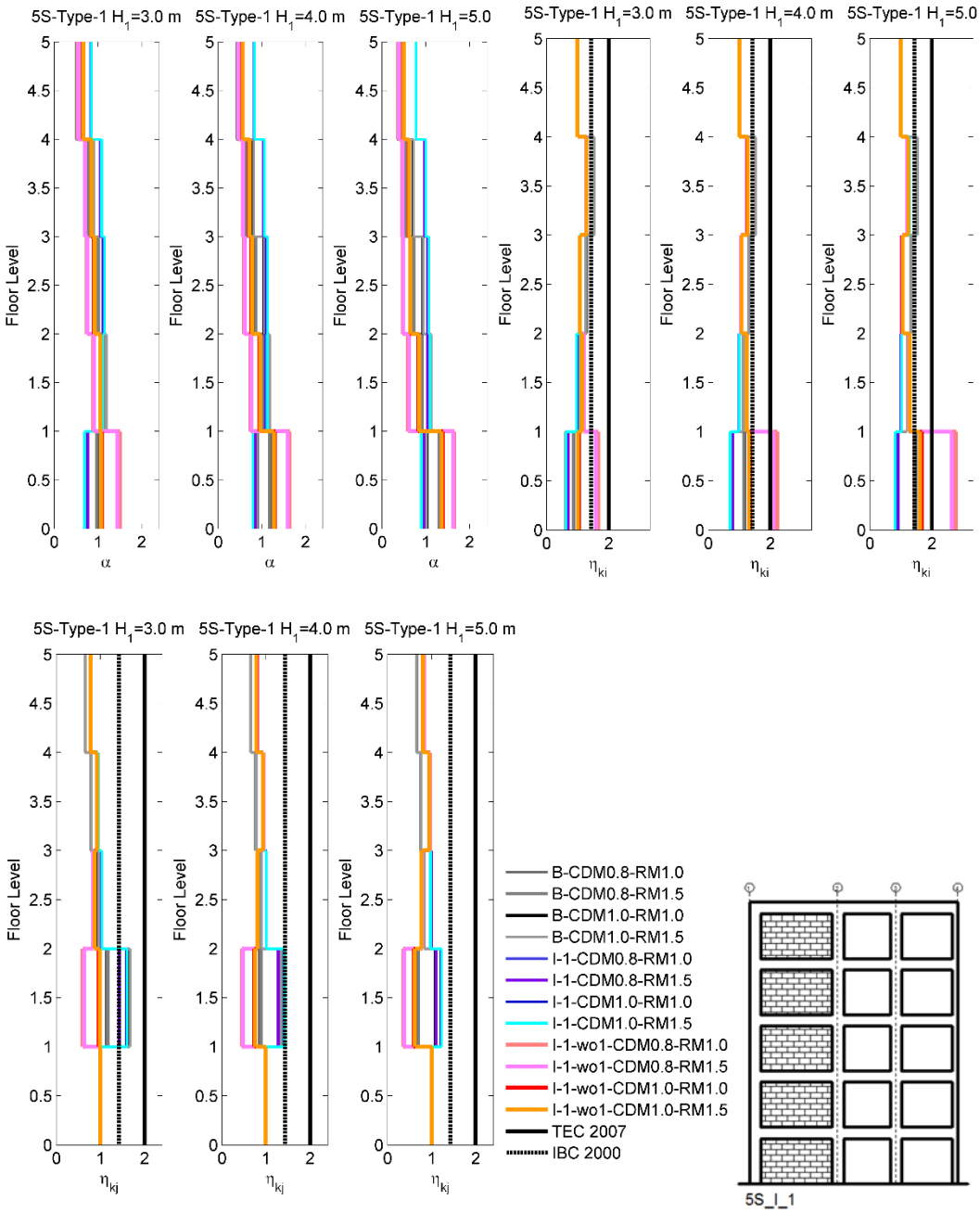

Figure A2-25 5 Story Frame; mod superposition analysis results for Type 1

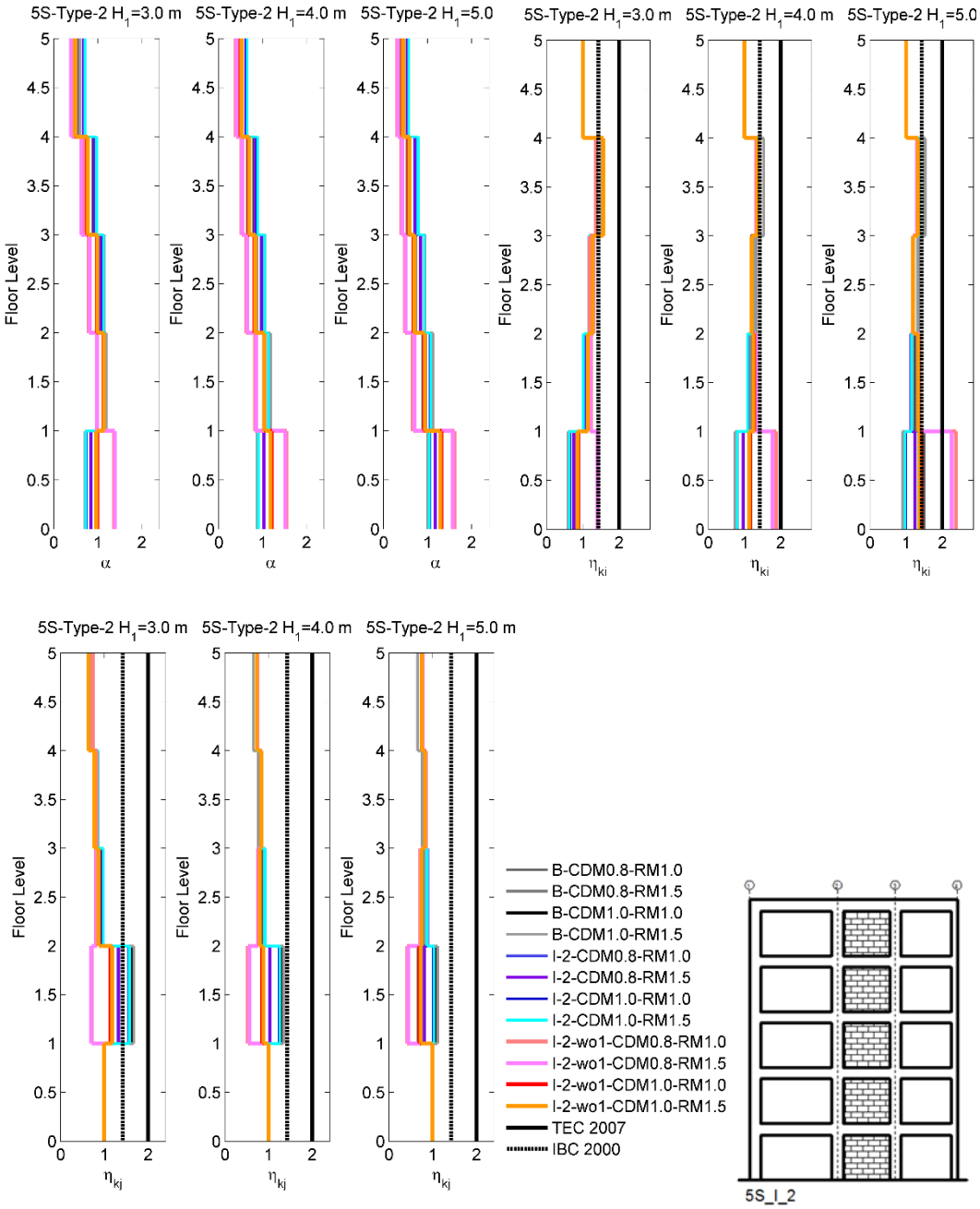

Figure A2-26 5 Story Frame; mod superposition analysis results for Type 2

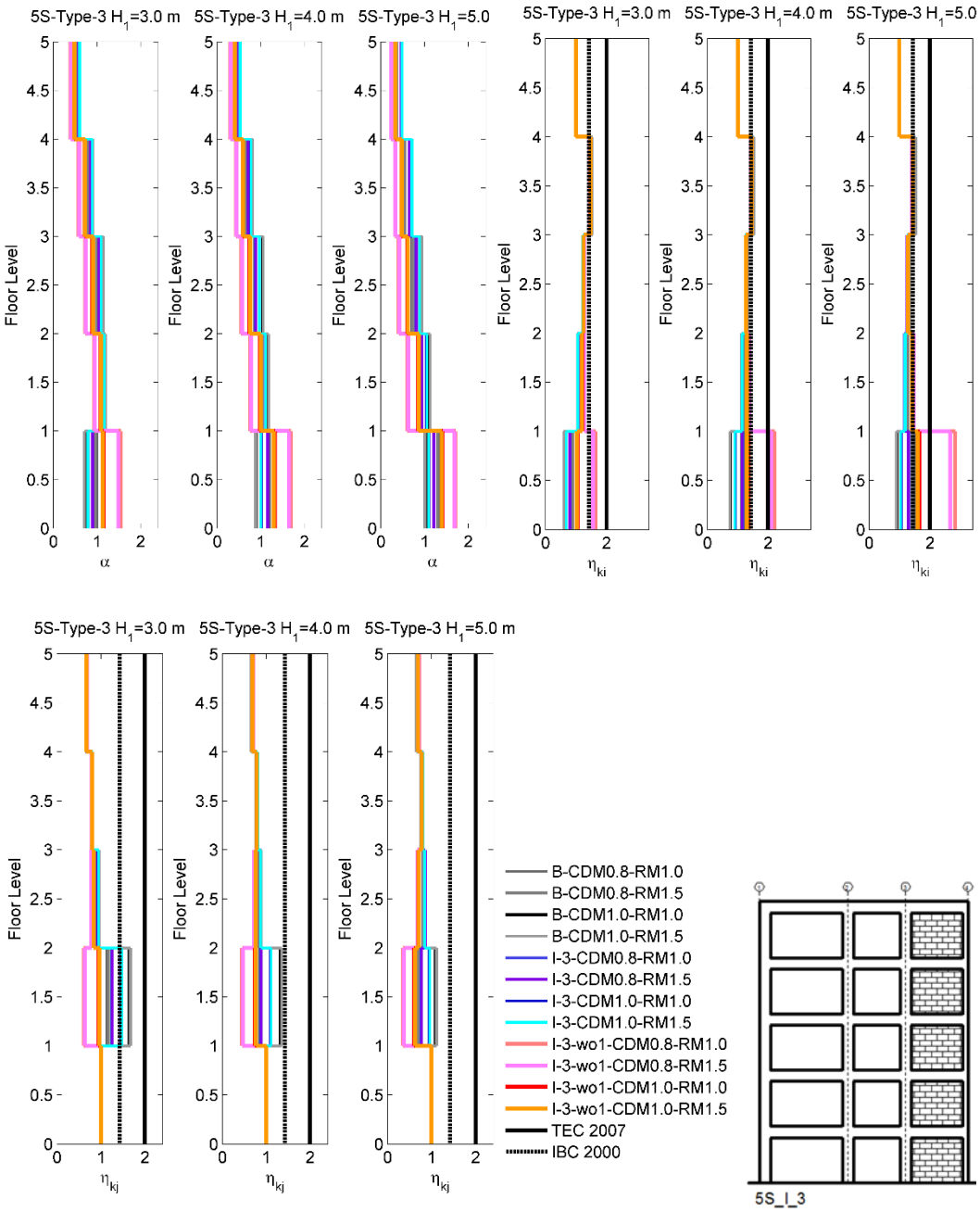

Figure A2-27 5 Story Frame; mod superposition analysis results for Type 3

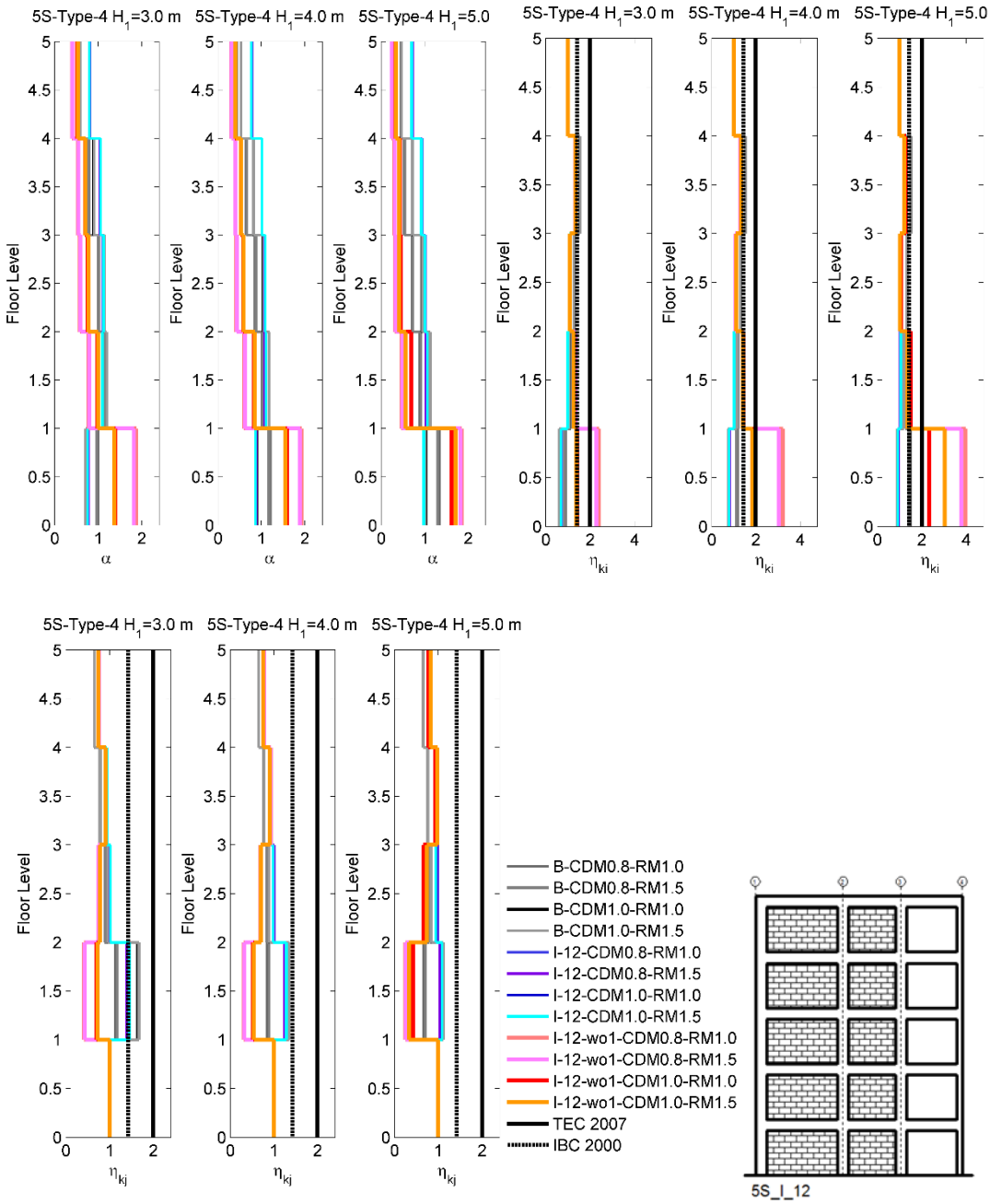

Figure A2-28 5 Story Frame; mod superposition analysis results for Type 4

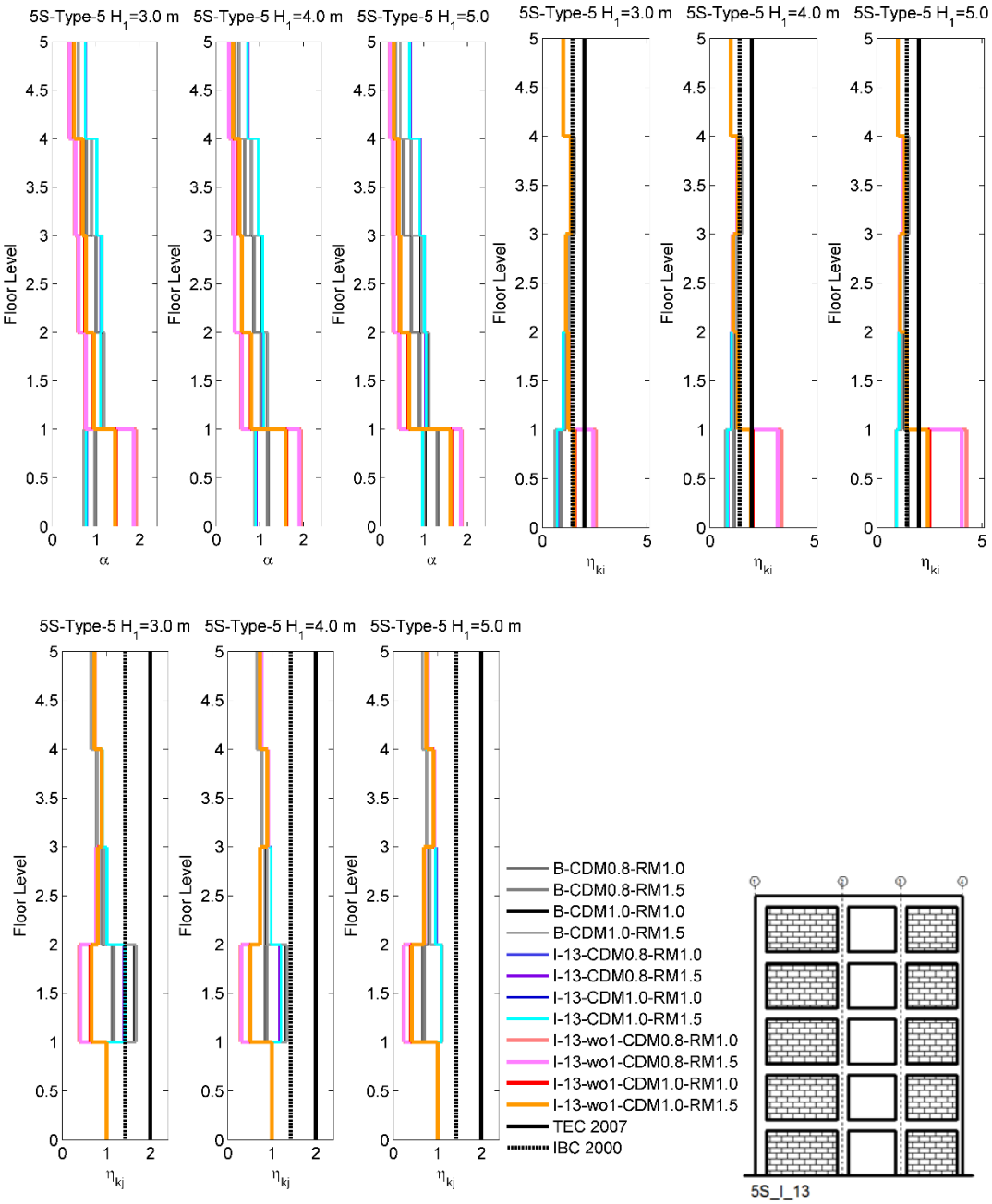

Figure A2-29 5 Story Frame; mod superposition analysis results for Type 5

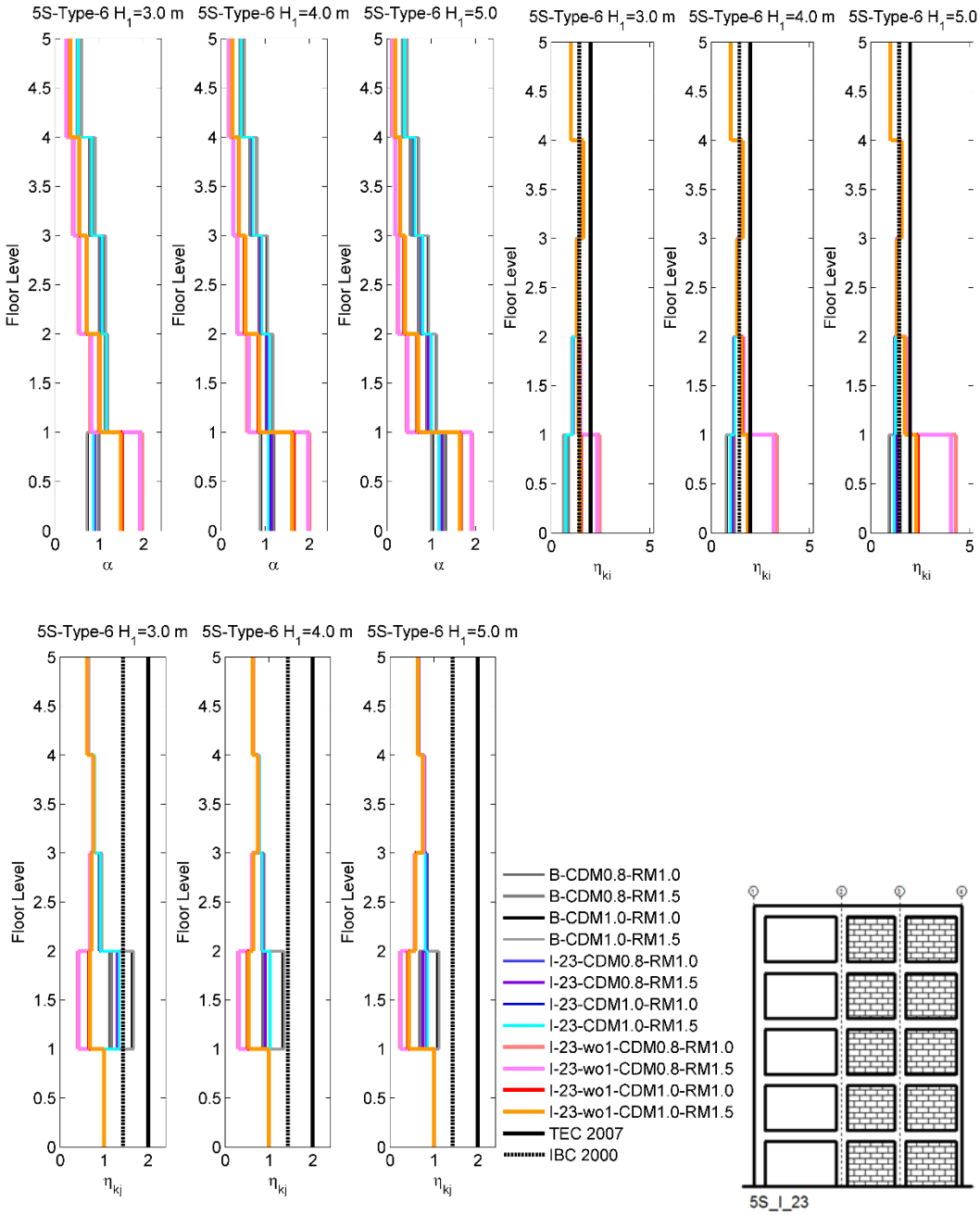

Figure A2-30 5 Story Frame; mod superposition analysis results for Type 6

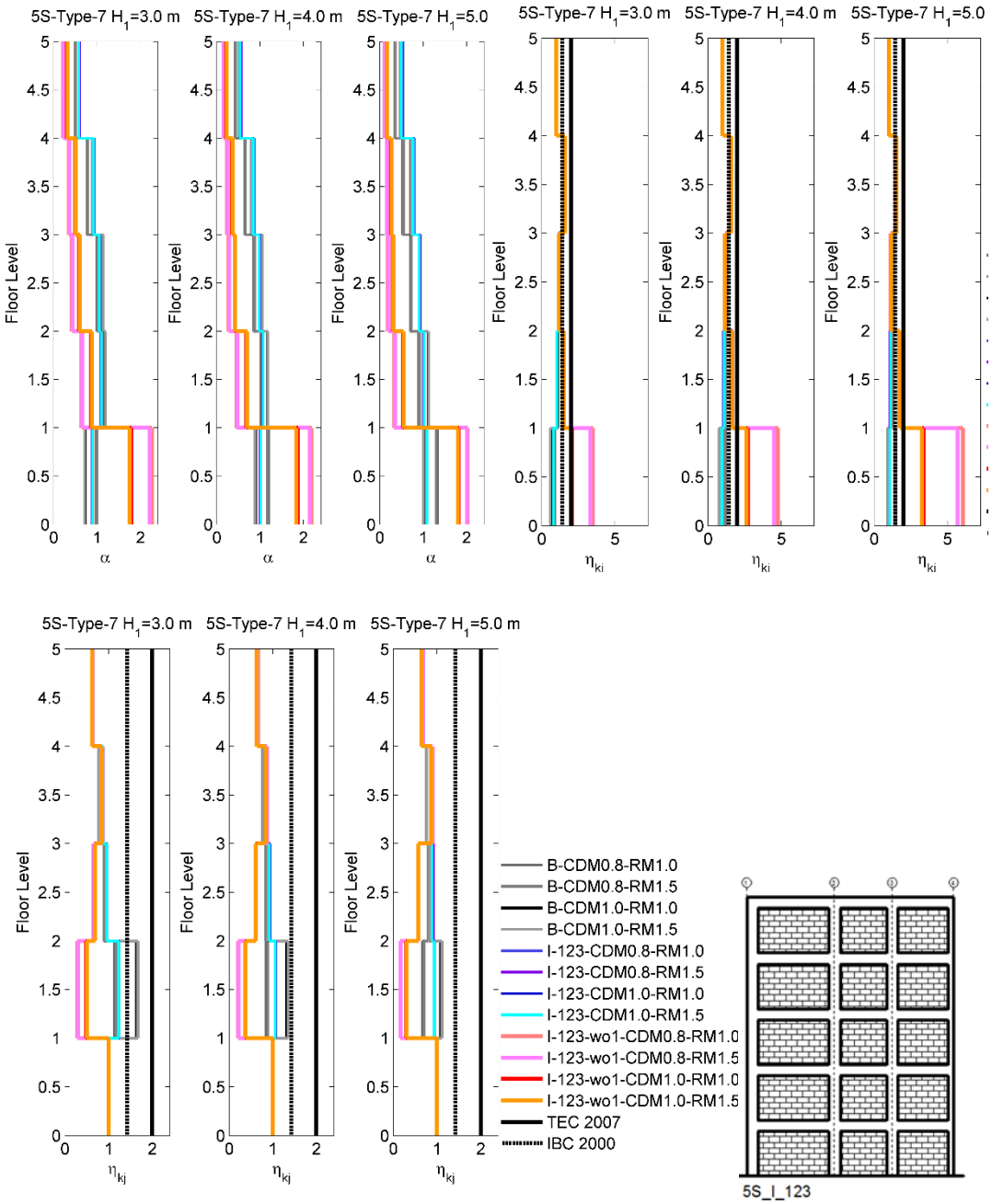

Figure A2-31 5 Story Frame; mod superposition analysis results for Type 7

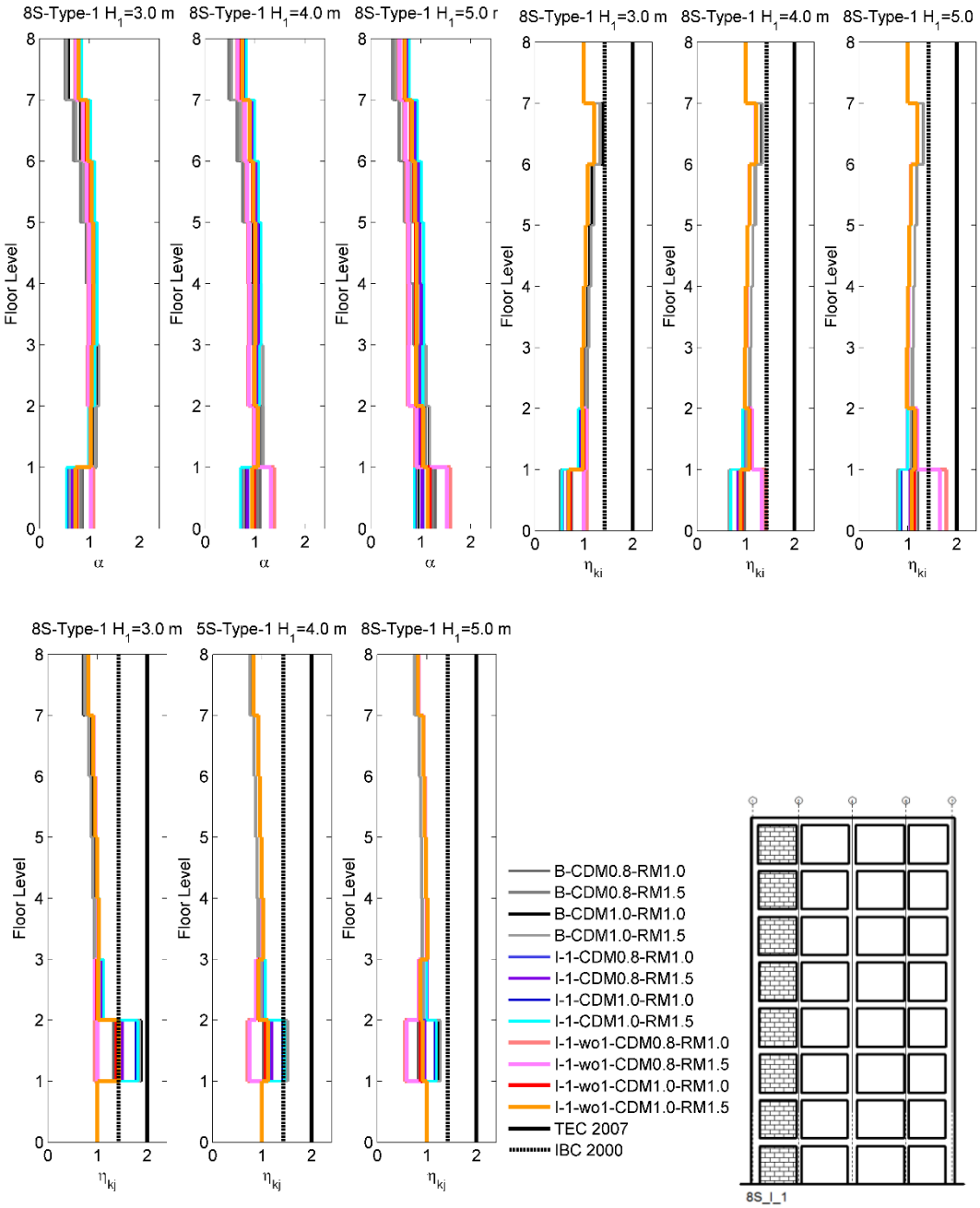

Figure A2-32 8 Story Frame; mod superposition analysis results for Type 1

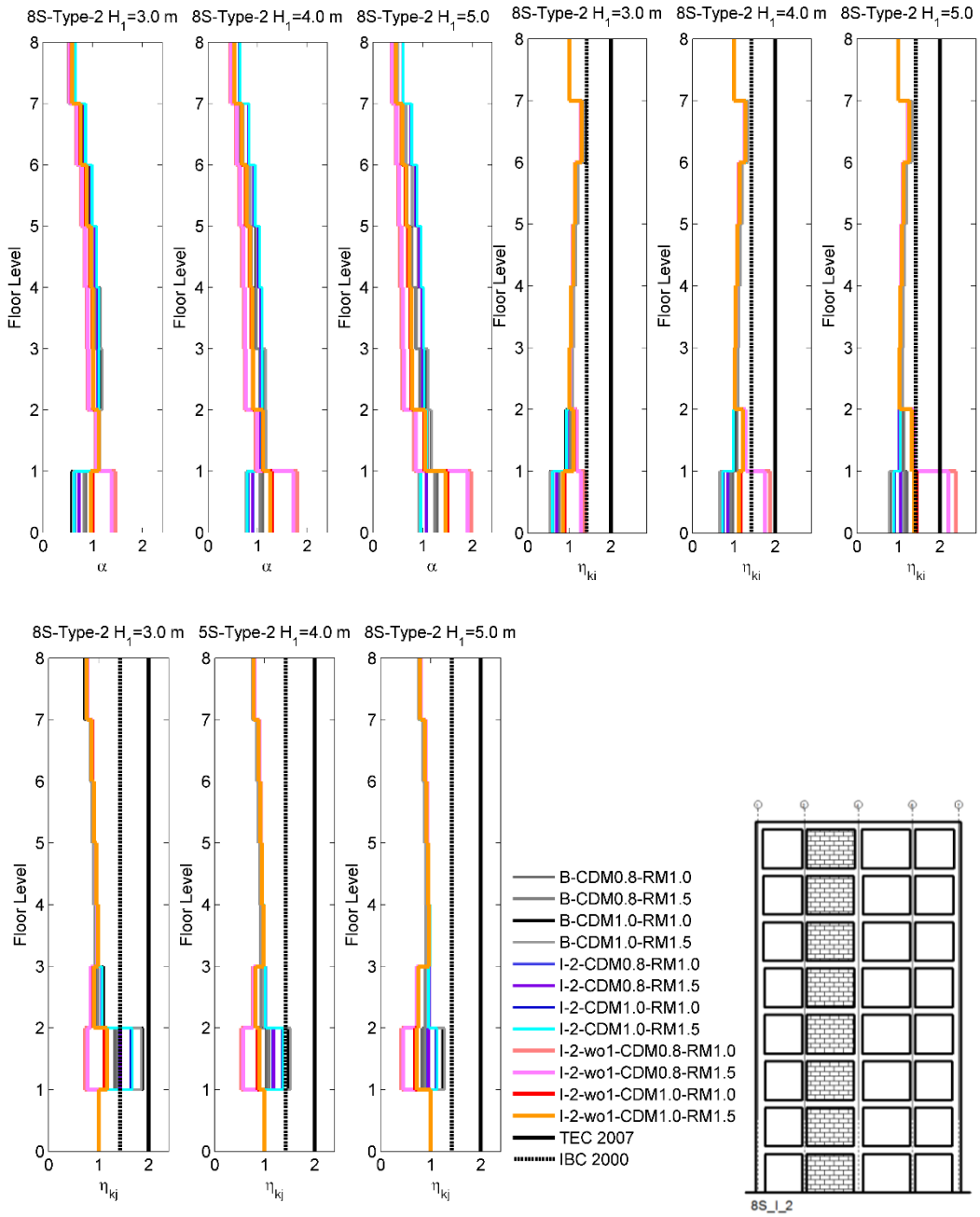

Figure A2-33 8 Story Frame; mod superposition analysis results for Type 2

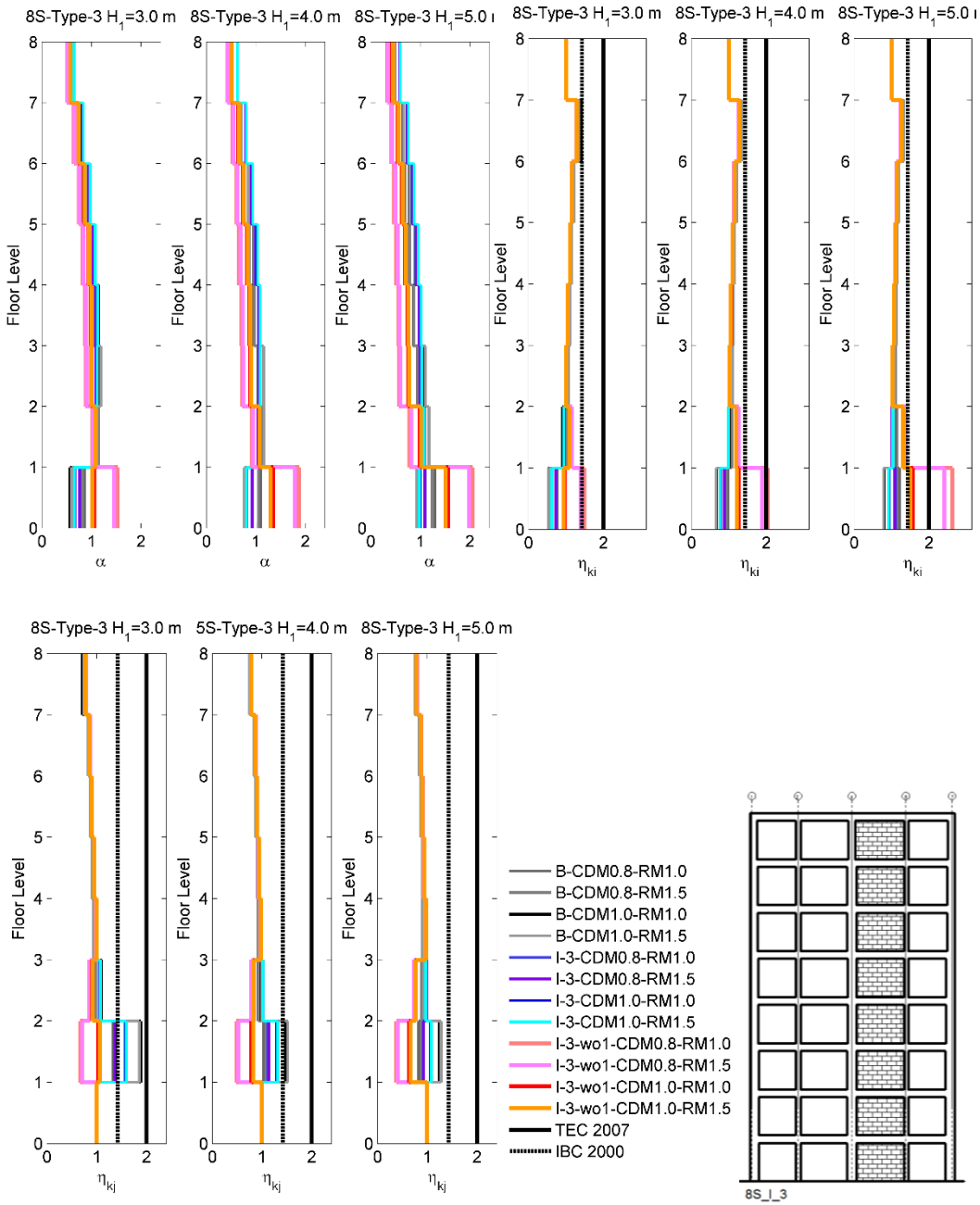

Figure A2-34 8 Story Frame; mod superposition analysis results for Type 3

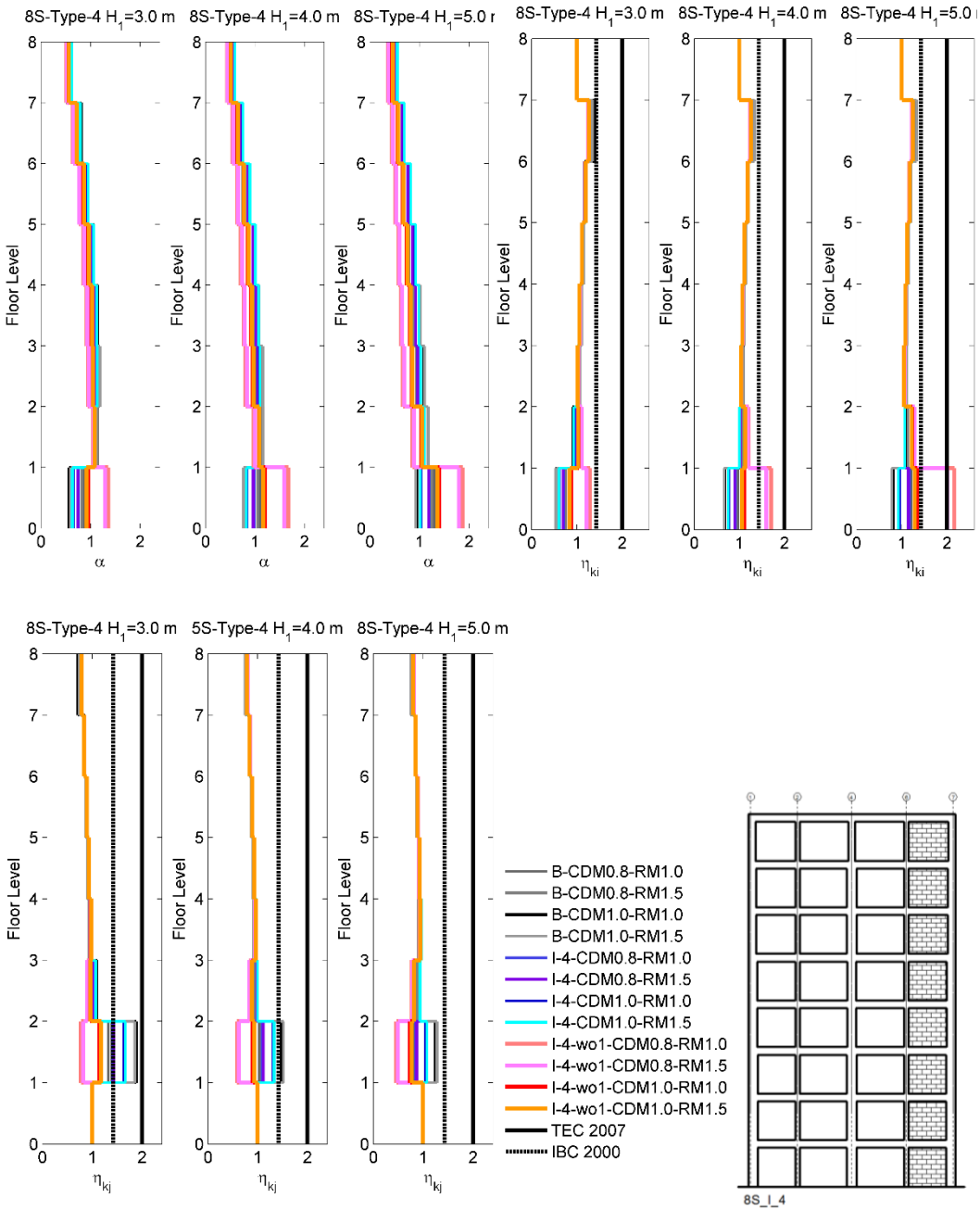

Figure A2-35 8 Story Frame; mod superposition analysis results for Type 4

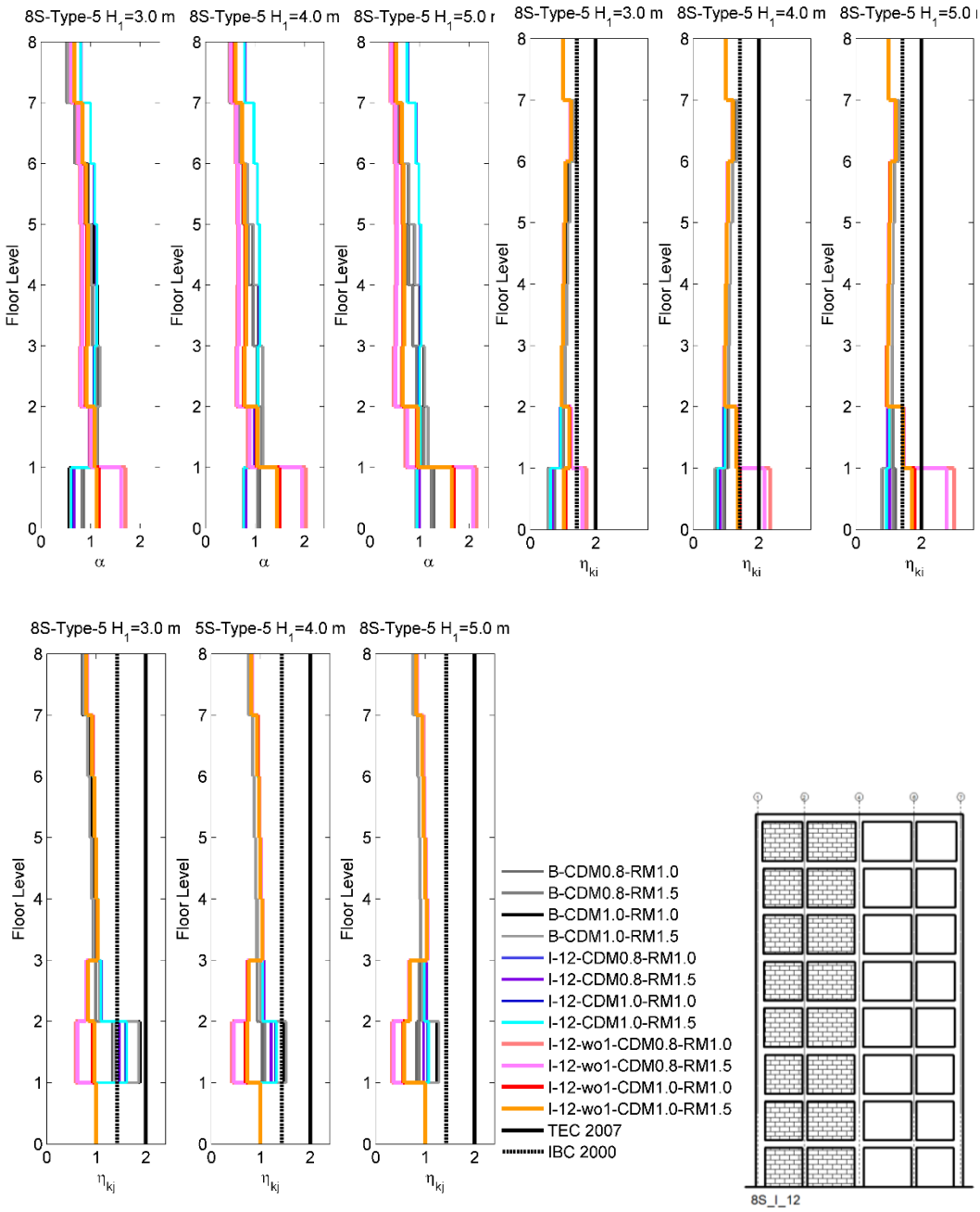

Figure A2-36 8 Story Frame; mod superposition analysis results for Type 5

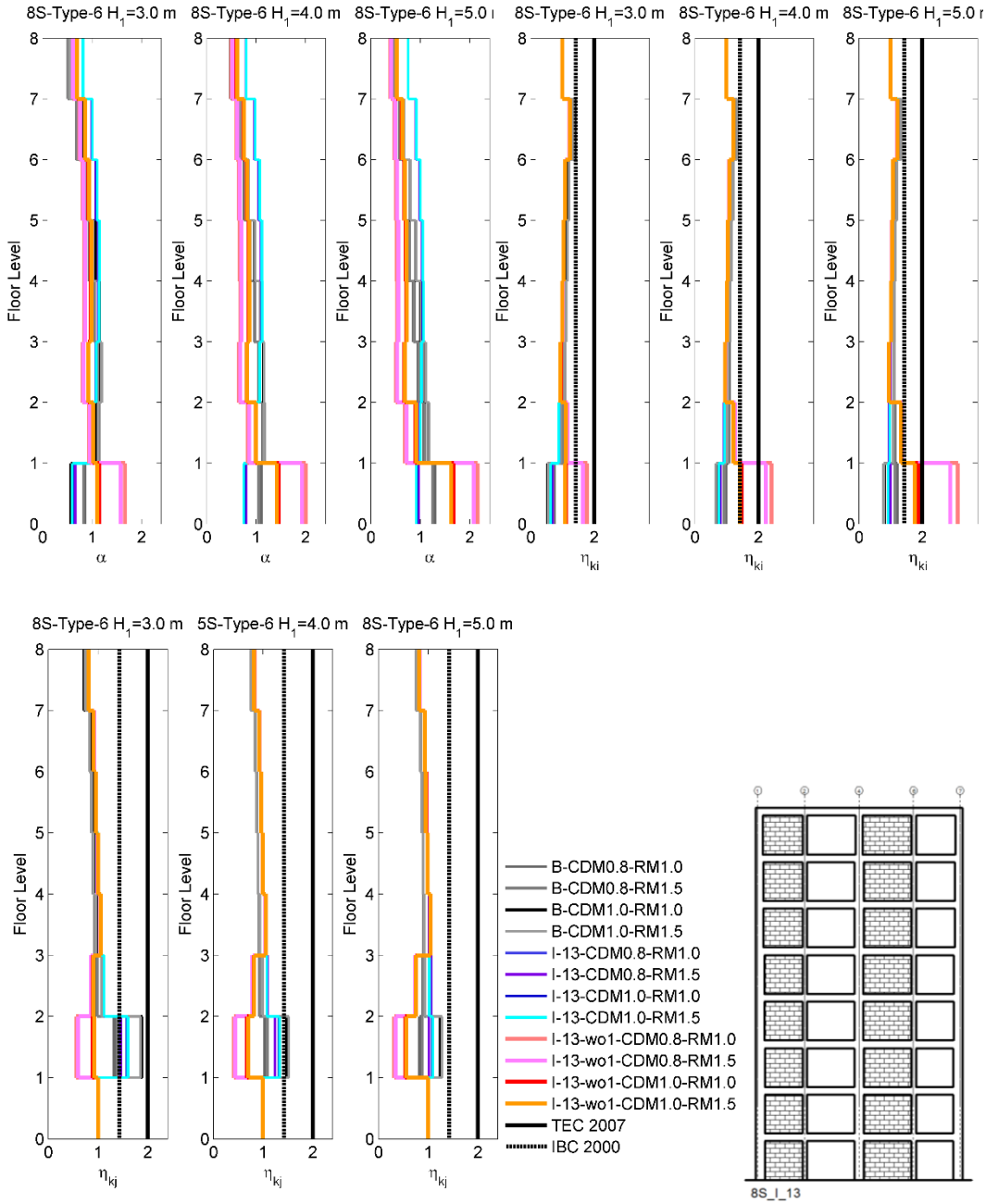

Figure A2-37 8 Story Frame; mod superposition analysis results for Type 6

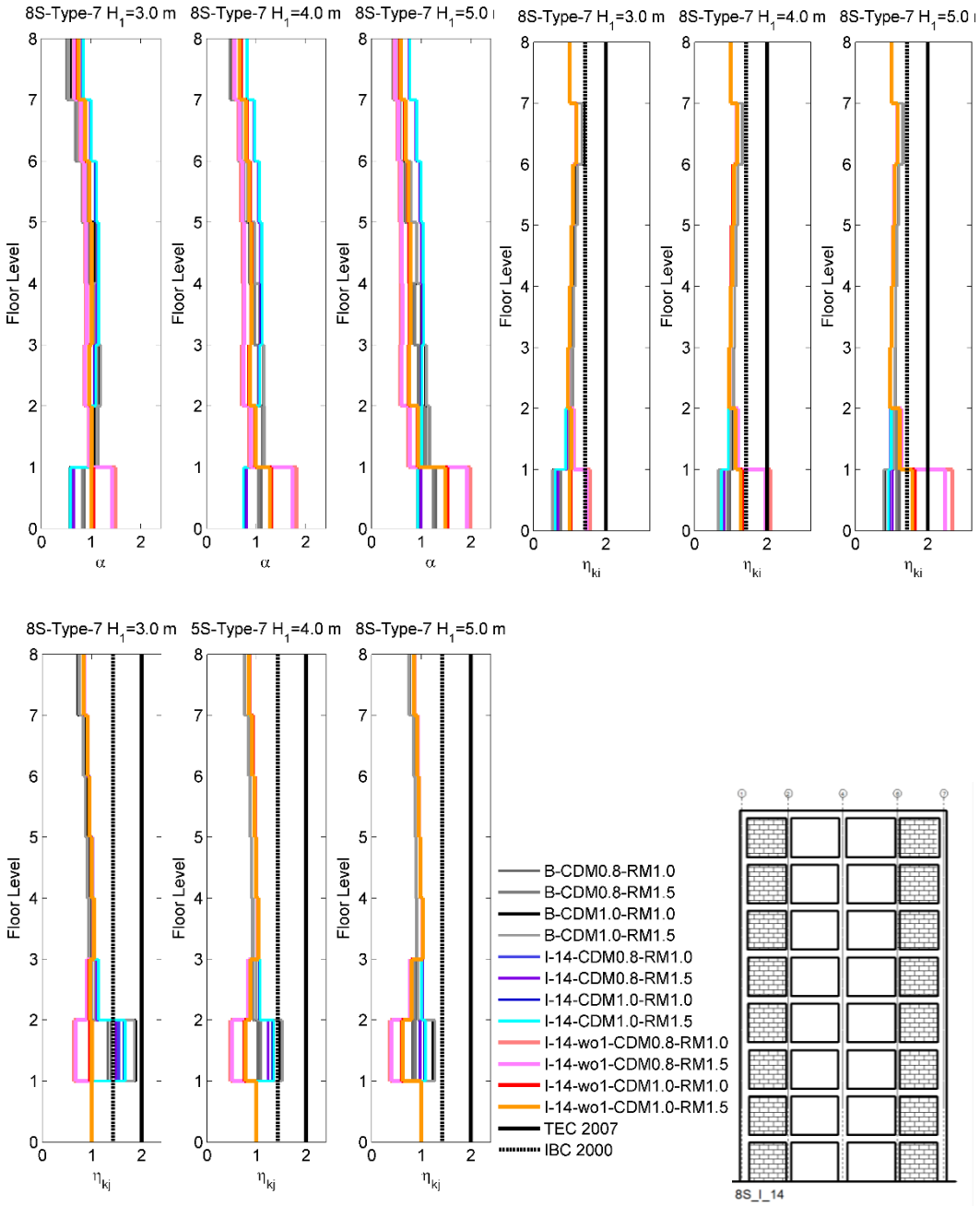

Figure A2-38 8 Story Frame; mod superposition analysis results for Type 7

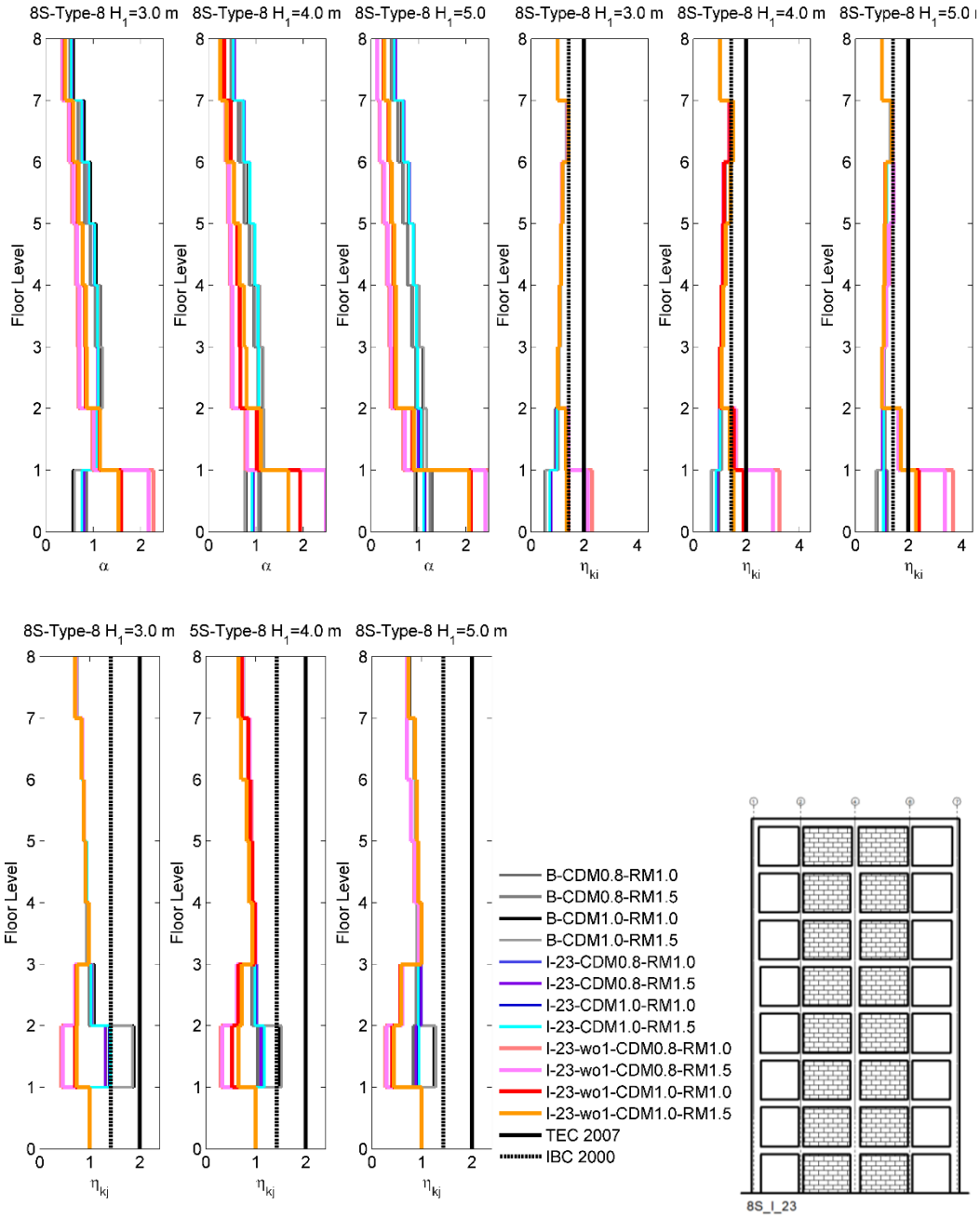

Figure A2-39 8 Story Frame; mod superposition analysis results for Type 8

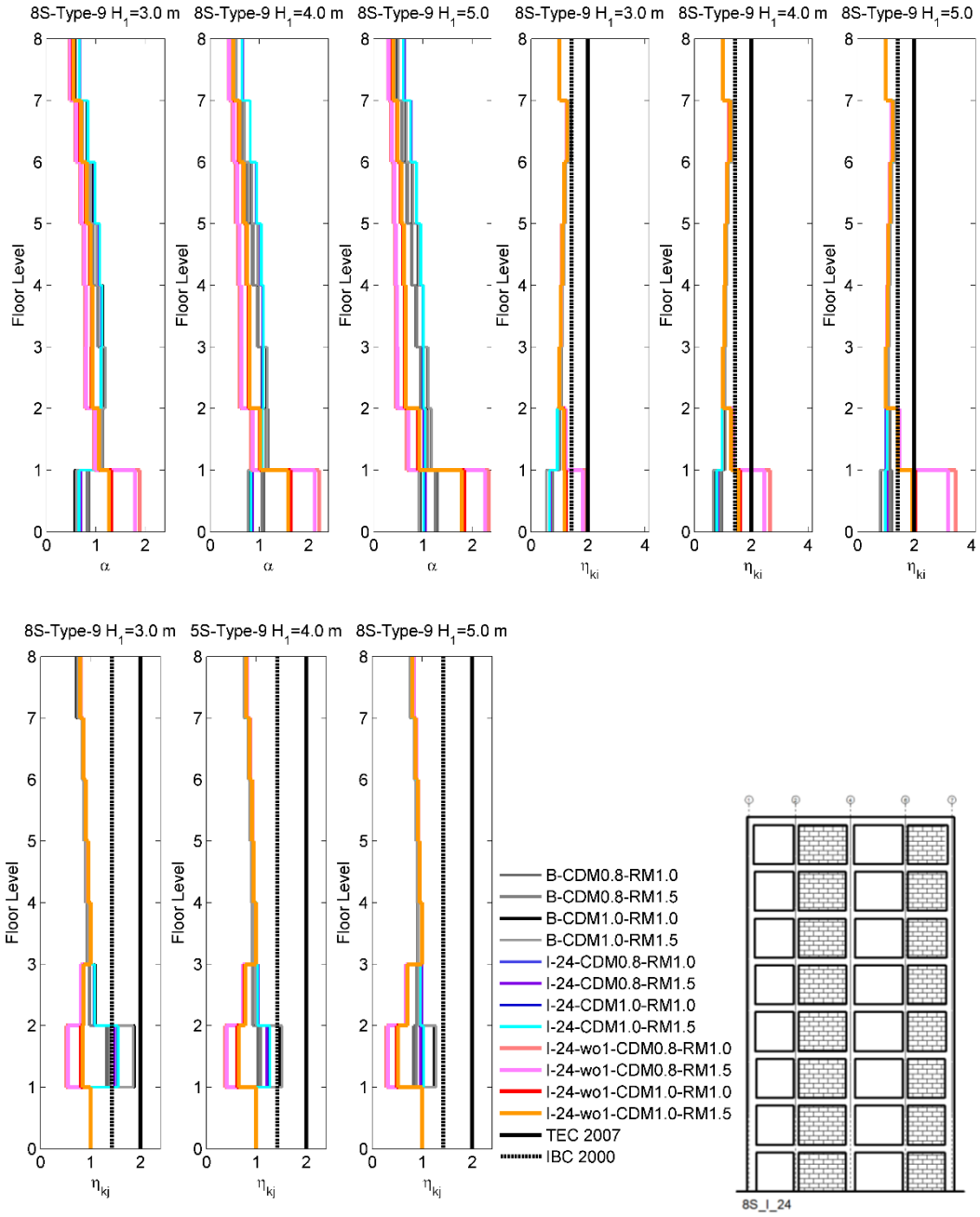

Figure A2-40 8 Story Frame; mod superposition analysis results for Type 9

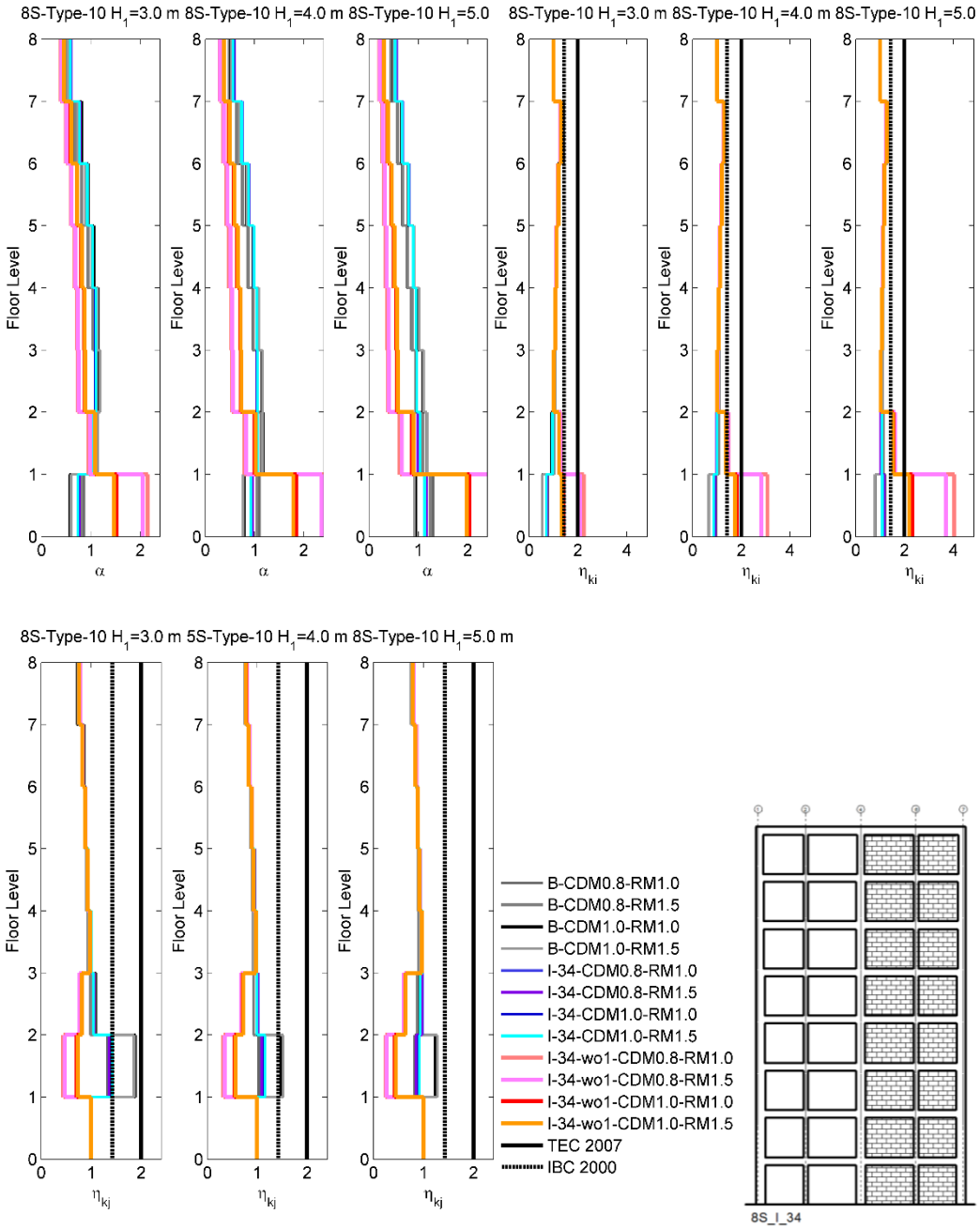

Figure A2-41 8 Story Frame; mod superposition analysis results for Type 10

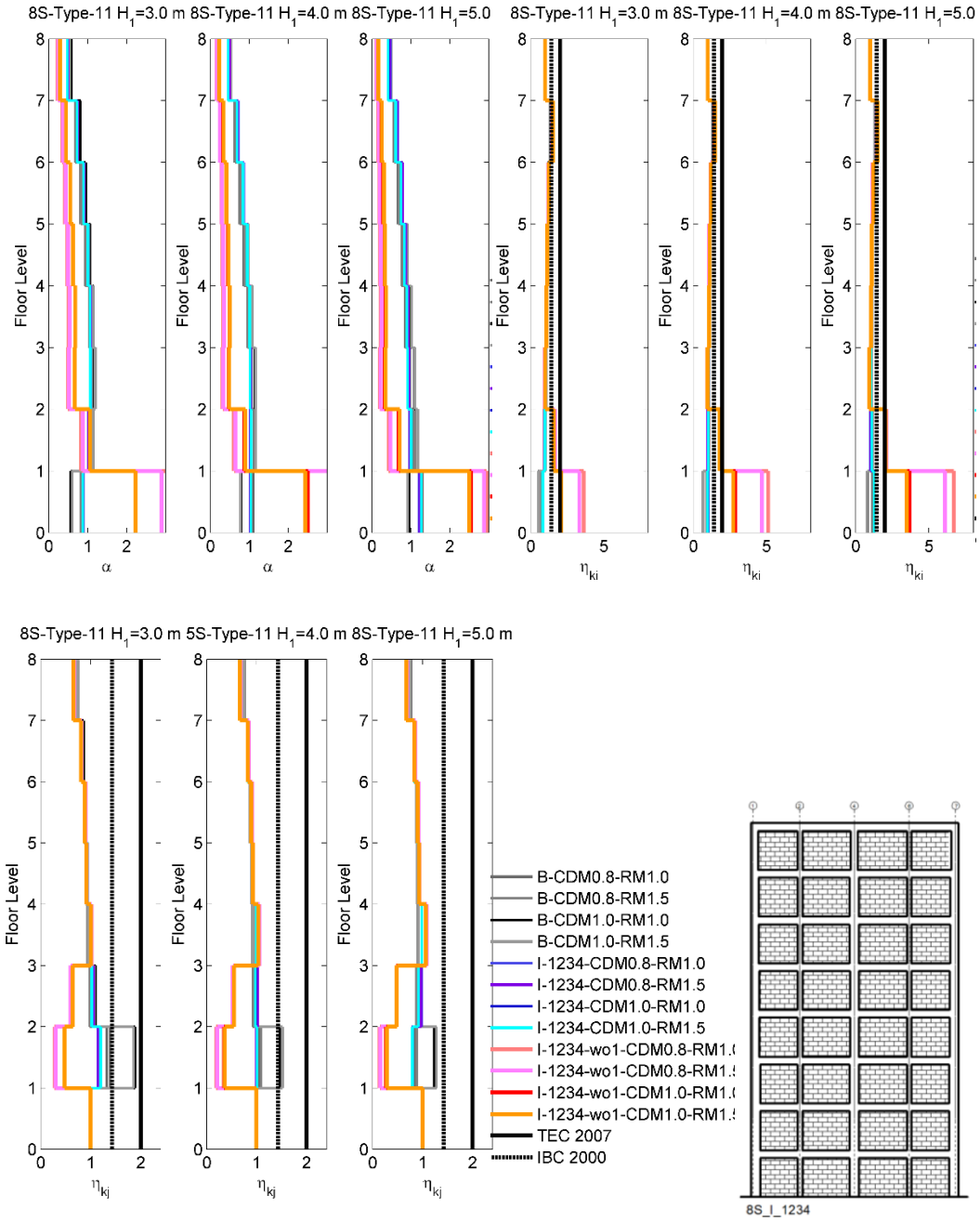

Figure A2-42 8 Story Frame; mod superposition analysis results for Type 11

A2.3 Pushover Analysis Results at Ultimate Point

Table A2-7 Soft story, weak story and max alpha values for 3 Story frame for pushover analysis results at Ultimate Point (UP)

Frame Type/ Story Level	$\eta_{ki,\ max}$	$\eta_{kj,\ max}$	α_{max}	$\alpha_{irregular}$	α_2
3S_B_H3.0_CDM0.8_RM1.0	2.880	1.000	1.272	0.795	2.862
3S_B_H3.0_CDM0.8_RM1.5	2.771	1.000	1.145	1.024	3.719
3S_B_H3.0_CDM1.0_RM1.0	2.462	1.000	1.125	1.000	4.069
3S_B_H3.0_CDM1.0_RM1.5	2.407	1.000	1.052	1.207	4.936
3S_B_H4.0_CDM0.8_RM1.0	3.513	1.000	1.322	0.796	2.376
3S_B_H4.0_CDM0.8_RM1.5	3.312	1.000	1.172	1.072	3.238
3S_B_H4.0_CDM1.0_RM1.0	3.293	1.000	1.126	1.139	4.051
3S_B_H4.0_CDM1.0_RM1.5	3.523	1.000	1.051	1.392	4.985
3S_B_H5.0_CDM0.8_RM1.0	3.817	1.000	1.349	0.890	2.164
3S_B_H5.0_CDM0.8_RM1.5	3.741	1.000	1.205	1.142	2.824
3S_B_H5.0_CDM1.0_RM1.0	3.886	1.000	1.145	1.348	4.119
3S_B_H5.0_CDM1.0_RM1.5	3.650	1.000	1.079	1.393	4.297
3S_I_1_H3.0_CDM0.8_RM1.0	15.584	1.000	1.557	0.433	10.677
3S_I_1_H3.0_CDM0.8_RM1.5	17.204	1.000	1.471	0.427	10.659
3S_I_1_H3.0_CDM1.0_RM1.0	23.060	1.000	1.131	0.407	11.158
3S_I_1_H3.0_CDM1.0_RM1.5	14.492	1.000	1.097	0.267	7.371
3S_I_1_H4.0_CDM0.8_RM1.0	13.629	1.000	1.344	0.522	10.724
3S_I_1_H4.0_CDM0.8_RM1.5	13.629	1.000	1.344	0.522	10.724
3S_I_1_H4.0_CDM1.0_RM1.0	15.620	1.000	1.107	0.397	9.156
3S_I_1_H4.0_CDM1.0_RM1.5	14.600	1.000	1.084	0.369	8.579
3S_I_1_H5.0_CDM0.8_RM1.0	12.038	1.000	1.278	0.554	9.582
3S_I_1_H5.0_CDM0.8_RM1.5	15.648	1.000	1.300	0.623	10.920
3S_I_1_H5.0_CDM1.0_RM1.0	19.256	1.000	1.258	0.646	12.653
3S_I_1_H5.0_CDM1.0_RM1.5	21.715	1.000	1.232	0.623	12.295
3S_I_1_wo_1_H3.0_CDM0.8_RM1.0	49.614	1.000	2.058	0.427	2.775
3S_I_1_wo_1_H3.0_CDM0.8_RM1.5	33.374	1.000	2.038	0.445	3.224
3S_I_1_wo_1_H3.0_CDM1.0_RM1.0	27.754	1.000	2.026	0.426	4.270
3S_I_1_wo_1_H3.0_CDM1.0_RM1.5	21.300	1.000	1.900	0.463	4.750
3S_I_1_wo_1_H4.0_CDM0.8_RM1.0	63.674	1.000	1.730	0.602	2.648
3S_I_1_wo_1_H4.0_CDM0.8_RM1.5	46.331	1.000	1.722	0.602	2.721
3S_I_1_wo_1_H4.0_CDM1.0_RM1.0	38.625	1.000	1.717	0.556	3.553
3S_I_1_wo_1_H4.0_CDM1.0_RM1.5	23.000	1.000	1.673	0.601	3.912
3S_I_1_wo_1_H5.0_CDM0.8_RM1.0	74.516	1.000	1.529	0.763	2.409
3S_I_1_wo_1_H5.0_CDM0.8_RM1.5	56.665	1.000	1.526	0.787	2.556
3S_I_1_wo_1_H5.0_CDM1.0_RM1.0	47.254	1.000	1.523	0.703	3.336
3S_I_1_wo_1_H5.0_CDM1.0_RM1.5	29.029	1.000	1.507	0.786	3.798
3S_I_2_H3.0_CDM0.8_RM1.0	9.148	1.000	1.612	0.208	5.919

3S_I_2_H3.0_CDM0.8_RM1.5	10.292	1.000	1.552	0.217	6.184
3S_I_2_H3.0_CDM1.0_RM1.0	11.488	1.000	1.483	0.231	6.834
3S_I_2_H3.0_CDM1.0_RM1.5	12.458	1.000	1.443	0.249	7.388
3S_I_2_H4.0_CDM0.8_RM1.0	8.982	1.000	1.473	0.286	6.637
3S_I_2_H4.0_CDM0.8_RM1.5	10.987	1.000	1.417	0.302	7.009
3S_I_2_H4.0_CDM1.0_RM1.0	12.863	1.000	1.371	0.323	7.764
3S_I_2_H4.0_CDM1.0_RM1.5	14.725	1.000	1.325	0.336	8.099
3S_I_2_H5.0_CDM0.8_RM1.0	8.318	1.000	1.419	0.414	7.755
3S_I_2_H5.0_CDM0.8_RM1.5	12.085	1.000	1.379	0.460	8.606
3S_I_2_H5.0_CDM1.0_RM1.0	14.276	1.000	1.330	0.460	8.894
3S_I_2_H5.0_CDM1.0_RM1.5	17.036	1.000	1.287	0.483	9.343
3S_I_2_wo_1_H3.0_CDM0.8_RM1.0	65.281	1.000	2.068	0.426	2.899
3S_I_2_wo_1_H3.0_CDM0.8_RM1.5	30.147	1.000	2.032	0.426	2.962
3S_I_2_wo_1_H3.0_CDM1.0_RM1.0	26.870	1.000	2.024	0.485	5.030
3S_I_2_wo_1_H3.0_CDM1.0_RM1.5	17.175	1.000	1.863	0.485	5.146
3S_I_2_wo_1_H4.0_CDM0.8_RM1.0	77.790	1.000	1.733	0.555	2.566
3S_I_2_wo_1_H4.0_CDM0.8_RM1.5	52.480	1.000	1.725	0.555	2.633
3S_I_2_wo_1_H4.0_CDM1.0_RM1.0	46.205	1.000	1.722	0.623	4.152
3S_I_2_wo_1_H4.0_CDM1.0_RM1.5	16.822	1.000	1.644	0.600	4.060
3S_I_2_wo_1_H5.0_CDM0.8_RM1.0	97.989	1.000	1.532	0.740	2.447
3S_I_2_wo_1_H5.0_CDM0.8_RM1.5	66.281	1.000	1.528	0.740	2.518
3S_I_2_wo_1_H5.0_CDM1.0_RM1.0	67.748	1.000	1.528	0.831	4.116
3S_I_2_wo_1_H5.0_CDM1.0_RM1.5	17.889	1.000	1.491	0.732	3.691
3S_I_12_H3.0_CDM0.8_RM1.0	11.367	1.000	1.703	0.222	10.839
3S_I_12_H3.0_CDM0.8_RM1.5	12.048	1.000	1.692	0.231	11.300
3S_I_12_H3.0_CDM1.0_RM1.0	12.015	1.000	1.727	0.249	12.433
3S_I_12_H3.0_CDM1.0_RM1.5	13.550	1.000	1.657	0.249	12.482
3S_I_12_H4.0_CDM0.8_RM1.0	12.581	1.000	1.489	0.353	14.988
3S_I_12_H4.0_CDM0.8_RM1.5	13.223	1.000	1.483	0.360	15.289
3S_I_12_H4.0_CDM1.0_RM1.0	13.790	1.000	1.473	0.369	16.060
3S_I_12_H4.0_CDM1.0_RM1.5	14.841	1.000	1.489	0.424	18.466
3S_I_12_H5.0_CDM0.8_RM1.0	13.194	1.000	1.378	0.553	20.039
3S_I_12_H5.0_CDM0.8_RM1.5	15.535	1.000	1.385	0.553	20.111
3S_I_12_H5.0_CDM1.0_RM1.0	14.812	1.000	1.367	0.553	20.684
3S_I_12_H5.0_CDM1.0_RM1.5	24.168	1.000	1.139	0.405	15.165
3S_I_12_wo_1_H3.0_CDM0.8_RM1.0	103.700	1.000	2.080	0.426	2.918
3S_I_12_wo_1_H3.0_CDM0.8_RM1.5	75.896	1.000	2.073	0.426	2.994
3S_I_12_wo_1_H3.0_CDM1.0_RM1.0	77.128	1.000	2.073	0.425	4.652
3S_I_12_wo_1_H3.0_CDM1.0_RM1.5	49.465	1.000	2.058	0.425	4.776
3S_I_12_wo_1_H4.0_CDM0.8_RM1.0	115.320	1.000	1.739	0.555	2.494
3S_I_12_wo_1_H4.0_CDM0.8_RM1.5	92.014	1.000	1.736	0.601	2.778
3S_I_12_wo_1_H4.0_CDM1.0_RM1.0	79.810	1.000	1.734	0.555	3.726
3S_I_12_wo_1_H4.0_CDM1.0_RM1.5	56.310	1.000	1.727	0.555	3.793

3S_I_12_wo_1_H5.0_CDM0.8_RM1.0	136.660	1.000	1.534	0.740	2.341
3S_I_12_wo_1_H5.0_CDM0.8_RM1.5	107.670	1.000	1.532	0.786	2.564
3S_I_12_wo_1_H5.0_CDM1.0_RM1.0	94.897	1.000	1.531	0.739	3.594
3S_I_12_wo_1_H5.0_CDM1.0_RM1.5	73.114	1.000	1.529	0.739	3.665

Table A2-8 Soft story, weak story and max alpha values for 5 Story frame for pushover analysis results at Ultimate Point (UP)

Frame Type/ Story Level	$\eta_{ki,\ max}$	$\eta_{kj,\ max}$	α_{max}	$\alpha_{irregular}$	α_2
5S_B_H3.0_CDM0.8_RM1.0	1.334	1.000	1.153	0.866	5.369
5S_B_H3.0_CDM0.8_RM1.5	1.217	1.000	1.084	1.135	7.083
5S_B_H3.0_CDM1.0_RM1.0	1.223	1.007	1.038	1.000	6.602
5S_B_H3.0_CDM1.0_RM1.5	1.098	1.138	1.059	1.662	11.019
5S_B_H4.0_CDM0.8_RM1.0	1.547	1.000	1.285	0.785	4.452
5S_B_H4.0_CDM0.8_RM1.5	1.257	1.000	1.090	1.189	6.807
5S_B_H4.0_CDM1.0_RM1.0	1.339	1.000	1.107	0.973	6.036
5S_B_H4.0_CDM1.0_RM1.5	1.122	1.046	1.036	1.764	11.004
5S_B_H5.0_CDM0.8_RM1.0	1.989	1.000	1.481	0.691	3.509
5S_B_H5.0_CDM0.8_RM1.5	1.418	1.000	1.178	1.098	5.651
5S_B_H5.0_CDM1.0_RM1.0	1.476	1.000	1.169	0.947	5.438
5S_B_H5.0_CDM1.0_RM1.5	1.137	1.003	1.033	1.996	11.551
5S_I_1_H3.0_CDM0.8_RM1.0	4.312	1.371	1.274	0.339	3.658
5S_I_1_H3.0_CDM0.8_RM1.5	4.315	1.630	1.280	0.352	3.845
5S_I_1_H3.0_CDM1.0_RM1.0	3.813	1.759	1.241	0.371	4.397
5S_I_1_H3.0_CDM1.0_RM1.5	3.464	2.177	1.331	0.371	4.428
5S_I_1_H4.0_CDM0.8_RM1.0	4.399	1.304	1.273	0.395	3.714
5S_I_1_H4.0_CDM0.8_RM1.5	4.264	1.521	1.306	0.390	3.709
5S_I_1_H4.0_CDM1.0_RM1.0	4.259	1.546	1.287	0.433	4.523
5S_I_1_H4.0_CDM1.0_RM1.5	3.607	1.917	1.291	0.433	4.561
5S_I_1_H5.0_CDM0.8_RM1.0	4.628	1.285	1.251	0.473	3.787
5S_I_1_H5.0_CDM0.8_RM1.5	4.401	1.442	1.293	0.446	3.620
5S_I_1_H5.0_CDM1.0_RM1.0	4.405	1.499	1.286	0.567	5.115
5S_I_1_H5.0_CDM1.0_RM1.5	4.028	1.840	1.324	0.581	5.286
5S_I_1_wo_1_H3.0_CDM0.8_RM1.0	3.683	1.000	2.389	0.339	2.867
5S_I_1_wo_1_H3.0_CDM0.8_RM1.5	5.459	1.000	1.292	0.406	3.487
5S_I_1_wo_1_H3.0_CDM1.0_RM1.0	5.398	1.000	1.298	0.406	4.116
5S_I_1_wo_1_H3.0_CDM1.0_RM1.5	4.622	1.159	1.245	0.371	3.813
5S_I_1_wo_1_H4.0_CDM0.8_RM1.0	8.805	1.000	2.481	0.366	2.561
5S_I_1_wo_1_H4.0_CDM0.8_RM1.5	5.117	1.000	1.620	0.617	4.408
5S_I_1_wo_1_H4.0_CDM1.0_RM1.0	4.551	1.000	1.586	0.554	4.589
5S_I_1_wo_1_H4.0_CDM1.0_RM1.5	6.199	1.000	1.219	0.985	8.241
5S_I_1_wo_1_H5.0_CDM0.8_RM1.0	13.383	1.000	2.237	0.447	2.588
5S_I_1_wo_1_H5.0_CDM0.8_RM1.5	5.191	1.000	2.045	0.501	2.975

5S_I_1_wo_1_H5.0_CDM1.0_RM1.0	4.048	1.000	1.965	0.474	3.418
5S_I_1_wo_1_H5.0_CDM1.0_RM1.5	5.976	1.000	1.465	0.864	6.317
5S_I_2_H3.0_CDM0.8_RM1.0	3.540	1.000	1.278	0.500	4.162
5S_I_2_H3.0_CDM0.8_RM1.5	1.511	1.482	1.152	0.594	4.975
5S_I_2_H3.0_CDM1.0_RM1.0	1.638	1.283	1.118	0.581	5.290
5S_I_2_H3.0_CDM1.0_RM1.5	1.253	2.152	1.304	0.621	5.696
5S_I_2_H4.0_CDM0.8_RM1.0	3.596	1.000	1.206	0.635	4.685
5S_I_2_H4.0_CDM0.8_RM1.5	1.669	1.434	1.173	0.702	5.217
5S_I_2_H4.0_CDM1.0_RM1.0	1.650	1.243	1.117	0.715	5.653
5S_I_2_H4.0_CDM1.0_RM1.5	1.269	1.802	1.278	0.742	5.840
5S_I_2_H5.0_CDM0.8_RM1.0	3.397	1.000	1.162	0.998	6.586
5S_I_2_H5.0_CDM0.8_RM1.5	1.619	1.289	1.158	0.890	5.925
5S_I_2_H5.0_CDM1.0_RM1.0	1.450	1.178	1.105	0.917	6.617
5S_I_2_H5.0_CDM1.0_RM1.5	1.121	1.493	1.198	1.671	12.132
5S_I_2_wo_1_H3.0_CDM0.8_RM1.0	3.738	1.000	1.331	0.638	4.800
5S_I_2_wo_1_H3.0_CDM0.8_RM1.5	5.519	1.000	1.706	0.520	5.791
5S_I_2_wo_1_H3.0_CDM1.0_RM1.0	4.127	1.000	2.292	0.332	4.094
5S_I_2_wo_1_H3.0_CDM1.0_RM1.5	6.423	1.151	1.445	0.844	10.466
5S_I_2_wo_1_H4.0_CDM0.8_RM1.0	4.192	1.000	2.176	0.407	2.672
5S_I_2_wo_1_H4.0_CDM0.8_RM1.5	4.159	1.000	1.258	0.840	5.604
5S_I_2_wo_1_H4.0_CDM1.0_RM1.0	4.169	1.000	1.253	0.729	5.475
5S_I_2_wo_1_H4.0_CDM1.0_RM1.5	1.888	1.049	1.098	0.885	6.701
5S_I_2_wo_1_H5.0_CDM0.8_RM1.0	6.632	1.000	2.096	0.461	2.591
5S_I_2_wo_1_H5.0_CDM0.8_RM1.5	3.781	1.000	1.510	0.716	4.112
5S_I_2_wo_1_H5.0_CDM1.0_RM1.0	3.779	1.000	1.460	0.644	4.325
5S_I_2_wo_1_H5.0_CDM1.0_RM1.5	4.040	1.000	1.170	1.140	7.747
5S_I_3_H3.0_CDM0.8_RM1.0	3.602	1.000	1.358	0.406	3.858
5S_I_3_H3.0_CDM0.8_RM1.5	3.066	1.442	1.184	0.527	5.055
5S_I_3_H3.0_CDM1.0_RM1.0	3.241	1.175	1.149	0.500	5.189
5S_I_3_H3.0_CDM1.0_RM1.5	1.499	2.220	1.301	0.527	5.506
5S_I_3_H4.0_CDM0.8_RM1.0	3.812	1.000	1.527	0.527	4.223
5S_I_3_H4.0_CDM0.8_RM1.5	4.057	1.145	1.198	0.581	4.686
5S_I_3_H4.0_CDM1.0_RM1.0	4.051	1.042	1.159	0.581	5.026
5S_I_3_H4.0_CDM1.0_RM1.5	1.718	1.625	1.209	0.675	5.897
5S_I_3_H5.0_CDM0.8_RM1.0	4.308	1.000	1.139	0.850	6.300
5S_I_3_H5.0_CDM0.8_RM1.5	2.115	1.405	1.194	0.963	7.183
5S_I_3_H5.0_CDM1.0_RM1.0	2.669	1.160	1.122	1.006	8.029
5S_I_3_H5.0_CDM1.0_RM1.5	1.951	1.612	1.219	0.790	6.348
5S_I_3_wo_1_H3.0_CDM0.8_RM1.0	4.813	1.000	1.387	0.554	4.541
5S_I_3_wo_1_H3.0_CDM0.8_RM1.5	3.615	1.000	1.424	0.285	2.361
5S_I_3_wo_1_H3.0_CDM1.0_RM1.0	3.280	1.000	1.141	0.715	6.525
5S_I_3_wo_1_H3.0_CDM1.0_RM1.5	2.403	1.205	1.111	0.648	5.986
5S_I_3_wo_1_H4.0_CDM0.8_RM1.0	4.505	1.000	2.220	0.379	2.695

5S_I_3_wo_1_H4.0_CDM0.8_RM1.5	3.490	1.000	1.674	0.272	1.962
5S_I_3_wo_1_H4.0_CDM1.0_RM1.0	4.656	1.000	1.397	0.581	4.741
5S_I_3_wo_1_H4.0_CDM1.0_RM1.5	2.279	1.036	1.092	1.068	8.789
5S_I_3_wo_1_H5.0_CDM0.8_RM1.0	7.097	1.000	2.118	0.433	2.611
5S_I_3_wo_1_H5.0_CDM0.8_RM1.5	2.978	1.000	1.734	0.285	1.758
5S_I_3_wo_1_H5.0_CDM1.0_RM1.0	4.070	1.000	1.495	0.581	4.222
5S_I_3_wo_1_H5.0_CDM1.0_RM1.5	5.046	1.000	1.213	1.084	7.968
5S_I_12_H3.0_CDM0.8_RM1.0	6.863	1.589	1.327	0.324	5.295
5S_I_12_H3.0_CDM0.8_RM1.5	6.759	1.684	1.325	0.297	4.892
5S_I_12_H3.0_CDM1.0_RM1.0	6.764	1.774	1.290	0.297	5.183
5S_I_12_H3.0_CDM1.0_RM1.5	6.624	2.167	1.374	0.292	5.115
5S_I_12_H4.0_CDM0.8_RM1.0	6.942	1.446	1.327	0.365	5.173
5S_I_12_H4.0_CDM0.8_RM1.5	6.989	1.650	1.345	0.351	5.024
5S_I_12_H4.0_CDM1.0_RM1.0	7.001	1.626	1.301	0.351	5.367
5S_I_12_H4.0_CDM1.0_RM1.5	6.786	1.947	1.335	0.338	5.192
5S_I_12_H5.0_CDM0.8_RM1.0	5.988	1.430	1.498	0.445	5.310
5S_I_12_H5.0_CDM0.8_RM1.5	7.006	1.485	1.348	0.405	4.874
5S_I_12_H5.0_CDM1.0_RM1.0	7.199	1.506	1.294	0.418	5.432
5S_I_12_H5.0_CDM1.0_RM1.5	7.122	1.716	1.330	0.392	5.119
5S_I_12_wo_1_H3.0_CDM0.8_RM1.0	13.365	1.000	3.146	0.257	2.612
5S_I_12_wo_1_H3.0_CDM0.8_RM1.5	4.075	1.000	1.984	0.338	3.542
5S_I_12_wo_1_H3.0_CDM1.0_RM1.0	3.850	1.000	1.807	0.314	4.158
5S_I_12_wo_1_H3.0_CDM1.0_RM1.5	6.343	1.000	1.671	0.553	7.449
5S_I_12_wo_1_H4.0_CDM0.8_RM1.0	25.039	1.000	2.677	0.338	2.738
5S_I_12_wo_1_H4.0_CDM0.8_RM1.5	8.472	1.000	2.503	0.364	3.015
5S_I_12_wo_1_H4.0_CDM1.0_RM1.0	6.364	1.000	2.417	0.352	3.462
5S_I_12_wo_1_H4.0_CDM1.0_RM1.5	4.623	1.000	1.614	0.378	3.812
5S_I_12_wo_1_H5.0_CDM0.8_RM1.0	32.048	1.000	2.316	0.419	2.735
5S_I_12_wo_1_H5.0_CDM0.8_RM1.5	13.473	1.000	2.249	0.446	2.995
5S_I_12_wo_1_H5.0_CDM1.0_RM1.0	9.837	1.000	2.207	0.419	3.487
5S_I_12_wo_1_H5.0_CDM1.0_RM1.5	5.747	1.000	1.659	0.500	4.865
5S_I_13_H3.0_CDM0.8_RM1.0	6.945	1.538	1.336	0.297	4.731
5S_I_13_H3.0_CDM0.8_RM1.5	7.032	1.709	1.331	0.292	4.686
5S_I_13_H3.0_CDM1.0_RM1.0	7.174	1.819	1.314	0.292	5.013
5S_I_13_H3.0_CDM1.0_RM1.5	7.318	2.276	1.408	0.297	5.136
5S_I_13_H4.0_CDM0.8_RM1.0	5.703	1.336	1.506	0.351	4.760
5S_I_13_H4.0_CDM0.8_RM1.5	7.049	1.493	1.366	0.351	4.808
5S_I_13_H4.0_CDM1.0_RM1.0	7.270	1.461	1.299	0.351	5.197
5S_I_13_H4.0_CDM1.0_RM1.5	7.332	1.739	1.317	0.338	5.032
5S_I_13_H5.0_CDM0.8_RM1.0	5.867	1.452	1.528	0.405	4.734
5S_I_13_H5.0_CDM0.8_RM1.5	6.980	1.568	1.403	0.405	4.781
5S_I_13_H5.0_CDM1.0_RM1.0	7.392	1.507	1.317	0.405	5.190
5S_I_13_H5.0_CDM1.0_RM1.5	7.521	1.769	1.349	0.391	5.055

5S_I_13_wo_1_H3.0_CDM0.8_RM1.0	13.722	1.000	3.155	0.244	2.458
5S_I_13_wo_1_H3.0_CDM0.8_RM1.5	2.876	1.000	2.312	0.155	1.614
5S_I_13_wo_1_H3.0_CDM1.0_RM1.0	4.826	1.000	1.838	0.338	4.460
5S_I_13_wo_1_H3.0_CDM1.0_RM1.5	4.170	1.000	1.623	0.338	4.534
5S_I_13_wo_1_H4.0_CDM0.8_RM1.0	25.808	1.000	2.678	0.311	2.523
5S_I_13_wo_1_H4.0_CDM0.8_RM1.5	5.222	1.000	2.338	0.169	1.399
5S_I_13_wo_1_H4.0_CDM1.0_RM1.0	6.860	1.000	2.445	0.338	3.316
5S_I_13_wo_1_H4.0_CDM1.0_RM1.5	5.214	1.000	1.657	0.378	3.794
5S_I_13_wo_1_H5.0_CDM0.8_RM1.0	34.444	1.000	2.319	0.405	2.656
5S_I_13_wo_1_H5.0_CDM0.8_RM1.5	8.960	1.000	2.177	0.214	1.446
5S_I_13_wo_1_H5.0_CDM1.0_RM1.0	10.958	1.000	2.222	0.395	3.311
5S_I_13_wo_1_H5.0_CDM1.0_RM1.5	6.546	1.000	1.722	0.510	4.346
5S_I_23_H3.0_CDM0.8_RM1.0	7.411	1.518	1.303	0.378	6.026
5S_I_23_H3.0_CDM0.8_RM1.5	7.317	1.766	1.317	0.364	5.839
5S_I_23_H3.0_CDM1.0_RM1.0	7.221	1.897	1.307	0.364	6.124
5S_I_23_H3.0_CDM1.0_RM1.5	7.047	2.330	1.370	0.351	5.924
5S_I_23_H4.0_CDM0.8_RM1.0	7.616	1.218	1.279	0.472	6.104
5S_I_23_H4.0_CDM0.8_RM1.5	7.816	1.563	1.323	0.010	0.125
5S_I_23_H4.0_CDM1.0_RM1.0	7.742	1.458	1.273	0.459	6.394
5S_I_23_H4.0_CDM1.0_RM1.5	7.495	1.876	1.332	0.432	6.056
5S_I_23_H5.0_CDM0.8_RM1.0	5.702	1.157	1.461	0.741	7.953
5S_I_23_H5.0_CDM0.8_RM1.5	7.768	1.483	1.332	0.504	5.451
5S_I_23_H5.0_CDM1.0_RM1.0	7.835	1.359	1.262	0.526	6.151
5S_I_23_H5.0_CDM1.0_RM1.5	7.603	1.725	1.333	0.499	5.881
5S_I_23_wo_1_H3.0_CDM0.8_RM1.0	7.066	1.000	2.893	0.271	2.760
5S_I_23_wo_1_H3.0_CDM0.8_RM1.5	4.082	1.000	1.696	0.392	4.061
5S_I_23_wo_1_H3.0_CDM1.0_RM1.0	4.393	1.000	1.680	0.445	5.763
5S_I_23_wo_1_H3.0_CDM1.0_RM1.5	5.158	1.000	1.587	0.634	8.325
5S_I_23_wo_1_H4.0_CDM0.8_RM1.0	14.334	1.000	2.605	0.338	2.864
5S_I_23_wo_1_H4.0_CDM0.8_RM1.5	4.753	1.000	2.302	0.393	3.398
5S_I_23_wo_1_H4.0_CDM1.0_RM1.0	3.846	1.000	2.203	0.378	3.820
5S_I_23_wo_1_H4.0_CDM1.0_RM1.5	6.399	1.000	1.559	0.720	7.343
5S_I_23_wo_1_H5.0_CDM0.8_RM1.0	22.770	1.000	2.293	0.432	2.983
5S_I_23_wo_1_H5.0_CDM0.8_RM1.5	7.661	1.000	2.164	0.473	3.348
5S_I_23_wo_1_H5.0_CDM1.0_RM1.0	6.041	1.000	2.111	0.446	3.877
5S_I_23_wo_1_H5.0_CDM1.0_RM1.5	5.363	1.000	1.511	0.567	4.997
5S_I_123_H3.0_CDM0.8_RM1.0	7.335	1.532	1.373	0.283	6.856
5S_I_123_H3.0_CDM0.8_RM1.5	7.834	1.727	1.323	0.283	6.885
5S_I_123_H3.0_CDM1.0_RM1.0	8.150	1.778	1.375	0.283	7.134
5S_I_123_H3.0_CDM1.0_RM1.5	8.318	2.164	1.490	0.283	7.157
5S_I_123_H4.0_CDM0.8_RM1.0	5.946	1.489	1.607	0.324	6.690
5S_I_123_H4.0_CDM0.8_RM1.5	6.307	2.037	1.837	0.351	7.283
5S_I_123_H4.0_CDM1.0_RM1.0	7.730	1.466	1.336	0.337	7.302

5S_I_123_H4.0_CDM1.0_RM1.5	8.271	1.703	1.313	0.324	7.038
5S_I_123_H5.0_CDM0.8_RM1.0	6.127	1.501	1.591	0.378	6.675
5S_I_123_H5.0_CDM0.8_RM1.5	6.368	1.780	1.690	0.364	6.470
5S_I_123_H5.0_CDM1.0_RM1.0	6.634	1.667	1.610	0.378	7.010
5S_I_123_H5.0_CDM1.0_RM1.5	8.251	1.737	1.366	0.378	7.039
5S_I_123_wo_1_H3.0_CDM0.8_RM1.0	28.962	1.000	3.307	0.230	2.804
5S_I_123_wo_1_H3.0_CDM0.8_RM1.5	10.391	1.000	3.092	0.257	3.250
5S_I_123_wo_1_H3.0_CDM1.0_RM1.0	7.765	1.000	2.982	0.249	4.150
5S_I_123_wo_1_H3.0_CDM1.0_RM1.5	5.221	1.000	1.915	0.293	4.983
5S_I_123_wo_1_H4.0_CDM0.8_RM1.0	38.016	1.000	2.715	0.308	2.829
5S_I_123_wo_1_H4.0_CDM0.8_RM1.5	21.924	1.000	2.666	0.324	3.055
5S_I_123_wo_1_H4.0_CDM1.0_RM1.0	16.706	1.000	2.635	0.324	3.796
5S_I_123_wo_1_H4.0_CDM1.0_RM1.5	5.217	1.000	2.374	0.364	4.378
5S_I_123_wo_1_H5.0_CDM0.8_RM1.0	47.532	1.000	2.336	0.405	2.910
5S_I_123_wo_1_H5.0_CDM0.8_RM1.5	30.838	1.000	2.315	0.419	3.102
5S_I_123_wo_1_H5.0_CDM1.0_RM1.0	24.545	1.000	2.301	0.392	3.723
5S_I_123_wo_1_H5.0_CDM1.0_RM1.5	8.561	1.000	2.194	0.432	4.179

Table A2-9 Soft story, weak story and max alpha values for 8 Story frame for pushover analysis results at Ultimate Point (UP)

Frame Type/ Story Level	$\eta_{ki,\,max}$	$\eta_{kj,\,max}$	α_{max}	$\alpha_{irregular}$	α_2
8S_B_H3.0_CDM0.8_RM1.0	1.368	1.156	1.100	0.812	3.668
8S_B_H3.0_CDM0.8_RM1.5	1.204	1.294	1.093	1.121	5.097
8S_B_H3.0_CDM1.0_RM1.0	1.228	1.259	1.102	1.000	4.966
8S_B_H3.0_CDM1.0_RM1.5	1.114	1.670	1.159	1.558	7.387
8S_B_H4.0_CDM0.8_RM1.0	1.494	1.104	1.146	0.744	3.181
8S_B_H4.0_CDM0.8_RM1.5	1.265	1.232	1.102	1.061	4.577
8S_B_H4.0_CDM1.0_RM1.0	1.345	1.194	1.105	0.880	4.000
8S_B_H4.0_CDM1.0_RM1.5	1.168	1.363	1.132	1.301	5.949
8S_B_H5.0_CDM0.8_RM1.0	1.696	1.037	1.183	0.684	2.729
8S_B_H5.0_CDM0.8_RM1.5	1.376	1.170	1.135	1.000	4.045
8S_B_H5.0_CDM1.0_RM1.0	1.447	1.139	1.126	0.819	3.556
8S_B_H5.0_CDM1.0_RM1.5	1.211	1.274	1.110	1.247	5.447
8S_I_1_H3.0_CDM0.8_RM1.0	4.424	1.853	1.343	0.438	2.423
8S_I_1_H3.0_CDM0.8_RM1.5	4.821	2.106	1.343	0.438	2.440
8S_I_1_H3.0_CDM1.0_RM1.0	4.960	2.286	1.397	0.438	2.555
8S_I_1_H3.0_CDM1.0_RM1.5	4.913	2.573	1.428	0.438	2.566
8S_I_1_H4.0_CDM0.8_RM1.0	4.442	1.655	1.308	0.499	2.574
8S_I_1_H4.0_CDM0.8_RM1.5	4.444	1.885	1.307	0.514	2.672
8S_I_1_H4.0_CDM1.0_RM1.0	4.010	1.964	1.334	0.529	2.920
8S_I_1_H4.0_CDM1.0_RM1.5	3.552	2.248	1.394	0.529	2.936

8S_I_1_H5.0_CDM0.8_RM1.0	3.410	1.244	1.435	0.544	2.635
8S_I_1_H5.0_CDM0.8_RM1.5	3.664	1.448	1.388	0.543	2.661
8S_I_1_H5.0_CDM1.0_RM1.0	3.843	1.432	1.331	0.559	2.940
8S_I_1_H5.0_CDM1.0_RM1.5	4.373	1.820	1.389	0.559	2.960
8S_I_1_wo_1_H3.0_CDM0.8_RM1.0	3.310	1.051	1.492	0.416	2.261
8S_I_1_wo_1_H3.0_CDM0.8_RM1.5	3.596	1.286	1.356	0.431	2.363
8S_I_1_wo_1_H3.0_CDM1.0_RM1.0	3.744	1.324	1.309	0.438	2.537
8S_I_1_wo_1_H3.0_CDM1.0_RM1.5	4.991	1.999	1.349	0.453	2.638
8S_I_1_wo_1_H4.0_CDM0.8_RM1.0	2.994	1.000	1.887	0.484	2.442
8S_I_1_wo_1_H4.0_CDM0.8_RM1.5	3.214	1.007	1.516	0.476	2.433
8S_I_1_wo_1_H4.0_CDM1.0_RM1.0	3.266	1.049	1.497	0.499	2.738
8S_I_1_wo_1_H4.0_CDM1.0_RM1.5	3.597	1.253	1.364	0.499	2.756
8S_I_1_wo_1_H5.0_CDM0.8_RM1.0	4.856	1.000	2.887	0.438	2.027
8S_I_1_wo_1_H5.0_CDM0.8_RM1.5	2.898	1.000	1.803	0.567	2.664
8S_I_1_wo_1_H5.0_CDM1.0_RM1.0	2.954	1.000	1.736	0.551	2.849
8S_I_1_wo_1_H5.0_CDM1.0_RM1.5	3.198	1.043	1.488	0.552	2.875
8S_I_2_H3.0_CDM0.8_RM1.0	4.569	1.526	1.346	0.369	2.732
8S_I_2_H3.0_CDM0.8_RM1.5	4.868	1.705	1.385	0.363	2.702
8S_I_2_H3.0_CDM1.0_RM1.0	5.227	1.831	1.427	0.363	2.800
8S_I_2_H3.0_CDM1.0_RM1.5	5.478	2.063	1.459	0.363	2.810
8S_I_2_H4.0_CDM0.8_RM1.0	4.367	1.357	1.271	0.438	3.077
8S_I_2_H4.0_CDM0.8_RM1.5	4.514	1.552	1.335	0.423	2.995
8S_I_2_H4.0_CDM1.0_RM1.0	4.659	1.587	1.380	0.416	3.073
8S_I_2_H4.0_CDM1.0_RM1.5	4.757	1.805	1.431	0.401	2.975
8S_I_2_H5.0_CDM0.8_RM1.0	3.932	1.233	1.275	0.514	3.418
8S_I_2_H5.0_CDM0.8_RM1.5	4.295	1.430	1.293	0.499	3.342
8S_I_2_H5.0_CDM1.0_RM1.0	4.580	1.396	1.284	0.499	3.531
8S_I_2_H5.0_CDM1.0_RM1.5	4.607	1.599	1.354	0.461	3.281
8S_I_2_wo_1_H3.0_CDM0.8_RM1.0	3.361	1.000	1.750	0.360	2.559
8S_I_2_wo_1_H3.0_CDM0.8_RM1.5	3.548	1.149	1.546	0.363	2.604
8S_I_2_wo_1_H3.0_CDM1.0_RM1.0	3.618	1.185	1.494	0.366	2.771
8S_I_2_wo_1_H3.0_CDM1.0_RM1.5	4.282	1.579	1.310	0.369	2.808
8S_I_2_wo_1_H4.0_CDM0.8_RM1.0	2.906	1.000	2.196	0.469	3.049
8S_I_2_wo_1_H4.0_CDM0.8_RM1.5	3.171	1.000	1.812	0.423	2.795
8S_I_2_wo_1_H4.0_CDM1.0_RM1.0	3.248	1.000	1.734	0.423	3.027
8S_I_2_wo_1_H4.0_CDM1.0_RM1.5	3.519	1.131	1.550	0.423	3.048
8S_I_2_wo_1_H5.0_CDM0.8_RM1.0	8.404	1.000	3.212	0.544	3.178
8S_I_2_wo_1_H5.0_CDM0.8_RM1.5	2.752	1.000	2.033	0.619	3.694
8S_I_2_wo_1_H5.0_CDM1.0_RM1.0	2.855	1.000	1.870	0.597	3.975
8S_I_2_wo_1_H5.0_CDM1.0_RM1.5	3.143	1.000	1.638	0.514	3.456
8S_I_3_H3.0_CDM0.8_RM1.0	4.765	1.376	1.373	0.384	2.898
8S_I_3_H3.0_CDM0.8_RM1.5	4.763	1.534	1.397	0.363	2.752
8S_I_3_H3.0_CDM1.0_RM1.0	5.393	1.619	1.435	0.363	2.850

8S_I_3_H3.0_CDM1.0_RM1.5	5.822	1.826	1.469	0.363	2.859
8S_I_3_H4.0_CDM0.8_RM1.0	4.423	1.268	1.269	0.438	3.137
8S_I_3_H4.0_CDM0.8_RM1.5	4.526	1.415	1.331	0.423	3.047
8S_I_3_H4.0_CDM1.0_RM1.0	4.684	1.446	1.386	0.415	3.123
8S_I_3_H4.0_CDM1.0_RM1.5	4.831	1.638	1.436	0.400	3.022
8S_I_3_H5.0_CDM0.8_RM1.0	4.137	1.165	1.242	0.513	3.475
8S_I_3_H5.0_CDM0.8_RM1.5	4.314	1.325	1.276	0.488	3.326
8S_I_3_H5.0_CDM1.0_RM1.0	4.557	1.317	1.277	0.483	3.466
8S_I_3_H5.0_CDM1.0_RM1.5	4.696	1.452	1.356	0.461	3.322
8S_I_3_wo_1_H3.0_CDM0.8_RM1.0	3.299	1.000	1.793	0.370	2.688
8S_I_3_wo_1_H3.0_CDM0.8_RM1.5	3.520	1.125	1.582	0.369	2.702
8S_I_3_wo_1_H3.0_CDM1.0_RM1.0	3.621	1.162	1.548	0.370	2.854
8S_I_3_wo_1_H3.0_CDM1.0_RM1.5	4.084	1.466	1.322	0.370	2.867
8S_I_3_wo_1_H4.0_CDM0.8_RM1.0	2.717	1.000	2.206	0.514	3.423
8S_I_3_wo_1_H4.0_CDM0.8_RM1.5	3.062	1.000	1.819	0.446	3.013
8S_I_3_wo_1_H4.0_CDM1.0_RM1.0	3.160	1.000	1.755	0.438	3.194
8S_I_3_wo_1_H4.0_CDM1.0_RM1.5	3.470	1.116	1.590	0.431	3.160
8S_I_3_wo_1_H5.0_CDM0.8_RM1.0	8.730	1.000	3.241	0.529	3.166
8S_I_3_wo_1_H5.0_CDM0.8_RM1.5	2.705	1.000	2.107	0.680	4.152
8S_I_3_wo_1_H5.0_CDM1.0_RM1.0	2.669	1.000	1.954	0.619	4.210
8S_I_3_wo_1_H5.0_CDM1.0_RM1.5	3.012	1.000	1.660	0.529	3.630
8S_I_4_H3.0_CDM0.8_RM1.0	4.129	1.894	1.373	0.438	2.925
8S_I_4_H3.0_CDM0.8_RM1.5	4.600	2.177	1.371	0.446	2.991
8S_I_4_H3.0_CDM1.0_RM1.0	4.819	2.190	1.414	0.446	3.098
8S_I_4_H3.0_CDM1.0_RM1.5	4.804	2.380	1.453	0.438	3.057
8S_I_4_H4.0_CDM0.8_RM1.0	3.896	1.623	1.374	0.499	3.149
8S_I_4_H4.0_CDM0.8_RM1.5	4.132	1.883	1.396	0.499	3.170
8S_I_4_H4.0_CDM1.0_RM1.0	4.436	1.959	1.397	0.514	3.415
8S_I_4_H4.0_CDM1.0_RM1.5	4.717	2.181	1.396	0.499	3.330
8S_I_4_H5.0_CDM0.8_RM1.0	3.592	1.358	1.450	0.589	3.471
8S_I_4_H5.0_CDM0.8_RM1.5	3.853	1.604	1.405	0.574	3.410
8S_I_4_H5.0_CDM1.0_RM1.0	3.966	1.513	1.357	0.574	3.609
8S_I_4_H5.0_CDM1.0_RM1.5	4.365	1.882	1.409	0.559	3.535
8S_I_4_wo_1_H3.0_CDM0.8_RM1.0	3.203	1.017	1.562	0.438	2.817
8S_I_4_wo_1_H3.0_CDM0.8_RM1.5	3.434	1.181	1.476	0.446	2.890
8S_I_4_wo_1_H3.0_CDM1.0_RM1.0	3.545	1.199	1.421	0.446	3.042
8S_I_4_wo_1_H3.0_CDM1.0_RM1.5	4.104	1.534	1.343	0.454	3.108
8S_I_4_wo_1_H4.0_CDM0.8_RM1.0	2.759	1.000	1.842	0.574	3.413
8S_I_4_wo_1_H4.0_CDM0.8_RM1.5	3.029	1.004	1.570	0.529	3.185
8S_I_4_wo_1_H4.0_CDM1.0_RM1.0	3.119	1.031	1.557	0.529	3.423
8S_I_4_wo_1_H4.0_CDM1.0_RM1.5	3.450	1.184	1.452	0.529	3.446
8S_I_4_wo_1_H5.0_CDM0.8_RM1.0	3.696	1.000	2.760	0.469	2.534
8S_I_4_wo_1_H5.0_CDM0.8_RM1.5	2.642	1.000	1.736	0.680	3.741

8S_I_4_wo_1_H5.0_CDM1.0_RM1.0	2.683	1.000	1.682	0.665	4.036
8S_I_4_wo_1_H5.0_CDM1.0_RM1.5	3.018	1.044	1.517	0.619	3.794
8S_I_12_H3.0_CDM0.8_RM1.0	4.462	1.547	1.350	0.325	2.705
8S_I_12_H3.0_CDM0.8_RM1.5	4.684	1.661	1.396	0.317	2.659
8S_I_12_H3.0_CDM1.0_RM1.0	4.884	1.729	1.471	0.317	2.768
8S_I_12_H3.0_CDM1.0_RM1.5	4.906	1.909	1.481	0.302	2.647
8S_I_12_H4.0_CDM0.8_RM1.0	4.153	1.449	1.431	0.378	2.960
8S_I_12_H4.0_CDM0.8_RM1.5	4.263	1.625	1.447	0.370	2.922
8S_I_12_H4.0_CDM1.0_RM1.0	4.415	1.609	1.412	0.362	3.010
8S_I_12_H4.0_CDM1.0_RM1.5	4.787	1.747	1.402	0.347	2.898
8S_I_12_H5.0_CDM0.8_RM1.0	4.040	1.186	1.377	0.445	3.254
8S_I_12_H5.0_CDM0.8_RM1.5	4.061	1.167	1.372	0.468	3.431
8S_I_12_H5.0_CDM1.0_RM1.0	4.192	1.434	1.438	0.430	3.360
8S_I_12_H5.0_CDM1.0_RM1.5	4.354	1.645	1.472	0.408	3.202
8S_I_12_wo_1_H3.0_CDM0.8_RM1.0	4.934	1.000	3.897	0.340	2.672
8S_I_12_wo_1_H3.0_CDM0.8_RM1.5	3.523	1.000	2.145	0.332	2.643
8S_I_12_wo_1_H3.0_CDM1.0_RM1.0	3.644	1.000	1.916	0.332	2.819
8S_I_12_wo_1_H3.0_CDM1.0_RM1.5	3.952	1.158	1.638	0.347	2.964
8S_I_12_wo_1_H4.0_CDM0.8_RM1.0	15.419	1.000	4.030	0.378	2.661
8S_I_12_wo_1_H4.0_CDM0.8_RM1.5	4.723	1.000	3.402	0.453	3.249
8S_I_12_wo_1_H4.0_CDM1.0_RM1.0	2.872	1.000	2.353	0.363	2.864
8S_I_12_wo_1_H4.0_CDM1.0_RM1.5	3.276	1.000	2.066	0.378	3.008
8S_I_12_wo_1_H5.0_CDM0.8_RM1.0	29.337	1.000	3.515	0.498	3.076
8S_I_12_wo_1_H5.0_CDM0.8_RM1.5	10.488	1.000	3.345	0.513	3.249
8S_I_12_wo_1_H5.0_CDM1.0_RM1.0	8.291	1.000	3.280	0.589	4.257
8S_I_12_wo_1_H5.0_CDM1.0_RM1.5	3.332	1.000	2.230	0.430	3.149
8S_I_13_H3.0_CDM0.8_RM1.0	4.326	1.240	1.362	0.325	2.610
8S_I_13_H3.0_CDM0.8_RM1.5	4.454	1.396	1.414	0.317	2.564
8S_I_13_H3.0_CDM1.0_RM1.0	4.392	1.483	1.435	0.302	2.539
8S_I_13_H3.0_CDM1.0_RM1.5	4.510	1.693	1.503	0.302	2.548
8S_I_13_H4.0_CDM0.8_RM1.0	3.996	1.205	1.355	0.385	2.936
8S_I_13_H4.0_CDM0.8_RM1.5	4.121	1.311	1.331	0.370	2.839
8S_I_13_H4.0_CDM1.0_RM1.0	4.334	1.334	1.361	0.362	2.909
8S_I_13_H4.0_CDM1.0_RM1.5	4.595	1.503	1.455	0.362	2.922
8S_I_13_H5.0_CDM0.8_RM1.0	3.825	1.057	1.278	0.453	3.245
8S_I_13_H5.0_CDM0.8_RM1.5	3.947	1.225	1.348	0.438	3.156
8S_I_13_H5.0_CDM1.0_RM1.0	3.960	1.266	1.360	0.438	3.321
8S_I_13_H5.0_CDM1.0_RM1.5	4.145	1.378	1.357	0.414	3.155
8S_I_13_wo_1_H3.0_CDM0.8_RM1.0	5.690	1.000	4.116	0.362	2.756
8S_I_13_wo_1_H3.0_CDM0.8_RM1.5	3.093	1.000	2.232	0.317	2.438
8S_I_13_wo_1_H3.0_CDM1.0_RM1.0	3.173	1.000	2.039	0.317	2.591
8S_I_13_wo_1_H3.0_CDM1.0_RM1.5	3.593	1.117	1.786	0.325	2.668
8S_I_13_wo_1_H4.0_CDM0.8_RM1.0	16.719	1.000	4.052	0.366	2.515

8S_I_13_wo_1_H4.0_CDM0.8_RM1.5	4.864	1.000	3.469	0.445	3.116
8S_I_13_wo_1_H4.0_CDM1.0_RM1.0	3.542	1.000	2.448	0.363	2.771
8S_I_13_wo_1_H4.0_CDM1.0_RM1.5	2.899	1.000	2.129	0.363	2.793
8S_I_13_wo_1_H5.0_CDM0.8_RM1.0	33.625	1.000	3.522	0.468	2.855
8S_I_13_wo_1_H5.0_CDM0.8_RM1.5	11.622	1.000	3.374	0.498	3.110
8S_I_13_wo_1_H5.0_CDM1.0_RM1.0	9.125	1.000	3.315	0.551	3.885
8S_I_13_wo_1_H5.0_CDM1.0_RM1.5	3.850	1.000	2.322	0.414	2.950
8S_I_14_H3.0_CDM0.8_RM1.0	4.214	1.712	1.433	0.340	2.437
8S_I_14_H3.0_CDM0.8_RM1.5	4.340	1.794	1.459	0.332	2.397
8S_I_14_H3.0_CDM1.0_RM1.0	4.476	1.862	1.508	0.325	2.428
8S_I_14_H3.0_CDM1.0_RM1.5	4.590	2.059	1.559	0.325	2.438
8S_I_14_H4.0_CDM0.8_RM1.0	4.077	1.693	1.483	0.393	2.655
8S_I_14_H4.0_CDM0.8_RM1.5	4.179	1.878	1.518	0.393	2.674
8S_I_14_H4.0_CDM1.0_RM1.0	4.325	1.735	1.477	0.385	2.751
8S_I_14_H4.0_CDM1.0_RM1.5	4.530	1.869	1.472	0.378	2.711
8S_I_14_H5.0_CDM0.8_RM1.0	3.868	1.399	1.581	0.453	2.855
8S_I_14_H5.0_CDM0.8_RM1.5	4.023	1.624	1.528	0.445	2.830
8S_I_14_H5.0_CDM1.0_RM1.0	4.083	1.585	1.466	0.453	3.049
8S_I_14_H5.0_CDM1.0_RM1.5	4.278	1.831	1.525	0.438	2.963
8S_I_14_wo_1_H3.0_CDM0.8_RM1.0	2.758	1.000	2.580	0.348	2.366
8S_I_14_wo_1_H3.0_CDM0.8_RM1.5	3.020	1.000	1.971	0.348	2.391
8S_I_14_wo_1_H3.0_CDM1.0_RM1.0	3.161	1.000	1.828	0.347	2.532
8S_I_14_wo_1_H3.0_CDM1.0_RM1.5	3.557	1.168	1.661	0.363	2.657
8S_I_14_wo_1_H4.0_CDM0.8_RM1.0	8.199	1.000	3.769	0.295	1.830
8S_I_14_wo_1_H4.0_CDM0.8_RM1.5	3.226	1.000	2.503	0.400	2.523
8S_I_14_wo_1_H4.0_CDM1.0_RM1.0	3.149	1.000	2.354	0.400	2.747
8S_I_14_wo_1_H4.0_CDM1.0_RM1.5	2.853	1.000	1.926	0.415	2.873
8S_I_14_wo_1_H5.0_CDM0.8_RM1.0	16.628	1.000	3.412	0.348	1.932
8S_I_14_wo_1_H5.0_CDM0.8_RM1.5	5.480	1.000	3.110	0.385	2.188
8S_I_14_wo_1_H5.0_CDM1.0_RM1.0	4.489	1.000	3.014	0.461	2.936
8S_I_14_wo_1_H5.0_CDM1.0_RM1.5	3.502	1.000	2.240	0.461	2.966
8S_I_23_H3.0_CDM0.8_RM1.0	4.969	1.194	1.311	0.317	3.491
8S_I_23_H3.0_CDM0.8_RM1.5	4.806	1.303	1.333	0.302	3.336
8S_I_23_H3.0_CDM1.0_RM1.0	4.822	1.390	1.376	0.295	3.331
8S_I_23_H3.0_CDM1.0_RM1.5	4.825	1.576	1.427	0.287	3.254
8S_I_23_H4.0_CDM0.8_RM1.0	4.421	1.160	1.301	0.384	4.049
8S_I_23_H4.0_CDM0.8_RM1.5	4.747	1.216	1.291	0.362	3.840
8S_I_23_H4.0_CDM1.0_RM1.0	5.309	1.271	1.356	0.362	3.952
8S_I_23_H4.0_CDM1.0_RM1.5	5.519	1.431	1.476	0.362	3.963
8S_I_23_H5.0_CDM0.8_RM1.0	4.128	1.090	1.262	0.445	4.412
8S_I_23_H5.0_CDM0.8_RM1.5	4.199	1.196	1.356	0.438	4.355
8S_I_23_H5.0_CDM1.0_RM1.0	4.235	1.196	1.330	0.415	4.269
8S_I_23_H5.0_CDM1.0_RM1.5	4.390	1.329	1.364	0.408	3.665

8S_I_23_wo_1_H3.0_CDM0.8_RM1.0	4.543	1.000	3.955	0.249	2.516
8S_I_23_wo_1_H3.0_CDM0.8_RM1.5	2.971	1.000	2.404	0.302	3.085
8S_I_23_wo_1_H3.0_CDM1.0_RM1.0	3.076	1.000	2.238	0.295	3.201
8S_I_23_wo_1_H3.0_CDM1.0_RM1.5	3.357	1.019	2.001	0.317	3.465
8S_I_23_wo_1_H4.0_CDM0.8_RM1.0	13.407	1.000	3.975	0.265	2.352
8S_I_23_wo_1_H4.0_CDM0.8_RM1.5	4.337	1.000	3.425	0.317	2.878
8S_I_23_wo_1_H4.0_CDM1.0_RM1.0	3.851	1.000	2.777	0.384	3.861
8S_I_23_wo_1_H4.0_CDM1.0_RM1.5	14.343	1.000	2.948	0.662	8.472
8S_I_23_wo_1_H5.0_CDM0.8_RM1.0	38.585	1.000	3.531	0.496	4.296
8S_I_23_wo_1_H5.0_CDM0.8_RM1.5	9.351	1.041	3.320	0.526	4.708
8S_I_23_wo_1_H5.0_CDM1.0_RM1.0	7.606	1.000	3.269	0.415	3.776
8S_I_23_wo_1_H5.0_CDM1.0_RM1.5	4.749	1.000	2.595	0.476	4.382
8S_I_24_H3.0_CDM0.8_RM1.0	4.261	1.435	1.397	0.325	2.949
8S_I_24_H3.0_CDM0.8_RM1.5	4.350	1.576	1.439	0.317	2.893
8S_I_24_H3.0_CDM1.0_RM1.0	4.455	1.640	1.481	0.310	2.913
8S_I_24_H3.0_CDM1.0_RM1.5	4.522	1.818	1.517	0.302	2.851
8S_I_24_H4.0_CDM0.8_RM1.0	4.121	1.396	1.420	0.393	3.395
8S_I_24_H4.0_CDM0.8_RM1.5	4.269	1.512	1.404	0.384	3.333
8S_I_24_H4.0_CDM1.0_RM1.0	4.386	1.474	1.392	0.369	3.318
8S_I_24_H4.0_CDM1.0_RM1.5	4.566	1.670	1.472	0.362	3.275
8S_I_24_H5.0_CDM0.8_RM1.0	3.996	1.285	1.431	0.461	3.741
8S_I_24_H5.0_CDM0.8_RM1.5	4.110	1.513	1.431	0.445	3.637
8S_I_24_H5.0_CDM1.0_RM1.0	4.180	1.389	1.422	0.445	3.788
8S_I_24_H5.0_CDM1.0_RM1.5	4.422	1.554	1.441	0.438	3.740
8S_I_24_wo_1_H3.0_CDM0.8_RM1.0	3.292	1.000	2.940	0.363	3.064
8S_I_24_wo_1_H3.0_CDM0.8_RM1.5	2.861	1.000	2.308	0.332	2.839
8S_I_24_wo_1_H3.0_CDM1.0_RM1.0	2.949	1.000	2.164	0.332	3.019
8S_I_24_wo_1_H3.0_CDM1.0_RM1.5	3.333	1.092	1.847	0.363	3.310
8S_I_24_wo_1_H4.0_CDM0.8_RM1.0	13.483	1.000	3.998	0.369	2.803
8S_I_24_wo_1_H4.0_CDM0.8_RM1.5	3.700	1.000	2.741	0.415	3.213
8S_I_24_wo_1_H4.0_CDM1.0_RM1.0	3.341	1.000	2.480	0.372	3.153
8S_I_24_wo_1_H4.0_CDM1.0_RM1.5	2.860	1.000	2.169	0.384	3.282
8S_I_24_wo_1_H5.0_CDM0.8_RM1.0	28.519	1.000	3.505	0.468	3.120
8S_I_24_wo_1_H5.0_CDM0.8_RM1.5	8.935	1.000	3.310	0.498	3.404
8S_I_24_wo_1_H5.0_CDM1.0_RM1.0	6.796	1.000	3.228	0.551	4.293
8S_I_24_wo_1_H5.0_CDM1.0_RM1.5	3.946	1.000	2.354	0.453	3.570
8S_I_34_H3.0_CDM0.8_RM1.0	4.221	1.340	1.419	0.325	3.336
8S_I_34_H3.0_CDM0.8_RM1.5	4.348	1.465	1.456	0.317	3.270
8S_I_34_H3.0_CDM1.0_RM1.0	4.484	1.504	1.491	0.310	3.271
8S_I_34_H3.0_CDM1.0_RM1.5	4.579	1.649	1.529	0.302	3.200
8S_I_34_H4.0_CDM0.8_RM1.0	4.200	1.283	1.433	0.384	3.748
8S_I_34_H4.0_CDM0.8_RM1.5	4.297	1.415	1.496	0.384	3.763
8S_I_34_H4.0_CDM1.0_RM1.0	4.363	1.392	1.449	0.365	3.693

8S_I_34_H4.0_CDM1.0_RM1.5	4.500	1.561	1.515	0.362	3.675
8S_I_34_H5.0_CDM0.8_RM1.0	4.078	1.285	1.424	0.460	4.207
8S_I_34_H5.0_CDM0.8_RM1.5	4.180	1.411	1.411	0.438	4.019
8S_I_34_H5.0_CDM1.0_RM1.0	4.259	1.348	1.436	0.438	4.166
8S_I_34_H5.0_CDM1.0_RM1.5	4.435	1.454	1.530	0.438	4.184
8S_I_34_wo_1_H3.0_CDM0.8_RM1.0	4.181	1.000	3.845	0.332	3.129
8S_I_34_wo_1_H3.0_CDM0.8_RM1.5	2.950	1.000	2.491	0.363	3.451
8S_I_34_wo_1_H3.0_CDM1.0_RM1.0	2.910	1.000	2.225	0.332	3.361
8S_I_34_wo_1_H3.0_CDM1.0_RM1.5	3.235	1.050	2.070	0.350	3.564
8S_I_34_wo_1_H4.0_CDM0.8_RM1.0	13.248	1.000	3.998	0.384	3.235
8S_I_34_wo_1_H4.0_CDM0.8_RM1.5	4.121	1.000	3.373	0.438	3.761
8S_I_34_wo_1_H4.0_CDM1.0_RM1.0	3.637	1.000	2.819	0.483	4.558
8S_I_34_wo_1_H4.0_CDM1.0_RM1.5	3.107	1.000	2.207	0.408	3.879
8S_I_34_wo_1_H5.0_CDM0.8_RM1.0	29.938	1.000	3.511	0.468	3.423
8S_I_34_wo_1_H5.0_CDM0.8_RM1.5	8.571	1.000	3.299	0.483	3.629
8S_I_34_wo_1_H5.0_CDM1.0_RM1.0	6.301	1.000	3.210	0.536	4.611
8S_I_34_wo_1_H5.0_CDM1.0_RM1.5	4.802	1.000	2.623	0.604	5.258
8S_I_1234_H3.0_CDM0.8_RM1.0	3.681	1.228	1.444	0.294	4.771
8S_I_1234_H3.0_CDM0.8_RM1.5	3.781	1.338	1.492	0.287	4.679
8S_I_1234_H3.0_CDM1.0_RM1.0	4.509	1.368	1.499	0.287	4.876
8S_I_1234_H3.0_CDM1.0_RM1.5	5.310	1.523	1.456	0.279	4.767
8S_I_1234_H4.0_CDM0.8_RM1.0	3.828	1.368	1.513	0.362	5.197
8S_I_1234_H4.0_CDM0.8_RM1.5	3.829	1.272	1.404	0.332	4.799
8S_I_1234_H4.0_CDM1.0_RM1.0	3.882	1.305	1.434	0.332	5.039
8S_I_1234_H4.0_CDM1.0_RM1.5	3.966	1.442	1.504	0.325	4.948
8S_I_1234_H5.0_CDM0.8_RM1.0	3.631	1.106	1.267	0.407	5.328
8S_I_1234_H5.0_CDM0.8_RM1.5	3.739	1.120	1.316	0.392	5.142
8S_I_1234_H5.0_CDM1.0_RM1.0	3.790	1.177	1.361	0.392	5.239
8S_I_1234_H5.0_CDM1.0_RM1.5	3.929	1.276	1.437	0.383	5.130
8S_I_1234_wo_1_H3.0_CDM0.8_RM1.0	25.181	1.047	5.125	0.175	2.194
8S_I_1234_wo_1_H3.0_CDM0.8_RM1.5	10.589	1.000	4.806	0.196	2.499
8S_I_1234_wo_1_H3.0_CDM1.0_RM1.0	6.969	1.000	4.606	0.233	3.217
8S_I_1234_wo_1_H3.0_CDM1.0_RM1.5	6.969	1.000	4.606	0.233	3.217
8S_I_1234_wo_1_H4.0_CDM0.8_RM1.0	40.188	1.150	4.206	0.249	2.603
8S_I_1234_wo_1_H4.0_CDM0.8_RM1.5	25.070	1.173	4.125	0.249	2.677
8S_I_1234_wo_1_H4.0_CDM1.0_RM1.0	19.962	1.195	4.097	0.279	3.458
8S_I_1234_wo_1_H4.0_CDM1.0_RM1.5	12.159	1.328	3.825	0.325	4.067
8S_I_1234_wo_1_H5.0_CDM0.8_RM1.0	52.339	1.289	3.561	0.325	2.747
8S_I_1234_wo_1_H5.0_CDM0.8_RM1.5	34.834	1.330	3.523	0.317	2.786
8S_I_1234_wo_1_H5.0_CDM1.0_RM1.0	33.932	1.390	3.524	0.362	3.884
8S_I_1234_wo_1_H5.0_CDM1.0_RM1.5	23.212	3.128	3.420	0.408	4.448

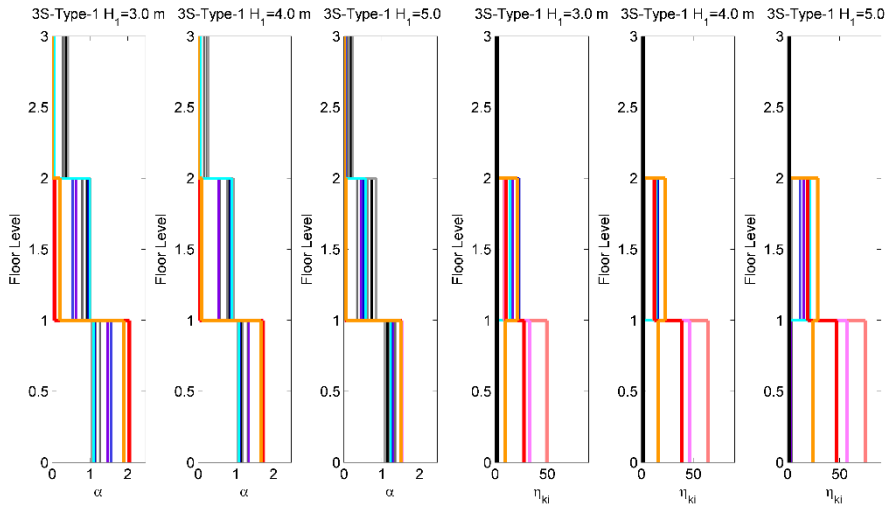
3S-Type-1 H1=3.0 m
3S-Type-1 H1=4.0 m
3S-Type-1 H1=5.0
3S-Type-1 H1=3.0 m
3S-Type-1 H1=4.0 m
3S-Type-1 H1=5.0
Floor Level
α
ηki

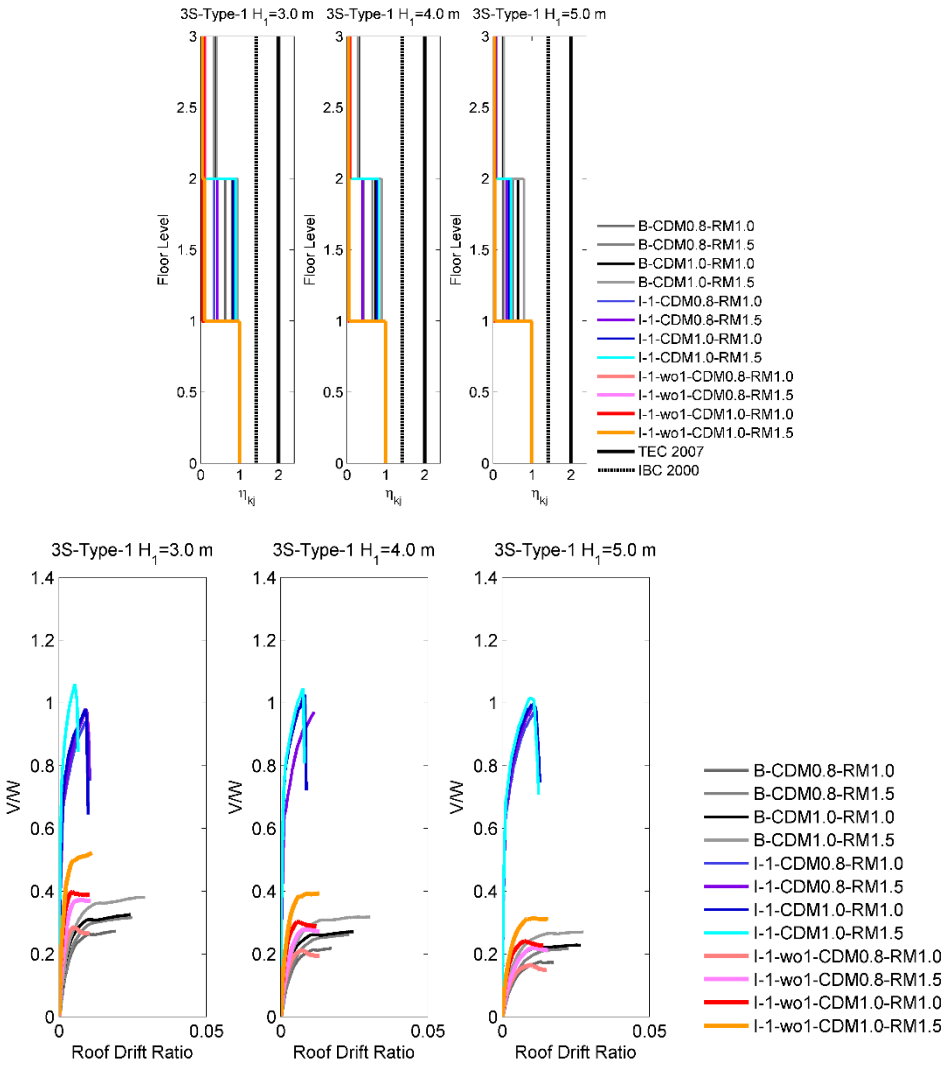

Figure A2-43 3 Story Frame; pushover analysis results at Ultimate Point for Type 1

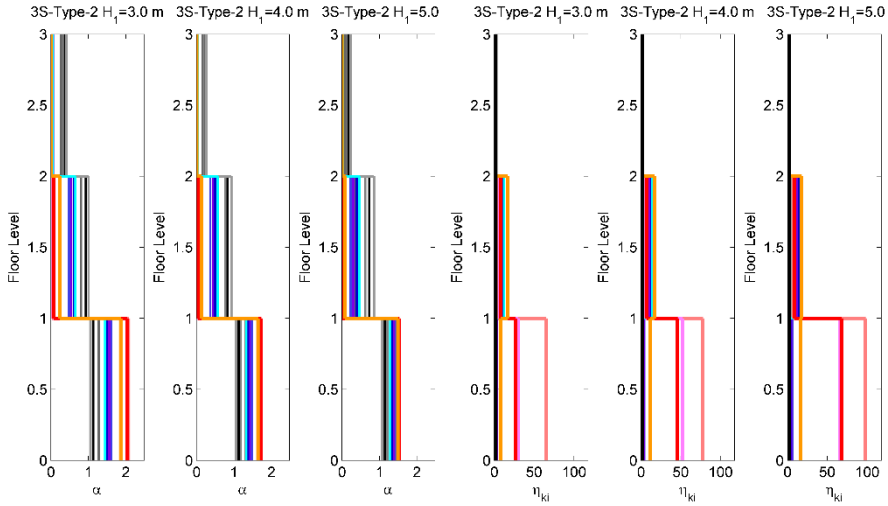

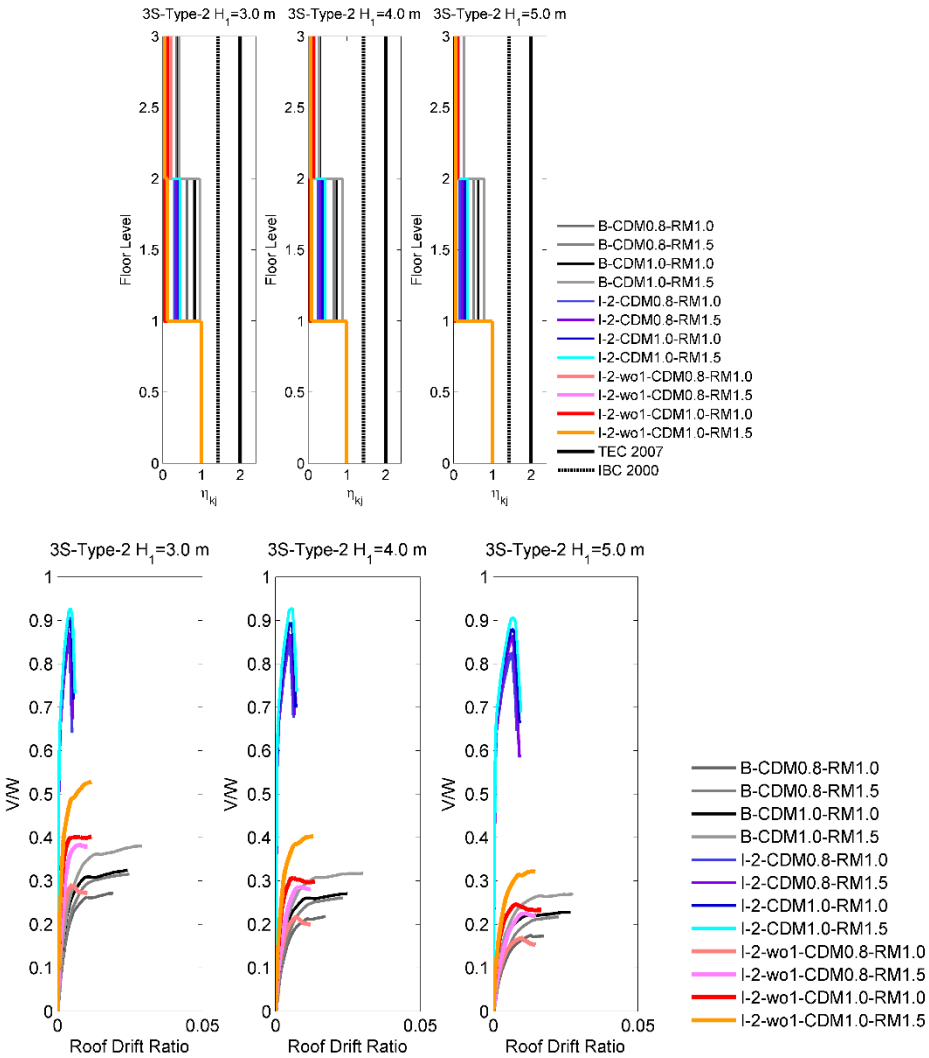

Figure A2-44 3 Story Frame; pushover analysis results at Ultimate Point for Type 2

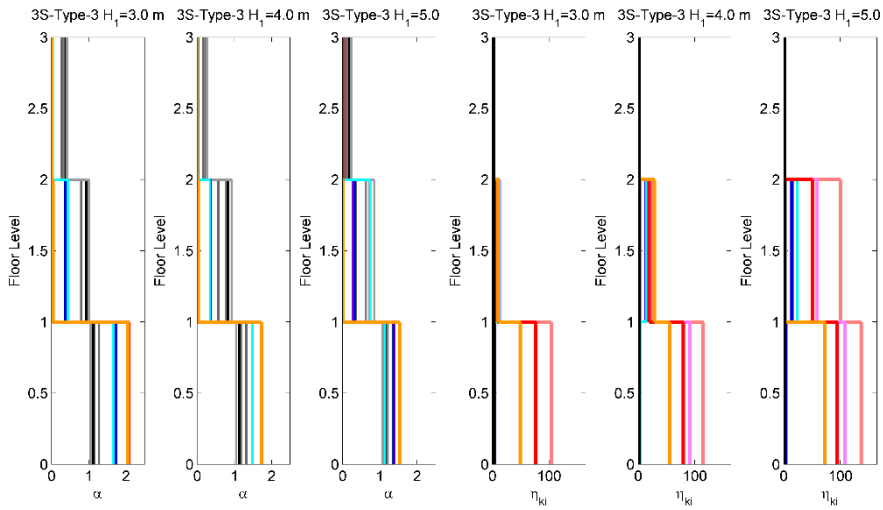

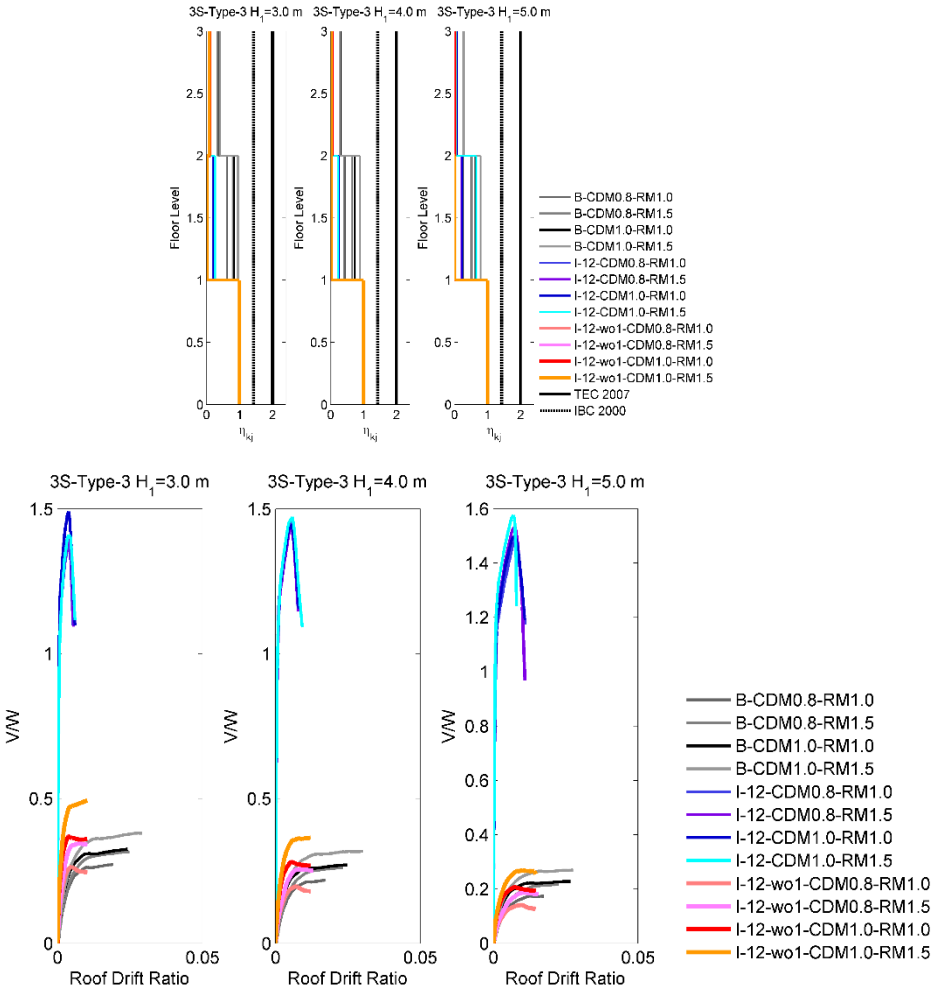

Figure A2-45 3 Story Frame; pushover analysis results for Type 3

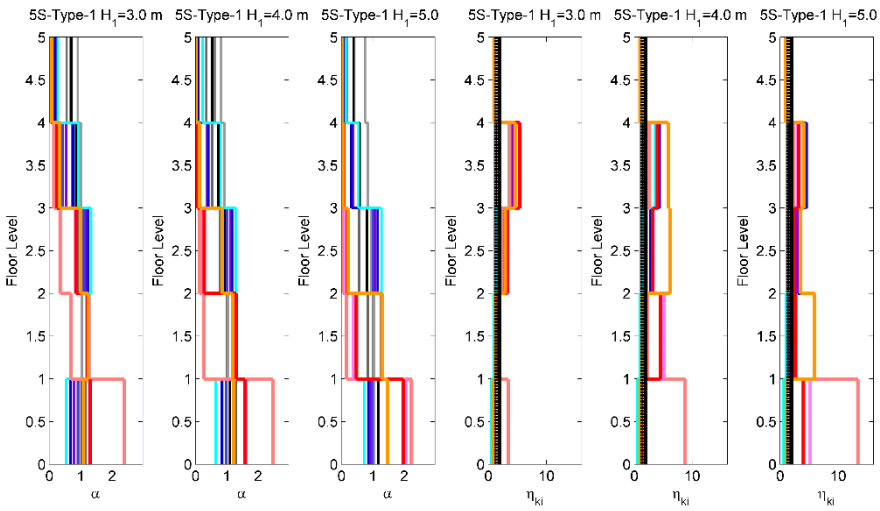

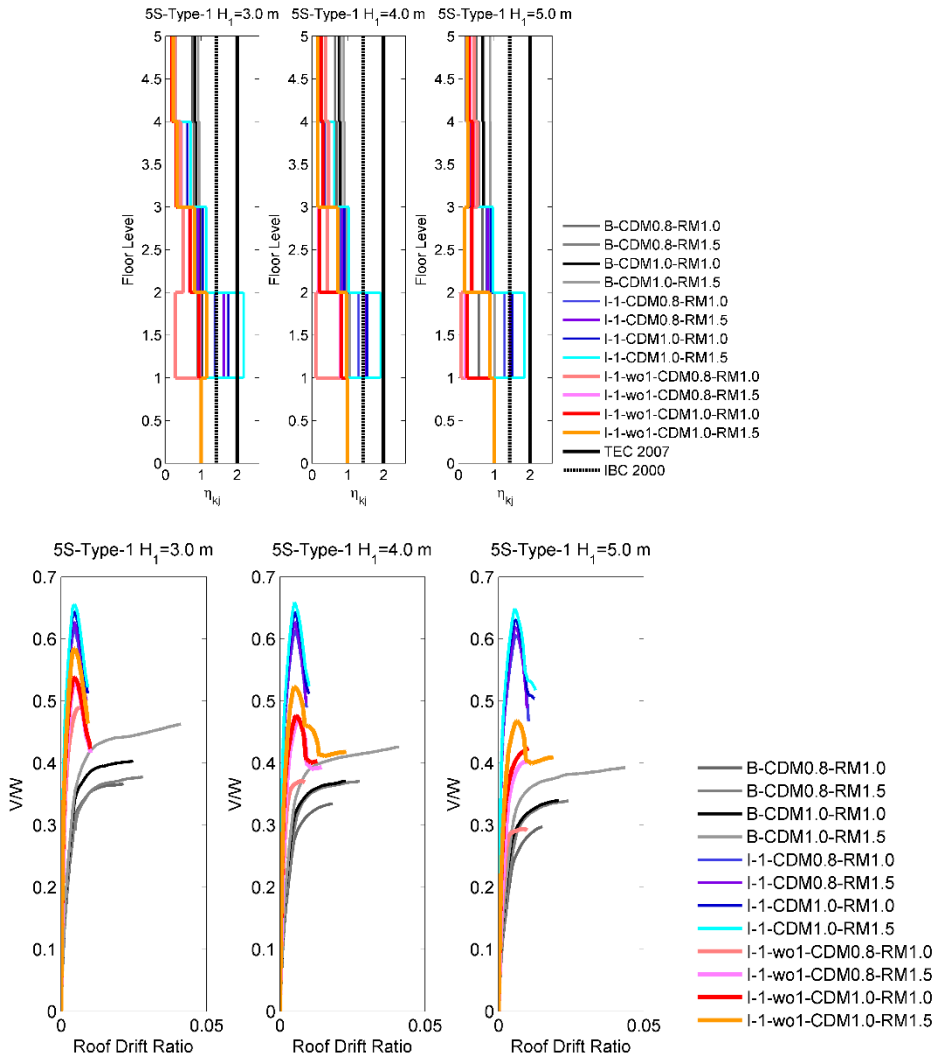

Figure A2-46 5 Story Frame; pushover analysis results at Ultimate Point for Type 1

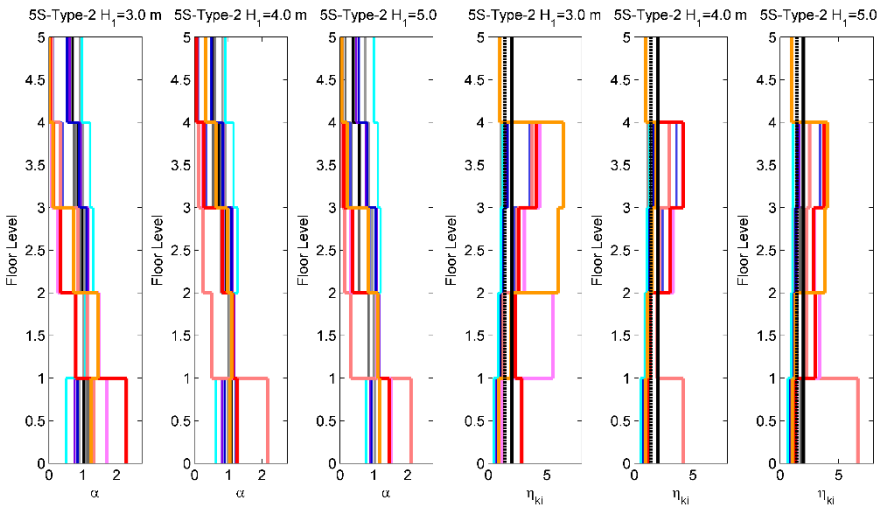

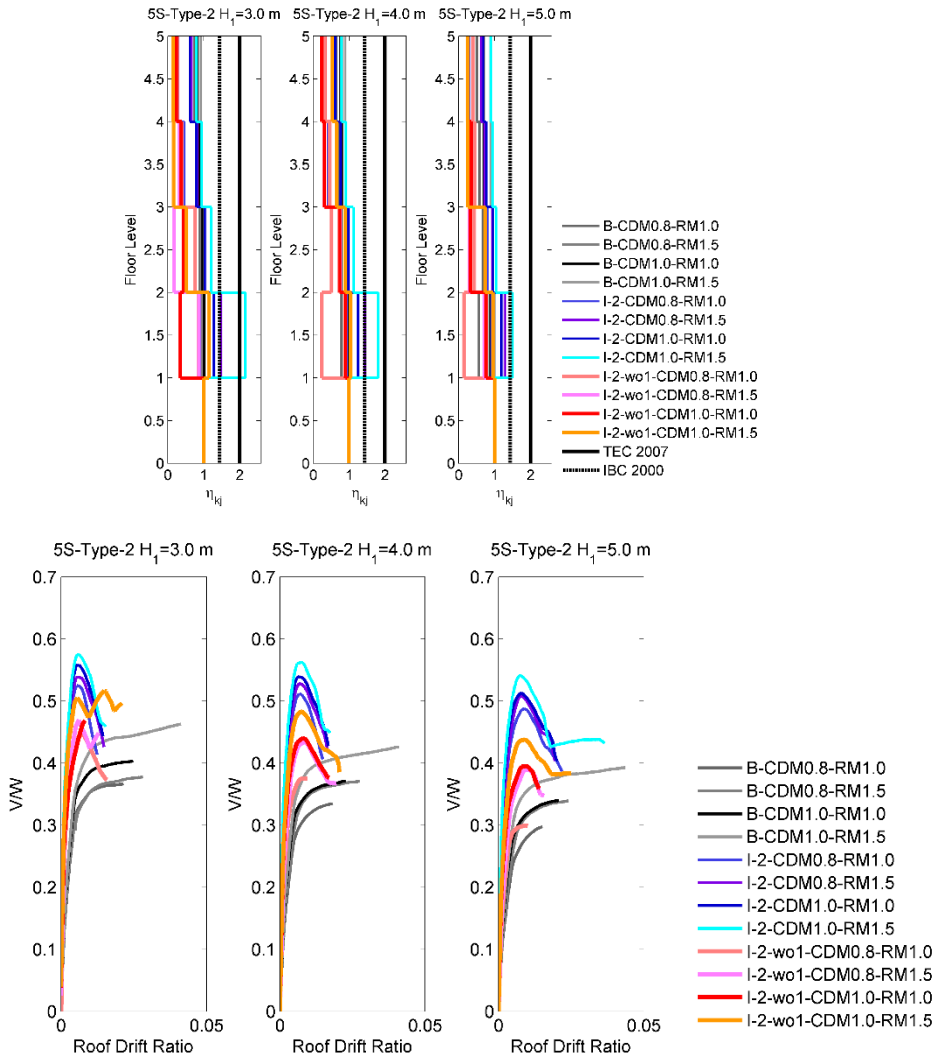

Figure A2-47 5 Story Frame; pushover analysis results for Type 2

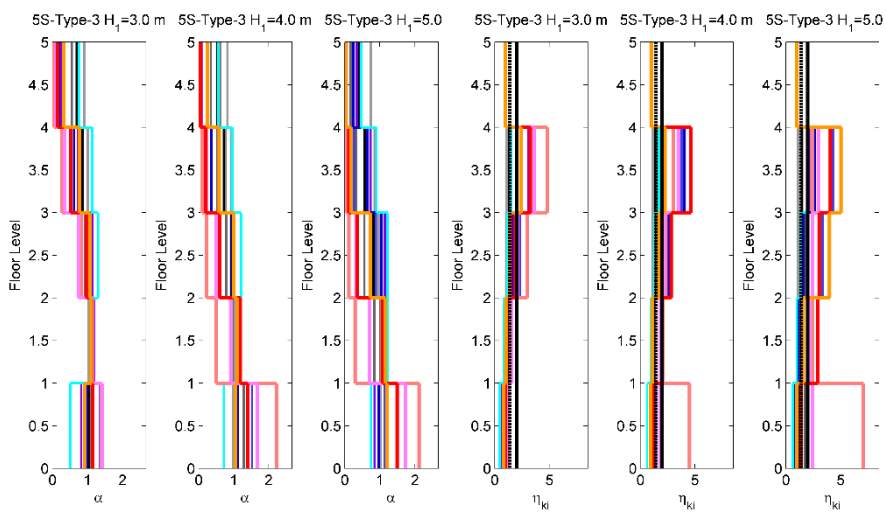

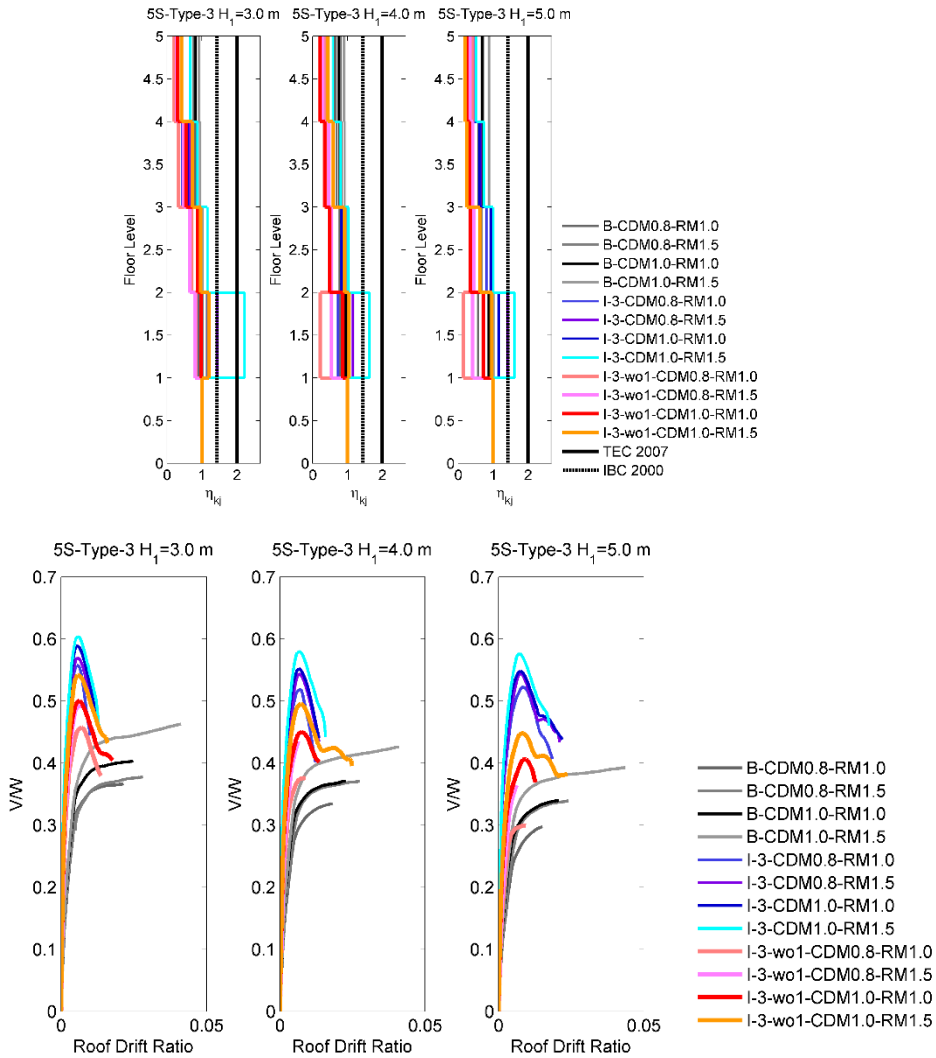

Figure A2-48 5 Story Frame; pushover analysis results at Ultimate Point for Type 3

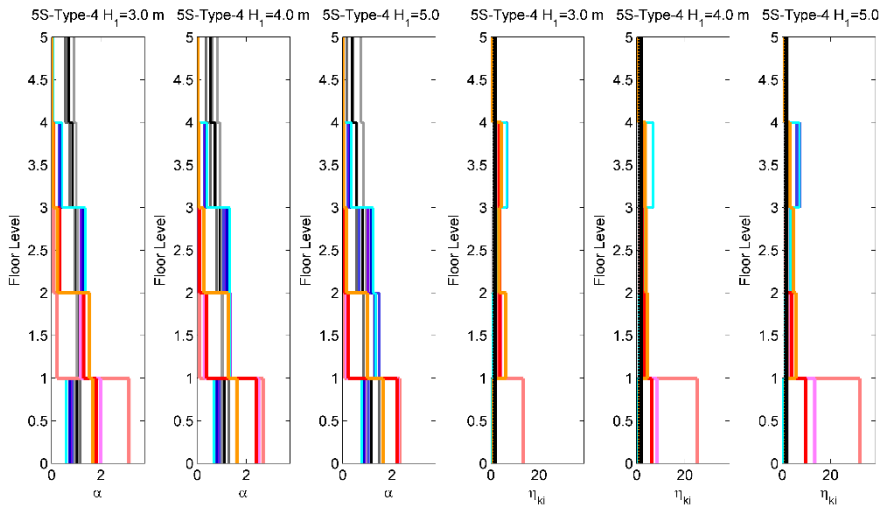

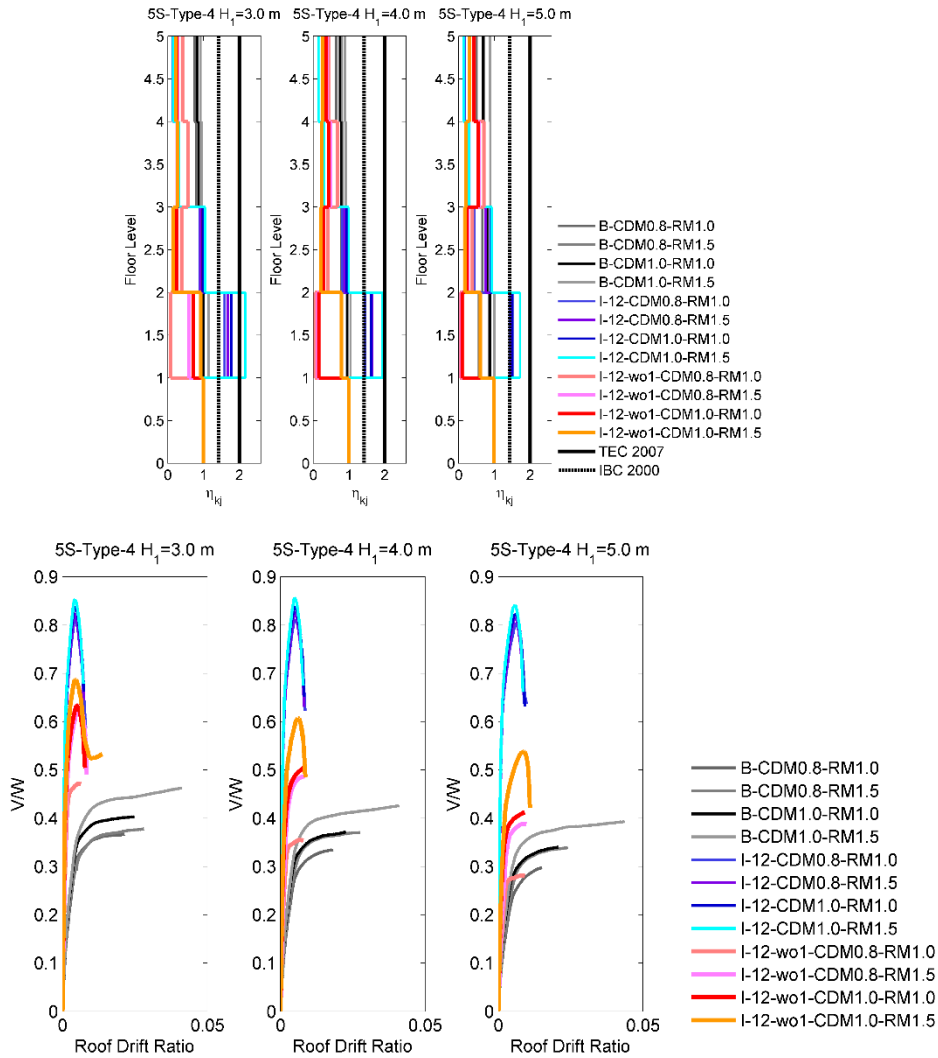

Figure A2-49 5 Story Frame; pushover analysis results at Ultimate Point for Type 4

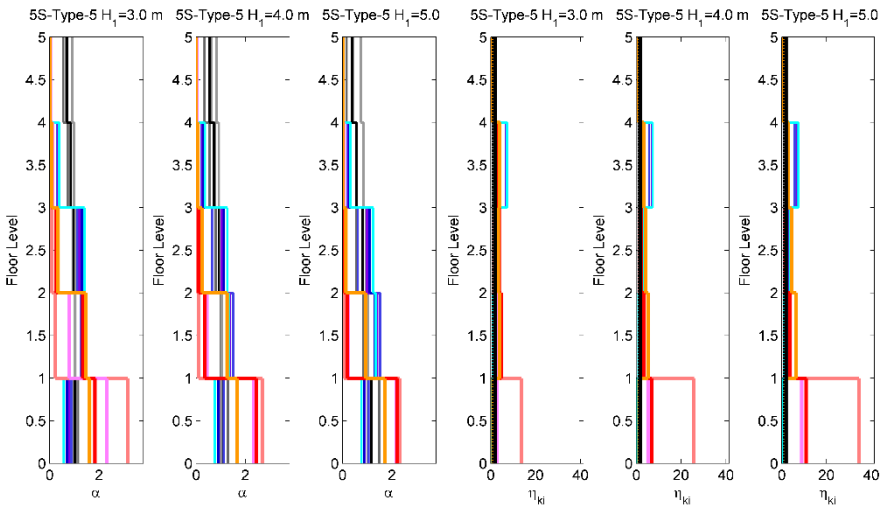

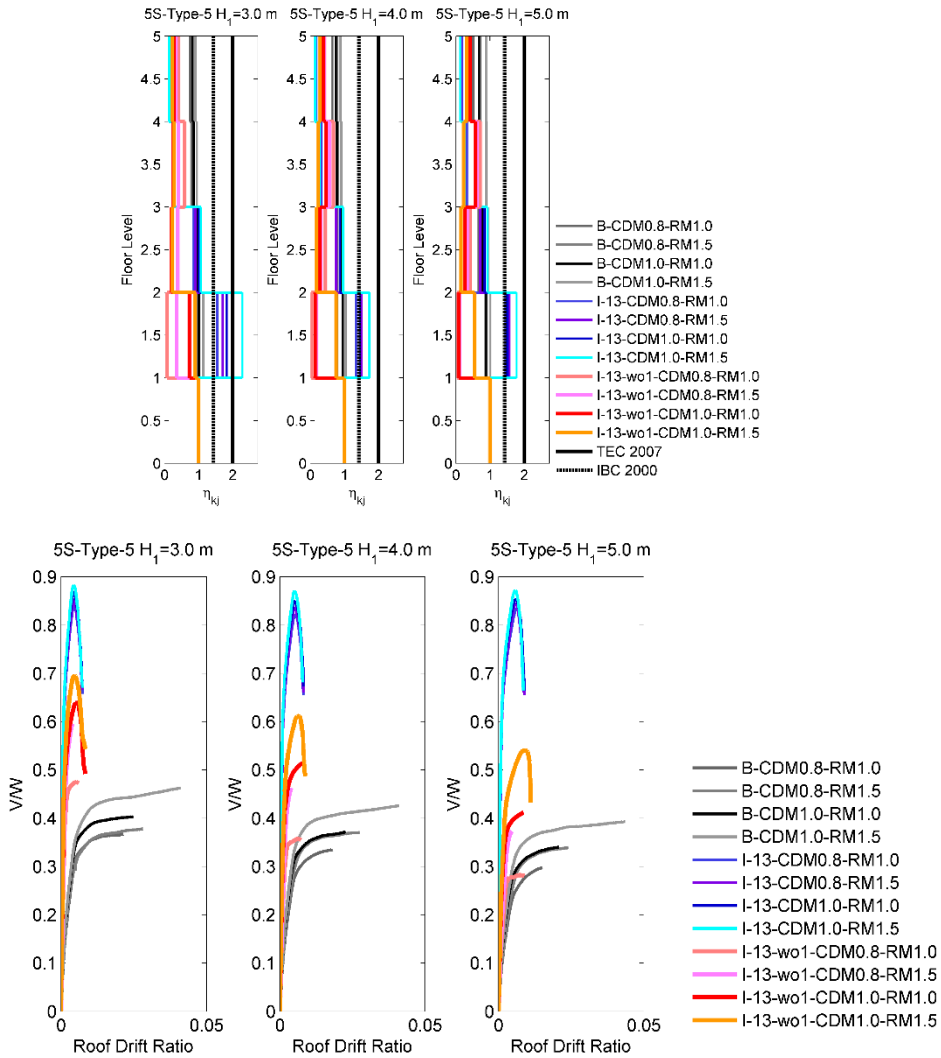

Figure A2-50 5 Story Frame; pushover analysis results at Ultimate Point for Type 5

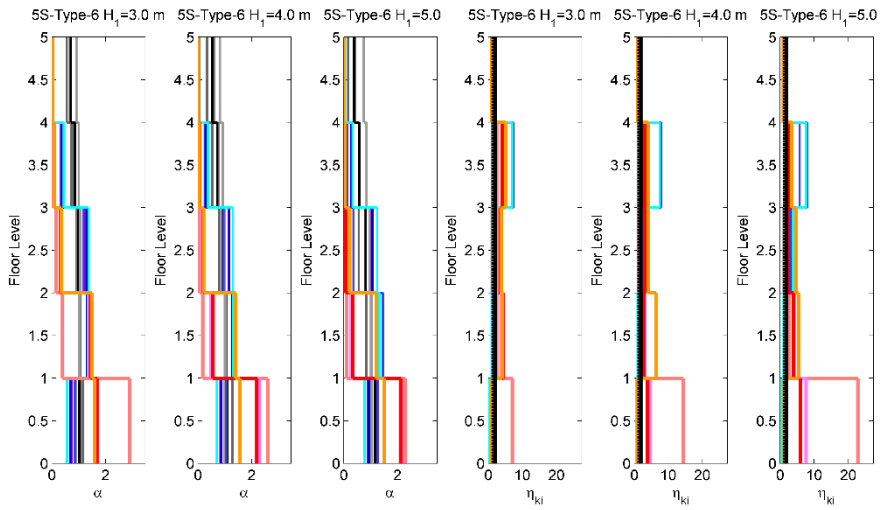

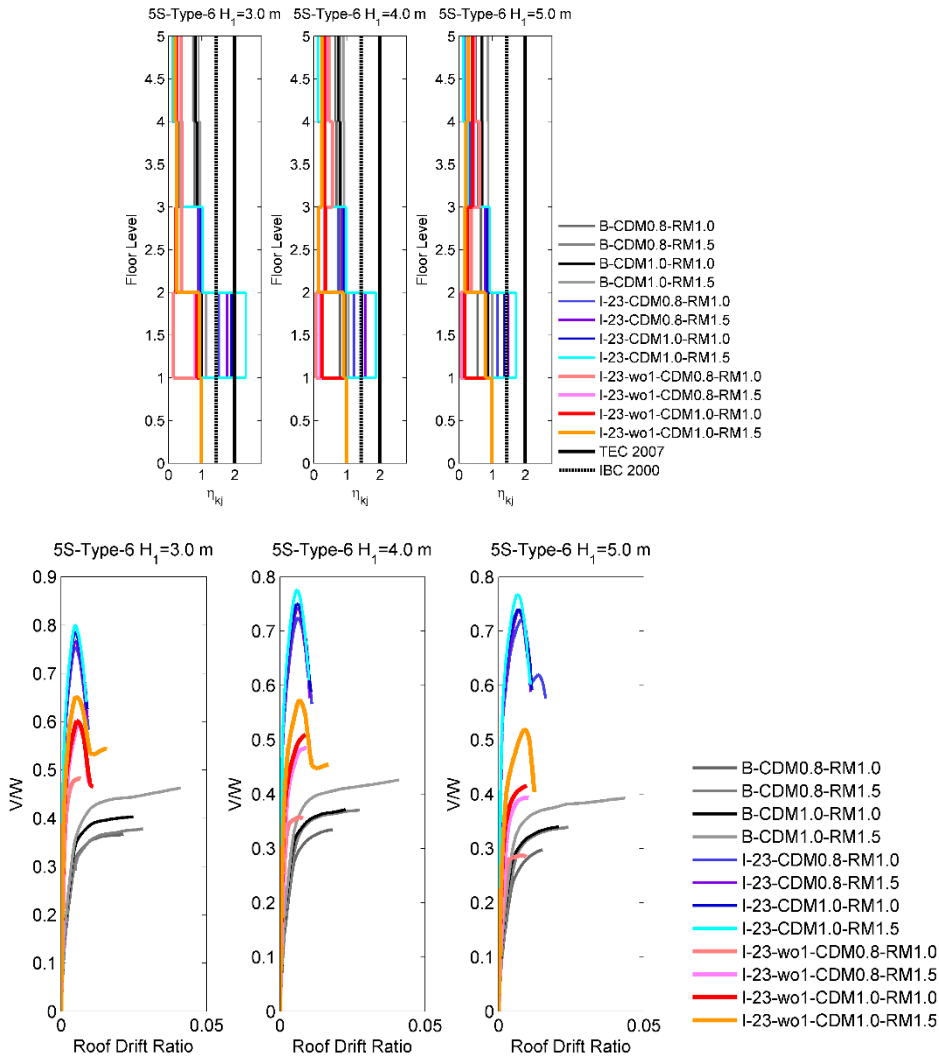

Figure A2-51 5 Story Frame; pushover analysis results at Ultimate Point for Type 6

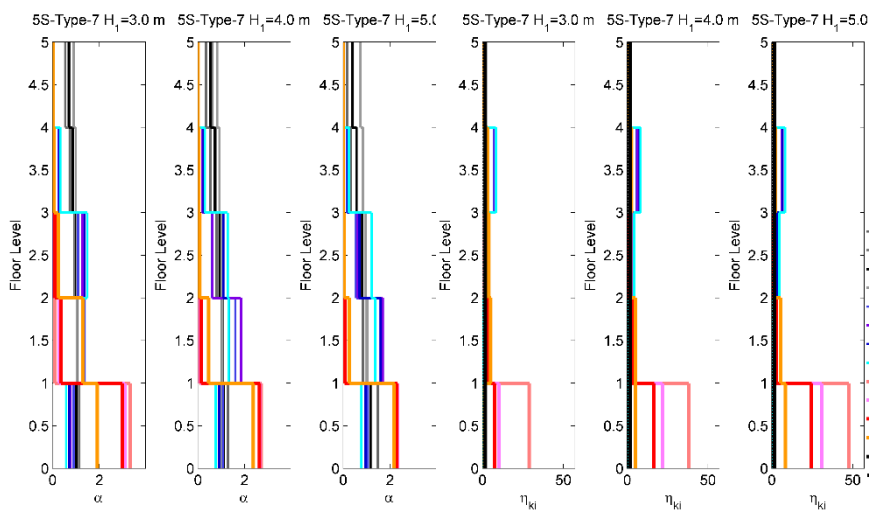

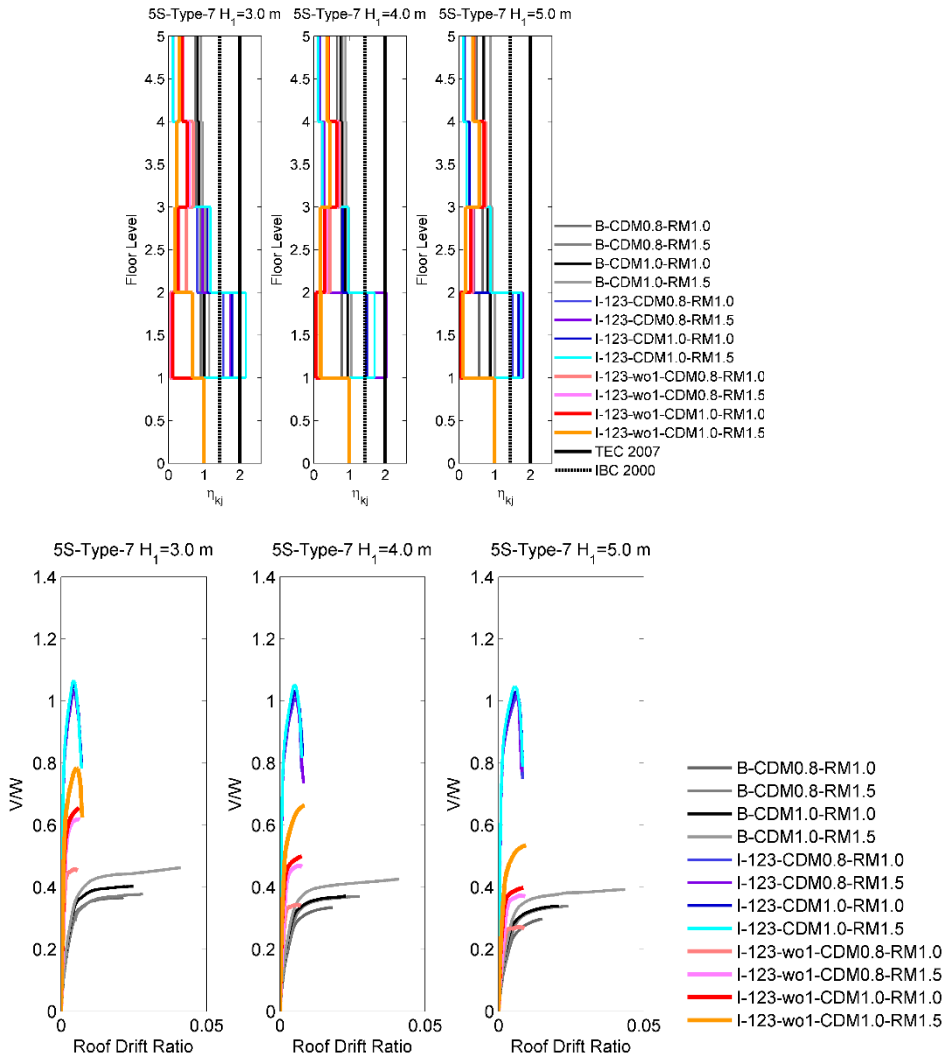

Figure A2-52 5 Story Frame; pushover analysis results at Ultimate Point for Type 7

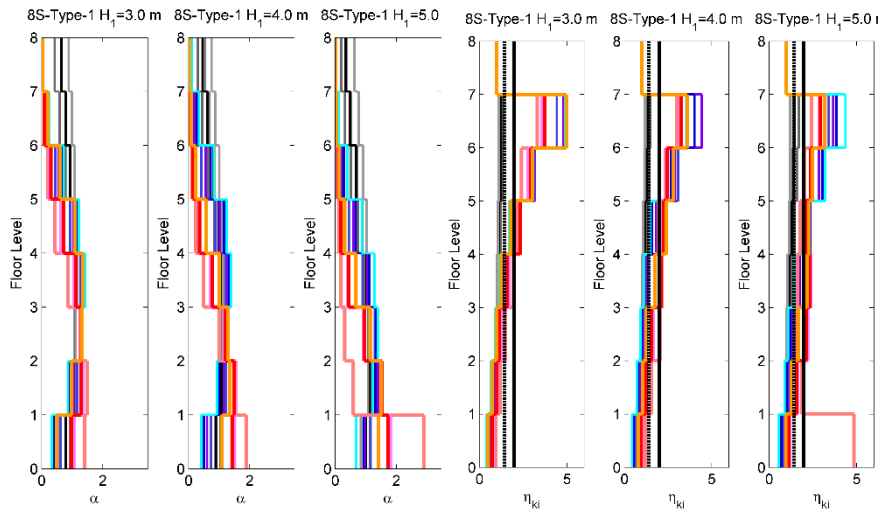

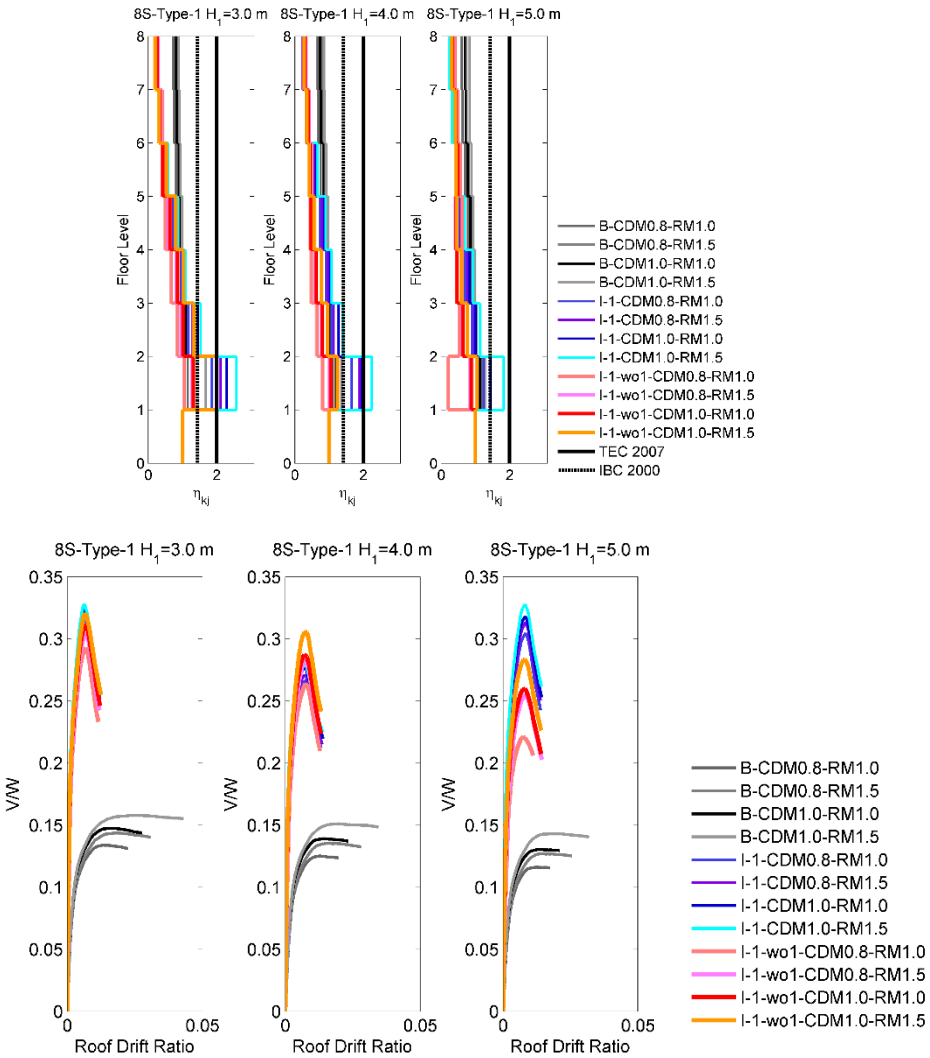

Figure A2-53 8 Story Frame; pushover analysis results at Ultimate Point for Type 1

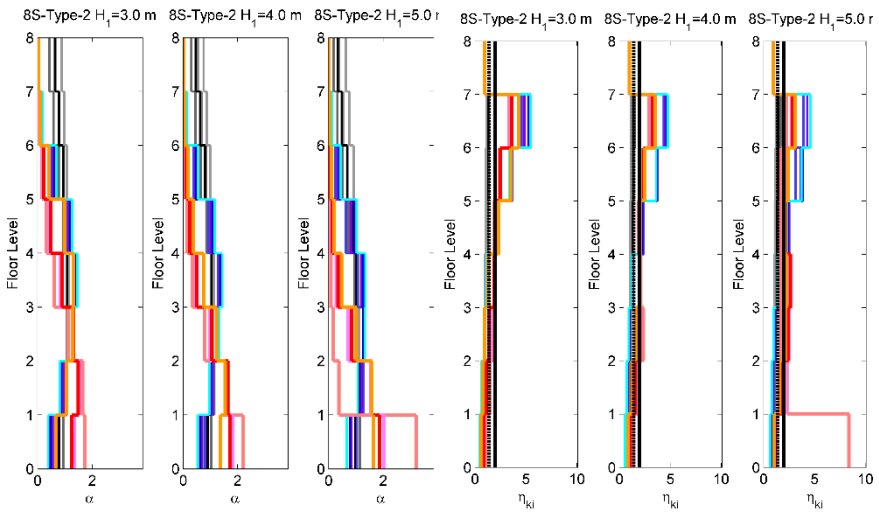

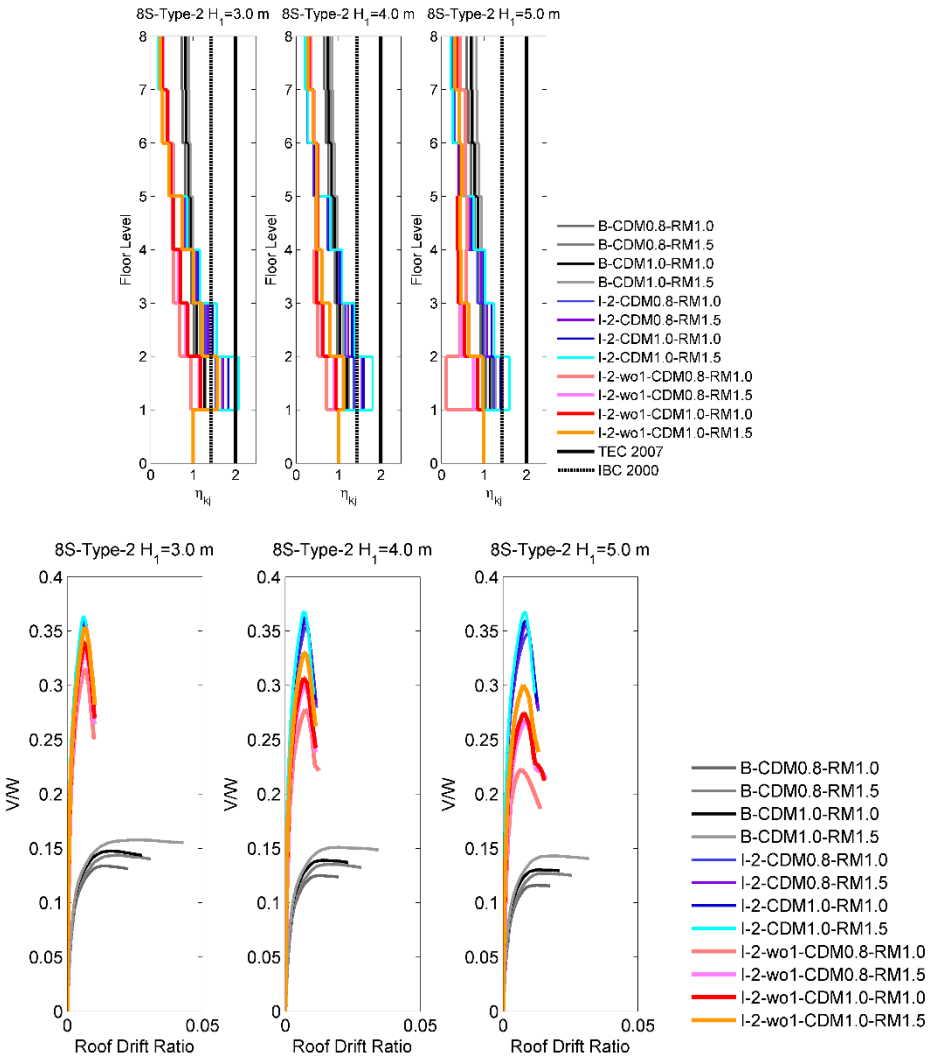

Figure A2-54 8 Story Frame; pushover analysis results at Ultimate Point for Type 2

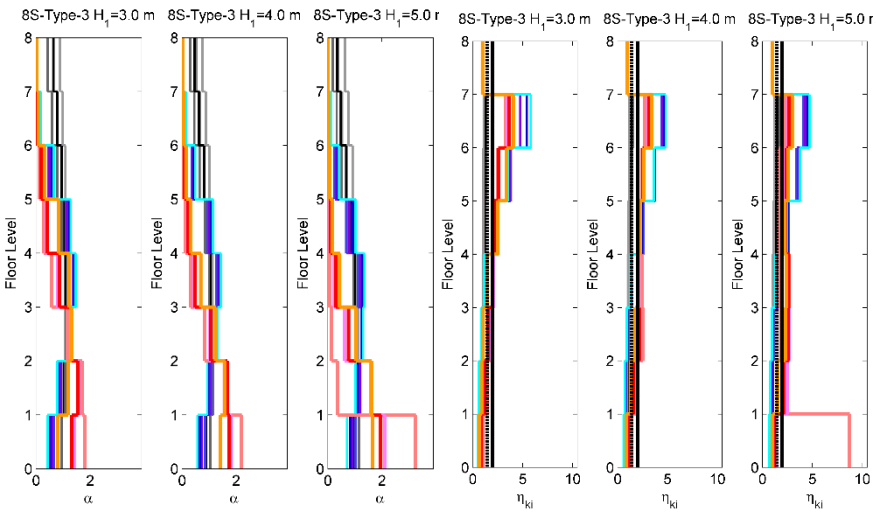

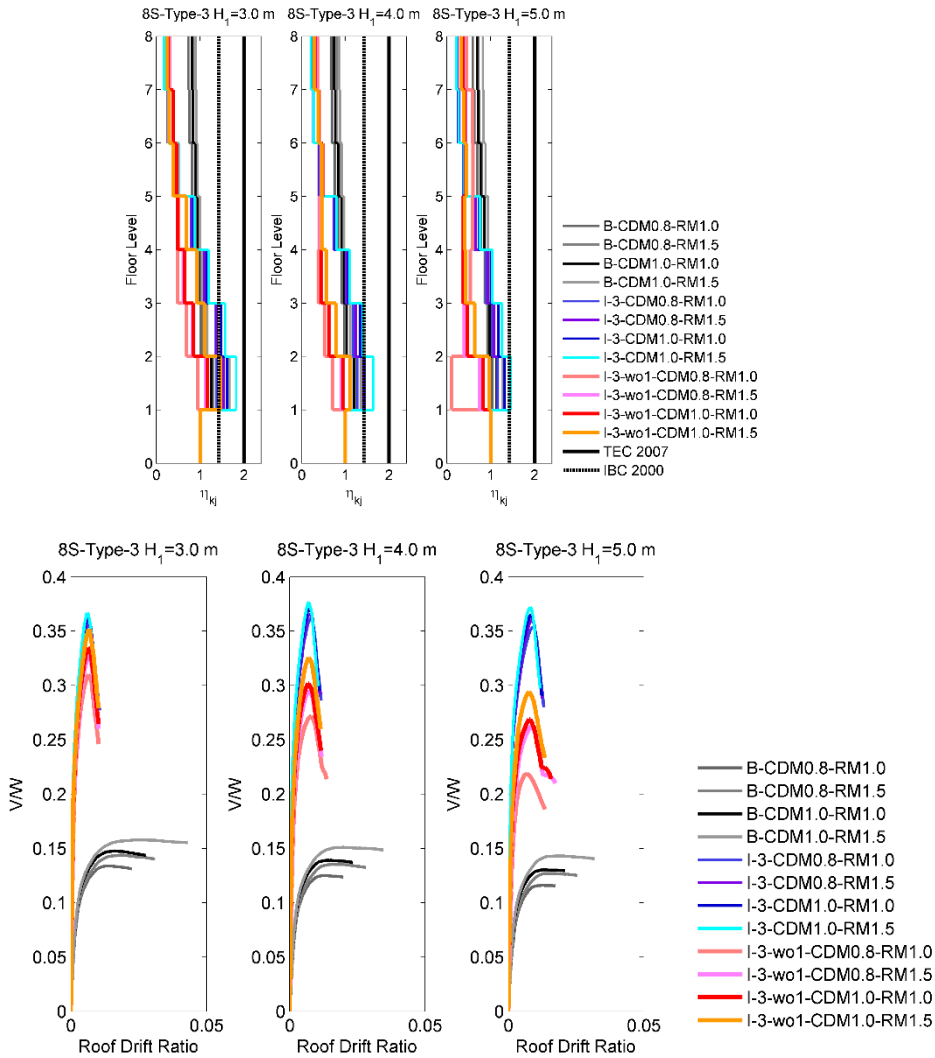

Figure A2-55 8 Story Frame; pushover analysis results at Ultimate Point for Type 3

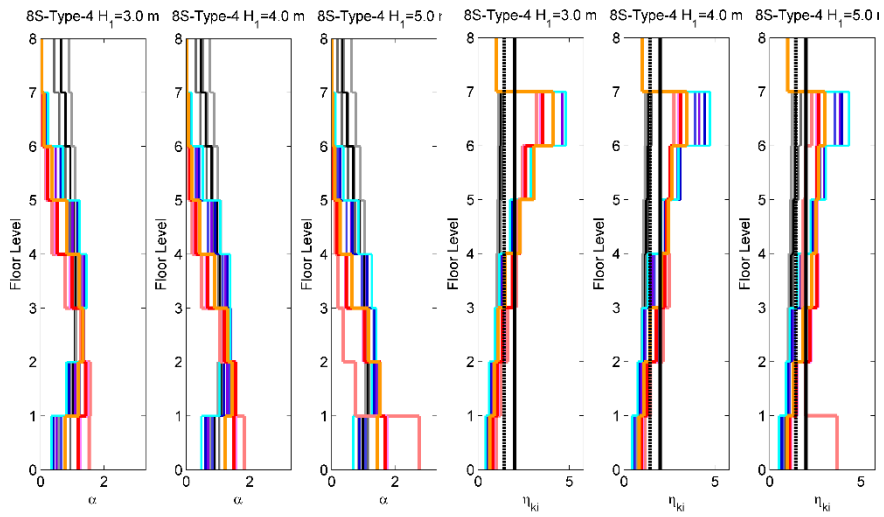

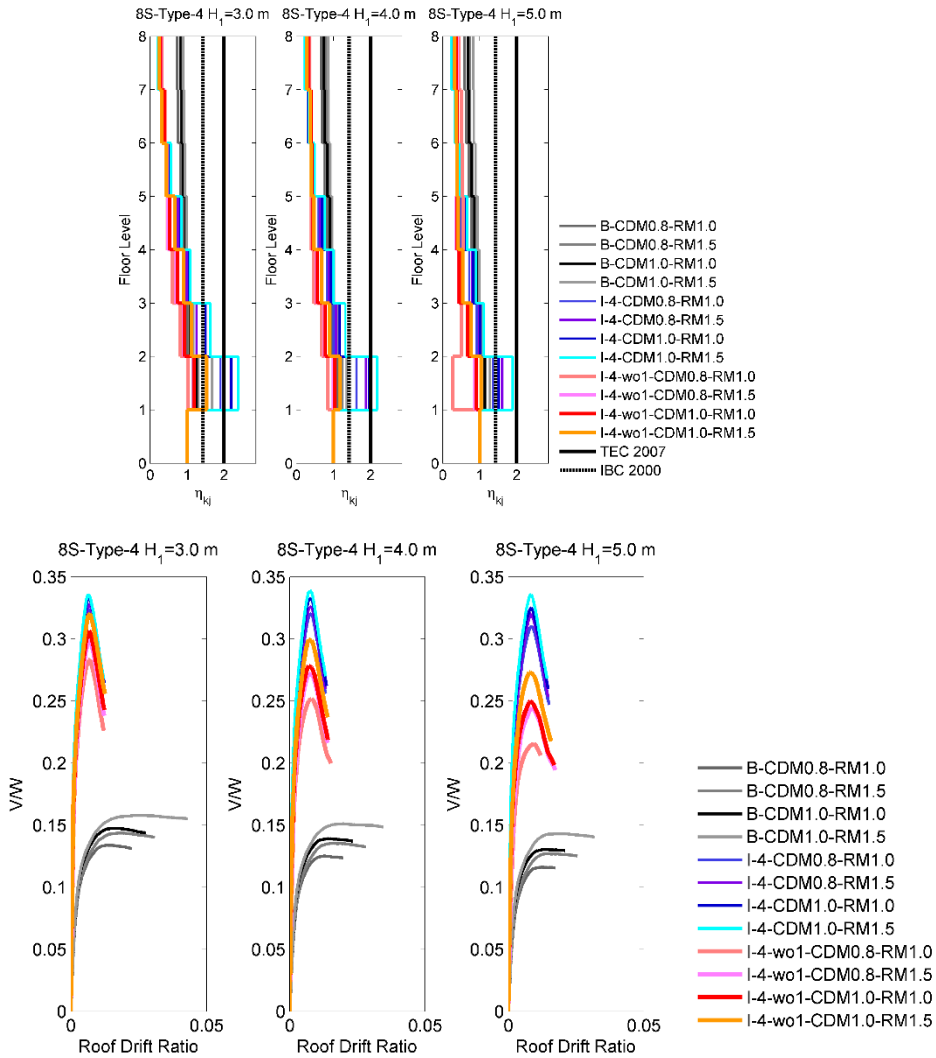

Figure A2-56 8 Story Frame; pushover analysis results at Ultimate Point for Type 4

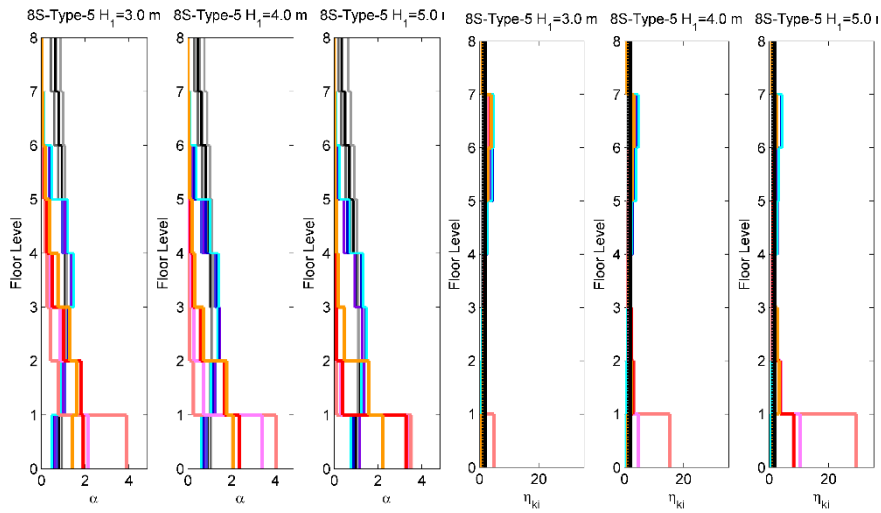

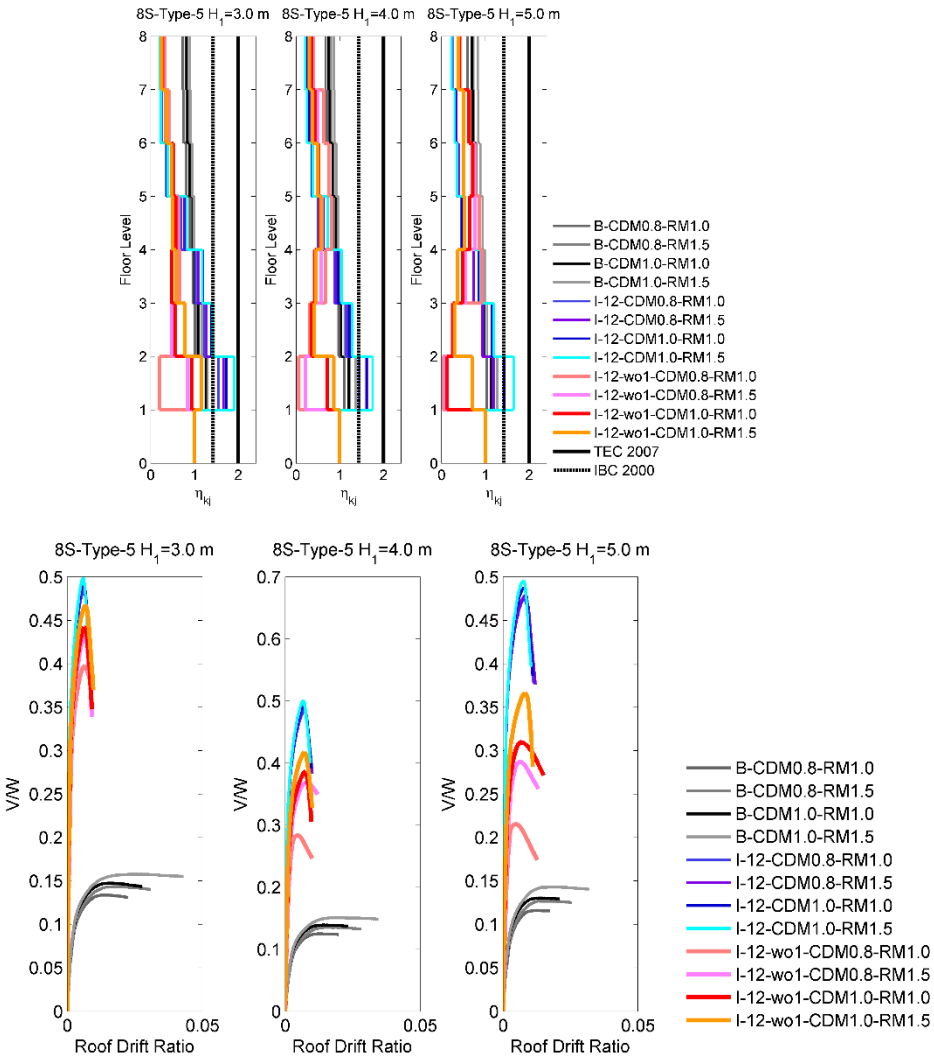

Figure A2-57 8 Story Frame; pushover analysis results at Ultimate Point for Type 5

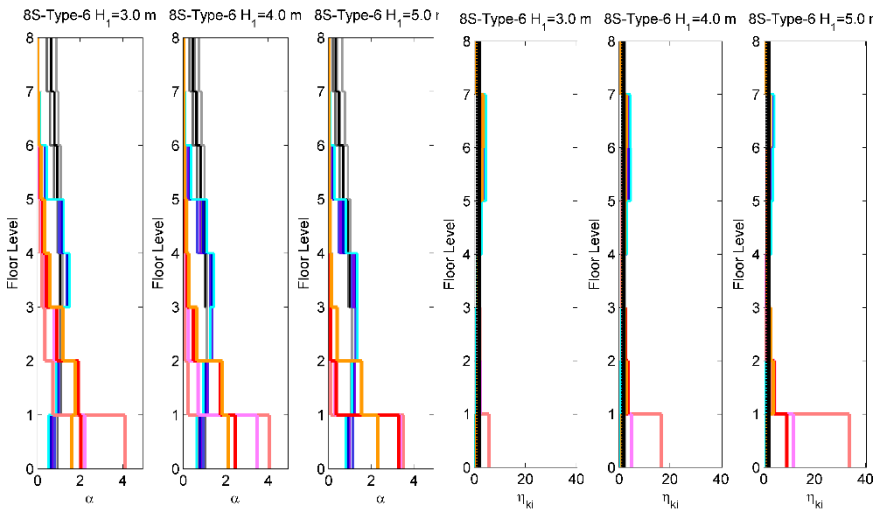

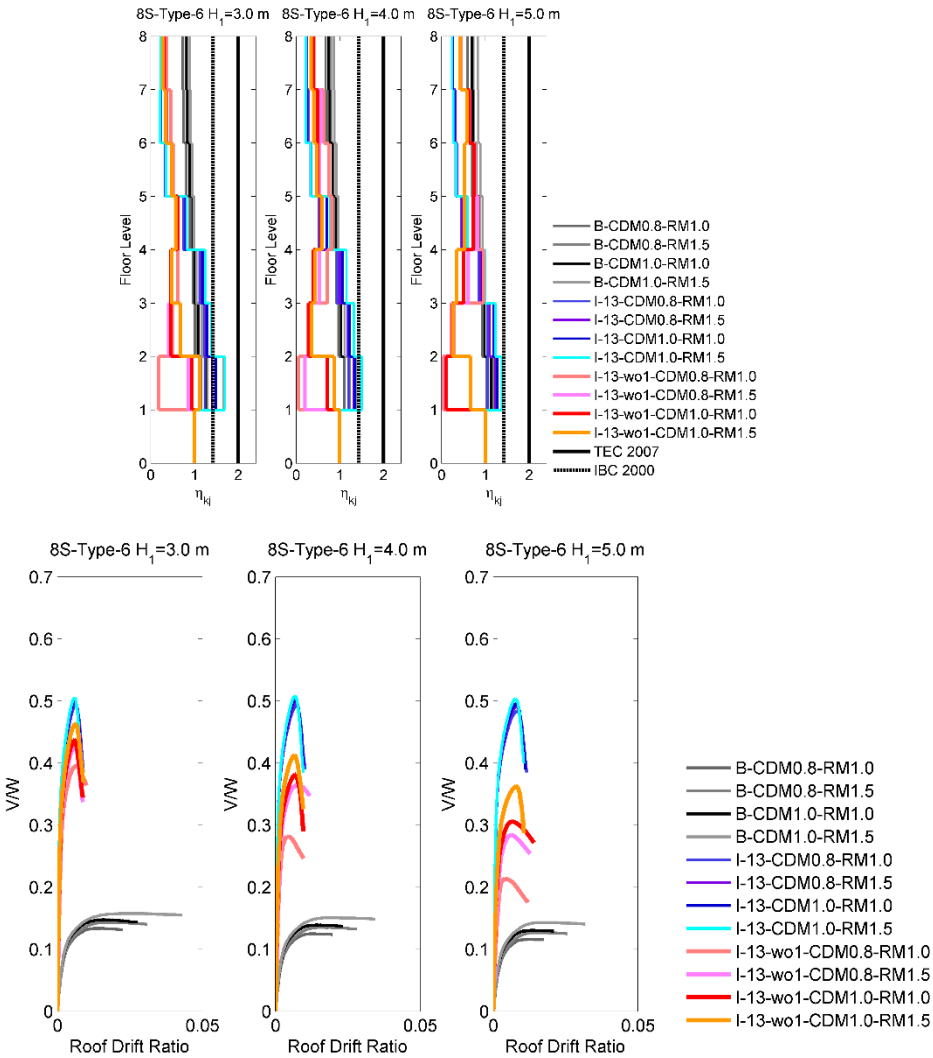

Figure A2-58 8 Story Frame; pushover analysis results at Ultimate Point for Type 6

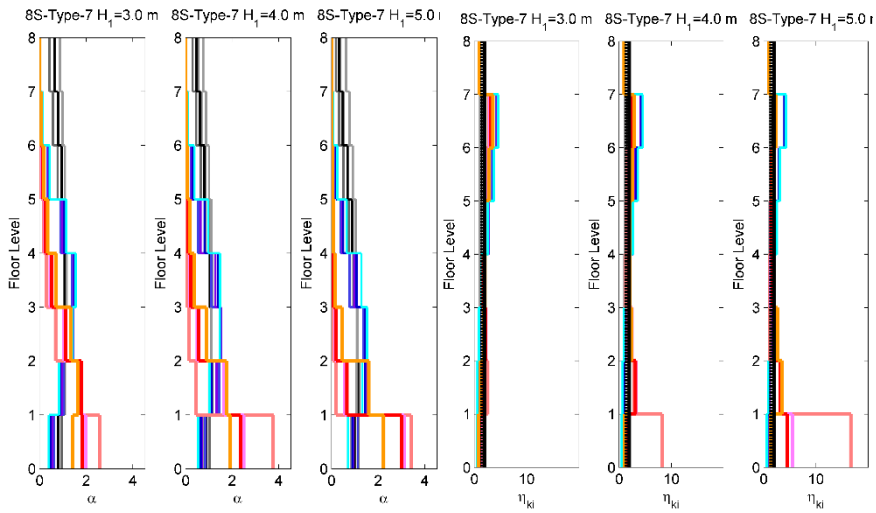

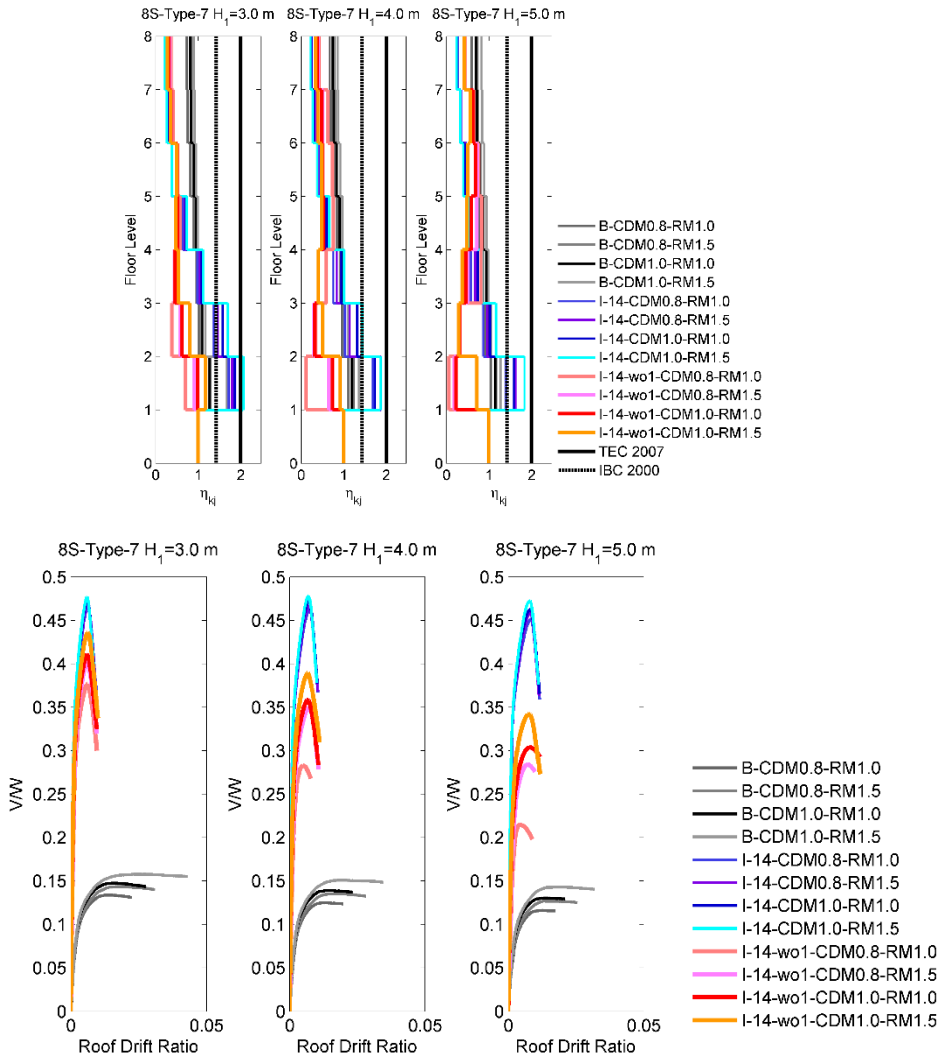

Figure A2-59 8 Story Frame; pushover analysis results at Ultimate Point for Type 7

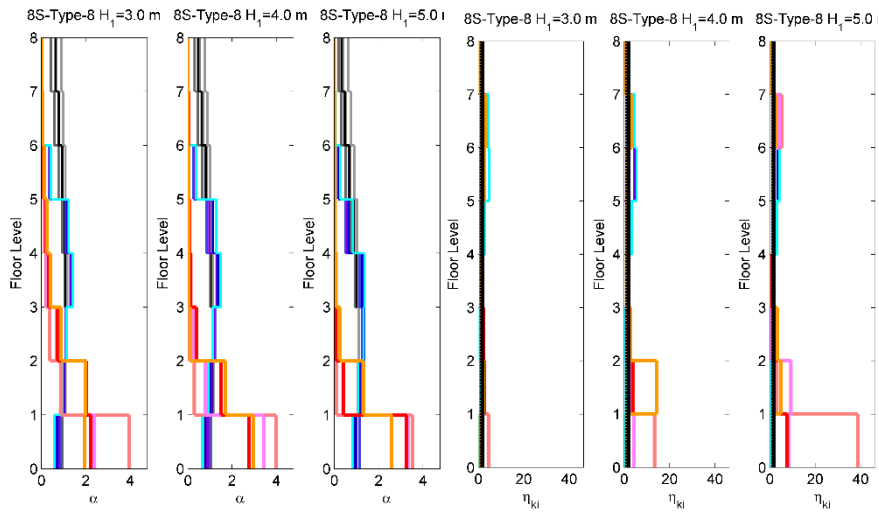

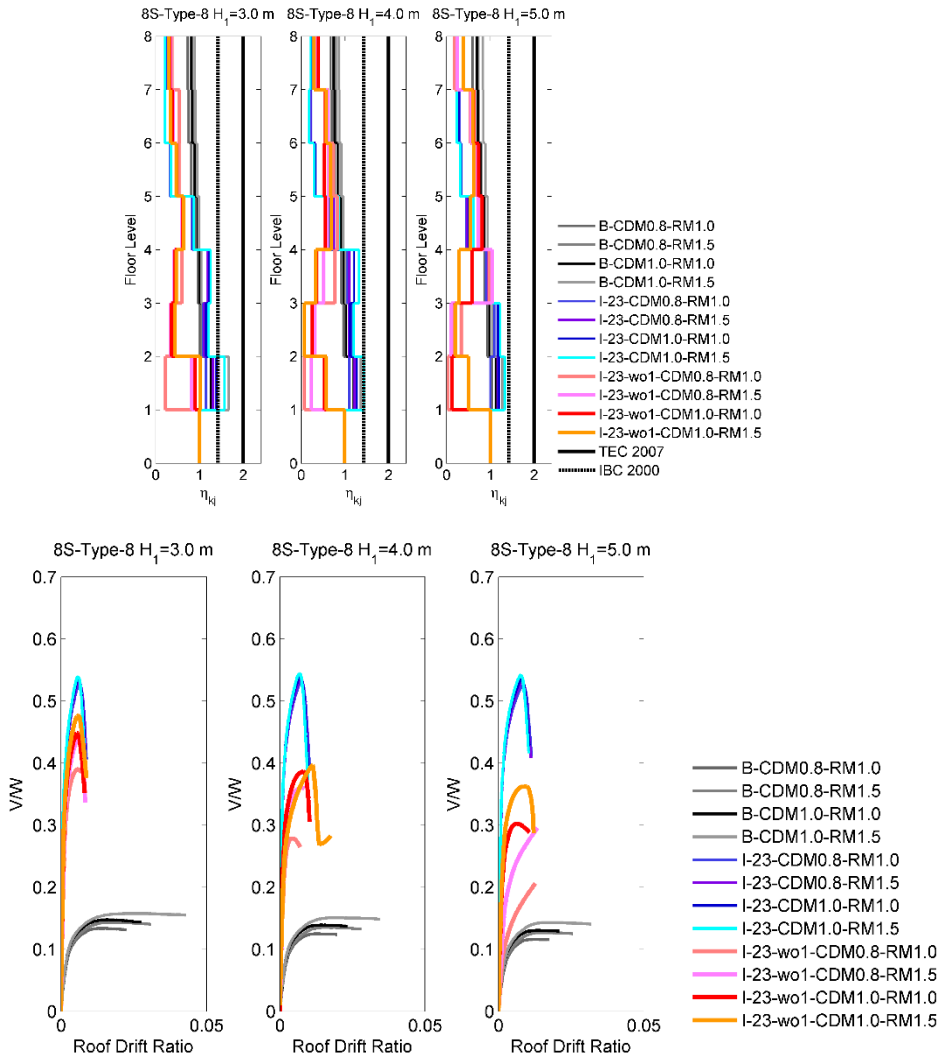

Figure A2-60 8 Story Frame; pushover analysis results at Ultimate Point for Type 8

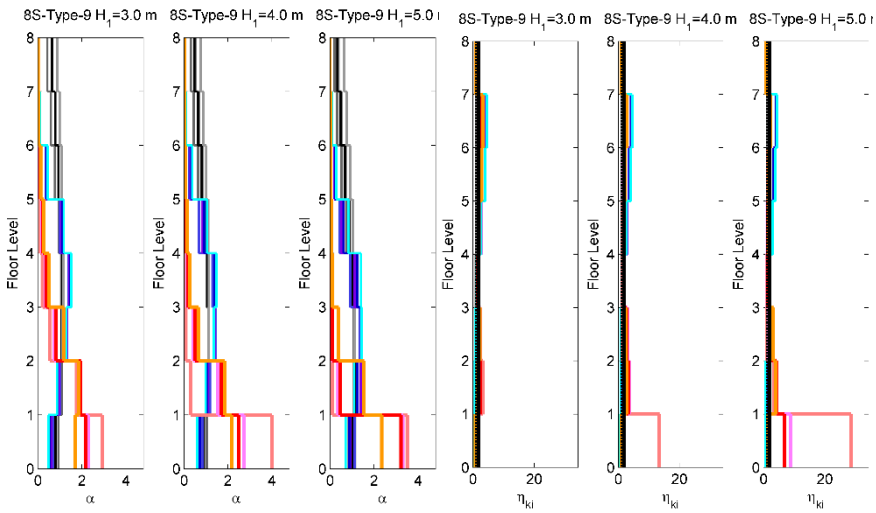

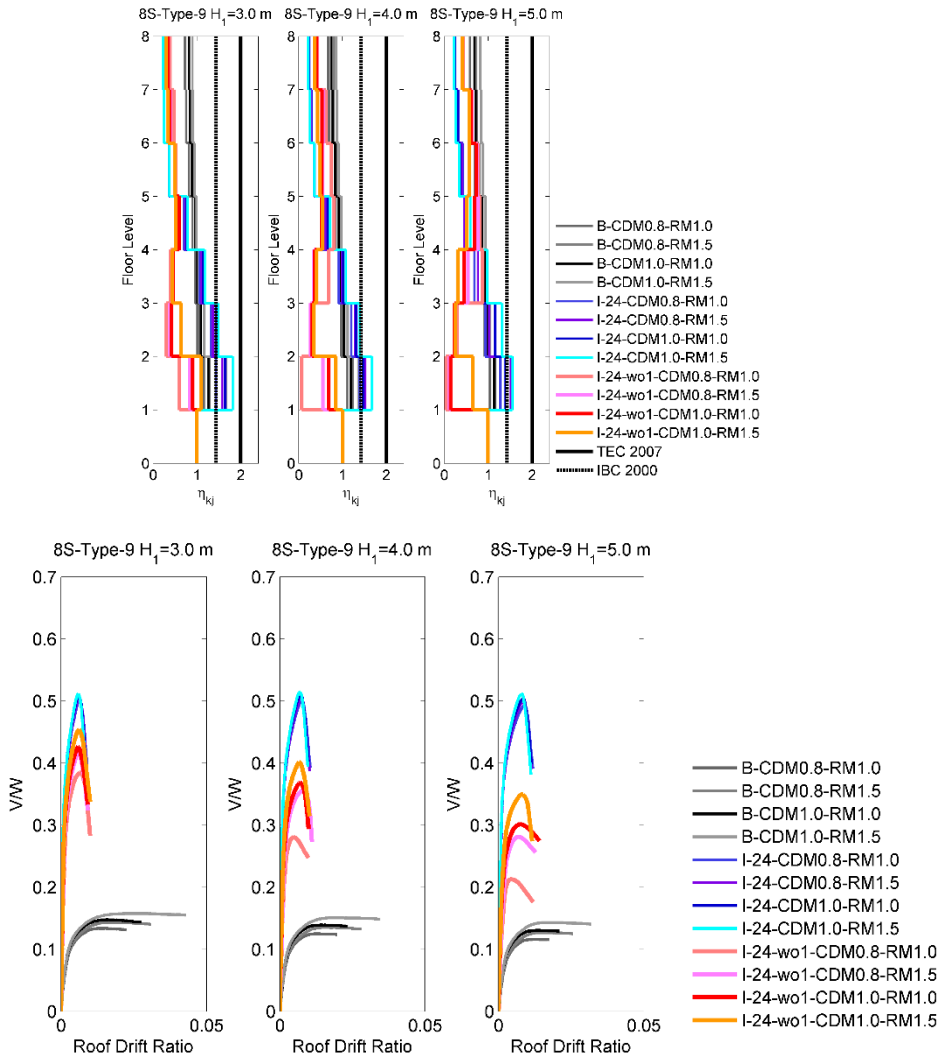

Figure A2-61 8 Story Frame; pushover analysis results at Ultimate Point for Type 9

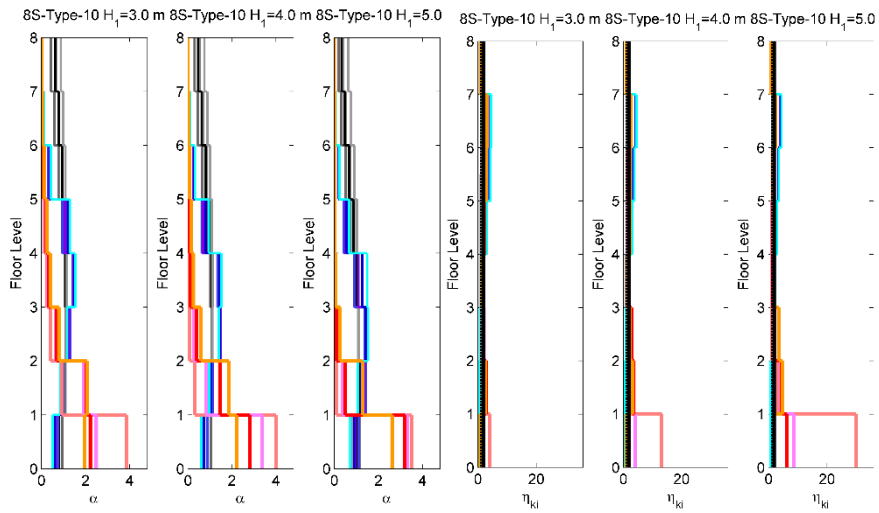

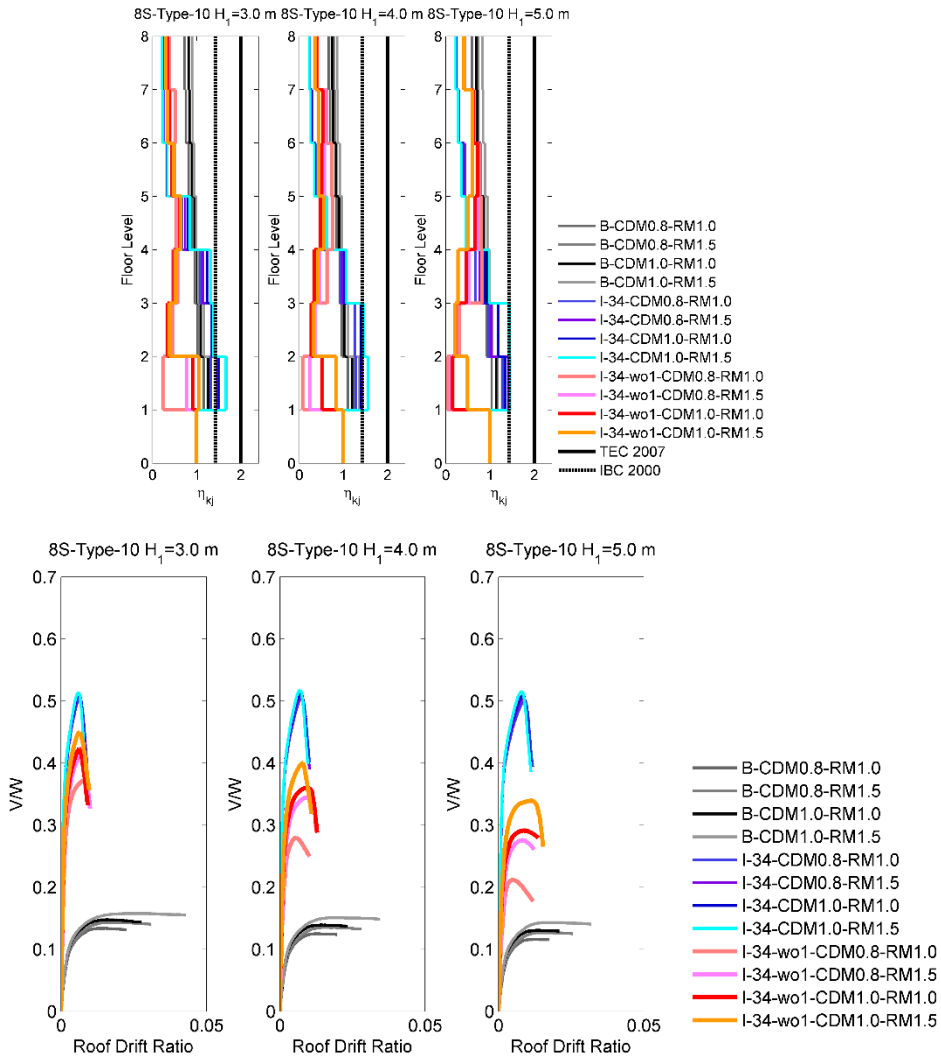

Figure A2-62 8 Story Frame; pushover analysis results at Ultimate Point for Type 10

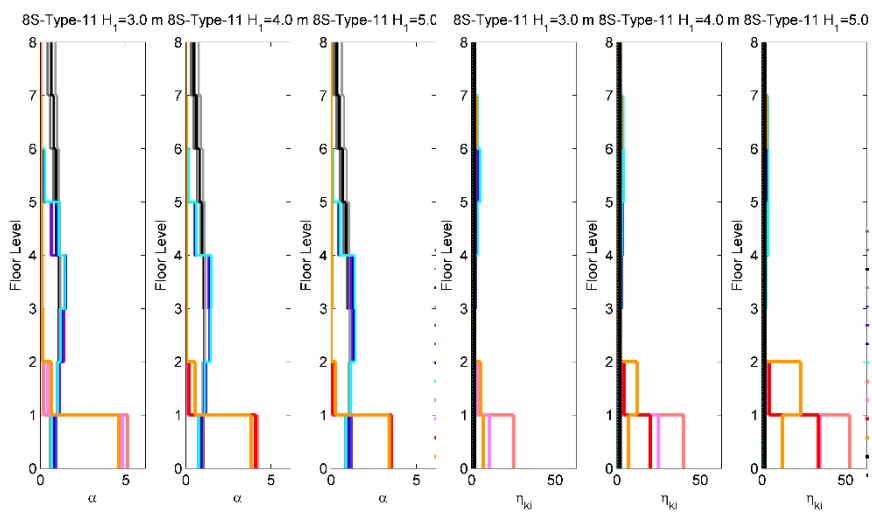

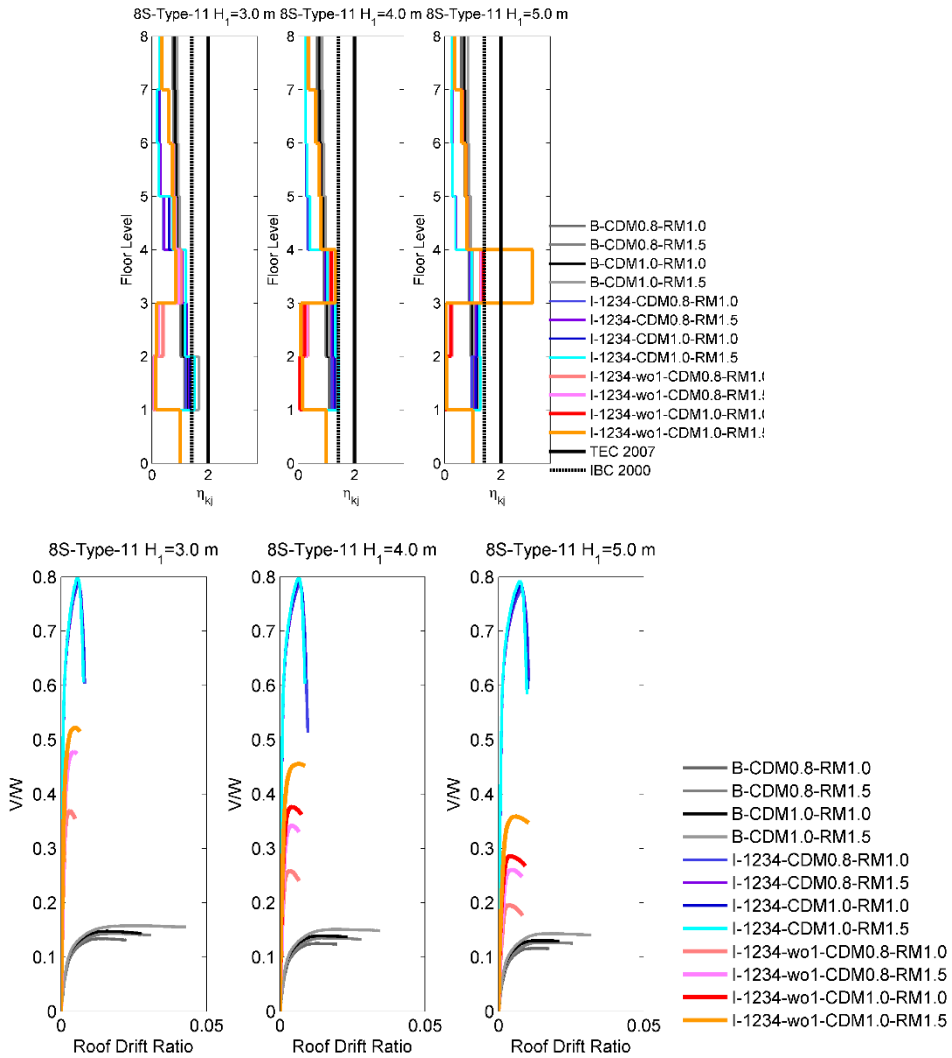

Figure A2-63 8 Story Frame; pushover analysis results at Ultimate Point for Type 11

A2.4 Pushover Analysis Results at Target Displacement

Target displacement is calculated according to ASCE 41-13, displacement coefficient method.

Table A2-10 Soft story, weak story and max alpha values for 3 Story frame for pushover analysis results at Target Displacement

Frame Type/ Story Level	$\eta_{ki,\ max}$	$\eta_{kj,\ max}$	α_{max}	$\alpha_{irregular}$	α_2
3S_B_H3.0_CDM0.8_RM1.0	2.580	1.000	1.226	1.123	1.257
3S_B_H3.0_CDM0.8_RM1.5	2.462	1.000	1.103	1.152	1.301
3S_B_H3.0_CDM1.0_RM1.0	2.271	1.000	1.031	1.000	1.265
3S_B_H3.0_CDM1.0_RM1.5	2.086	1.178	1.107	1.000	1.272
3S_B_H4.0_CDM0.8_RM1.0	3.020	1.000	1.307	1.527	1.416
3S_B_H4.0_CDM0.8_RM1.5	2.895	1.000	1.188	1.409	1.323
3S_B_H4.0_CDM1.0_RM1.0	2.700	1.000	1.093	1.182	1.307
3S_B_H4.0_CDM1.0_RM1.5	2.549	1.000	1.017	1.182	1.316
3S_B_H5.0_CDM0.8_RM1.0	3.186	1.000	1.317	1.827	1.382
3S_B_H5.0_CDM0.8_RM1.5	3.295	1.000	1.232	1.827	1.405
3S_B_H5.0_CDM1.0_RM1.0	3.125	1.000	1.143	1.527	1.451
3S_B_H5.0_CDM1.0_RM1.5	2.945	1.000	1.075	1.408	1.350
3S_I_1_H3.0_CDM0.8_RM1.0	5.505	1.000	1.406	0.201	1.541
3S_I_1_H3.0_CDM0.8_RM1.5	5.849	1.000	1.382	0.216	1.674
3S_I_1_H3.0_CDM1.0_RM1.0	5.648	1.000	1.276	0.171	1.459
3S_I_1_H3.0_CDM1.0_RM1.5	3.661	1.000	1.282	0.121	1.036
3S_I_1_H4.0_CDM0.8_RM1.0	5.169	1.000	1.293	0.216	1.378
3S_I_1_H4.0_CDM0.8_RM1.5	5.169	1.000	1.293	0.216	1.378
3S_I_1_H4.0_CDM1.0_RM1.0	4.097	1.000	1.229	0.156	1.118
3S_I_1_H4.0_CDM1.0_RM1.5	4.132	1.000	1.214	0.153	1.104
3S_I_1_H5.0_CDM0.8_RM1.0	5.260	1.000	1.229	0.245	1.319
3S_I_1_H5.0_CDM0.8_RM1.5	5.344	1.000	1.221	0.245	1.337
3S_I_1_H5.0_CDM1.0_RM1.0	5.683	1.000	1.156	0.215	1.312
3S_I_1_H5.0_CDM1.0_RM1.5	5.755	1.000	1.133	0.206	1.267
3S_I_1_wo_1_H3.0_CDM0.8_RM1.0	28.125	1.000	2.027	0.811	1.640
3S_I_1_wo_1_H3.0_CDM0.8_RM1.5	16.997	1.000	1.982	0.707	1.593
3S_I_1_wo_1_H3.0_CDM1.0_RM1.0	11.984	1.000	1.937	0.573	1.785
3S_I_1_wo_1_H3.0_CDM1.0_RM1.5	11.046	1.000	1.842	0.529	1.686
3S_I_1_wo_1_H4.0_CDM0.8_RM1.0	34.657	1.000	1.713	1.094	1.496
3S_I_1_wo_1_H4.0_CDM0.8_RM1.5	28.429	1.000	1.705	1.197	1.683
3S_I_1_wo_1_H4.0_CDM1.0_RM1.0	17.513	1.000	1.678	0.811	1.614
3S_I_1_wo_1_H4.0_CDM1.0_RM1.5	13.592	1.000	1.644	0.749	1.516
3S_I_1_wo_1_H5.0_CDM0.8_RM1.0	42.967	1.000	1.521	1.436	1.409

3S_I_1_wo_1_H5.0_CDM0.8_RM1.5	33.485	1.000	1.516	1.472	1.487
3S_I_1_wo_1_H5.0_CDM1.0_RM1.0	20.851	1.000	1.501	0.976	1.440
3S_I_1_wo_1_H5.0_CDM1.0_RM1.5	19.285	1.000	1.490	0.976	1.467
3S_I_2_H3.0_CDM0.8_RM1.0	3.660	1.000	1.363	0.151	1.337
3S_I_2_H3.0_CDM0.8_RM1.5	3.752	1.000	1.336	0.151	1.338
3S_I_2_H3.0_CDM1.0_RM1.0	3.979	1.000	1.251	0.151	1.390
3S_I_2_H3.0_CDM1.0_RM1.5	3.765	1.000	1.222	0.136	1.256
3S_I_2_H4.0_CDM0.8_RM1.0	3.716	1.000	1.309	0.195	1.410
3S_I_2_H4.0_CDM0.8_RM1.5	3.671	1.000	1.279	0.181	1.303
3S_I_2_H4.0_CDM1.0_RM1.0	4.053	1.000	1.204	0.181	1.351
3S_I_2_H4.0_CDM1.0_RM1.5	3.802	1.000	1.202	0.165	1.238
3S_I_2_H5.0_CDM0.8_RM1.0	3.663	1.000	1.276	0.225	1.308
3S_I_2_H5.0_CDM0.8_RM1.5	3.764	1.000	1.264	0.225	1.307
3S_I_2_H5.0_CDM1.0_RM1.0	4.030	1.000	1.210	0.210	1.262
3S_I_2_H5.0_CDM1.0_RM1.5	4.174	1.000	1.193	0.210	1.263
3S_I_2_wo_1_H3.0_CDM0.8_RM1.0	32.563	1.000	2.036	0.719	1.522
3S_I_2_wo_1_H3.0_CDM0.8_RM1.5	19.360	1.000	1.995	0.704	1.524
3S_I_2_wo_1_H3.0_CDM1.0_RM1.0	11.714	1.000	1.932	0.525	1.694
3S_I_2_wo_1_H3.0_CDM1.0_RM1.5	7.742	1.000	1.838	0.525	1.733
3S_I_2_wo_1_H4.0_CDM0.8_RM1.0	43.551	1.000	1.720	1.046	1.504
3S_I_2_wo_1_H4.0_CDM0.8_RM1.5	33.197	1.000	1.711	1.120	1.652
3S_I_2_wo_1_H4.0_CDM1.0_RM1.0	20.600	1.000	1.689	0.719	1.490
3S_I_2_wo_1_H4.0_CDM1.0_RM1.5	11.014	1.000	1.638	0.749	1.575
3S_I_2_wo_1_H5.0_CDM0.8_RM1.0	59.422	1.000	1.526	1.492	1.535
3S_I_2_wo_1_H5.0_CDM0.8_RM1.5	42.281	1.000	1.521	1.457	1.542
3S_I_2_wo_1_H5.0_CDM1.0_RM1.0	27.207	1.000	1.510	0.980	1.510
3S_I_2_wo_1_H5.0_CDM1.0_RM1.5	17.312	1.000	1.493	0.980	1.537
3S_I_12_H3.0_CDM0.8_RM1.0	3.432	1.000	1.479	0.093	1.407
3S_I_12_H3.0_CDM0.8_RM1.5	3.414	1.000	1.413	0.078	1.183
3S_I_12_H3.0_CDM1.0_RM1.0	3.100	1.000	1.362	0.076	1.184
3S_I_12_H3.0_CDM1.0_RM1.5	3.990	1.000	1.426	0.093	1.450
3S_I_12_H4.0_CDM0.8_RM1.0	3.500	1.000	1.297	0.093	1.226
3S_I_12_H4.0_CDM0.8_RM1.5	3.801	1.000	1.297	0.096	1.263
3S_I_12_H4.0_CDM1.0_RM1.0	3.860	1.000	1.272	0.094	1.268
3S_I_12_H4.0_CDM1.0_RM1.5	3.889	1.000	1.267	0.094	1.268
3S_I_12_H5.0_CDM0.8_RM1.0	3.948	1.000	1.271	0.124	1.396
3S_I_12_H5.0_CDM0.8_RM1.5	3.591	1.000	1.255	0.108	1.218
3S_I_12_H5.0_CDM1.0_RM1.0	4.003	1.000	1.240	0.109	1.266
3S_I_12_H5.0_CDM1.0_RM1.5	3.401	1.000	1.237	0.107	1.243
3S_I_12_wo_1_H3.0_CDM0.8_RM1.0	59.393	1.000	2.065	0.808	1.722
3S_I_12_wo_1_H3.0_CDM0.8_RM1.5	40.955	1.000	2.050	0.720	1.573
3S_I_12_wo_1_H3.0_CDM1.0_RM1.0	29.576	1.000	2.031	0.525	1.786
3S_I_12_wo_1_H3.0_CDM1.0_RM1.5	23.389	1.000	2.013	0.525	1.833

3S_I_12_wo_1_H4.0_CDM0.8_RM1.0	65.870	1.000	1.730	1.062	1.483
3S_I_12_wo_1_H4.0_CDM0.8_RM1.5	51.633	1.000	1.725	1.051	1.509
3S_I_12_wo_1_H4.0_CDM1.0_RM1.0	35.199	1.000	1.714	0.786	1.641
3S_I_12_wo_1_H4.0_CDM1.0_RM1.5	28.167	1.000	1.705	0.750	1.595
3S_I_12_wo_1_H5.0_CDM0.8_RM1.0	86.685	1.000	1.531	1.567	1.542
3S_I_12_wo_1_H5.0_CDM0.8_RM1.5	68.969	1.000	1.528	1.597	1.620
3S_I_12_wo_1_H5.0_CDM1.0_RM1.0	52.773	1.000	1.521	1.048	1.584
3S_I_12_wo_1_H5.0_CDM1.0_RM1.5	38.980	1.000	1.517	1.048	1.615

Table A2-11 Soft story, weak story and max alpha values for 5 Story frame for pushover analysis results at Target Displacement

Frame Type/ Story Level	$\eta_{ki,\,max}$	$\eta_{kj,\,max}$	α_{max}	$\alpha_{irregular}$	α_2
5S_B_H3.0_CDM0.8_RM1.0	1.869	1.005	1.119	1.103	1.448
5S_B_H3.0_CDM0.8_RM1.5	1.880	1.000	1.171	1.103	1.458
5S_B_H3.0_CDM1.0_RM1.0	1.810	1.312	1.157	1.000	1.398
5S_B_H3.0_CDM1.0_RM1.5	1.765	1.515	1.170	1.000	1.404
5S_B_H4.0_CDM0.8_RM1.0	1.953	1.000	1.352	1.358	1.630
5S_B_H4.0_CDM0.8_RM1.5	1.919	1.000	1.149	1.193	1.446
5S_B_H4.0_CDM1.0_RM1.0	1.898	1.059	1.132	1.103	1.448
5S_B_H4.0_CDM1.0_RM1.5	1.860	1.242	1.172	1.166	1.540
5S_B_H5.0_CDM0.8_RM1.0	2.007	1.000	1.478	1.550	1.666
5S_B_H5.0_CDM0.8_RM1.5	1.980	1.000	1.262	1.422	1.551
5S_B_H5.0_CDM1.0_RM1.0	1.973	1.000	1.203	1.358	1.652
5S_B_H5.0_CDM1.0_RM1.5	1.937	1.085	1.143	1.320	1.618
5S_I_1_H3.0_CDM0.8_RM1.0	3.295	1.051	1.175	0.443	1.013
5S_I_1_H3.0_CDM0.8_RM1.5	3.287	1.126	1.193	0.442	1.024
5S_I_1_H3.0_CDM1.0_RM1.0	3.260	1.330	1.222	0.430	1.079
5S_I_1_H3.0_CDM1.0_RM1.5	3.279	1.411	1.230	0.468	1.183
5S_I_1_H4.0_CDM0.8_RM1.0	3.175	1.000	1.185	0.443	0.881
5S_I_1_H4.0_CDM0.8_RM1.5	3.216	1.008	1.143	0.443	0.892
5S_I_1_H4.0_CDM1.0_RM1.0	3.296	1.211	1.207	0.430	0.951
5S_I_1_H4.0_CDM1.0_RM1.5	3.328	1.279	1.223	0.430	0.959
5S_I_1_H5.0_CDM0.8_RM1.0	3.068	1.000	1.244	0.468	0.793
5S_I_1_H5.0_CDM0.8_RM1.5	3.180	1.000	1.202	0.506	0.870
5S_I_1_H5.0_CDM1.0_RM1.0	3.289	1.083	1.156	0.493	0.942
5S_I_1_H5.0_CDM1.0_RM1.5	3.330	1.146	1.181	0.493	0.951
5S_I_1_wo_1_H3.0_CDM0.8_RM1.0	3.073	1.000	1.954	0.622	1.114
5S_I_1_wo_1_H3.0_CDM0.8_RM1.5	3.323	1.000	1.583	0.596	1.084
5S_I_1_wo_1_H3.0_CDM1.0_RM1.0	3.336	1.000	1.411	0.545	1.170
5S_I_1_wo_1_H3.0_CDM1.0_RM1.5	3.359	1.000	1.231	0.520	1.131
5S_I_1_wo_1_H4.0_CDM0.8_RM1.0	3.753	1.000	2.143	0.737	1.092
5S_I_1_wo_1_H4.0_CDM0.8_RM1.5	2.970	1.000	1.830	0.737	1.114

5S_I_1_wo_1_H4.0_CDM1.0_RM1.0	2.936	1.000	1.653	0.597	1.047
5S_I_1_wo_1_H4.0_CDM1.0_RM1.5	3.214	1.000	1.430	0.622	1.103
5S_I_1_wo_1_H5.0_CDM0.8_RM1.0	6.672	1.000	2.107	0.992	1.217
5S_I_1_wo_1_H5.0_CDM0.8_RM1.5	3.265	1.000	1.881	0.967	1.216
5S_I_1_wo_1_H5.0_CDM1.0_RM1.0	2.609	1.000	1.743	0.738	1.127
5S_I_1_wo_1_H5.0_CDM1.0_RM1.5	2.966	1.000	1.549	0.737	1.142
5S_I_2_H3.0_CDM0.8_RM1.0	2.833	1.047	1.165	0.583	1.028
5S_I_2_H3.0_CDM0.8_RM1.5	2.815	1.136	1.185	0.583	1.034
5S_I_2_H3.0_CDM1.0_RM1.0	2.772	1.320	1.205	0.583	1.125
5S_I_2_H3.0_CDM1.0_RM1.5	2.758	1.437	1.220	0.526	1.022
5S_I_2_H4.0_CDM0.8_RM1.0	2.876	1.000	1.251	0.584	0.912
5S_I_2_H4.0_CDM0.8_RM1.5	2.883	1.000	1.180	0.584	0.919
5S_I_2_H4.0_CDM1.0_RM1.0	2.876	1.140	1.183	0.584	0.977
5S_I_2_H4.0_CDM1.0_RM1.5	2.853	1.225	1.205	0.584	0.973
5S_I_2_H5.0_CDM0.8_RM1.0	2.857	1.000	1.369	0.736	1.029
5S_I_2_H5.0_CDM0.8_RM1.5	2.930	1.000	1.288	0.736	1.038
5S_I_2_H5.0_CDM1.0_RM1.0	2.939	1.000	1.142	0.737	1.125
5S_I_2_H5.0_CDM1.0_RM1.5	2.934	1.057	1.148	0.737	1.133
5S_I_2_wo_1_H3.0_CDM0.8_RM1.0	2.967	1.000	1.619	0.738	1.176
5S_I_2_wo_1_H3.0_CDM0.8_RM1.5	3.466	1.000	1.916	0.705	1.660
5S_I_2_wo_1_H3.0_CDM1.0_RM1.0	3.239	1.000	2.243	0.706	1.841
5S_I_2_wo_1_H3.0_CDM1.0_RM1.5	3.629	1.000	1.480	0.579	1.522
5S_I_2_wo_1_H4.0_CDM0.8_RM1.0	2.623	1.000	1.815	0.777	1.081
5S_I_2_wo_1_H4.0_CDM0.8_RM1.5	2.786	1.000	1.579	0.739	1.044
5S_I_2_wo_1_H4.0_CDM1.0_RM1.0	2.912	1.000	1.425	0.738	1.174
5S_I_2_wo_1_H4.0_CDM1.0_RM1.5	3.014	1.000	1.267	0.738	1.183
5S_I_2_wo_1_H5.0_CDM0.8_RM1.0	3.359	1.000	1.872	0.994	1.184
5S_I_2_wo_1_H5.0_CDM0.8_RM1.5	2.755	1.000	1.665	1.096	1.332
5S_I_2_wo_1_H5.0_CDM1.0_RM1.0	2.636	1.000	1.515	0.765	1.089
5S_I_2_wo_1_H5.0_CDM1.0_RM1.5	2.781	1.000	1.382	0.765	1.100
5S_I_3_H3.0_CDM0.8_RM1.0	3.150	1.012	1.159	0.518	1.043
5S_I_3_H3.0_CDM0.8_RM1.5	3.189	1.096	1.180	0.582	1.182
5S_I_3_H3.0_CDM1.0_RM1.0	3.147	1.282	1.208	0.518	1.139
5S_I_3_H3.0_CDM1.0_RM1.5	3.127	1.378	1.218	0.518	1.147
5S_I_3_H4.0_CDM0.8_RM1.0	2.961	1.000	1.389	0.582	0.988
5S_I_3_H4.0_CDM0.8_RM1.5	3.085	1.000	1.300	0.607	1.038
5S_I_3_H4.0_CDM1.0_RM1.0	3.168	1.010	1.154	0.582	1.067
5S_I_3_H4.0_CDM1.0_RM1.5	3.196	1.091	1.180	0.582	1.077
5S_I_3_H5.0_CDM0.8_RM1.0	2.783	1.000	1.384	0.582	0.914
5S_I_3_H5.0_CDM0.8_RM1.5	2.864	1.000	1.310	0.582	0.920
5S_I_3_H5.0_CDM1.0_RM1.0	3.027	1.000	1.155	0.582	0.984
5S_I_3_H5.0_CDM1.0_RM1.5	3.082	1.038	1.145	0.582	0.990
5S_I_3_wo_1_H3.0_CDM0.8_RM1.0	3.193	1.000	1.744	0.774	1.344

5S_I_3_wo_1_H3.0_CDM0.8_RM1.5	3.308	1.000	1.463	0.736	1.291
5S_I_3_wo_1_H3.0_CDM1.0_RM1.0	3.176	1.000	1.327	0.583	1.126
5S_I_3_wo_1_H3.0_CDM1.0_RM1.5	3.222	1.000	1.201	0.583	1.140
5S_I_3_wo_1_H4.0_CDM0.8_RM1.0	2.622	1.000	1.906	0.775	1.166
5S_I_3_wo_1_H4.0_CDM0.8_RM1.5	2.874	1.000	1.654	0.737	1.127
5S_I_3_wo_1_H4.0_CDM1.0_RM1.0	3.024	1.000	1.512	0.736	1.273
5S_I_3_wo_1_H4.0_CDM1.0_RM1.5	3.223	1.000	1.339	0.736	1.283
5S_I_3_wo_1_H5.0_CDM0.8_RM1.0	3.859	1.000	1.933	0.972	1.240
5S_I_3_wo_1_H5.0_CDM0.8_RM1.5	2.665	1.000	1.722	0.967	1.261
5S_I_3_wo_1_H5.0_CDM1.0_RM1.0	2.646	1.000	1.587	0.775	1.193
5S_I_3_wo_1_H5.0_CDM1.0_RM1.5	2.805	1.000	1.448	0.737	1.147
5S_I_12_H3.0_CDM0.8_RM1.0	3.373	1.038	1.195	0.350	1.210
5S_I_12_H3.0_CDM0.8_RM1.5	3.309	1.098	1.211	0.325	1.130
5S_I_12_H3.0_CDM1.0_RM1.0	3.527	1.280	1.245	0.350	1.291
5S_I_12_H3.0_CDM1.0_RM1.5	3.447	1.354	1.256	0.324	1.204
5S_I_12_H4.0_CDM0.8_RM1.0	3.140	1.001	1.156	0.325	0.975
5S_I_12_H4.0_CDM0.8_RM1.5	3.169	1.050	1.177	0.325	0.983
5S_I_12_H4.0_CDM1.0_RM1.0	3.273	1.222	1.232	0.325	1.050
5S_I_12_H4.0_CDM1.0_RM1.5	3.298	1.266	1.244	0.325	1.057
5S_I_12_H5.0_CDM0.8_RM1.0	3.224	1.000	1.233	0.414	1.044
5S_I_12_H5.0_CDM0.8_RM1.5	3.269	1.000	1.192	0.414	1.054
5S_I_12_H5.0_CDM1.0_RM1.0	3.391	1.084	1.174	0.414	1.137
5S_I_12_H5.0_CDM1.0_RM1.5	3.426	1.136	1.196	0.414	1.145
5S_I_12_wo_1_H3.0_CDM0.8_RM1.0	5.888	1.000	2.771	0.515	1.109
5S_I_12_wo_1_H3.0_CDM0.8_RM1.5	2.792	1.000	2.238	0.579	1.285
5S_I_12_wo_1_H3.0_CDM1.0_RM1.0	2.769	1.000	1.984	0.453	1.270
5S_I_12_wo_1_H3.0_CDM1.0_RM1.5	3.102	1.000	1.645	0.453	1.291
5S_I_12_wo_1_H4.0_CDM0.8_RM1.0	13.487	1.000	2.577	0.834	1.430
5S_I_12_wo_1_H4.0_CDM0.8_RM1.5	4.629	1.000	2.287	0.727	1.276
5S_I_12_wo_1_H4.0_CDM1.0_RM1.0	3.212	1.000	2.112	0.581	1.210
5S_I_12_wo_1_H4.0_CDM1.0_RM1.5	2.685	1.000	1.858	0.517	1.103
5S_I_12_wo_1_H5.0_CDM0.8_RM1.0	15.499	1.000	2.250	0.923	1.277
5S_I_12_wo_1_H5.0_CDM0.8_RM1.5	7.463	1.000	2.140	0.834	1.187
5S_I_12_wo_1_H5.0_CDM1.0_RM1.0	4.912	1.000	2.042	0.734	1.293
5S_I_12_wo_1_H5.0_CDM1.0_RM1.5	3.579	1.000	1.884	0.734	1.513
5S_I_13_H3.0_CDM0.8_RM1.0	3.330	1.000	1.199	0.349	1.177
5S_I_13_H3.0_CDM0.8_RM1.5	3.369	1.053	1.205	0.349	1.188
5S_I_13_H3.0_CDM1.0_RM1.0	3.530	1.232	1.241	0.349	1.270
5S_I_13_H3.0_CDM1.0_RM1.5	3.243	1.297	1.250	0.286	1.045
5S_I_13_H4.0_CDM0.8_RM1.0	2.999	1.000	1.340	0.349	1.004
5S_I_13_H4.0_CDM0.8_RM1.5	3.054	1.000	1.285	0.349	1.013
5S_I_13_H4.0_CDM1.0_RM1.0	3.203	1.033	1.182	0.349	1.095
5S_I_13_H4.0_CDM1.0_RM1.5	3.249	1.095	1.204	0.349	1.103

5S_I_13_H5.0_CDM0.8_RM1.0	3.226	1.000	1.283	0.451	1.117
5S_I_13_H5.0_CDM0.8_RM1.5	3.286	1.000	1.233	0.451	1.128
5S_I_13_H5.0_CDM1.0_RM1.0	3.435	1.038	1.160	0.451	1.225
5S_I_13_H5.0_CDM1.0_RM1.5	3.488	1.103	1.189	0.451	1.234
5S_I_13_wo_1_H3.0_CDM0.8_RM1.0	6.279	1.000	2.808	0.516	1.102
5S_I_13_wo_1_H3.0_CDM0.8_RM1.5	2.880	1.000	2.300	0.516	1.138
5S_I_13_wo_1_H3.0_CDM1.0_RM1.0	2.655	1.000	2.097	0.452	1.264
5S_I_13_wo_1_H3.0_CDM1.0_RM1.5	2.917	1.000	1.757	0.452	1.285
5S_I_13_wo_1_H4.0_CDM0.8_RM1.0	13.873	1.000	2.577	0.771	1.323
5S_I_13_wo_1_H4.0_CDM0.8_RM1.5	5.129	1.000	2.327	0.733	1.287
5S_I_13_wo_1_H4.0_CDM1.0_RM1.0	3.690	1.000	2.183	0.580	1.204
5S_I_13_wo_1_H4.0_CDM1.0_RM1.5	2.939	1.000	1.946	0.580	1.231
5S_I_13_wo_1_H5.0_CDM0.8_RM1.0	17.055	1.000	2.259	0.924	1.282
5S_I_13_wo_1_H5.0_CDM0.8_RM1.5	8.707	1.000	2.171	0.962	1.373
5S_I_13_wo_1_H5.0_CDM1.0_RM1.0	5.884	1.000	2.085	0.733	1.302
5S_I_13_wo_1_H5.0_CDM1.0_RM1.5	3.684	1.000	1.933	0.732	1.320
5S_I_23_H3.0_CDM0.8_RM1.0	3.460	1.000	1.188	0.451	1.522
5S_I_23_H3.0_CDM0.8_RM1.5	3.519	1.070	1.204	0.451	1.529
5S_I_23_H3.0_CDM1.0_RM1.0	3.216	1.273	1.246	0.349	1.242
5S_I_23_H3.0_CDM1.0_RM1.5	3.261	1.344	1.255	0.349	1.247
5S_I_23_H4.0_CDM0.8_RM1.0	2.731	1.000	1.402	0.369	1.011
5S_I_23_H4.0_CDM0.8_RM1.5	3.047	1.000	1.329	0.451	1.242
5S_I_23_H4.0_CDM1.0_RM1.0	3.218	1.000	1.175	0.451	1.331
5S_I_23_H4.0_CDM1.0_RM1.5	3.296	1.075	1.202	0.451	1.339
5S_I_23_H5.0_CDM0.8_RM1.0	2.780	1.000	1.375	0.451	1.024
5S_I_23_H5.0_CDM0.8_RM1.5	2.857	1.000	1.311	0.451	1.032
5S_I_23_H5.0_CDM1.0_RM1.0	3.029	1.000	1.166	0.451	1.117
5S_I_23_H5.0_CDM1.0_RM1.5	3.085	1.041	1.166	0.451	1.125
5S_I_23_wo_1_H3.0_CDM0.8_RM1.0	4.019	1.000	2.550	0.732	1.581
5S_I_23_wo_1_H3.0_CDM0.8_RM1.5	2.593	1.000	2.025	0.516	1.133
5S_I_23_wo_1_H3.0_CDM1.0_RM1.0	2.725	1.000	1.865	0.516	1.413
5S_I_23_wo_1_H3.0_CDM1.0_RM1.5	3.053	1.000	1.580	0.516	1.434
5S_I_23_wo_1_H4.0_CDM0.8_RM1.0	8.619	1.000	2.485	0.923	1.656
5S_I_23_wo_1_H4.0_CDM0.8_RM1.5	3.335	1.000	2.126	0.733	1.341
5S_I_23_wo_1_H4.0_CDM1.0_RM1.0	2.882	1.000	1.989	0.732	1.566
5S_I_23_wo_1_H4.0_CDM1.0_RM1.5	2.749	1.000	1.755	0.732	1.582
5S_I_23_wo_1_H5.0_CDM0.8_RM1.0	11.280	1.000	2.207	0.962	1.406
5S_I_23_wo_1_H5.0_CDM0.8_RM1.5	4.935	1.000	2.046	0.924	1.386
5S_I_23_wo_1_H5.0_CDM1.0_RM1.0	3.611	1.000	1.946	0.733	1.350
5S_I_23_wo_1_H5.0_CDM1.0_RM1.5	3.182	1.000	1.785	0.733	1.369
5S_I_123_H3.0_CDM0.8_RM1.0	2.980	1.000	1.214	0.259	1.326
5S_I_123_H3.0_CDM0.8_RM1.5	3.008	1.028	1.210	0.259	1.332
5S_I_123_H3.0_CDM1.0_RM1.0	3.125	1.187	1.249	0.259	1.380

5S_I_123_H3.0_CDM1.0_RM1.5	3.158	1.239	1.260	0.259	1.384
5S_I_123_H4.0_CDM0.8_RM1.0	2.872	1.000	1.277	0.259	1.133
5S_I_123_H4.0_CDM0.8_RM1.5	2.886	1.000	1.247	0.259	1.139
5S_I_123_H4.0_CDM1.0_RM1.0	2.938	1.038	1.190	0.259	1.188
5S_I_123_H4.0_CDM1.0_RM1.5	2.949	1.071	1.204	0.259	1.192
5S_I_123_H5.0_CDM0.8_RM1.0	2.976	1.000	1.233	0.323	1.207
5S_I_123_H5.0_CDM0.8_RM1.5	2.990	1.000	1.208	0.323	1.213
5S_I_123_H5.0_CDM1.0_RM1.0	3.029	1.013	1.157	0.323	1.268
5S_I_123_H5.0_CDM1.0_RM1.5	3.043	1.050	1.177	0.323	1.273
5S_I_123_wo_1_H3.0_CDM0.8_RM1.0	15.697	1.000	3.158	0.603	1.558
5S_I_123_wo_1_H3.0_CDM0.8_RM1.5	5.672	1.000	2.757	0.451	1.208
5S_I_123_wo_1_H3.0_CDM1.0_RM1.0	4.184	1.000	2.599	0.451	1.592
5S_I_123_wo_1_H3.0_CDM1.0_RM1.5	2.880	1.000	2.260	0.413	1.485
5S_I_123_wo_1_H4.0_CDM0.8_RM1.0	19.933	1.000	2.641	0.757	1.471
5S_I_123_wo_1_H4.0_CDM0.8_RM1.5	11.592	1.000	2.550	0.731	1.459
5S_I_123_wo_1_H4.0_CDM1.0_RM1.0	8.509	1.000	2.473	0.604	1.497
5S_I_123_wo_1_H4.0_CDM1.0_RM1.5	4.354	1.000	2.253	0.513	1.306
5S_I_123_wo_1_H5.0_CDM0.8_RM1.0	25.820	1.000	2.300	1.024	1.557
5S_I_123_wo_1_H5.0_CDM0.8_RM1.5	14.347	1.000	2.242	0.834	1.308
5S_I_123_wo_1_H5.0_CDM1.0_RM1.0	11.402	1.000	2.210	0.732	1.473
5S_I_123_wo_1_H5.0_CDM1.0_RM1.5	6.284	1.000	2.108	0.732	1.498

Table A2-12 Soft story, weak story and max alpha values for 8 Story frame for pushover analysis results at Target Displacement

Frame Type/ Story Level	$\eta_{ki,\,max}$	$\eta_{kj,\,max}$	α_{max}	$\alpha_{irregular}$	α_2
8S_B_H3.0_CDM0.8_RM1.0	1.823	1.463	1.186	1.060	1.215
8S_B_H3.0_CDM0.8_RM1.5	1.792	1.605	1.196	1.060	1.223
8S_B_H3.0_CDM1.0_RM1.0	1.770	1.770	1.209	1.000	1.190
8S_B_H3.0_CDM1.0_RM1.5	1.745	1.973	1.227	1.000	1.203
8S_B_H4.0_CDM0.8_RM1.0	1.908	1.278	1.226	1.090	1.182
8S_B_H4.0_CDM0.8_RM1.5	1.865	1.403	1.206	1.120	1.226
8S_B_H4.0_CDM1.0_RM1.0	1.845	1.508	1.207	1.030	1.189
8S_B_H4.0_CDM1.0_RM1.5	1.813	1.651	1.224	1.030	1.195
8S_B_H5.0_CDM0.8_RM1.0	1.945	1.136	1.244	1.210	1.225
8S_B_H5.0_CDM0.8_RM1.5	1.928	1.260	1.248	1.180	1.210
8S_B_H5.0_CDM1.0_RM1.0	1.909	1.344	1.218	1.090	1.200
8S_B_H5.0_CDM1.0_RM1.5	1.888	1.464	1.210	1.060	1.175
8S_I_1_H3.0_CDM0.8_RM1.0	2.873	1.355	1.254	0.450	0.631
8S_I_1_H3.0_CDM0.8_RM1.5	2.893	1.458	1.251	0.450	0.635
8S_I_1_H3.0_CDM1.0_RM1.0	2.911	1.664	1.288	0.432	0.639
8S_I_1_H3.0_CDM1.0_RM1.5	2.907	1.781	1.304	0.420	0.624

8S_I_1_H4.0_CDM0.8_RM1.0	2.854	1.215	1.279	0.480	0.628
8S_I_1_H4.0_CDM0.8_RM1.5	2.881	1.306	1.278	0.480	0.633
8S_I_1_H4.0_CDM1.0_RM1.0	2.892	1.465	1.270	0.450	0.631
8S_I_1_H4.0_CDM1.0_RM1.5	2.915	1.559	1.289	0.450	0.634
8S_I_1_H5.0_CDM0.8_RM1.0	2.697	1.000	1.320	0.509	0.626
8S_I_1_H5.0_CDM0.8_RM1.5	2.739	1.040	1.269	0.509	0.633
8S_I_1_H5.0_CDM1.0_RM1.0	2.767	1.212	1.289	0.480	0.640
8S_I_1_H5.0_CDM1.0_RM1.5	2.796	1.295	1.292	0.480	0.644
8S_I_1_wo_1_H3.0_CDM0.8_RM1.0	2.718	1.000	1.447	0.462	0.637
8S_I_1_wo_1_H3.0_CDM0.8_RM1.5	2.749	1.066	1.360	0.450	0.626
8S_I_1_wo_1_H3.0_CDM1.0_RM1.0	2.816	1.243	1.330	0.450	0.661
8S_I_1_wo_1_H3.0_CDM1.0_RM1.5	2.855	1.375	1.305	0.450	0.664
8S_I_1_wo_1_H4.0_CDM0.8_RM1.0	2.601	1.000	1.887	0.599	0.767
8S_I_1_wo_1_H4.0_CDM0.8_RM1.5	2.642	1.000	1.606	0.540	0.700
8S_I_1_wo_1_H4.0_CDM1.0_RM1.0	2.695	1.000	1.383	0.510	0.710
8S_I_1_wo_1_H4.0_CDM1.0_RM1.5	2.767	1.116	1.372	0.510	0.715
8S_I_1_wo_1_H5.0_CDM0.8_RM1.0	2.284	1.000	2.312	0.718	0.842
8S_I_1_wo_1_H5.0_CDM0.8_RM1.5	2.534	1.000	1.888	0.718	0.856
8S_I_1_wo_1_H5.0_CDM1.0_RM1.0	2.478	1.000	1.695	0.569	0.746
8S_I_1_wo_1_H5.0_CDM1.0_RM1.5	2.614	1.000	1.470	0.569	0.753
8S_I_2_H3.0_CDM0.8_RM1.0	2.851	1.289	1.309	0.360	0.677
8S_I_2_H3.0_CDM0.8_RM1.5	3.000	1.378	1.296	0.420	0.793
8S_I_2_H3.0_CDM1.0_RM1.0	3.053	1.557	1.269	0.420	0.822
8S_I_2_H3.0_CDM1.0_RM1.5	2.951	1.678	1.293	0.360	0.708
8S_I_2_H4.0_CDM0.8_RM1.0	2.858	1.125	1.299	0.420	0.748
8S_I_2_H4.0_CDM0.8_RM1.5	2.887	1.208	1.308	0.420	0.754
8S_I_2_H4.0_CDM1.0_RM1.0	2.955	1.381	1.292	0.420	0.788
8S_I_2_H4.0_CDM1.0_RM1.5	2.979	1.465	1.288	0.420	0.791
8S_I_2_H5.0_CDM0.8_RM1.0	2.756	1.000	1.308	0.450	0.759
8S_I_2_H5.0_CDM0.8_RM1.5	2.736	1.042	1.275	0.420	0.714
8S_I_2_H5.0_CDM1.0_RM1.0	2.829	1.213	1.300	0.420	0.754
8S_I_2_H5.0_CDM1.0_RM1.5	2.859	1.286	1.307	0.420	0.759
8S_I_2_wo_1_H3.0_CDM0.8_RM1.0	2.912	1.000	1.651	0.539	0.972
8S_I_2_wo_1_H3.0_CDM0.8_RM1.5	2.830	1.000	1.459	0.450	0.819
8S_I_2_wo_1_H3.0_CDM1.0_RM1.0	2.855	1.136	1.427	0.420	0.807
8S_I_2_wo_1_H3.0_CDM1.0_RM1.5	2.914	1.261	1.403	0.420	0.811
8S_I_2_wo_1_H4.0_CDM0.8_RM1.0	2.475	1.000	2.207	0.539	0.890
8S_I_2_wo_1_H4.0_CDM0.8_RM1.5	2.590	1.000	1.849	0.510	0.854
8S_I_2_wo_1_H4.0_CDM1.0_RM1.0	2.597	1.000	1.620	0.450	0.817
8S_I_2_wo_1_H4.0_CDM1.0_RM1.5	2.684	1.011	1.452	0.450	0.822
8S_I_2_wo_1_H5.0_CDM0.8_RM1.0	2.626	1.000	2.514	0.635	0.941
8S_I_2_wo_1_H5.0_CDM0.8_RM1.5	2.460	1.000	2.117	0.718	1.086
8S_I_2_wo_1_H5.0_CDM1.0_RM1.0	2.431	1.000	1.918	0.575	0.972

8S_I_2_wo_1_H5.0_CDM1.0_RM1.5	2.570	1.000	1.657	0.551	0.941
8S_I_3_H3.0_CDM0.8_RM1.0	2.956	1.136	1.285	0.419	0.803
8S_I_3_H3.0_CDM0.8_RM1.5	2.992	1.229	1.284	0.419	0.807
8S_I_3_H3.0_CDM1.0_RM1.0	2.899	1.419	1.268	0.360	0.717
8S_I_3_H3.0_CDM1.0_RM1.5	2.927	1.513	1.258	0.360	0.720
8S_I_3_H4.0_CDM0.8_RM1.0	2.745	1.005	1.266	0.396	0.718
8S_I_3_H4.0_CDM0.8_RM1.5	2.835	1.082	1.278	0.419	0.766
8S_I_3_H4.0_CDM1.0_RM1.0	2.996	1.244	1.274	0.449	0.856
8S_I_3_H4.0_CDM1.0_RM1.5	3.033	1.331	1.272	0.449	0.860
8S_I_3_H5.0_CDM0.8_RM1.0	2.663	1.000	1.413	0.419	0.720
8S_I_3_H5.0_CDM0.8_RM1.5	2.691	1.000	1.327	0.419	0.725
8S_I_3_H5.0_CDM1.0_RM1.0	2.823	1.088	1.263	0.449	0.817
8S_I_3_H5.0_CDM1.0_RM1.5	2.864	1.166	1.275	0.449	0.821
8S_I_3_wo_1_H3.0_CDM0.8_RM1.0	2.654	1.000	1.865	0.449	0.828
8S_I_3_wo_1_H3.0_CDM0.8_RM1.5	2.721	1.000	1.606	0.449	0.835
8S_I_3_wo_1_H3.0_CDM1.0_RM1.0	2.828	1.053	1.444	0.449	0.878
8S_I_3_wo_1_H3.0_CDM1.0_RM1.5	2.914	1.177	1.423	0.449	0.883
8S_I_3_wo_1_H4.0_CDM0.8_RM1.0	2.472	1.000	2.376	0.598	1.012
8S_I_3_wo_1_H4.0_CDM0.8_RM1.5	2.610	1.000	1.960	0.574	0.985
8S_I_3_wo_1_H4.0_CDM1.0_RM1.0	2.539	1.000	1.765	0.450	0.831
8S_I_3_wo_1_H4.0_CDM1.0_RM1.5	2.620	1.000	1.558	0.450	0.837
8S_I_3_wo_1_H5.0_CDM0.8_RM1.0	2.988	1.000	2.649	0.688	1.044
8S_I_3_wo_1_H5.0_CDM0.8_RM1.5	2.328	1.000	2.256	0.628	0.974
8S_I_3_wo_1_H5.0_CDM1.0_RM1.0	2.404	1.000	2.065	0.628	1.083
8S_I_3_wo_1_H5.0_CDM1.0_RM1.5	2.447	1.000	1.799	0.509	0.887
8S_I_4_H3.0_CDM0.8_RM1.0	2.774	1.342	1.257	0.450	0.762
8S_I_4_H3.0_CDM0.8_RM1.5	2.799	1.442	1.249	0.450	0.766
8S_I_4_H3.0_CDM1.0_RM1.0	2.867	1.615	1.282	0.450	0.793
8S_I_4_H3.0_CDM1.0_RM1.5	2.999	1.727	1.293	0.492	0.870
8S_I_4_H4.0_CDM0.8_RM1.0	2.694	1.142	1.290	0.492	0.788
8S_I_4_H4.0_CDM0.8_RM1.5	2.648	1.238	1.300	0.450	0.726
8S_I_4_H4.0_CDM1.0_RM1.0	2.805	1.395	1.268	0.492	0.829
8S_I_4_H4.0_CDM1.0_RM1.5	2.697	1.507	1.267	0.420	0.712
8S_I_4_H5.0_CDM0.8_RM1.0	2.515	1.000	1.322	0.510	0.762
8S_I_4_H5.0_CDM0.8_RM1.5	2.533	1.053	1.292	0.492	0.741
8S_I_4_H5.0_CDM1.0_RM1.0	2.634	1.217	1.302	0.492	0.784
8S_I_4_H5.0_CDM1.0_RM1.5	2.677	1.306	1.305	0.492	0.789
8S_I_4_wo_1_H3.0_CDM0.8_RM1.0	2.562	1.000	1.620	0.510	0.831
8S_I_4_wo_1_H3.0_CDM0.8_RM1.5	2.617	1.000	1.421	0.492	0.809
8S_I_4_wo_1_H3.0_CDM1.0_RM1.0	2.713	1.087	1.329	0.492	0.851
8S_I_4_wo_1_H3.0_CDM1.0_RM1.5	2.778	1.204	1.304	0.492	0.855
8S_I_4_wo_1_H4.0_CDM0.8_RM1.0	2.421	1.000	2.049	0.689	1.038
8S_I_4_wo_1_H4.0_CDM0.8_RM1.5	2.599	1.000	1.700	0.689	1.052

8S_I_4_wo_1_H4.0_CDM1.0_RM1.0	2.702	1.000	1.537	0.688	1.130
8S_I_4_wo_1_H4.0_CDM1.0_RM1.5	2.756	1.024	1.354	0.629	1.040
8S_I_4_wo_1_H5.0_CDM0.8_RM1.0	2.318	1.000	2.377	0.867	1.189
8S_I_4_wo_1_H5.0_CDM0.8_RM1.5	2.347	1.000	1.984	0.778	1.086
8S_I_4_wo_1_H5.0_CDM1.0_RM1.0	2.310	1.000	1.821	0.629	0.969
8S_I_4_wo_1_H5.0_CDM1.0_RM1.5	2.429	1.000	1.573	0.629	0.978
8S_I_12_H3.0_CDM0.8_RM1.0	2.954	1.264	1.320	0.300	0.633
8S_I_12_H3.0_CDM0.8_RM1.5	2.975	1.342	1.323	0.300	0.637
8S_I_12_H3.0_CDM1.0_RM1.0	3.028	1.506	1.300	0.300	0.663
8S_I_12_H3.0_CDM1.0_RM1.5	3.048	1.594	1.302	0.300	0.666
8S_I_12_H4.0_CDM0.8_RM1.0	2.905	1.107	1.301	0.329	0.655
8S_I_12_H4.0_CDM0.8_RM1.5	2.926	1.174	1.316	0.329	0.660
8S_I_12_H4.0_CDM1.0_RM1.0	2.984	1.315	1.322	0.329	0.694
8S_I_12_H4.0_CDM1.0_RM1.5	3.007	1.386	1.325	0.329	0.697
8S_I_12_H5.0_CDM0.8_RM1.0	2.964	1.000	1.317	0.418	0.775
8S_I_12_H5.0_CDM0.8_RM1.5	2.789	1.000	1.347	0.359	0.668
8S_I_12_H5.0_CDM1.0_RM1.0	3.061	1.144	1.309	0.418	0.829
8S_I_12_H5.0_CDM1.0_RM1.5	3.093	1.213	1.324	0.419	0.834
8S_I_12_wo_1_H3.0_CDM0.8_RM1.0	2.607	1.000	2.662	0.419	0.835
8S_I_12_wo_1_H3.0_CDM0.8_RM1.5	2.775	1.000	2.062	0.419	0.845
8S_I_12_wo_1_H3.0_CDM1.0_RM1.0	2.751	1.000	1.773	0.359	0.773
8S_I_12_wo_1_H3.0_CDM1.0_RM1.5	3.020	1.049	1.522	0.419	0.906
8S_I_12_wo_1_H4.0_CDM0.8_RM1.0	4.213	1.000	3.295	0.490	0.876
8S_I_12_wo_1_H4.0_CDM0.8_RM1.5	2.562	1.000	2.717	0.490	0.892
8S_I_12_wo_1_H4.0_CDM1.0_RM1.0	2.571	1.000	2.423	0.449	0.899
8S_I_12_wo_1_H4.0_CDM1.0_RM1.5	2.600	1.000	2.001	0.419	0.847
8S_I_12_wo_1_H5.0_CDM0.8_RM1.0	8.439	1.000	3.222	0.669	1.047
8S_I_12_wo_1_H5.0_CDM0.8_RM1.5	3.575	1.000	2.840	0.568	0.911
8S_I_12_wo_1_H5.0_CDM1.0_RM1.0	3.417	1.000	2.653	0.490	0.899
8S_I_12_wo_1_H5.0_CDM1.0_RM1.5	2.765	1.000	2.345	0.490	0.910
8S_I_13_H3.0_CDM0.8_RM1.0	2.948	1.132	1.318	0.359	0.732
8S_I_13_H3.0_CDM0.8_RM1.5	2.829	1.211	1.325	0.299	0.614
8S_I_13_H3.0_CDM1.0_RM1.0	2.943	1.371	1.315	0.329	0.701
8S_I_13_H3.0_CDM1.0_RM1.5	2.884	1.444	1.319	0.299	0.640
8S_I_13_H4.0_CDM0.8_RM1.0	2.777	1.014	1.277	0.329	0.636
8S_I_13_H4.0_CDM0.8_RM1.5	2.792	1.076	1.296	0.329	0.641
8S_I_13_H4.0_CDM1.0_RM1.0	2.835	1.216	1.319	0.329	0.670
8S_I_13_H4.0_CDM1.0_RM1.5	2.851	1.279	1.326	0.329	0.673
8S_I_13_H5.0_CDM0.8_RM1.0	2.533	1.000	1.422	0.329	0.598
8S_I_13_H5.0_CDM0.8_RM1.5	2.656	1.000	1.339	0.388	0.710
8S_I_13_H5.0_CDM1.0_RM1.0	2.583	1.022	1.268	0.329	0.633
8S_I_13_H5.0_CDM1.0_RM1.5	2.597	1.079	1.289	0.329	0.637
8S_I_13_wo_1_H3.0_CDM0.8_RM1.0	2.533	1.000	2.844	0.389	0.750

8S_I_13_wo_1_H3.0_CDM0.8_RM1.5	2.585	1.000	2.261	0.389	0.758
8S_I_13_wo_1_H3.0_CDM1.0_RM1.0	2.672	1.000	1.911	0.389	0.806
8S_I_13_wo_1_H3.0_CDM1.0_RM1.5	2.643	1.000	1.684	0.329	0.686
8S_I_13_wo_1_H4.0_CDM0.8_RM1.0	5.047	1.000	3.426	0.508	0.886
8S_I_13_wo_1_H4.0_CDM0.8_RM1.5	2.673	1.000	2.853	0.508	0.901
8S_I_13_wo_1_H4.0_CDM1.0_RM1.0	2.537	1.000	2.576	0.419	0.812
8S_I_13_wo_1_H4.0_CDM1.0_RM1.5	2.531	1.000	2.193	0.359	0.702
8S_I_13_wo_1_H5.0_CDM0.8_RM1.0	9.312	1.000	3.230	0.597	0.924
8S_I_13_wo_1_H5.0_CDM0.8_RM1.5	4.118	1.000	2.924	0.597	0.945
8S_I_13_wo_1_H5.0_CDM1.0_RM1.0	3.638	1.000	2.739	0.508	0.908
8S_I_13_wo_1_H5.0_CDM1.0_RM1.5	3.124	1.000	2.456	0.449	0.811
8S_I_14_H3.0_CDM0.8_RM1.0	2.942	1.318	1.270	0.419	0.761
8S_I_14_H3.0_CDM0.8_RM1.5	2.965	1.413	1.266	0.419	0.766
8S_I_14_H3.0_CDM1.0_RM1.0	3.033	1.561	1.300	0.419	0.794
8S_I_14_H3.0_CDM1.0_RM1.5	3.067	1.670	1.317	0.419	0.797
8S_I_14_H4.0_CDM0.8_RM1.0	2.697	1.150	1.296	0.359	0.616
8S_I_14_H4.0_CDM0.8_RM1.5	2.830	1.239	1.306	0.419	0.723
8S_I_14_H4.0_CDM1.0_RM1.0	2.885	1.377	1.288	0.419	0.758
8S_I_14_H4.0_CDM1.0_RM1.5	2.911	1.468	1.285	0.419	0.762
8S_I_14_H5.0_CDM0.8_RM1.0	2.754	1.000	1.323	0.490	0.783
8S_I_14_H5.0_CDM0.8_RM1.5	2.686	1.044	1.292	0.419	0.675
8S_I_14_H5.0_CDM1.0_RM1.0	2.739	1.189	1.312	0.419	0.715
8S_I_14_H5.0_CDM1.0_RM1.5	2.764	1.264	1.321	0.419	0.718
8S_I_14_wo_1_H3.0_CDM0.8_RM1.0	2.462	1.000	2.556	0.449	0.775
8S_I_14_wo_1_H3.0_CDM0.8_RM1.5	2.549	1.000	2.047	0.419	0.731
8S_I_14_wo_1_H3.0_CDM1.0_RM1.0	2.622	1.000	1.745	0.419	0.774
8S_I_14_wo_1_H3.0_CDM1.0_RM1.5	2.703	1.000	1.478	0.419	0.778
8S_I_14_wo_1_H4.0_CDM0.8_RM1.0	3.639	1.000	3.167	0.508	0.800
8S_I_14_wo_1_H4.0_CDM0.8_RM1.5	2.416	1.000	2.640	0.479	0.765
8S_I_14_wo_1_H4.0_CDM1.0_RM1.0	2.419	1.000	2.380	0.419	0.729
8S_I_14_wo_1_H4.0_CDM1.0_RM1.5	2.442	1.000	1.991	0.419	0.735
8S_I_14_wo_1_H5.0_CDM0.8_RM1.0	7.000	1.000	3.130	0.633	0.893
8S_I_14_wo_1_H5.0_CDM0.8_RM1.5	3.528	1.000	2.794	0.657	0.946
8S_I_14_wo_1_H5.0_CDM1.0_RM1.0	3.293	1.000	2.606	0.479	0.774
8S_I_14_wo_1_H5.0_CDM1.0_RM1.5	2.665	1.000	2.311	0.479	0.782
8S_I_23_H3.0_CDM0.8_RM1.0	2.797	1.085	1.343	0.264	0.736
8S_I_23_H3.0_CDM0.8_RM1.5	2.904	1.161	1.359	0.299	0.839
8S_I_23_H3.0_CDM1.0_RM1.0	2.940	1.309	1.360	0.299	0.859
8S_I_23_H3.0_CDM1.0_RM1.5	2.859	1.373	1.361	0.264	0.758
8S_I_23_H4.0_CDM0.8_RM1.0	2.811	1.000	1.296	0.299	0.802
8S_I_23_H4.0_CDM0.8_RM1.5	2.824	1.054	1.313	0.299	0.805
8S_I_23_H4.0_CDM1.0_RM1.0	2.859	1.182	1.341	0.299	0.828
8S_I_23_H4.0_CDM1.0_RM1.5	2.872	1.237	1.352	0.299	0.831

8S_I_23_H5.0_CDM0.8_RM1.0	2.684	1.000	1.414	0.299	0.752
8S_I_23_H5.0_CDM0.8_RM1.5	2.773	1.000	1.353	0.329	0.830
8S_I_23_H5.0_CDM1.0_RM1.0	2.733	1.016	1.282	0.299	0.781
8S_I_23_H5.0_CDM1.0_RM1.5	2.747	1.066	1.302	0.299	0.683
8S_I_23_wo_1_H3.0_CDM0.8_RM1.0	2.617	1.000	3.175	0.389	0.995
8S_I_23_wo_1_H3.0_CDM0.8_RM1.5	2.646	1.000	2.534	0.389	1.007
8S_I_23_wo_1_H3.0_CDM1.0_RM1.0	2.644	1.000	2.181	0.329	0.908
8S_I_23_wo_1_H3.0_CDM1.0_RM1.5	2.680	1.000	1.856	0.329	0.913
8S_I_23_wo_1_H4.0_CDM0.8_RM1.0	6.106	1.000	3.562	0.508	1.145
8S_I_23_wo_1_H4.0_CDM0.8_RM1.5	3.184	1.000	3.042	0.449	1.032
8S_I_23_wo_1_H4.0_CDM1.0_RM1.0	3.021	1.000	2.769	0.389	0.993
8S_I_23_wo_1_H4.0_CDM1.0_RM1.5	4.492	1.000	3.267	0.500	1.622
8S_I_23_wo_1_H5.0_CDM0.8_RM1.0	24.020	1.005	3.473	0.974	2.140
8S_I_23_wo_1_H5.0_CDM0.8_RM1.5	8.704	1.124	3.261	0.730	1.658
8S_I_23_wo_1_H5.0_CDM1.0_RM1.0	4.072	1.000	2.842	0.508	1.172
8S_I_23_wo_1_H5.0_CDM1.0_RM1.5	3.722	1.000	2.586	0.508	1.187
8S_I_24_H3.0_CDM0.8_RM1.0	2.718	1.253	1.316	0.300	0.690
8S_I_24_H3.0_CDM0.8_RM1.5	2.731	1.337	1.319	0.300	0.693
8S_I_24_H3.0_CDM1.0_RM1.0	2.762	1.473	1.292	0.300	0.715
8S_I_24_H3.0_CDM1.0_RM1.5	2.774	1.556	1.307	0.300	0.717
8S_I_24_H4.0_CDM0.8_RM1.0	2.686	1.135	1.316	0.329	0.723
8S_I_24_H4.0_CDM0.8_RM1.5	2.701	1.209	1.329	0.329	0.726
8S_I_24_H4.0_CDM1.0_RM1.0	2.741	1.351	1.321	0.329	0.752
8S_I_24_H4.0_CDM1.0_RM1.5	2.752	1.413	1.325	0.329	0.755
8S_I_24_H5.0_CDM0.8_RM1.0	2.627	1.000	1.315	0.359	0.740
8S_I_24_H5.0_CDM0.8_RM1.5	2.644	1.035	1.297	0.359	0.744
8S_I_24_H5.0_CDM1.0_RM1.0	2.632	1.159	1.324	0.329	0.711
8S_I_24_H5.0_CDM1.0_RM1.5	2.644	1.211	1.338	0.329	0.714
8S_I_24_wo_1_H3.0_CDM0.8_RM1.0	2.469	1.000	2.889	0.449	0.962
8S_I_24_wo_1_H3.0_CDM0.8_RM1.5	2.507	1.000	2.341	0.389	0.843
8S_I_24_wo_1_H3.0_CDM1.0_RM1.0	2.500	1.000	2.048	0.330	0.760
8S_I_24_wo_1_H3.0_CDM1.0_RM1.5	2.585	1.000	1.725	0.359	0.832
8S_I_24_wo_1_H4.0_CDM0.8_RM1.0	4.342	1.000	3.334	0.508	0.980
8S_I_24_wo_1_H4.0_CDM0.8_RM1.5	2.816	1.000	2.854	0.508	0.997
8S_I_24_wo_1_H4.0_CDM1.0_RM1.0	2.674	1.000	2.596	0.389	0.838
8S_I_24_wo_1_H4.0_CDM1.0_RM1.5	2.468	1.000	2.195	0.449	0.974
8S_I_24_wo_1_H5.0_CDM0.8_RM1.0	8.382	1.000	3.201	0.627	1.060
8S_I_24_wo_1_H5.0_CDM0.8_RM1.5	3.791	1.000	2.877	0.574	0.994
8S_I_24_wo_1_H5.0_CDM1.0_RM1.0	3.752	1.000	2.713	0.508	1.005
8S_I_24_wo_1_H5.0_CDM1.0_RM1.5	3.214	1.000	2.457	0.508	1.016
8S_I_34_H3.0_CDM0.8_RM1.0	2.767	1.169	1.313	0.299	0.780
8S_I_34_H3.0_CDM0.8_RM1.5	2.777	1.243	1.319	0.299	0.783
8S_I_34_H3.0_CDM1.0_RM1.0	2.806	1.387	1.297	0.299	0.802

8S_I_34_H3.0_CDM1.0_RM1.5	2.816	1.466	1.295	0.299	0.804
8S_I_34_H4.0_CDM0.8_RM1.0	2.742	1.074	1.297	0.329	0.816
8S_I_34_H4.0_CDM0.8_RM1.5	2.754	1.140	1.311	0.329	0.819
8S_I_34_H4.0_CDM1.0_RM1.0	2.788	1.274	1.312	0.329	0.844
8S_I_34_H4.0_CDM1.0_RM1.5	2.800	1.345	1.317	0.329	0.846
8S_I_34_H5.0_CDM0.8_RM1.0	2.726	1.000	1.381	0.388	0.901
8S_I_34_H5.0_CDM0.8_RM1.5	2.661	1.000	1.300	0.329	0.766
8S_I_34_H5.0_CDM1.0_RM1.0	2.697	1.096	1.299	0.329	0.794
8S_I_34_H5.0_CDM1.0_RM1.5	2.709	1.151	1.314	0.329	0.798
8S_I_34_wo_1_H3.0_CDM0.8_RM1.0	2.885	1.000	3.311	0.508	1.213
8S_I_34_wo_1_H3.0_CDM0.8_RM1.5	2.552	1.000	2.719	0.419	1.011
8S_I_34_wo_1_H3.0_CDM1.0_RM1.0	2.577	1.000	2.367	0.389	0.998
8S_I_34_wo_1_H3.0_CDM1.0_RM1.5	2.629	1.000	2.012	0.389	1.003
8S_I_34_wo_1_H4.0_CDM0.8_RM1.0	5.039	1.000	3.438	0.508	1.086
8S_I_34_wo_1_H4.0_CDM0.8_RM1.5	3.000	1.000	3.033	0.508	1.107
8S_I_34_wo_1_H4.0_CDM1.0_RM1.0	2.847	1.000	2.803	0.449	1.073
8S_I_34_wo_1_H4.0_CDM1.0_RM1.5	2.497	1.000	2.460	0.389	0.939
8S_I_34_wo_1_H5.0_CDM0.8_RM1.0	9.931	1.000	3.261	0.687	1.273
8S_I_34_wo_1_H5.0_CDM0.8_RM1.5	4.590	1.000	2.983	0.597	1.138
8S_I_34_wo_1_H5.0_CDM1.0_RM1.0	3.792	1.000	2.832	0.508	1.109
8S_I_34_wo_1_H5.0_CDM1.0_RM1.5	3.553	1.000	2.612	0.508	1.122
8S_I_1234_H3.0_CDM0.8_RM1.0	2.867	1.007	1.359	0.209	0.861
8S_I_1234_H3.0_CDM0.8_RM1.5	2.869	1.065	1.379	0.209	0.867
8S_I_1234_H3.0_CDM1.0_RM1.0	2.872	1.176	1.396	0.209	0.903
8S_I_1234_H3.0_CDM1.0_RM1.5	2.874	1.237	1.408	0.209	0.907
8S_I_1234_H4.0_CDM0.8_RM1.0	2.867	1.000	1.418	0.239	0.870
8S_I_1234_H4.0_CDM0.8_RM1.5	2.867	1.000	1.375	0.239	0.877
8S_I_1234_H4.0_CDM1.0_RM1.0	2.871	1.057	1.360	0.239	0.921
8S_I_1234_H4.0_CDM1.0_RM1.5	2.870	1.097	1.380	0.233	0.902
8S_I_1234_H5.0_CDM0.8_RM1.0	2.843	1.000	1.650	0.239	0.793
8S_I_1234_H5.0_CDM0.8_RM1.5	2.842	1.000	1.609	0.239	0.795
8S_I_1234_H5.0_CDM1.0_RM1.0	2.843	1.000	1.536	0.239	0.810
8S_I_1234_H5.0_CDM1.0_RM1.5	2.843	1.000	1.500	0.239	0.812
8S_I_1234_wo_1_H3.0_CDM0.8_RM1.0	11.710	1.038	4.658	0.358	1.138
8S_I_1234_wo_1_H3.0_CDM0.8_RM1.5	5.716	1.011	4.131	0.329	1.061
8S_I_1234_wo_1_H3.0_CDM1.0_RM1.0	3.834	1.000	3.731	0.299	1.049
8S_I_1234_wo_1_H3.0_CDM1.0_RM1.5	3.834	1.000	3.731	0.299	1.049
8S_I_1234_wo_1_H4.0_CDM0.8_RM1.0	16.881	1.129	3.986	0.448	1.186
8S_I_1234_wo_1_H4.0_CDM0.8_RM1.5	10.460	1.171	3.802	0.418	1.139
8S_I_1234_wo_1_H4.0_CDM1.0_RM1.0	7.680	1.188	3.661	0.388	1.219
8S_I_1234_wo_1_H4.0_CDM1.0_RM1.5	4.708	1.146	3.406	0.388	1.234
8S_I_1234_wo_1_H5.0_CDM0.8_RM1.0	22.007	1.246	3.453	0.573	1.229
8S_I_1234_wo_1_H5.0_CDM0.8_RM1.5	15.011	1.294	3.375	0.561	1.250

8S_I_1234_wo_1_H5.0_CDM1.0_RM1.0	9.839	1.323	3.253	0.418	1.137
8S_I_1234_wo_1_H5.0_CDM1.0_RM1.5	7.193	1.367	3.158	0.448	1.240

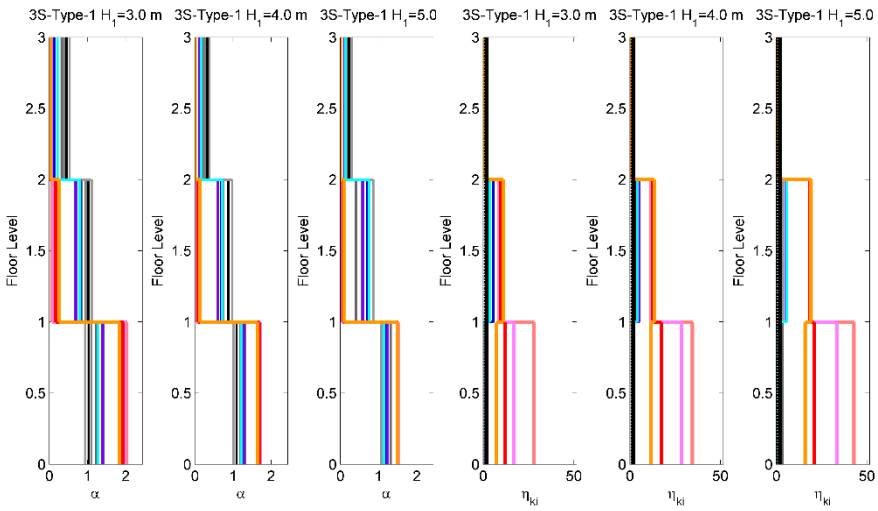

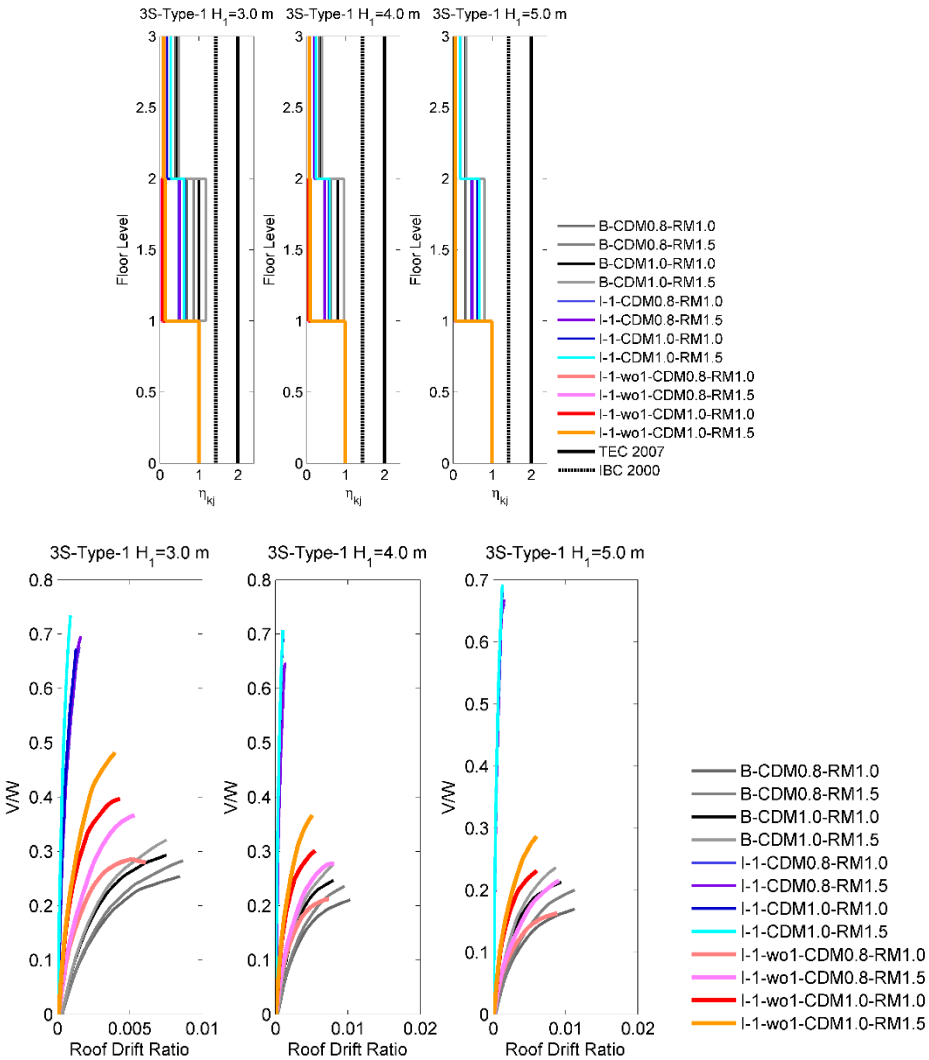

Figure A2-64 3 Story Frame; pushover analysis results at target displacement for Type 1

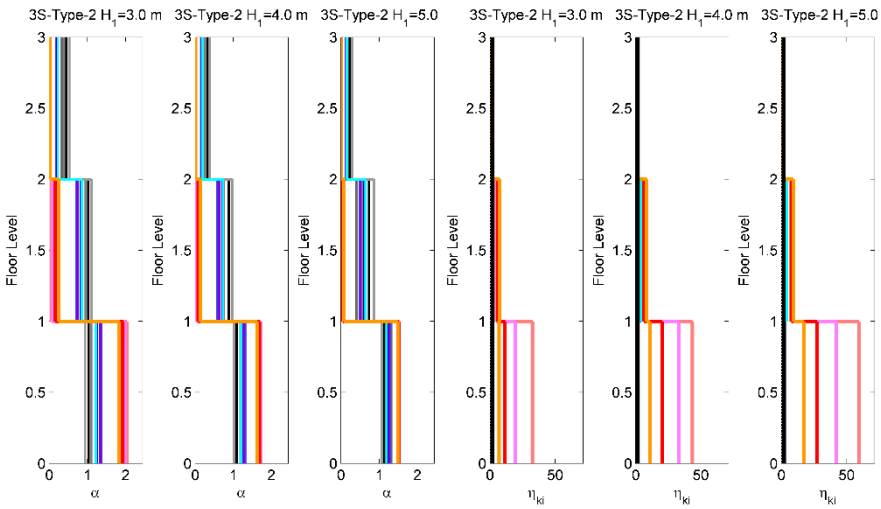

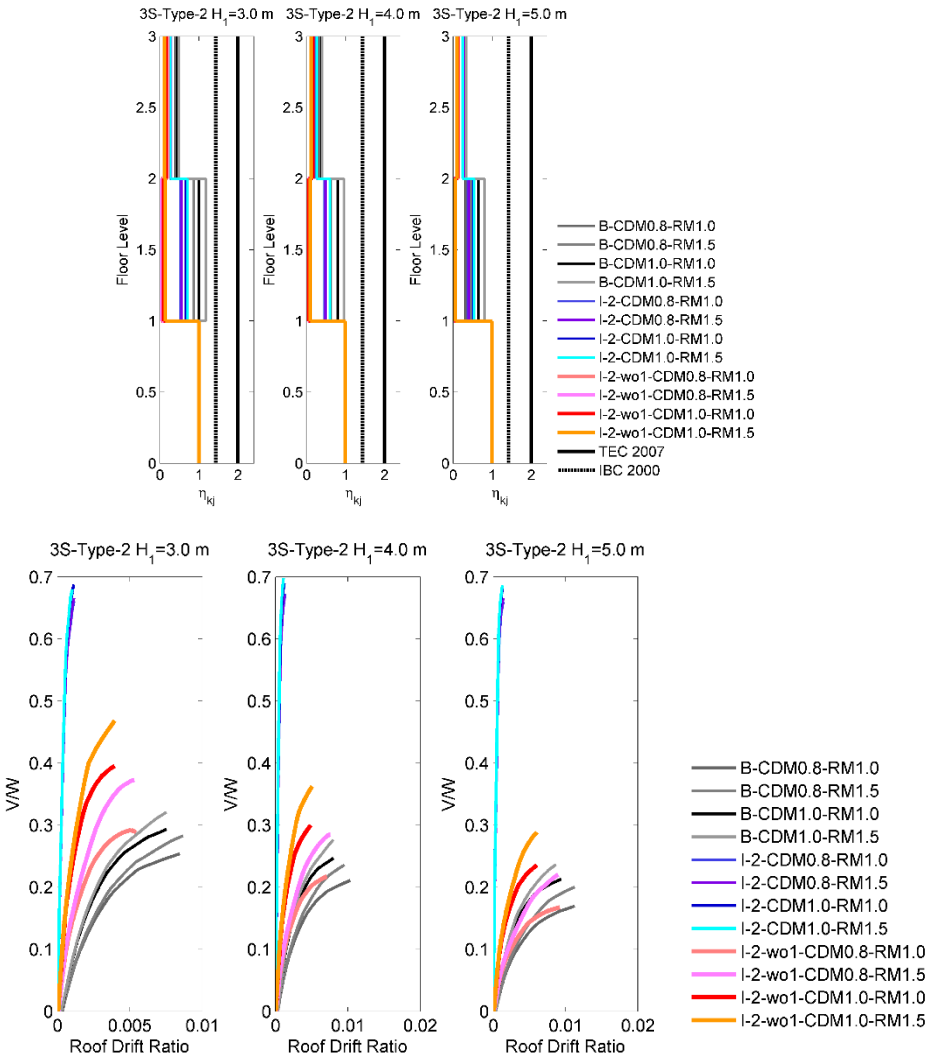

Figure A2-65 3 Story Frame; pushover analysis results at target displacement for Type 2

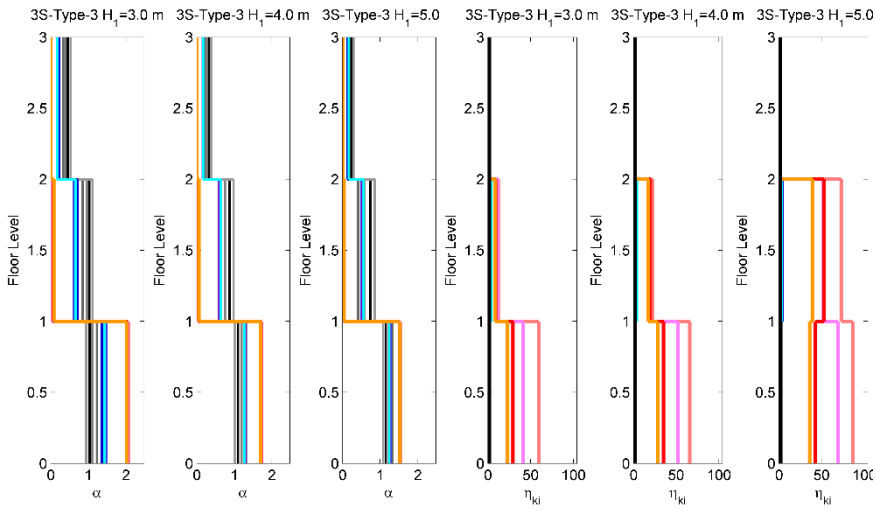

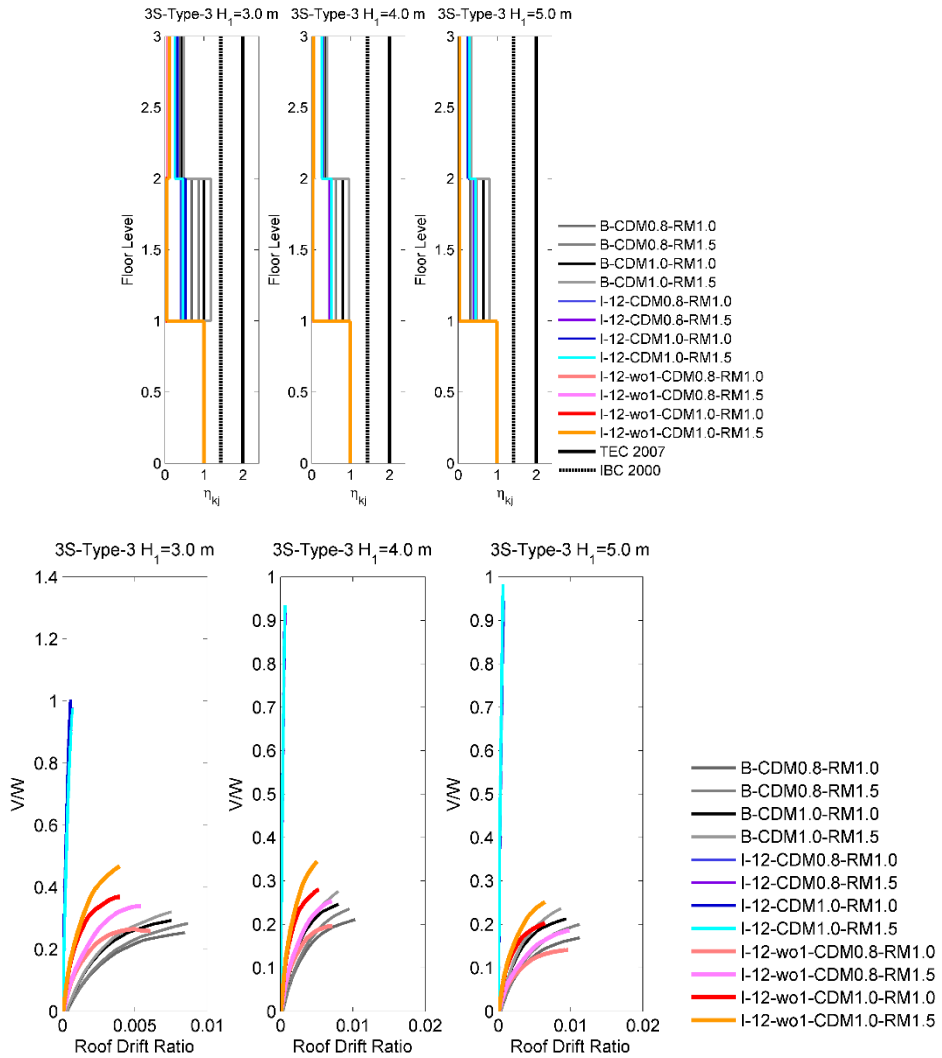

Figure A2-66 3 Story Frame; pushover analysis results at target displacement for Type 3

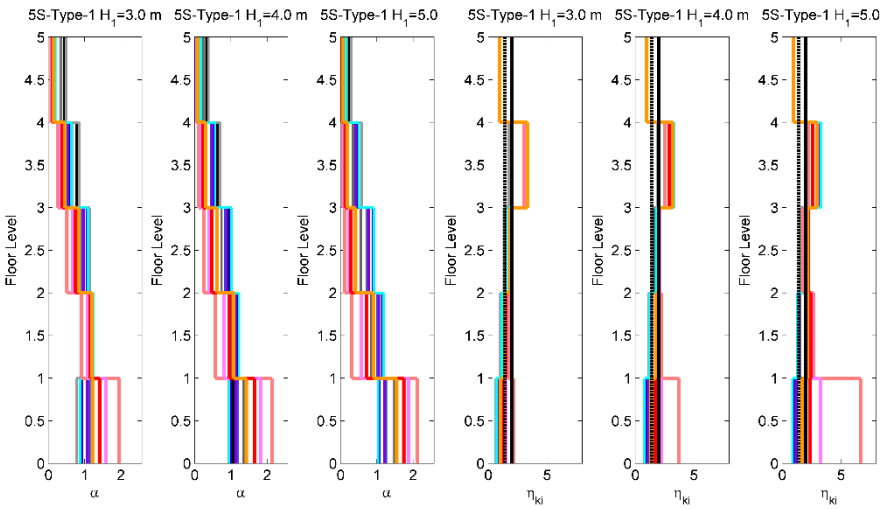

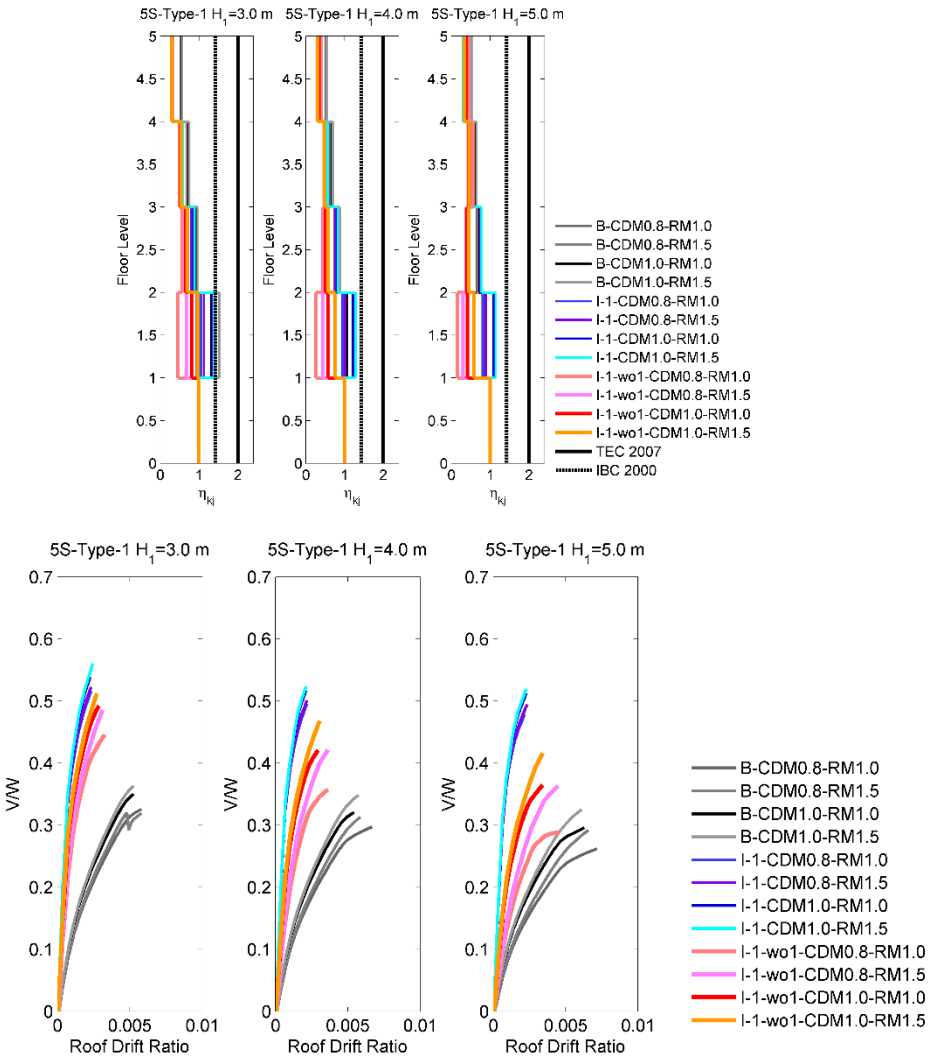

Figure A2-67 5 Story Frame; pushover analysis results at target displacement for Type 1

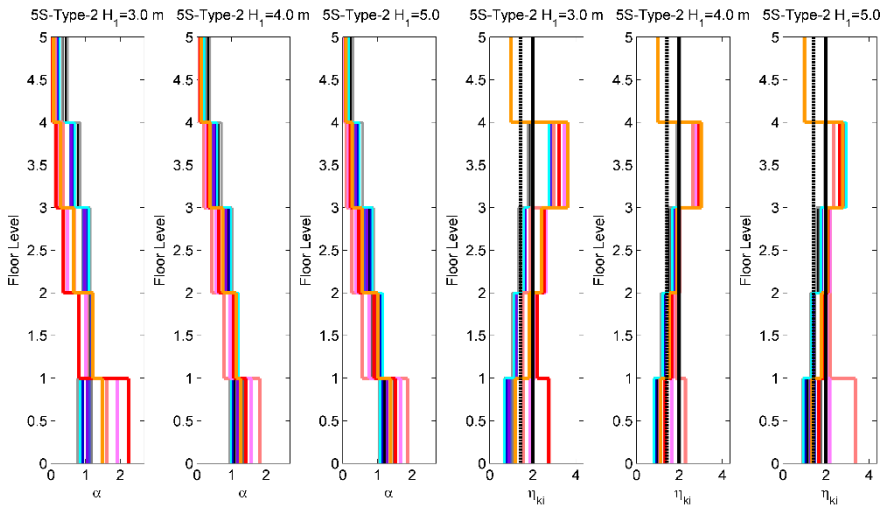

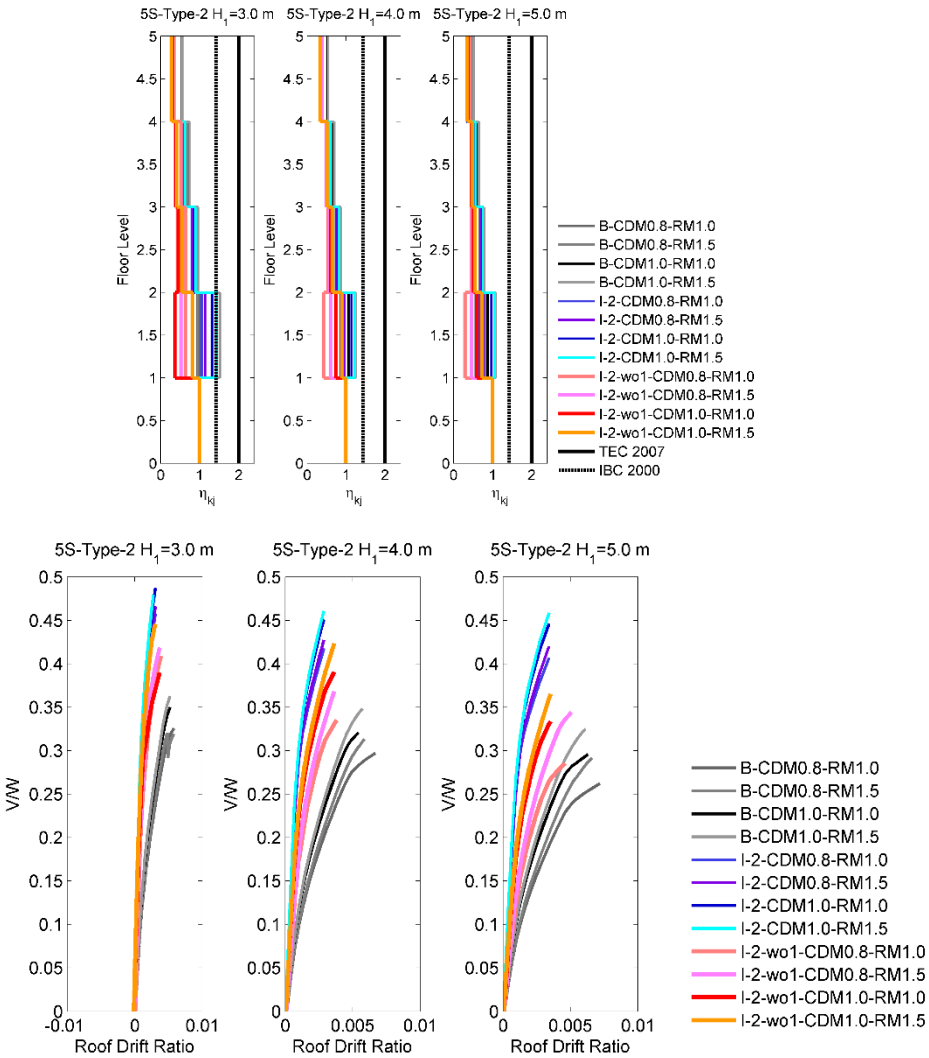

Figure A2-68 5 Story Frame; pushover analysis results at target displacement for Type 2

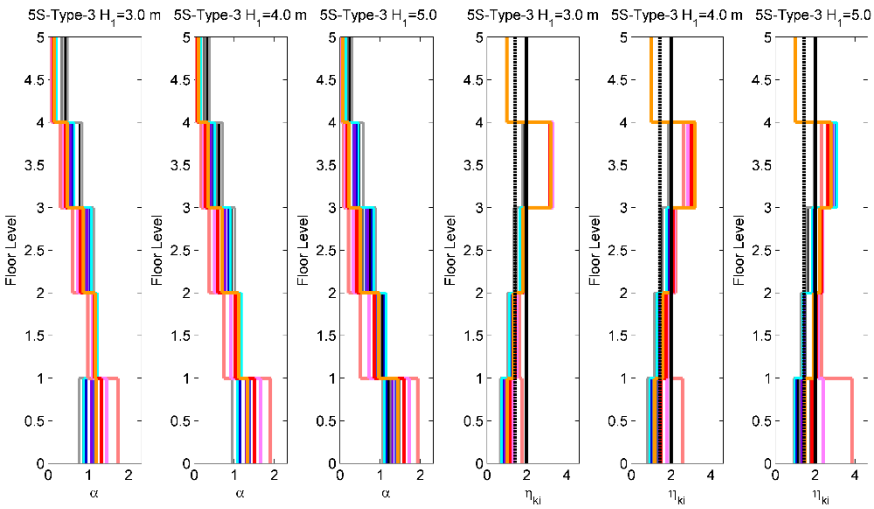

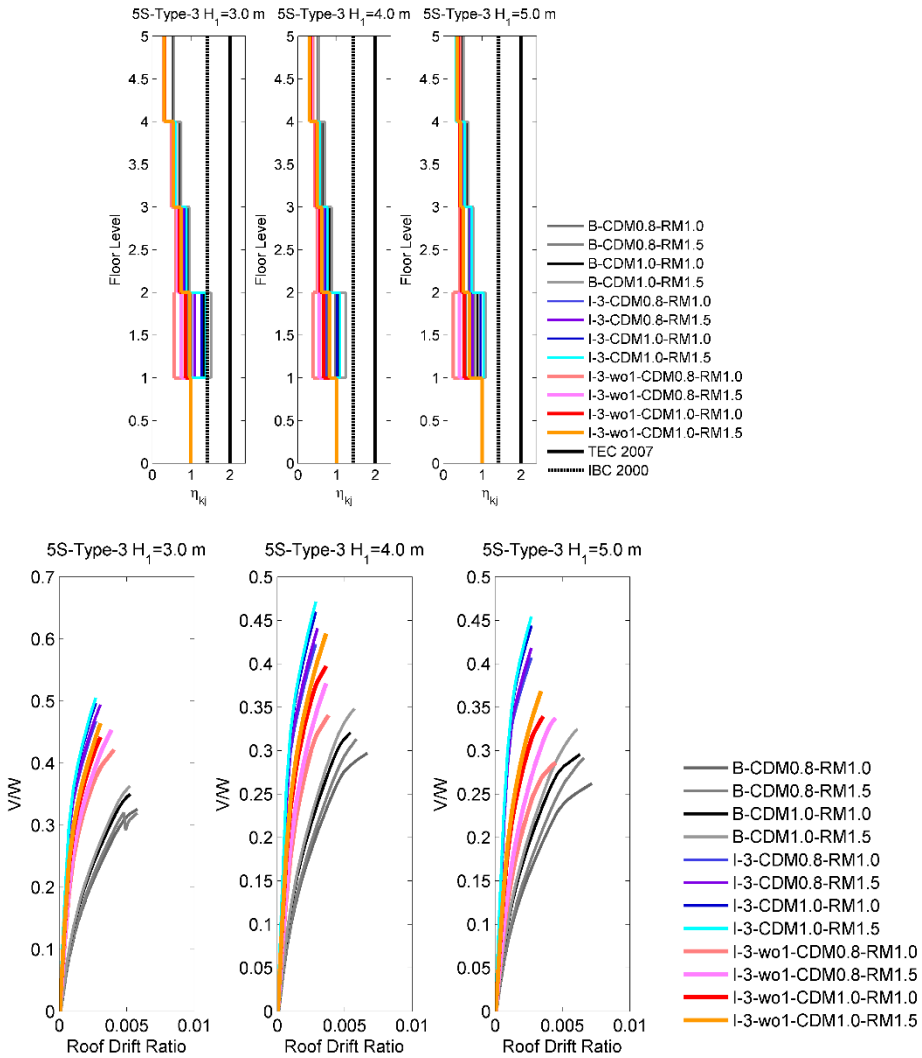

Figure A2-69 5 Story Frame; pushover analysis results at target displacement for Type 3

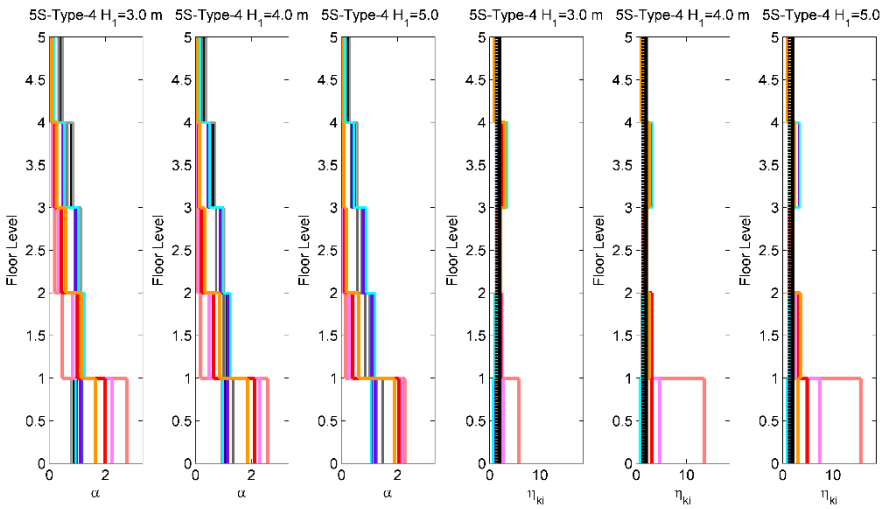

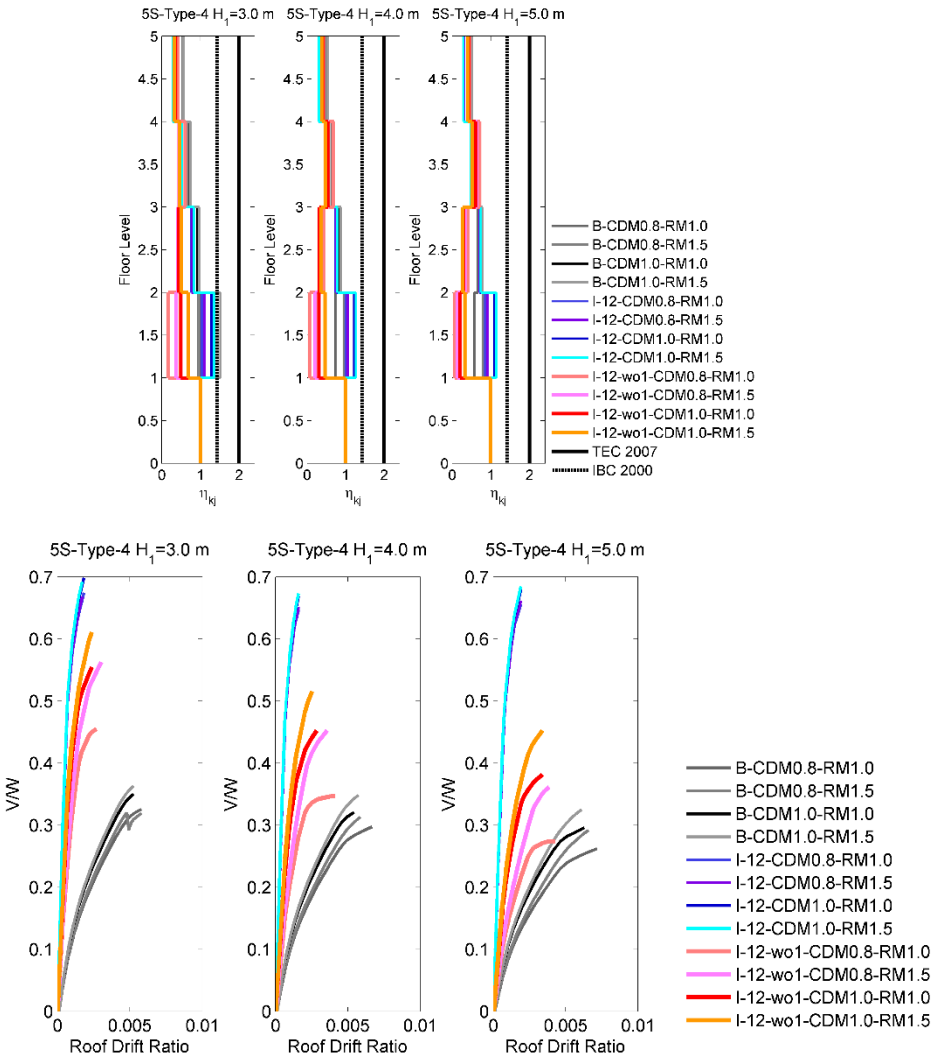

Figure A2-70 5 Story Frame; pushover analysis results at target displacement for Type 4

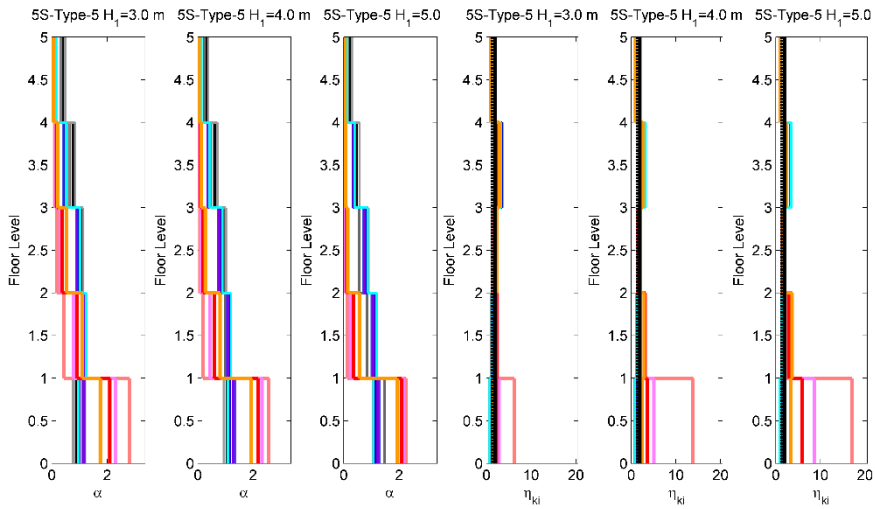

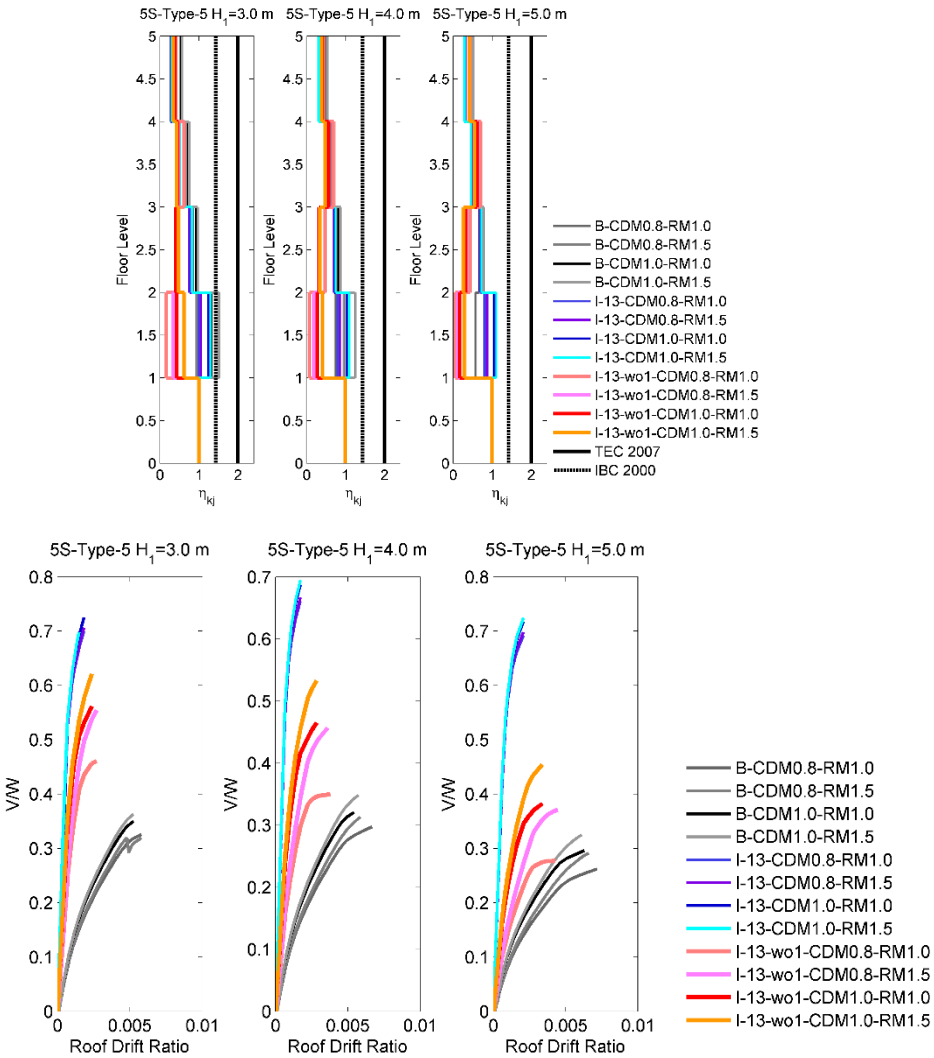

Figure A2-71 5 Story Frame; pushover analysis results at target displacement for Type 5

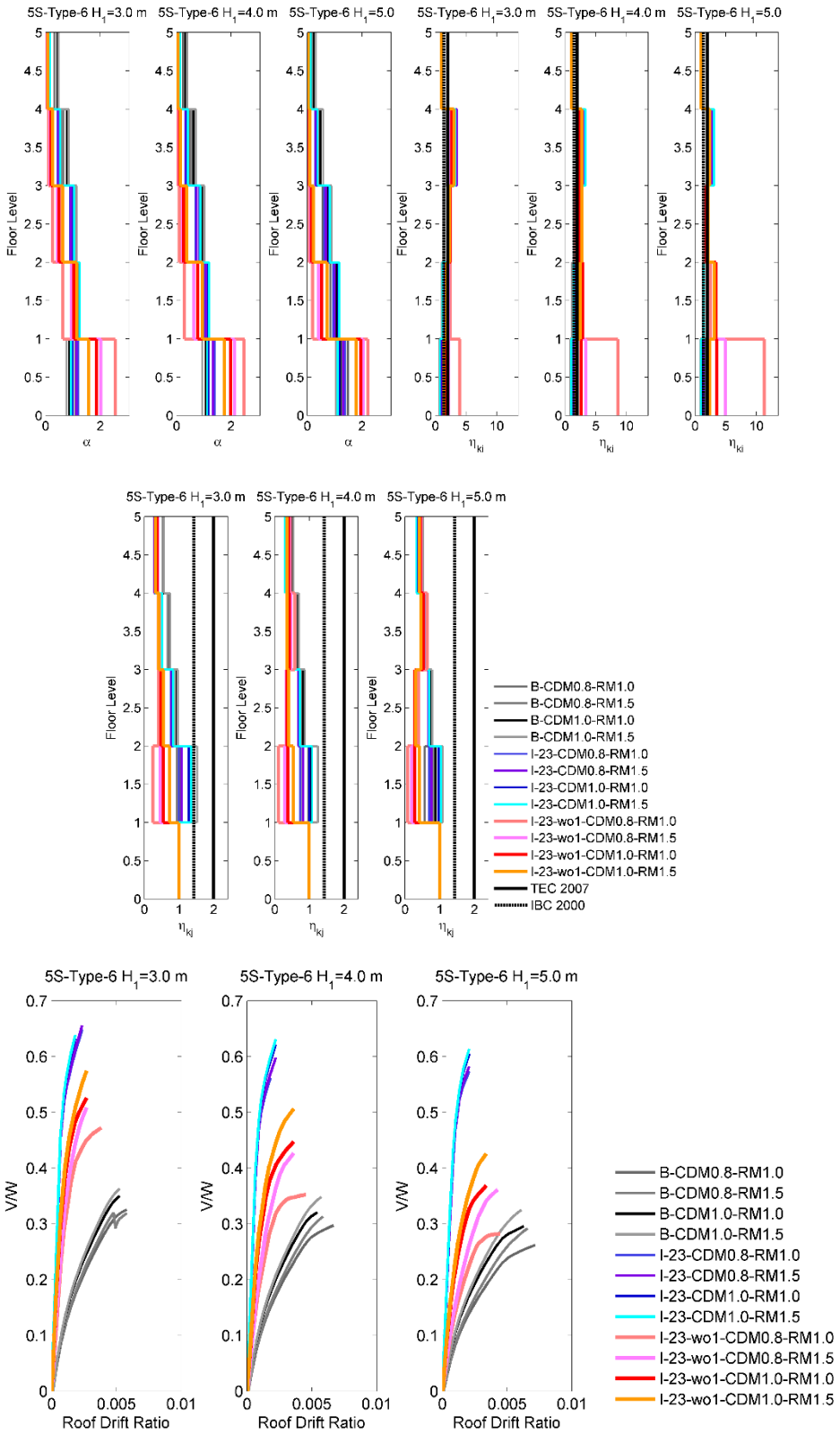

Figure A2-72 5 Story Frame; pushover analysis results at target displacement for Type 6

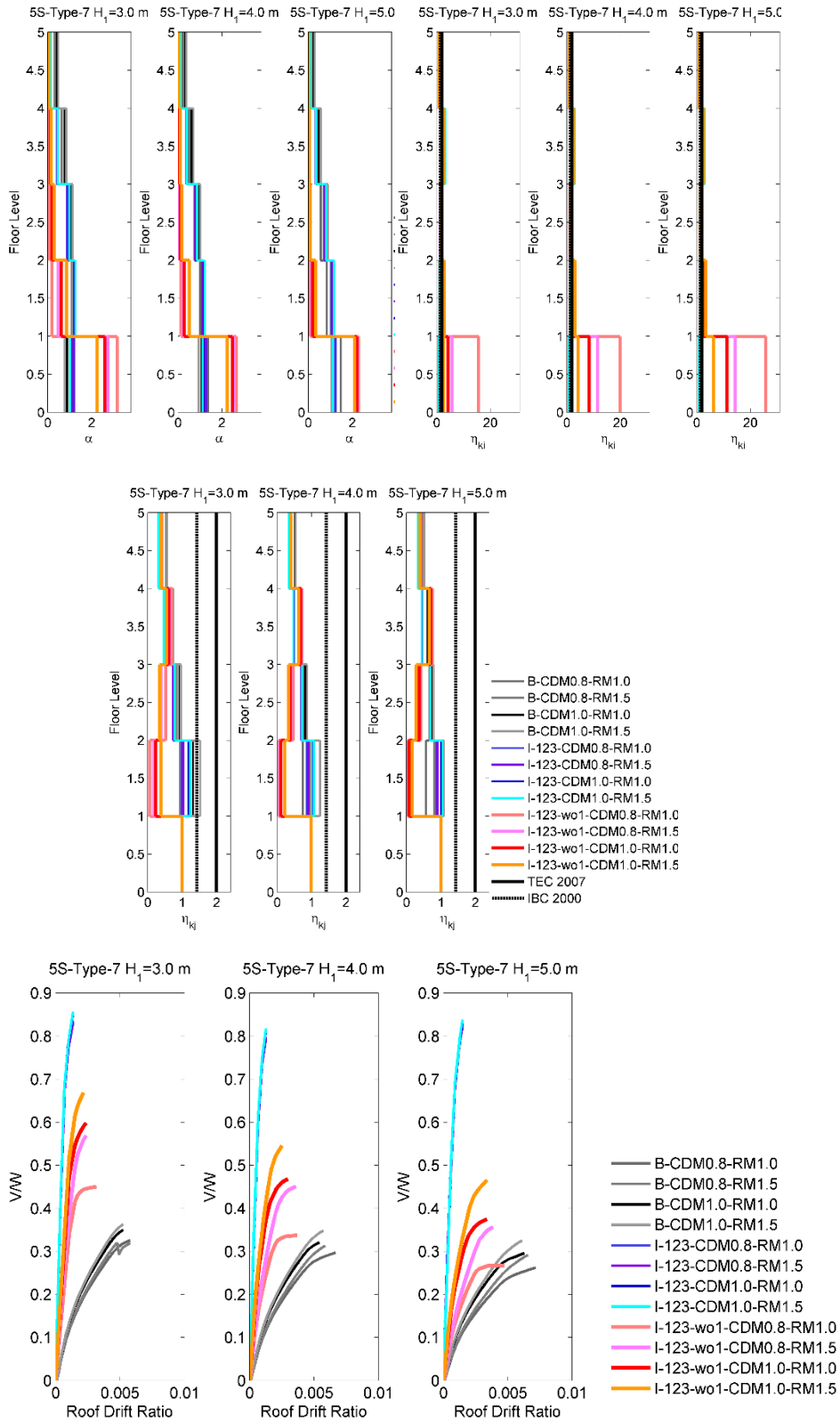

Figure A2-73 5 Story Frame; pushover analysis results at target displacement for Type 7

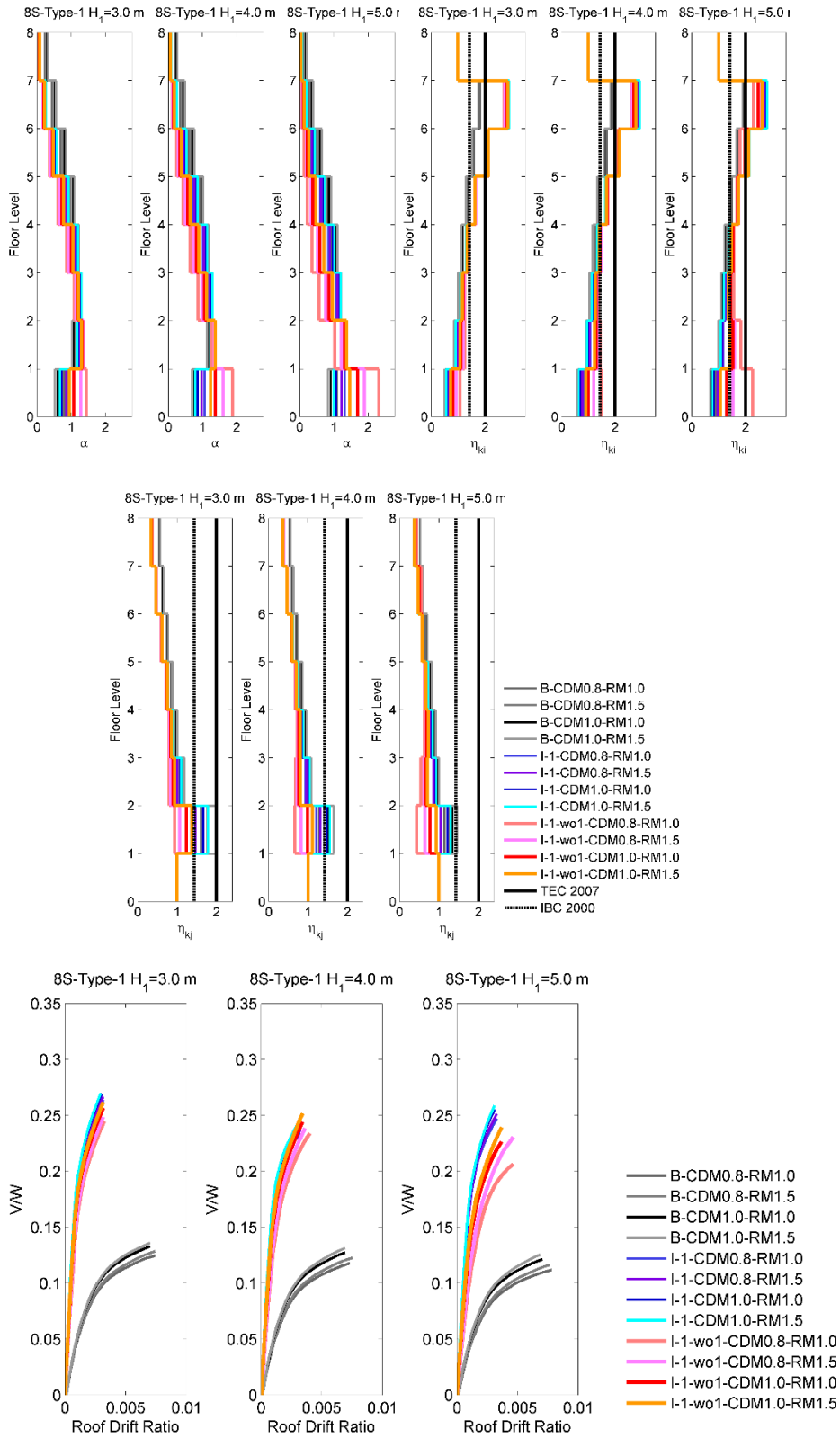

Figure A2-74 8 Story Frame; pushover analysis results at target displacement for Type 1

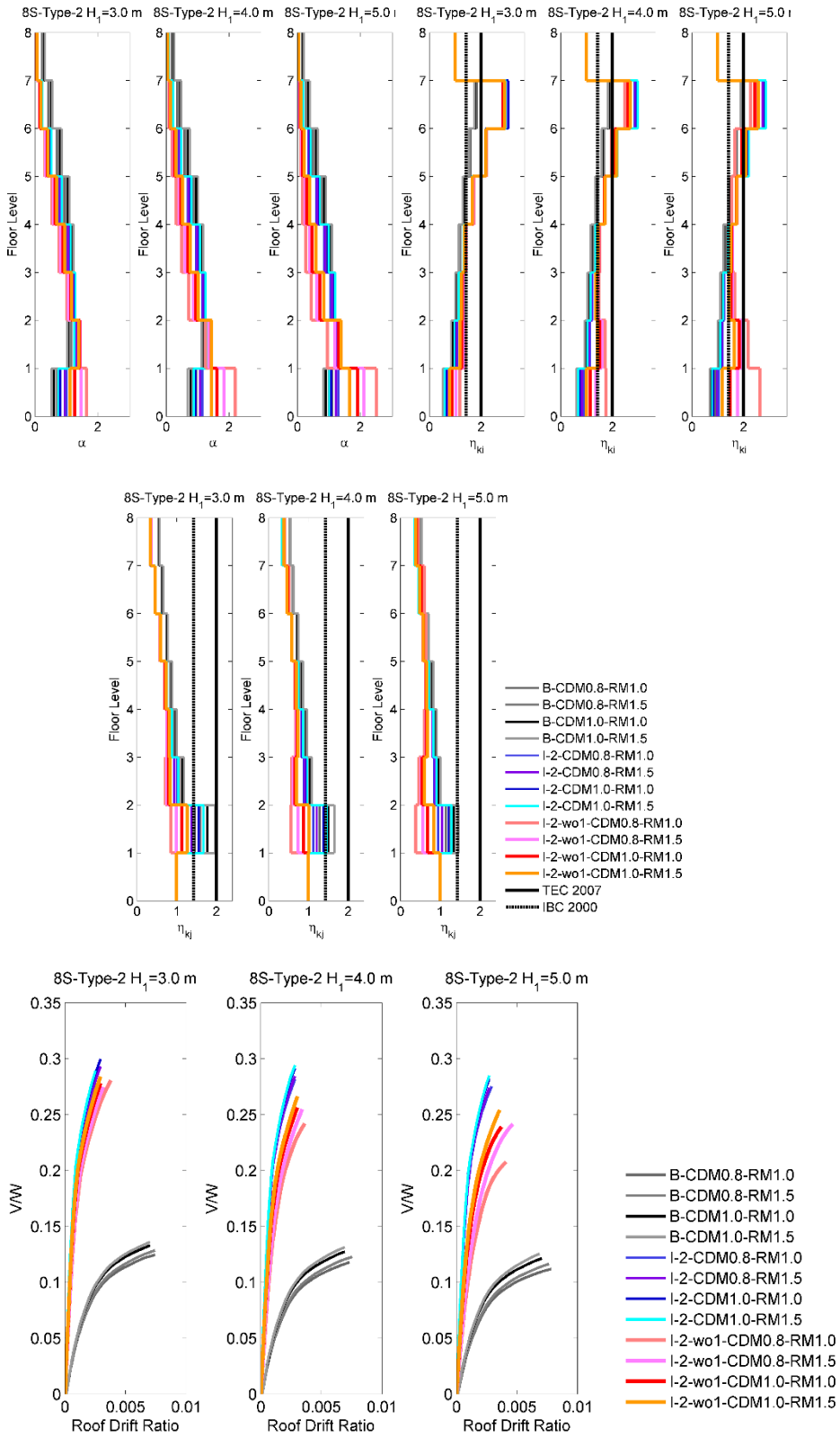

Figure A2-75 8 Story Frame; pushover analysis results at target displacement for Type 2

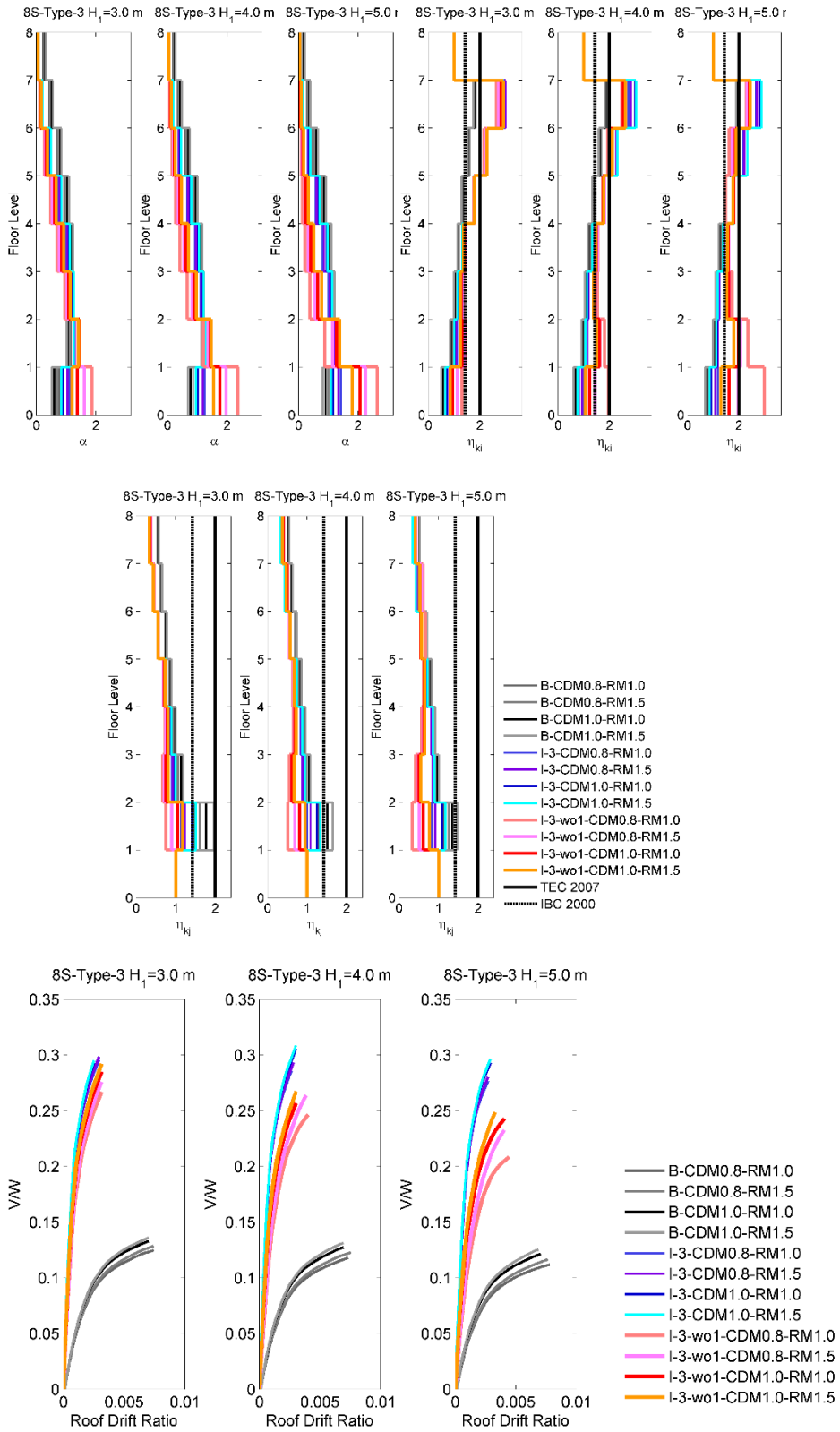

Figure A2-76 8 Story Frame; pushover analysis results at target displacement for Type 3

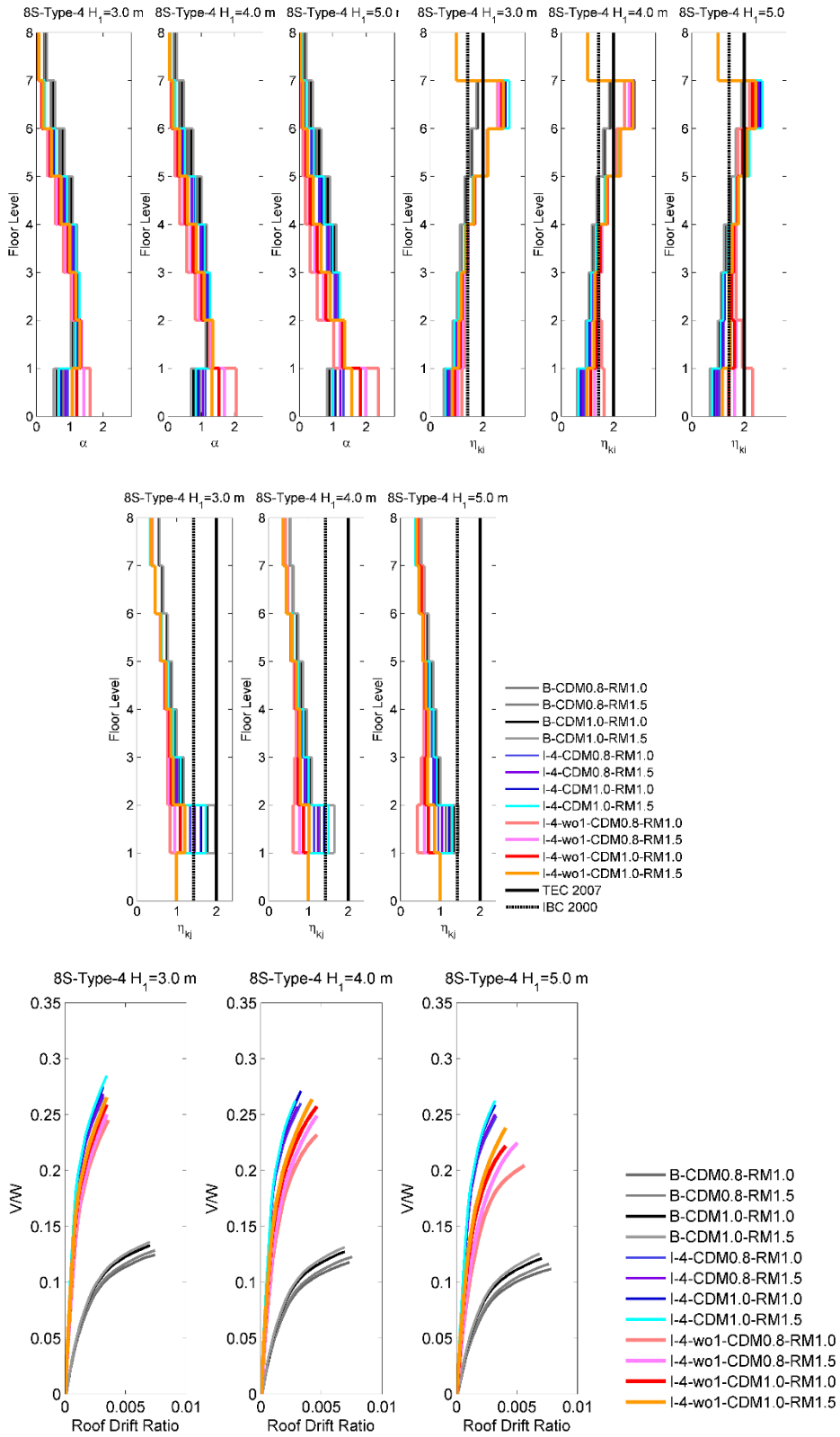

Figure A2-77 8 Story Frame; pushover analysis results at target displacement for Type 4

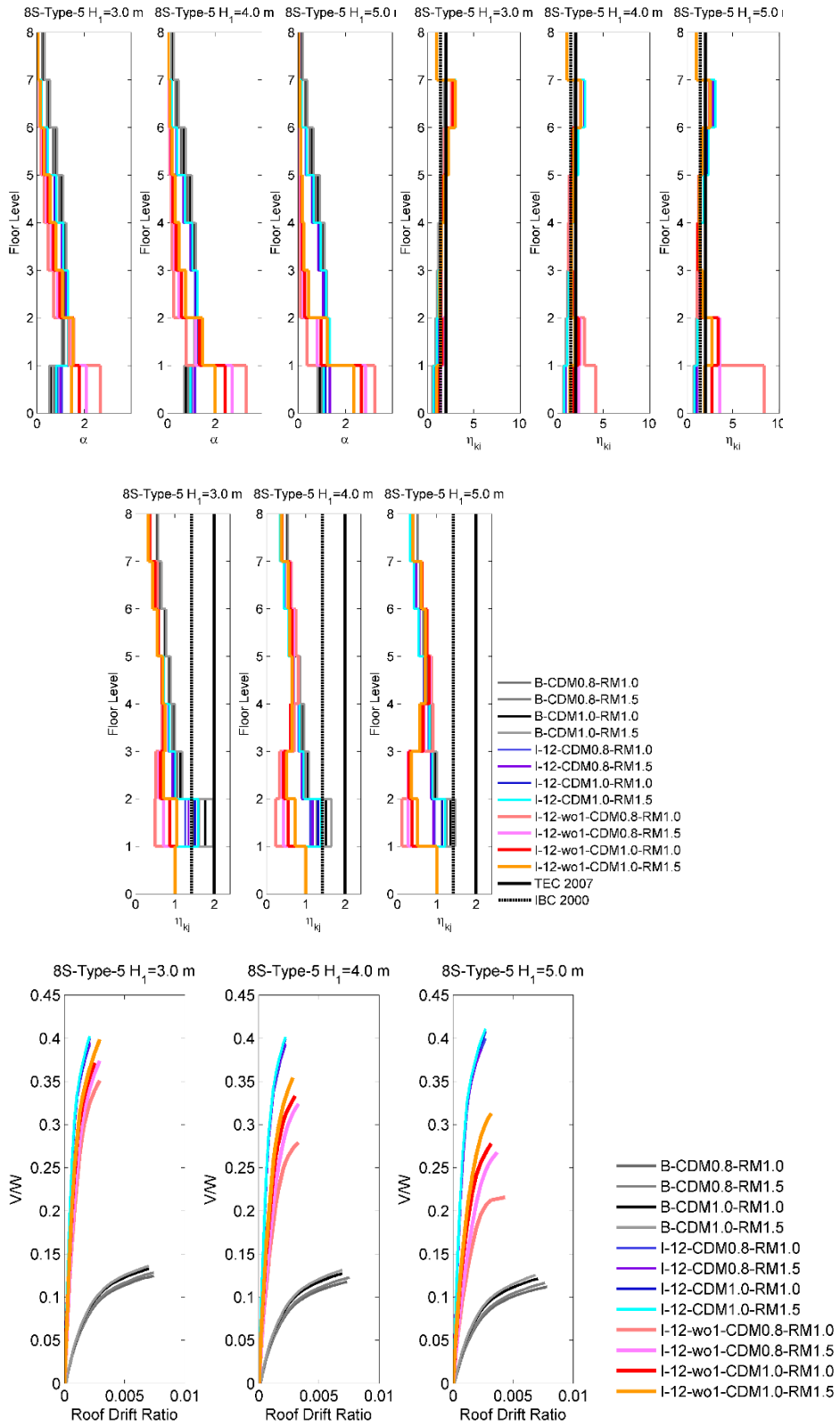

Figure A2-78 8 Story Frame; pushover analysis results at target displacement for Type 5

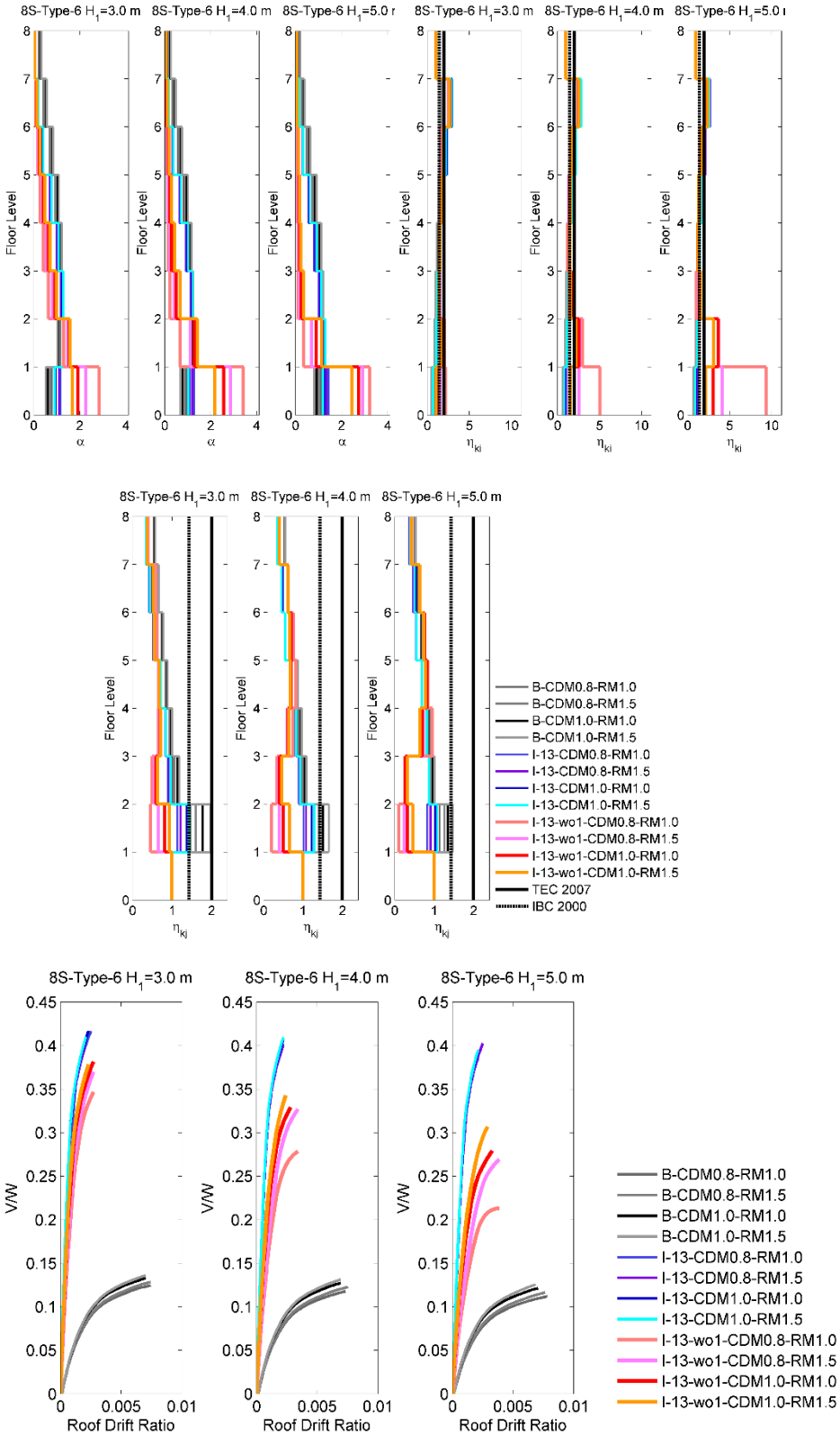

Figure A2-79 8 Story Frame; pushover analysis results at target displacement for Type 6

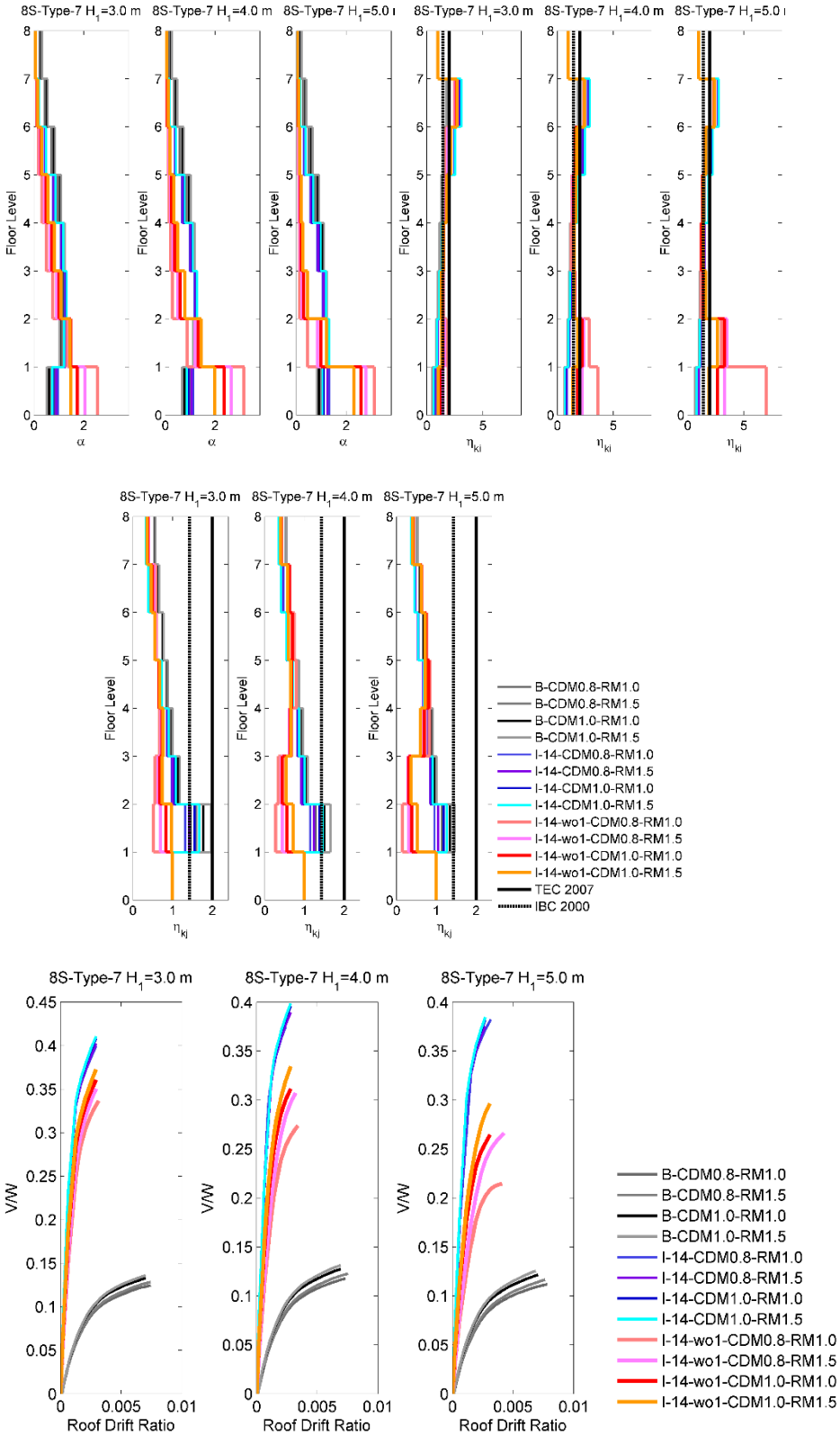

Figure A2-80 8 Story Frame; pushover analysis results at target displacement for Type 7

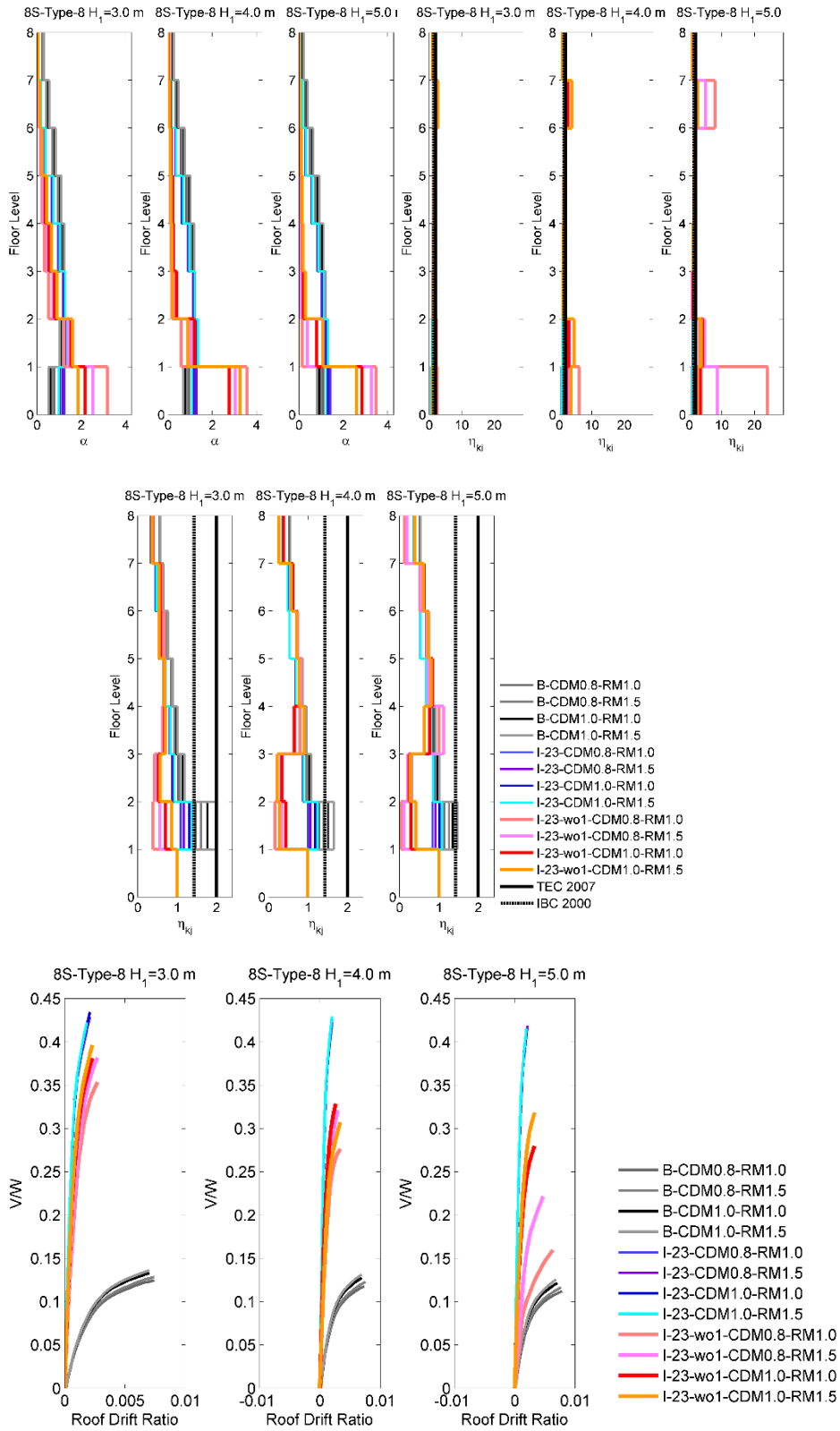

Figure A2-81 8 Story Frame; pushover analysis results at target displacement for Type 8

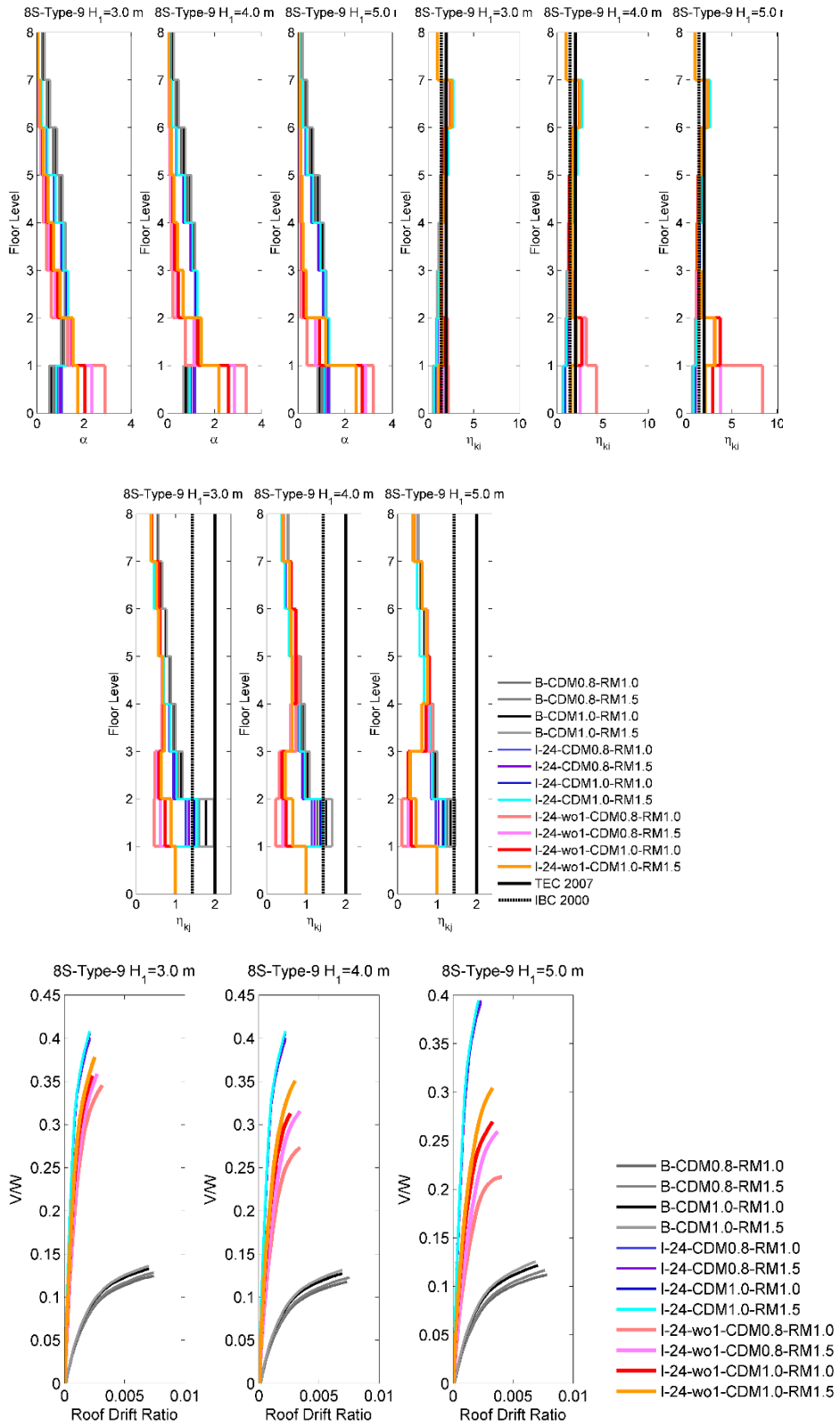

Figure A2-82 8 Story Frame; pushover analysis results at target displacement for Type 9

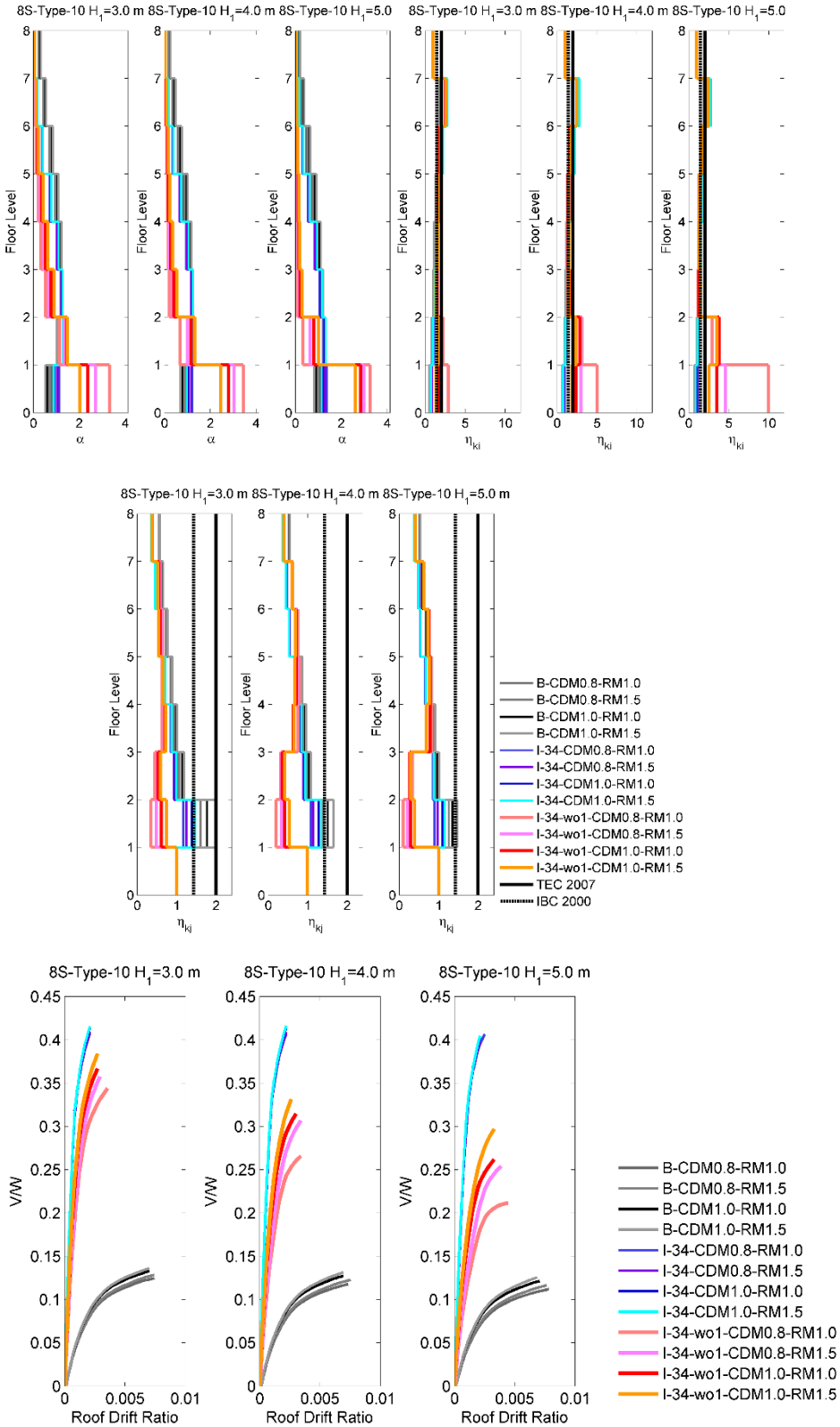

Figure A2-83 8 Story Frame; pushover analysis results at target displacement for Type 10

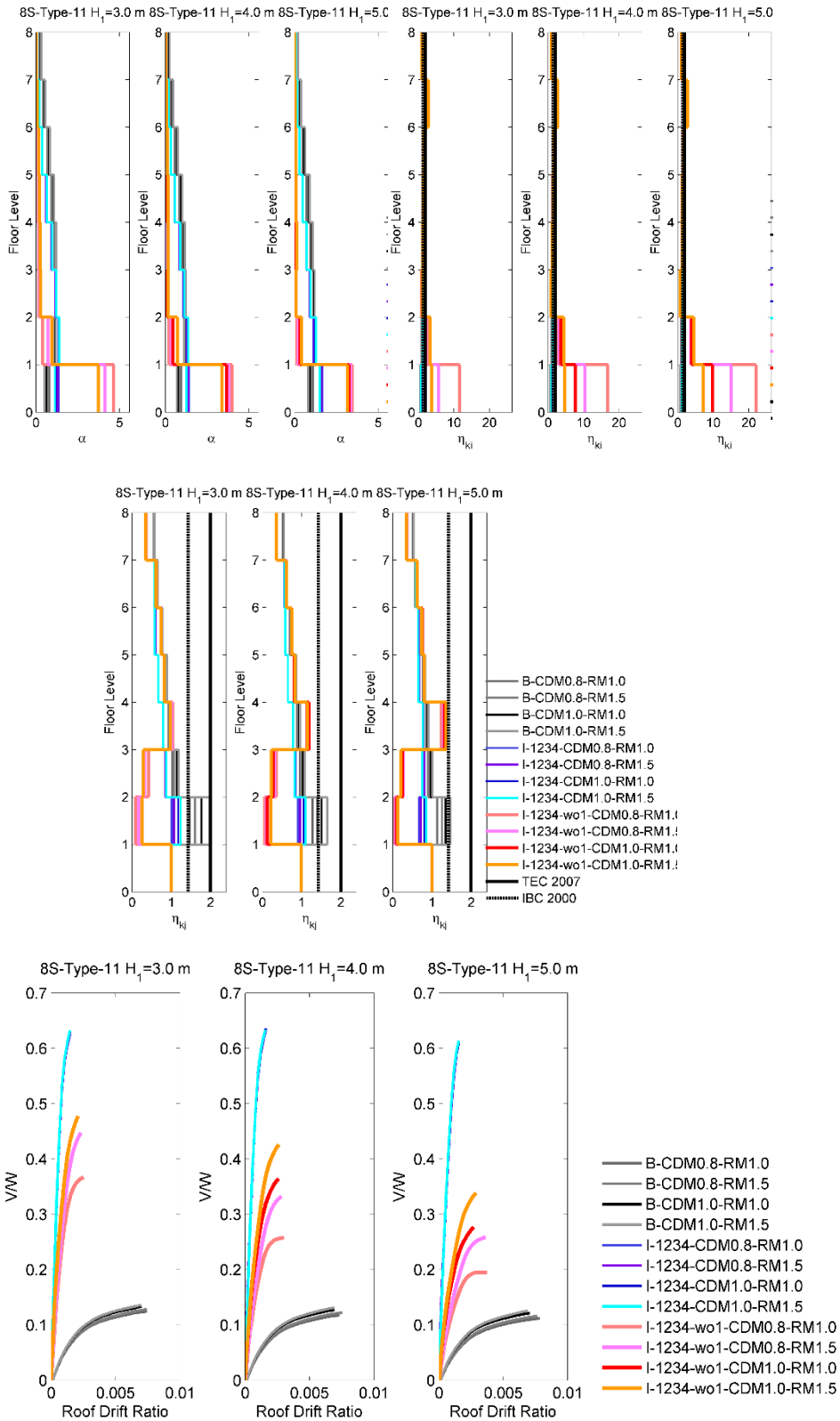

Figure A2-84 8 Story Frame; pushover analysis results at target displacement for Type 11

A3. PUSHOVER CURVES FOR EACH FRAME AT DIFFERENT PERFORMANCE POINTS

This part includes a folder, named as “VesileHatunAkansel _PhD_APPENDIX_C”, in the DVD attachment. Every frame has immediate occupancy (IO), ultimate point (which is CP in the figures) and Target. Immediate occupancy is calculated if any one of the column end yields. Ultimate point limit is calculated if one of the predefined failure criterions exist. These failure criterions are defined as; shear failure for column ends, 20% reduction in the base shear or if any one of the columns ends exceed 10 times of the yield curvature. Target displacement is calculated according to ASCE 41-13, displacement coefficient method. In APPENDIX C folder, in some of the cases, IO and Target cases match. , some of the cases, Ultimate Point (UltP) matches with IO again due to assumed global failure criteria of the 20% reduction in base shear. These cases occur at the infilled frames.

CURRICULUM VITAE

Education

Bachelor degree: Dicle University, Civil Engineering Department, (2002-2006)

Master Thesis: Middle East Technical University, Civil Engineering Department, (2008-2011), "Fragility of a shear wall building with torsional irregularity".

Advisor: Prof. Dr. Polat Gülkan.

Co-Advisor: Prof. Dr. Ahmet Yakut

Journal Papers

National

1. V. H. Akansel, İ. Kazaz, A. Yakut ve P. Gülkan, 2010, "Perde duvarlı binaların deprem etkileri altındaki davranışlarının modellenmesi ve simulasyonu", *Dicle Üniversitesi Mühendislik Fakültesi Mühendislik Dergisi*, Cilt:1, Sayı:1, Aralık, ISSN: 1309-8640, s. 31-40.

International

1. V. H. Akansel, G. Ameri, A. Askan, A. Caner, B. Erdil, Ö. Kale and D. Okuyucu, ,2012, *"23 October 2011 Mw 7.1 Van (Eastern Turkey) Earthquake: Characteristics of Recorded Strong Ground Motions and Post-Earthquake Condition Assessment of Infrastructure and Cultural Heritage",*

2. Dilek Okuyucu, Ozkan Kale, Barış Erdil, Alp Caner, M.ASCE, P.E., Ayşegül Askan and Vesile Akansel, 2012, *"Evaluation of Turkish Seismic Bridge Design Practice Resulting in a Successful Seismic Performance of Highway Bridges at the Van Earthquake, Mw=7.2, October 2011",*

Conference Papers

National

1. İ.Kazaz, V.Akansel ve P. Gülkan, 2009, *"Deprem dayanırlığı için eşsiz bir örnek: Diyarbakır Şeyh Mutahhar Camisi'nin dört ayaklı minaresi"*, Uluslararası Katılımlı Tarihi Yapıların Güçlendirilmesi ve Geleceğe Güvenle Devredilemesi Sempozyumu – II, 15-17 Ekim 2009, Diyarbakır, Türkiye

2. V. H. Akansel, İ. Kazaz, A. Yakut ve P. Gülkan, 2010, *"Perde duvarlı binaların deprem etkileri altındaki davranışlarının modellenmesi ve simulasyonu",* Bilimde Modern Yöntemler Sempozyumu-BMYS 2010,14–16 Ekim, Dicle Üniversitesi Kongre Merkezi.

3. V. H. Akansel, A. Yakut, İ. Kazaz ve P. Gülkan, 2011*, "Perde duvarlı bir model binanın dinamik davranışına yönelik parametrik bir çalışma"*, 1. Türkiye Deprem Mühendisliği ve Sismoloji Konferansı, 11-14 Ekim, ODTÜ, ANKARA.

4. Demirel, İ. O., Akansel, V. H., Bankir, Ş., Geneş, M. C., Erberik, M. A., & Yakut, A. ANTAKYA'DAKİ YIĞMA BİNALARIN ÖZELLİKLERİNİN DEPREM PERFORMANSI AÇISINDAN ANALİTİK OLARAK DEĞERLENDİRİLMESİ, 2. Türkiye Deprem Mühendisliği ve Sismoloji Konferansı, 25-27 Eylül 2013 – MKÜ – HATAY.

International

1. İ. Kazaz, V.H. Akansel, and P. Gülkan, 2011, *"Collapse Simulation of a Four-Legged Masonry Minaret"*, WCCE-ECCE-TCCE Joint Conference-2, Seismic Protection of Cultural Heritage, 31October-1 November, Antalya.

2. S. Nazirzadeh , A. Yakut, V. H. Akansel, İ. Kazaz, 2011, "*Numerical Modeling of an Unsymmetrical Building tested on Shaking Table"*, ASEM'11, Advanced Structural Engineering and Mechanics, 18-22 September, Seoul, Korea.

3. V. H. Akansel, A. Yakut, İ. Kazaz ve P. Gülkan, 2012, *"Fragility of Shear Wall Buildings with Torsional Irregularity"*, 15. WCEE, 24 – 28 Eylül, Lisbon, Portugal.

4. S. Nazirzadeh , A. Yakut, V. H. Akansel, İ. Kazaz, 2012, "*Numerical Modeling of an Unsymmetrical Building tested on Shaking Table"*, 15. WCEE, 24 – 28 Eylül, Lisbon, Portugal.

5. Kazaz, İ., Akansel, V., Gülkan, P., & Kazaz, E. *"Seismic behavior of a four-legged masonry minaret.",* 15. WCEE, 24 – 28 Eylül, Lisbon, Portugal.

6. V. Akansel, G. Ameri, A. Askan, A. Caner, B. Erdil, Ö. Kale and D. Okuyucu, ,2012, *"23 October 2011 Mw 7.1 Van (Eastern Turkey) Earthquake: Characteristics of Recorded Strong Ground Motions and Post-Earthquake Condition Assessment of Infrastructure and Cultural Heritage",* SSA

7. V. H. Akansel, J. P. Moehle, 2017. "Assessment of the collapse risk of infill walled buildings", 16th WCEE, Santiago, Chile, 9-13 Ocak.

8. V. H. Akansel, A. Yakut and J. P. Moehle, 2017. "Effect of infill walls on structural behavior of rc buildings with vertical irregularties", 16th WCEE, Santiago, Chile, 9-13 Ocak.

9. V. H. Akansel, A. Yakut and P. Gülkan, 2017. "Effects of openings on the collapse risk of infilled RC buildings", 4.UDMSK, Eskişehir, Turkey.

10. L. Mazılıgüney, K. Kadaş, and V. H. Akansel, 2017. "Fragility curves for reinforced concrete school buildings in turkey due to repeated earthquakes", 4.UDMSK, Eskişehir, Turkey.

Scholarship

2214-A “Research Fellowship during Ph.D.” Grantee for 2014 2.Term to study with Prof. Dr. Jack Moehle from University of California, Berkeley for 1 year (2015-2016).

Email: vesileakansel@gmail.com